

Supplementary Information for:

Hyoliths with pedicles constrain the origin of the  
brachiopod body plan

*Haijing Sun, Martin R. Smith, Han Zeng, Fangchen Zhao, Guoxiang Li and Maoyan Zhu*

*2018-06-19*

# Contents

<b>Supplementary Text</b>	<b>4</b>
<b>1 Phylogenetic dataset</b>	<b>5</b>
<b>2 Fitch parsimony</b>	<b>7</b>
2.1 Results . . . . .	12
<b>3 Corrected parsimony</b>	<b>14</b>
3.1 Search parameters . . . . .	14
3.2 Analysis . . . . .	14
3.3 Results . . . . .	15
<b>4 Bayesian analysis</b>	<b>22</b>
4.1 Parameter estimates . . . . .	23
4.2 Results . . . . .	23
<b>5 Character reconstructions</b>	<b>25</b>
5.1 Brephic shell . . . . .	27
5.2 Larval chaetae: Paired bundles [9] . . . . .	41
5.3 Adult setae [10] . . . . .	42
5.4 Body organization . . . . .	53
5.5 Pedicle . . . . .	59
5.6 Mantle canals . . . . .	70
5.7 Perioral tentacular apparatus . . . . .	79
5.8 Digestive tract . . . . .	96
5.9 Digestive tract: Anus . . . . .	103
5.10 Sclerites . . . . .	108
5.11 Sclerites: Bivalved [67] . . . . .	110
5.12 Sclerites: Dorsal valve . . . . .	143
5.13 Sclerites: Ventral valve . . . . .	162
5.14 Sclerites: Ornament . . . . .	191
5.15 Sclerites: Composition . . . . .	197
5.16 Sclerites: Structure . . . . .	206
5.17 Gametes . . . . .	218
5.18 Gametes: Egg . . . . .	223
5.19 Gametes: Spermatozoa . . . . .	227
5.20 Embryo . . . . .	241
5.21 Larva: Apical organ . . . . .	247
5.22 Larva: Cilia . . . . .	258
5.23 Ciliary ultrastructure . . . . .	265
5.24 Nephridia . . . . .	281
5.25 Cuticle . . . . .	286

5.26 Muscles . . . . .	292
5.27 Glands . . . . .	294
5.28 Nervous system . . . . .	296
<b>6 Taxonomic implications</b>	<b>305</b>
<b>Supplementary Figures</b>	<b>307</b>
<b>Supplementary Table</b>	<b>311</b>
<b>Bibliography</b>	<b>312</b>

# Supplementary Text

This document contains supplementary material to Sun et al. (2018b). It is best viewed in HTML format at [ms609.github.io/hyoliths](https://ms609.github.io/hyoliths).

It describes the morphological dataset and the results of tree searches using Fitch parsimony and a Bayesian method: approaches that are subject to errors resulting from logically incoherent treatment of inapplicable data (Maddison, 1993). We also present the results of tree searches with the algorithm described by Brazeau et al. (2018), which reduces error due to inapplicable data in a parsimony setting. Finally, we document how each character is parsimoniously reconstructed on an optimal tree.

Supplementary figures and tables appear after the text.

# Chapter 1

## Phylogenetic dataset

Analysis was performed on a new matrix of 54 lophotrochozoan taxa, coded for 225 morphological characters (129 neomorphic, 96 transformational). The matrix can be viewed interactively at Morphobank (project 2800) [This dataset will be released on publication of the paper. Referee access is available by logging in to MorphoBank using the e-mail address and password given in the manuscript.]; a static version can be downloaded directly :

- [raw.githubusercontent.com/ms609/hyoliths/master/mbank\\_X24932\\_6-19-2018\\_744.nex](https://raw.githubusercontent.com/ms609/hyoliths/master/mbank_X24932_6-19-2018_744.nex) (Nexus format)
- [raw.githubusercontent.com/ms609/hyoliths/master/mbank\\_X24932\\_6-15-2018\\_519.tnt](https://raw.githubusercontent.com/ms609/hyoliths/master/mbank_X24932_6-15-2018_519.tnt) (TNT format).

Taxa include sipunculans and molluscs, which have previously been interpreted as having affinities with hyoliths. Other lophotrochozoan groups help to constrain the outgroup topology, and a diversity of brachiozoans helps to resolve the position of hyoliths within this group.

Characters are coded following the recommendations of Brazeau et al. (2018):

- We have employed reductive coding, using a distinct state to mark character inapplicability. Character specifications follow the structural syntax of Sereno (2007) in order to highlight ontological dependence between characters and emphasize the structure of the dataset.
- We have distinguished between neomorphic and transformational characters (*sensu* Sereno, 2007) by reserving the token 0 to refer to the absence of a neomorphic (i.e. presence/absence) character. The states of transformational characters (i.e. characters that describe a property of a feature) are represented by the tokens 1, 2, 3, ...
- We code the absence of neomorphic ontologically dependent characters (*sensu* Vogt, 2017) as absence, rather than inapplicability.

The complete dataset comprises 4975 character codings, plus 1133 inapplicable codings. (The amount and quality of data that *is* coded is more instructive than the number of cells that are ambiguous (Wiens, 1998, 2003), which, for completeness, is 6042). Of the 225 characters, the number that were coded with an applicable token for each taxon is:

<u>Acanthotretella spinosa</u>	70	<u>Gasconsia</u>	70	<u>Novocrania</u>	186
<u>Alisina</u>	84	<u>Glyptoria</u>	73	<u>Orthis</u>	70
<u>Amathia</u>	157	<u>Halkieria evangelista</u>	65	<u>Paramicrocornus</u>	57
<u>Antigonambonites planus</u>	85	<u>Haplophrentis carinatus</u>	82	<u>Paterimitra</u>	67
<u>Askepasma toddense</u>	78	<u>Heliomedusa orienta</u>	67	<u>Pauxillites</u>	56
<u>Bactrotheca</u>	53	<u>Kutorgina chengjiangensis</u>	84	<u>Pedunculotheca diana</u>	63
<u>Botsfordia</u>	75	<u>Lingula</u>	205	<u>Pelagodiscus atlanticus</u>	166
<u>Clupeafumosus socialis</u>	76	<u>Lingulellotreta malongensis</u>	87	<u>Phoronis</u>	169
<u>Conotheca</u>	60	<u>Lingulosacculus</u>	60	<u>Salanygolina</u>	79
<u>Coolinia pecten</u>	80	<u>Longtancunella chengjiangensis</u>	61	<u>Serpula</u>	170
<u>Cotyledion tylodes</u>	65	<u>Loxosomella</u>	164	<u>Siphonobolus priscus</u>	74
<u>Craniops</u>	66	<u>Maxilites</u>	61	<u>Sipunculus</u>	168
<u>Cupitheca holocyclata</u>	63	<u>Mickwitzia muralensis</u>	72	<u>Terebratulina</u>	184
<u>Dailyatia</u>	55	<u>Micrina</u>	71	<u>Tomteluva perturbata</u>	58
<u>Dentalium</u>	169	<u>Micromitra</u>	81	<u>Tonicella</u>	188
<u>Eccentrotheca</u>	54	<u>Mummpikia nuda</u>	55	<u>Ussunia</u>	53
<u>Eoobolus</u>	81	<u>Namacalathus</u>	59	<u>Wiwaxia corrugata</u>	75
<u>Flustra</u>	168	<u>Nisusia sulcata</u>	80	<u>Yuganotheca elegans</u>	56

# Chapter 2

## Fitch parsimony

Parsimony search with the Fitch (1971) algorithm was conducted in TNT v1.5 (Goloboff and Catalano, 2016) using Ratchet and tree drifting heuristics (Goloboff, 1999; Nixon, 1999), repeating the search until the optimal score had been hit by 1500 independent searches:

```
xmult:rat25 drift25 hits 1500 level 4 chklevel 5;
```

Searches were conducted under equal weights and results saved to file:

```
piwe-; xmult; /* Conduct search with equal weighting */  
tsav *TNT/ew.tre;sav;tsav/; /* Save results to file */
```

Node support was estimated by calculating the proportion of jackknife replicates in which each group occurred, using 5000 symmetric resampling iterations, following the recommendations of Kopuchian and Ramírez (2010) and Simmons and Freudenstein (2011).

```
var: nt; /* Define a variable to track tree address */  
nelsen *; /* Generate strict consensus tree */  
set nt ntrees; ttag=; /* Prepare for resampling */  
resample=sym 5000 frequency from 'nt'; /* Symmetric resampling, counting frequencies */  
log TNT/ew.sym; ttag/; log/; /* Write results to log */  
keep 0; ttag-; hold 10000; /* Clear memory */
```

Further searches were conducted under extended implied weighting (Goloboff, 1997, 2014), under the concavity constants 3, 4.5, 7, 10.5, 16 and 24:

```
xpiwe=; /* Enable extended implied weighting */  
piwe=3; xmult; /* Conduct analysis at k = 3 */  
tsav *TNT/xpiwe3.tre; sav; tsav/; /* Save results to file */  
nelsen *; set nt ntrees; ttag=; /* Prepare for resampling */  
resample=frequency from 'nt'; /* Symmetric resampling */  
log TNT/xpiwe3.sym; ttag/; log/; /* Write results to log */  
keep 0; ttag-; hold 10000; /* Clear memory */  
/* Repeat this block for each value of k */
```

Results can be replicated by:

- Downloading the data in TNT format: [raw.githubusercontent.com/ms609/hyoliths/master/mbank\\_X24932\\_6-15-2018\\_519.tnt](https://raw.githubusercontent.com/ms609/hyoliths/master/mbank_X24932_6-15-2018_519.tnt).
- Saving the script above to the same directory, with the filename **tnt.run**.
- Opening TNT, typing **piwe=** before you load the downloaded dataset (to enable extended implied weighting), then typing **tnt** into the command box to run the script.

We acknowledge the Willi Hennig Society for their sponsorship of the TNT software.

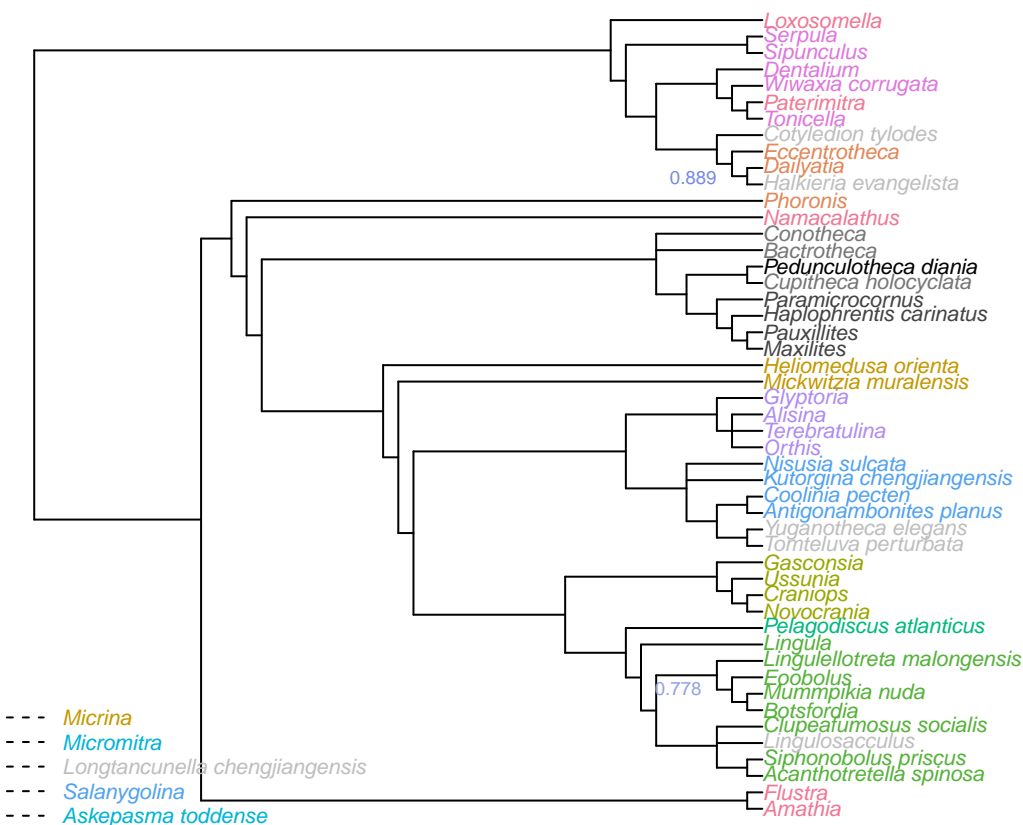


Figure 2.1: Majority-rule consensus of all trees that are optimal under implied weights. Each node is labelled with its frequency in the set of all optimal trees under all examined values of  $k$ , where less than 100%.

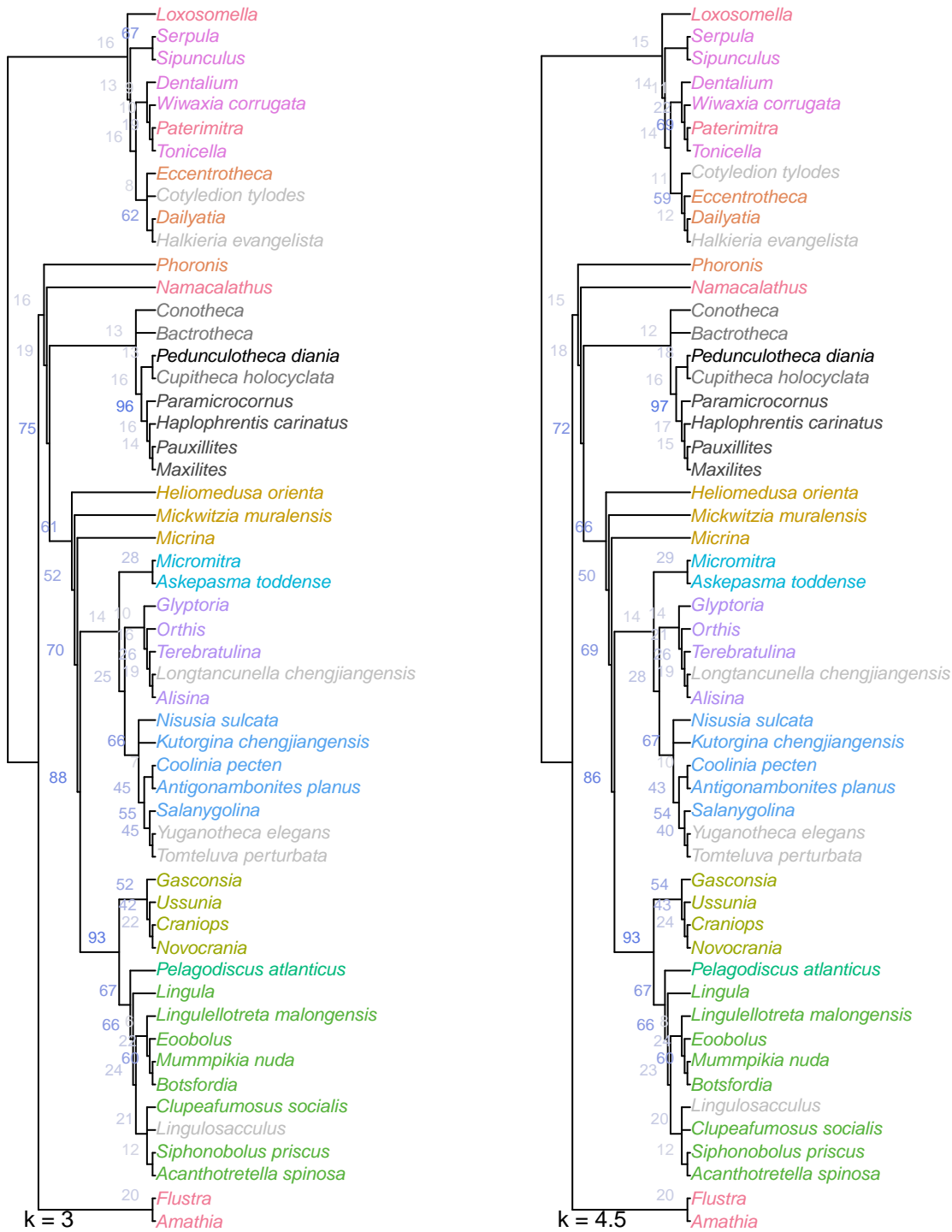
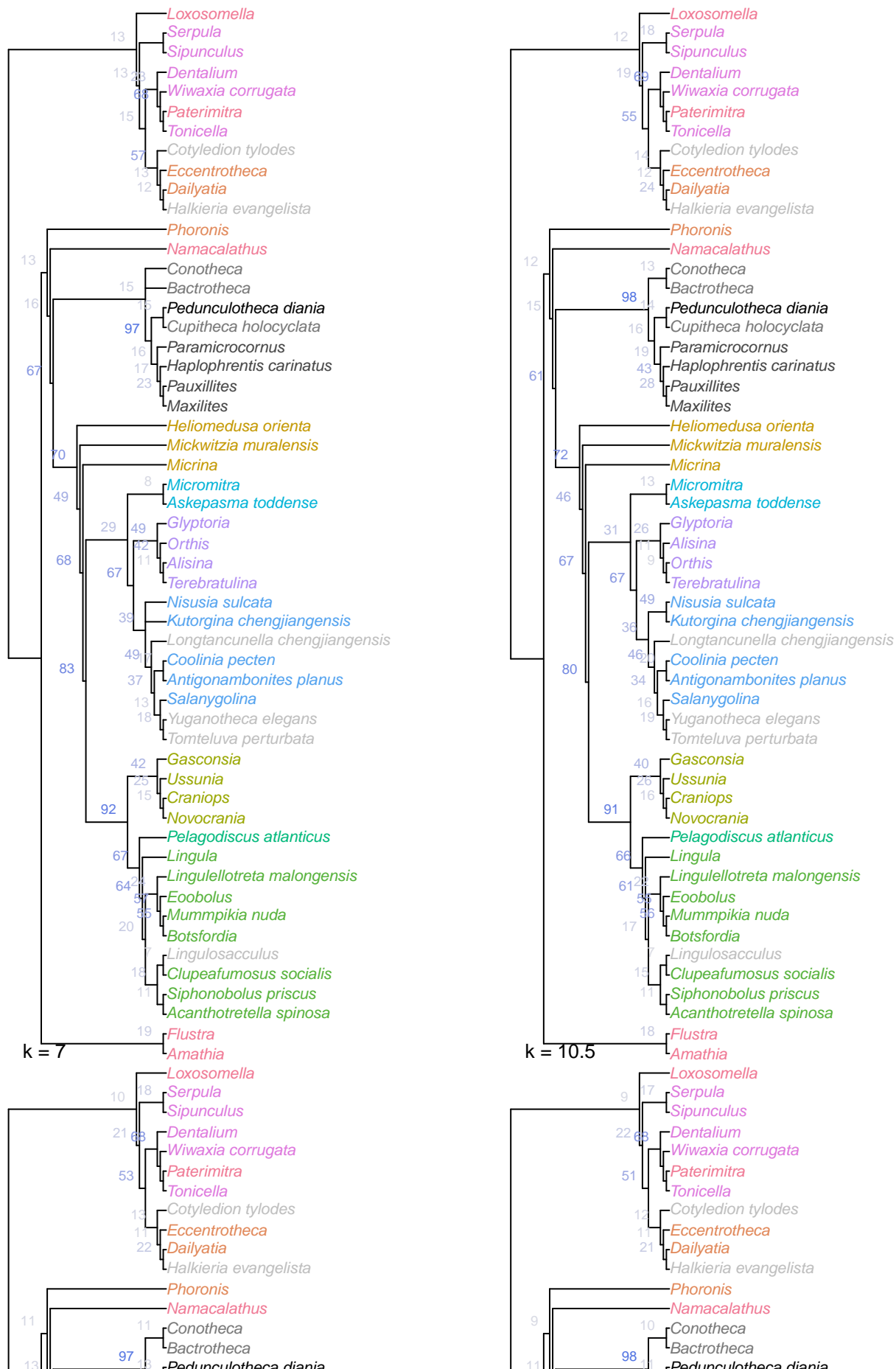


Figure 2.2: Strict consensus of all optimal trees under Fitch parsimony with implied weighting at  $k = 3$  and  $4.5$ . Nodes labelled with jackknife frequencies (%).



## 2.1 Results



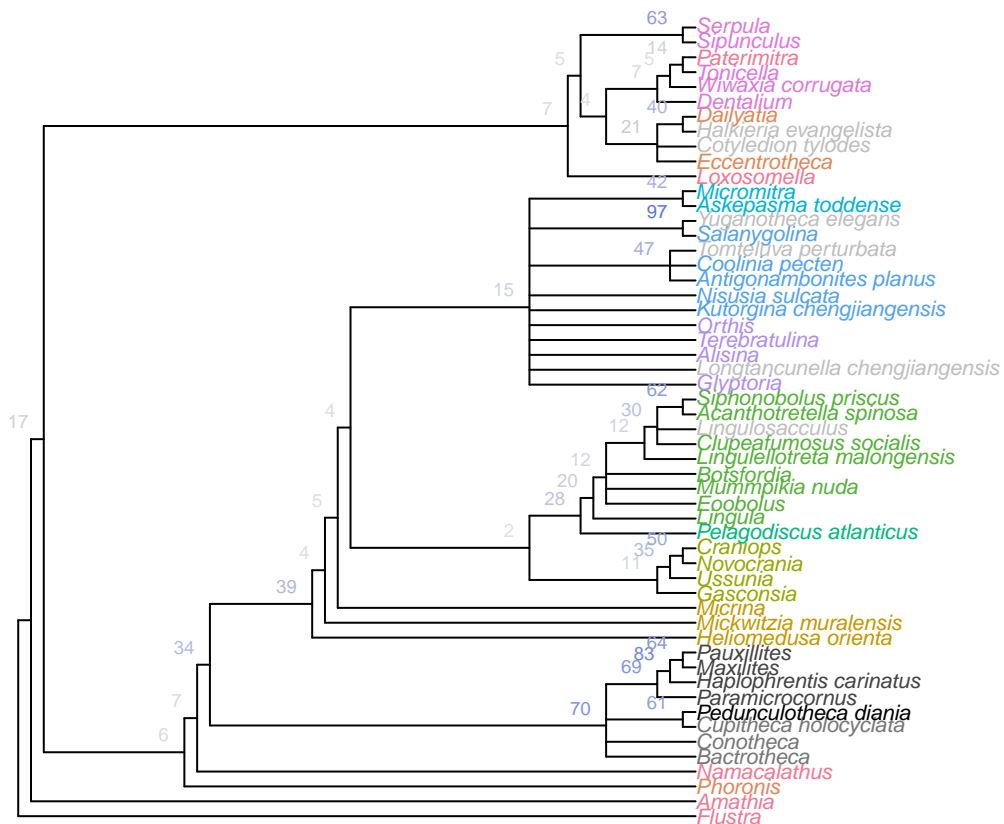


Figure 2.3: Consensus of all trees that are optimal under equally weighted Fitch parsimony. Nodes labelled with jackknife frequencies (%).

# Chapter 3

## Corrected parsimony

The phylogenetic dataset contains a considerable proportion of inapplicable codings (1133, = 18.5% of 6108 non-ambiguous tokens; 9.3% of 12150 total cells), which are known to introduce error and bias to phylogenetic reconstruction when the Fitch algorithm is employed (Maddison, 1993; Brazeau et al., 2018). As such, we used the R package *TreeSearch* v0.1.2 (Smith, 2018) to conduct phylogenetic tree search with a tree-scoring algorithm that avoids logically impossible character transformations when handling inapplicable data (Brazeau et al., 2018), implemented in the *MorphyLib* C library (Brazeau et al., 2017).

### 3.1 Search parameters

Heuristic searches were conducted using the parsimony ratchet (Nixon, 1999) under equal and implied weights (Goloboff, 1997). The consensus tree presented in the main manuscript represents a strict consensus of all trees that are most parsimonious under one or more of the concavity constants ( $k$ ) 3, 4.5, 7, 10.5, 16 and 24, an approach that has been shown to produce higher accuracy (i.e. more nodes and quartets resolved correctly) than equal weights at any given level of precision (Smith, 2017).

### 3.2 Analysis

The R commands used to conduct the analysis are reproduced below. The results can most readily be replicated using the R markdown files (.Rmd) used to generate these pages: in Rstudio, run [raw.githubusercontent.com/ms609/hyoliths/master/index.Rmd](https://raw.githubusercontent.com/ms609/hyoliths/master/index.Rmd), then run each block in [raw.githubusercontent.com/ms609/hyoliths/master/14\\_TreeSearch.Rmd](https://raw.githubusercontent.com/ms609/hyoliths/master/14_TreeSearch.Rmd). The complete analysis will take several hours.

#### 3.2.1 Initialize and load data

```
# Load data from locally downloaded copy of MorphoBank matrix
my_data <- ReadAsPhyDat(nexusFile)
my_data[ignored_taxa] <- NULL
iw_data <- PrepareDataIW(my_data)
```

### 3.2.2 Generate starting tree

Start by quickly rearranging a neighbour-joining tree, rooted on the outgroup.

```
nj.tree <- NJTree(my_data)
rooted.tree <- EnforceOutgroup(nj.tree, outgroup)
start.tree <- TreeSearch(tree=rooted.tree, dataset=my_data, maxIter=3000,
                           EdgeSwapper=RootedNNISwap, verbosity=0)
```

### 3.2.3 Implied weights analysis

The position of the root does not affect tree score, so we keep it fixed (using RootedXXXSwap functions) to avoid unnecessary swaps.

```
for (k in kValues) {
  iw.tree <- IW Ratchet(start.tree, iw_data, concavity=k,
                         ratchHits = 20, ratchIter=4000, searchHits=56,
                         swappers=list(RootedTBRSwap, RootedSPRSwap, RootedNNISwap),
                         verbosity=0L)
  score <- IWScore(iw.tree, iw_data, concavity=k)
  # Write a single best tree
  write.nexus(iw.tree,
              file=paste0("TreeSearch/hy_iw_k", k, "_",
                          signif(score, 5), ".nex", collapse=''))
  
  iw.consensus <- IW RatchetConsensus(iw.tree, iw_data, concavity=k,
                                         swappers=list(RootedTBRSwap, RootedNNISwap),
                                         searchHits=55, searchIter=4000, nSearch=250, verbosity=0L)
  write.nexus(iw.consensus,
              file=paste0("TreeSearch/hy_iw_k", k, "_",
                          signif(IWScore(iw.tree, iw_data, concavity=k), 5),
                          ".all.nex", collapse=''))
}
```

### 3.2.4 Equal weights analysis

```
ew.tree <- Ratchet(start.tree, my_data, verbosity=0L,
                     ratchHits = 20, ratchIter=4000, searchHits=55, # ratchHits = 20 not enough
                     swappers=list(RootedTBRSwap, RootedSPRSwap, RootedNNISwap))
ew.consensus <- RatchetConsensus(ew.tree, my_data, nSearch=250, searchHits = 85,
                                   swappers=list(RootedTBRSwap, RootedNNISwap),
                                   verbosity=0L)
write.nexus(ew.consensus, file=paste0(collapse=' ', "TreeSearch/hy_ew_",
                                       Fitch(ew.tree, my_data), ".nex"))
```

## 3.3 Results

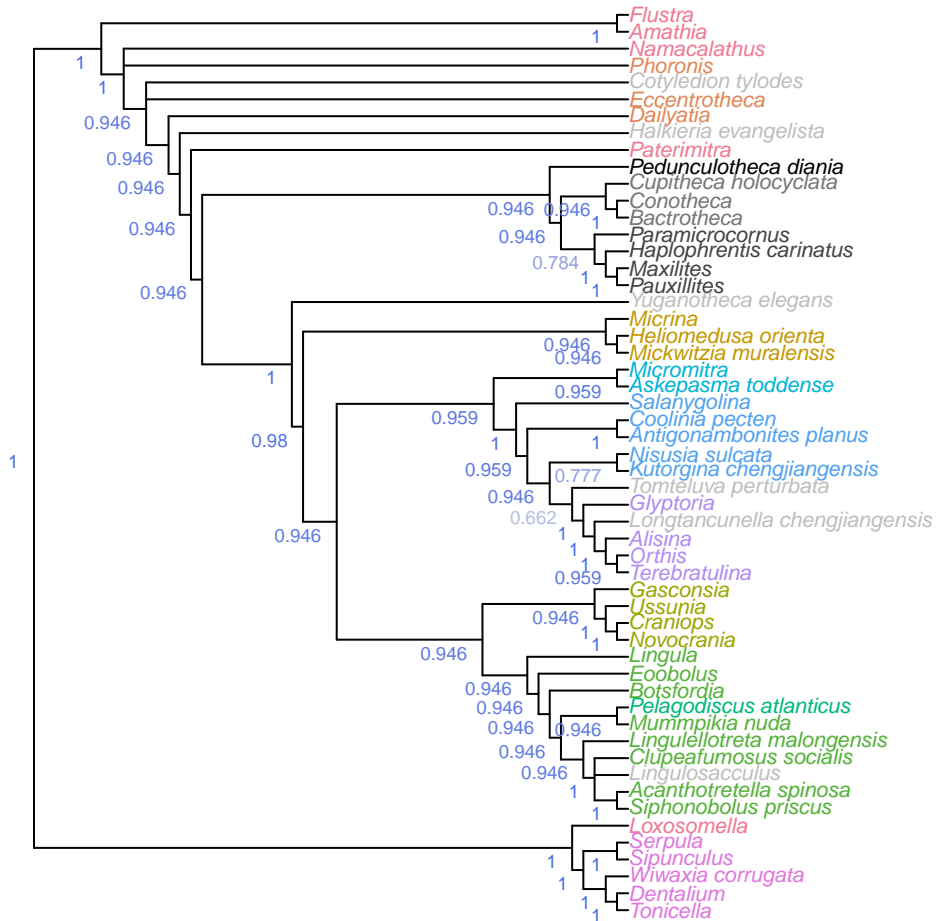


Figure 3.1: Consensus of all parsimony trees, under equal and implied weights. Node labels denote the frequency of each clade in most parsimonious trees under all analytical conditions.

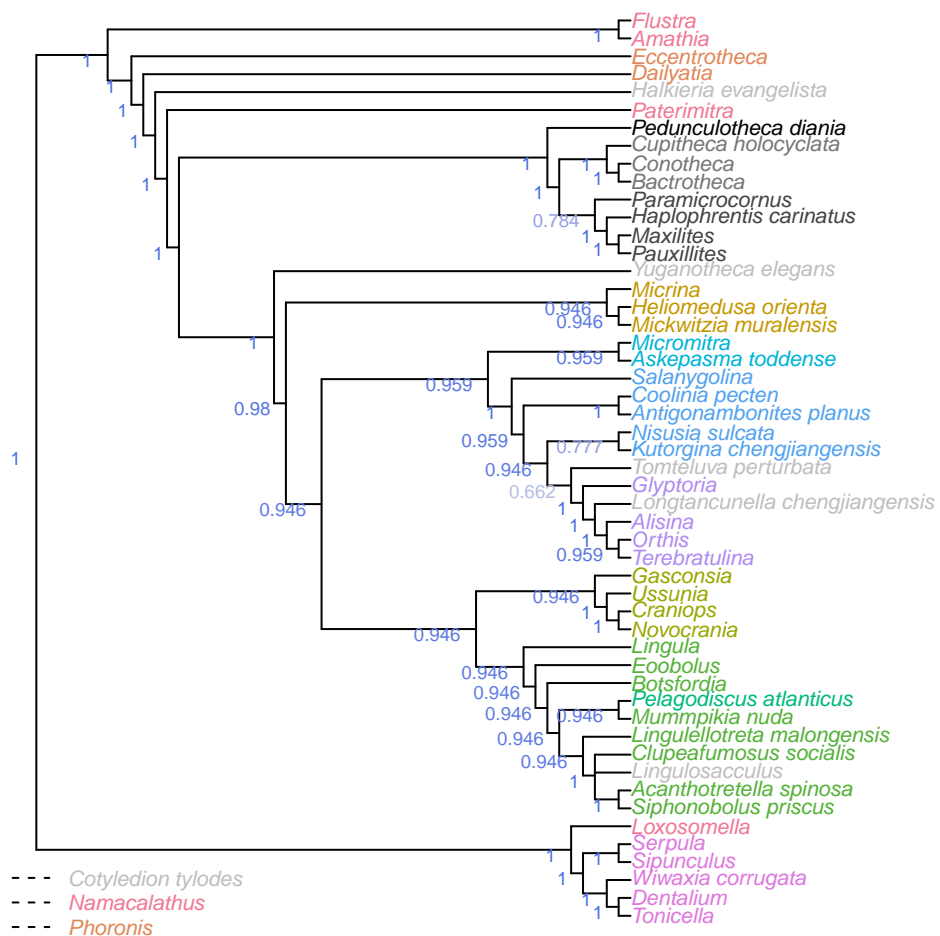


Figure 3.2: Consensus of same trees, with taxa pruned before constructing consensus to give context to clade support. Node labels denote the frequency of each clade in most parsimonious trees under all analytical conditions.

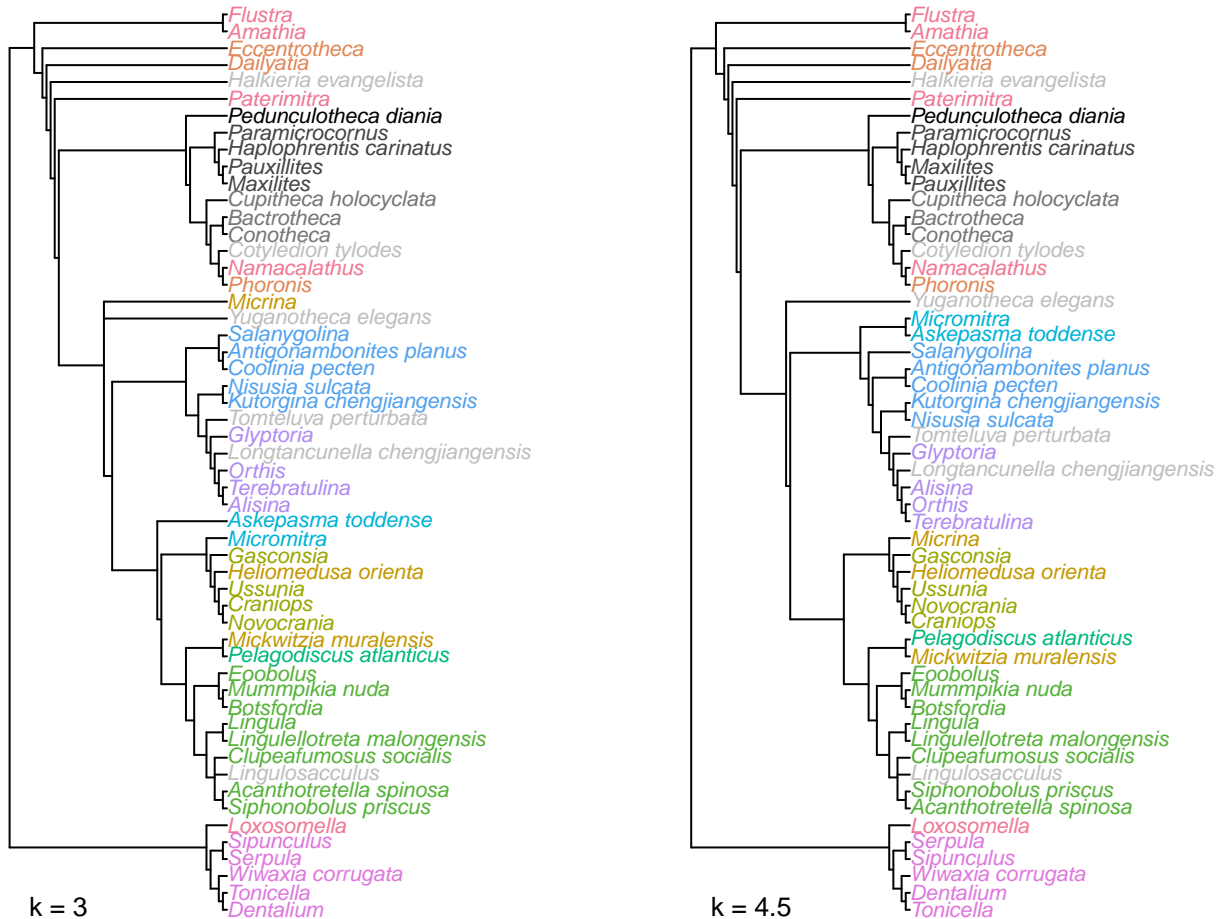


Figure 3.3: Strict consensus trees of implied weights analyses at  $k = 3$  and 4.5.

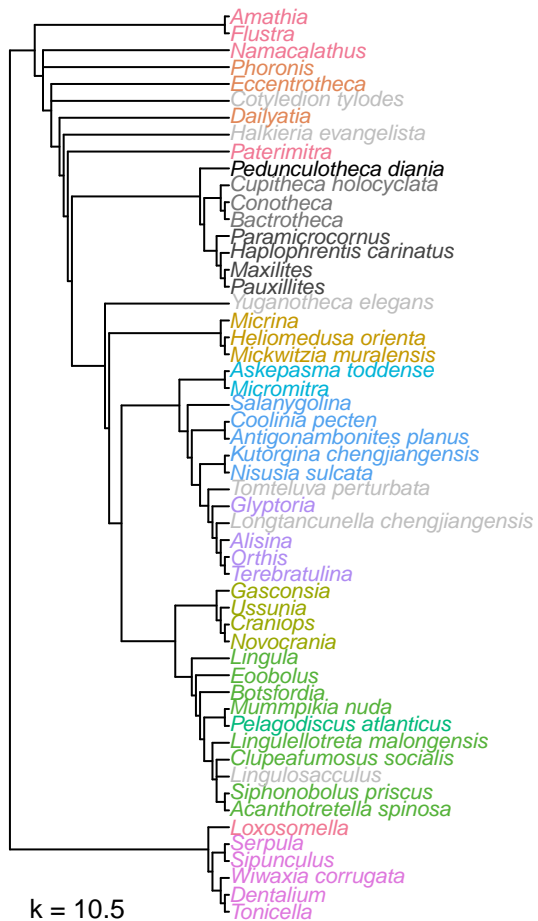


Figure 3.4: Strict consensus trees of implied weights analyses at  $k = 7$  and 10.5.

```
##  
## > Results not available for panel 3
```

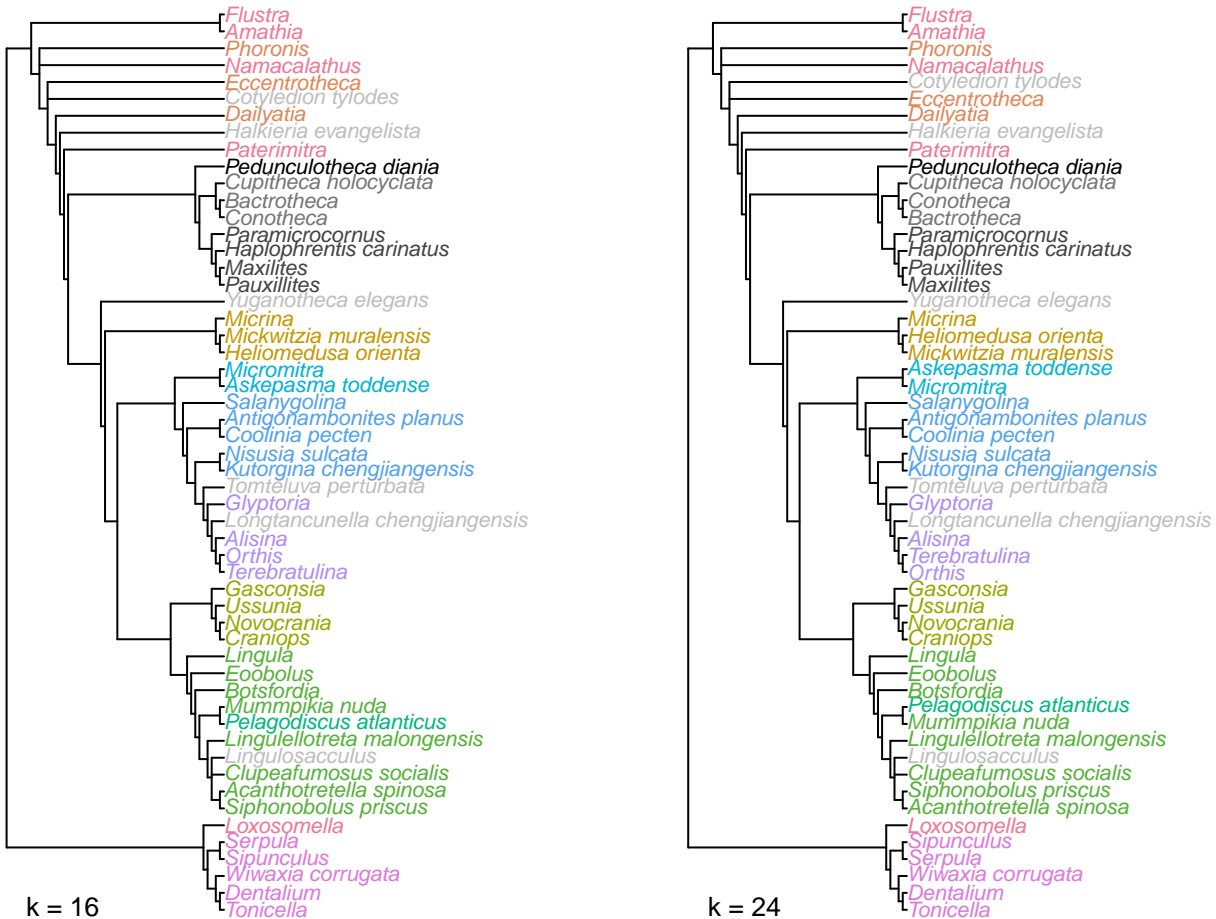


Figure 3.5: Strict consensus trees of implied weights analyses at  $k = 16$  and  $24$ .

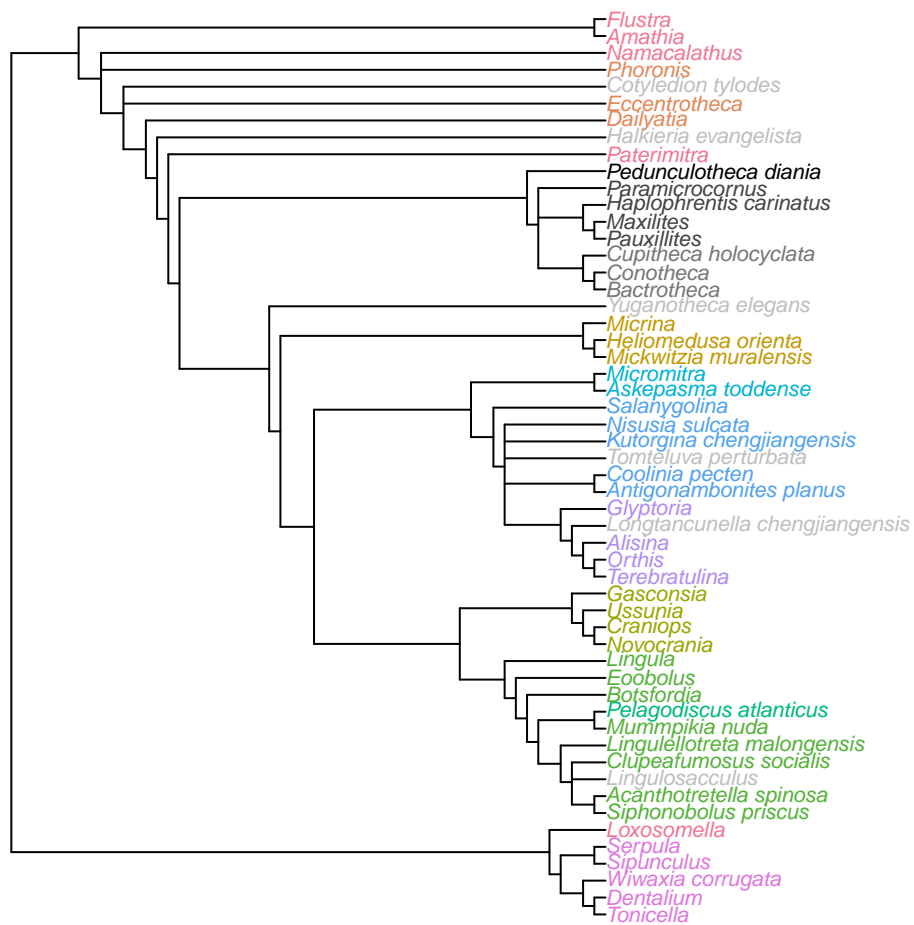


Figure 3.6: Strict consensus of most parsimonious trees under equally weighted parsimony

# Chapter 4

## Bayesian analysis

Bayesian search was conducted in MrBayes v3.2.6 (Ronquist et al., 2012) using the Mk model (Lewis, 2001) with gamma-distributed rate variation across characters:

```
lset coding=variable rates=gamma;
```

Branch length was drawn from a dirichlet prior distribution, which is less informative than an exponential model (Rannala et al., 2012), but requires a prior mean tree length within about two orders of magnitude of the true value (Zhang et al., 2012). To satisfy this latter criterion, we specified the prior mean tree length to be equal to the length of the most parsimonious tree under equal weights, using a Dirichlet prior with  $\alpha_T = 1$ ,  $\beta_T = 1/(equal\ weights\ tree\ length/number\ of\ characters)$ ,  $\alpha = c = 1$ :

```
prset brlenspr = unconstrained: gammadir(1, 0.35, 1, 1);
```

Neomorphic and transformational characters (*sensu* Sereno, 2007) were allocated to two separate partitions whose proportion of invariant characters and gamma shape parameters were allowed to vary independently:

```
charset Neomorphic = 1 6 7 9 10 15 18 19 20 21 22 24 26 29 30 34 35 37 38 40 43 44 45 48 49 53  
54 55 56 57 58 59 60 61 65 66 67 69 70 72 77 79 80 81 82 84 87 88 89 92 93 94 95 98 99 100 101  
102 103 107 109 110 112 119 120 122 123 126 127 130 137 138 139 140 141 142 143 144 148 150  
151 153 154 155 156 157 158 160 164 168 170 174 175 176 177 179 180 181 182 183 184 185 186  
187 188 190 192 193 196 199 202 203 204 205 206 207 209 210 211 212 214 215 216 217 218 219  
220 222 225;
```

```
charset Transformational = 2 3 4 5 8 11 12 13 14 16 17 23 25 27 28 31 32 33 36 39 41 42 46 47  
50 51 52 62 63 64 68 71 73 74 75 76 78 83 85 86 90 91 96 97 104 105 106 108 111 113 114 115  
116 117 118 121 124 125 128 129 131 132 133 134 135 136 145 146 147 149 152 159 161 162 163  
165 166 167 169 171 172 173 178 189 191 194 195 197 198 200 201 208 213 221 223 224;
```

```
partition chartype = 2: Neomorphic, Transformational;
```

```
set partition = chartype;
```

```
unlink shape=(all) pinvar=(all);
```

Neomorphic characters were not assumed to have a symmetrical transition rate – that is, the probability of the absent → present transition was allowed to differ from that of the present → absent transition, being drawn from a uniform prior:

```
prset applyto=(1) symdirhyperpr=fixed(1.0);
```

The rate of variation in neomorphic characters was also allowed to vary from that of transformational characters:

```
prset applyto=(1) ratepr=variable;
```

*Loxosomella* was selected as an outgroup:

```
outgroup Loxosomella;
```

Four MrBayes runs were executed, each sampling eight chains for 5 000 000 generations, with samples taken every 500 generations. The first 10% of samples were discarded as burn-in.

```
mcmcp ngen=5000000 samplefreq=500 nruns=4 nchains=8 burninfrac=0.1;
```

A posterior tree topology was derived from the combined posterior sample of all runs. Convergence was indicated by PSRF = 1.00 and an estimated sample size of > 200 for each parameter. Nodes are labelled with posterior probabilities; recall that caution must be applied when interpreting these values (Yang and Zhu, 2018).

The Nexus file used to generate these results in MrBayes can be [raw.githubusercontent.com/ms609/hyoliths/master/MrBayes/](https://raw.githubusercontent.com/ms609/hyoliths/master/MrBayes/) and run in MrBayes by typing `exe path/to/download`.

## 4.1 Parameter estimates

Parameter	Mean	Variance	minESS	avgESS	PSRF
TL{all}	9.980	0.50100	5440	5970	0.99999
m{1}	0.462	0.00265	3100	3720	0.99999

## 4.2 Results

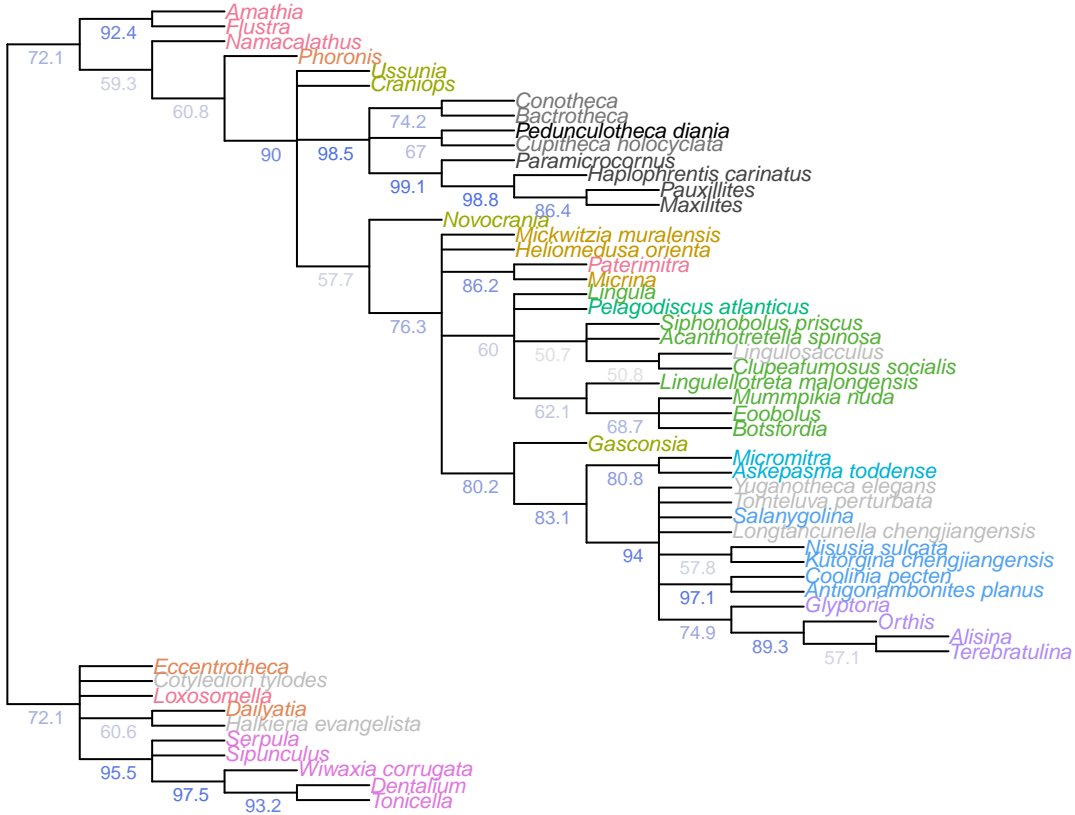


Figure 4.1: Results of Bayesian analysis, posterior probability &gt; 50%, all taxa

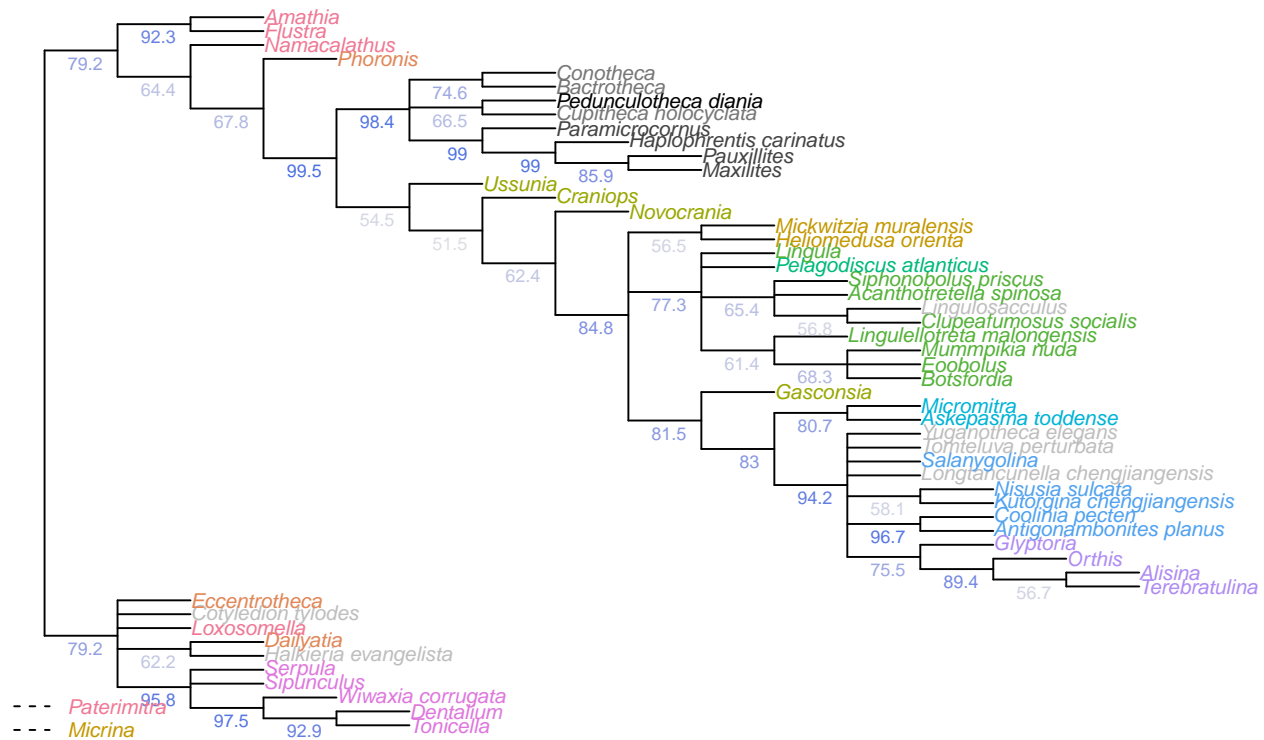


Figure 4.2: Results of Bayesian analysis, posterior probability &gt; 50%, wildcard taxa pruned

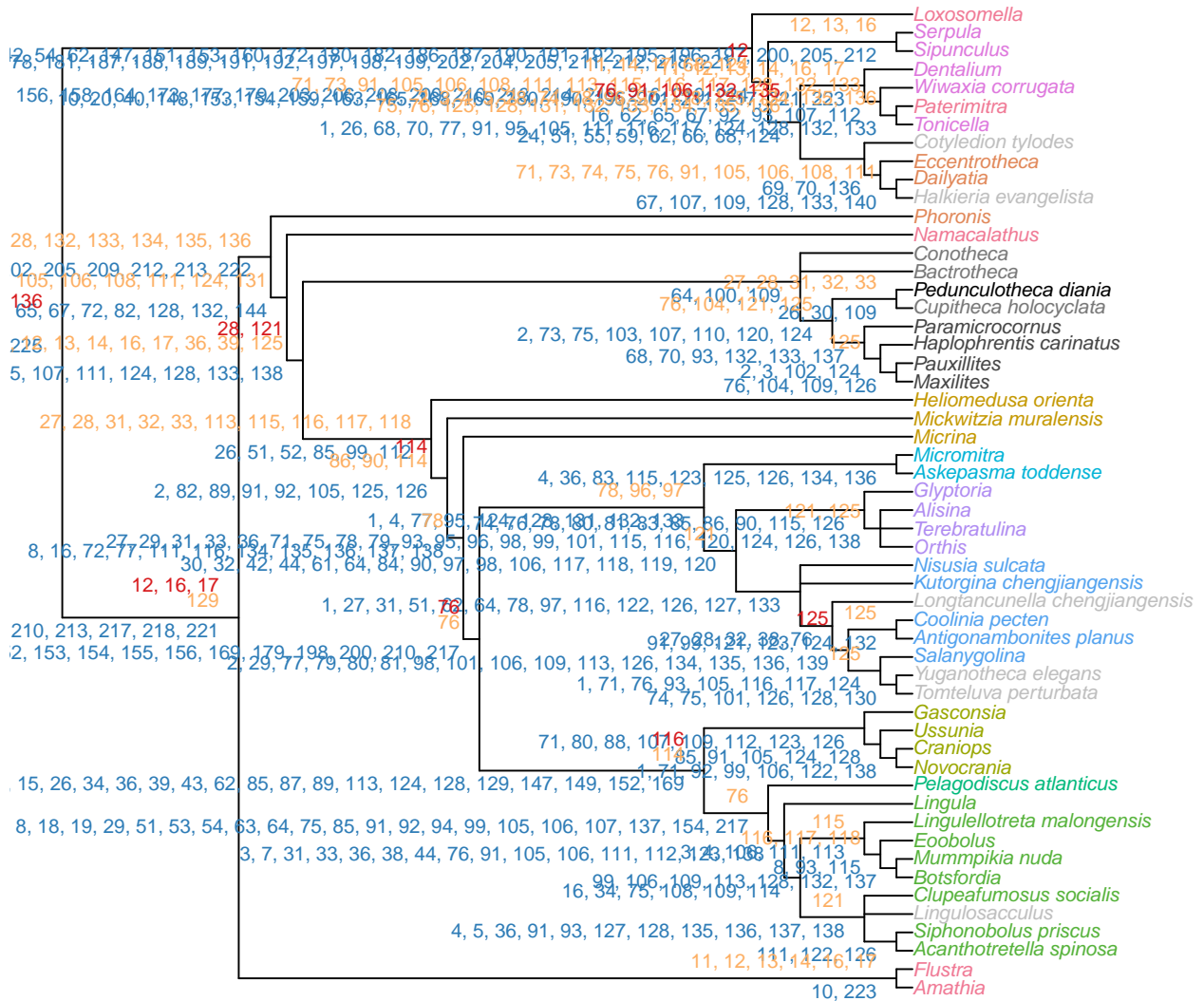
# Chapter 5

## Character reconstructions

This page provides definitions for each of the characters in our matrix, and justifies codings in particular taxa where relevant. Further citations for codings that are not discussed in the text can be viewed by browsing the morphological dataset on MorphoBank (project 2800). [This dataset will be released on publication of the paper. Referee access is available by logging in to MorphoBank using the e-mail address and password given in the manuscript.]

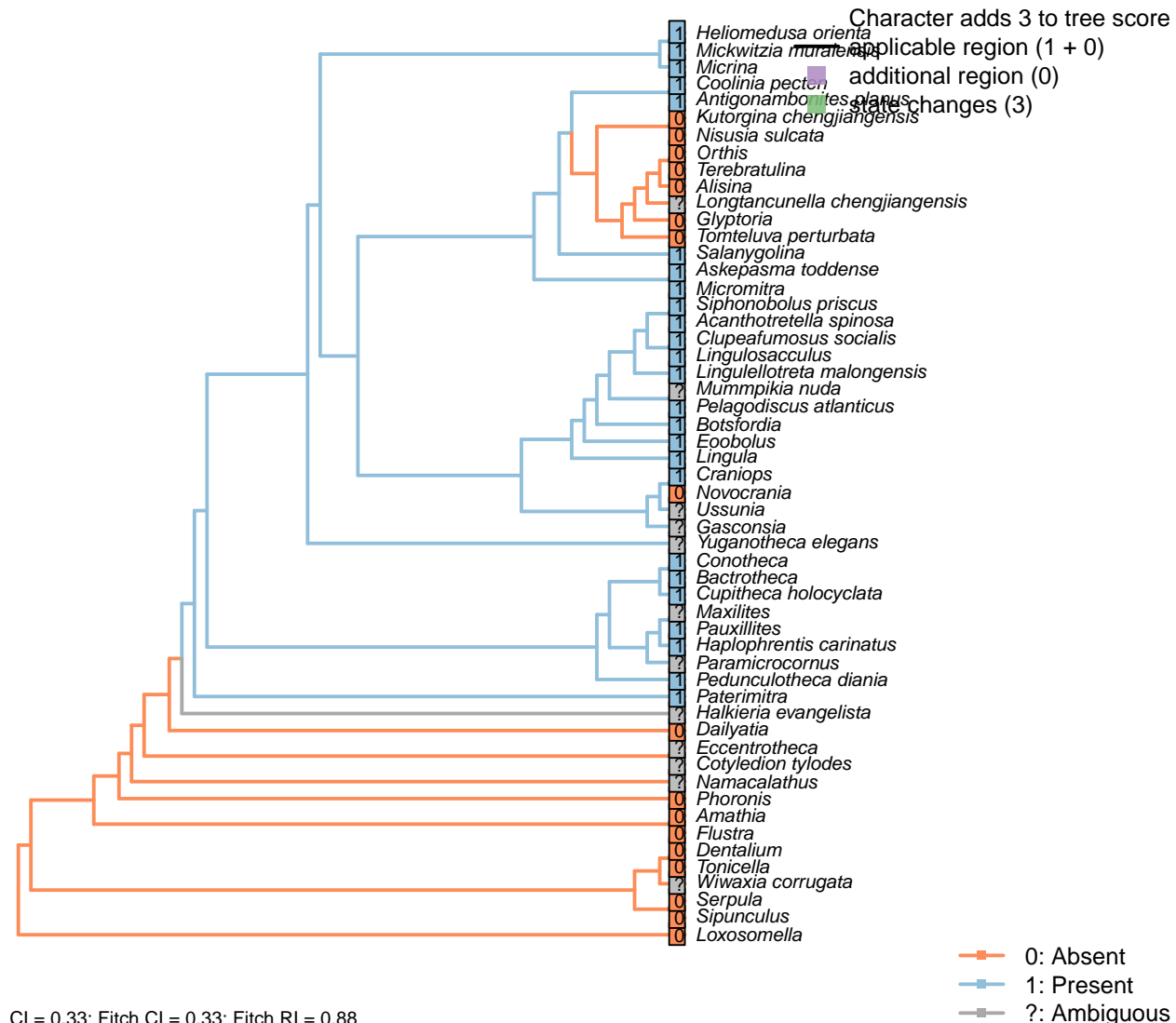
Alongside its definition, each character has been mapped onto a tree. Here, we have arbitrarily selected one most parsimonious tree obtained under implied weighting. Other trees can be viewed in the HTML version of this document at [ms609.github.io/hyoliths](https://ms609.github.io/hyoliths). Each tip is labelled according to its coding in the matrix. These states have been used to reconstruct the condition of each internal node, using the parsimony method of Brazeau et al. (2018) as implemented in the *R* package *Inapp*.

We emphasize that different trees will give different reconstructions. The character mappings are not intended to definitively establish how each character evolved, but to help the reader quickly establish how each character has been coded, and to visualize at a glance how each character fits onto a given tree.



## 5.1 Brephic shell

### [1] Embryonic shell



#### Character 1: Brephic shell: Embryonic shell

0: Absent

1: Present

Neomorphic character.

The embryonic shell or protegulum is secreted by the embryo immediately before hatching.

*Amathia*: Reed and Cloney (1982).

*Clupeafumosus socialis*: Described by Topper *et al.* (2013a).

*Conotheca*: (Wrona, 2003).

*Dentalium*: The shell does not form until the trochophore larval stage, which has been exquisitely described in Antalis (Wanninger and Haszprunar, 2001).

This shell field is initially disc-like, subsequently expanding to fuse ventrally and produce the cylindrical

protoconch. The prototroch is clearly delineated from the telotroch in post-metamorphic juveniles (Wanninger and Haszprunar, 2001).

*Gasconsia*: The earliest shell is not described by Hanken and Harper (1985) or Watkins (2002).

*Loxosomella*: Absent, with no possible equivalent (Nielsen, 1966).

*Namacalathus*: Inapplicable insofar as reproduction occurs by budding; there is no evidence for a free-living larval stage. Nevertheless, the presence of a sexual reproductive phase in addition to asexual reproduction cannot be discounted.

*Novocrania*: Shell not secreted until after metamorphosis (Popov et al., 2010). Freeman & Lundelius (1999) report a *Craniops*-like larval shell in fossil “Crania”, but observe that Quaternary [Novo]crania no longer exhibit a larval shell.

*Paramicrocornus*: “The initial part of the conch appears to be a simple apex without clearly delineated protoconch” (Zhang et al., 2018), though it is not clear from illustrated figures whether an embryonic shell contiguous with the adult shell was present.

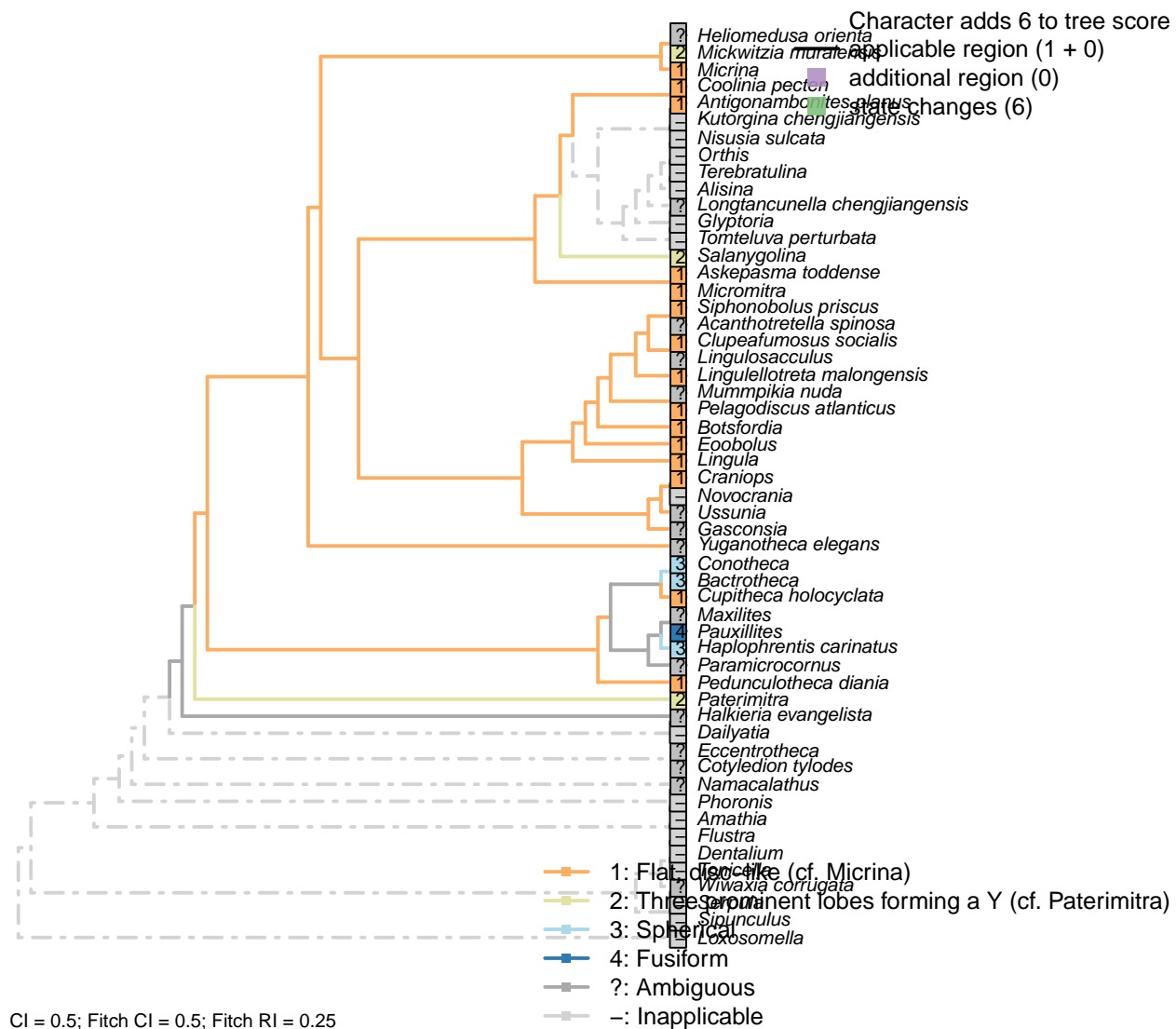
*Pauxillites*: Coded following *Recilites* (Dzik, 1978), a fellow member of Pauxillitidae (Marek, 1967).

*Tonicella*: On hatching, the polyplacophoran larva lacks a shell field.

Shell fields develop during the trochophore larva stage. The larva of the chiton *Mopalia* has two distinct shell fields: that anterior to the prototroch will develop into the first shell plate; the one posterior to the prototroch becomes the subsequent plates (Wanninger and Haszprunar, 2002a).

This disc-shaped posterior plate, whose position corresponds to the conchiferan shell field, bears a polygonal ornament and is subdivided by a series of grooves that prefigure the adult shell plates (Wanninger and Haszprunar, 2002a).

## [2] Morphology



### Character 2: Brephic shell: Morphology

- 1: Flat, disc-like (cf. *Micrina*)
  - 2: Three prominent lobes forming a Y (cf. *Paterimitra*)
  - 3: Spherical
  - 4: Fusiform
- Transformational character.

The brephic shell is the shell possessed by the young organism (see Ushatinskaya and Korovnikov, 2016, and references therein for discussion of terminology).

*Micrina* resembles linguliforms (Holmer et al., 2011): in both, the brephic mitral shell has one pair of setal sacs enclosed by lateral lobes, whereas the brephic ventral shell has two lateral setal tubes.

*Paterimitra* and *Salanygolina* have “identical” ventral brephic shells (Holmer et al., 2011), resembling the shape of a ship’s propeller.

*Haplophrentis* is coded following typical hyoliths, which have a spherical brephic shell; *Pedunculotheca*’s, in

contrast, is seemingly cap-shaped.

*Askepasma toddense*: Renoid – see fig. 4B3 in Topper et al. (2013b).

*Clupeafumosus socialis*: The flat larval shell of *Clupeafumosus* resembles that of *Micrina* in outline (Topper et al., 2013a; cf. Holmer et al., 2011).

*Conotheca*: (Wrona, 2003).

*Coolinia pecten*: See fig. 3 in Bassett and Popov (2017).

*Craniops*: The embryonic shell is more or less circular in outline – see Freeman and Lundelius (1999), fig. 6A.

*Cupitheca holocyclata*: The impression of the larval shell on the operculum is flat and disc-like (Skovsted et al., 2016). The fusiform ‘protoconch’ (Sun et al., 2018a) likely represents a larval (rather than biphic) shell.

*Lingula*: See fig. 159 in Williams et al. (1997).

*Lingulellotreta malongensis*: Disc-like (Li and Holmer, 2004).

*Mickwitzia muralensis*: Trifoliate appearance results from prominent attachment rudiment and bunching of setal sacs (Balthasar, 2009).

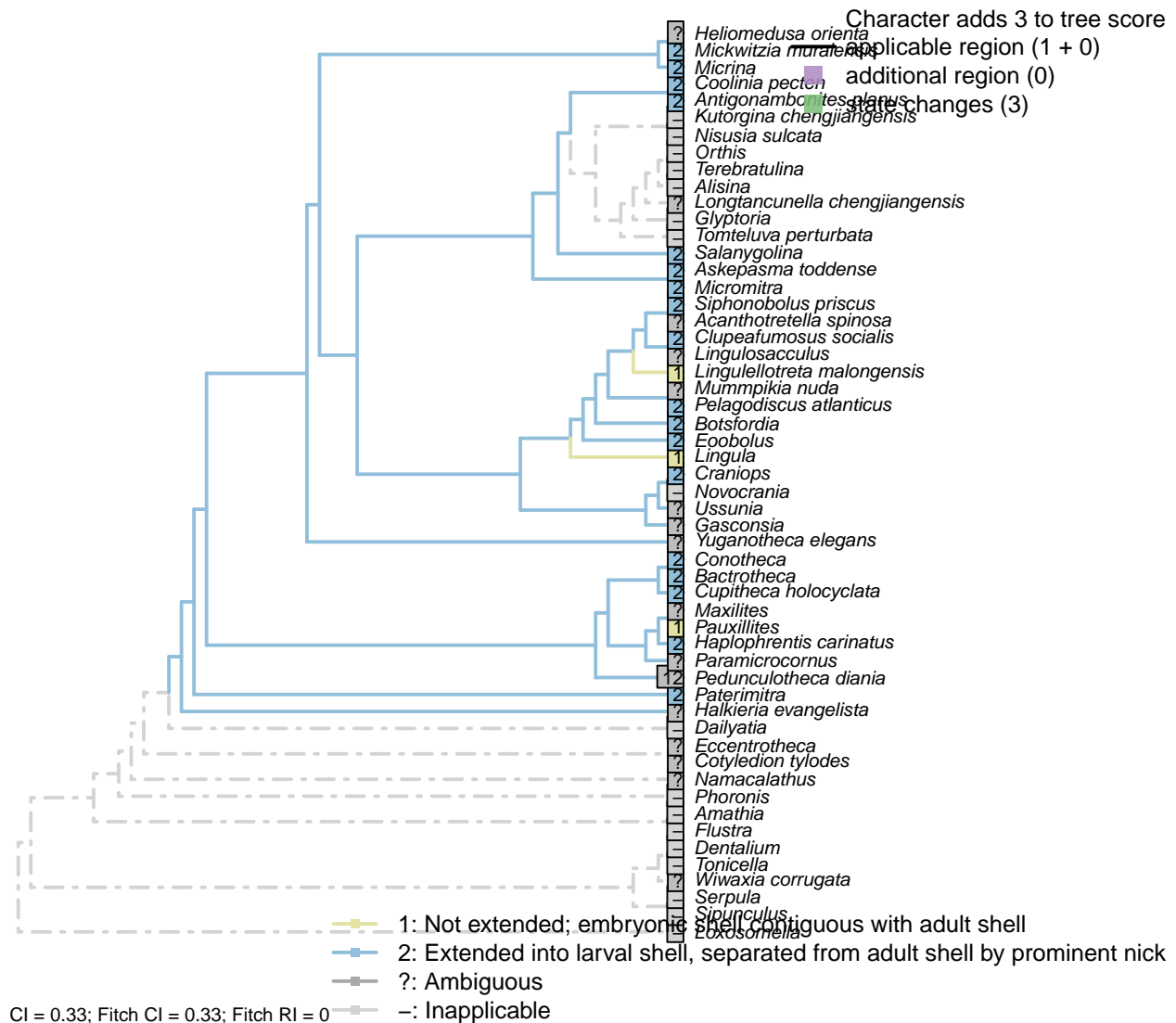
*Micromitra*: Subtriangular – essentially round.

*Pauxillites*: Fusiform, following *Recilites* (Pauxillitidae) (Dzik, 1978).

*Pelagodiscus atlanticus*: See e.g. fig 169 in Williams et al. (1997).

*Tonicella*: Disc-like, subdivided by transverse grooves (Wanninger and Haszprunar, 2002a).

### [3] Embryonic shell extended in larvae



#### Character 3: Brephic shell: Embryonic shell extended in larvae

- 1: Not extended; embryonic shell contiguous with adult shell
- 2: Extended into larval shell, separated from adult shell by prominent nick
- Transformational character.

Many taxa add to their embryonic shell (the protegulum possessed by the embryo upon hatching) during the larval phase of their life cycle. The shell that exists at metamorphosis, marked by a halo or nick point, is variously termed the “first formed shell”, “metamorphic shell” or “larval shell” (Bassett and Popov, 2017).

*Bactrotheca*: There is a small ridge and a change in surface ornament at the end of the larval shell (Dzik,

1980).

*Clupeafumosus socialis*: Described by Topper *et al.* (2013a).

*Conotheca*: Prominent nick (Wrona, 2003, figs 5G-H, 6a1).

*Craniops*: Prominent nick; see Freeman and Lundelius (1999), fig. 6A.

*Cupitheca holocyclata*: Prominent nick (Skovsted *et al.*, 2016).

*Eoobolus*: Nick point indicated by arrows in fig. 1 of Balthasar (2009).

*Lingulellotreta malongensis*: No prominent nick point (Holmer *et al.*, 1997; Li and Holmer, 2004).

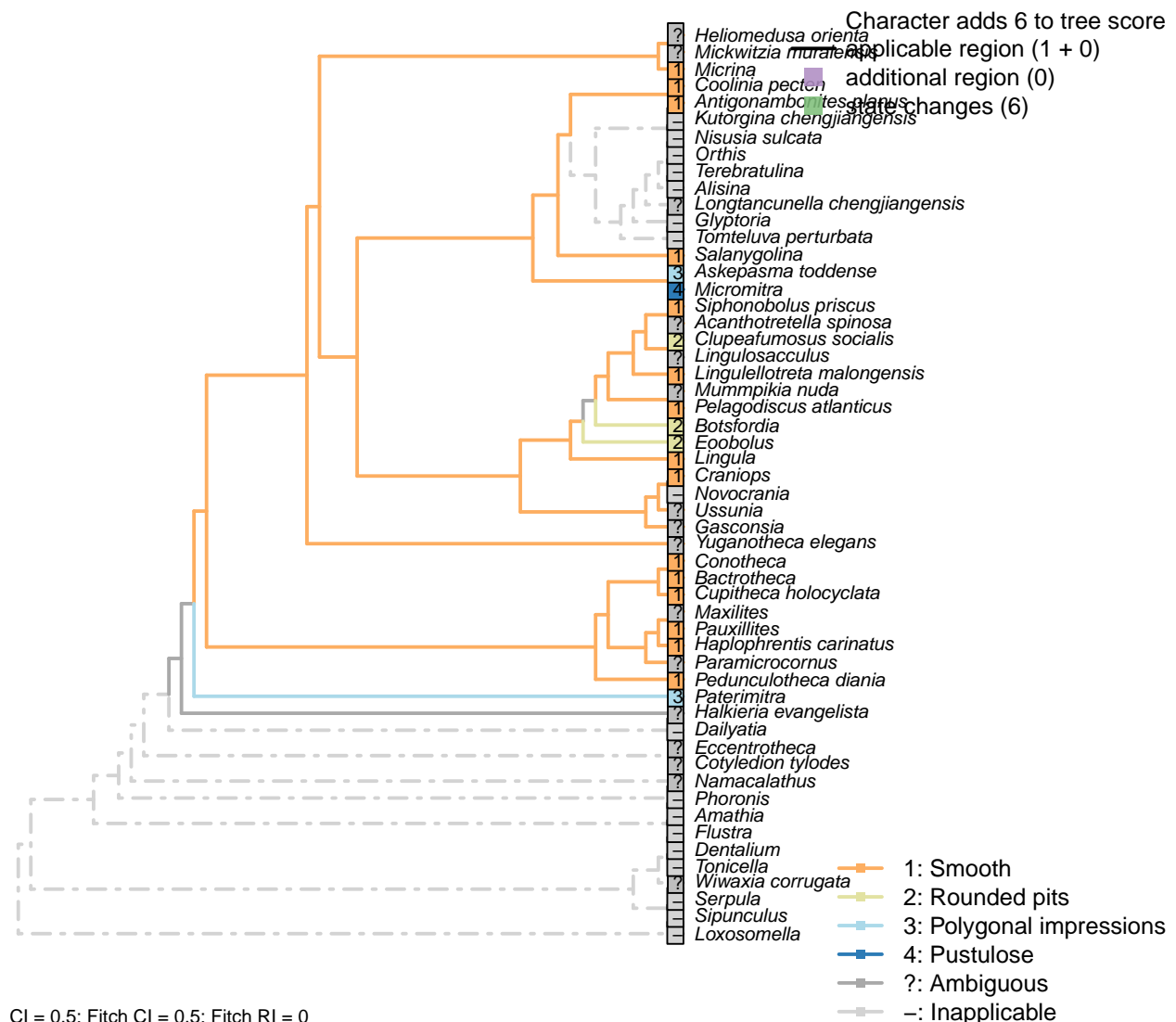
*Paramicrocornus*: Not clearly delineated (Zhang *et al.*, 2018), so either inapplicable or undifferentiated.

*Pauxillites*: No prominent nick in *Recilites* (Pauxillitidae) (Dzik, 1978).

*Pedunculotheca diania*: The flattened region at the umbo of the ventral valve in smaller specimens conceivably represents an embryonic shell, though it may alternatively represent a cicatrix or colleplax-like structure.

*Tonicella*: Wanninger and Haszprunar (2002a).

#### [4] Surface ornament



##### Character 4: Brephic shell: Surface ornament

- 1: Smooth
  - 2: Rounded pits
  - 3: Polygonal impressions
  - 4: Pustulose
- Transformational character.

Pitting of the larval shell characterises acrotretids and their relatives. Pustules occur on Paterinidae. See Character 3 in Williams *et al.* (2000) tables 5–6.

*Askepasma toddense*: Indented with hexagonal pits (Williams *et al.*, 1998b, appendix 2).

*Clupeafumosus socialis*: “Larval shells on both valves [...] are covered by fine, shallow pits” – Topper *et al.*

(2013a).

*Conotheca*: (Wrona, 2003).

*Cupitheca holocyclata*: Perfectly smooth (Skovsted et al., 2016).

*Eoobolus*: Pitted (Williams et al., 2000, table 8).

*Pelagodiscus atlanticus*, *Lingula*: Smooth, following family-level codings of Williams et al. (2000), table 6.

*Lingulellotreta malongensis*: Smooth (Holmer et al., 1997; Li and Holmer, 2004).

*Micrina*: Smooth (Holmer et al., 2011).

*Micromitra*: Pustulose in Paterinidae (Williams et al., 2000, table 6).

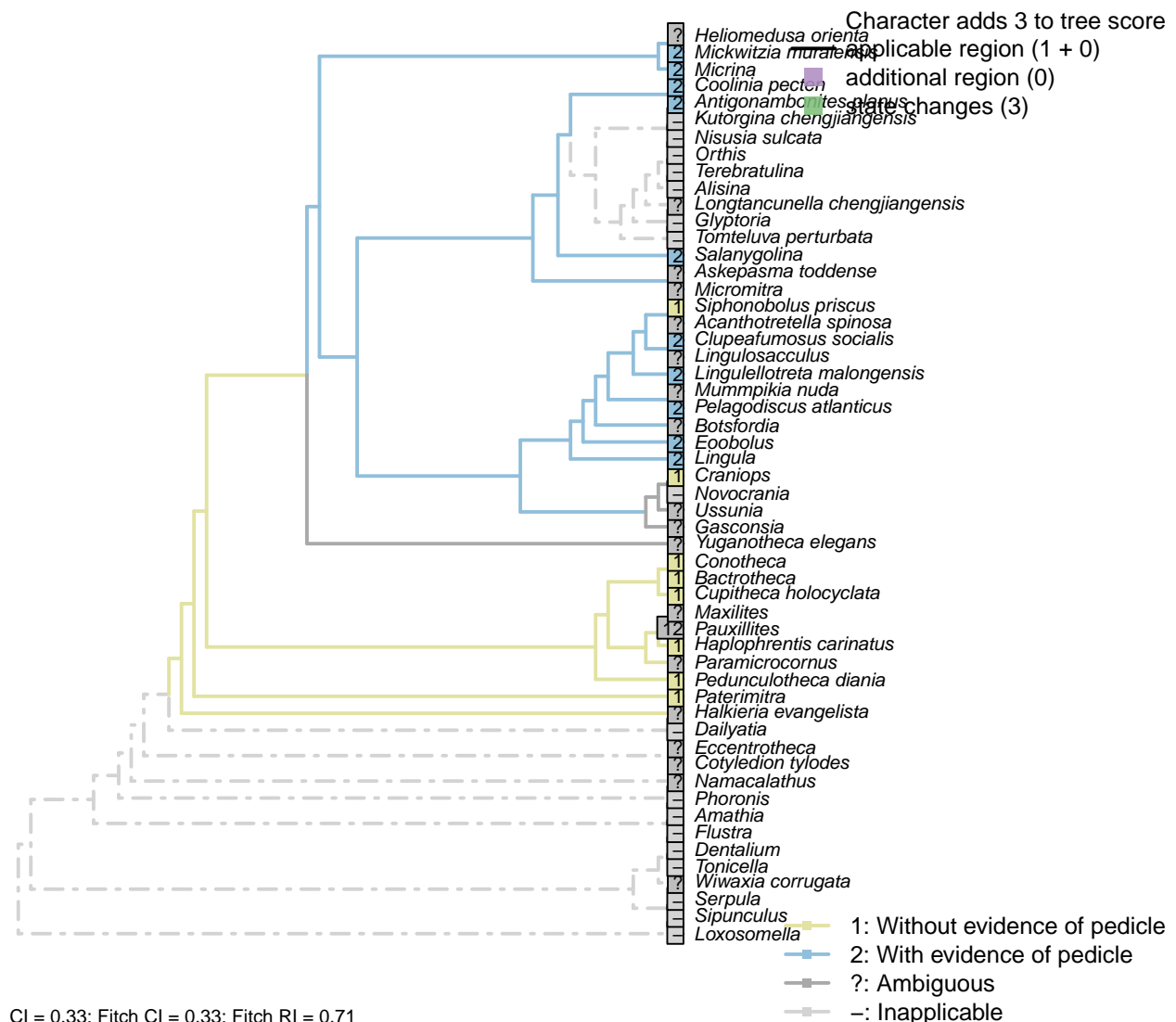
*Paterimitra*: Polygonal texture present (Holmer et al., 2011), as in the adult shell.

*Pauxillites*: Essentially smooth in *Recilites* (Pauxillitidae) (Dzik, 1978).

*Salanygolina*: Smooth (Holmer et al., 2009).

*Siphonobolus priscus*: “Smooth brepthic shell” – Popov et al. (2009).

## [5] Larval attachment structure



### Character 5: Brephic shell: Larval attachment structure

- 1: Without evidence of pedicle
- 2: With evidence of pedicle
- Transformational character.

Embryonic shells of *Micrina* and certain linguliforms exhibit a transversely folded posterior extension that speaks of the original presence of a pedicle in the embryo.

This is independent of the presence of an adult pedicle, which may arise after metamorphosis.

*Clupeafumosus socialis*: The larval shell embraces the pedicle foramen, suggesting a larval attachment. See fig. 4 of Topper *et al.* (2013a).

*Conotheca*: (Wrona, 2003).

*Cupitheca holocykleta*: A pedicle is not inferred by Skovsted *et al.* (2016), and is difficult to reconcile with

the apical morphology documented by Sun et al. (2018a).

*Eoobolus*: Lobe related to the attachment rudiment (Balthasar, 2009, fig. 2).

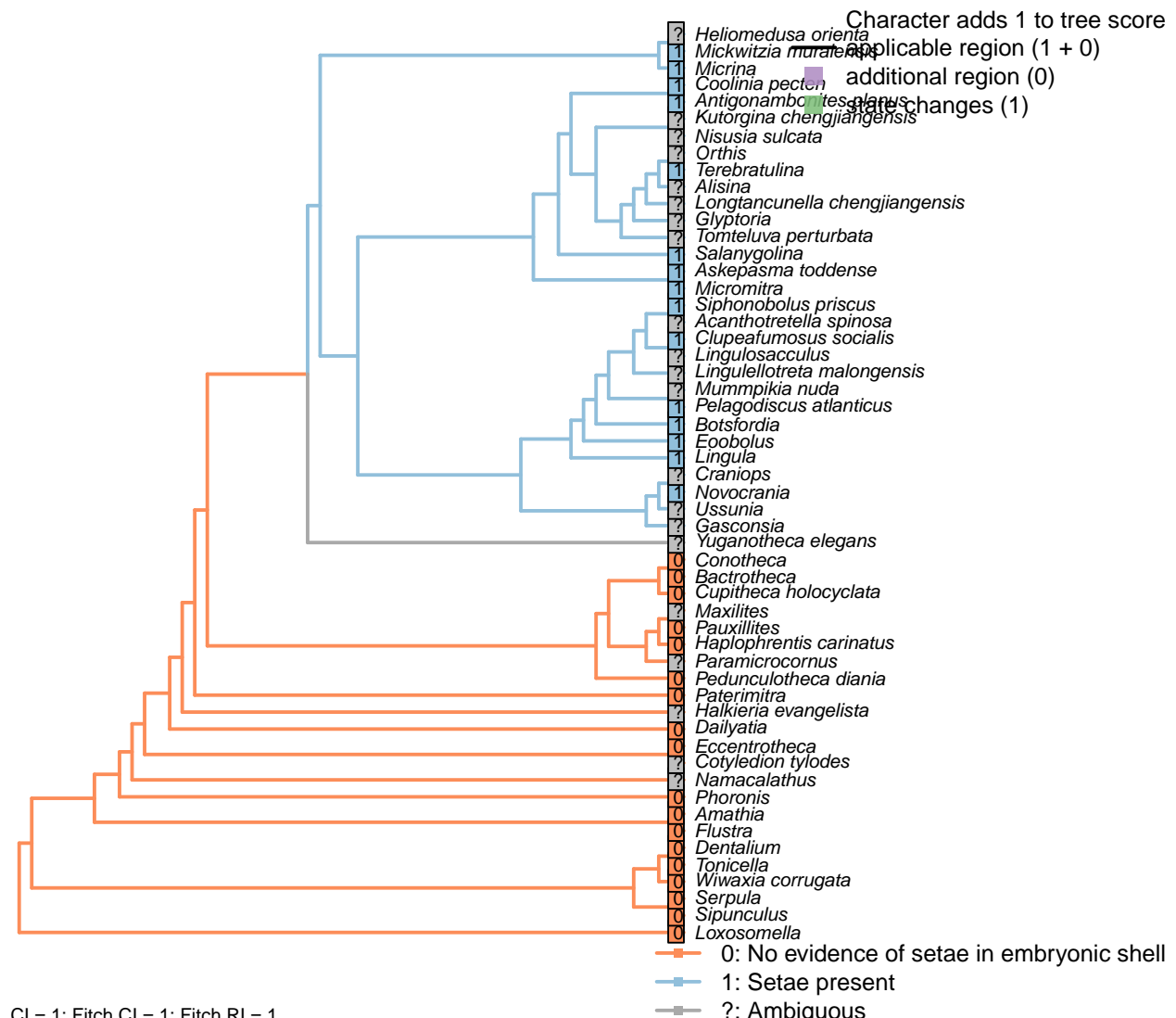
*Lingulellotreta malongensis*: The pedicle foramen intersects the brepthic shell (Holmer et al., 1997; Li and Holmer, 2004), suggesting larval attachment.

*Mickwitzia muralensis*: Note the posterior lobe related to the attachment rudiment in fig. 2 of Balthasar (2009).

*Pauxillites*: Distal extension of *Recilites* (Pauxillitidae) has plausible similarity to pedicle (Dzik, 1978), but deemed unlikely. Coded as ambiguous.

*Siphonobolus priscus*: Interpreted as having planktotrophic (and thus non-attached) larvae (Popov et al., 2009).

## [6] Setulose



CI = 1; Fitch CI = 1; Fitch RI = 1

Character 6: Brepthic shell: Setulose

- 0: No evidence of setae in embryonic shell
  - 1: Setae present
- Neomorphic character.

The protogulum of *Micrina* is penetrated with canals that were originally associated with setae, a character that it has in common with linguliforms (Holmer et al., 2011).

*Botsfordia*: “One specimen shows fine capillae running laterally from the posterior tubercles on the dorsal valve (Pl. 3, fig. 5b). This is possibly the imprints of setae.” – Ushatinskaya and Korovnikov (2016).

*Clupeafumosus socialis*: Setal bundles interpreted as present in acrotretids by Ushatinskaya (2016).

*Conotheca*: (Wrona, 2003).

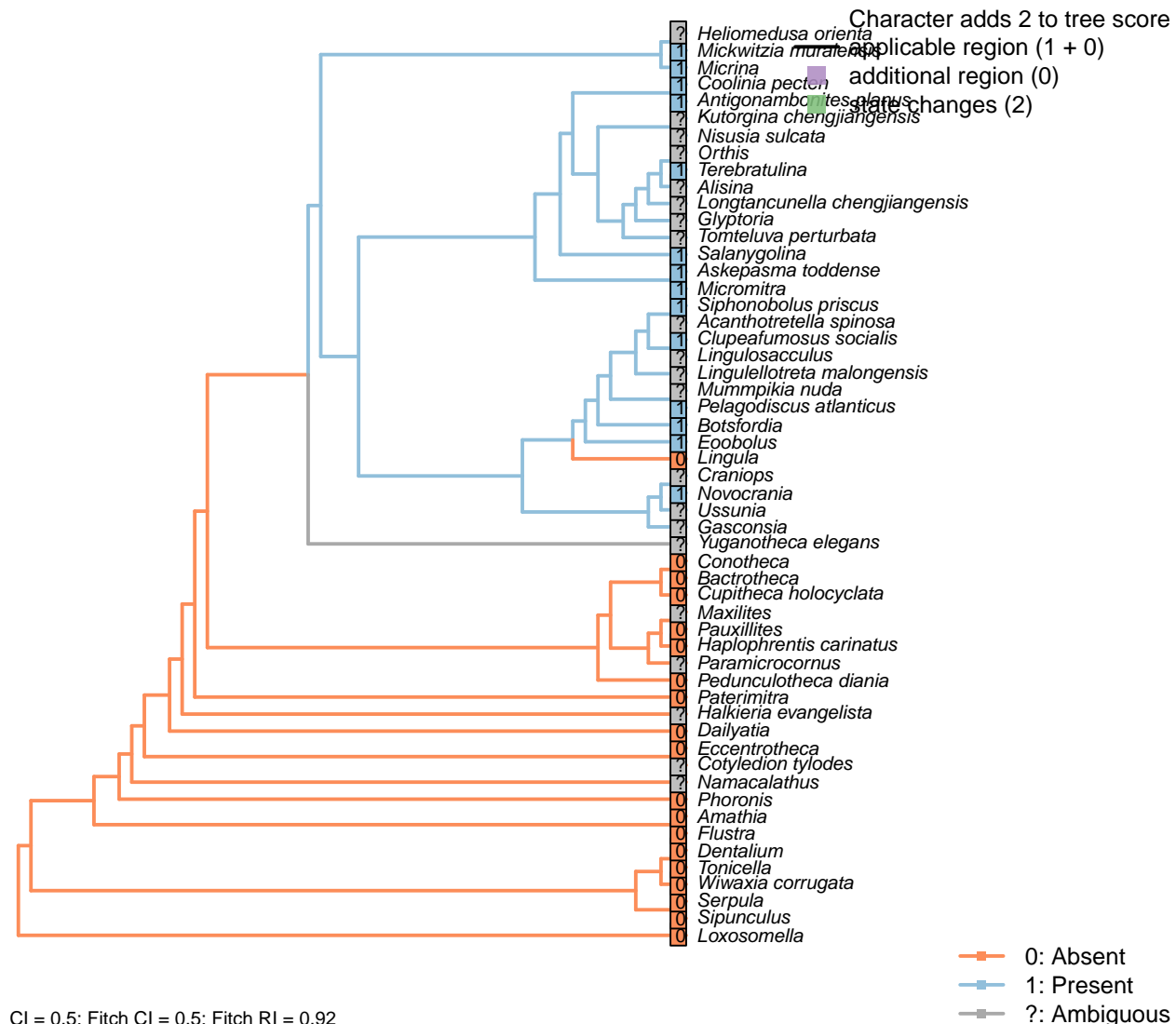
*Cupitheca holocyclata*: Absent (Skovsted et al., 2016).

*Lingulellotreta malongensis*: Possible suggestion of setal sacs present on brephic shell (Holmer et al., 1997; Li and Holmer, 2004), but outline inadequately preserved to code with confidence; treated as ambiguous.

*Mickwitzia muralensis*: Four setal sacs.

*Pauxillites*: Following *Recilites* (Pauxillitidae) (Dzik, 1978).

## [7] Setal sacs



### Character 7: Brethic shell: Setal sacs

0: Absent

1: Present

Neomorphic character.

Setal sacs are recognizable as raised lumps on the juvenile shell (see Bassett and Popov, 2017).

*Micrina* and linguliforms have setal sacs on their mitral/dorsal embryonic shell, whereas these are absent in *Paterimitra* (Holmer et al., 2011).

*Bactrotheca*: Following *Bactrotheca* (Dzik, 1980).

*Botsfordia*: A single pair of low tubercles are (Ushatinskaya and Korovnikov, 2016, state "may be") located in the middle region of the dorsal and the ventral brethic valve; these are interpreted as a single pair of setal

sacs, with the identity of the (dorsally unpaired) tubercles uncertain.

*Clupeafumosus socialis*: Setal bundles interpreted as present in acrotretids by Ushatinskaya (2016).

*Conotheca*: (Wrona, 2003).

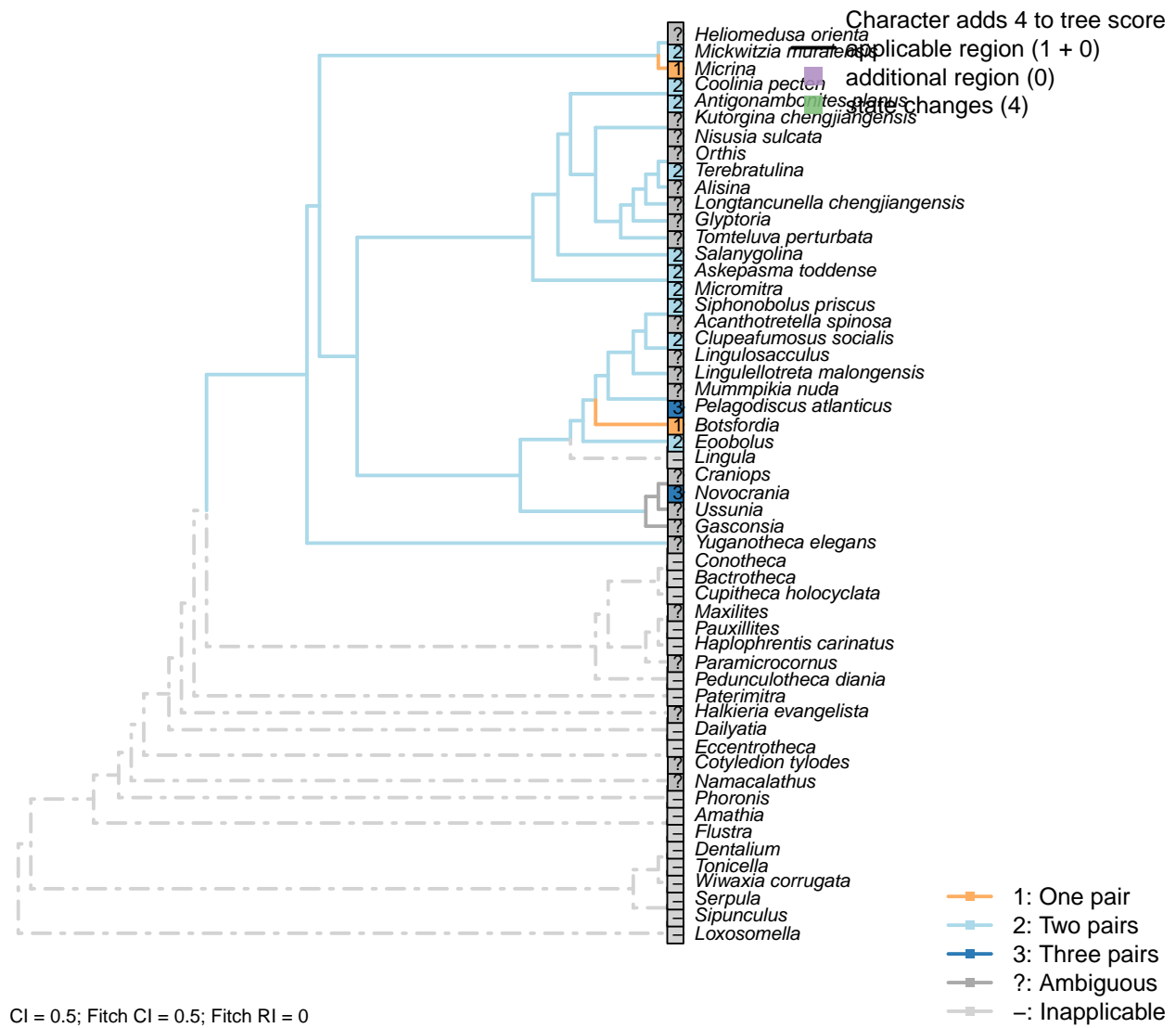
*Lingula*: Lingulids' larval setae are not arranged in bundles (Carlson, 1995).

*Lingulellotreta malongensis*: Possible suggestion of setal sacs present on brephic shell (Holmer et al., 1997; Li and Holmer, 2004), but outline inadequately preserved to code with confidence; treated as ambiguous.

*Novocrania, Pelagodiscus atlanticus*: Three pairs (Carlson, 1995).

*Pauxillites*: Following *Recilites* (Pauxillitidae) (Dzik, 1978).

## [8] Number



### Character 8: Brephic shell: Setal sacs: Number

1: One pair

2: Two pairs

3: Three pairs  
Transformational character.

Two pairs on e.g. *Coolina*; one on e.g. *Micrina*.

*Botsfordia*: “larval shell with one to three apical tubercles in ventral valve and two in dorsal valve” (Williams et al., 2000) – if these correspond to setal sacs, then we interpret this as equivalent to one pair.

In *B. minuta*, the ventral valve bears a single medial tubercle (which in figured material seems to have two bilaterally symmetrical fields), whereas the dorsal valve bears two apical tubercles (Li and Holmer, 2004) – supporting the interpretation of a single pair of setal sacs.

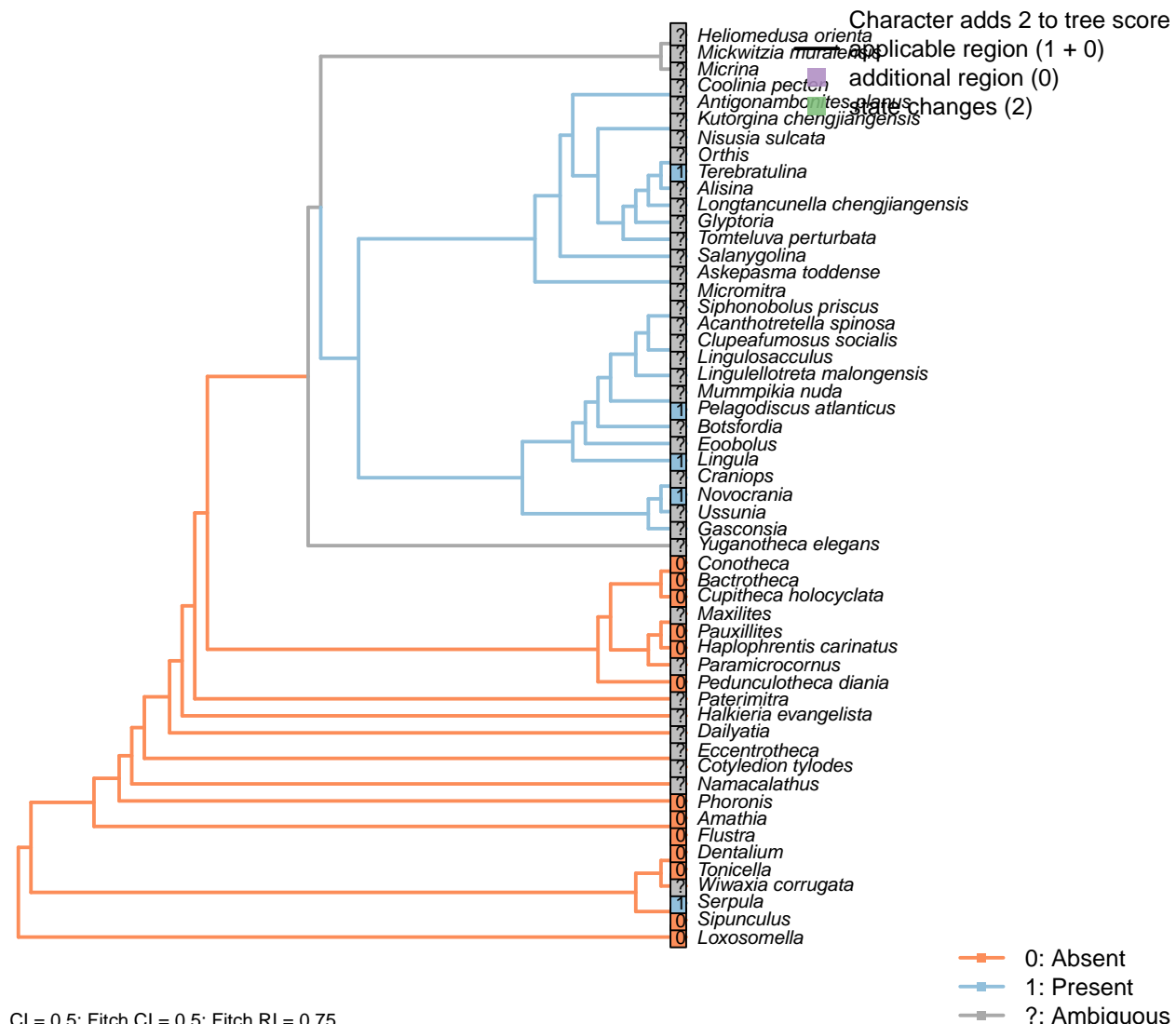
*Clupeafumosus socialis*: Two pairs identified in acrotretids by Ushatinskaya (2016).

*Mickwitzia muralensis*: See fig. 2 in Balthasar (2009).

*Novocrania*, *Pelagodiscus atlanticus*: Three pairs (Carlson, 1995).

*Siphonobolus priscus*: Two pairs of setal sacs (Popov et al., 2009).

## 5.2 Larval chaetae: Paired bundles [9]



### Character 9: Larval chaetae: Paired bundles

0: Absent

1: Present

Neomorphic character.

Annelid chaetae are equivalent to the bundled setae expressed in certain brachiopod larvae. See character 12 in Vinther et al. (2008).

*Amathia*: (Reed and Cloney, 1982).

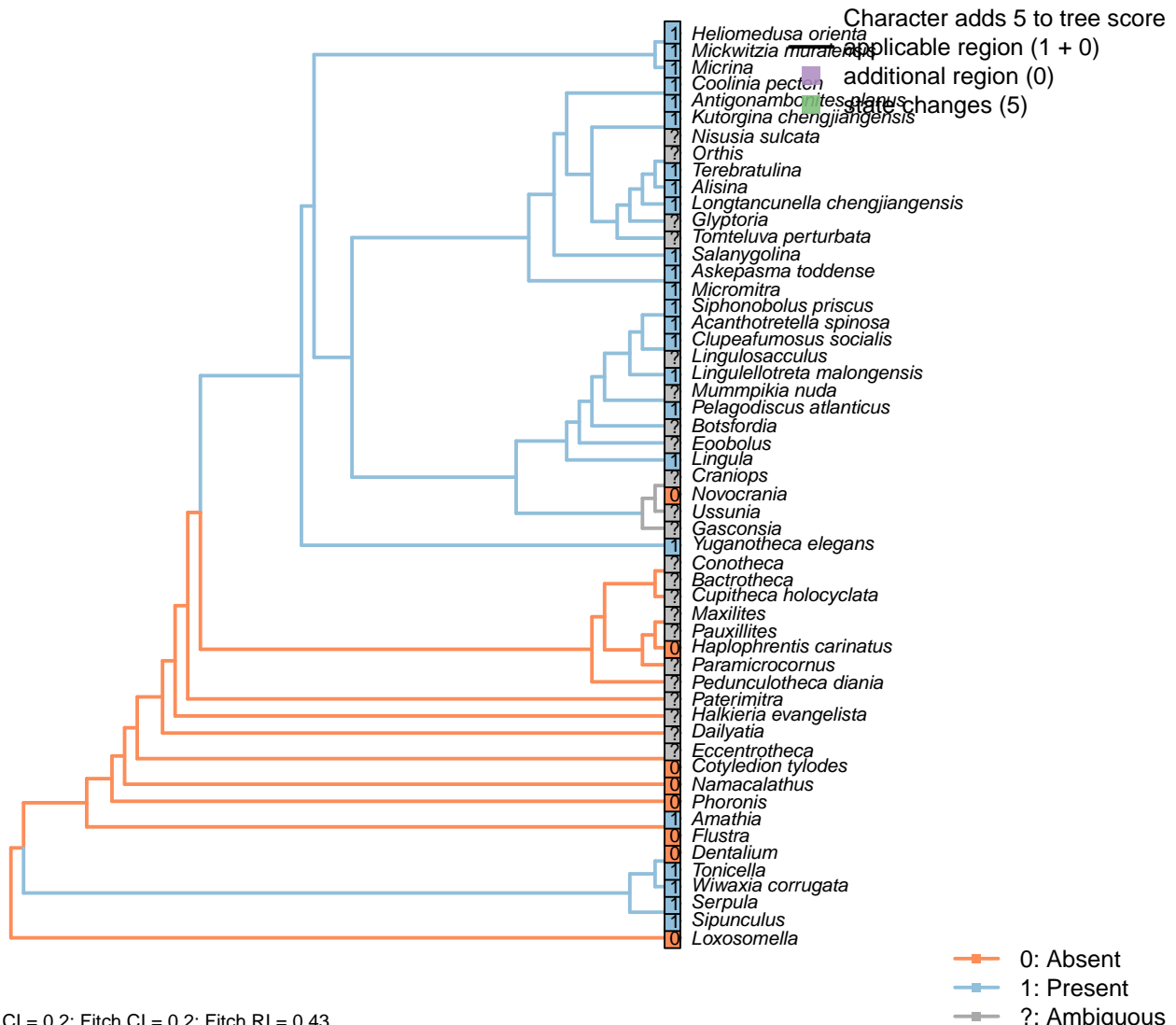
*Flustra*: Absent (Zimmer and Woollacott, 2013).

*Pauxillites*: Following *Recilites* (Pauxillitidae) (Dzik, 1978).

*Serpula*: Lüter (2000) contends that annelid larvae lack setae, but chaetae are present on day 16 of the larval development of *Serpula* (Keay, 2007).

*Terebratulina*: Williams et al. (1997).

### 5.3 Adult setae [10]



#### Character 10: Adult setae

0: Absent

1: Present

Neomorphic character.

Lüter (2000) demonstrates that the setae of larval and adult brachiopods exhibit fundamental structural differences and are conceivably not homologous structures. Larval setae are thus described separately.

Although preservation of setae in fossil brachiopods is exceptional, their presence can be inferred from shelly material (see Holmer and Caron, 2006).

*Acanthotretella spinosa*: Note that the setae do not obviously emerge from tubes, leading Holmer and Caron to question their homology with the setae of other taxa (*Heliomedusa*, *Mickwitzia*).

Both valves of *Acanthotretella* were covered by long spine-like and shell penetrating setae. The setae of *A.*

*decaius* are usually preserved along anterior and anterolateral margins (Hu et al., 2010).

*Amathia*: The teeth of the Bryozoan gizzard have been homologized with annelid setae (Gordon, 1975).

*Clupeafumosus socialis*: Setal bundles interpreted as present in acrotretids by Ushatinskaya (2016).

*Flustra*: A gizzard is not present in all bryozoans, and has not been reported in *Flustra*.

*Haplophrentis carinatus*: Not observed (Moysiuk et al., 2017), despite suitable preservation.

*Lingulellotreta malongensis*: “Setae appear short, delicate, and are closely fringed with the entire mantle margin, hardly extending beyond the edge of shell” – Zhang et al. (2005).

*Novocrania*: “Adult craniids are without setae (a feature shared with the thecideides, the shells of which are also cemented).” – Williams et al. (2007).

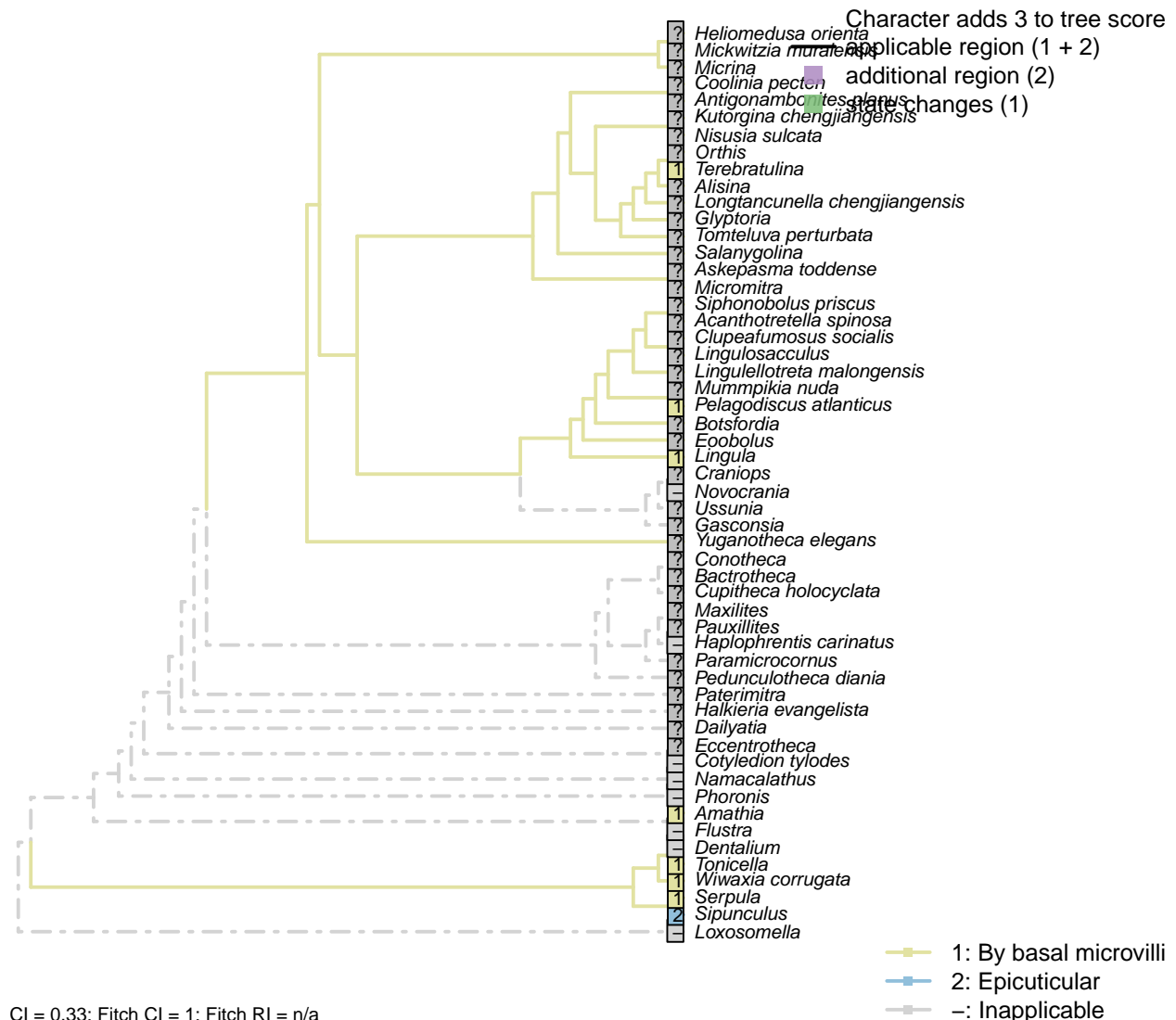
*Siphonobolus priscus*: Phosphatised setae emerge from hollow spines (Popov et al., 2009).

*Sipunculus*: The absence of chitin or microvillar lineations in sipunculan hooks argues against their interpretation as setae, but they are coded as conceivable homologues, with these characteristics treated separately.

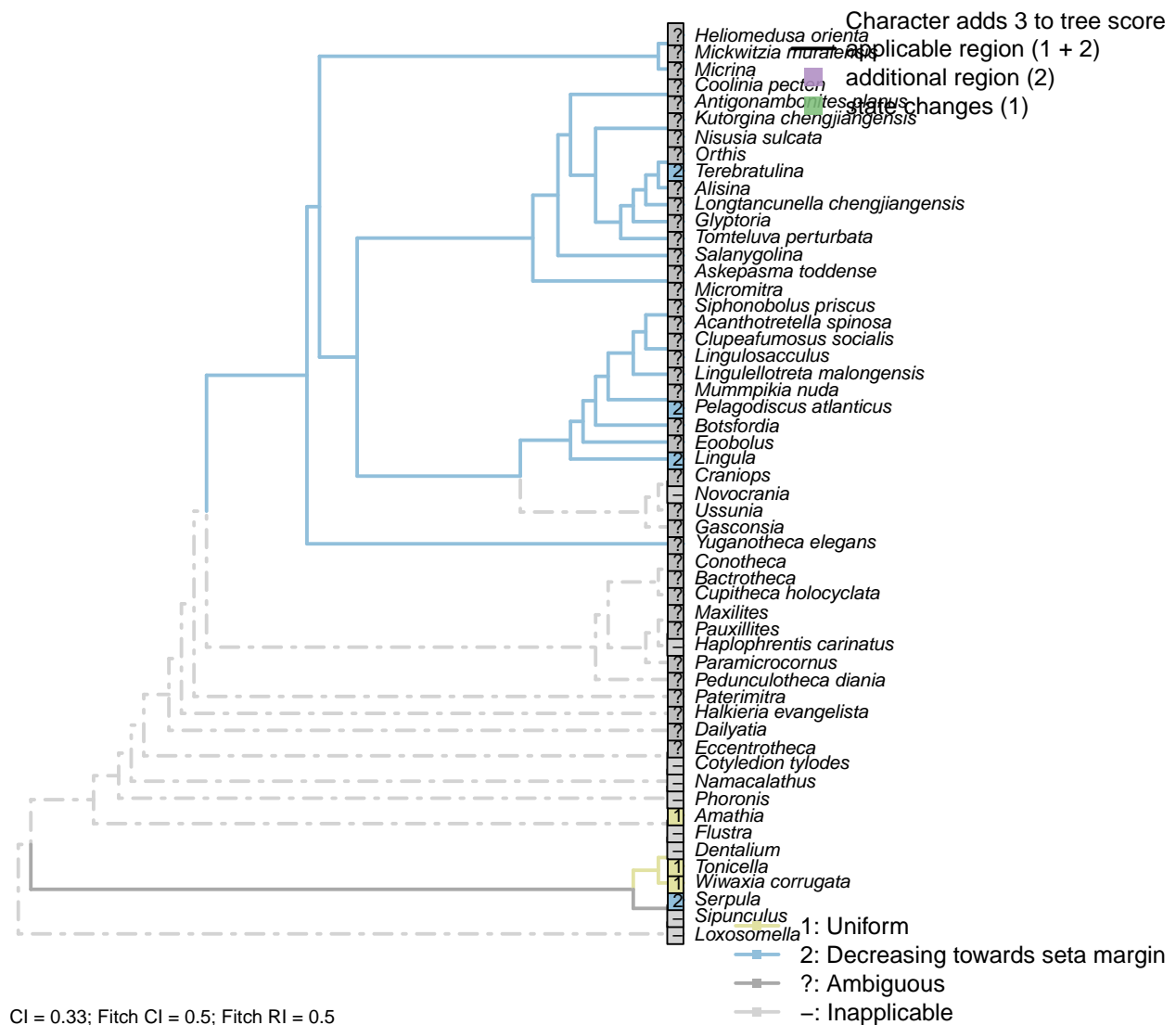
*Tonicella*: The girdle elements of certain polyplacophorans are chitinous and secreted by microvilli (Fischer et al., 1980; Leise and Cloney, 1982; Leise, 1988); it is therefore likely that they are homologous with the setae of other lophotrochozoans.

*Wiwaxia corrugata*: Sclerites likely correspond with lophotrochozoan setae (Butterfield, 1990; Smith, 2014; Zhang et al., 2015).

## [11] Secretion



## [12] Microvillar diameter

**Character 12: Adult setae: Secretion: Microvillar diameter**

1: Uniform

2: Decreasing towards seta margin

Transformational character.

The diameter of secretory microvilli may vary across the diameter of a seta (Smith, 2014).

*Amathia*: No trend in microvillar size (Gordon, 1975).

*Lingula*: Widest in centre (Lüter, 2000).

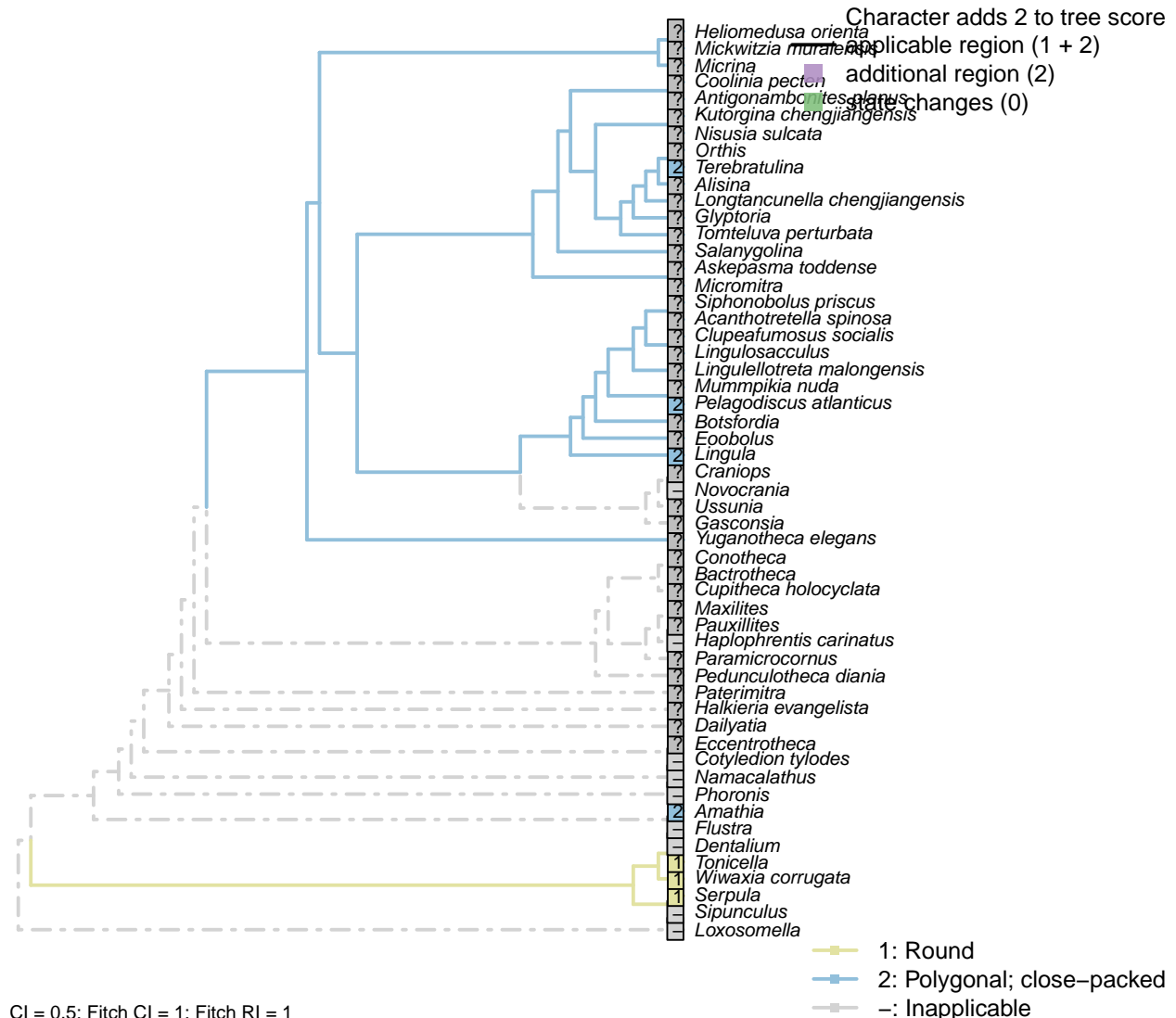
*Pelagodiscus atlanticus*: Slight decrease towards margin in *Discinisca* (Lüter, 2003).

*Serpula*: Following *Scolelepis* (Hausen, 2005); *Diasoma* (Orrrage, 1971).

*Terebratulina*: Decreases towards margin in *Terebratalia* larvae (Gustus and Cloney, 1972).

*Tonicella*: Uniform (Fischer et al., 1980; Leise and Cloney, 1982).

### [13] Microvillar canal aspect



Lüter (2000) distinguishes between the polygonal outline of microvillar canals in adult brachiopod setae and

the oval outline of larval setae.

*Amathia*: Polygonal (Gordon, 1975).

*Lingula*: Polygonal (Lüter, 2000).

*Pelagodiscus atlanticus*: Reported as hexagonal in *Discina* (Lüter, 2000).

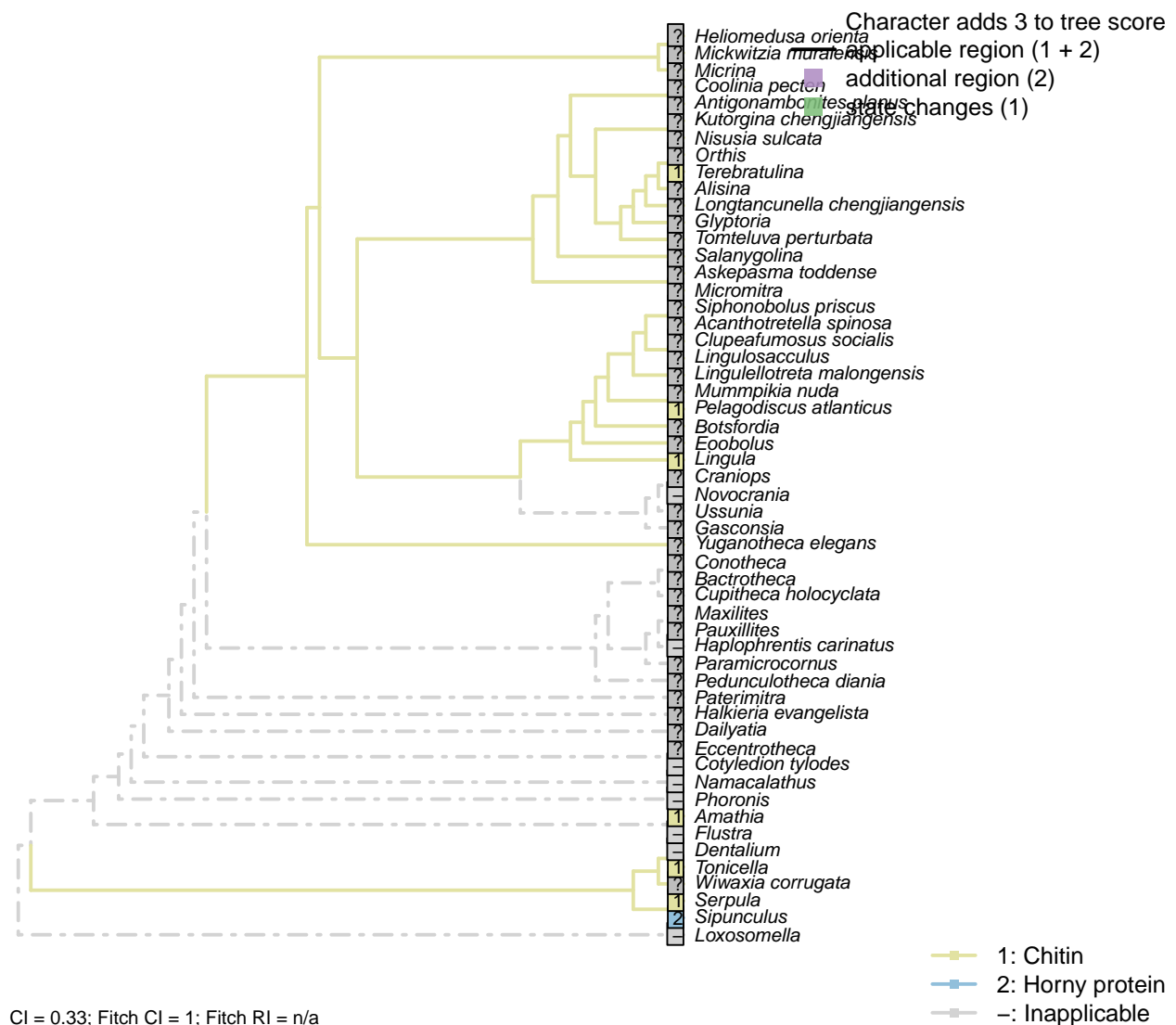
*Serpula*: Annelid setae are prominently round, with gaps between each microvillar chamber (Orrhage, 1971).

*Terebratulina*: Polygonal in *Calloria* (Lüter, 2000).

*Tonicella*: Round (Fischer et al., 1980).

*Wiwaxia corrugata*: The loose spacing of pyrite infills of microvillar canals in *Wiwaxia* sclerites (Smith, 2014) argues against a close-packed arrangement.

## [14] Composition



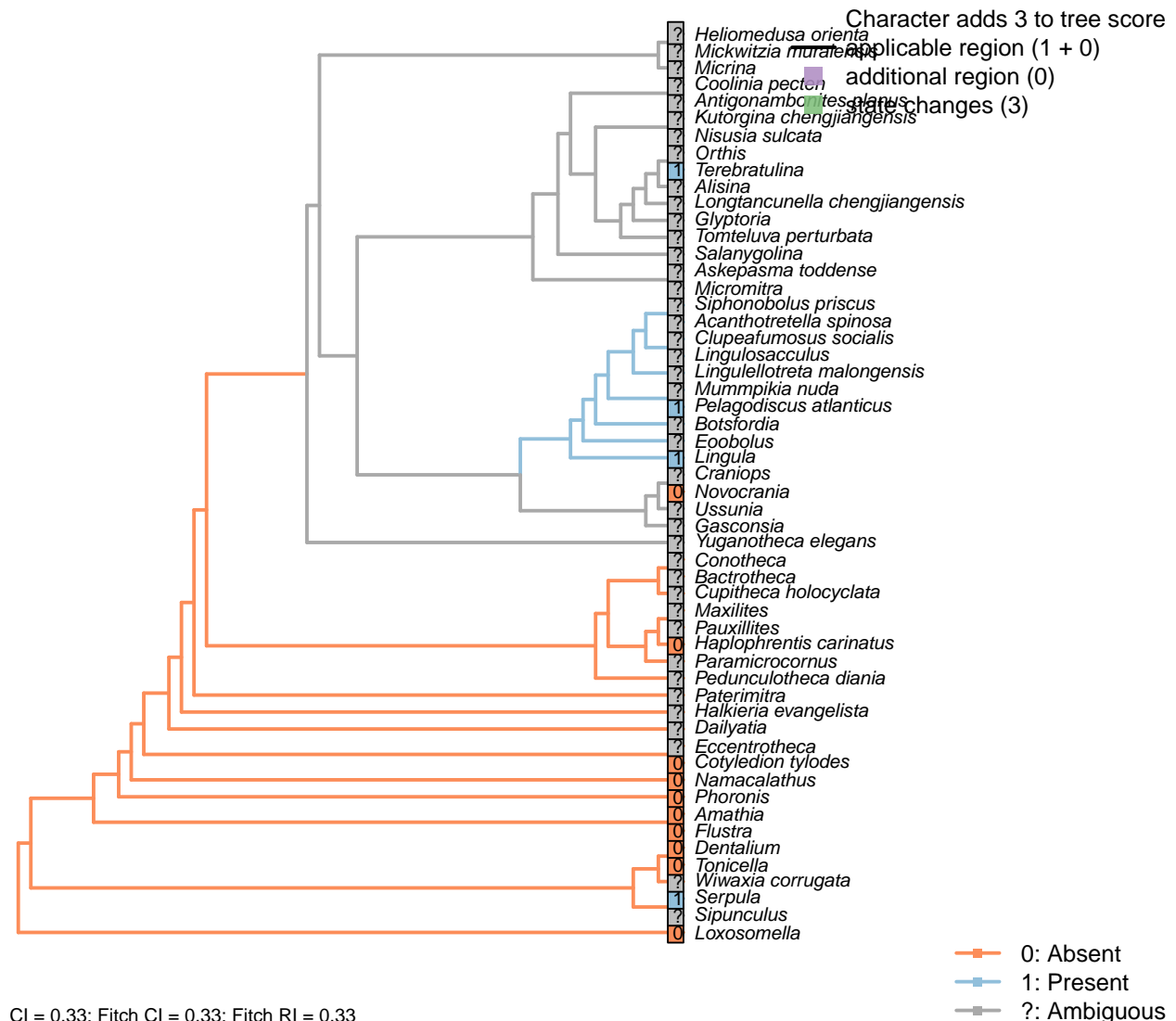
Character 14: Adult setae: Composition

- 1: Chitin
- 2: Horny protein
- Transformational character.

The majority of lophotrochozoan sclerites are chitinous, occasionally hosting secondary biominerals.

*Sipunculus*: Enzymatic test for chitin proved negative (Rice, 1993).

## [15] Enamel



### Character 15: Adult setae: Enamel

- 0: Absent
- 1: Present
- Neomorphic character.

Certain setae are encapsulated in a 20 nm wide electron dense layer, termed “enamel” by Gustus and Cloney (1973). Enamel may be absent in larval setae (Lüter, 2003); this character refers to the condition in adult

setae.

*Amathia*: Not evident (Gordon, 1975).

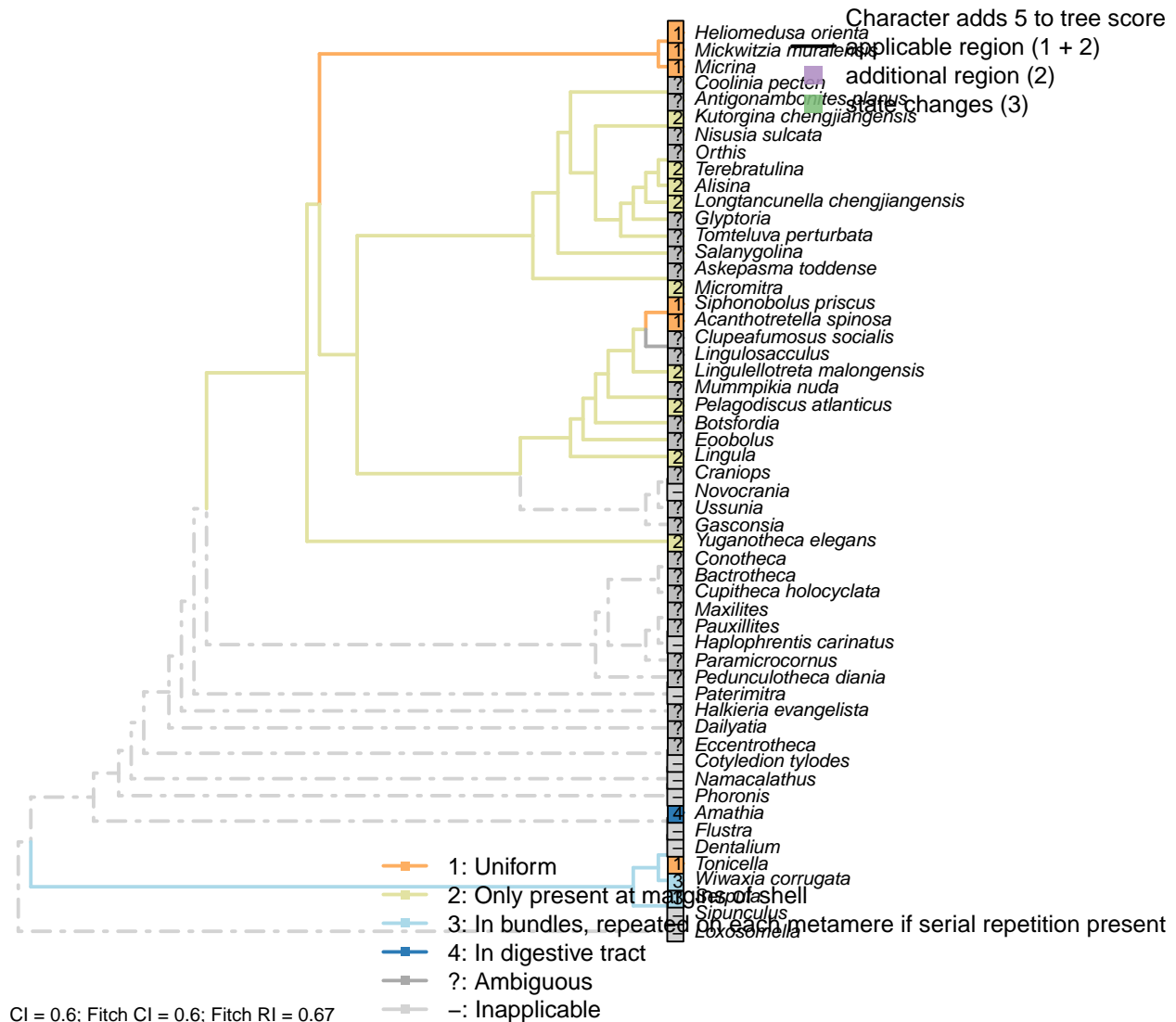
*Pelagodiscus atlanticus*: Enamel layer apparent in Discina (Williams et al., 1997, fig. 47.1).

*Serpula*: Present in *Nereis* (Gustus and Cloney, 1973).

*Terebratulina*: Present in the terebratulid *Calloria* (and the Rhynchonellid *Notosaria*) (Lüter, 2000).

*Tonicella*: Not evident (Leise, 1988; Fischer et al., 1980).

## [16] Distribution



### Character 16: Adult setae: Distribution

- 1: Uniform
  - 2: Only present at margins of shell
  - 3: In bundles, repeated on each metamere if serial repetition present
  - 4: In digestive tract
- Transformational character.

Setae penetrate the valves of many brachiopods. In certain taxa, they are apparent only at the margins of the valves, in association with the commissure, being reduced or lost over the surface of the shell.

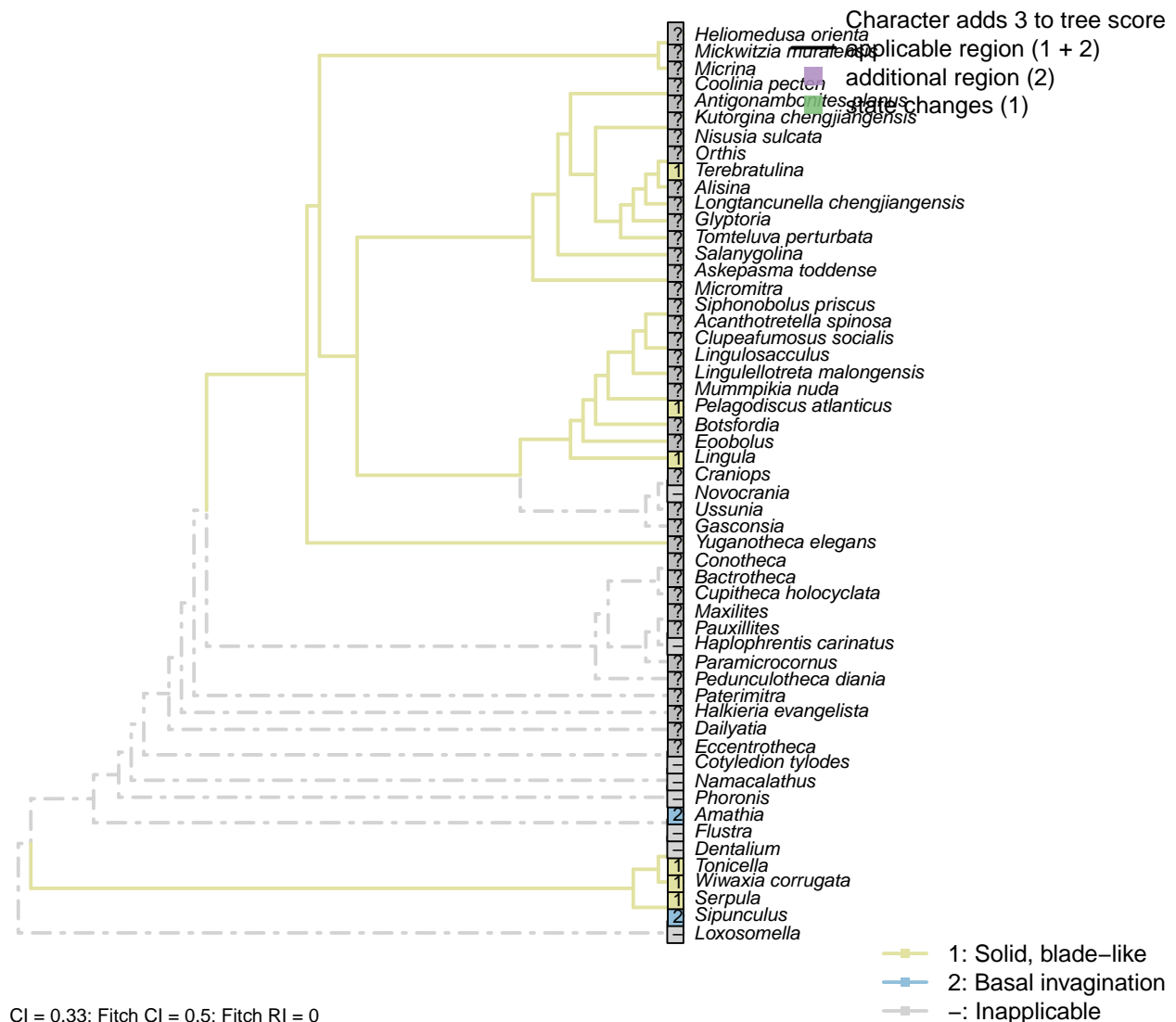
*Eccentrotheca*: Skovsted *et al.* (2011) assumed the setae may have been present along the margin of the adapical opening, but there is no fossil evidence.

*Heliomedusa orienta*: Throughout the shell – see Williams *et al.* (2007) – causing the pustulose appearance remarked upon by Chen *et al.* (2007).

*Lingulellotreta malongensis*: At margin of shell (Zhang *et al.*, 2005).

*Tonicella*: Uniformly distributed around girdle (though not within shell) with no serial repetition (Vinther and Nielsen, 2005; Leise, 1988).

## [17] Constitution



### Character 17: Adult setae: Constitution

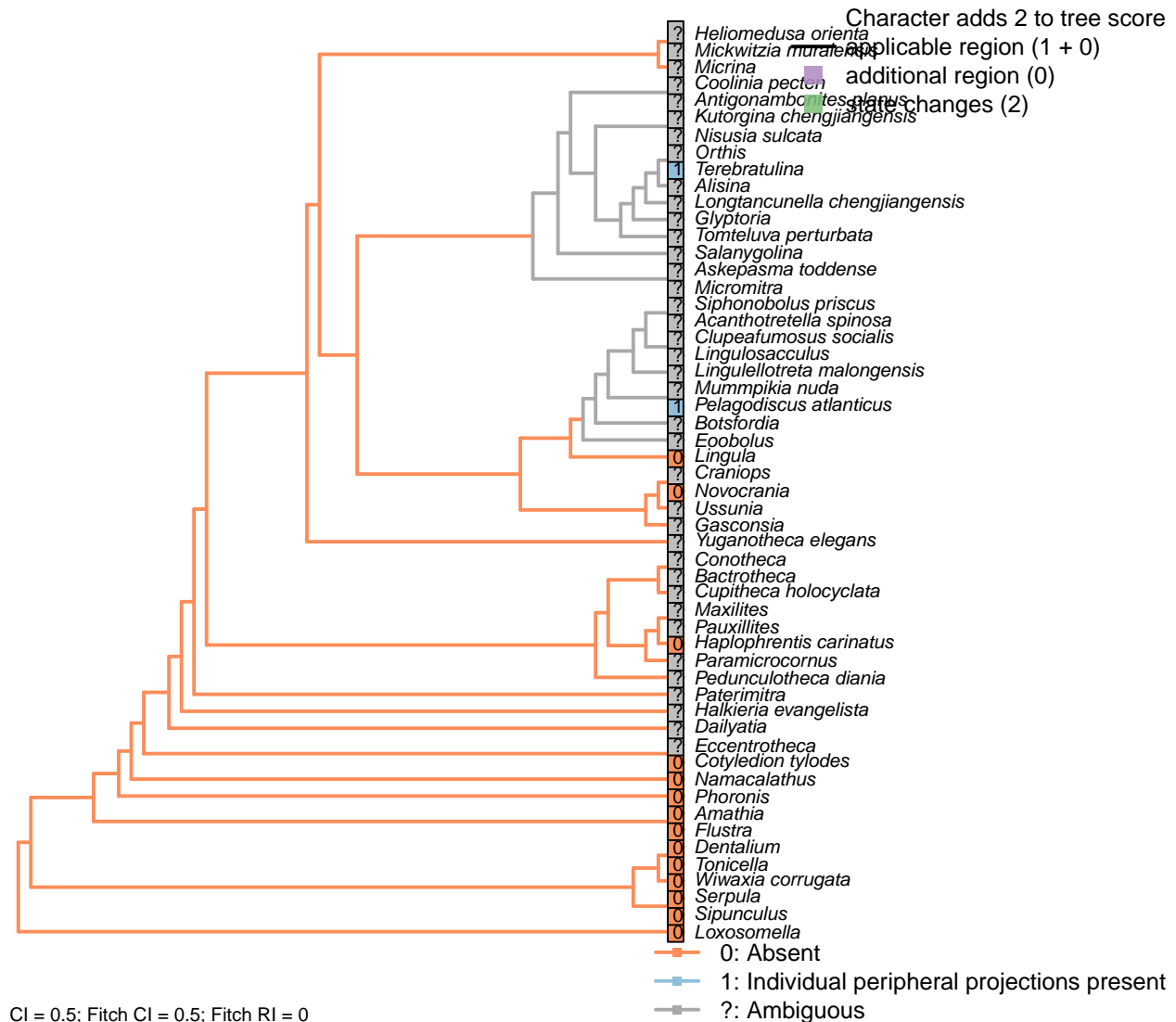
- 1: Solid, blade-like
- 2: Basal invagination

Transformational character.

Sipunculan “setae” are basally invaginated, suggesting that they may not be homologous with annelid chaetae.

*Amathia*: Cytoplasmic intrusion into a central cavity (Gordon, 1975).

## [18] Projecting knobs



Terebratulids and discinids instead exhibit knob-like individual spines These are distinct from the rings of spines that fringe lingulid setae.

*Lingula*: Lüter (2000).

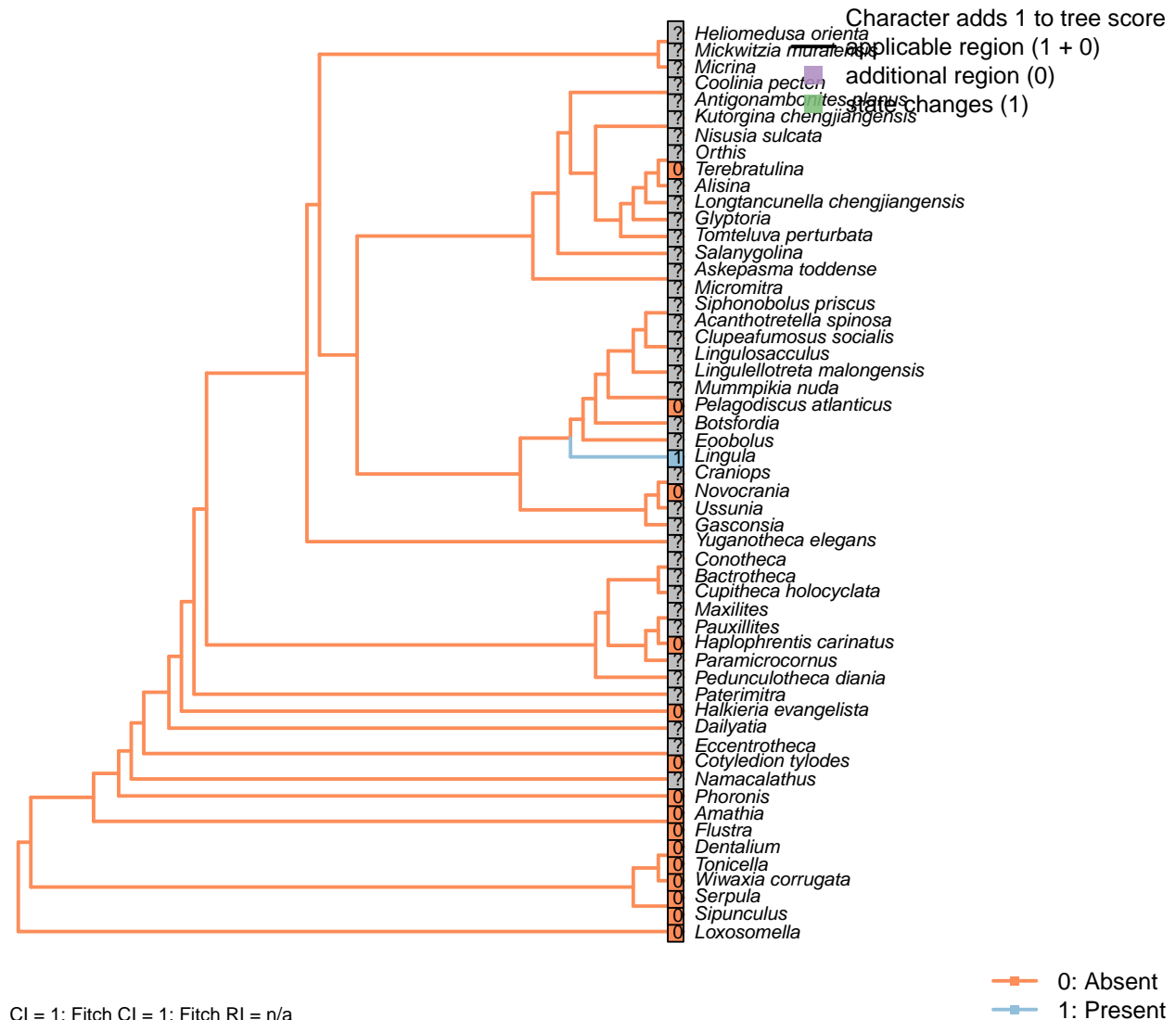
*Pelagodiscus atlanticus*: *Discinisca* sports individual peripheral spines (Williams et al., 1997; Lüter, 2003).

Note that the “embryonic” setae of Discinids correspond to the “larval setae” of other brachiopods, and the “larval setae” of juvenile discinids correspond to adult setae (Lüter, 2003).

*Serpula*: Surface smooth (Sun and Qiu, 2012).

*Terebratulina*: Individual peripheral spines (in *Calloria*; Lüter, 2000).

### [19] Circling coronae



CI = 1; Fitch CI = 1; Fitch RI = n/a

#### Character 19: Adult setae: Circling coronae

0: Absent

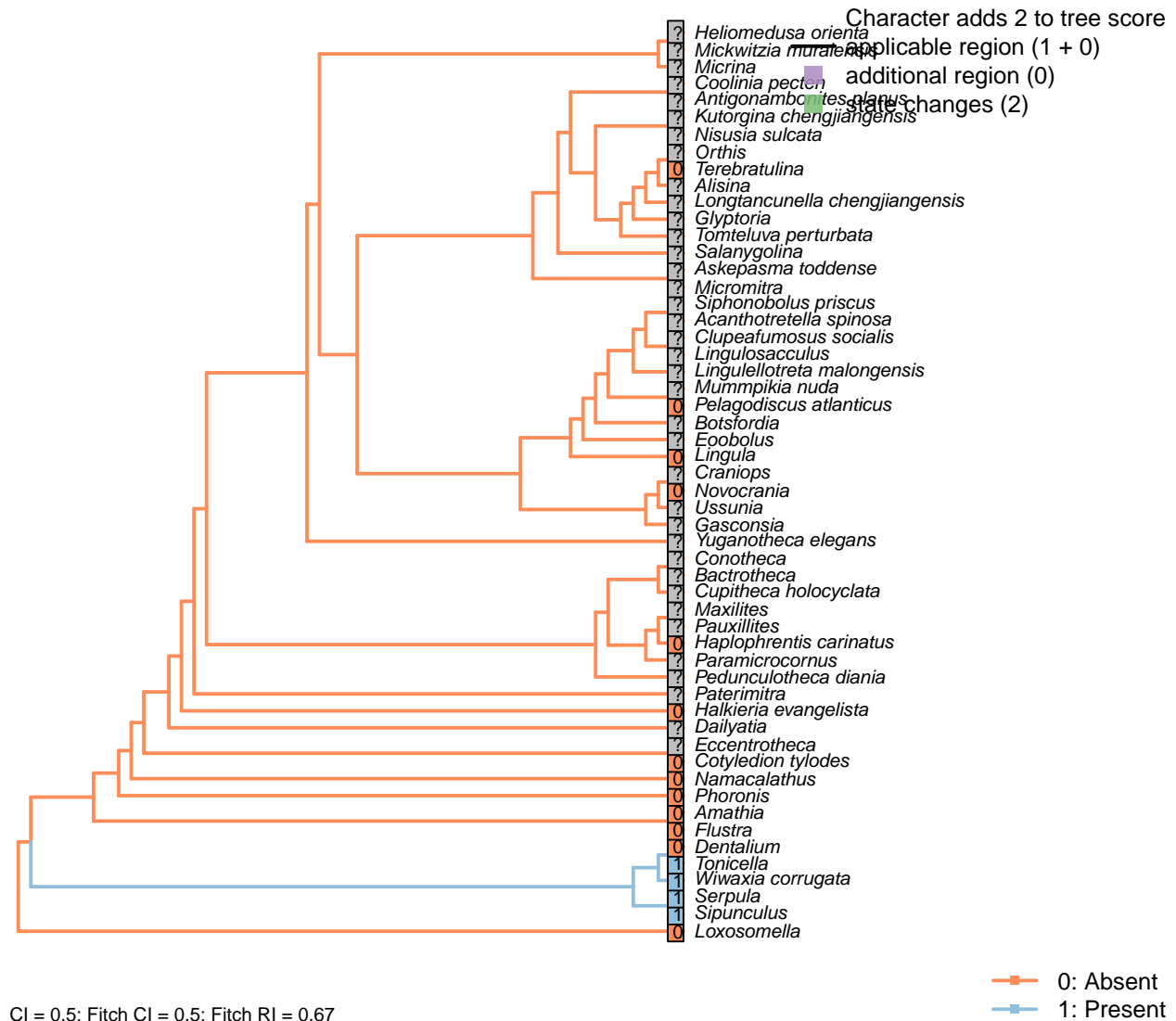
1: Present

Neomorphic character.

Lingulid setae bear crown-like rings of fine spines delimiting vertical sections, recalling the nodes of *Equisetum* stems. These arise by the addition of an additional circlet of microvilli (see Lüter, 2000, fig. 1e).

## 5.4 Body organization

### [20] Serial repetition



#### Character 20: Body organization: Serial repetition

0: Absent

1: Present

Neomorphic character.

Serial repetition in adult, whether expressed in valves, soft tissues or exoskeletal elements. See character 13 in Rouse (1999); 19 in Vinther et al. (2008); 38 in Haszprunar (1996); 40–41 in Sutton and Sigwart (2012); Wanninger (2009).

*Bactrotheca, Conotheca, Maxilites, Pauxillites*: The soft anatomy of this taxon is unknown, so it is impossible to rule out the presence of serial repetition.

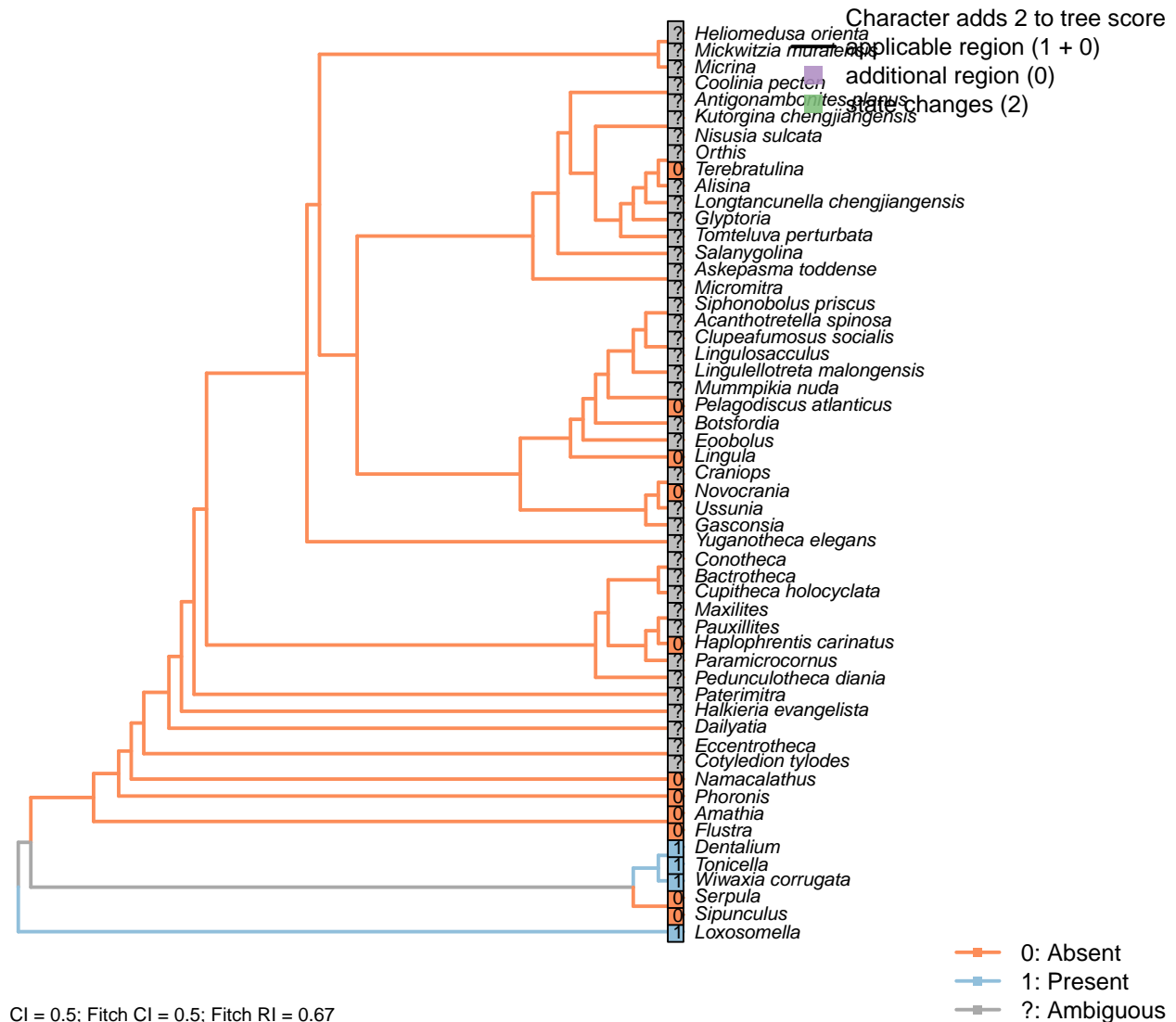
*Dailyatia*: Unknown whether sclerites are serially repeated, or whether metameres were present in underlying

soft anatomy.

*Halkieria evangelista*: Elements of the *Halkieria* scleritome adhere to a quincunx arrangement, with different spacing of elements in each zone; there is no evidence of a metameric arrangement.

*Namacalathus*: Not evident.

## [21] Foot



### Character 21: Body organization: Foot

0: Absent

1: Present

Neomorphic character.

See characters 8 in Haszprunar (1996); 4 in Vinther et al. (2008); 137 in Rouse (1999); 21 in Buckland-Nicks (2008); 37 in Sutton and Sigwart (2012); 1, 3 and 4 in Haszprunar and Wanninger (2008).

It is assumed that the adult foot is homologous with (and thus contingent on) the larval foot.

*Cotyledion tylodes*: The stalk may conceivably be homologous with the entoproct foot, but the evidence for

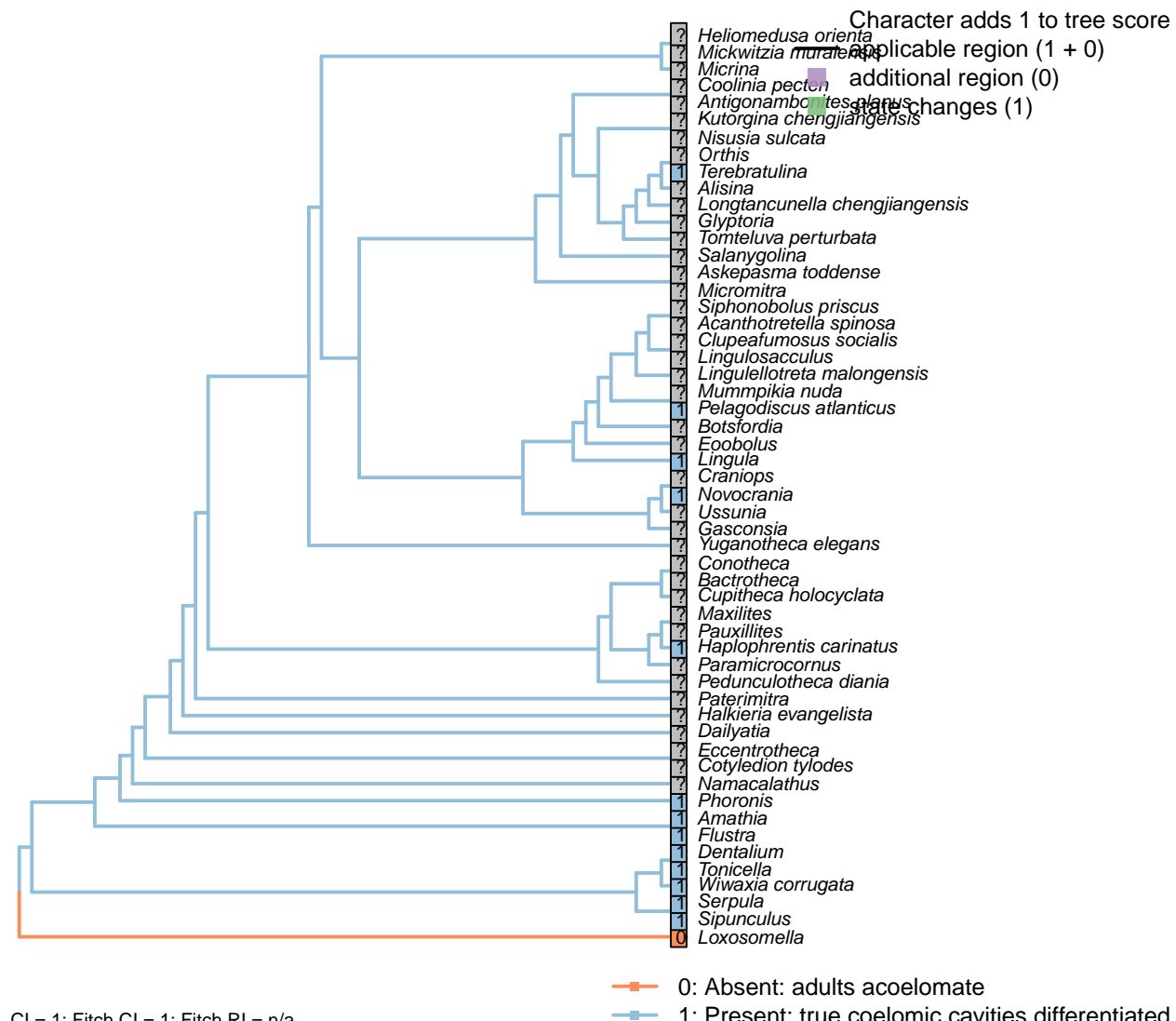
homology is weak.

*Halkieria evangelista*: The ventral surface of *Halkieria* is unarmoured, but its soft anatomy is unknown.

*Loxosomella*: See Haszprunar and Wanninger (2008).

*Sipunculus*: LISTED AS PRESENT IN Smith (2012a): WHY?.

## [22] Coelom



### Character 22: Body organization: Coelom

0: Absent: adults acelomate

1: Present: true coelomic cavities differentiated

Neomorphic character.

*Bactrotheca*, *Conotheca*, *Maxillites*, *Pauxillites*: The soft anatomy of this taxon is unknown, so it is impossible

to determine the presence of a coelom.

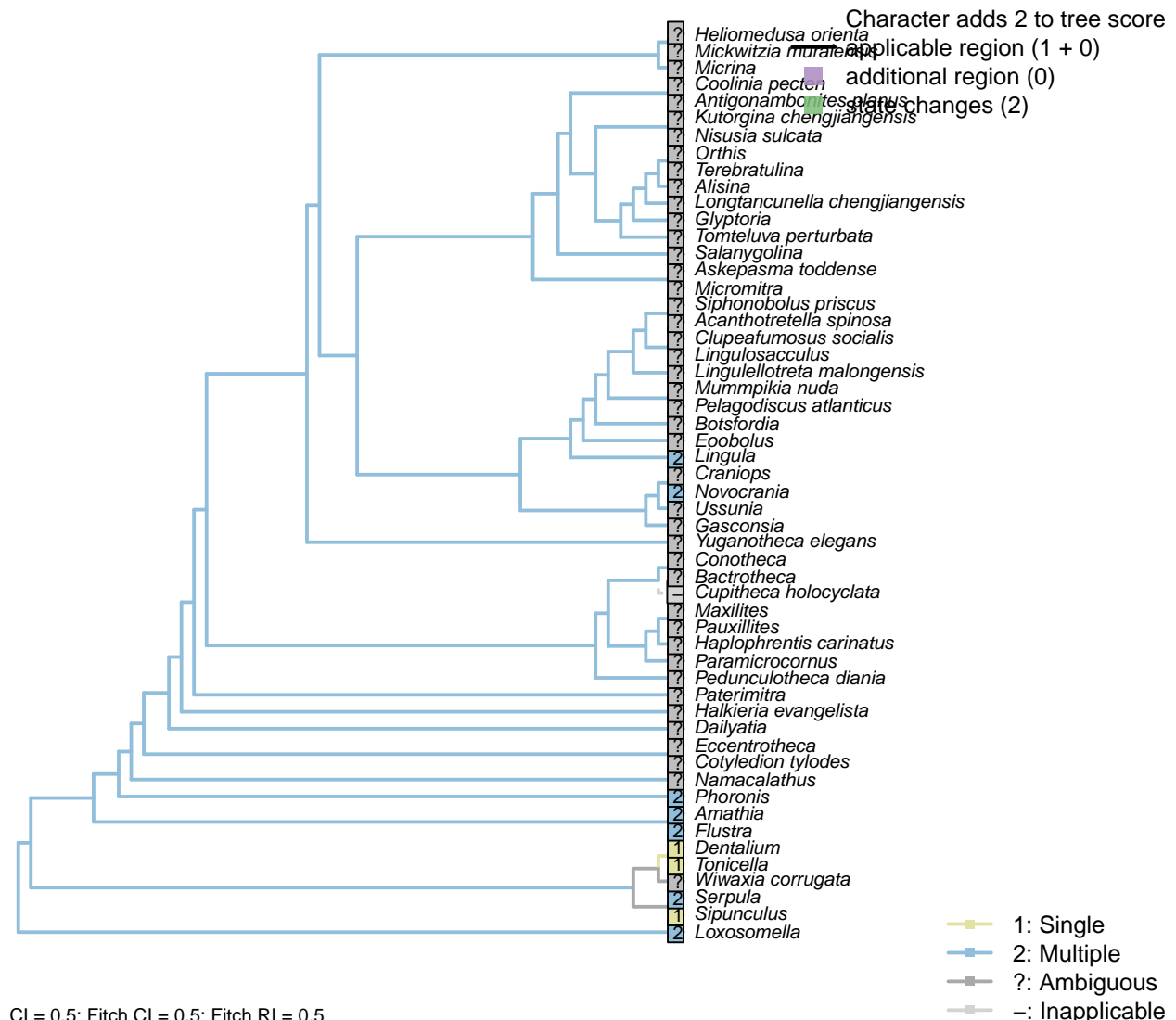
*Flustra*: “Adult ectoprocts differentiate true coelomic cavities” – Fuchs and Wanninger (2008).

*Haplophrentis carinatus*: Internal cavities indicated by differentiation of internal organs (see Moysiuk et al., 2017).

*Loxosomella*: “Adult entoprocts are acoelomate” – Fuchs and Wanninger (2008).

*Phoronis*: Temereva (2017).

## [23] Number



### Character 23: Body organization: Coelomoducts: Number

1: Single

2: Multiple

Transformational character.

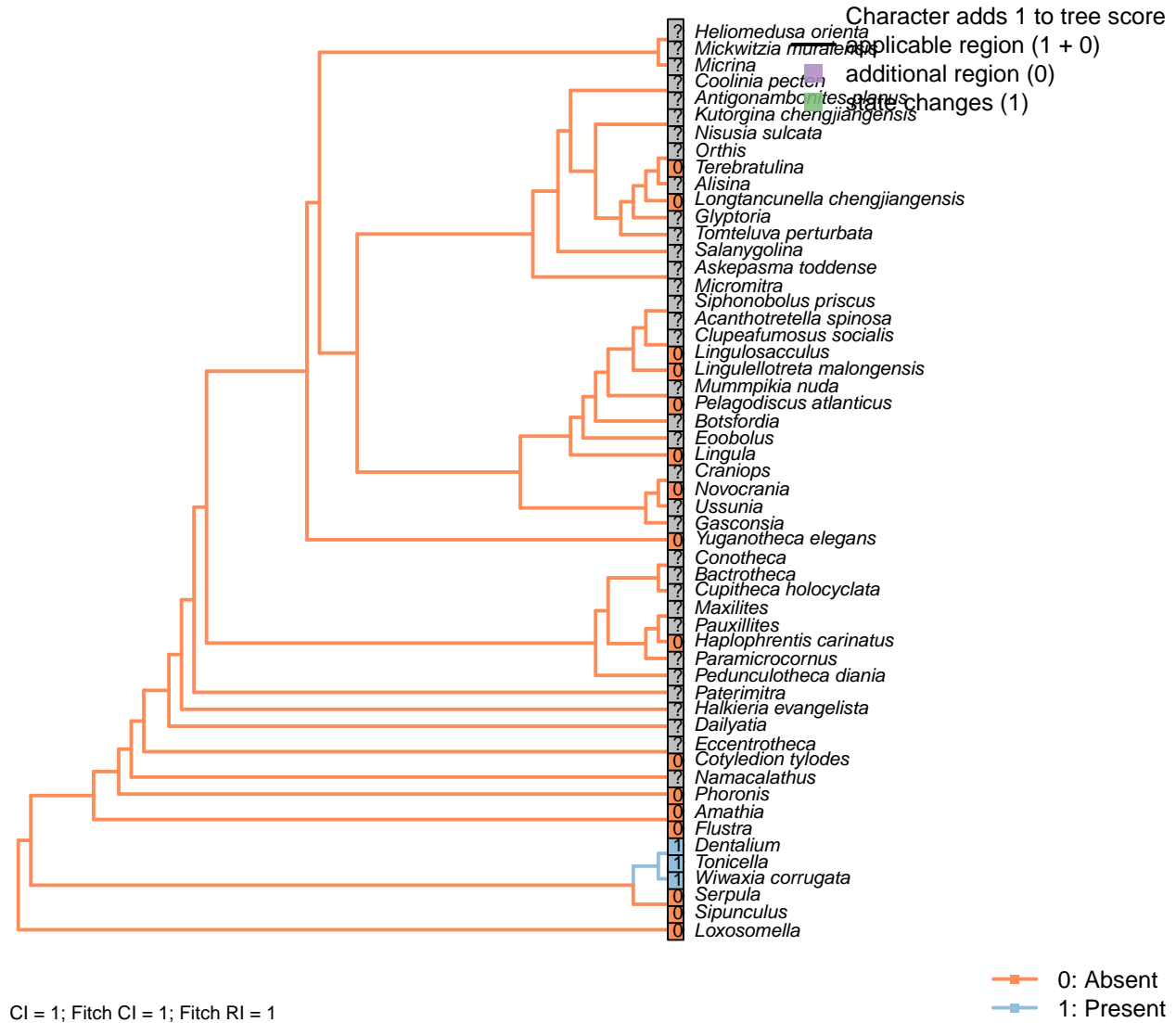
Character 27 in Haszprunar (2000). Coelomoducts are excretory organs derived from the coelom, also in some cases serving as genital ducts (gonoducts); they replace (and may resemble) nephridia (Goodrich, 1945).

*Flustra*: Multiple ciliated ducts leading to a common gonopore (Goodrich, 1945).

*Loxosomella*: Two coelomoducts pass outwards, meet, and open by a common pore (Goodrich, 1945).

*Phoronis*: “large coelomic funnels serving as genital ducts” (Goodrich, 1945).

## [24] Gills



### Character 24: Body organization: Gills

0: Absent

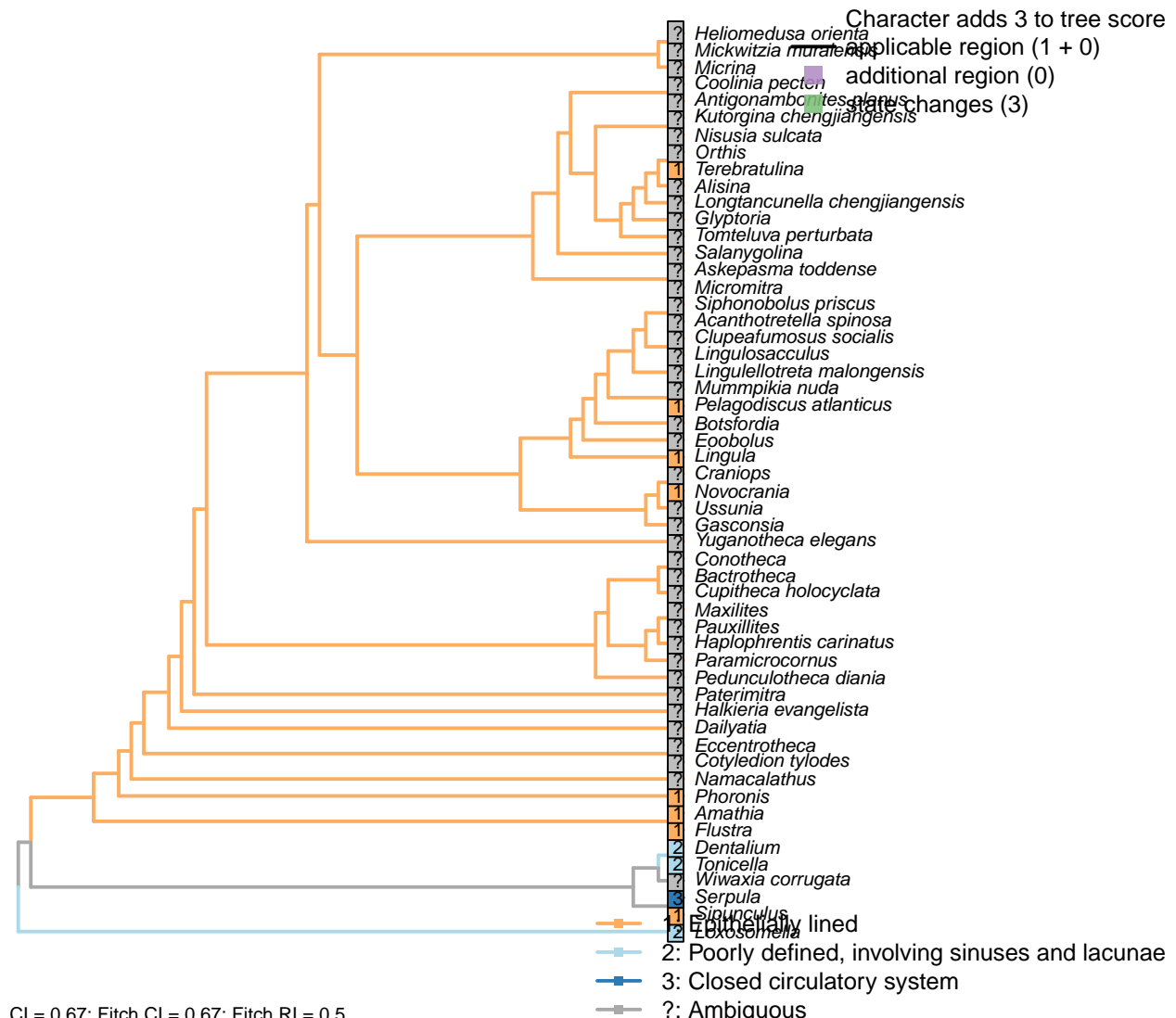
1: Present

Neomorphic character.

Gills (or ctenidia) surround the molluscan foot.

Character 1.59–60, 2.09, 4.49 in von Salvini-Plawen and Steiner (1996); 10–11 in Haszprunar (2000); 45 in Sutton and Sigwart (2012).

## [25] Circulatory system



### Character 25: Body organization: Circulatory system

- 1: Epithelialy lined
  - 2: Poorly defined, involving sinuses and lacunae
  - 3: Closed circulatory system
- Transformational character.

After character 23 in Haszprunar (1996); 24 in Haszprunar (2000); 41 in Rouse (1999); 16 in Scheltema (1993); 16 in Vinther et al. (2008); 5 in Haszprunar and Wanninger (2008).

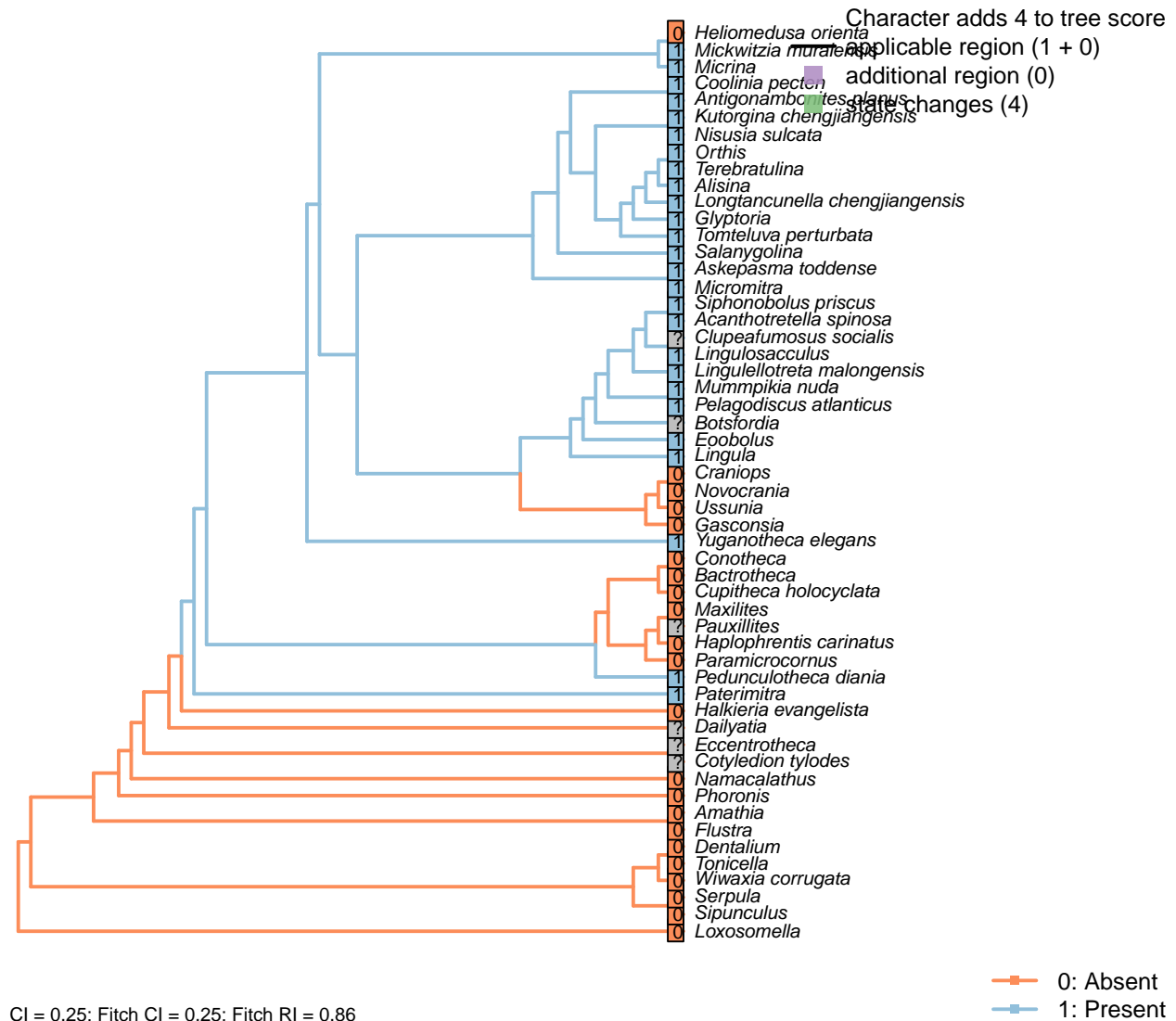
*Flustra, Amathia*: As Brachiopods, sipunculans and relatives (Ruppert and Carle, 1983).

*Loxosomella, Tonicella, Dentalium*: See Haszprunar and Wanninger (2008).

*Sipunculus*: Open circulatory system.

## 5.5 Pedicle

### [26] Presence



The brachiopod pedicle is a fleshy protuberance that emerges from the posterior part of the body wall – as denoted in fossil taxa by its occurrence between the dorsal and ventral valves.

It is important to distinguish the pedicle from the “pedicle sheath”, a tubular extension of the umbo that grows by accretion from an isolated portion of the ventral mantle. For discussion see Holmer et al. (2018b) and Bassett and Popov (2017).

*Acanthotretella spinosa*: The attachment structure of *Acanthotretella* originates at the margin of the dorsal and ventral valves; although it emerges from the umbo of the ventral valve, the presence of an internal pedicle tube betrays its identity as a pedicle, rather than a pedicle sheath.

The pedicle of *Acanthotretella* emerges from a short extension of the umbo of the ventral valve. This extension is contiguous with the valve and presumably grew by accretion; its position and continuity with the valve suggest its interpretation as a pedicle sheath that is superseded as an attachment structure. On the other hand, its continuity with the internal pedicle tube suggests that it may represent an independent organ.

*Bactrotheca*: The apex of *Bactrotheca deleta* is pointed (Novak, 1891).

*Botsfordia*: Pedicle foramen was not necessarily occupied by a pedicle (though it presumably was).

*Clupeafumosus socialis*: A pedicle was presumably present, but only the foramen is preserved.

*Cotyledion tylodes*: The stalk is conceivably homologous with the brachiopod pedicle, but this possibility is impossible to test.

*Craniops*: Attached apically by cementation.

*Cupitheca holocyclus*: Not possible to reconcile with decollation.

*Flustra*: Grows directly onto the substrate.

*Heliomedusa orienta*: “It seems unlikely that *H. orienta* possessed a pedicle that attached it to the soft seafloor, like most other Chengjiang brachiopods.” ...

“The putative pedicle illustrated by Chen *et al.* (2007, Figs 4, 6, 7) in fact is the mold of a three-dimensionally preserved visceral cavity” – Zhang *et al.* (2009).

*Lingulosacculus*: The absence of a pedicle is inferred from the absence of an internal pedicle tube, and the absence of a pedicle at the hinge.

*Loxosomella*: The stalk corresponds to the molluscan foot, rather than a pedicle.

*Mickwitzia muralensis*: An attachment structure is inferred based on the presence of an opening (Balthasar, 2004); this is assumed to have been homologous with the brachiopod pedicle.

*Micrina*: The prominent foramen between artificially articulated valves is taken to imply the presence of a pedicle (Holmer *et al.*, 2008).

*Micromitra*: The presence of a pedicle is indicated by the propensity of *Micromitra* to attach to hard substrates, such as sponge spicules (Holmer and Caron, 2006).

*Namacalathus*: There is no obvious way to homologise the attachment structure with the ventral pedicle of brachiopods.

*Nisusia sulcata*: Has a pedicle, rather than a pedicle sheath as in *Kutorgina* (Holmer *et al.*, 2018a,b).

*Paterimitra*: “*Paterimitra* is interpreted to have attached to hard substrates via a pedicle that emerged through the small posterior opening” – Skovsted *et al.* (2009).

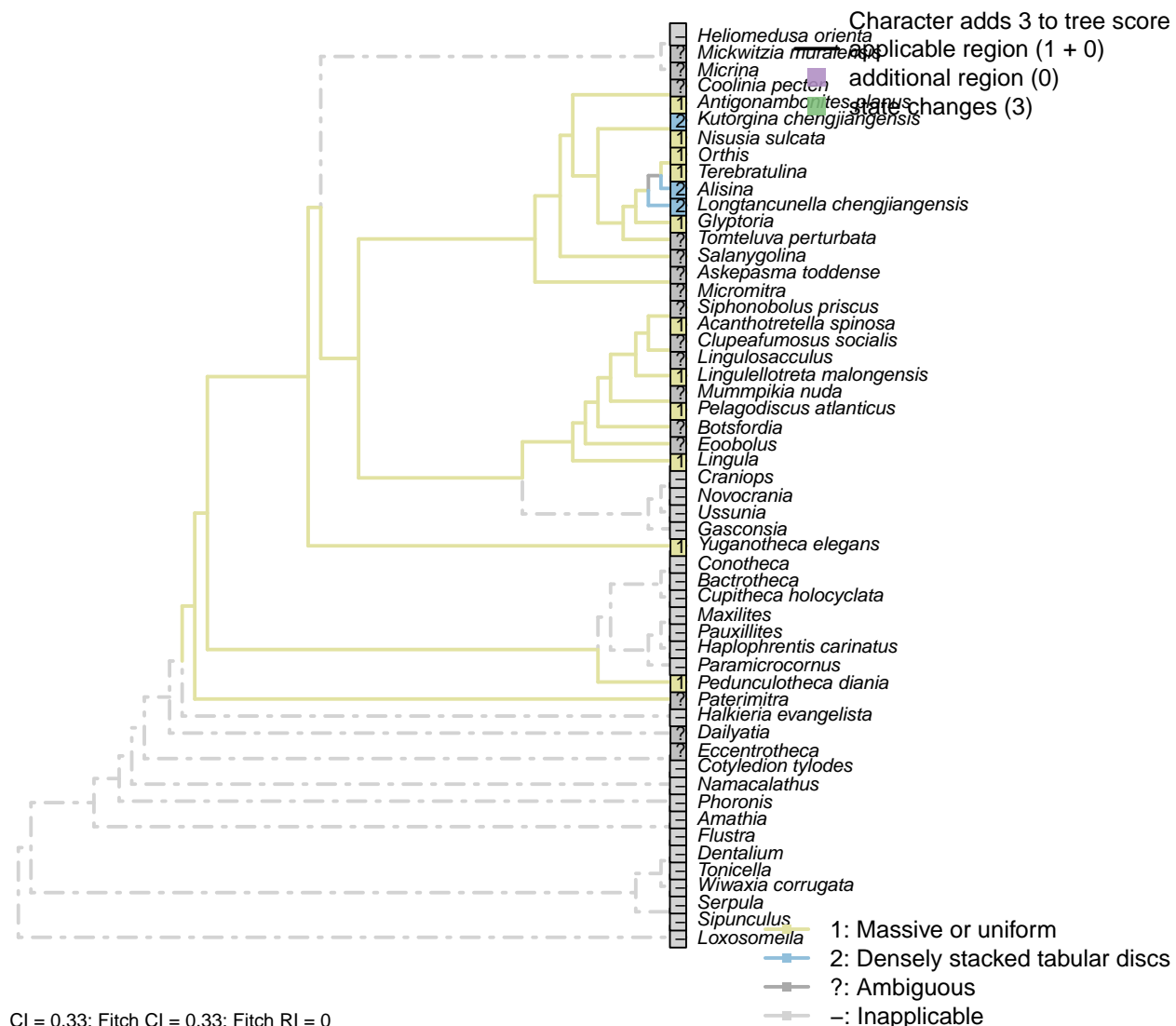
*Pauxillites*: Uncertain: specimens in Valent and Corbacho (2015) do not unambiguously show apical termination.

*Phoronis*: The tube-bearing stalk of phoronids arises as an eversion of the metastomal sac, a markedly different origin from the brachiopod pedicle, which arises from a terminal attachment disc (Young, 2002); the structures are of dubious homology.

*Siphonobolus priscus*: Presumed present, based on ventral foramen with colleplax.

*Sipunculus*: Absent; there is no clear basis to homologise the larval attachment structure of certain sipunculans with a pedicle.

## [27] Constitution



### Character 27: Pedicle: Constitution

- 1: Massive or uniform
  - 2: Densely stacked tabular discs
  - ?: Ambiguous
  - : Inapplicable
- Transformational character.

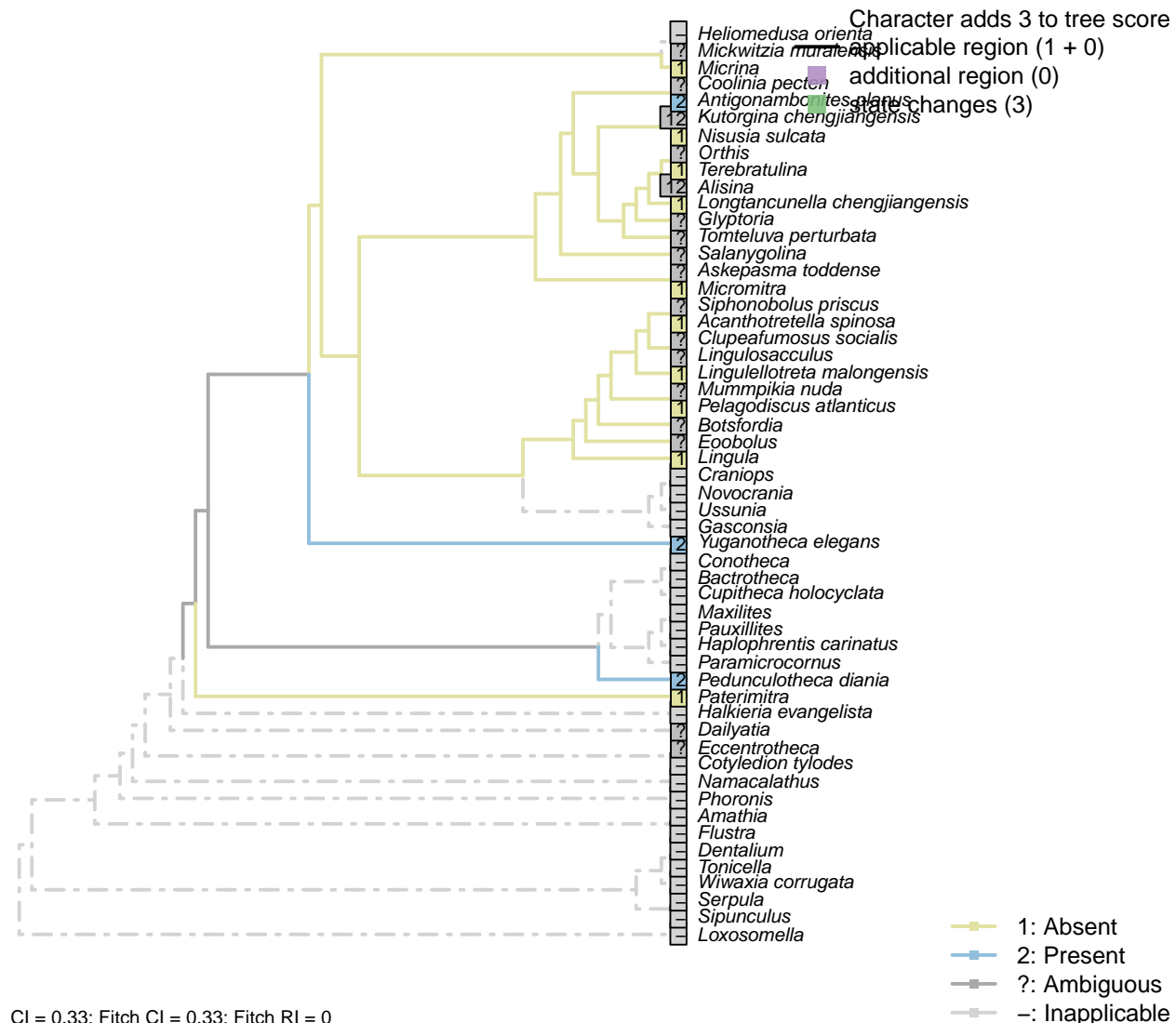
The pedicle of certain chengjiang rhynchonelliforms comprises “densely stacked, three dimensionally preserved, tabular discs” (Holmer et al., 2018a).

This contrasts with the uniform (‘massive’) pedicles of living taxa.

*Antigonambonites planus*: Biomineralized (Holmer et al., 2018a).

*Terebratulina*: Extant rhynchonellid pedicles are massive, consisting of a thick outer chitinous cuticle, a pedicle epithelium, and a core composed of collagen fibres and cartilage-like connective tissue (Holmer et al., 2018a).

## [28] Biomineralization



### Character 28: Pedicle: Biomineralization

1: Absent

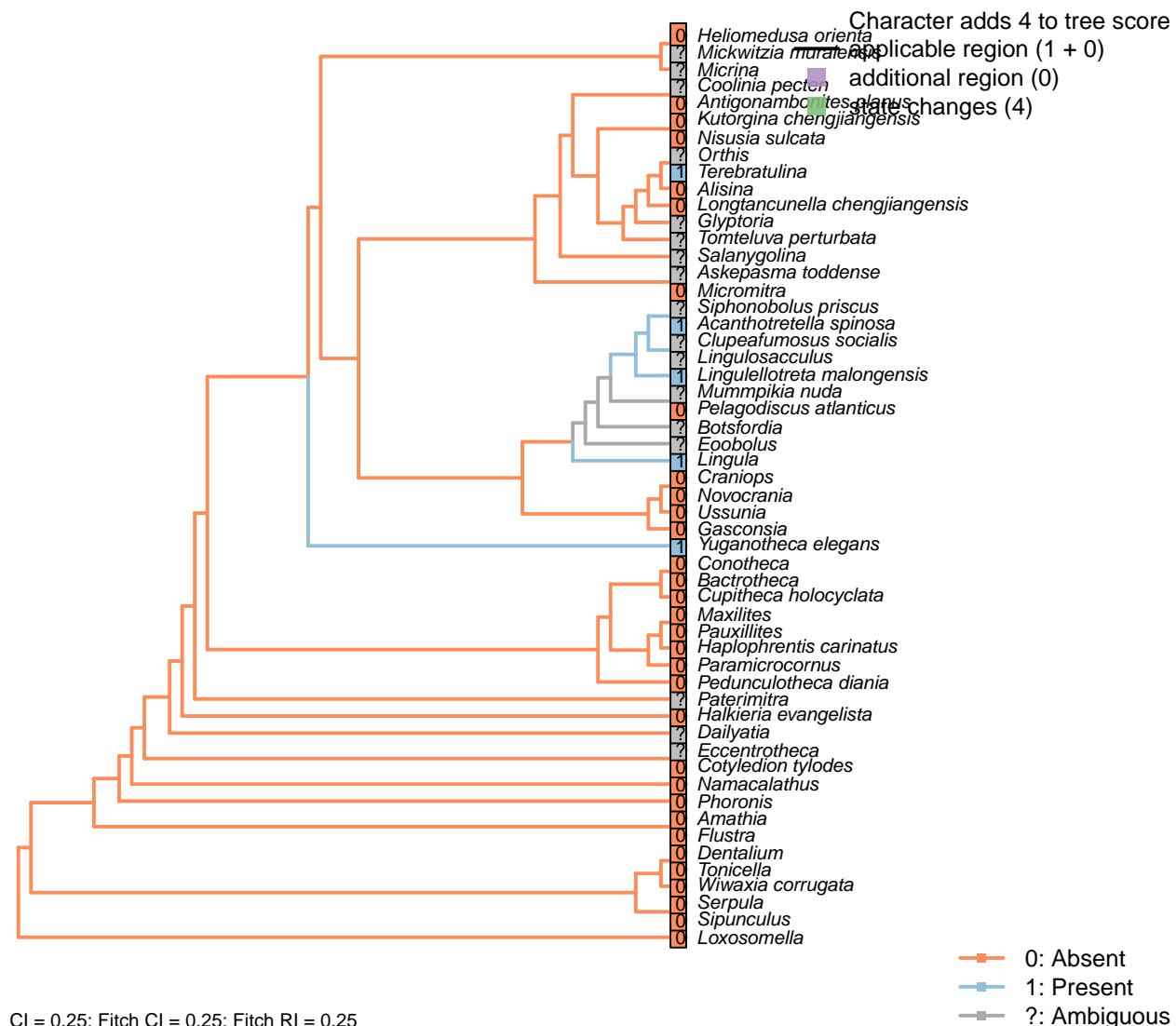
2: Present

Transformational character.

*Kutorgina chengjiangensis*: The tabular discs that make up the pedicle “clearly have a pronounced three-dimensional preservation and may have been partly mineralized.” –Holmer et al. (2018b).

*Micromitra*: A pedicle has not been observed in biomimeticized material (Williams et al., 1998b), indicating an originally non-mineralized constitution.

## [29] Bulb



## Character 29: Pedicle: Bulb

0: Absent

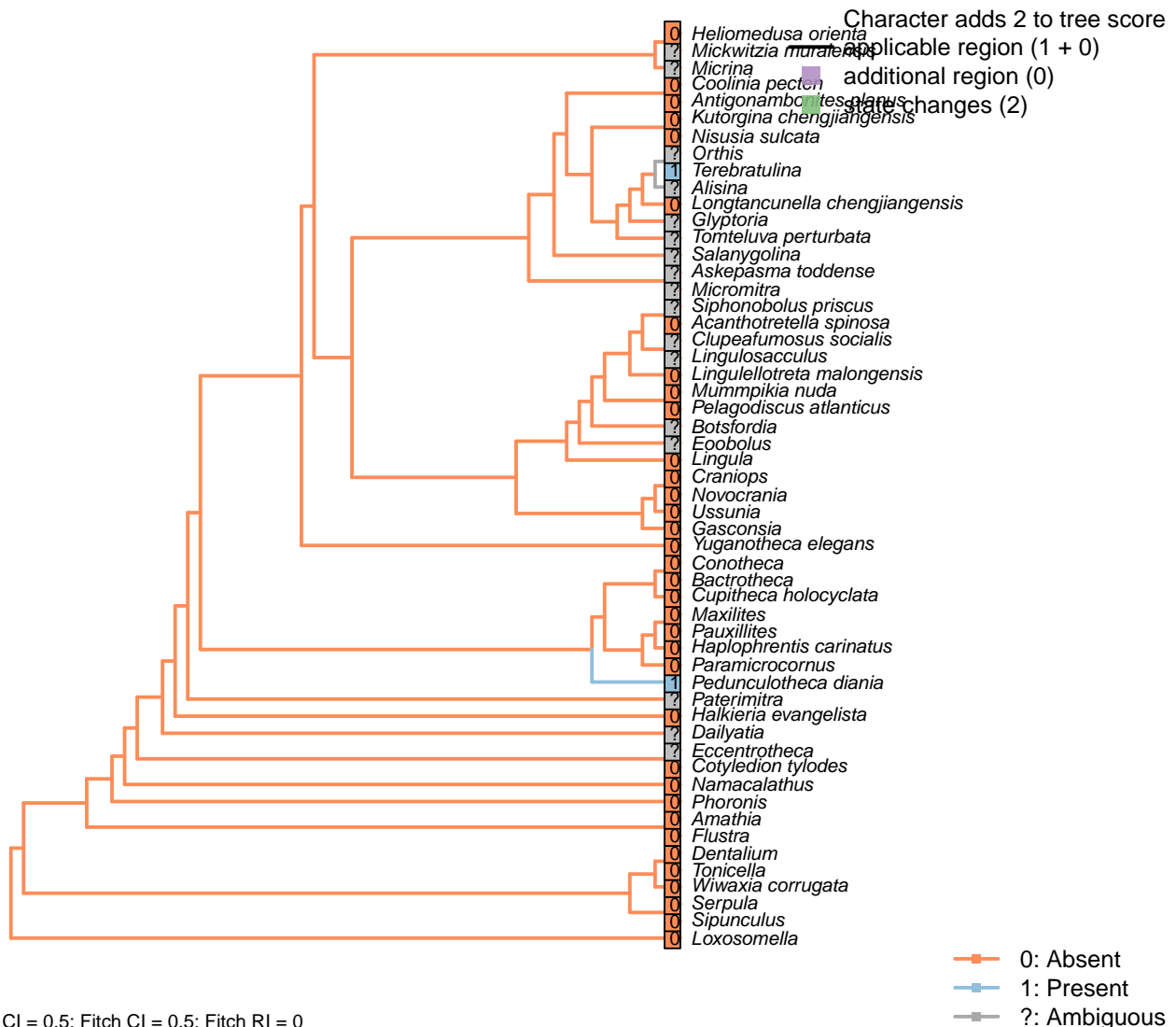
1: Present

Neomorphic character.

A bulb is an expanded region of the distal pedicle, often embedded into the sediment to improve anchorage.

*Acanthotretella spinosa*: Holmer and Caron (2006) interpret the presence of a bulb as tentative; we score it as ambiguous.

### [30] Distal rootlets



#### Character 30: Pedicle: Distal rootlets

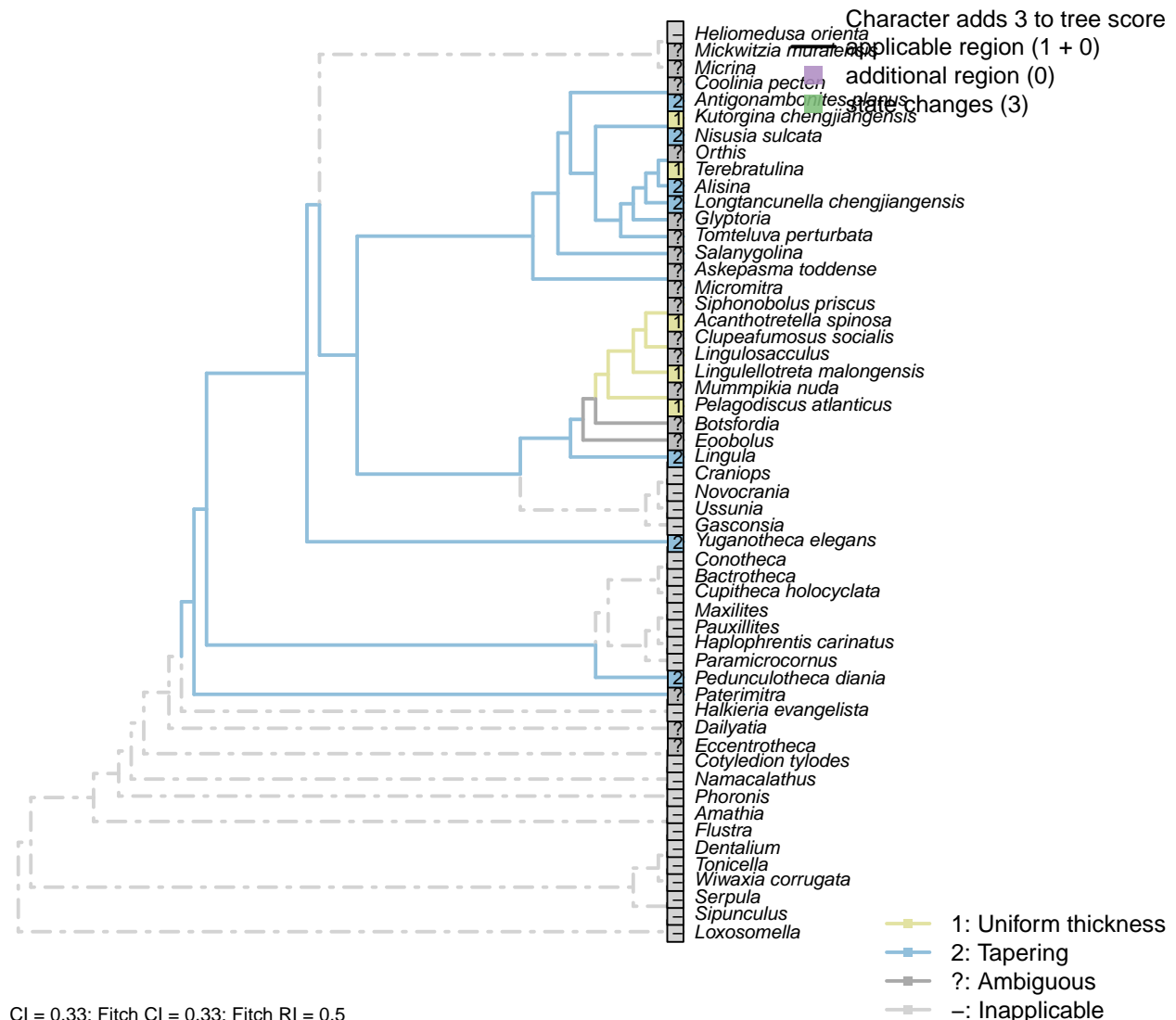
0: Absent

1: Present

Neomorphic character.

Observed in *Pedunculotheca* and *Bethia* (Sutton et al., 2005).

### [31] Tapering



#### Character 31: Pedicle: Tapering

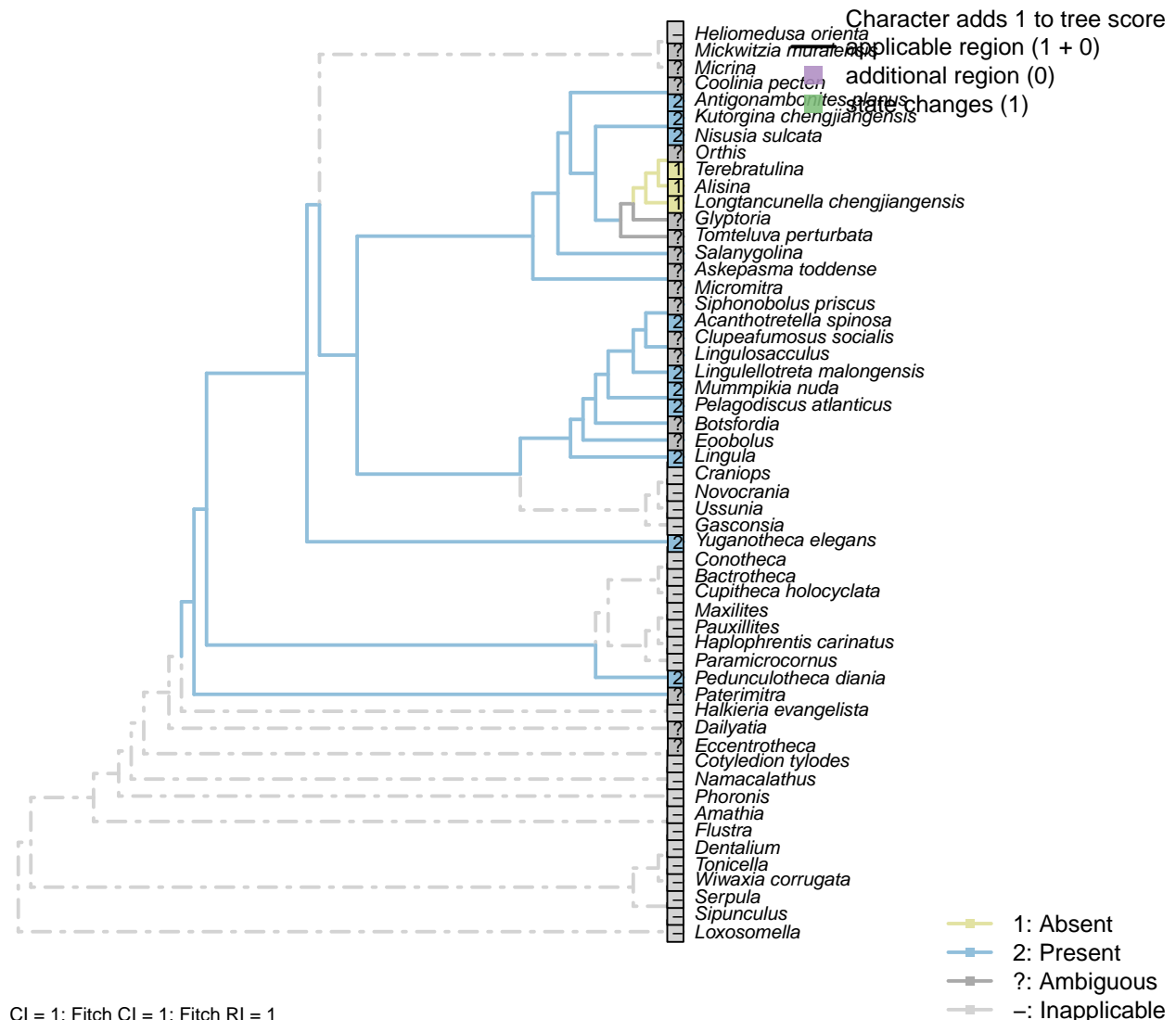
- 1: Uniform thickness
  - 2: Tapering
  - ?: Ambiguous
  - : Inapplicable
- Transformational character.

Holmer *et al.* (2018b) remark that the tapering aspect of the *Nisusia* pedicle recalls that of certain Chengjiang taxa (*Alisina*, *Longtancunella*) whilst distinguishing it from many other taxa (*Eichwaldia*, *Bethia*) in which the pedicle is a constant thickness.

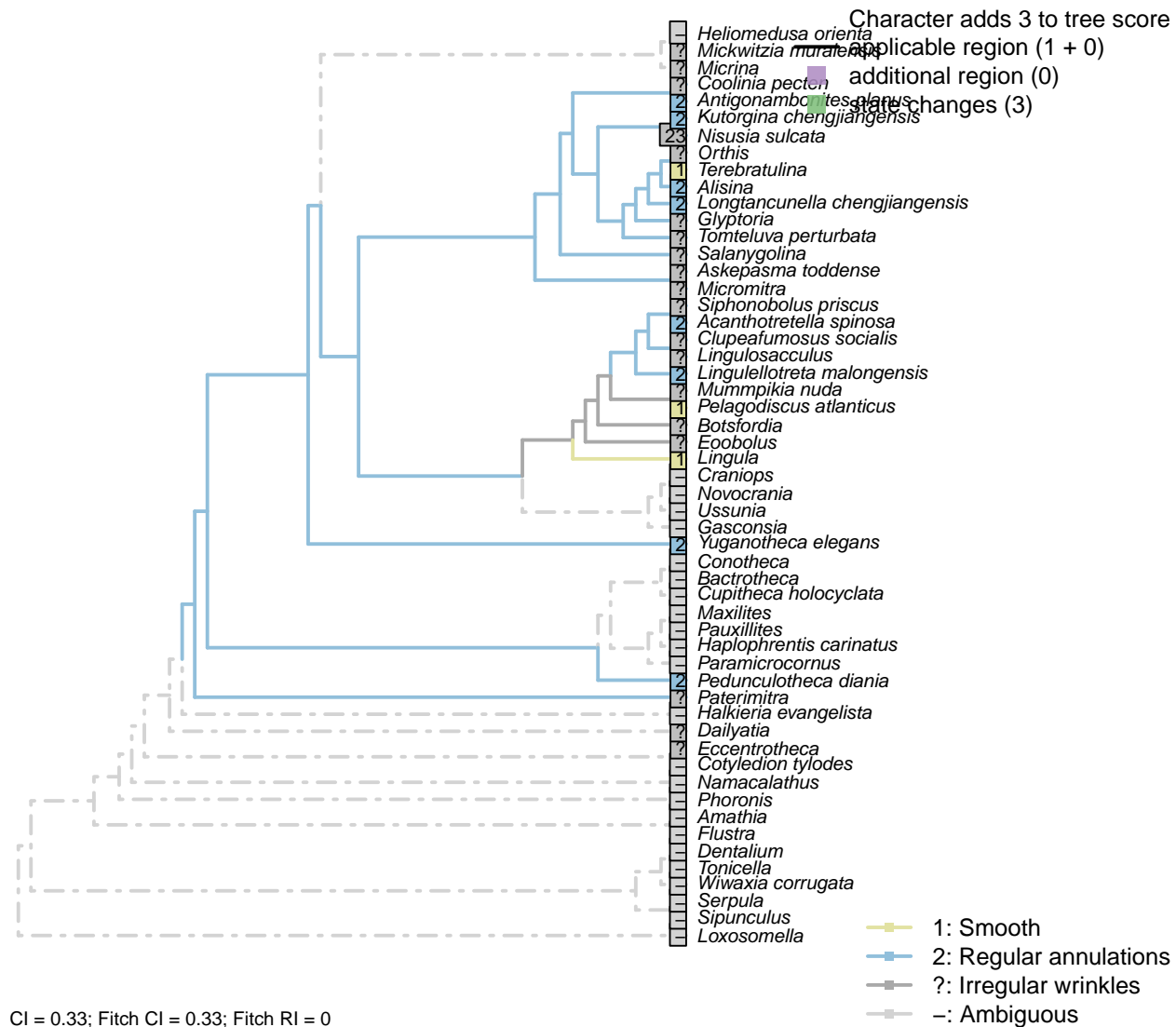
*Antigonambonites planus*: Tapered pedicle sheath with holdfast.

*Pedunculotheca diania*: The pedicle thickness gradually tapers from the apex of the shell to the holdfast.

## [32] Coelomic region



### [33] Surface ornament



is strongly annulated and distally tapering" – Holmer et al. (2018a).

*Kutorgina chengjiangensis*: "Pronounced concentric annular discs disposed at intervals of 0.6–1.0 mm" – Zhang et al. (2007b).

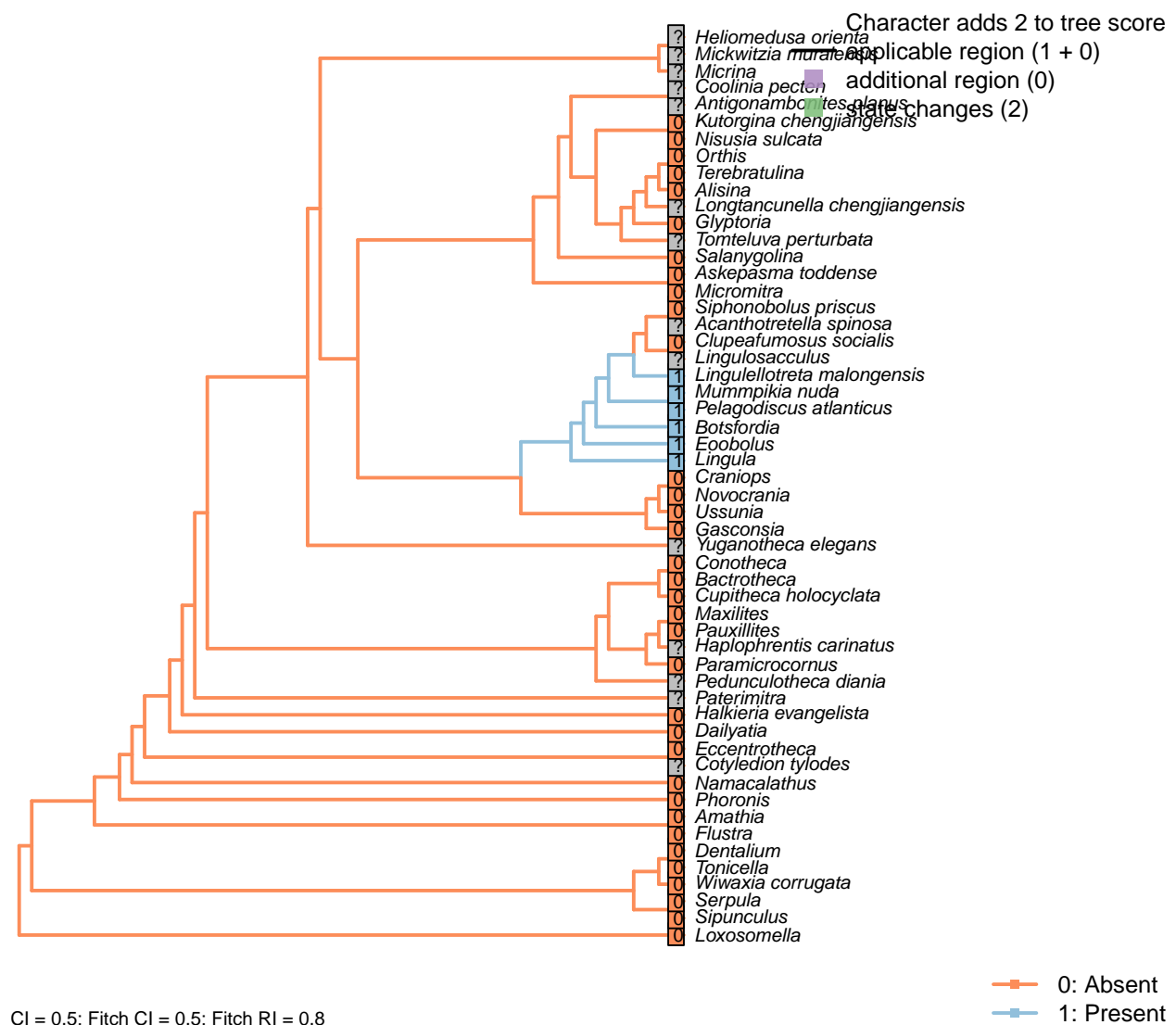
*Lingulellotreta malongensis*: Regularly annotated (see fig. 14.9 in Hou et al., 2017).

*Longtancunella chengjiangensis*: "The preserved pedicle has condensed annulations" – Zhang et al. (2011a).

*Nisusia sulcata*: The "strong annulations" vary significantly in transverse thickness (Holmer et al., 2018a), so it is not clear whether these represent true annulations or wrinkles.

*Yuganotheca elegans*: Annulations present in median collar.

### [34] Nerve impression



CI = 0.5; Fitch CI = 0.5; Fitch RI = 0.8

#### Character 34: Pedicle: Nerve impression

0: Absent

1: Present

Neomorphic character.

In certain taxa the impression of the pedicle nerve is evident in the shell. See character 28 in Williams *et al.* (1998b) appendix 1. Care must be taken not to code an impression as absent when the preservational quality is insufficient to safely infer a genuine absence. Treated as neomorphic as the presence of an innervation is considered a derived state.

*Alisina*: Not described by Williams *et al.* (2000).

*Askepasma toddense*, *Micromitra*, *Glyptoria*, *Kutorgina chengjiangensis*, *Salanygolina*: Following Williams *et al.* (1998b), appendix 2.

*Botsfordia*: Documented by Skovsted *et al.* (2017).

*Clupeafumosus socialis*: Coded as absent in Acrotretidae (Williams *et al.*, 2000, table 6).

*Lingula*: Present in many lingulids (Williams *et al.*, 2000), and coded as present in Lingulidae (Williams *et al.*, 2000, table 6).

*Lingulellotreta malongensis*: Coded as present in Lingulellotretidae (Williams *et al.*, 2000, table 6).

*Mummpikia nuda*: Balthasar (2008, p. 274) identifies a canal as a probable impression of a pedicle nerve.

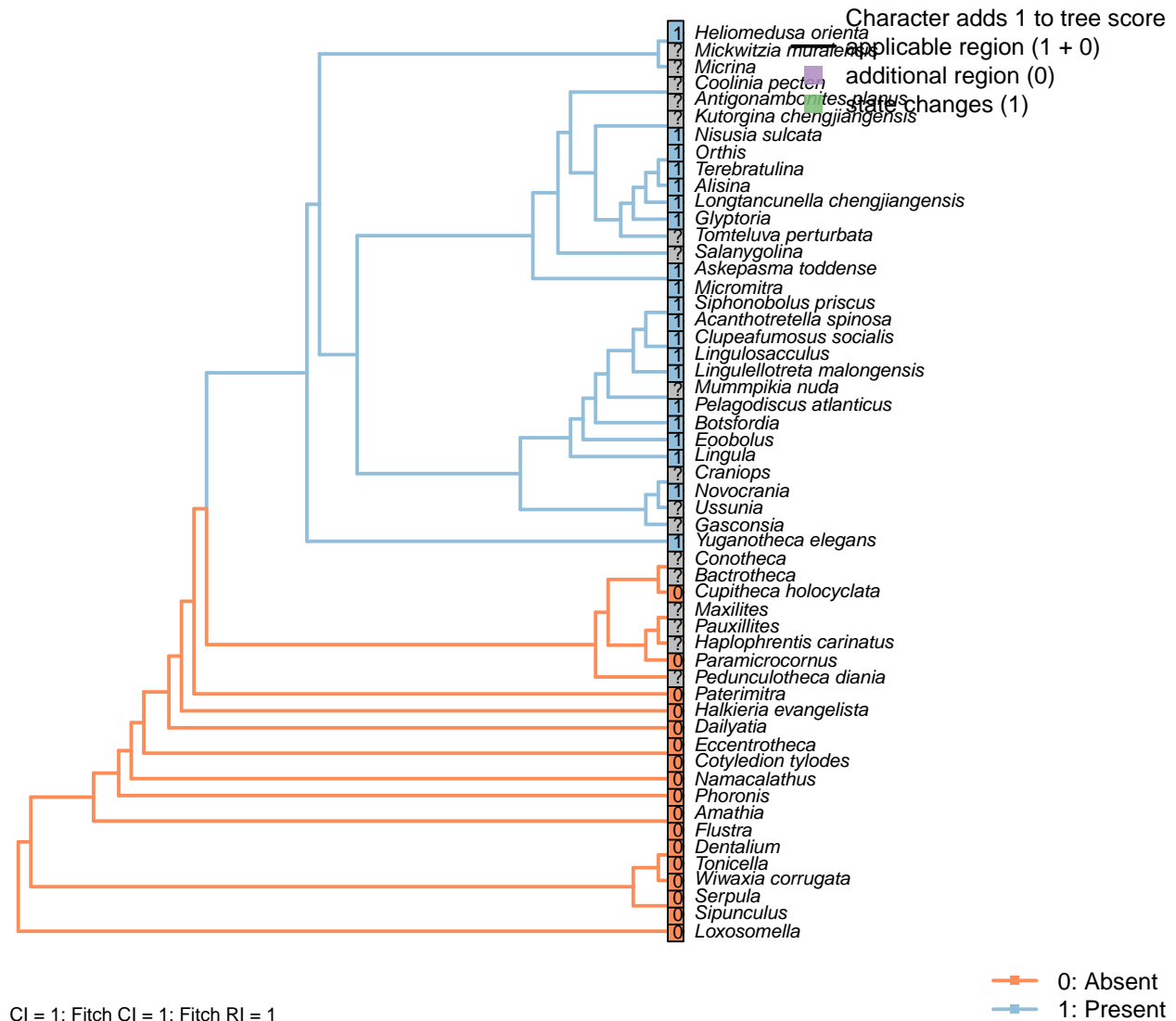
*Nisusia sulcata*, *Orthis*: Not reported in Williams *et al.* (2000).

*Pelagodiscus atlanticus*: Coded as present in Discinidae (Williams *et al.*, 2000, table 6).

*Siphonobolus priscus*: Coded as absent in Siphonotretidae (Williams *et al.*, 2000, table 6).

## 5.6 Mantle canals

### [35] Presence



Whether impressed on a shell or expressed solely in soft tissue.

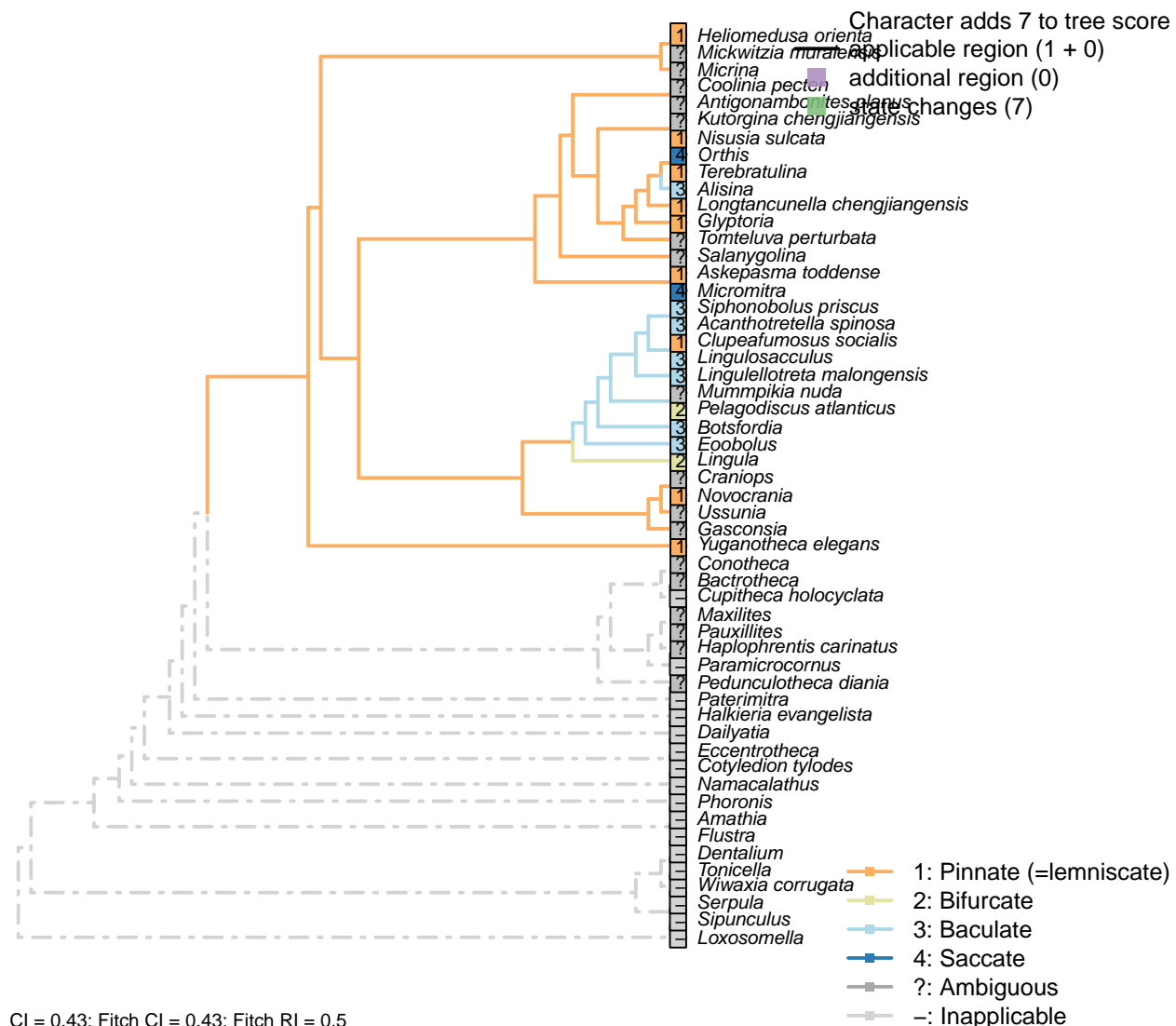
*Cupitheca holocyclus*: Not observed despite excellent preservation.

*Paramicrocornus*: Not impressed on valves, despite fine preservation of muscular attachment (Zhang et al., 2018).

*Paterimitra*: Not evident.

*Ussunia*: Not preserved along muscle scars (Nikitin and Popov, 1984), presumably owing to quality of preservation rather than genuine absence.

## [36] Morphology



### Character 36: Mantle canals: Morphology

1: Pinnate (=lemniscate)

2: Bifurcate

3: Baculate

4: Saccate

Transformational character.

The morphology of dorsal and ventral canals is identical in all included taxa, so is assumed not to be independent – hence the use of a single character (contra Williams et al., 2000).

For a description of terms see Williams et al. (1997, 2000).

Pinnate = “rapidly branch into a number of subequal, radially disposed canals”

Bifurcate = “*vascula lateralia* in both valves divide immediately after leaving the body cavity”

Baculate = “extend forward without any major dichotomy or bifurcation” (Williams et al., 1997, p. 418)

Saccate = “pouchlike sinuses lying wholly posterior to the arcuate *vascula media*” (ibid., p412).

*Acanthotretella spinosa*: Following Table 6, for Siphonotretidae, in Williams *et al.* (2000).

*Alisina, Nisusia sulcata*: Following Table 15 in Williams *et al.* (2000).

*Antigonambonites planus*: Not reported in Treatise (Williams *et al.*, 2000).

*Askepasma toddense*: Described as pinnate (at least in ventral valve) by Williams *et al.* (1998b, p. 250).

*Botsfordia, Eoobolus*: Following Williams *et al.* (1998b), appendix 2, and Williams *et al.* (2000), table 8.

*Clupeafumosus socialis*: Following Table 8 (for Acrotreta) in Williams *et al.* (2000), and the general pinnate condition for acrotretoids stated in Williams *et al.* (1997), p. 420.

*Coolinia pecten*: Not reported in Williams *et al.* (2000).

*Craniops*: Not reported from fossil material.

*Gasconsia*: Williams *et al.* (2000, table 15) appear to use Palaeotrimmerella (as drawn in Williams *et al.*, 1997) as a model for *Gasconsia*, which pre-supposes a close relationship. We are not aware of any report of mantle canals from *Gasconsia* itself.

*Glyptoria*: Following appendix 2 (char. 21) in Williams *et al.* (1998b).

*Heliomedusa orienta*: Described as pinnate by Jin & Wang (1992).

*Novocrania, Kutorgina chengiangensis*: Following table 15 in Williams *et al.* (2000) (for *Neocrania*).

*Lingula, Lingulellotreta malongensis*: Following table 6 in Williams *et al.* (2000).

*Lingulosacculus*: Baculate *vascula media* – Balthasar & Butterfield (2009).

*Longtancunella chengiangensis*: Reported by Zhang *et al.* (2007c, 2011T) though the interpretation is tentative.

*Micromitra*: Described as saccate by Williams *et al.* (1998b).

*Mummpikia nuda*: “Poorly resolved” – Balthasar (2008).

*Orthis*: Sacculate (sometimes digitate in dorsal valve) (Williams *et al.*, 2000, p716).

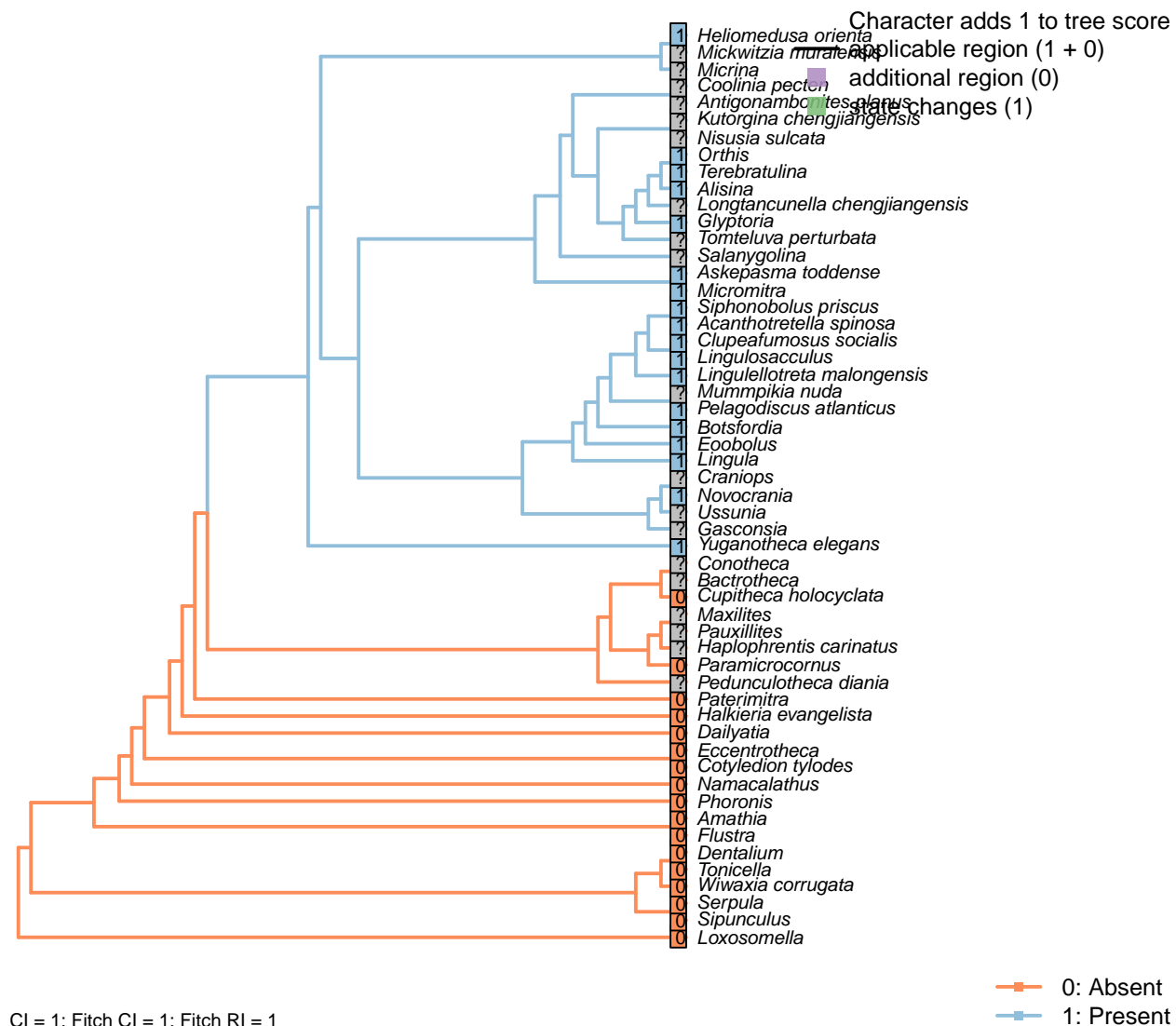
*Pelagodiscus atlanticus*: Following table 6, for Discinidae, in Williams *et al.* (2000).

*Salanygolina*: Coded uncertain in appendix 2 in Williams *et al.* (1998b).

*Siphonobolus priscus*: Interpreted as baculate, following Havlicek (1982).

*Terebratulina*: “In modern terebratulides, the *vascula media* are subordinate to the lemniscate or pinnate *vascula genitalia*” – Williams *et al.* (1997).

*Tomteluva perturbata*: Preservation not adequate to evaluate (Streng *et al.*, 2016).

[37] *vascula lateralia*

CI = 1; Fitch CI = 1; Fitch RI = 1

0: Absent  
1: Present

Character 37: Mantle canals: *vascula lateralia*

0: Absent

1: Present

Neomorphic character.

We treat the *vascula lateralia* as equivalent to the *vascula genitalia* of articulated brachiopods, allowing phylogenetic analysis to test their proposed homology.

Williams *et al.* (1997) write: “The mantle canal system of most of the organophosphate-shelled species consists of a single pair of main trunks in the ventral mantle (*vascula lateralia*) and two pairs in the dorsal mantle, one pair (*vascula lateralia*) occupying a similar position to the single pair in the ventral mantle and a second pair projecting from the body cavity near the midline of the valve. This latter pair may be termed the *vascula media*, but whether they are strictly homologous with the *vascula media* of articulated brachiopods is a matter of opinion. It is also impossible to assert that the *vascula lateralia* are the homologues of the *vascula myaria* or *genitalia* of articulated species, although they are likely to be so as they arise in a comparable position.”

"In inarticulated brachiopods, two main mantle canals (*vascula lateralia*) emerge from the main body cavity through muscular valves and bifurcate distally to produce an increasingly dense array of blindly ending branches near the periphery of the mantle (fig. 71.1–71.2)."

*Acanthotretella spinosa*: Following table 8 (which records presence in Siphonotreta) in Williams *et al.* (2000).

*Alisina, Kutorgina chengjiangensis, Nisusia sulcata*: Following table 15 in Williams *et al.* (2000).

*Askepasma toddense, Micromitra*: "Laurie (1987) has shown that arcuate *vascula media* were present in the mantles of both valves as were pouchlike *vascula genitalia*, especially in the ventral valve" – Williams *et al.* (1997).

*Botsfordia*: Following Popov (1992).

*Clupeafumosus socialis*: Presence indicated in Table 8 (for Acrotreta) in Williams *et al.* (2000).

*Gasconsia*: Williams *et al.* (2000, table 15) appear to use Palaeotrimerella (as drawn in Williams *et al.*, 1997) as a model for *Gasconsia*, which pre-supposes a close relationship. We are not aware of any report of mantle canals from *Gasconsia* itself.

*Heliomedusa orienta*: Present: Williams *et al.* (2000); Jin & Wang (1992).

*Lingulellotreta malongensis*: Present (Williams *et al.*, 2000).

*Longtancunella chengjiangensis*: Presence is possible but requires interpretation that is not unambiguous:

"In the dorsal valve, there can be seen two baculate grooves that arise from the anterior body wall at an antero-lateral position. These two grooves (Figs 4H, 5D) could be taken to represent the *vascula lateralia*" – Zhang *et al.* (2007c).

*Novocrania*: Following table 15 in Williams *et al.* (2000) (for *Neocrania*), who write that "Holocene craniides have only a single pair of main trunks in both valves, corresponding to the *vascula lateralia*". Williams *et al.* (2007) reiterate this position (p. 2875), at least for the ventral valve.

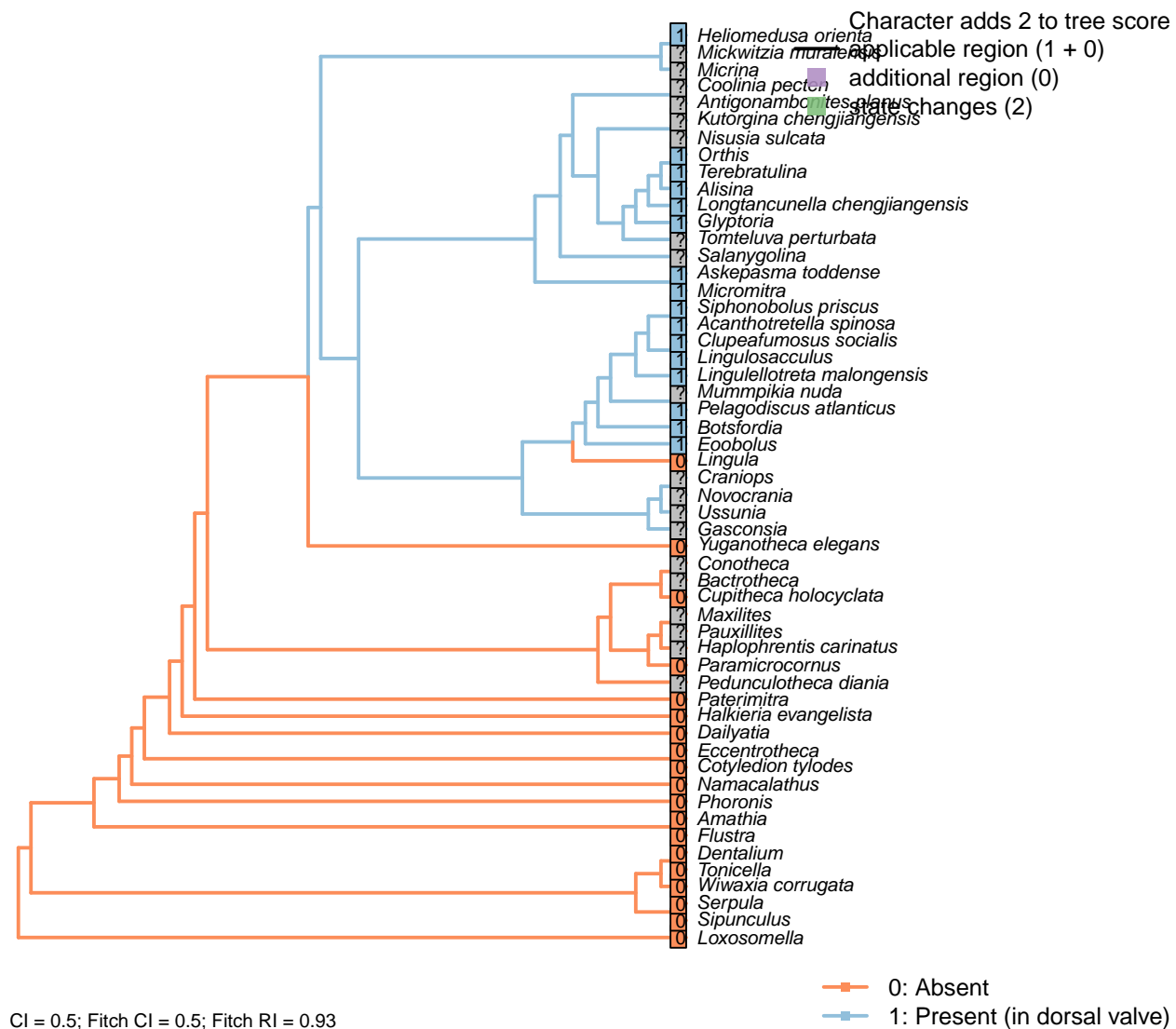
*Terebratulina, Orthis*: = *vascula genitalia*.

*Pelagodiscus atlanticus*: Following *Lochkothele* (Discinidae), Fig. 43.4a in Williams *et al.* (2000).

*Siphonobolus priscus*: Noted in *Siphonobolus* by Williams *et al.* (2000), with reference to Havlicek (1982).

*Tomteluva perturbata*: Preservation not adequate to evaluate (Streng *et al.*, 2016).

*Yuganotheca elegans*: Based on the figures and sketches in Zhang *et al.* (2014) (and supplementary material), the mantle canals are interpreted as lateral, with no clear *vascula media* present.

[38] *vascula media*Character 38: Mantle canals: *vascula media*

0: Absent

1: Present (in dorsal valve)

Neomorphic character.

Williams *et al.* (1997) note that in addition to the *vascula lateralia*, “*Discinisca* has two additional mantle canals emanating from the body cavity into the dorsal mantle (*vascula media*).”

These structures are only evident in the dorsal valve for the included taxa, so only a single character is

necessary.

*Acanthotretella spinosa*: Following table 6 (for Siphonotretidae) in Williams *et al.* (2000).

*Alisina, Kutorgina chengjiangensis, Nisusia sulcata*: Following table 15 in Williams *et al.* (2000).

*Askepasma toddense*: Following table 6 (for Paterinidae) in Williams *et al.* (2000).

*Botsfordia*: Following Popov (1992, fig. 2).

*Clupeafumosus socialis*: Following *Hadrotreta* schematic in Williams *et al.* (2000).

*Eoobolus*: Fig. 5 in Balthasar (2009).

*Gasconsia*: Williams *et al.* (2000, table 15) appear to use *Palaeotrimerella* (as drawn in Williams *et al.*, 1997) as a model for *Gasconsia*, which pre-supposes a close relationship. We are not aware of any report of mantle canals from *Gasconsia* itself.

*Glyptoria*: Present and divergent (Williams *et al.*, 2000).

*Heliomedusa orienta*: Present: Williams *et al.* (2000) p162, Jin & Wang (1992).

*Lingula, Lingulellotreta malongensis*: Following table 6 in Williams *et al.* (2000).

*Longtancunella chengjiangensis*: Reported by Zhang *et al.* (2007c) though the interpretation is tentative.

*Micromitra*: Reported by Williams *et al.* (1998b).

*Novocrania*: Williams *et al.* (2000) write “Holocene craniides have only a single pair of main trunks in both valves, corresponding to the *vascula lateralia*” – an observation reflected in their table 15 (for *Neocrania*). But in contrast, Williams *et al.* (2007), p. 2875, identify the dorsal valve’s canals as a *vascula media* in living craniids (though both are *lateralia* in Ordovician craniides). This character is therefore coded as ambiguous.

*Orthis*: From idealised morphology in Williams *et al.* (2000).

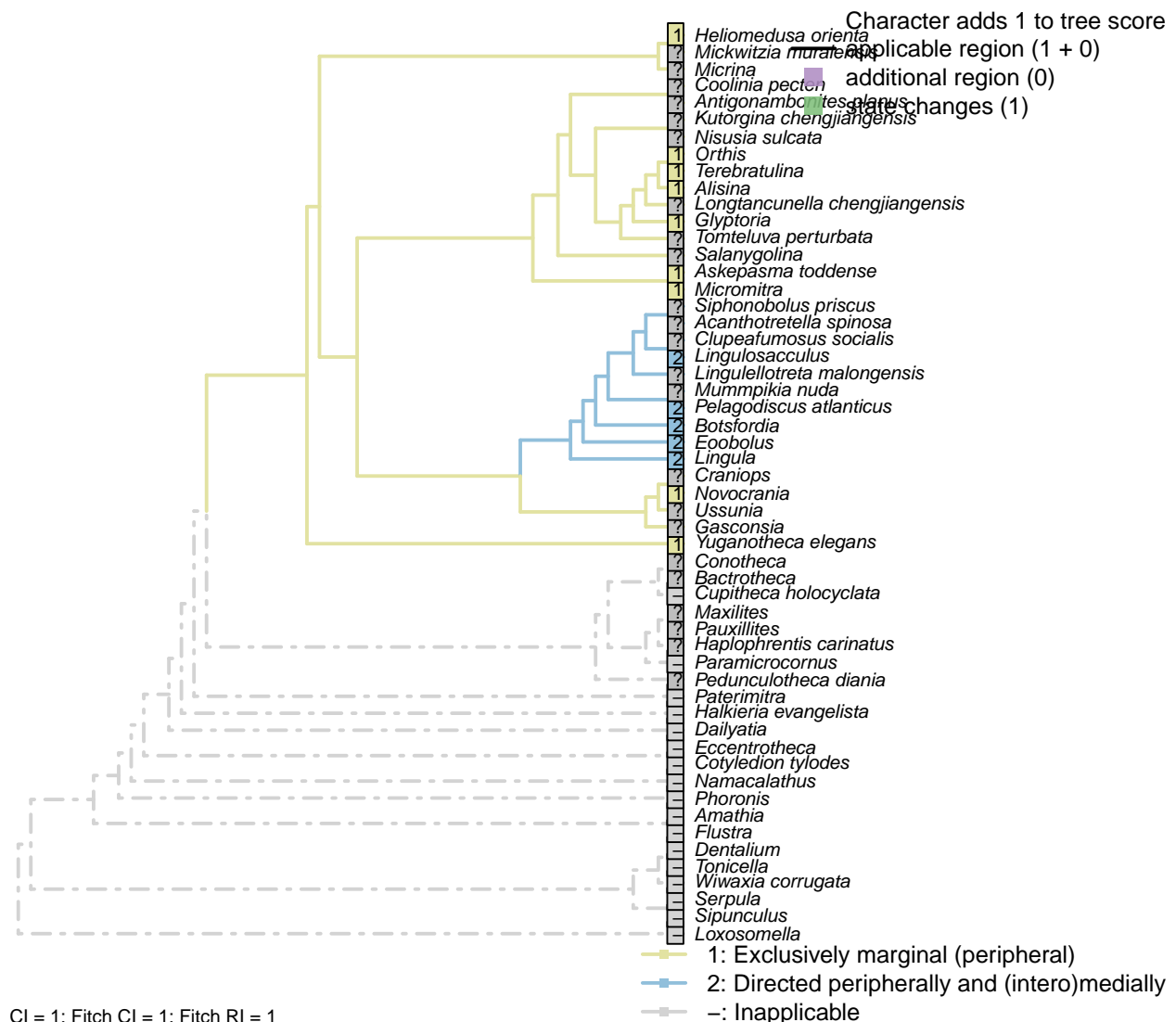
*Pelagodiscus atlanticus*: Following table 6 (for Discinidae) in Williams *et al.* (2000).

*Siphonobolus priscus*: Noted in *Siphonobolus* by Havlicek (1982).

*Terebratulina*: “In modern terebratulides, the *vascula media* are subordinate to the lemniscate or pinnate *vascula genitalia*” – Williams *et al.* (1997) p417.

*Tomteluva perturbata*: Preservation not adequate to evaluate (Streng *et al.*, 2016).

*Yuganotheca elegans*: Based on the figures and sketches in Zhang *et al.* (2014) (and supplementary material), the mantle canals are interpreted as lateral, with no clear *vascula media* present.

[39] *vascula terminalia***Character 39: Mantle canals: *vascula terminalia***

- 1: Exclusively marginal (peripheral)
- 2: Directed peripherally and (intero)medially
- Transformational character.

Presumed to be connected with setal follicles in life (Williams et al., 1998b). See Williams *et al.* (2000) for

discussion.

*Acanthotretella spinosa*: Preservation not clear enough to score with certainty (Holmer and Caron, 2006).

*Alisina*: Interomedial *vascula terminalia* not reported by Williams *et al.* (2000).

*Askepasma toddense, Micromitra*: Peripheral only (Williams *et al.*, 1998b, 2000).

*Botsfordia, Eoobolus*: Following Williams *et al.* (1998b), appendix 2.

*Glyptoria*: Following appendix 2 in Williams *et al.* (1998b).

*Heliomedusa orienta*: Inferred from Jin & Wang (1992).

*Kutorgina chengjiangensis, Salanygolina*: Coded uncertain in appendix 2 in Williams *et al.* (1998b).

*Lingula*: Peripheral and medial for all Lingulata (Williams *et al.*, 2000).

*Lingulellotreta malongensis*: Not described in Williams *et al.* (2000).

*Lingulosacculus*: Strong indication of medially directed *vascula terminalia* from *vascula lateralia*; see fig. 1.A1 in Balthasar and Butterfield (2009).

*Novocrania*: Peripheral only (Williams *et al.*, 2000, p.158).

*Orthis*: See schematics in Williams *et al.* (2000).

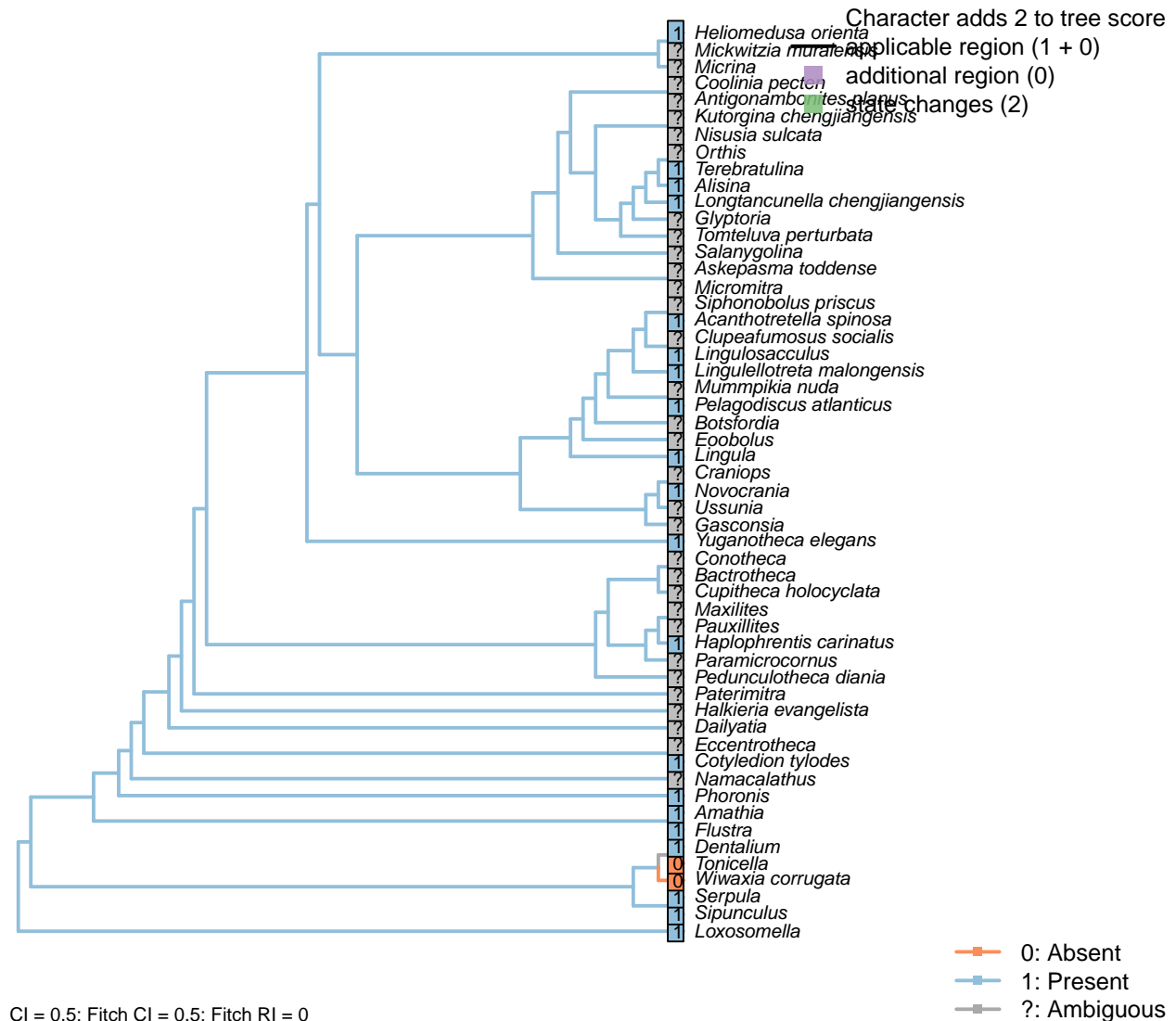
*Pelagodiscus atlanticus*: Following *Lochkothele* (Discinidae), fig. 43.4a in Williams *et al.* (2000).

*Siphonobolus priscus*: Not reported in Havlicek (1982) or Williams *et al.* (2000).

*Terebratulina*: Following idealised plectolophous terebratulid of Emig (1992).

## 5.7 Perioral tentacular apparatus

[40] Presence



The lophophore is a ring of tentacles that surrounds the mouth. Temereva (2017) suggests that true lophophores must also encompass the anus, which excludes the tentacular apparatus of entoprocts from the definition; as homology between the tentacular apparatuses of entoprocts and other lophophorates has often been assumed, we prefer to take a more inclusive stance and code the structures as potentially homologous.

It is unlikely that the tentacles of annelids and sipunculans correspond to the lophophore, yet homology is not inconceivable. In order that the tentacular apparatus of *Haplophrentis* can be compared with both organs without prejudice, we capture the presence of a tentacular apparatus in this very broad character,

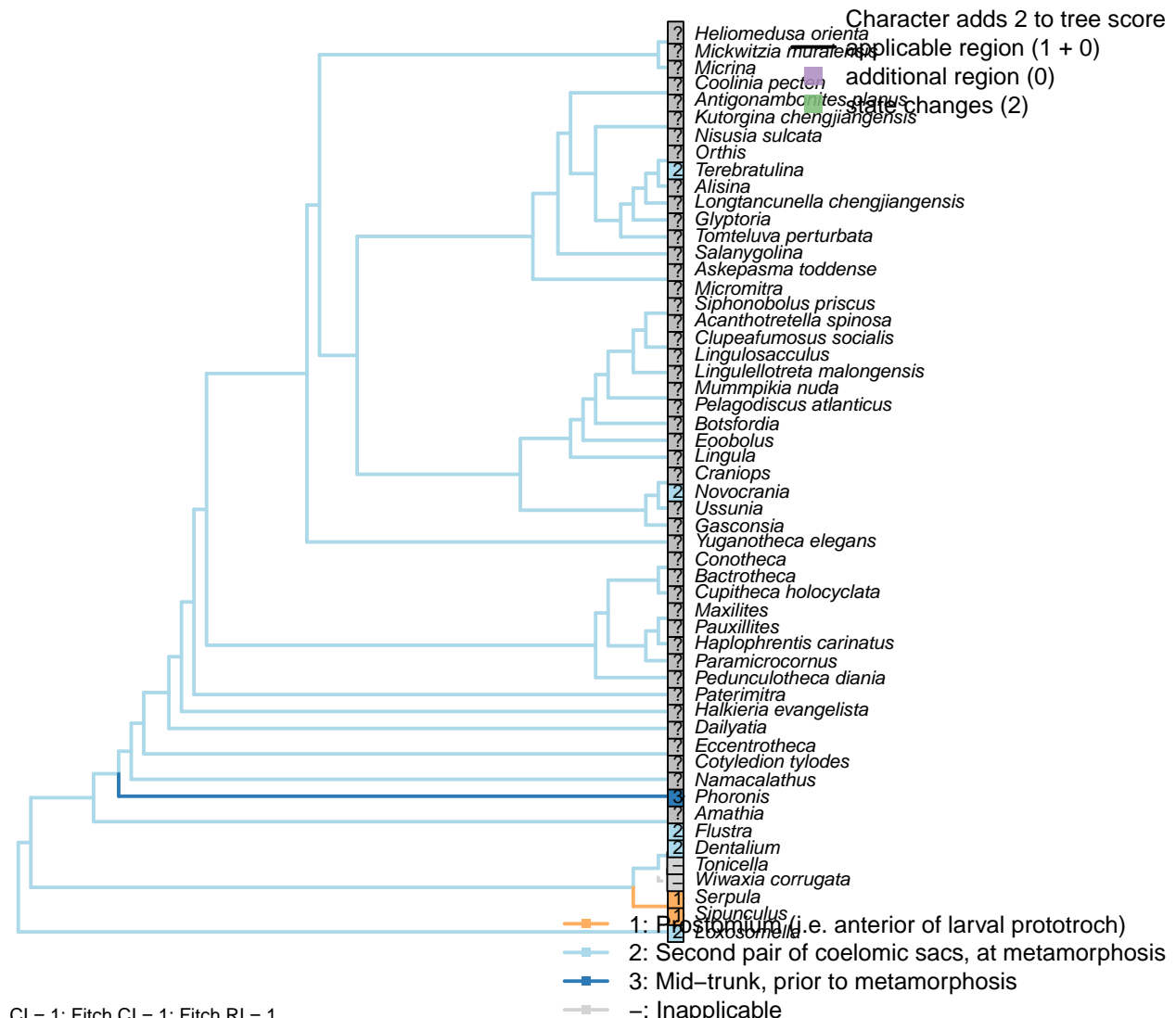
with arguments against homology reflected in separate transformation series.

*Cotyledion tylodes*: The tentacular crown (Zhang et al., 2013) is interpreted as a lophophore.

*Dentalium*: The scaphopod captacula is conceivably equivalent to the tentacular apparatus of other lophotrochozoans. It is developmentally pre-oral, and has tentatively been homologised with the pre-oral tentacles of Monoplacophora and Gastropoda (Steiner, 1992), though their musculature and late development suggests instead that they may derive from the molluscan foot, as do the arms of cephalopods (Wanninger and Haszprunar, 2002b).

*Haplophrentis carinatus*: Moysiuk et al. (2017).

## [41] Origin



### Character 41: Perioral tentacular apparatus: Origin

- 1: Prostomium (i.e. anterior of larval prototroch)
  - 2: Second pair of coelomic sacs, at metamorphosis
  - 3: Mid-trunk, prior to metamorphosis
- Transformational character.

The tentacles of annelids and sipunculans originate from a dorsal pair of buds on the prostomium (Adrianov et al., 2006), whereas the brachiopod lophophore arises from the second pair of coelomic sacs (Nielsen, 1991).

*Dentalium*: The captacula arise close to the mouth after metamorphosis (Wanninger and Haszprunar, 2002b), in a position not dissimilar from that of the phoronid tentacles (Santagata, 2004).

*Flustra*: The tentacles appear at metamorphosis, seemingly from below the corona (=prototroch) (Young, 2002).

*Loxosomella*: Arising after metamorphosis (Nielsen, 1971).

*Novocrania*: “At metamorphosis [...] the second pair of coelomic sacs develop small attachment areas at the edge of the dorsal valve and become the lophophore coelom” (Nielsen, 1991)

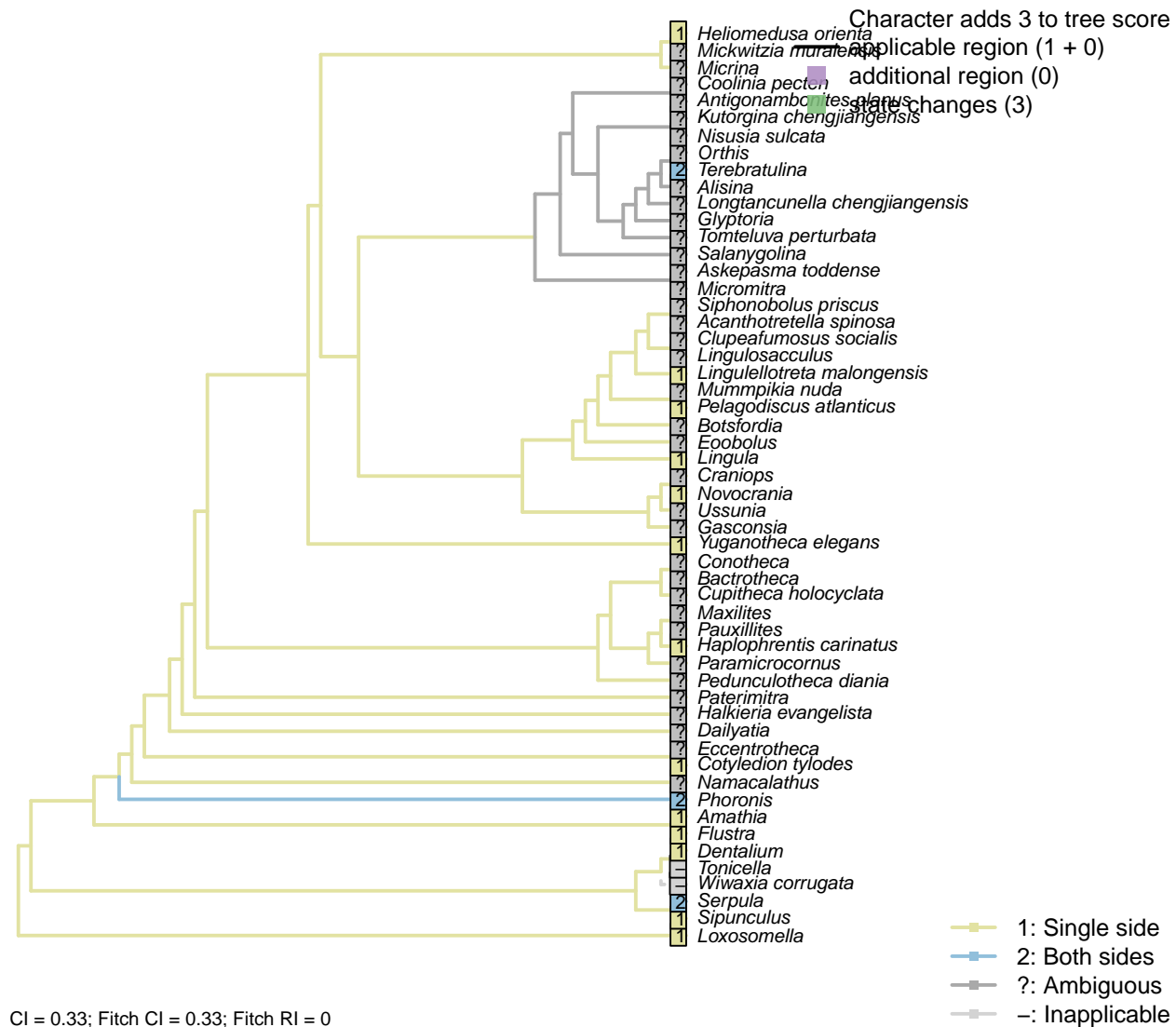
“The larval lobes are retained during the first steps of metamorphosis and are subsequently remodeled to form the lophophore and other adult organs” – Altenburger et al. (2013).

*Phoronis*: At the posterior of the head, at the late larval stage (Santagata, 2004).

*Sipunculus*: (Adrianov et al., 2006).

*Terebratulina*: Lophophore of *Terebratalia* arises post metamorphosis (Young, 2002); lophophore conceivably arising from vesicular bodies at base of apical lobe?.

## [42] Tentacle disposition



Tentacles may occur along one or both sides of the axis of the lophophore arm (Carlson, 1995).

*Acanthotretella spinosa*: Preservation insufficient to evaluate (Holmer and Caron, 2006).

*Alisina*, *Lingulosacculus*, *Longtancunella chengjiangensis*: Preservation inadequate.

*Amathia*: Single side (Temereva and Kosevich, 2016).

*Cotyledion tylodes*: Tentacles seemingly occupy a single side of the lophophore (Zhang et al., 2013).

*Dentalium*: On rim of basal lobe only (Morton, 1959).

*Flustra*: Both sides (Schwaha and Wanninger, 2015; Shunkina et al., 2015).

*Heliomedusa orienta*: “Each lophophoral arm bears a row of long, slender flexible tentacles” – Zhang et al.

(2009).

*Kutorgina chengjiangensis*: Tentacles “cannot be confidently demonstrated in the available specimens.” – Zhang et al. (2007b).

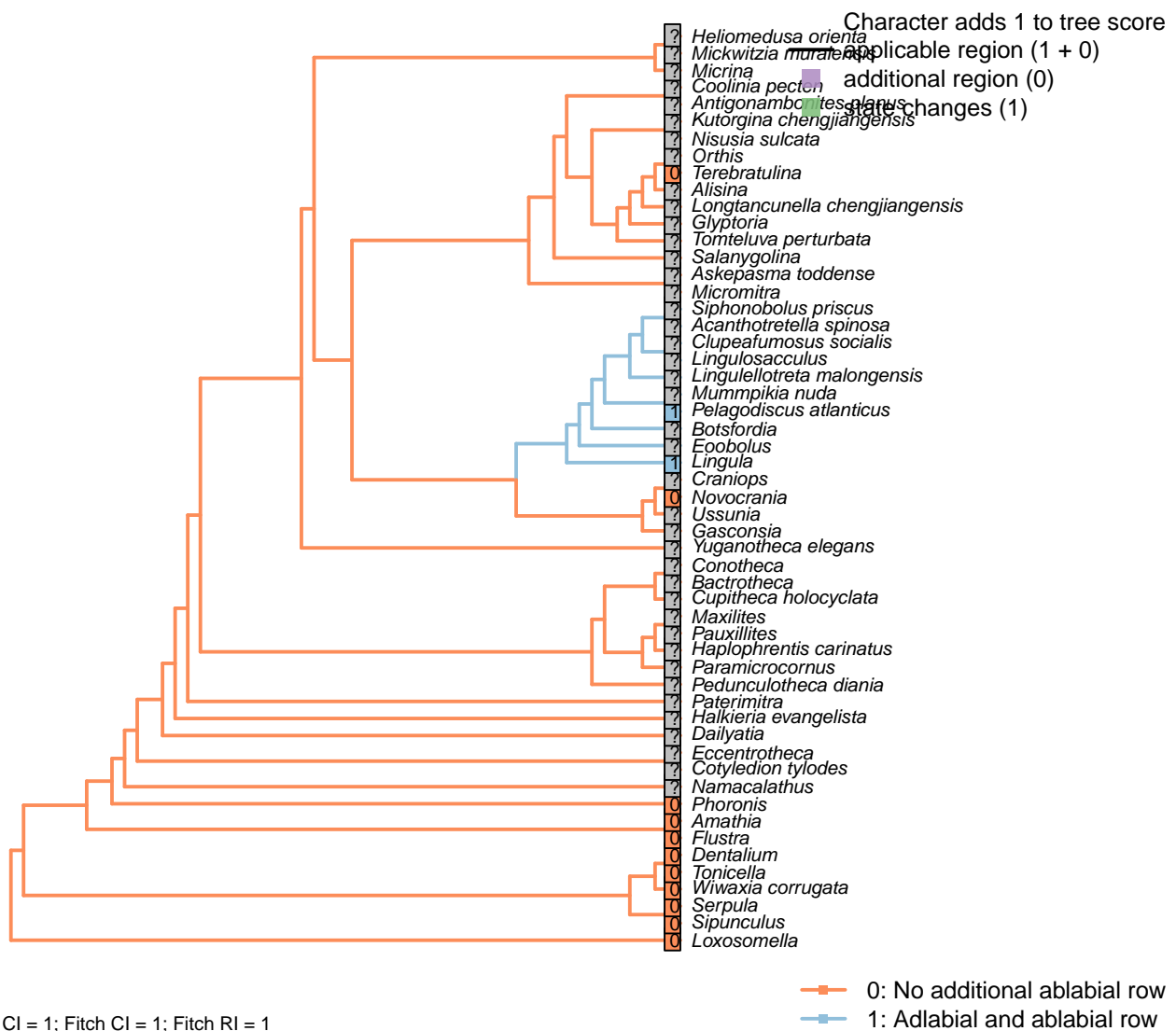
*Novocrania*, *Pelagodiscus atlanticus*, *Lingula*, *Terebratulina*, *Phoronis*: Following coding for higher group in Carlson (1995), appendix 1, character 36.

*Lingulellotreta malongensis*: “The tentacles are clearly visible, and closely arranged in a single palisade” – Zhang et al. (2004).

*Loxosomella*: Single side (Nielsen, 1966).

*Sipunculus*: Both sides in tentacle-breathers such as *Themiste* (Ruppert and Rice, 1995; Adrianov et al., 2006); only one side in *Sipunculus* (Ruppert and Rice, 1995; Adrianov et al., 2006).

#### [43] Tentacle rows per side in trocholophic stage



**Character 43: Perioral tentacular apparatus: Tentacle rows per side in trocholophic stage**

- 0: No additional ablabial row  
 1: Adlabial and ablabial row  
 Neomorphic character.

After Carlson (1995), character 37. Lophophore tentacles are commonly arranged into an ablabial and adlabial row, with ablabial tentacles sometimes added later in development.

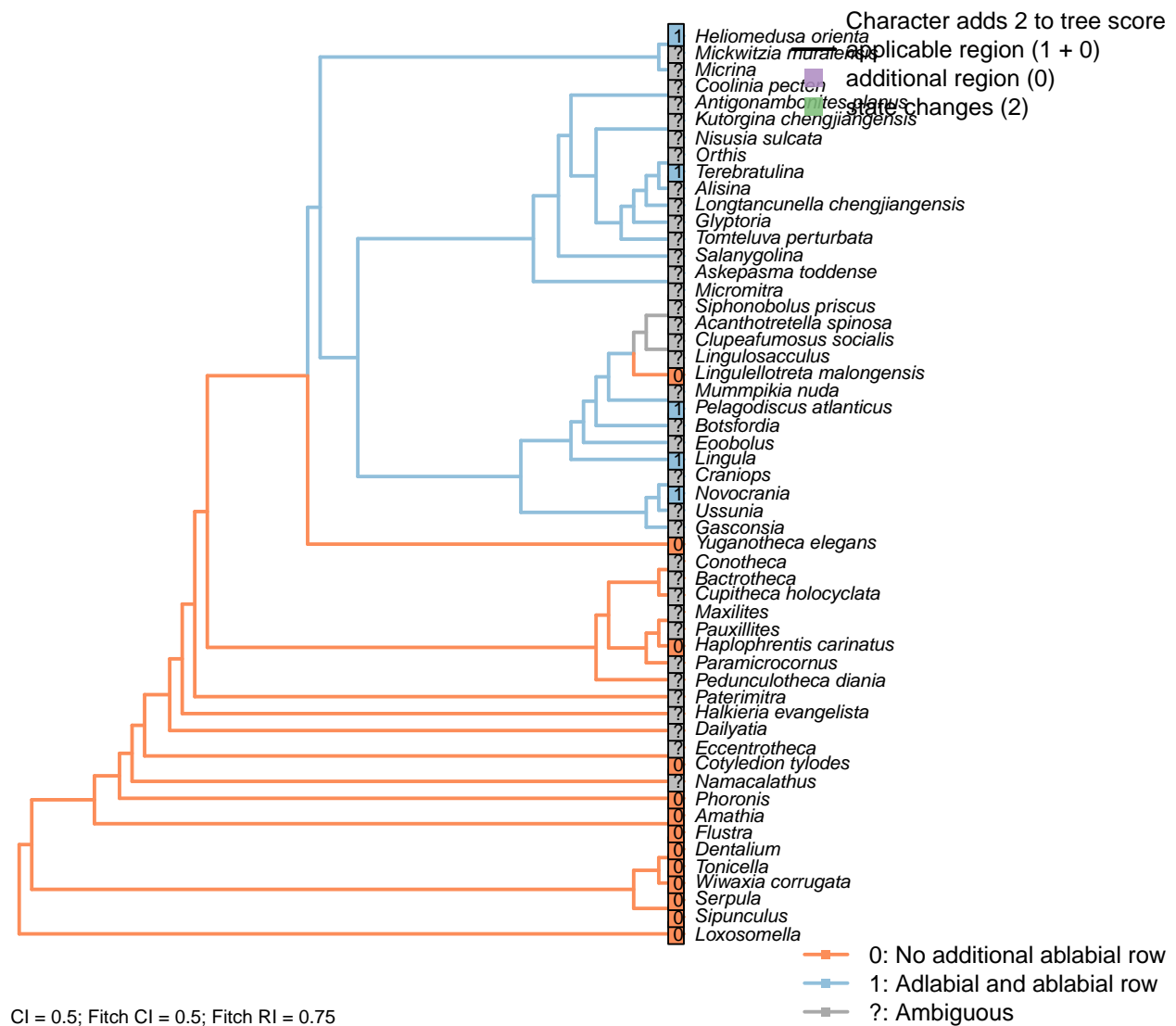
*Amathia*: (Temereva and Kosevich, 2016).

*Loxosomella*, *Flustra*: Inapplicable.

*Pelagodiscus atlanticus*, *Lingula*, *Terebratulina*, *Phoronis*: Following coding for higher taxon in Carlson (1995), appendix 1, character 37.

*Novocrania*: Following coding for higher taxon in Carlson (1995), appendix 1, character 37. Also states in Williams et al. (2000), p. 158.

#### [44] Tentacle rows per side in post-trocholophe stage



**Character 44: Perioral tentacular apparatus: Tentacle rows per side in post-trocholophe stage**

- 0: No additional ablabial row  
1: Adlabial and ablabial row  
Neomorphic character.

After Carlson (1995), character 37. Lophophore tentacles are commonly arranged into an ablabial and adlabial row, with ablabial tentacles sometimes added later in development (and thus interpreted as a neomorphic addition).

*Acanthotretella spinosa*: Preservation insufficient to evaluate (Holmer and Caron, 2006).

*Amathia*: (Temereva and Kosevich, 2016).

*Cotyledion tylodes*: Additional row not evident (Zhang et al., 2013).

*Helio medusa orienta*: “The lophophoral arms bear laterofrontal tentacles with a double row of cilia along their lateral edge, as in extant lingulid brachiopods” – Zhang et al. (2009).

*Kutorgina chengjiangensis*: Tentacles “cannot be confidently demonstrated in the available specimens.” – Zhang et al. (2007b).

*Novocrania*, *Pelagodiscus atlanticus*, *Lingula*, *Terebratulina*, *Phoronis*: Following coding for higher taxon in Carlson (1995), appendix 1, character 37.

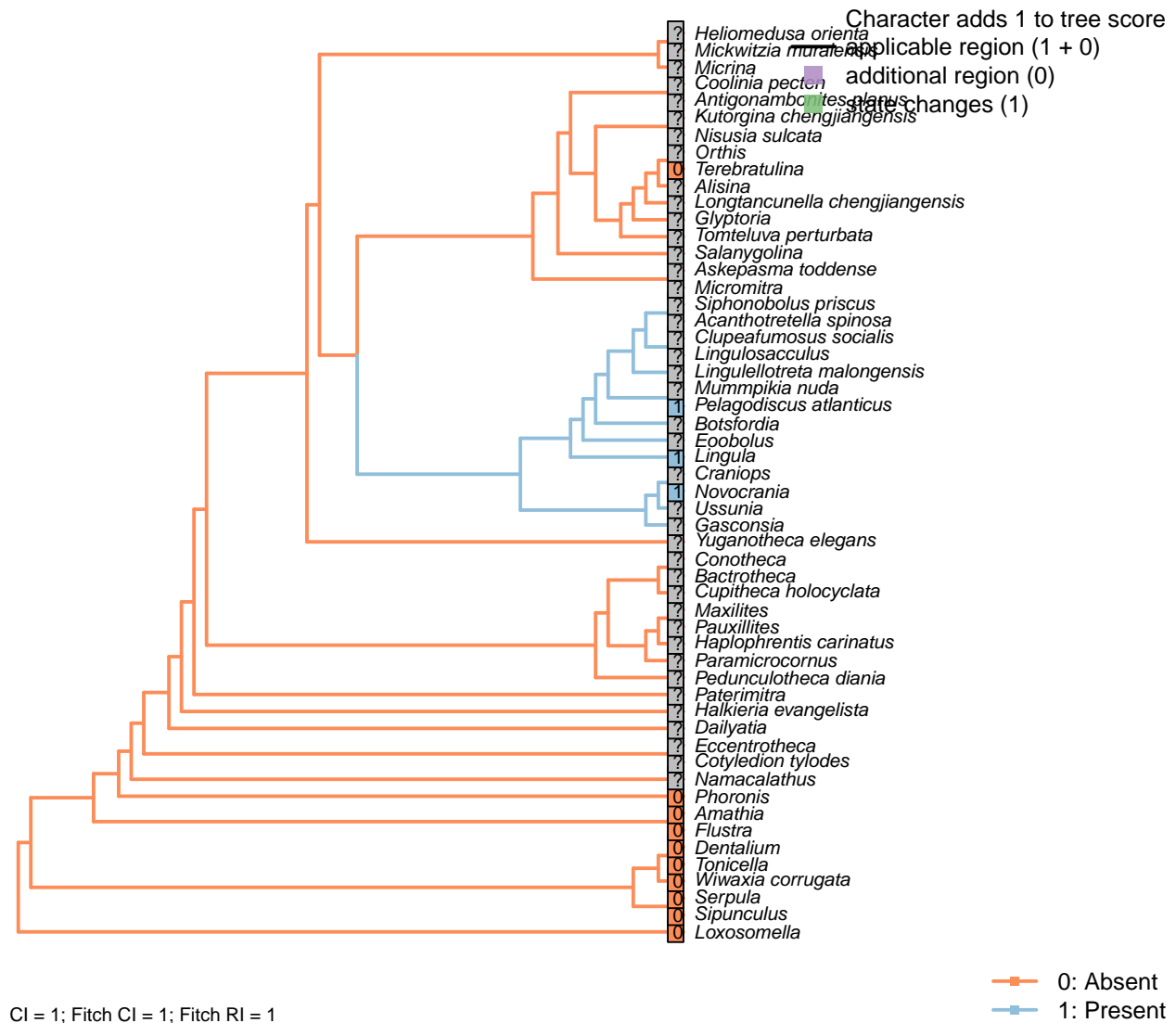
*Lingulellotreta malongensis*: Single palisade (Zhang et al., 2004).

*Lingulosacculus*: Preservation insufficient to evaluate.

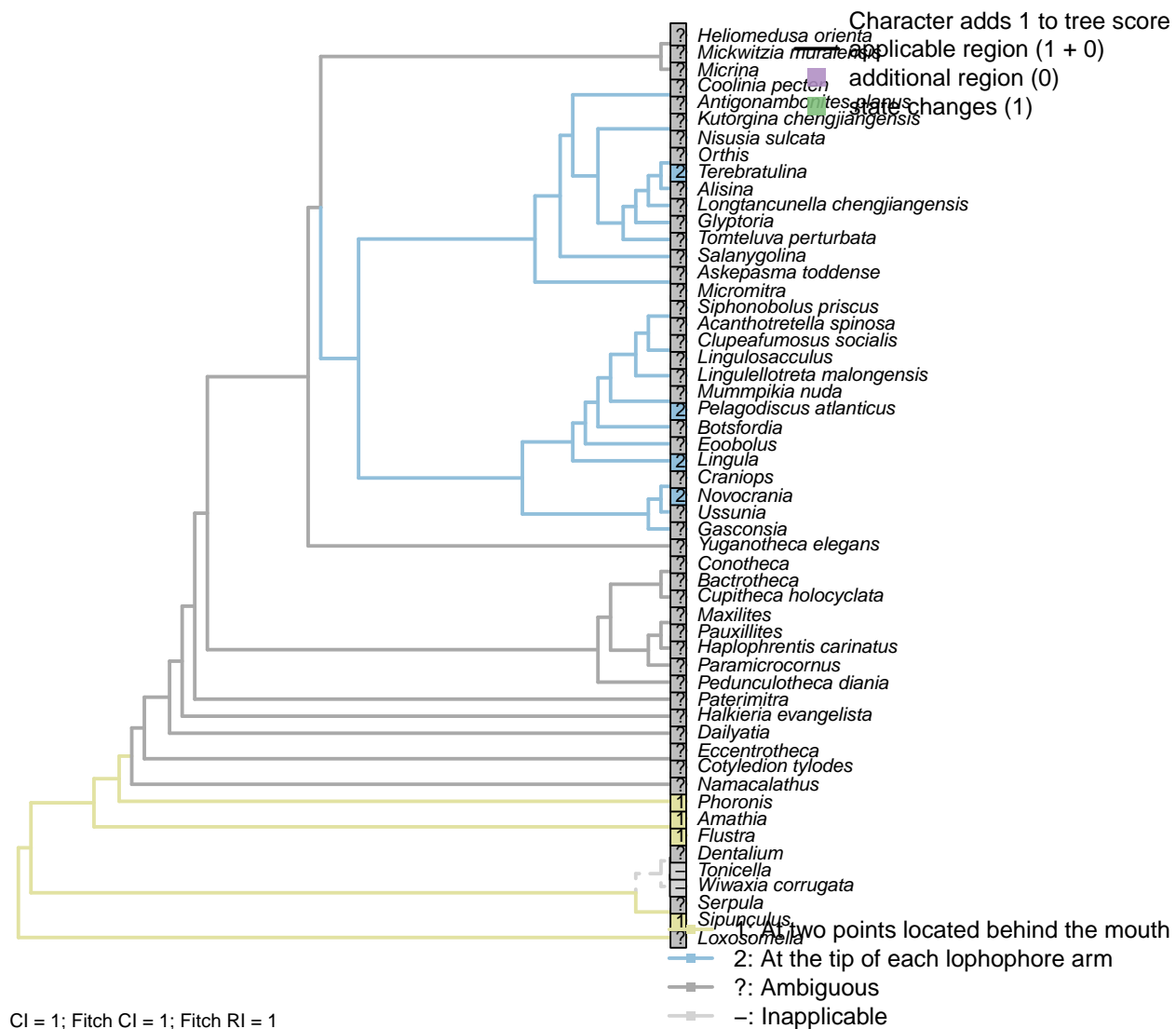
*Loxosomella*: Nielsen (1966).

*Yuganotheca elegans*: “helical lophophore fringed with a single row of thick, widely spaced, parallel-sided and hollow tentacles” – Zhang et al. (2014).

### [45] Median tentacle in early development



## [46] Site of tentacle addition

**Character 46: Perioral tentacular apparatus: Site of tentacle addition**

- 1: At two points located behind the mouth
  - 2: At the tip of each lophophore arm
- Transformational character.

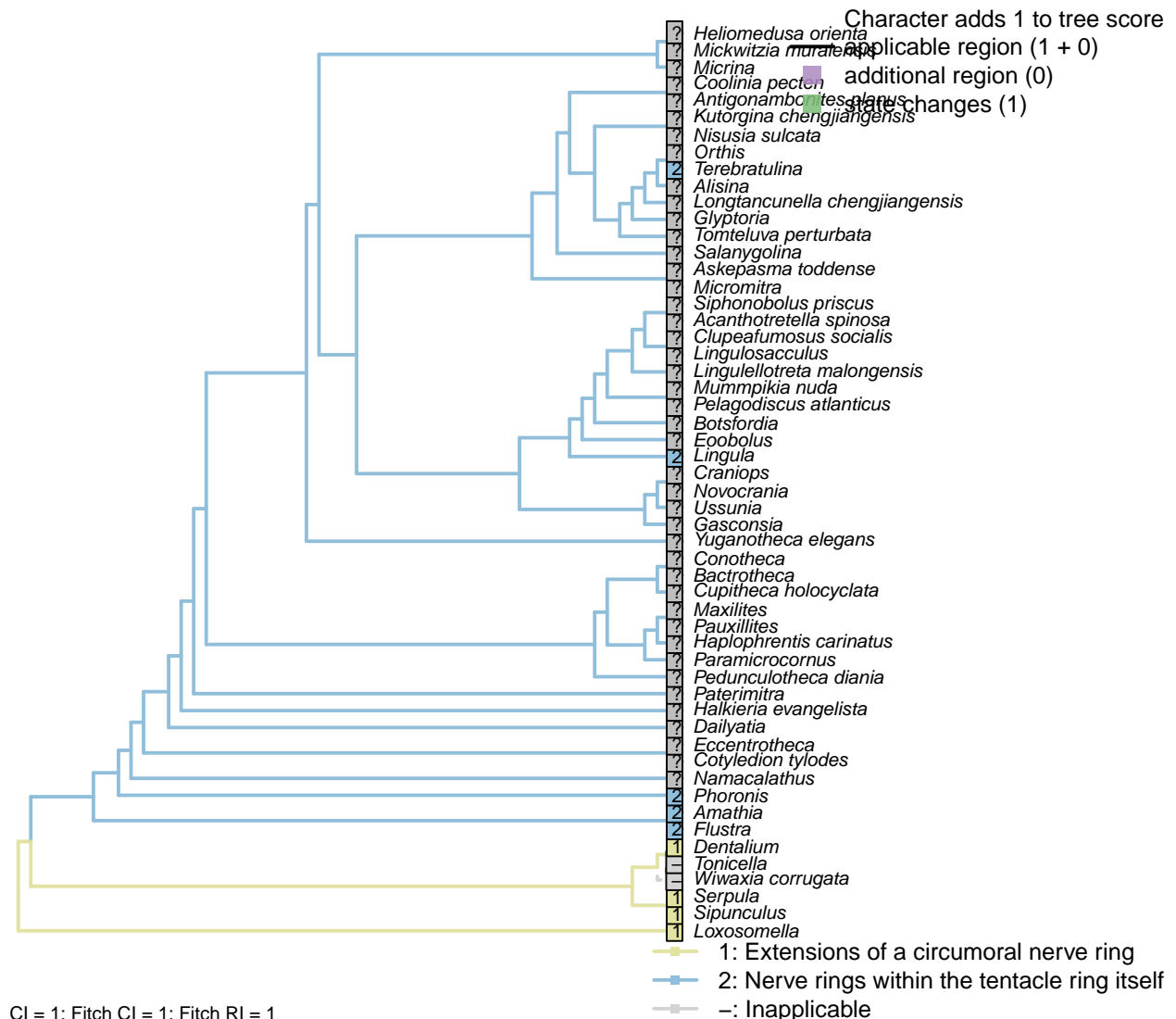
Following Temereva (2017).

*Flustra, Amathia, Novocrania, Pelagodiscus atlanticus, Lingula, Terebratulina*: Following Temereva (2017).

*Phoronis*: Following Temereva (2017) – though in larvae, tentacles are added at the tips of the developing lophophore.

*Sipunculus*: New branches added at each lateral extreme, behind mouth (Adrianov et al., 2006).

## [47] Innervation



### Character 47: Perioral tentacular apparatus: Innervation

- 1: Extensions of a circumoral nerve ring
  - 2: Nerve rings within the tentacle ring itself
- Transformational character.

Annelid tentacles are innervated by palp nerves (Orrhage and Müller, 2005); lophophores ancestrally contained a pair of nerve rings (Temereva, 2017).

*Flustra, Amathia*: Following Temereva (2017).

*Dentalium*: The captacula each bear an individual nerve fibre emanating from the cerebral ganglia, which is also associated with the circumoesophageal nerve ring (Sumner-Rooney et al., 2015), recalling the situation in annelids and sipunculans.

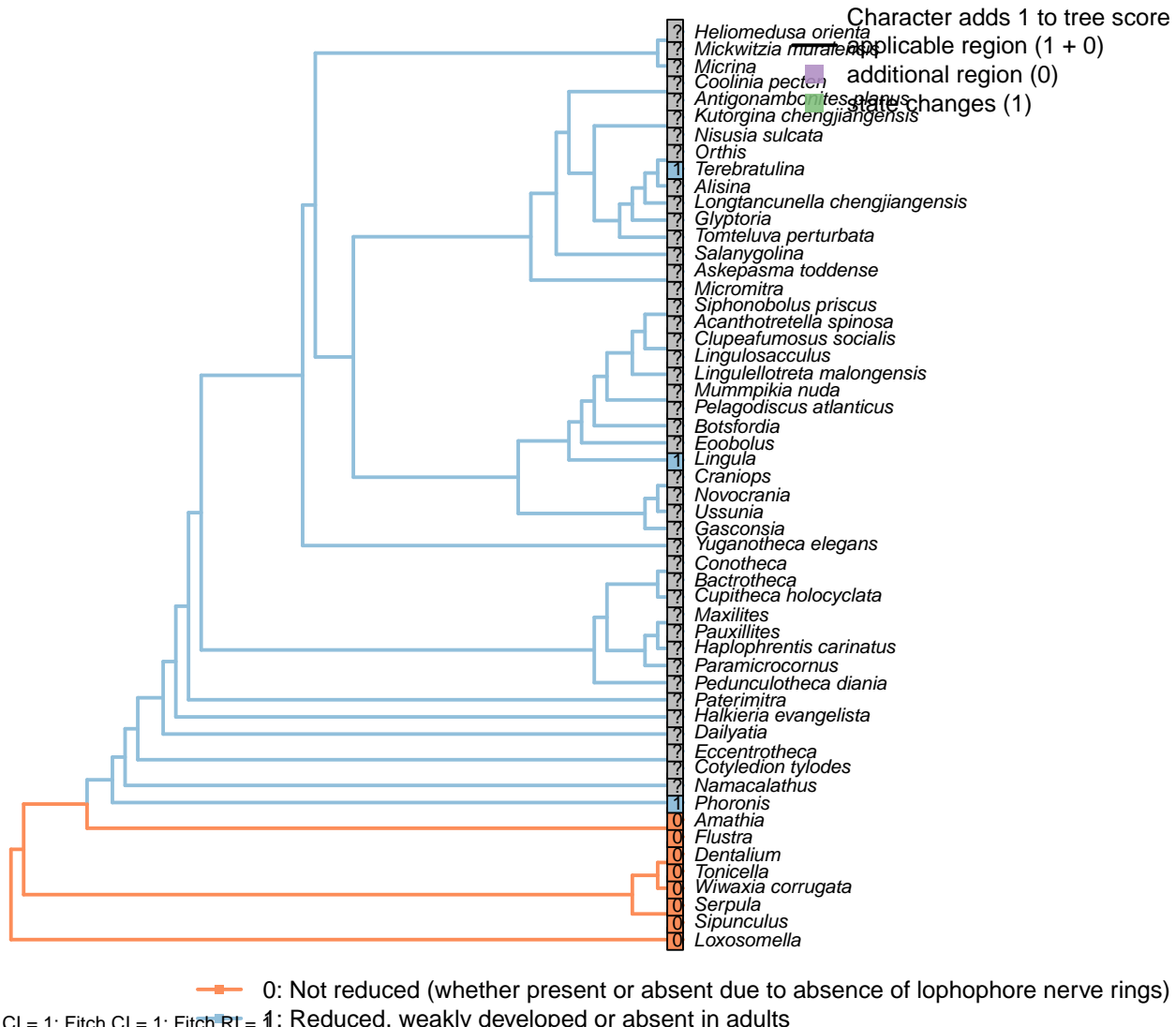
*Loxosomella*: Tentacle nerves originate laterally from the cerebral ganglion, branching three times and leading

to a single nerve within each tentacle (Fuchs et al., 2006).

*Serpula*: Orrhage and Müller (2005).

*Sipunculus*: Rice (1993).

#### [48] Inner nerve ring



#### Character 48: Perioral tentacular apparatus: Inner nerve ring

0: Not reduced (whether present or absent due to absence of lophophore nerve rings)

1: Reduced, weakly developed or absent in adults

Neomorphic character.

Juvenile lophophorates exhibit two nerve rings in the tentacles; one of these rings is often reduced or lost at

adulthood (Temereva, 2017).

*Flustra, Amathia*: Following Temereva (2017).

*Lingula*: Temereva and Kuzmina (2017).

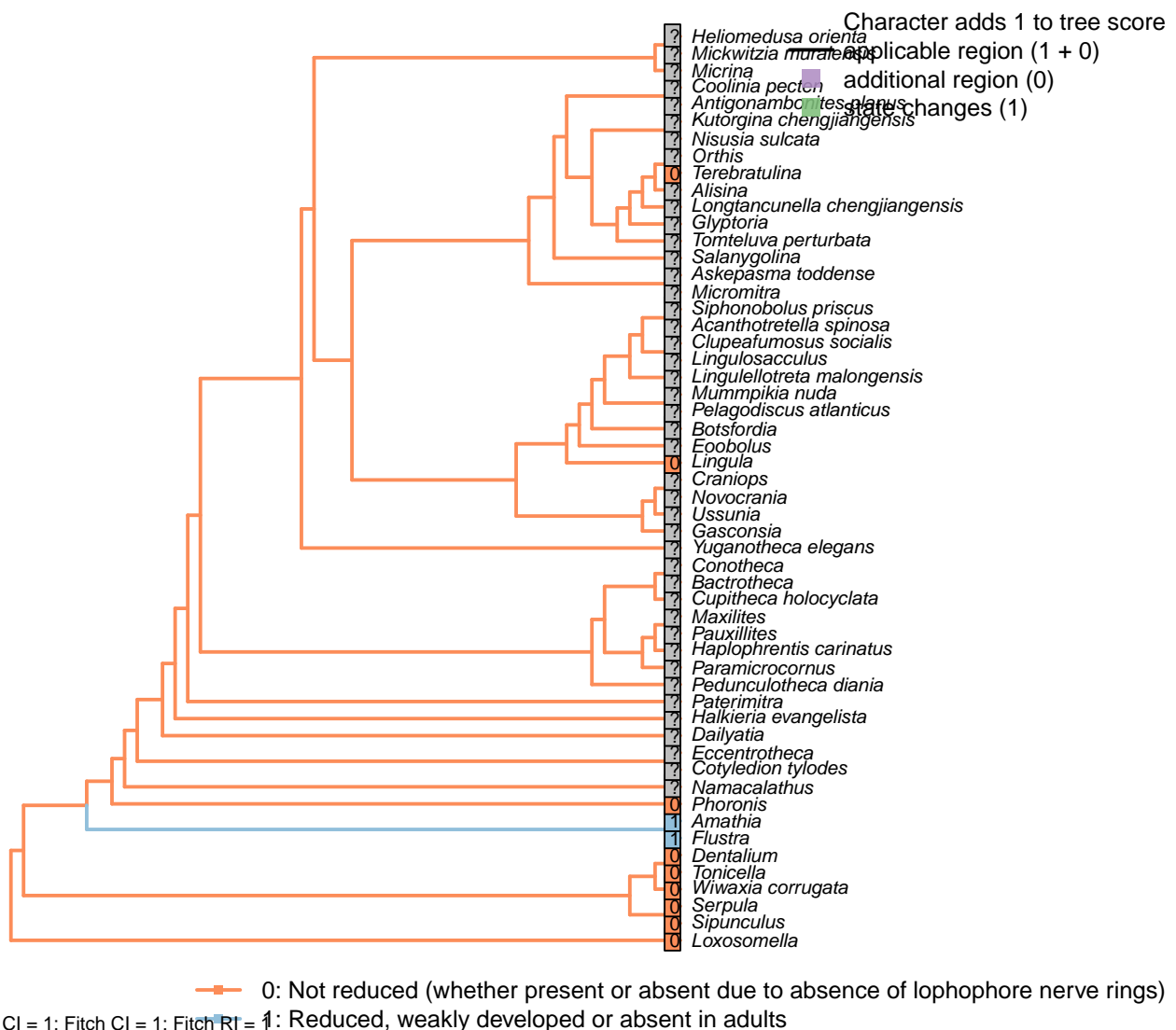
*Loxosomella*: Nerves present in tentacles, but not forming rings (Fuchs et al., 2006).

*Novocrania*: Probably only a single ring is present, but only available illustrations are 19th century sketches (Lüter, 2016).

*Phoronis*: (Temereva, 2017).

*Terebratulina*: In *Gryphus* (Temereva and Kuzmina, 2017).

## [49] Outer nerve ring



### Character 49: Perioral tentacular apparatus: Outer nerve ring

0: Not reduced (whether present or absent due to absence of lophophore nerve rings)

1: Reduced, weakly developed or absent in adults

Neomorphic character.

Juvenile lophophorates exhibit two nerve rings in the tentacles; one of these rings is often reduced or lost at adulthood (Temereva, 2017).

*Amathia*: Following Temereva (2017); only one tentacle nerve ring evident in Temereva and Kosevich (2016).

*Flustra*: “Most species of bryozoans have only the inner” nerve ring – Temereva (2017).

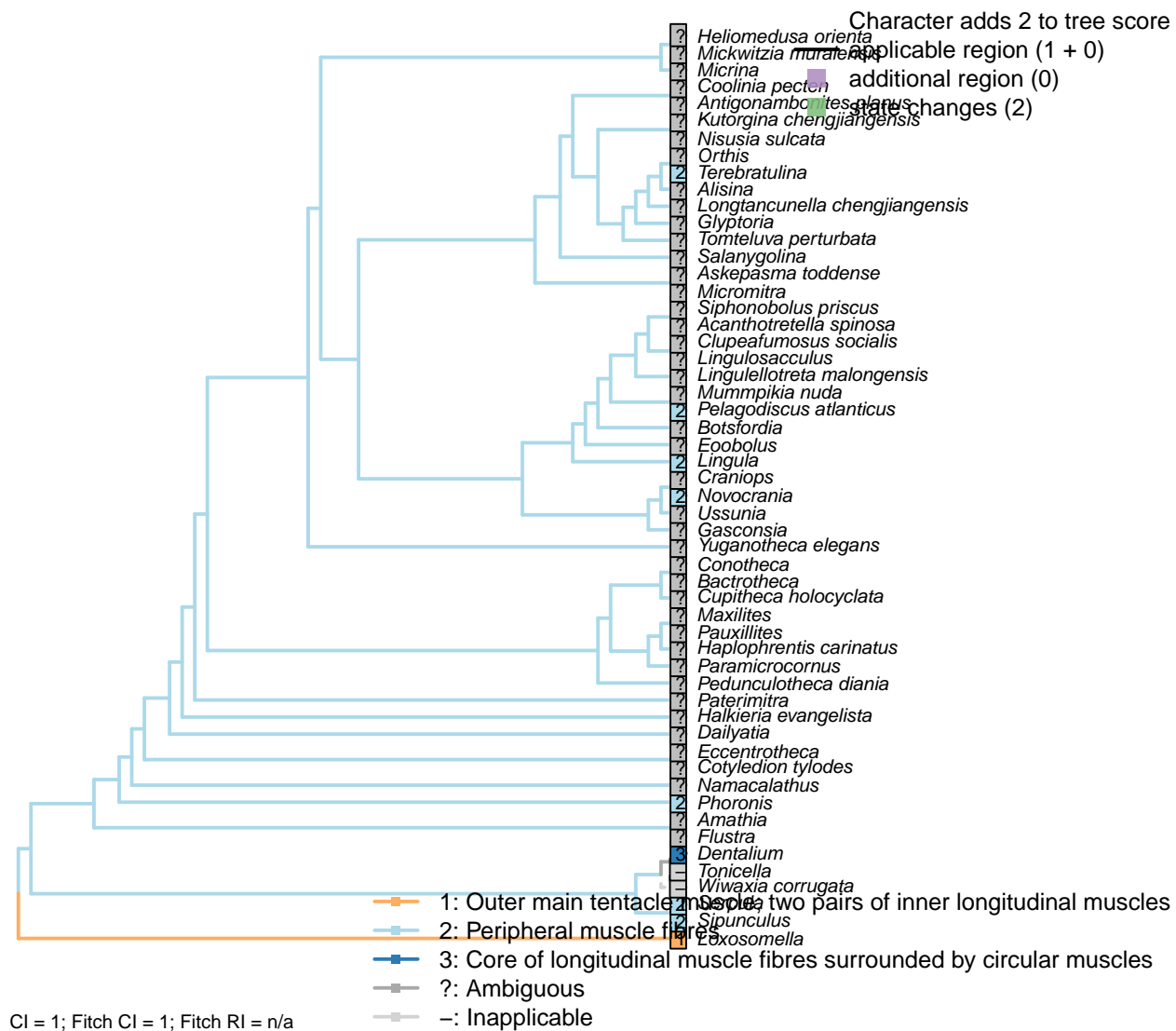
*Lingula*, *Terebratulina*: Temereva (2017).

*Loxosomella*: Nerves present in tentacles, but not forming rings (Fuchs et al., 2006).

*Novocrania*: Probably only a single ring is present, but only available illustrations are 19th century sketches (Lüter, 2016).

*Phoronis*: Temereva and Kuzmina (2017).

## [50] Musculature



Character 50: Perioral tentacular apparatus: Musculature

- 1: Outer main tentacle muscle; two pairs of inner longitudinal muscles
  - 2: Peripheral muscle fibres
  - 3: Core of longitudinal muscle fibres surrounded by circular muscles
- Transformational character.

*Dentalium*: Six to eight elongate muscle cells in core (Shimek, 1988), surrounded by circular muscles (Byrum and Ruppert, 1994).

*Novocrania, Pelagodiscus atlanticus, Lingula, Terebratulina*: “Inner coelomic epithelium underlain by muscle fibers, or in the tentacles, myoepithelial cells.” – Williams et al. (1997).

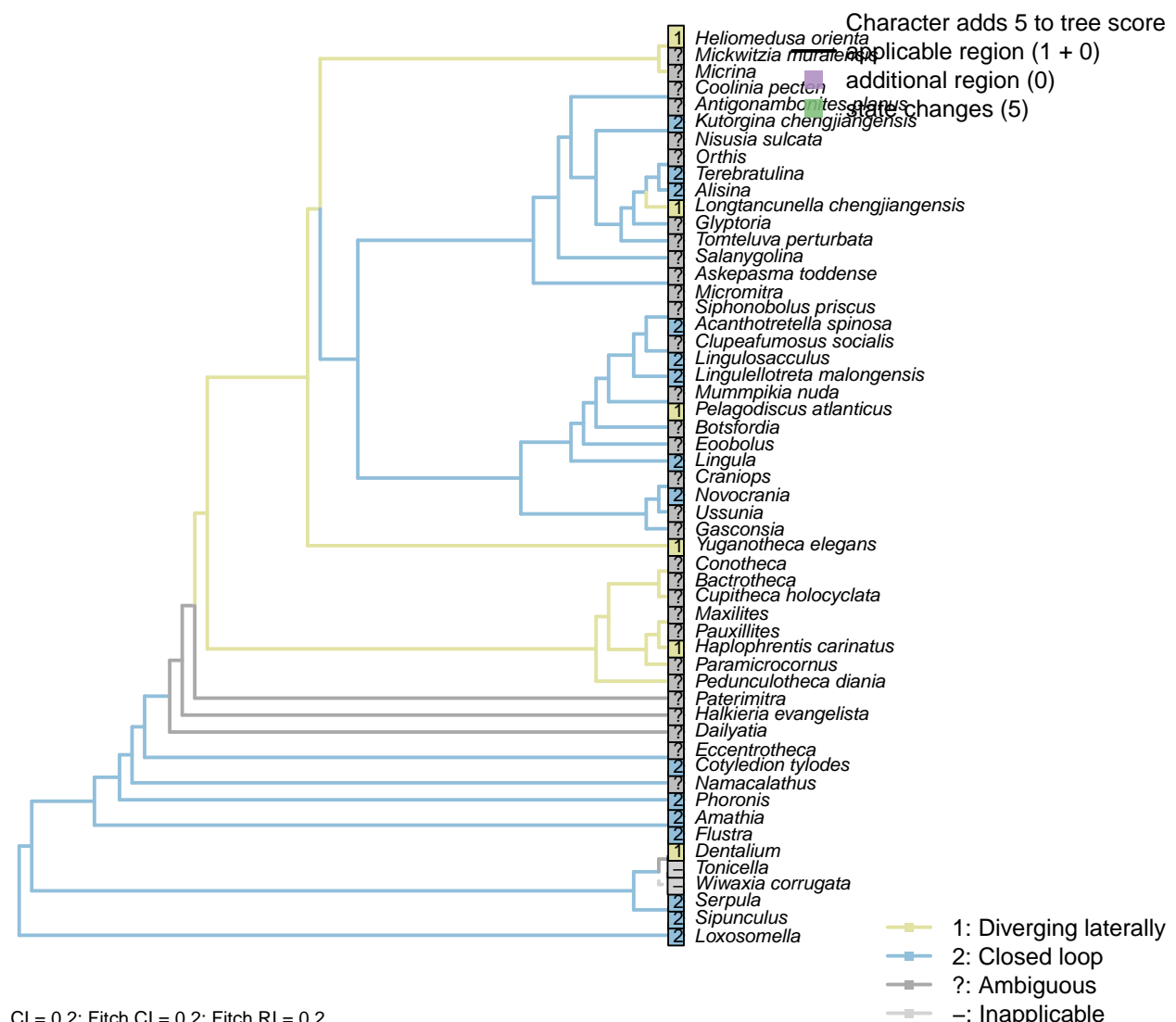
*Loxosomella*: Outer main tentacle muscle; two pairs of inner longitudinal muscles (Fuchs et al., 2006).

*Phoronis*: (Pardos et al., 1991).

*Serpula*: Peripheral muscle fibres (Hanson, 1949).

*Sipunculus*: Peripheral to main tentacle cavity (Pilger, 1982).

## [51] Forms closed loop



**Character 51: Perioral tentacular apparatus: Forms closed loop**

- 1: Diverging laterally
  - 2: Closed loop
- Transformational character.

Whereas the lophophore of crown-group brachiopods typically forms a closed loop, those of *Haplophrentis* and *Helio medusa* diverge laterally (Moysiuk et al., 2017).

*Amathia*: Ends of arms meet to form closed loop (Temereva and Kosevich, 2016).

*Cotyledion tylodes*: Tentacles form almost complete circular crown.

*Lingulosacculus*: Two diverging arms of the lophophore are preserved (Balthasar and Butterfield, 2009).

*Longtancunella chengjiangensis*: Two distinct, diverging arms reconstructed by Zhang et al. (2007c).

*Loxosomella*: Nielsen (1966).

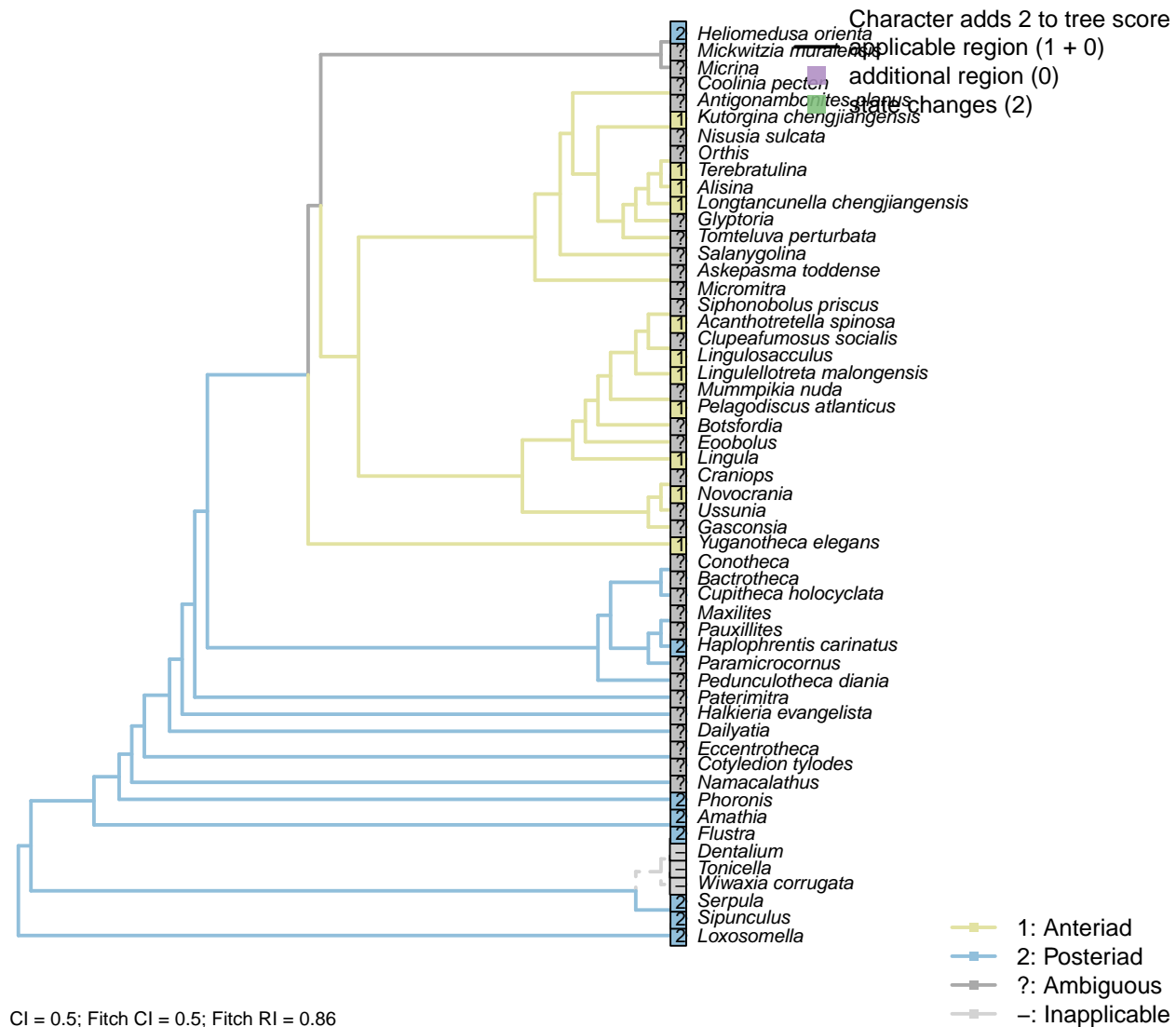
*Namacalathus*: The existence of a lophophore is speculative.

*Nisusia sulcata*: No specimens of *Nisusia* preserve the lophophore.

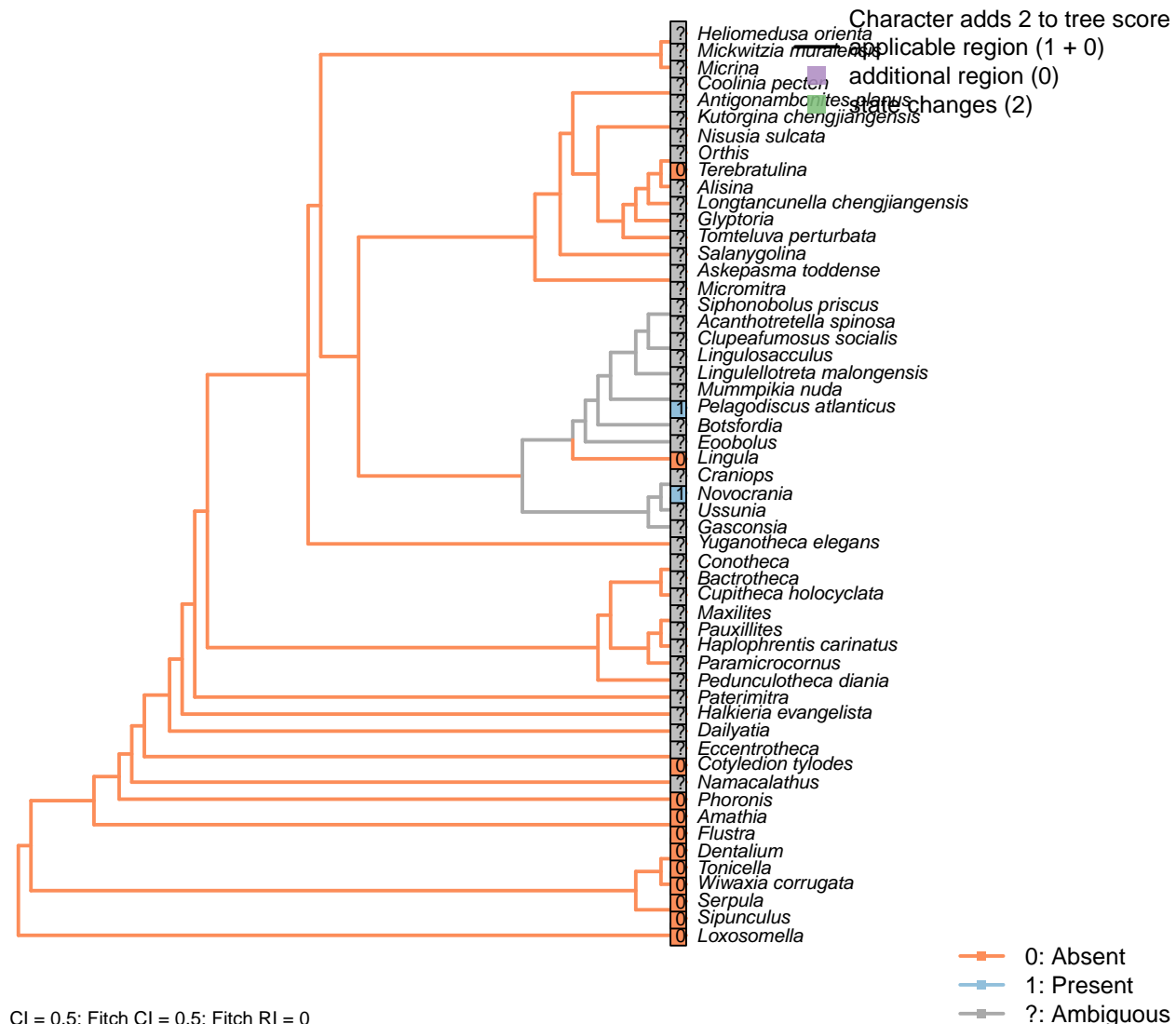
*Phoronis*: Two lophophore arms rather than a single continuous loop, but with tips close together to form functional loop (Torrey, 1901).

*Sipunculus, Serpula*: Growing to encircle mouth in adults.

## [52] Coiling direction



## [53] Adjustor muscle



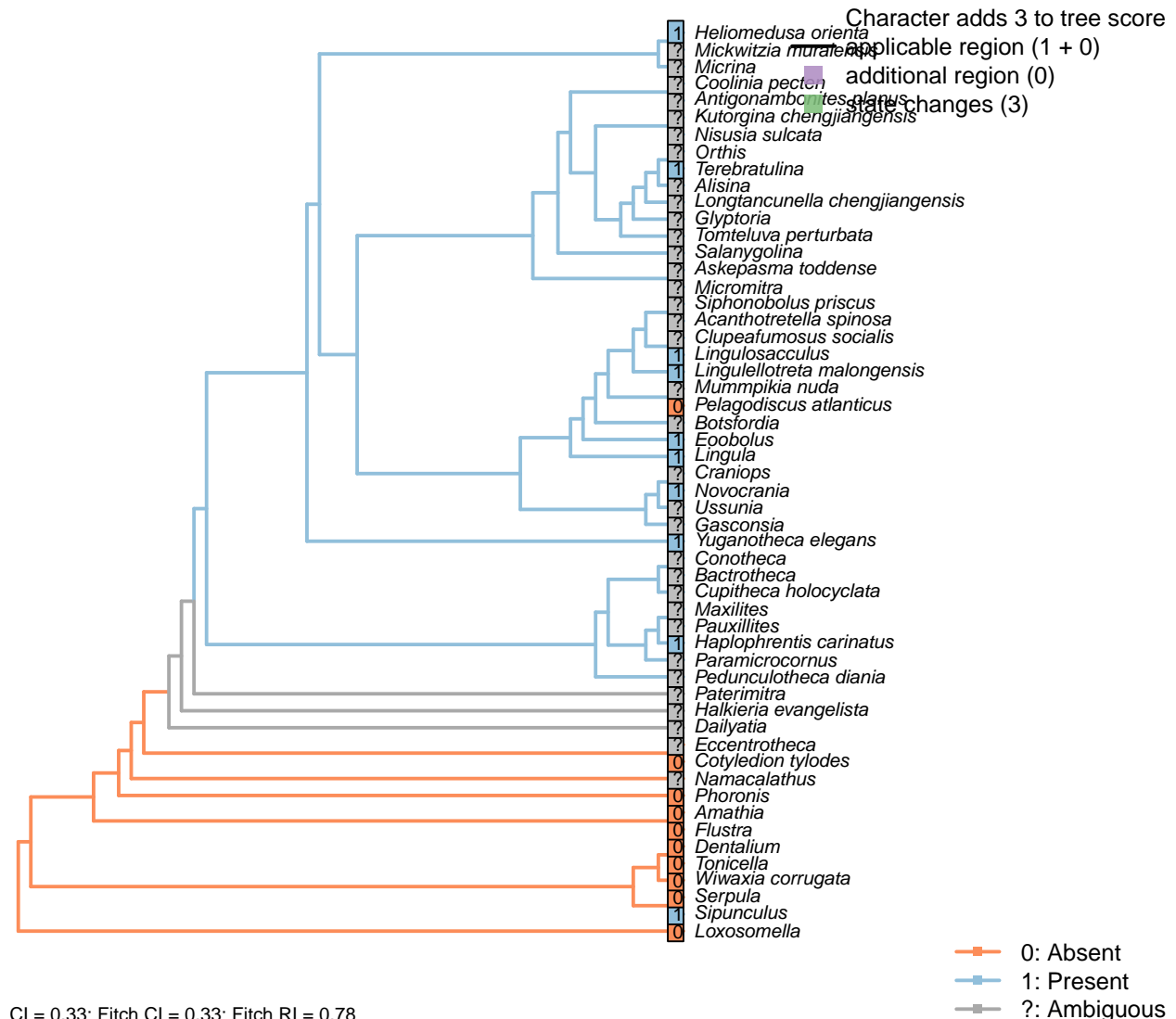
Following character 55 in Carlson (1995). Not possible to code in most fossil taxa.

*Namacalathus, Haplophrentis carinatus, Pedunculotheca diania, Dailyatia, Acanthotretella spinosa, Alisina, Askepasma toddense, Micromitra, Antigonambonites planus, Clupeafumosus socialis, Coolinia pecten, Eccentrotheca, Gasconsia, Glyptoria, Heliomedusa orienta, Kutorgina chengjiangensis, Lingulosacculus, Lingulellotreta malongensis, Longtancunella chengjiangensis, Micrina, Mummpikia nuda, Nisusia sulcata, Orthis, Paterimitra, Salanygolina, Tomteluva perturbata, Yuganotheca elegans*: Preservation not adequate to evaluate presence or absence of this muscle.

*Novocrania, Pelagodiscus atlanticus, Lingula, Terebratulina, Phoronis*: Following coding for higher taxon in Carlson (1995), appendix 1, character 55.

## 5.8 Digestive tract

### [54] Prominent pharynx



**Character 54: Digestive tract: Prominent pharynx**

0: Absent

1: Present

Neomorphic character.

Hyoliths exhibit a prominent protrusible muscular pharynx at the base of the lophophore (Moysiuk et al., 2017). This is considered as potentially equivalent to the anterior projection of the visceral cavity in *Heliomedusa*, and, by extension, in *Lingulosacculus* and *Lingulellotreta*.

*Eoobolus*: Prominent extension of dorsal visceral platform (Balthasar, 2009).

*Heliomedusa orienta*: Corresponding to the “neck” of the vase-shaped visceral cavity reported by Zhang et al. (2009).

*Lingulellotreta malongensis*: An anterior projection of the visceral area is noted by Williams et al. (2000)

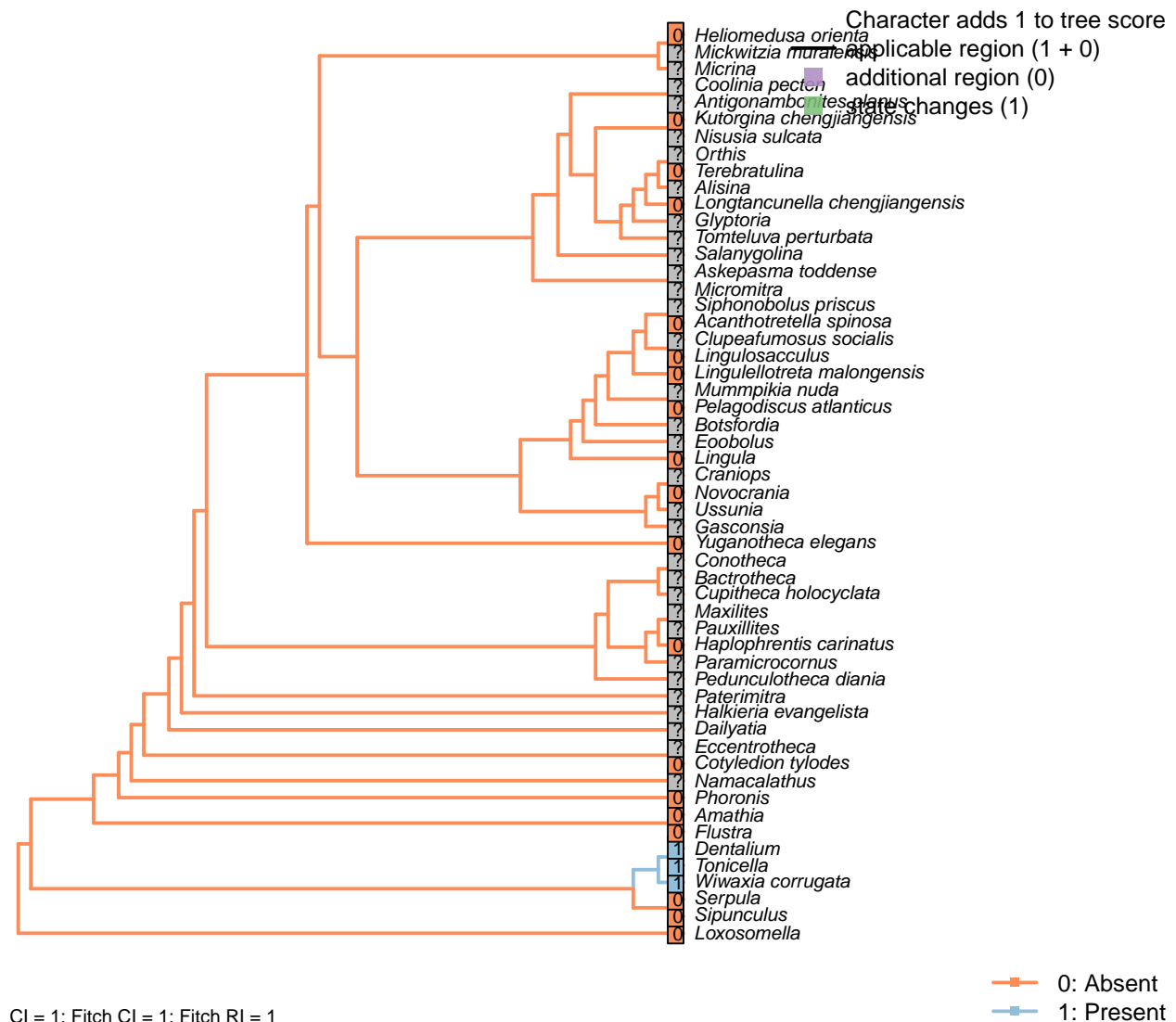
and considered equivalent to that observed in *Lingulosacculus* (Balthasar and Butterfield, 2009).

*Lingulosacculus*: The prominent anterior extension of the visceral area noted by Balthasar & Butterfield (2009) is considered as potentially homologous with that of *Heliomedusa* (Zhang et al., 2009) and, by extension, *Haplophrentis* (Moysiuk et al., 2017).

*Sipunculus*: Eversible pharynx (introvert).

*Yuganotheca elegans*: Possibly present, following interpretation of mouth (see fig. 2c, d in Zhang et al., 2014).

## [55] Radula



### Character 55: Digestive tract: Radula

0: Absent

1: Present

Neomorphic character.

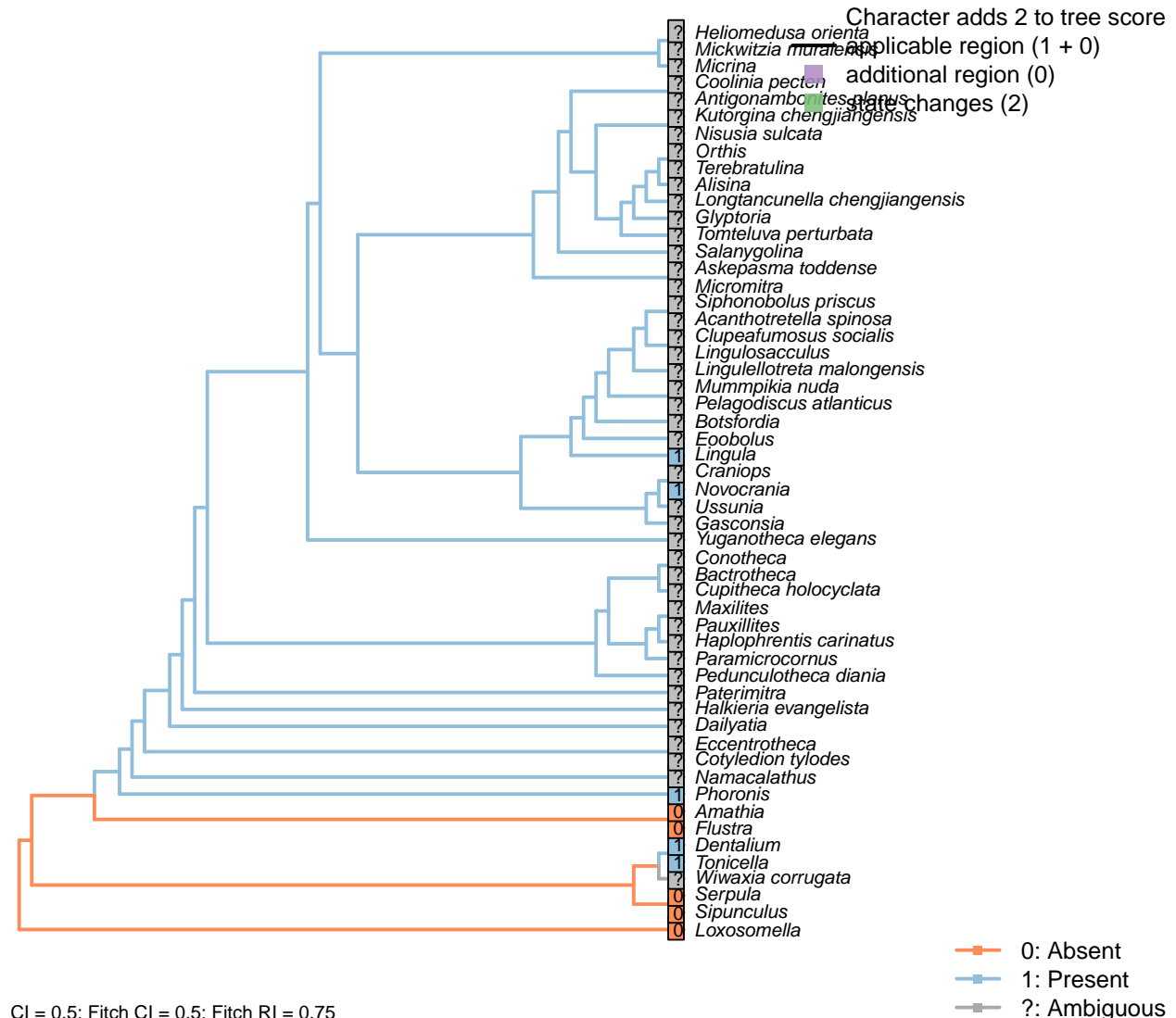
Any apparatus comprising multiple denticulate rows arranged serially in the sagittal plane is treated as

potentially homologous with the molluscan radula.

*Haplophrentis carinatus*, *Acanthotretella spinosa*, *Heliomedusa orienta*, *Kutorgina chengjiangensis*, *Lingulosacculus*, *Lingulellotreta malongensis*, *Longtancunella chengjiangensis*, *Yuganotheca elegans*: No candidate observed despite exceptional preservation.

*Wiwaxia corrugata*: Smith (2012b).

## [56] Oesophageal folds



### Character 56: Digestive tract: Oesophageal folds

0: Absent

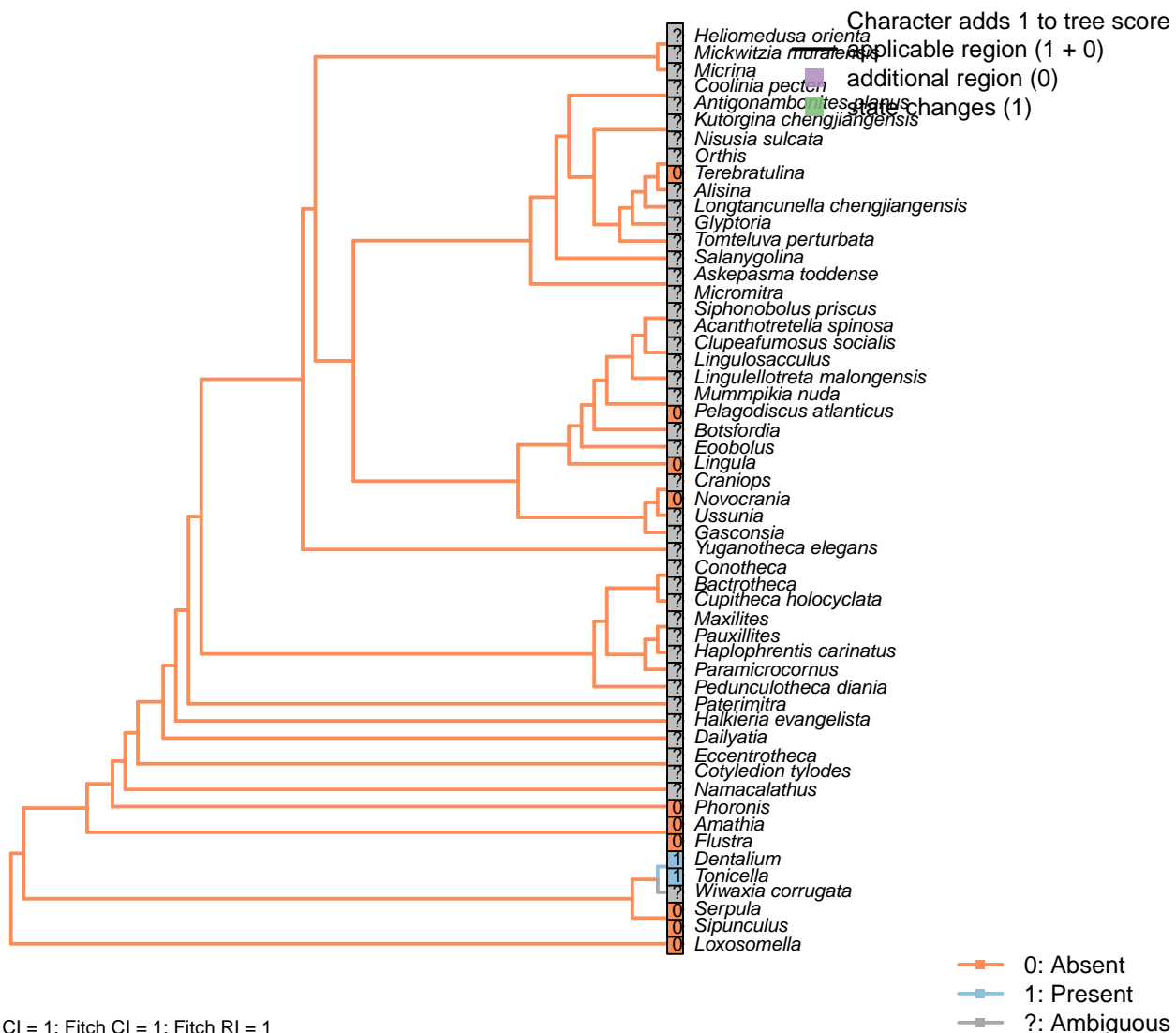
1: Present

Neomorphic character.

Following character 86 in Giribet and Wheeler (2002).

*Phoronis*: Ciliated ridge in oesophagus (Torrey, 1901).

## [57] Oral sphincter



## Character 57: Digestive tract: Oral sphincter

0: Absent

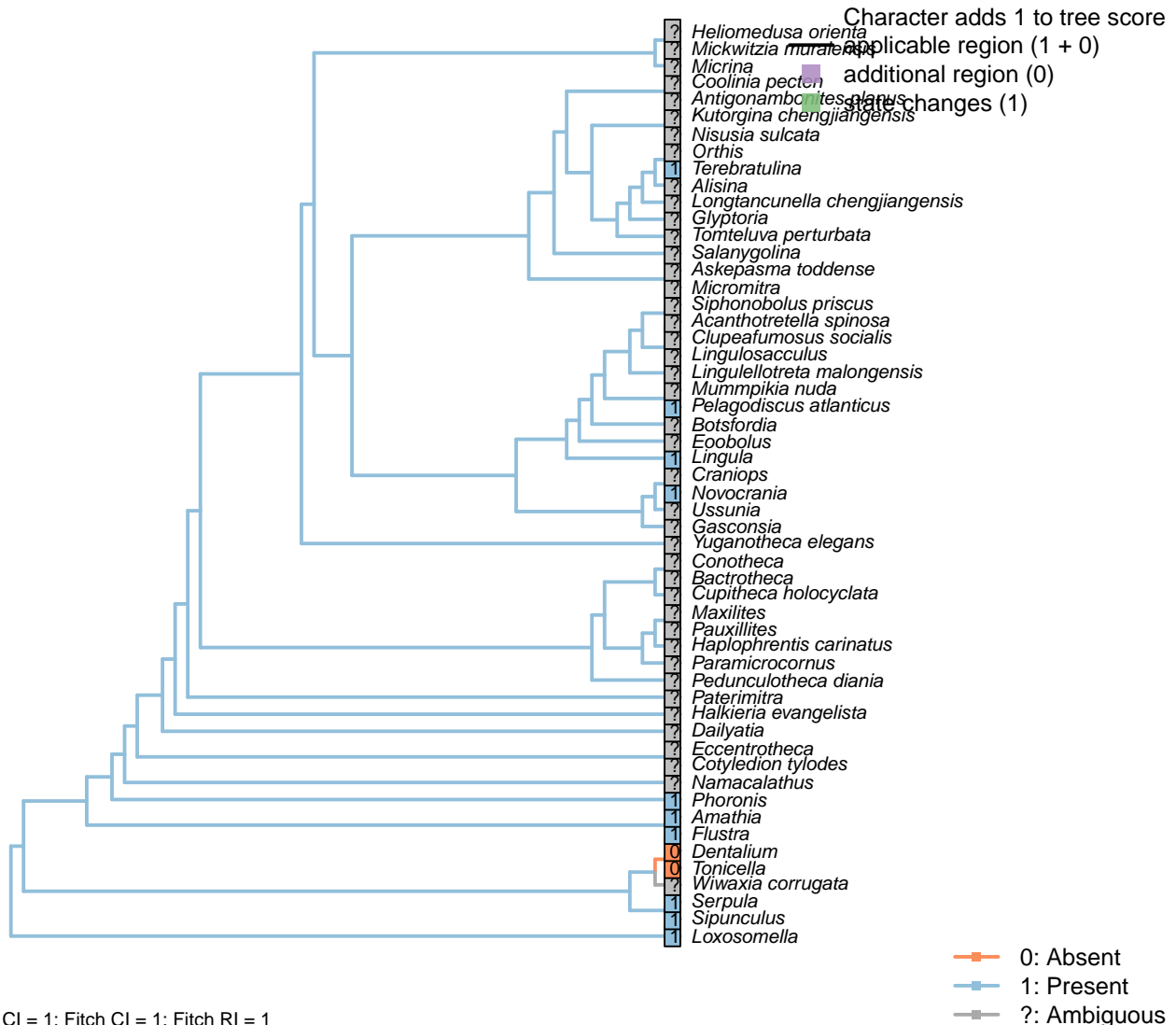
1: Present

Neomorphic character.

Character 133 in Grobe (2007).

*Dentalium*: Present, but secondarily reduced.

## [58] Locomotory cilia



## Character 58: Digestive tract: Foregut: Locomotory cilia

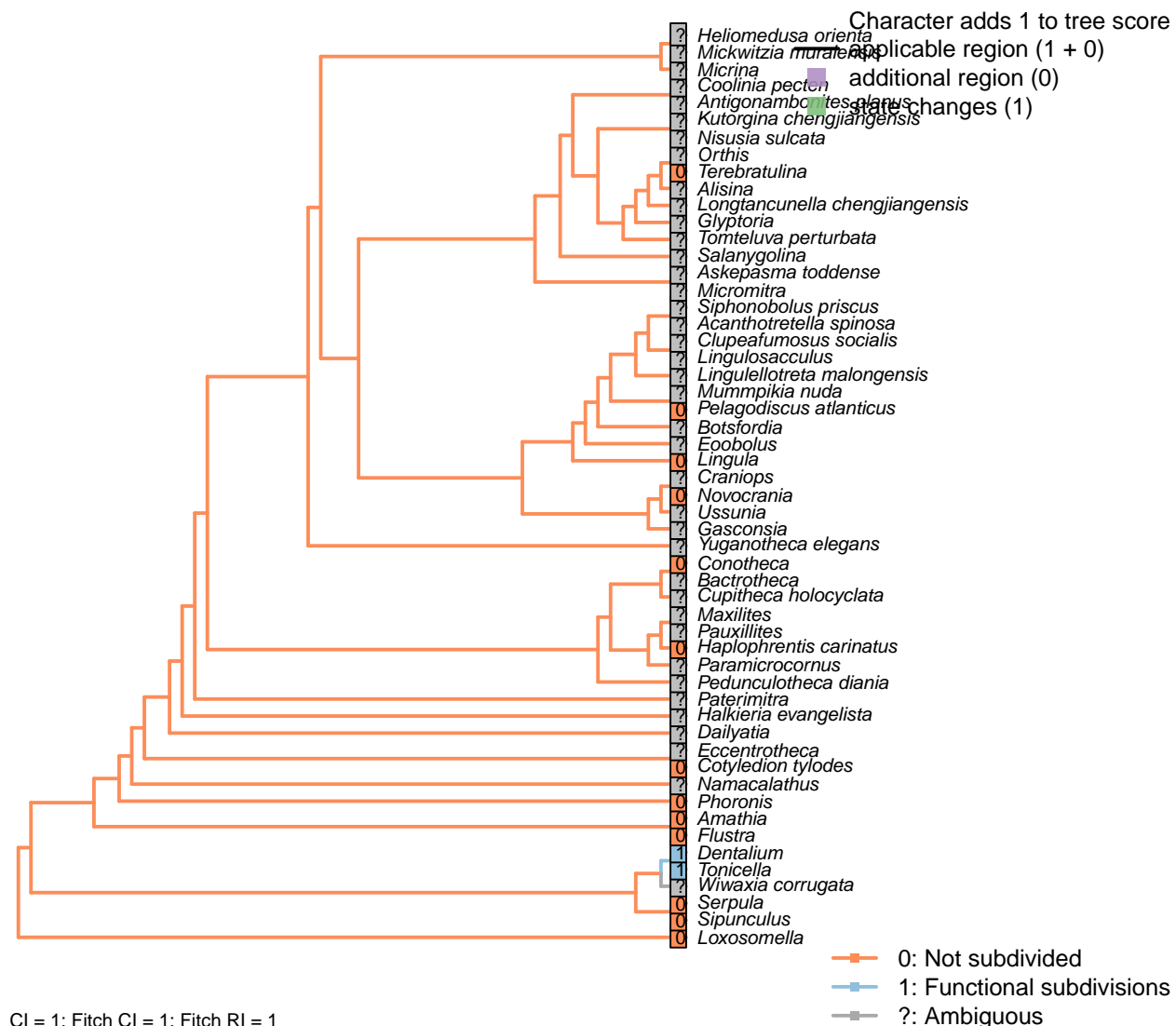
0: Absent

1: Present

Neomorphic character.

Character 66 in Haszprunar (2000).

## [59] Subdivisions



### Character 59: Digestive tract: Midgut: Subdivisions

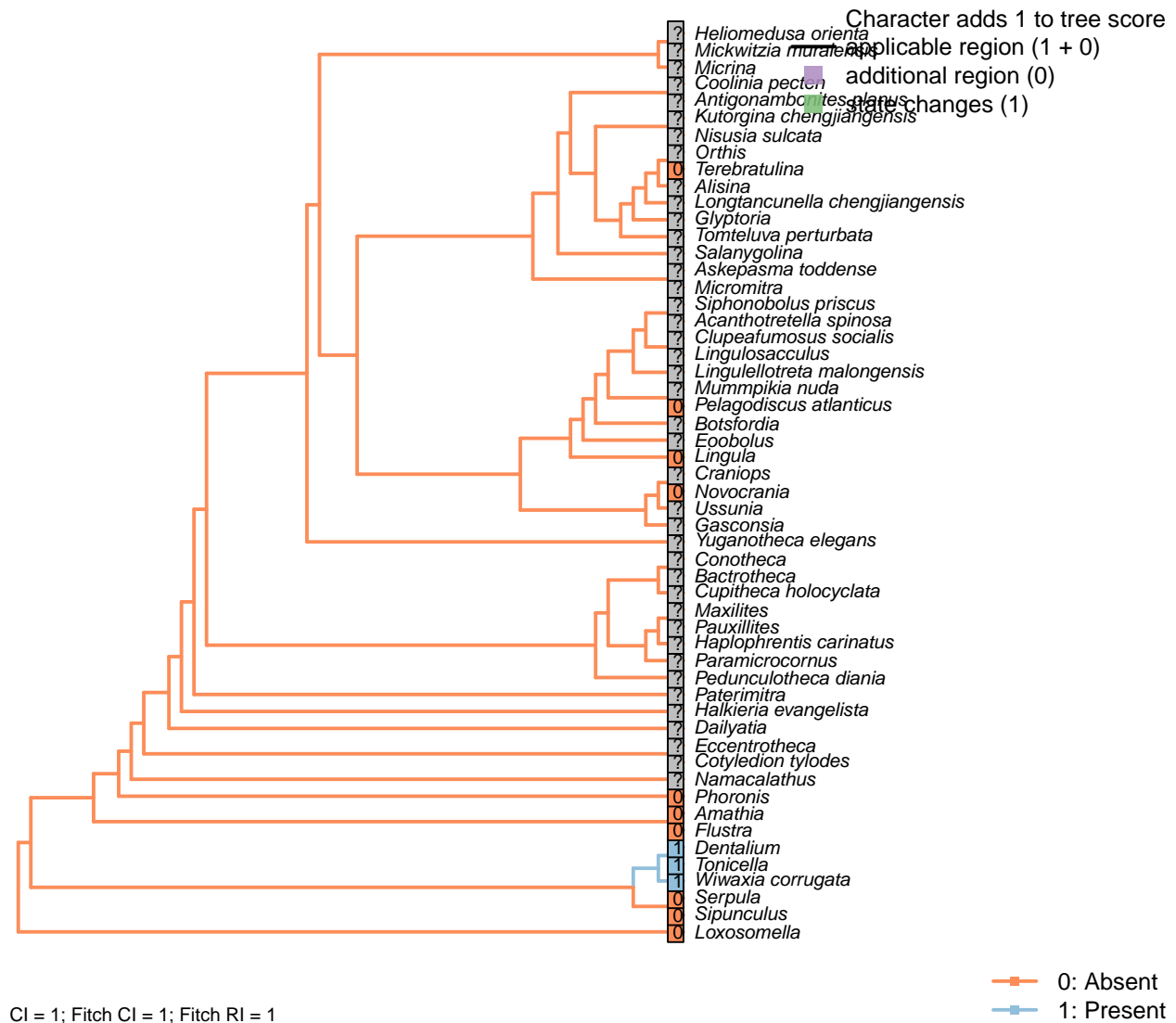
- 0: Not subdivided
- 1: Functional subdivisions
- Neomorphic character.

The molluscan midgut is functionally subdivided into a sorting area (stomach), digestion area (midgut sac or gland), and transport tube (intestine). Characters 42 in Haszprunar (2000), 1.38 in von Salvini-Plawen and Steiner (1996).

*Conotheca*: (Devaere et al., 2014).

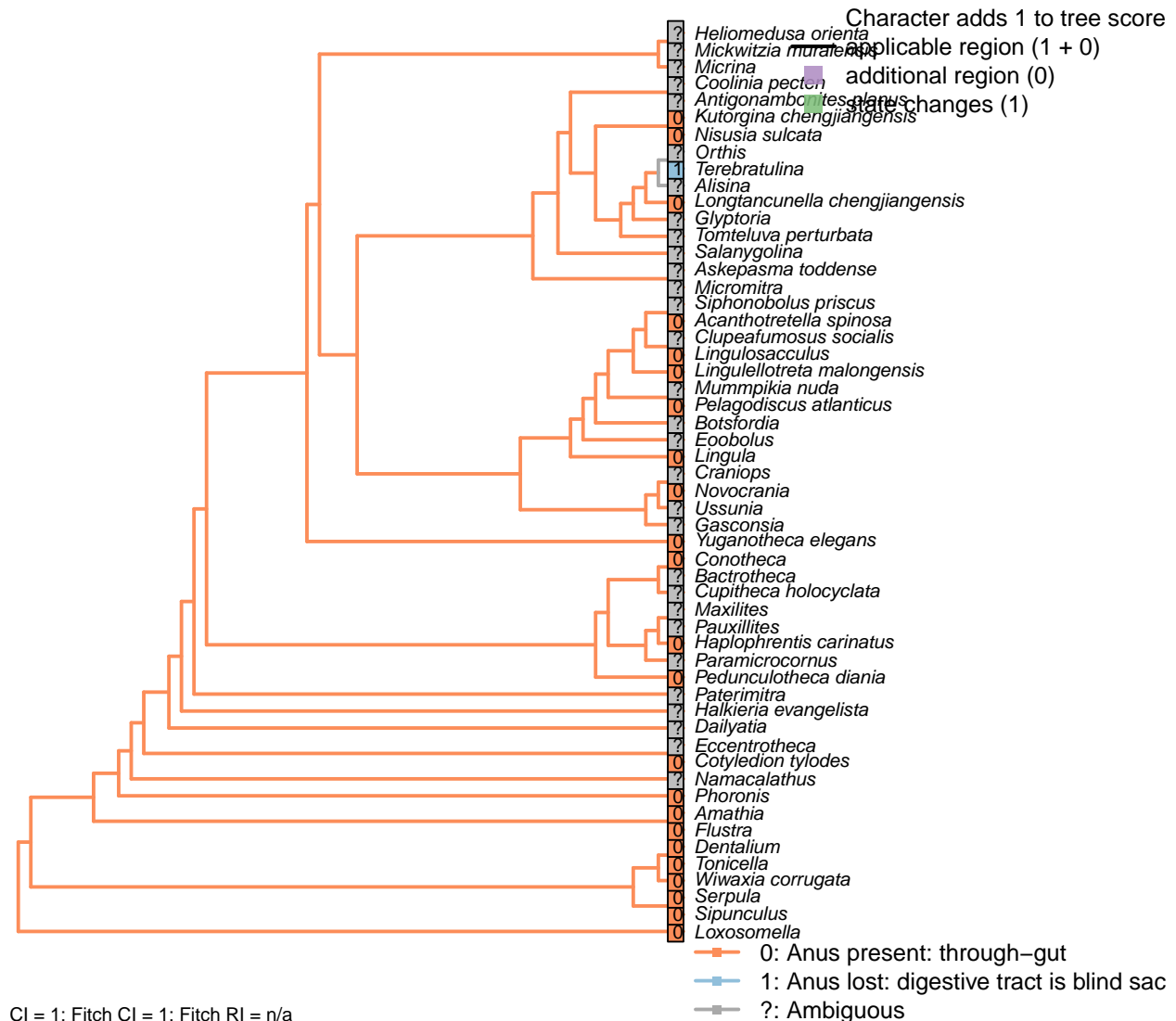
*Wiwaxia corrugata*: Subdivided, presumably functionally, but with some ambiguity [Smith (2012b); Smith 2014].

## [60] Glands



## 5.9 Digestive tract: Anus

### [61] Presence



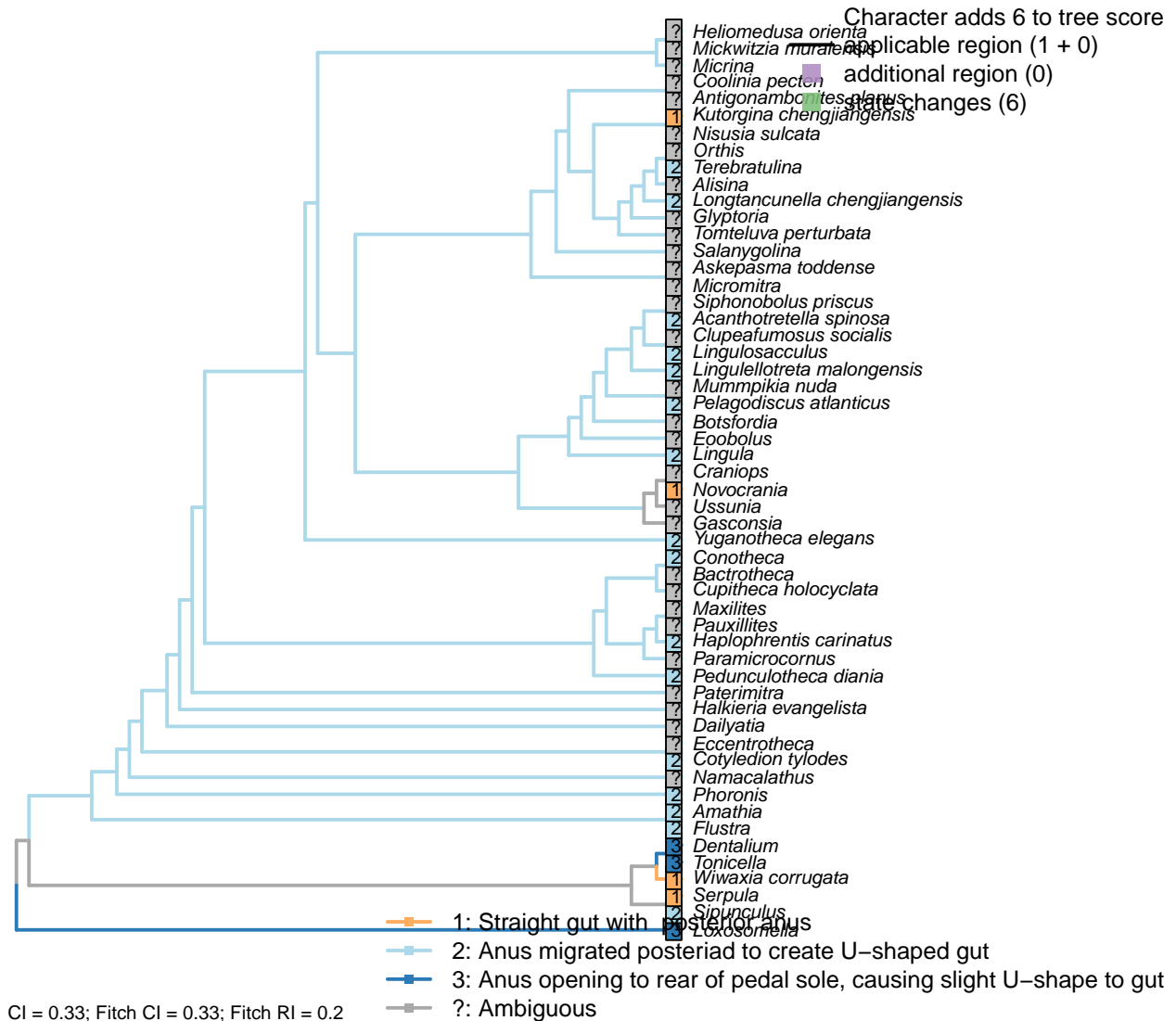
The digestive tract may either constitute a blind sac, or a through gut with anus. The loss of an anus is known to be derived within spiralia, so this character is treated as neomorphic.

*Conotheca*: (Devaere et al., 2014).

*Glyptoria*: Scored according to familial level feature.

*Kutorgina chengjiangensis*: Although “the possibility of a blind ending may not be completely eliminated [...] the weight of evidence [...] leads us to reject the possibility of a blind-ending intestine” – Zhang et al. (2007b), p. 1399.

## [62] Location



### Character 62: Digestive tract: Anus: Location

- 1: Straight gut with posterior anus
  - 2: Anus migrated posteriad to create U-shaped gut
  - 3: Anus opening to rear of pedal sole, causing slight U-shape to gut
- Transformational character.

"The relative position of the mouth and anus in the larvae of brachiopods and phoronids is similar: posterior anus and anterior mouth" – Williams et al. (2007), p. 2884

See also character 6 in Haszprunar and Wanninger (2008).

*Conotheca*: (Devaere et al., 2014).

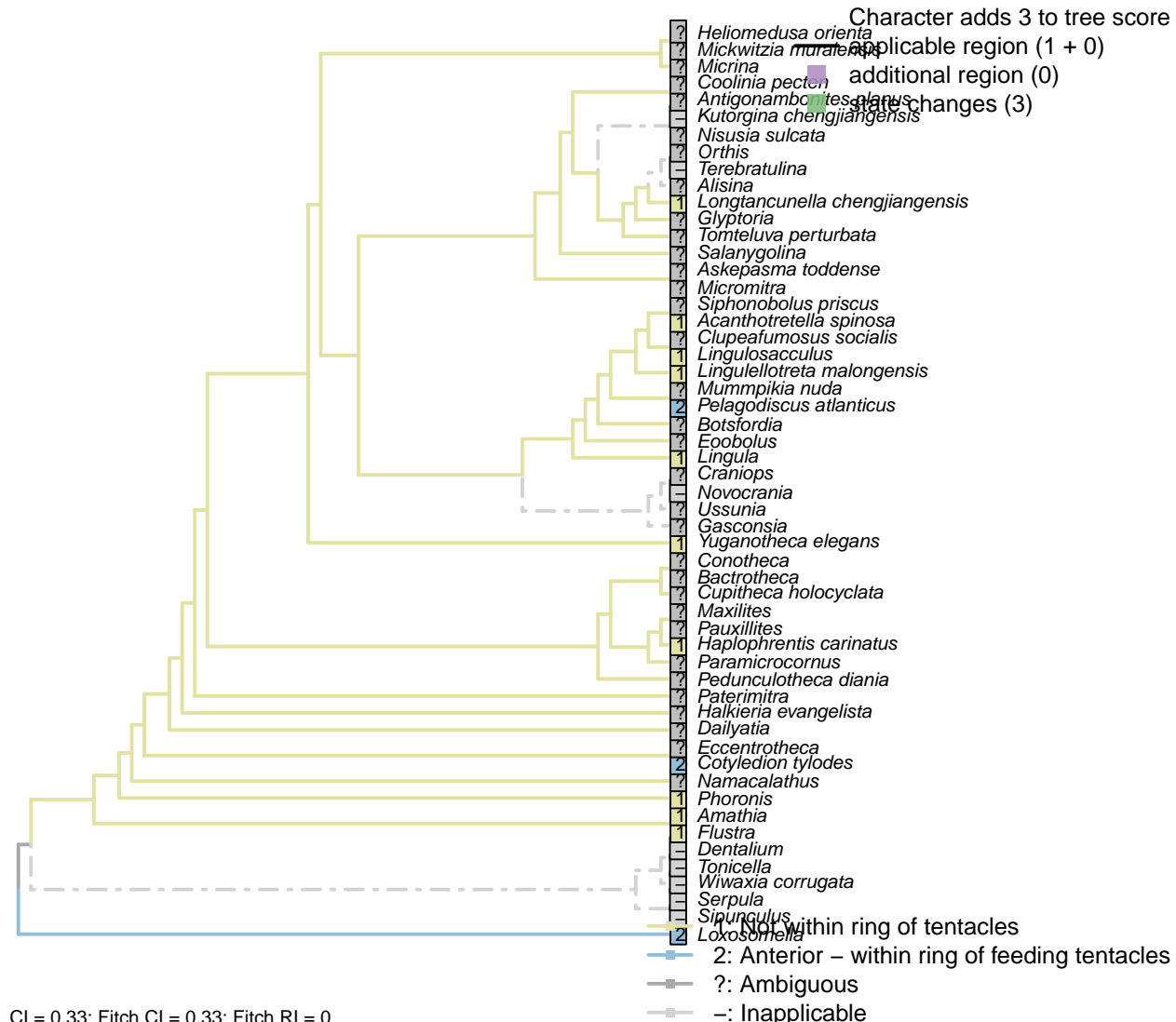
*Dentalium*: The U-shaped gut of scaphopods arises by exaggeration of the dorsal surface, rather than migration of the anus (Steiner, 1992).

*Kutorgina chengjiangensis*: "Five specimens have an exceptionally preserved digestive tract, dorsally curved,

with a putative dorso-terminal anus located near the proximal end of a pedicle" – Zhang et al. (2007b).

*Terebratulina*: "In rhynchonelliforms, the gut curves somewhat into a C-shape and the (blind) anus becomes posteroventral in position." – Williams et al. (2007), p. 2884.

### [63] Migration: Within ring of tentacles



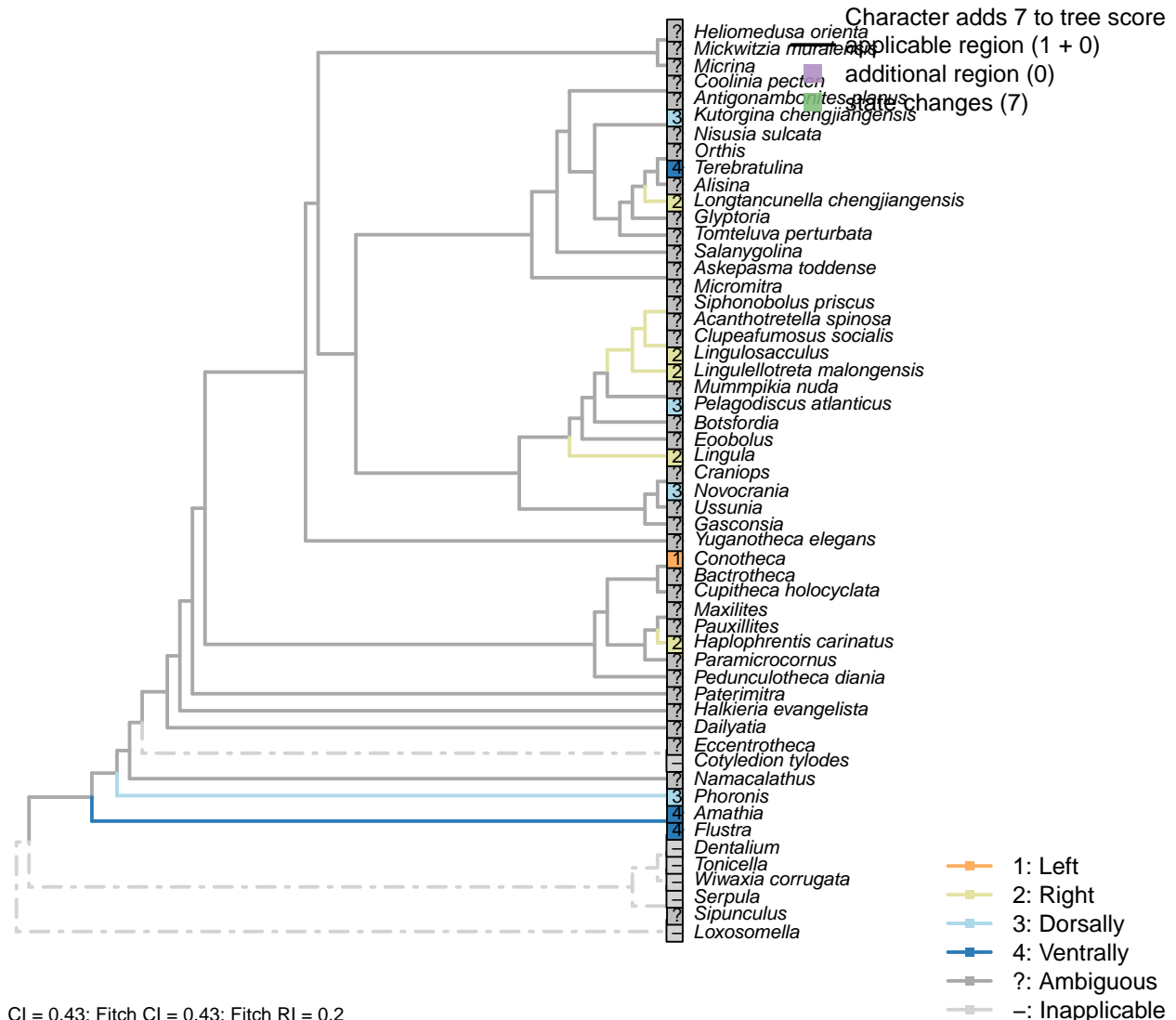
#### Character 63: Digestive tract: Anus: Migration: Within ring of tentacles

- 1: Not within ring of tentacles
  - 2: Anterior - within ring of feeding tentacles
- Transformational character.

A migrated anus may be located laterally or within the lophophore ring (as in entoprocts).

*Kutorgina chengjiangensis*: "Presumed to terminate in a functional anus located near the proximal end of the pedicle." – Zhang et al. (2007b).

## [64] Migration: Position



### Character 64: Digestive tract: Anus: Migration: Position

- 1: Left
- 2: Right
- 3: Dorsally
- 4: Ventrally

Transformational character.

If the anus is not within the ring of tentacles, in which direction is it oriented?.

*Flustra, Amathia*: Anus remains on ventral surface. Arguably, rather than the anus migrating, the dorsal surface of the animal has become extended.

*Conotheca*: Opening to left in Devaere et al. (2014), fig. 5A.

*Dentalium*: An alternative interpretation would be that the posterior of the scaphopod has been extended to generate the relatively anterior position of the originally ventral anus.

*Haplophrentis carinatus*: Opening to the right – see figures 1, 3, and extended data 5 in Moysiuk et al. (2017).

The text states in error that the anus is to the left of the midline.

*Kutorgina chengjiangensis*: “Five specimens have an exceptionally preserved digestive tract, dorsally curved, with a putative dorso-terminal anus located near the proximal end of a pedicle” – Zhang et al. (2007b).

*Lingula*: “In the lingulids, the [intestine] follows an oblique course anteriorly to open at the anus on the right body wall.” – Williams et al. (1997), p. 89.

*Lingulellotreta malongensis*: “finally terminating in an anal opening on the right anterior body wall” (Zhang et al., 2007a, p.66).

*Lingulosacculus*: “This same arrangement occurs in *L. nuda*, with the looped dark line tracking the same course as the exceptionally preserved guts of Chengjiang lingulellotretids, including the median position of its posterior loop and the sharp right turn as it exits the posterior extension of the ventral valve” (Balthasar and Butterfield, 2009, p.310).

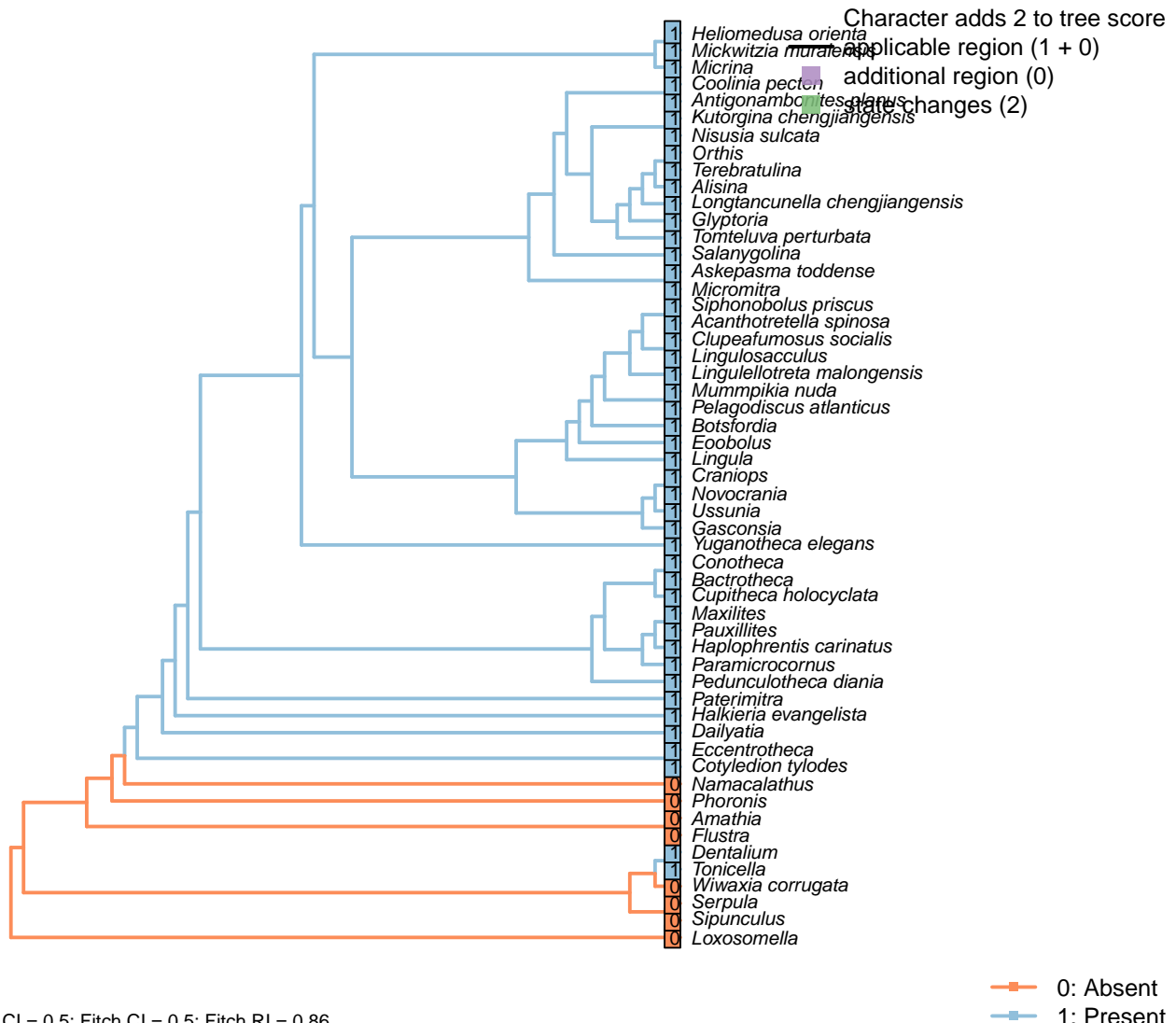
*Longtancunella chengjiangensis*: “The intestine extends posteriorly, and then turns right to continue as a tortuous strand, finally terminating at the latero-median position of the anterior body wall” – Zhang et al. (2007c).

*Terebratulina*: “In rhynchonelliforms, the gut curves somewhat into a C-shape and the (blind) anus becomes posteroventral in position.” – Williams et al. (2007), p. 2884.

*Yuganotheca elegans*: The identification of the “very poorly impressed possible anus at the lateral side of the anterior body wall” is not yet confident, so this character is coded as not presently available.

## 5.10 Sclerites

### [65] Present in adult



and hence the brachiopods (Zhao et al., 2017).

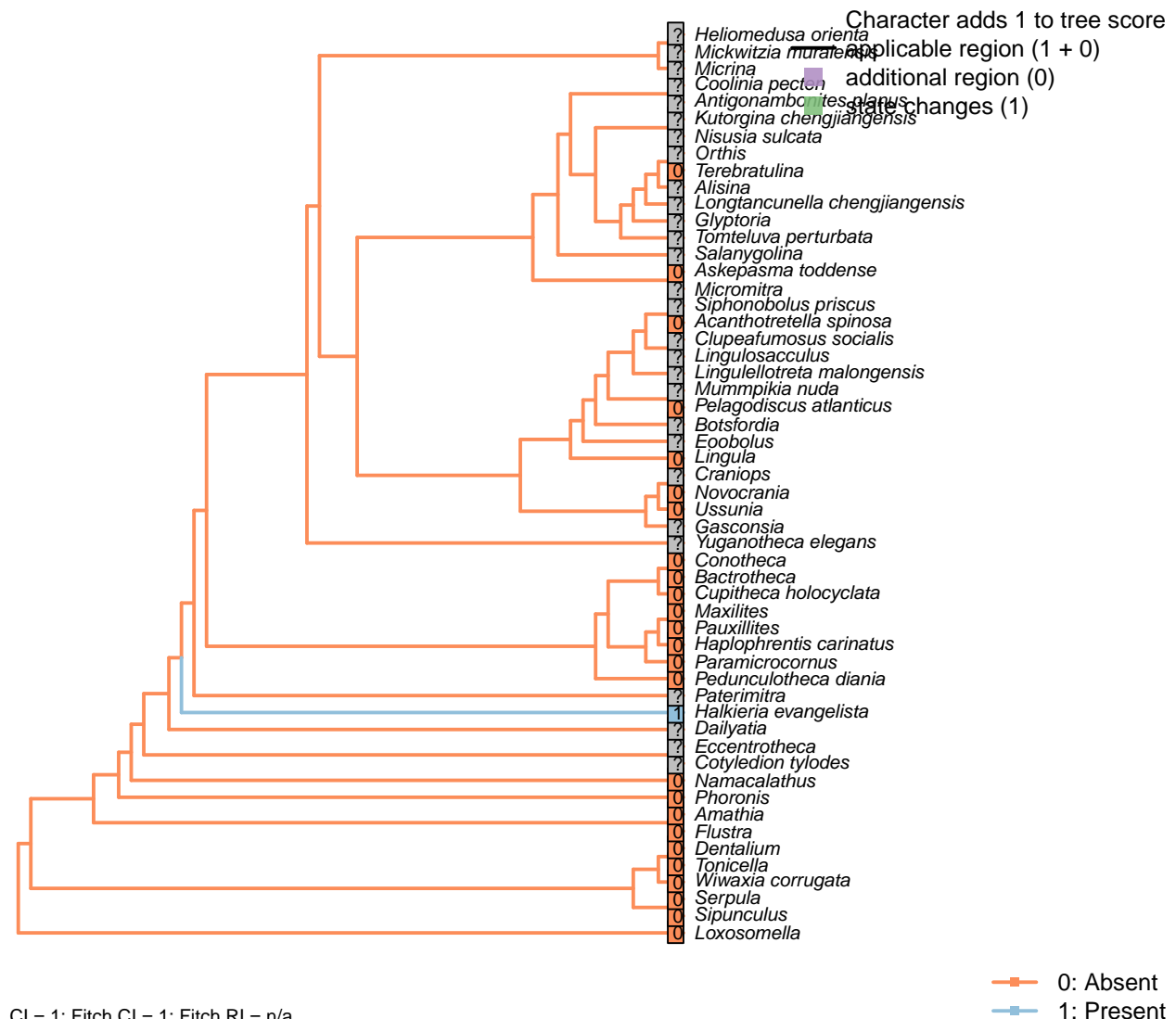
*Namacalathus*: The mineralized endoskeleton of *Namacalathus* is not interpreted as a sclerite.

*Serpula*: Annelid setae are not considered to represent potential homologues with the brachiopod shell.

*Sipunculus*: Hooks are present, though the absence of chitin or microvillar impressions indicates that they are not homologous with those of other lophotrochozoans.

*Wiwaxia corrugata*: The scales of *Wiwaxia* are treated as homologous with the chaetae of annelids and brachiopods (Butterfield, 1990; Smith, 2014; Zhang et al., 2015), rather than brachiopod shell.

## [66] Periodically shed and replaced



### Character 66: Sclerites: Periodically shed and replaced

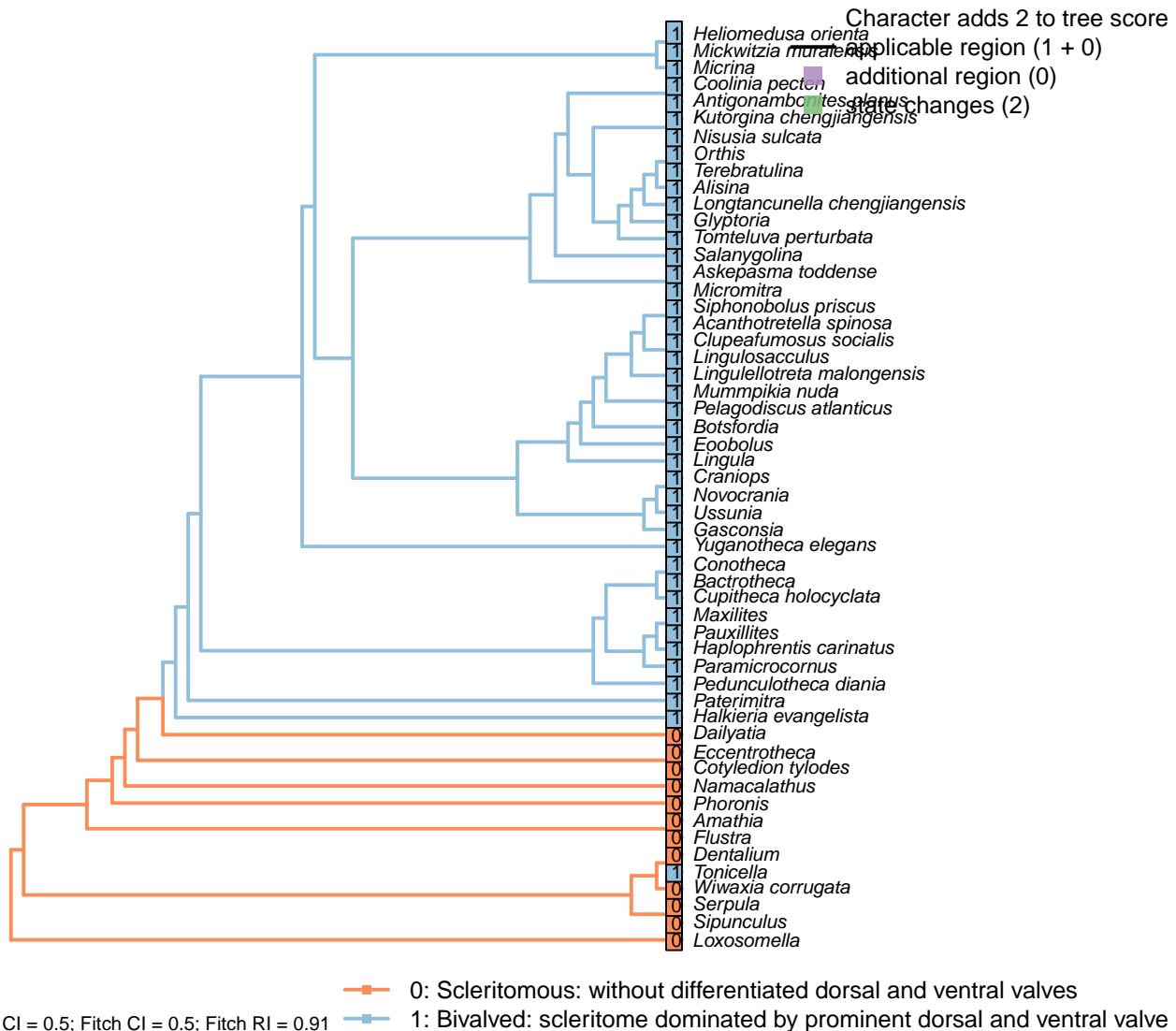
0: Absent

1: Present

Neomorphic character.

Certain taxa periodically slough and replace some of their individual sclerites during growth.

## 5.11 Sclerites: Bivalved [67]



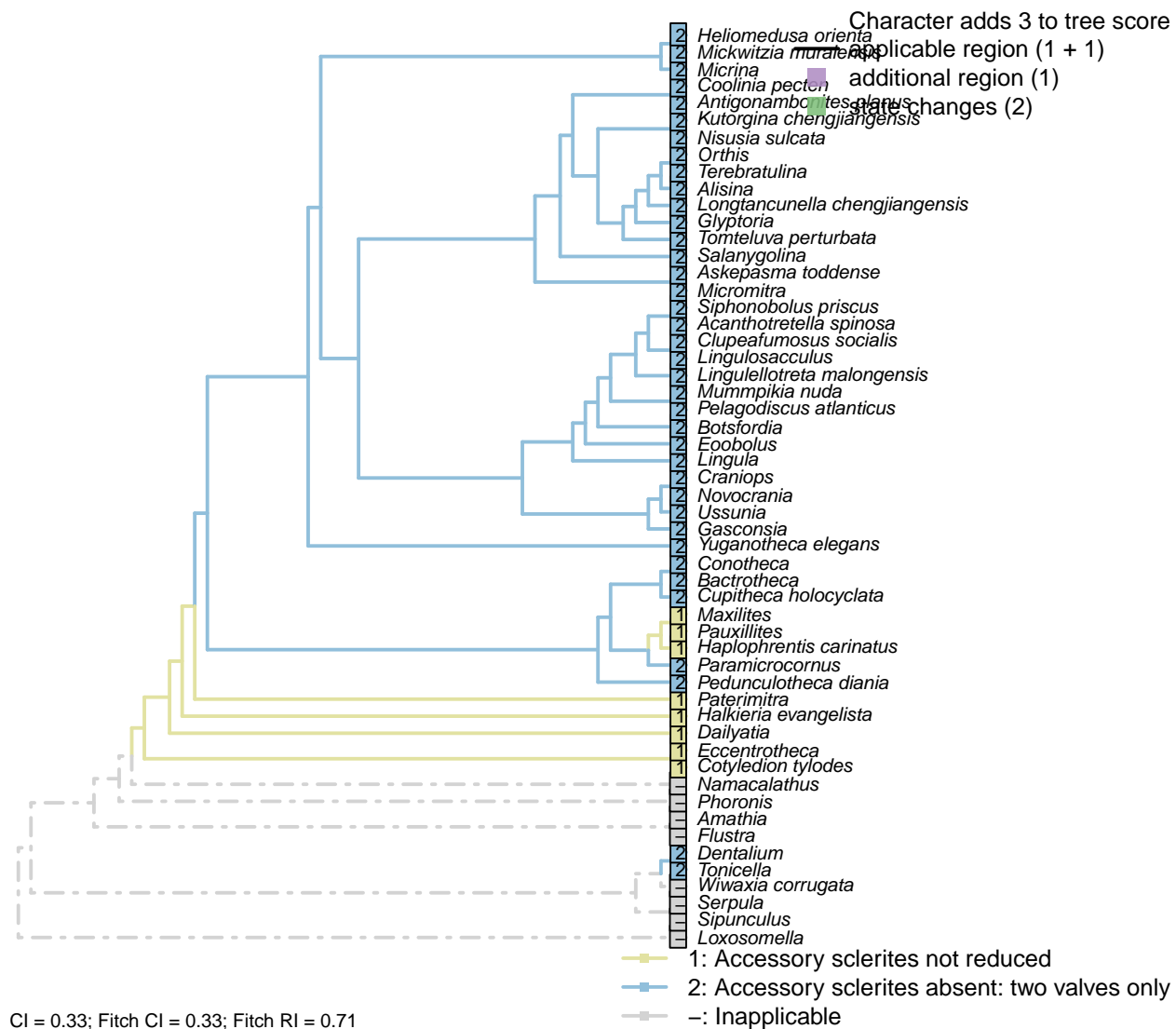
### Character 67: Sclerites: Bivalved

- 0: Scleritomous: without differentiated dorsal and ventral valves
  - 1: Bivalved: scleritome dominated by prominent dorsal and ventral valve
- Neomorphic character.

Scleritome dominated by prominent differentiated dorsal and ventral valves.

*Tonicella*: As larvae, polyplacophorans exhibit an anterior and a posterior shell field (Wanninger and Haszprunar, 2002a); subsequent subdivision of the posterior field gives rise to the posterior seven valves. *Tonicella* is thus tentatively coded as ‘bivalved’ to reflect the potential (if perhaps unlikely) homology with the paired elements of brachiopods.

## [68] Reduced

**Character 68: Sclerites: Accessory sclerites: Reduced**

- 1: Accessory sclerites not reduced
  - 2: Accessory sclerites absent: two valves only
- Transformational character.

Taxa in the bivalved condition may retain sclerites as small additional elements, such as the L-elements of *Paterimitra* (Skovsted et al., 2015). Hyolithid helens are coded as potentially homologous to these elements (following Moysiuk et al., 2017).

This character is treated as neomorphic, with accessory sclerites ancestrally present, recognizing the likely origin of brachiozoans (and Lophotrochozoans more generally) from a scleritomous organism.

*Conotheca*: [Reference needed: not found, but does this necessarily mean that they were absent?].

*Cupitheca holocyclus*: Helens never observed and considered absent (Skovsted et al., 2016).

*Dentalium*: The scaphopod valve arises posterior of the prototroch and is thus homologous with the posterior

valves of Chiton, assuming that molluscan shell fields are homologous features.

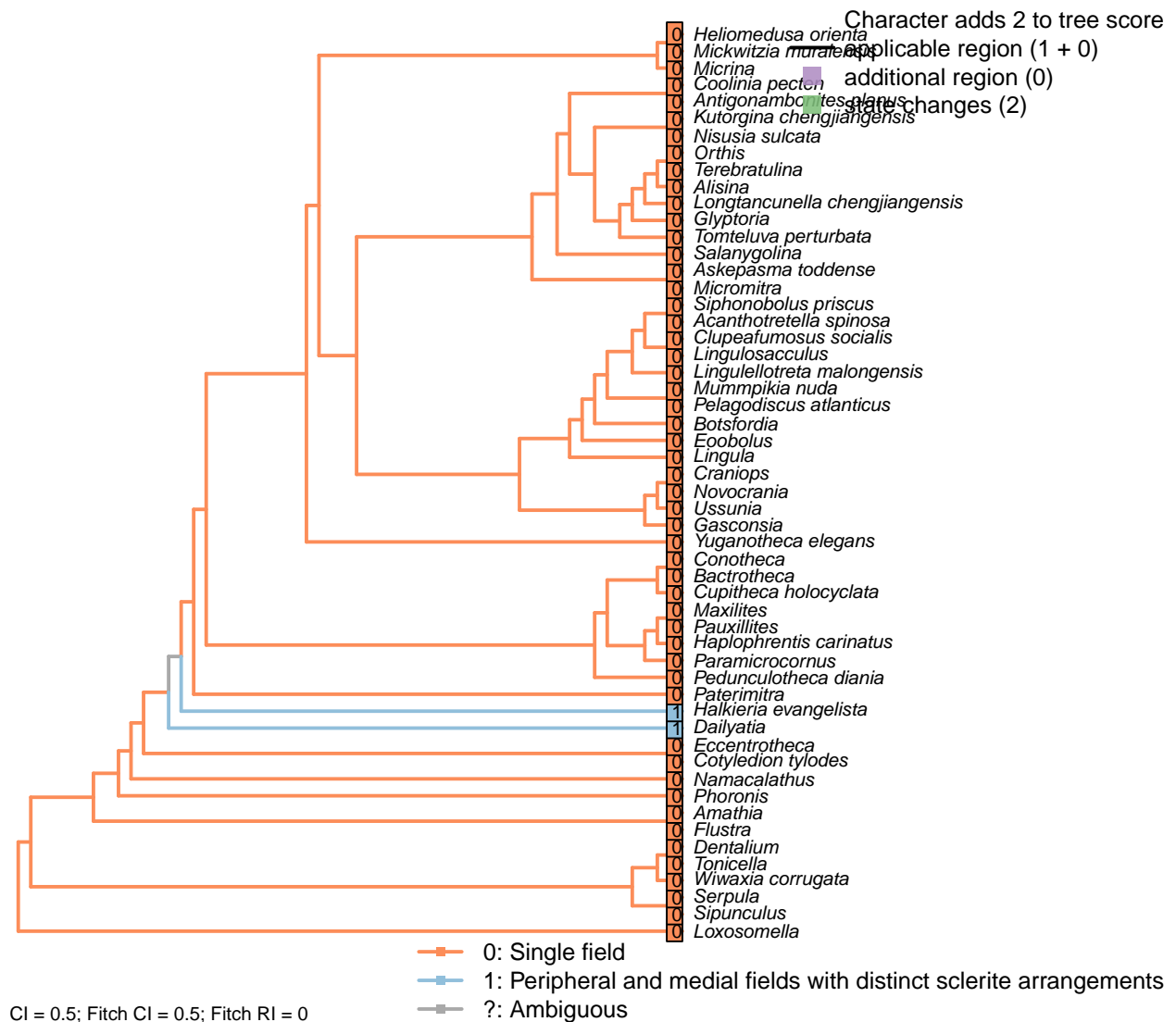
*Paramicrocornus*: Helens absent, with no possible insertion point (Zhang et al., 2018).

*Paterimitra*: L-sclerites (Skovsted et al., 2009).

*Pauxillites*: Not found by Valent and Corbacho (2015) or Marek (1966), but reconstructed as present by Marek (1976).

*Tonicella*: The intermediate shell plates arise by subdivision of the posterior shell field (Wanninger and Haszprunar, 2002a), and are thus treated as equivalent to the posterior valve rather than as distinct elements. The girdle elements are homologous with annelid chaetae / brachiopod setae (Leise and Cloney, 1982), rather than sclerites.

## [69] Arrangement



### Character 69: Sclerites: Accessory sclerites: Arrangement

0: Single field

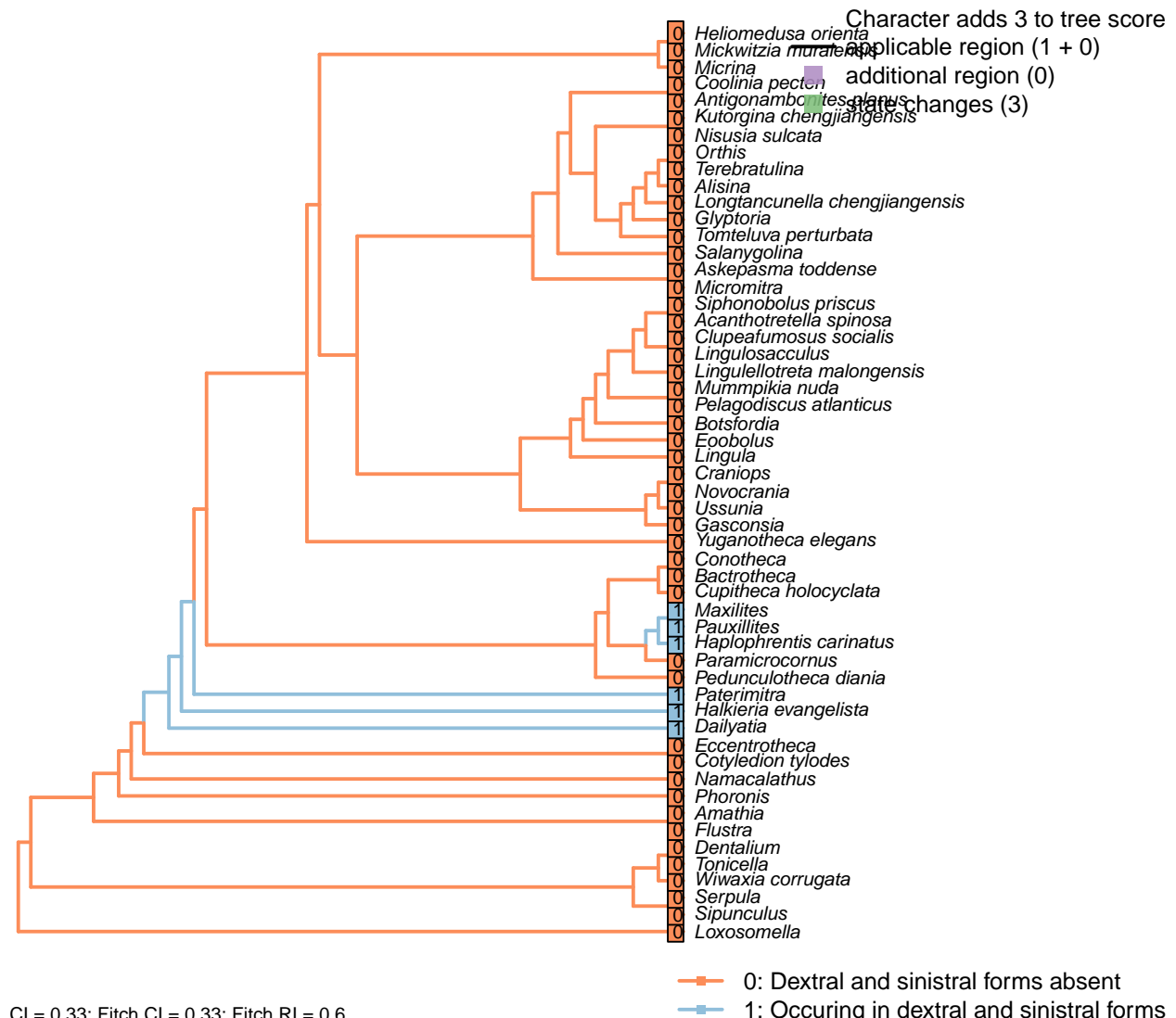
1: Peripheral and medial fields with distinct sclerite arrangements

Neomorphic character.

Following Zhao et al. (2017).

*Dailyatia*: Following the reconstruction of Skovsted et al. (2015).

## [70] Symmetry



### Character 70: Sclerites: Accessory sclerites: Symmetry

0: Dextral and sinistral forms absent

1: Occuring in dextral and sinistral forms

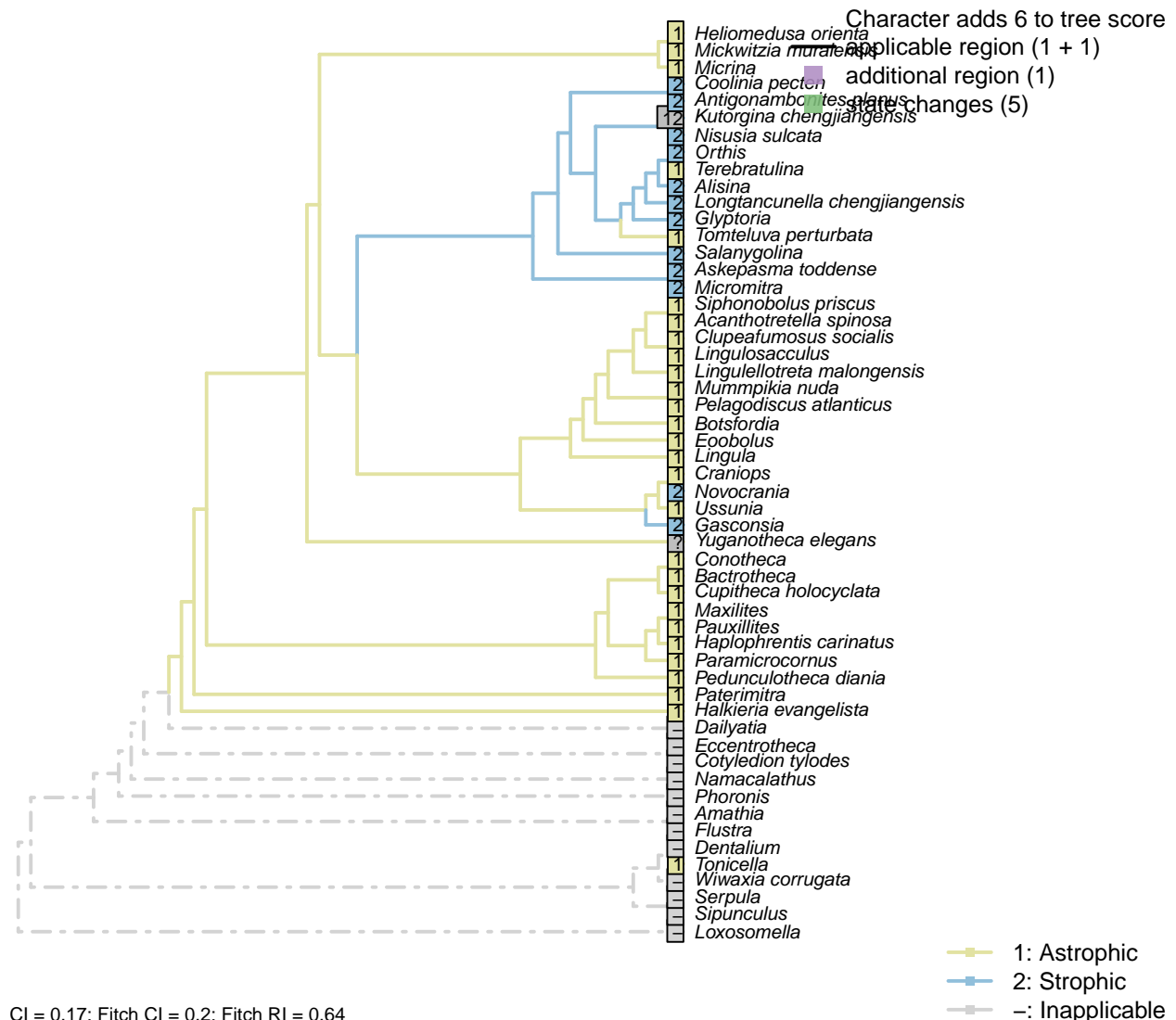
Neomorphic character.

Following Zhao et al. (2017).

*Eccentrotheca*: Skovsted et al. (2008).

*Haplophrentis carinatus*, *Maxilites*, *Pauxillites*: Helens are symmetrical.

## [71] Hinge line shape



(Holmer et al., 2014).

*Halkieria evangelista, Mickwitzia muralensis*: Non-strophic.

*Kutorgina chengjiangensis*: Williams et al. (1998b) (appendix 2) and Williams et al. (2000) (p. 208) consider the hinge of *Kutorgina* to be strophic, whereas Bassett *et al.* (2001) argue for an astrophic interpretation – whilst noting that the arrangement is prominently different from other astrophic taxa. We therefore code this taxon as ambiguous.

*Longtancunella chengjiangensis*: “*Longtancunella* has an oval to subcircular shell with a very short strophic hinge line” – Zhang et al. (2011a).

*Micrina*: Non-strophic: see Holmer et al. (2008).

*Nisusia sulcata*: “The strophic, articulated shells of the Kutorginata rotated on simple hinge mechanisms that are different from those of other rhynchonelliforms” (Williams et al., 2000, p. 208).

*Novocrania*: Craniides have a strophic posterior valve edge (Williams et al., 2007, table 39 on p. 2853): *Novocrania*’s “dorsal posterior margin” is “straight” (Williams et al., 2000, p. 171).

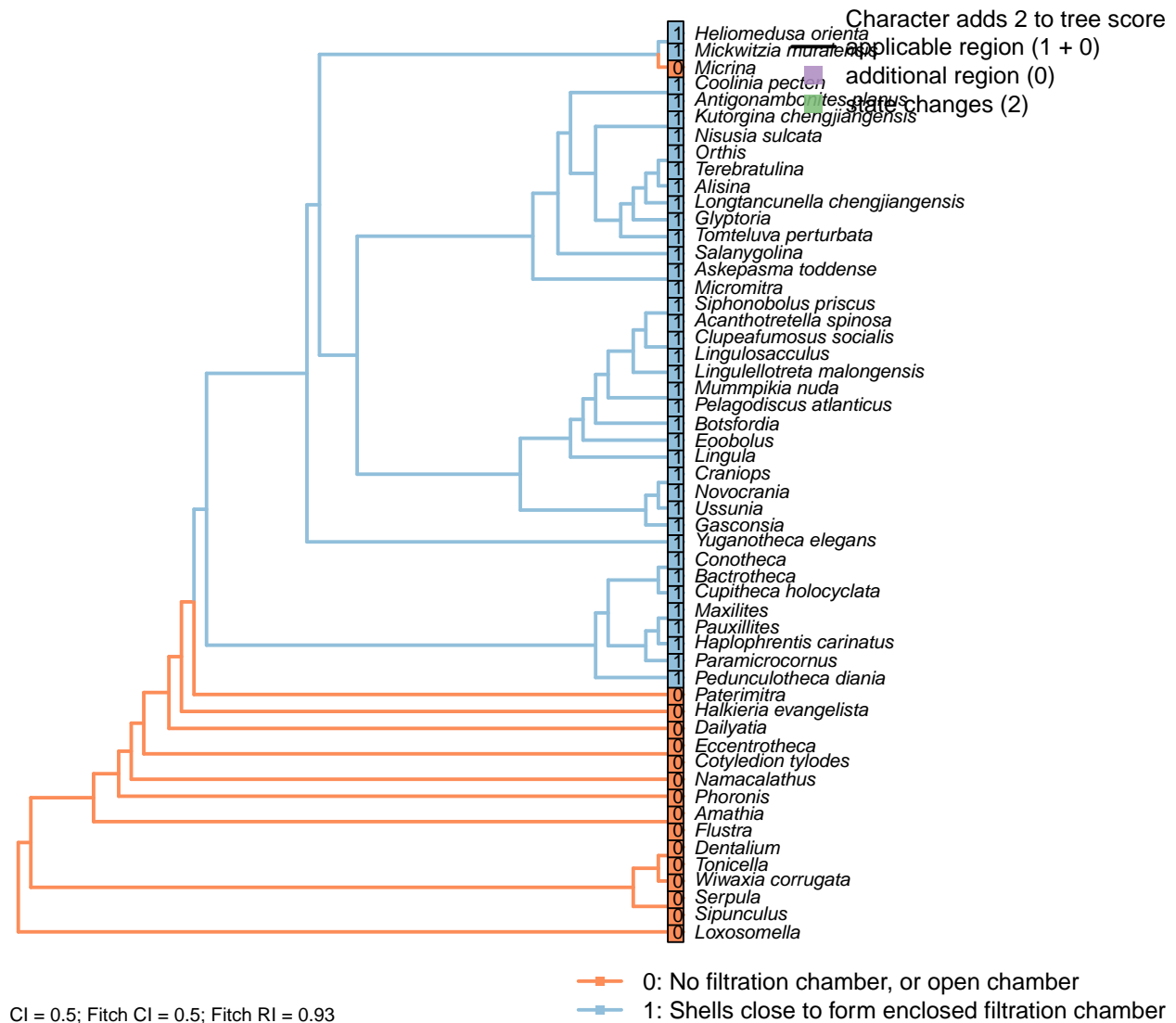
*Salanygolina*: Coded as strophic in Williams *et al.* (1998b); see Holmer et al. (2009).

*Tomteluva perturbata*: “Tomteluvid taxa all have a strongly ventribiconvex, astrophic shell with a unisulcate commissure” – Streng et al. (2016), p5.

*Tonicella*: A linear hinge articulation does not exist between valves 1 and 2; nor would it exist between valves 1 and 8 were these adjacent (Connors et al., 2012).

*Yuganotheca elegans*: Not evident from fossil material; the possibility of a short strophic hinge line (as in *Longtancunella*) is difficult to discount.

## [72] Enclosing filtration chamber

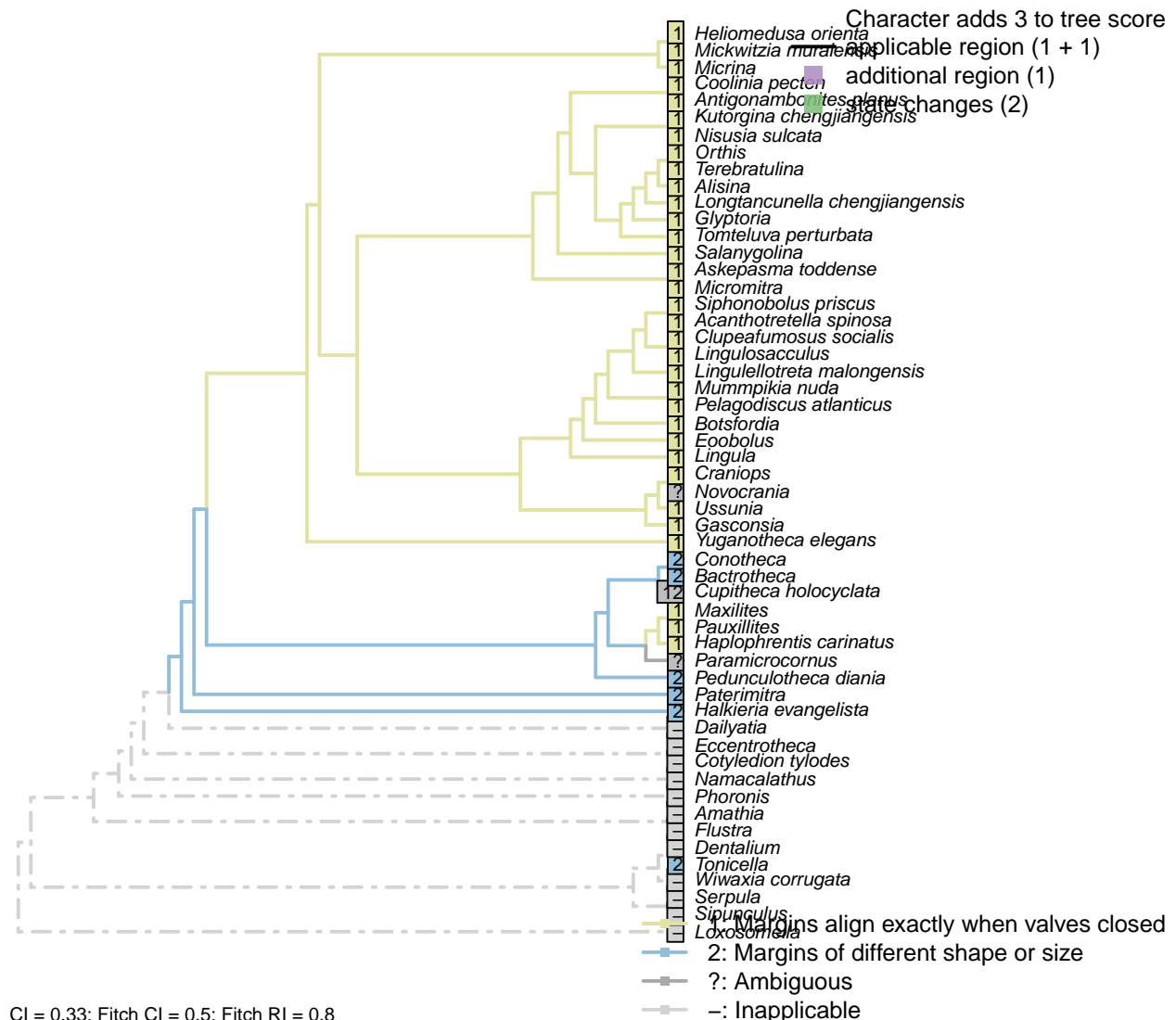


### Character 72: Sclerites: Bivalved: Enclosing filtration chamber

- 0: No filtration chamber, or open chamber
  - 1: Shells close to form enclosed filtration chamber
- Neomorphic character.

In crown-group brachiopods, the two primary shells close to form an enclosed filtration chamber. Further down the stem, taxa such as *Micrina* do not.

### [73] Commissure: Exact correspondence of valve margins



#### Character 73: Sclerites: Bivalved: Commissure: Exact correspondence of valve margins

- 1: Margins align exactly when valves closed
  - 2: Margins of different shape or size
- Transformational character.

Orthothecid hyoliths can retract their operculum into their conical shell, in contrast to most other taxa, where the valves align exactly when they are closed, save perhaps for a pedicle notch or, in the case of hyolithids, depressions that allow the lenses to protrude. Refers only to two prominent valves, not to additional sclerites of e.g. Eccentrotheca.

*Bactrotheca*: Operculum interpreted as sitting inside conical shell (Marek, 1976).

*Conotheca*: “The diameter of orthothecid opercula is generally slightly smaller than the diameter of the conch aperture. This observation is confirmed [in *Conotheca*] and further supported by the recurrent presence of opercula preserved withdrawn inside the conch” – Devaere et al. (2014).

*Cupitheca holocyclus*: “The width range of opercula matches that of the apertures” (Sun et al., 2018a), but

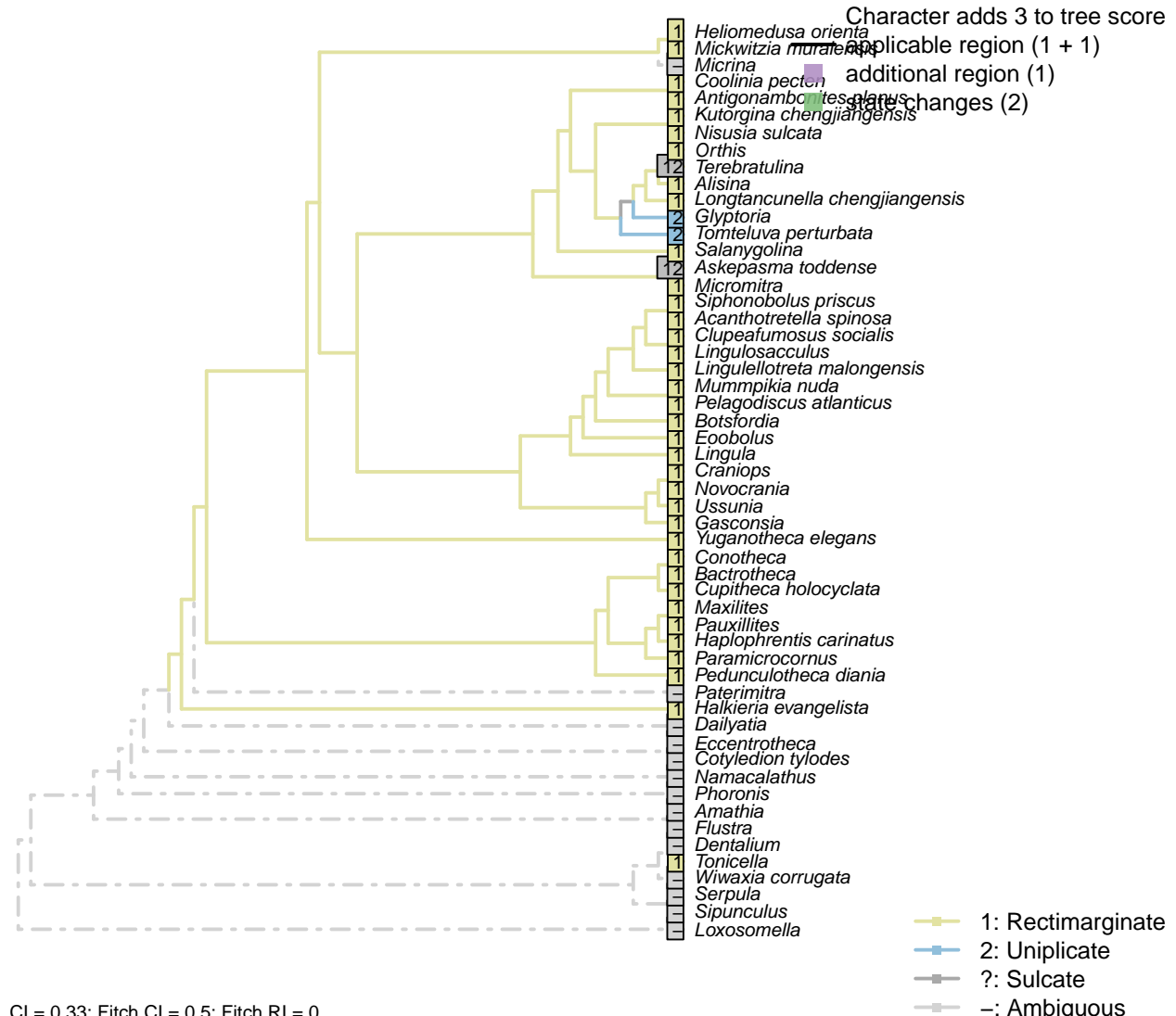
it is not possible to determine whether this is an exact match or whether the operculum may have been slightly smaller, and hence retractable, as anticipated for orthothecids.

*Maxilites*: Martí Mus and Bergström (2005).

*Paramicrocornus*: Articulated specimens unknown.

*Pauxillites*: Following depiction in Marek (1976).

## [74] Commissure: Sulcate



### Character 74: Sclerites: Bivalved: Commissure: Sulcate

1: Rectimarginate

2: Uniplicate

3: Sulcate

Transformational character.

The anterior commissure can be rectimarginate (i.e. straight), uniplicate (i.e. median sulcus in ventral valve),

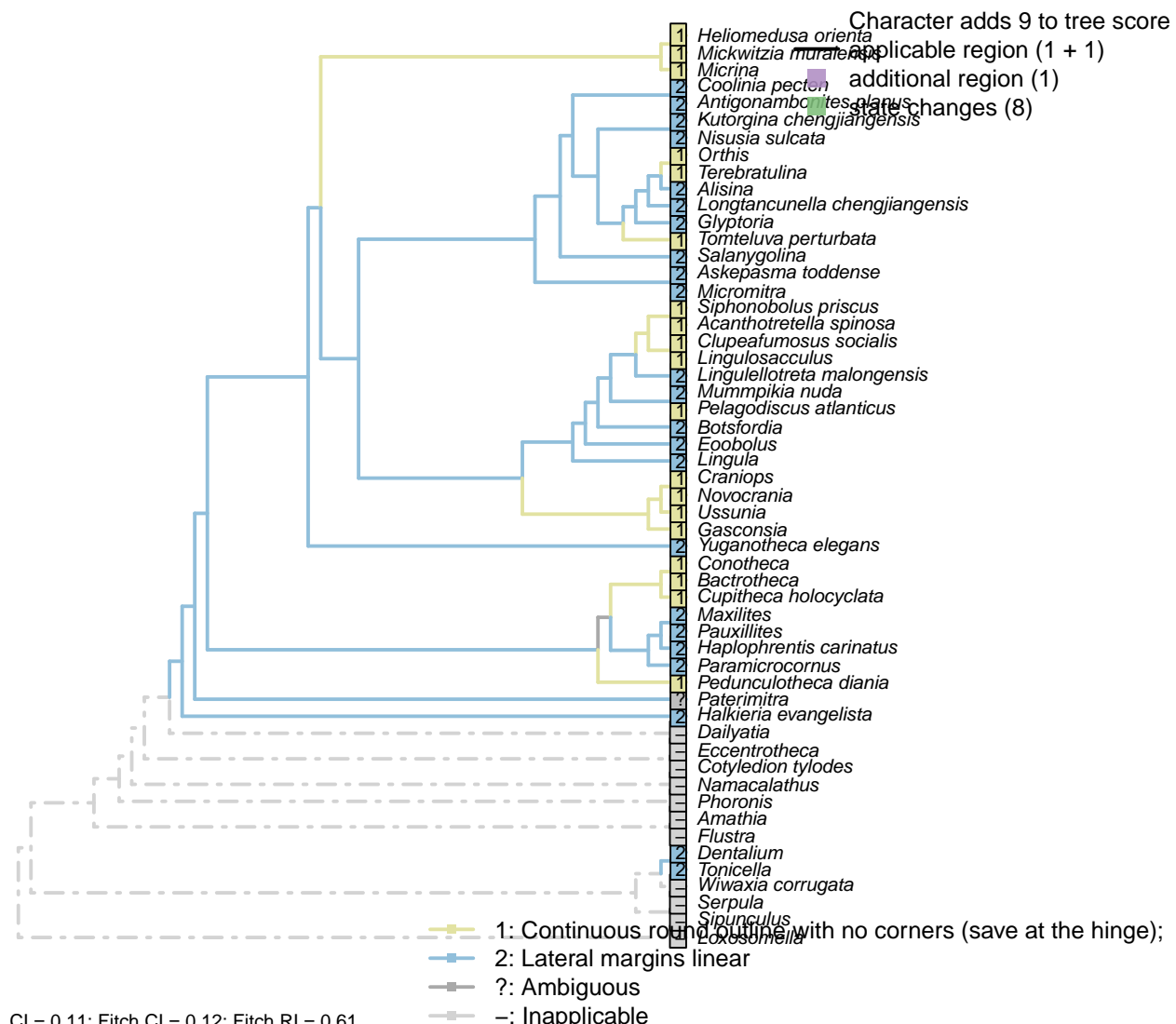
or sulcate (with median sulcus in dorsal valve).

*Askepasma toddense*: Coded as rectimarginate in Williams et al. (1998b), though note that the “ventral valve weakly to moderately sulcate” (Topper et al., 2013b); a similar description is provided by Williams et al. (2000). Coded as ambiguous for these two states accordingly.

*Micromitra*, *Glyptoria*, *Kutorgina chengjiangensis*, *Salanygolina*: Following appendix 2 in Williams et al. (1998b).

*Terebratulina*: “Anterior commissure rectimarginate to uniplicate” – uniplicate in fig. 1425.1c of Williams et al. (2006).

## [75] Commissure: Circular



Shape of the commissure in plan view, ignoring any deflection arising due to articulation at the hinge (e.g. delthyrium/notothyrium). This character seeks to discriminate the essentially conical ‘conchs’ of orthothecid hyoliths from the polygonal ‘conchs’ of hyolithids. Triangular and oblong outlines are not distinguished, as this is not entirely independent of the strophic/astrophic nature of the hinge.

*Acanthotretella spinosa*: Round (Holmer and Caron, 2006).

*Alisina*: Sub-triangular (Zhang et al., 2011b).

*Askepasma toddense*, *Antigonambonites planus*, *Coolinia pecten*, *Glyptoria*, *Nisusia sulcata*: Lateral margins subparallel, cf. *Askepasma* (Williams et al., 2000).

*Bactrotheca*: Operculum essentially round, though becoming flattened on functionally ventral surface (Dzik, 1980).

*Botsfordia*: Diverging lateral margins (Li and Holmer, 2004).

*Clupeafumosus socialis*: Round (Topper et al., 2013a).

*Craniops*, *Siphonobolus priscus*: Round (Williams et al., 2000).

*Dentalium*: Opening essentially polygonal (a rolled rectangle).

*Eoobolus*: Essentially triangular (Williams et al., 2000).

*Gasconsia*: Round, hinge notwithstanding (Hanken and Harper, 1985).

*Halkieria evangelista*: Anterior shell essentially triangular.

*Kutorgina chengjiangensis*: Lateral margins subparallel (Williams et al., 2000, fig. 125); clear angular corners in *K. chengjiangensis* (Holmer et al., 2018b).

*Lingulellotreta malongensis*: Linear, diverging lateral margins (Zhang et al., 2007a).

*Lingulosacculus*: Round (Balthasar and Butterfield, 2009).

*Mickwitzia muralensis*: Round (Balthasar, 2004).

*Micrina*: Mitral valve aperture essentially round (Holmer et al., 2008).

*Micromitra*: Lateral margins subparallel, cf. *Askepasma* (Robson and Pratt, 2001).

*Mummpikia nuda*: Polygonal (Balthasar, 2008).

*Novocrania*, *Pelagodiscus atlanticus*: Essentially round (Williams et al., 2000).

*Orthis*: Essentially round, hinge notwithstanding (Williams et al., 2000, fig. 523).

*Paramicrocornus*: Polygonal (Zhang et al., 2018).

*Paterimitra*: Broad posterior sinus: not directly comparable with brachiopod condition.

*Pauxillites*: Subtriangular (Malinky, 1987).

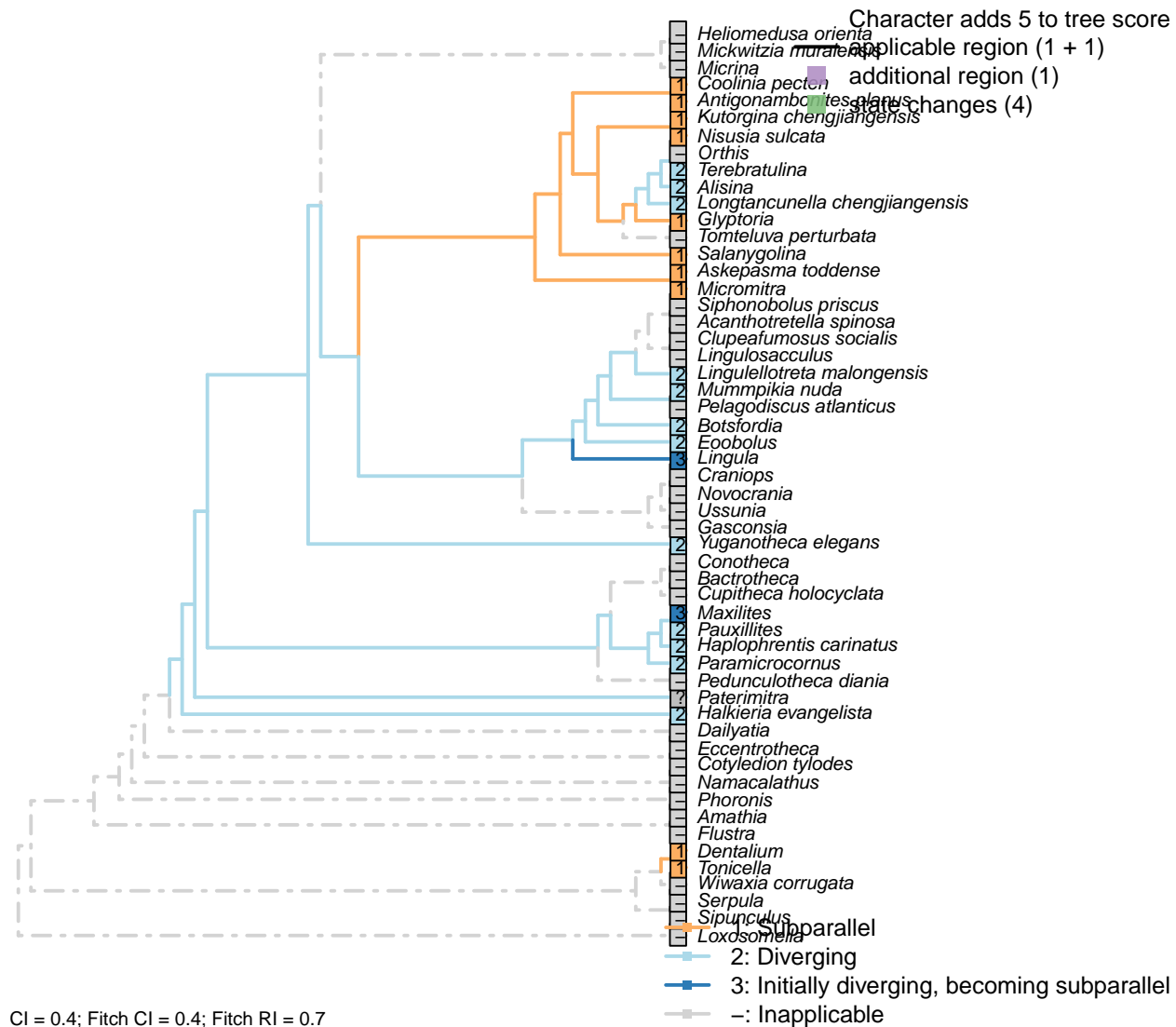
*Salanygolina*: Short subparallel stretch of lateral sides of adult shell (Holmer et al., 2009, fig. 1a), recalling D-shaped profile of *Askepasma*.

*Tomteluva perturbata*: Essentially round, sulcus notwithstanding (Streng et al., 2016).

*Ussunia*: Essentially round, hinge notwithstanding (Williams et al., 2000).

*Yuganotheca elegans*: Polygonal (Zhang et al., 2014).

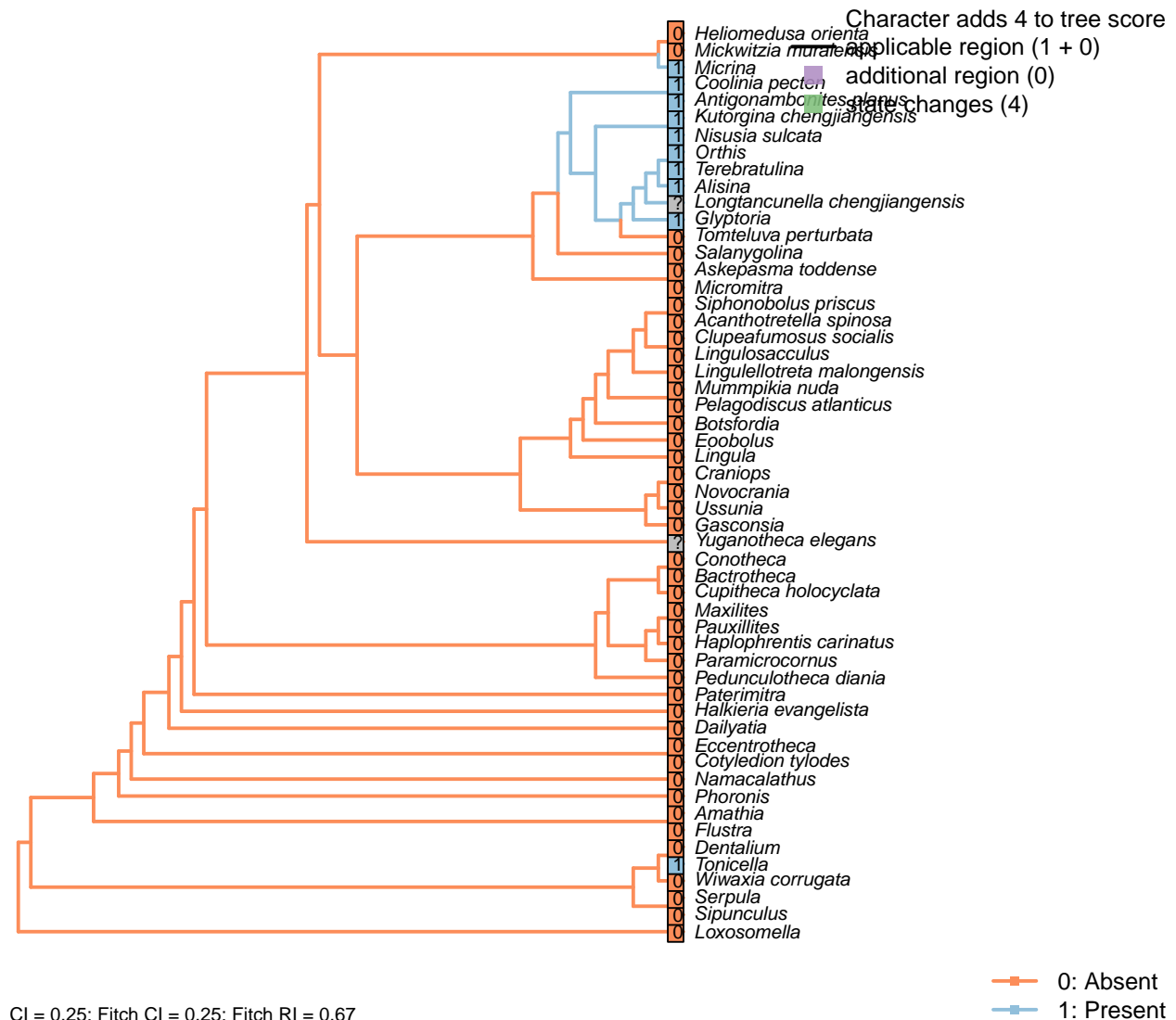
## [76] Commissure: Lateral margins



If lateral margins are linear, are the subparallel (i.e. commissure profile oblong, with long hinge) or diverging (i.e. commissure profile triangular, with short hinge)?

*Maxilites*: Initially diverging, becoming subparallel (Martí Mus and Bergström, 2005).

## [77] Apophyses



### Character 77: Sclerites: Bivalved: Apophyses

0: Absent

1: Present

Neomorphic character.

*Micrina*, like many brachiopods, bears tooth-like structures or processes that articulate the two primary valves. Caution must be applied before taxa are coded as “absent”, as teeth can be subtle and may be overlooked.

*Alisina*: “Strophic articulation with paired, ventral denticles, composed of secondary shell” – definition of family Trematobolidae in Williams et al. (2000).

*Clupeafumosus socialis*: No articulating processes evident or reported by Topper et al. (2013a).

*Gasconsia*: “Articulatory structure comprising ventral cardinal socket and dorsal hinge plate [...] The shape of the shell probably correlates strongly with the unique type of articulation, which consists of a dorsal hinge plate that fits tightly into a cardinal socket in the ventral valve, with a concave homeodeltidium in the center

of the ventral interarea” – Williams et al. (2000), p.184, concerning order Trimerellida.

*Kutorgina chengjiangensis*, *Nisusia sulcata*: Kutorginata don’t have teeth or dental sockets, but their shells are articulated by “two triangular plates formed by dorsal interarea, bearing oblique ridges on the inner sides” (Williams et al., 2000, p. 211); this simple hinge mechanism is different from other rhynchonelliforms (Williams et al., 2000, p.208), but serves an equivalent purpose and is thus potentially homologous. We thus code kutorginids as present, using a subsequent character to capture difference in tooth morphology.

*Mickwitzia muralensis*: Not reported by or evident in Balthasar (2004).

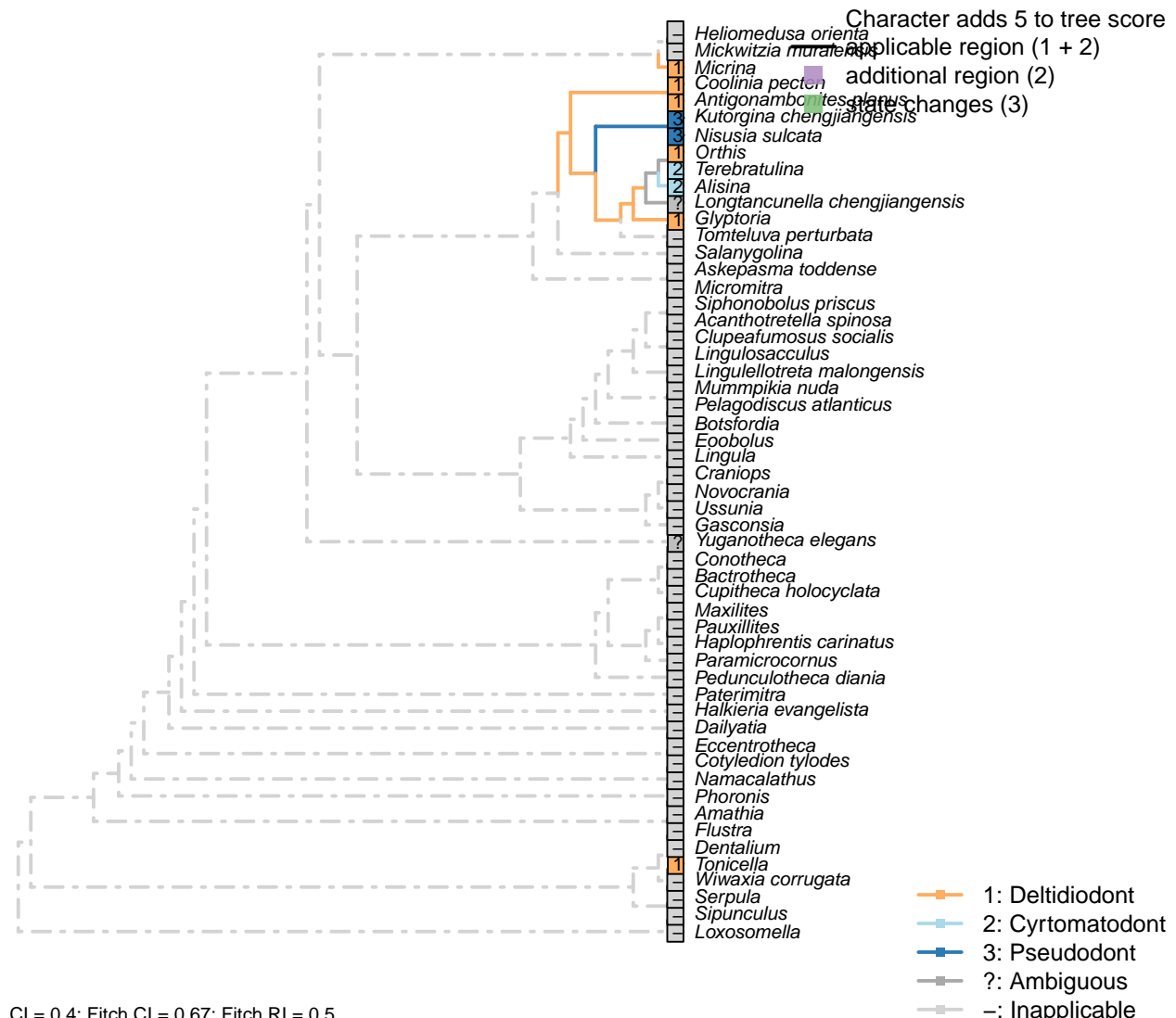
*Mummpikia nuda*: No articulation structures are evident; instead, the propareas are rotated inwards (Balthasar, 2008). The definition of Family Obolellidae in Williams et al. (2000) notes that articulation may be lacking or vestigial in the group.

*Tomteluva perturbata*: Tomteluvids [...] lack articulation structures such as teeth and sockets (Streng et al., 2016).

*Tonicella*: The sutural laminae correspond in function and position to brachiopod apophyses (Connors et al., 2012), and so are coded as potentially homologous.

*Ussunia*: “articulatory structures poorly developed” – Williams et al. (2000), p. 192.

## [78] Apophyses: Morphology



### Character 78: Sclerites: Bivalved: Apophyses: Morphology

- 1: Deltidiodont
  - 2: Cyrtomatodont
  - 3: Pseudodont
- Transformational character.

Deltidiodont teeth are simple hinge teeth developed by the distal accretion of secondary shell; Cyrtomatodont teeth are knoblike or hook-shaped hinge teeth developed by differential secretion and resorption of the secondary shell (fig. 322 in Williams et al., 1997).

Kutorginata (here represented by *Kutorgina* and *Nisusia*) don't have teeth (apophyses) or dental sockets, but their shells are articulated by "two triangular plates formed by dorsal interarea, bearing oblique ridges on the inner sides" (Williams et al., 2000, p. 211); this simple hinge mechanism is different from other rhynchonelliforms [Williams et al. (2000), p.208; table 13 character 30], and is described as a "pseudodont

articulation" (Holmer et al., 2018a).

*Antigonambonites planus*, *Glyptoria*: Coded as deltidiodont in Benedetto (2009).

*Kutorgina chengjiangensis*: "Articulation characterized by two triangular plates formed by dorsal interarea, bearing oblique ridges on the inner sides" – Williams et al. (2000), p. 211.

*Micrina*: The simple knob-like teeth of *Micrina* show no evidence of resprobtion or the hook-like shape that characterises Cyrtomatodont teeth.

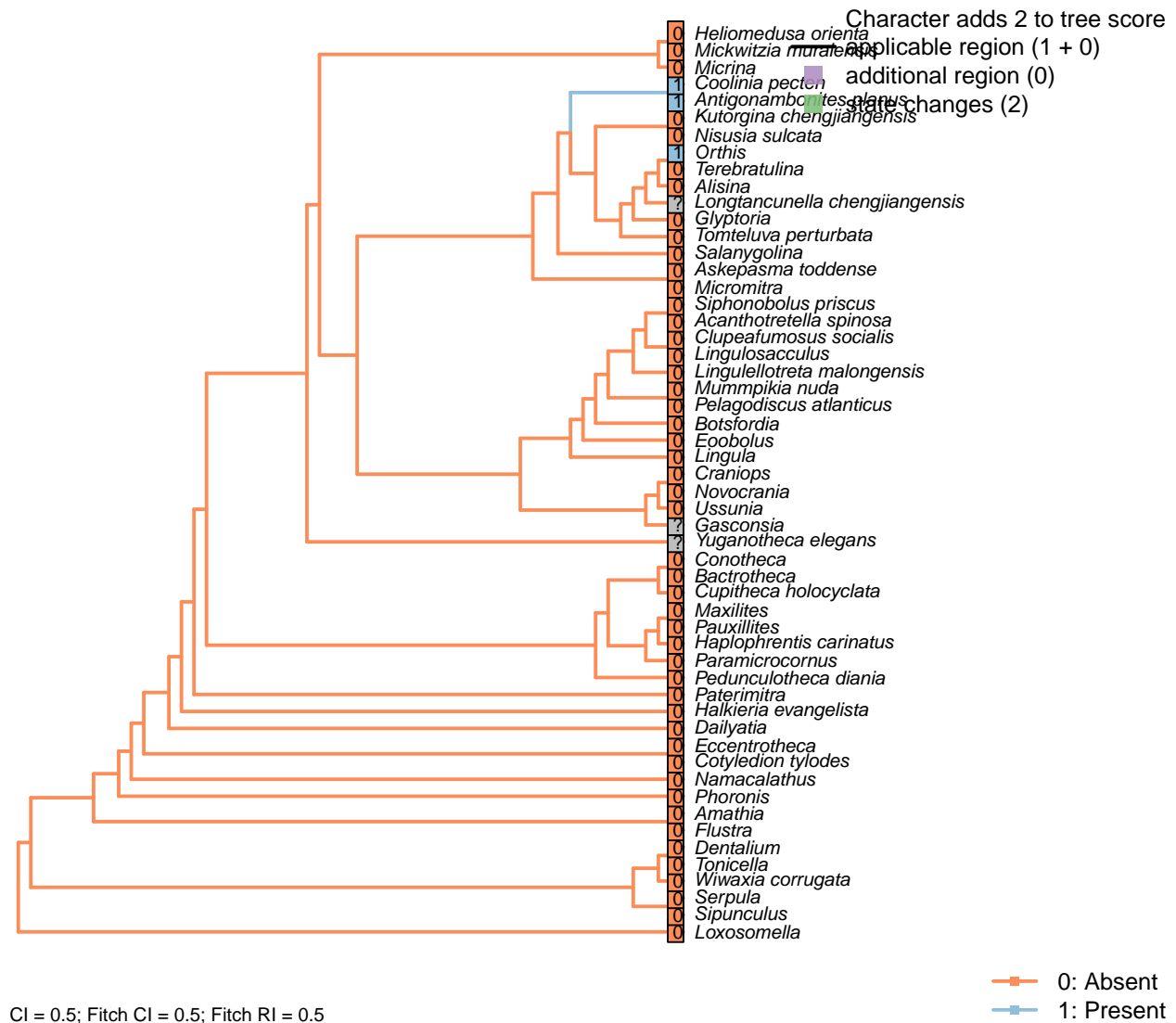
*Nisusia sulcata*: The 'teeth' are formed by the distal lateral extensions from the ventral pseudodeltidium fitting into the 'sockets' on the inner side of the dorsal interarea (Holmer et al., 2018a). [Coded as "deltidiodont teeth absent" in Benedetto (2009)].

*Orthis*: Coded as deltidiodont (in *Eoorthis*) in Benedetto (2009).

*Terebratulina*: Cyrtomatodont – see fig. 322 in Williams et al. (2000).

*Tonicella*: Chiton apophyses (sutural laminae) are accretions deriving from the ventral shell layer of the intermediate and tail valves (Schwabe, 2010), so correspond to the deltidiodont situation in brachiopods.

## [79] Apophyses: Dental plates



### Character 79: Sclerites: Bivalved: Apophyses: Dental plates

0: Absent

1: Present

Neomorphic character.

Williams et al. (1997) (p362) write: “Teeth [...] are commonly supported by a pair of variably disposed plates also built up exclusively of secondary shell and known as dental plates (Fig. 323.1, 323.3).”

Dewing (2001) elaborates: “Dental plates are near-vertical, narrow sheets of shell tissue between the antero-medial edge of the teeth and floor of the ventral valve. They are a composite structure, resulting from the growth of teeth over the ridge that bounds the ventral-valve muscle field.”

Williams et al. (2000) (p.201) write: “The denticles lack supporting structures in all Obolellida, but in Naukatida they are supported by an arcuate plate below the interarea, the anterise (Fig. 119.3a).”

The anterise is conceivably homologous with the dental plates, thus the presence of either is coded “present”

for this character.

*Antigonambonites planus*: Coded as present (well developed) in Benedetto (2009).

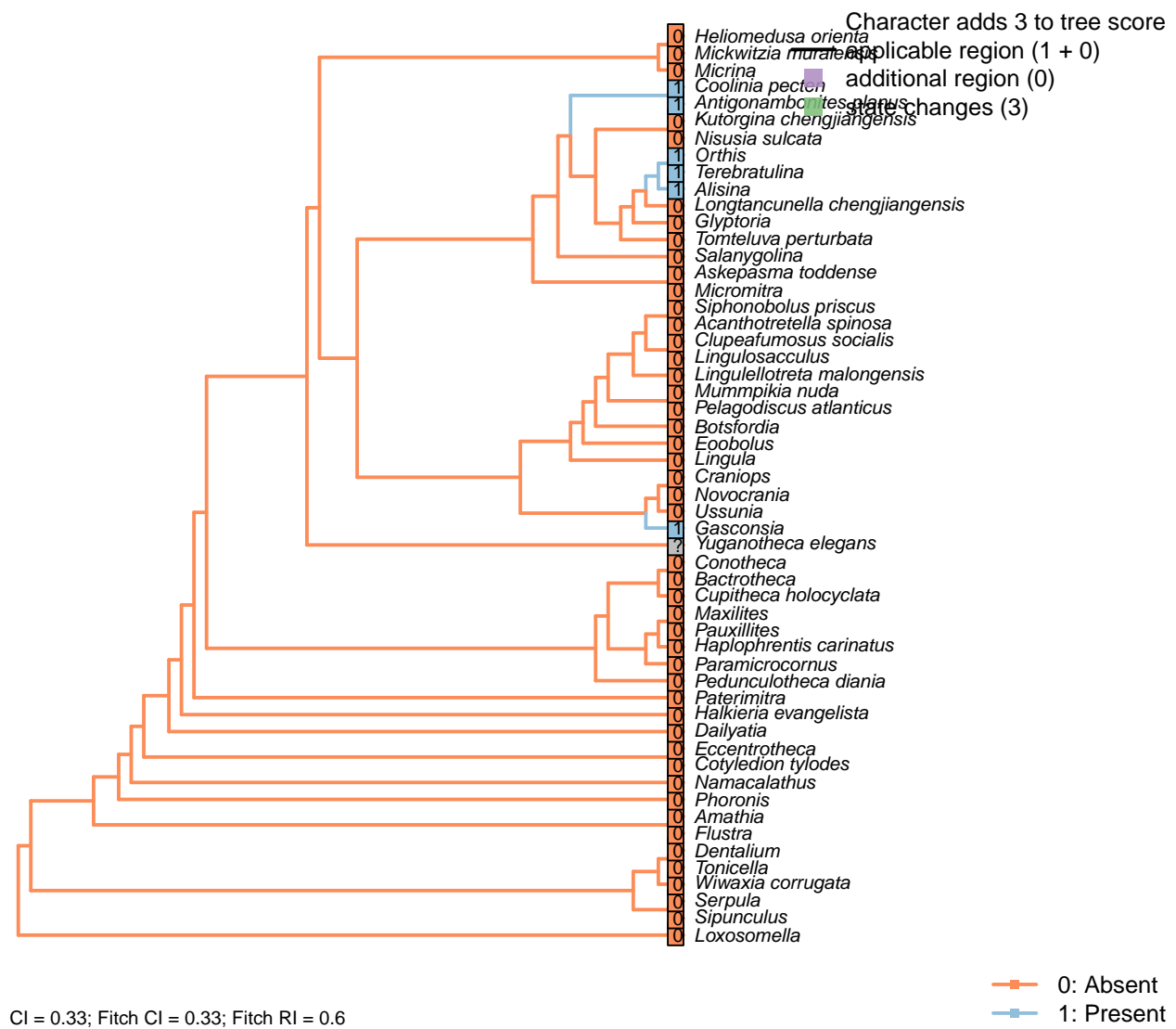
*Coolinia pecten*: Coded as present following Dewing (2001), who seems to use the term Strophomenoids to encompass *Coolinia*, and attests to the presence of dental plates.

*Gasconsia*: Coded ambiguous to reflect the possibility that the hinge plate in trimerellids is homologous to the dental plates of other taxa, and has replaced the teeth themselves as the primary articulatory mechanism (see Williams et al., 2000, p. 184, for details of the articulation).

*Glyptoria, Nisusia sulcata*: Coded as absent in Benedetto (2009).

*Orthis*: Coded as present (short and recessive, in *Eoorthis*) in Benedetto (2009).

## [80] Sockets



CI = 0.33; Fitch CI = 0.33; Fitch RI = 0.6

### Character 80: Sclerites: Bivalved: Sockets

0: Absent

1: Present

Neomorphic character.

Simplified from Bassett *et al.* (2001) character 16.

This character is independent of apophyses, as several taxa bear sockets without corresponding teeth; the function of these sockets is unknown.

See figs 323ff in Williams *et al.* (1997).

*Alisina*: “bearing sockets, bounded by low ridges” – Williams *et al.* (2000).

*Antigonambonites planus*: Coded as present in Benedetto (2009).

*Gasconsia*: “Articulatory structure comprising ventral cardinal socket and dorsal hinge plate” – Williams *et al.* (2000), p. 184.

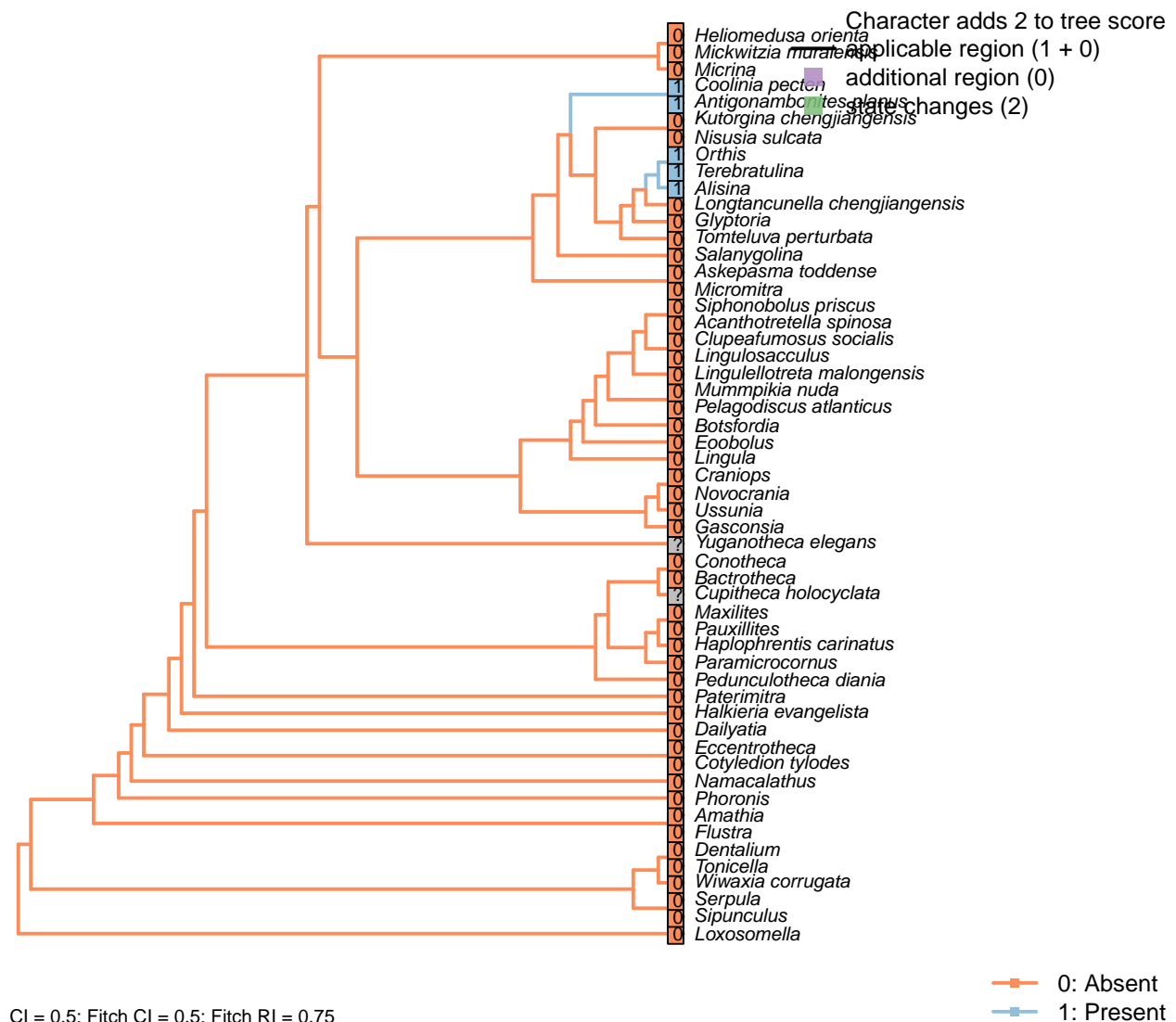
*Glyptoria, Nisusia sulcata*: Coded as absent in Benedetto (2009).

*Mickwitzia muralensis*: Not reported by or evident in Balthasar (2004).

*Tomteluva perturbata*: Tomteluvids [...] lack articulation structures such as teeth and sockets (Streng *et al.*, 2016).

*Ussunia*: Following table 15 in Williams *et al.* (2000).

## [81] Socket ridges



## Character 81: Sclerites: Bivalved: Socket ridges

0: Absent

1: Present

Neomorphic character.

After Bassett *et al.* (2001) character 17. May be difficult to distinguish from a brachiophore (see Fig 323 in Williams *et al.*, 1997), so the two structures are not distinguished here.

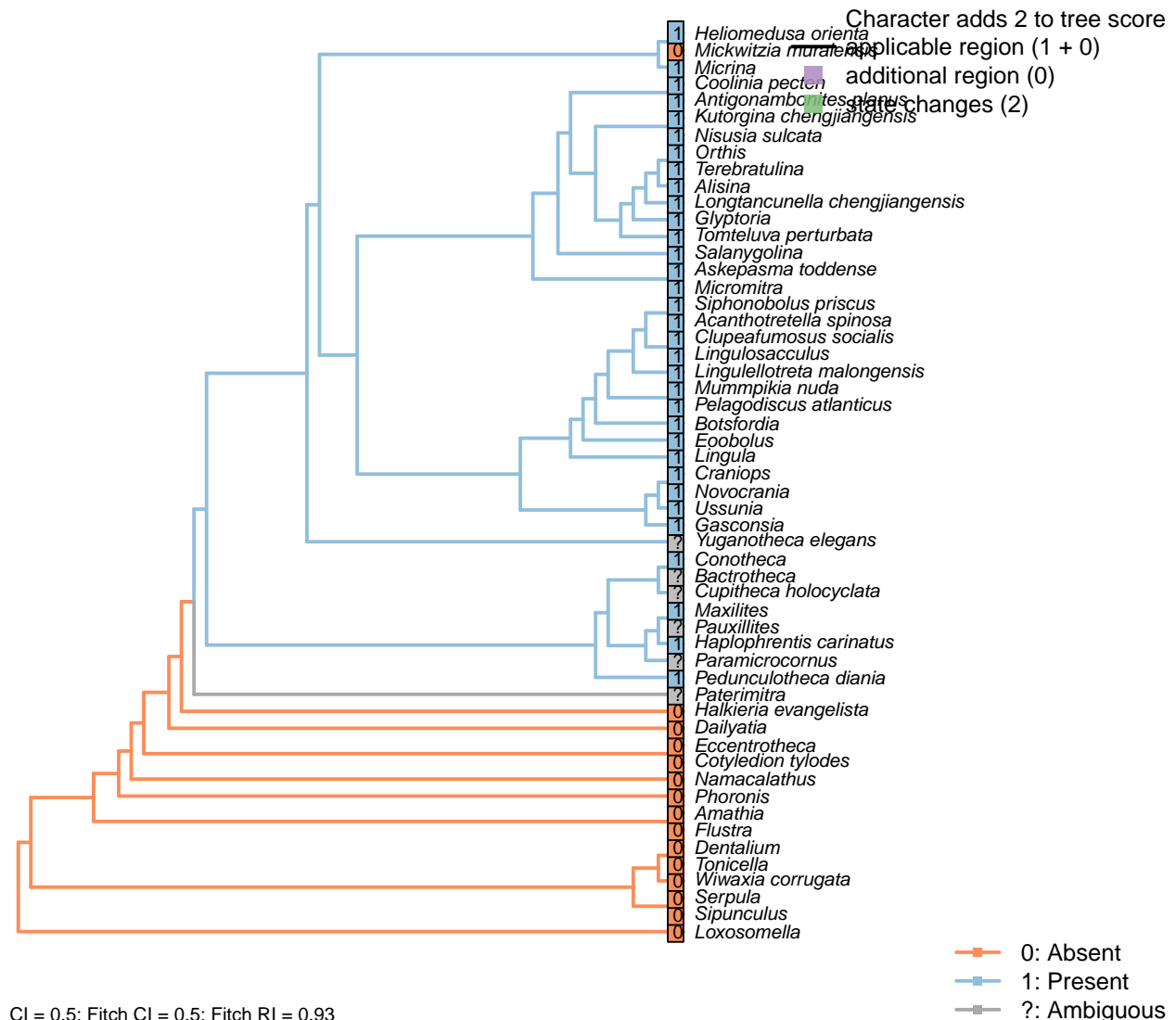
*Alisina*: “bearing sockets, bounded by low ridges” – Williams *et al.* (2000).

*Antigonambonites planus*: Coded as present in Benedetto (2009).

*Glyptoria*, *Nisusia sulcata*: Coded as absent in Benedetto (2009).

*Tomteluva perturbata*: Tomteluvids [...] lack articulation structures such as teeth and sockets (Streng *et al.*, 2016).

## [82] Muscle scars: Ventral



## Character 82: Sclerites: Bivalved: Muscle scars: Ventral

0: Absent

1: Present

Neomorphic character.

After Bassett *et al.* (2001) character 6.*Alisina*: Muscle scars scored based on *Alisina comleyensis* (Bassett *et al.*, 2001).*Bactrotheca*: "Muscle scars were not found" – Valent *et al.* (2012).*Conotheca*: [Reference needed].*Halkieria evangelista*: Muscle scars are known from the Type A, but not Type B, morphs of the halkieriid

*Oikozetetes* (Paterson et al., 2009; Jacquet et al., 2014).

*Mickwitzia muralensis*: Scars absent; instead, cones ornament shell's internal surface.

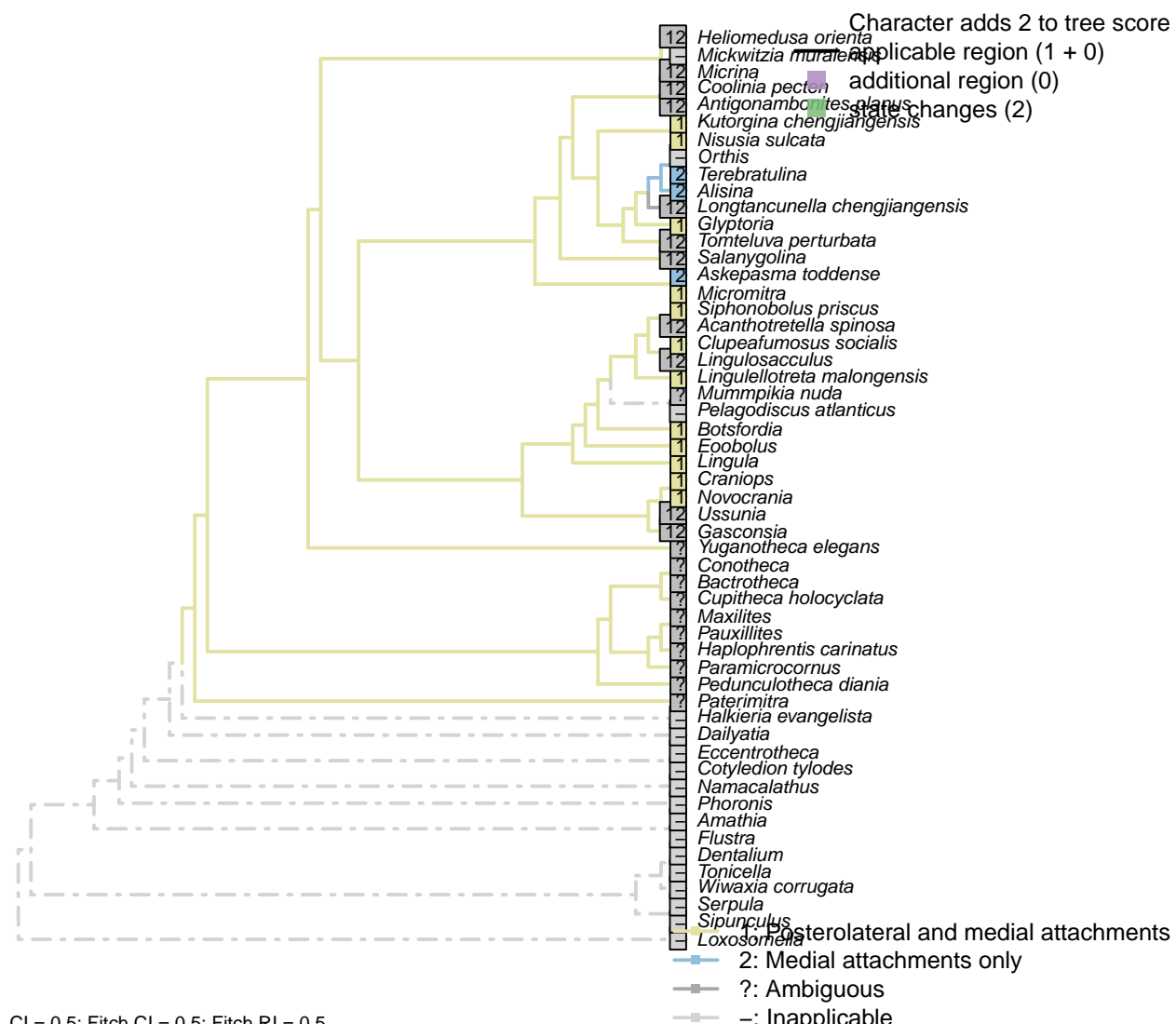
*Micrina*: Prominent ventral muscle scars – see e.g. Holmer et al. (2008), fig. 1f.

*Paramicrocornus*: Not preserved in conchs, though likely present (by analogy with *Maxilites*) (Zhang et al., 2018).

*Tonicella*: Absent (Schwabe, 2010).

*Ussunia*: Scars preserved on ventral valve (Nikitin and Popov, 1984).

### [83] Muscle scars: Ventral: Position



CI = 0.5; Fitch CI = 0.5; Fitch RI = 0.5

#### Character 83: Sclerites: Bivalved: Muscle scars: Ventral: Position

1: Posterolateral and medial attachments

2: Medial attachments only

Transformational character.

Muscles can attach to the ventral valve posterolaterally to, as well as between, the *vascula lateralia* (Popov, 1992).

*Acanthotretella spinosa*: “Individual muscle scars cannot be distinguished” – Holmer and Caron (2006).

*Alisina*: Following reconstruction of Gorjansky & Popov (1986).

*Askepasma toddense*: Restricted to medial field, following the interpretation of the musculature presented by Williams *et al.* (2000), fig. 81.

*Clupeafumosus socialis*: Coded following *Hadrotreta*, as illustrated in Popov (1992).

*Craniops*: See fig. 89 in Williams *et al.* (2000).

*Eoobolus*: The ‘laterals’ of Balthasar (2009, fig. 5) are situated almost upon the *vascula lateralia*; they are interpreted as sitting posterolateral to them.

*Gasconsia*: Musculature described in Hanken & Harper (1985), but location of mantle canals unknown.

*Glyptoria*: Posterolateral reflected by diductor attachments; see fig. 18.3.2 in Bassett *et al.* (2001).

*Kutorgina chengjiangensis*: Following situation in *Nisusia*; see fig. 18.2 in Bassett *et al.* (2001).

*Lingulellotreta malongensis*: See fig. 5 in Holmer *et al.* (1997).

*Micromitra*: Posteriomedial muscle field (Williams *et al.*, 1998b, text-fig. 6) treated as equivalent to postero-lateral muscles.

*Nisusia sulcata*: Posterolateral diductors (fig. 18.2 in Bassett *et al.*, 2001).

*Novocrania*: Posterior adductor muscles attach posterolaterally to ventral mantle canal (Robinson, 2014).

*Orthis*: Not applicable: *vascula lateralia* not comparable to those of other taxa.

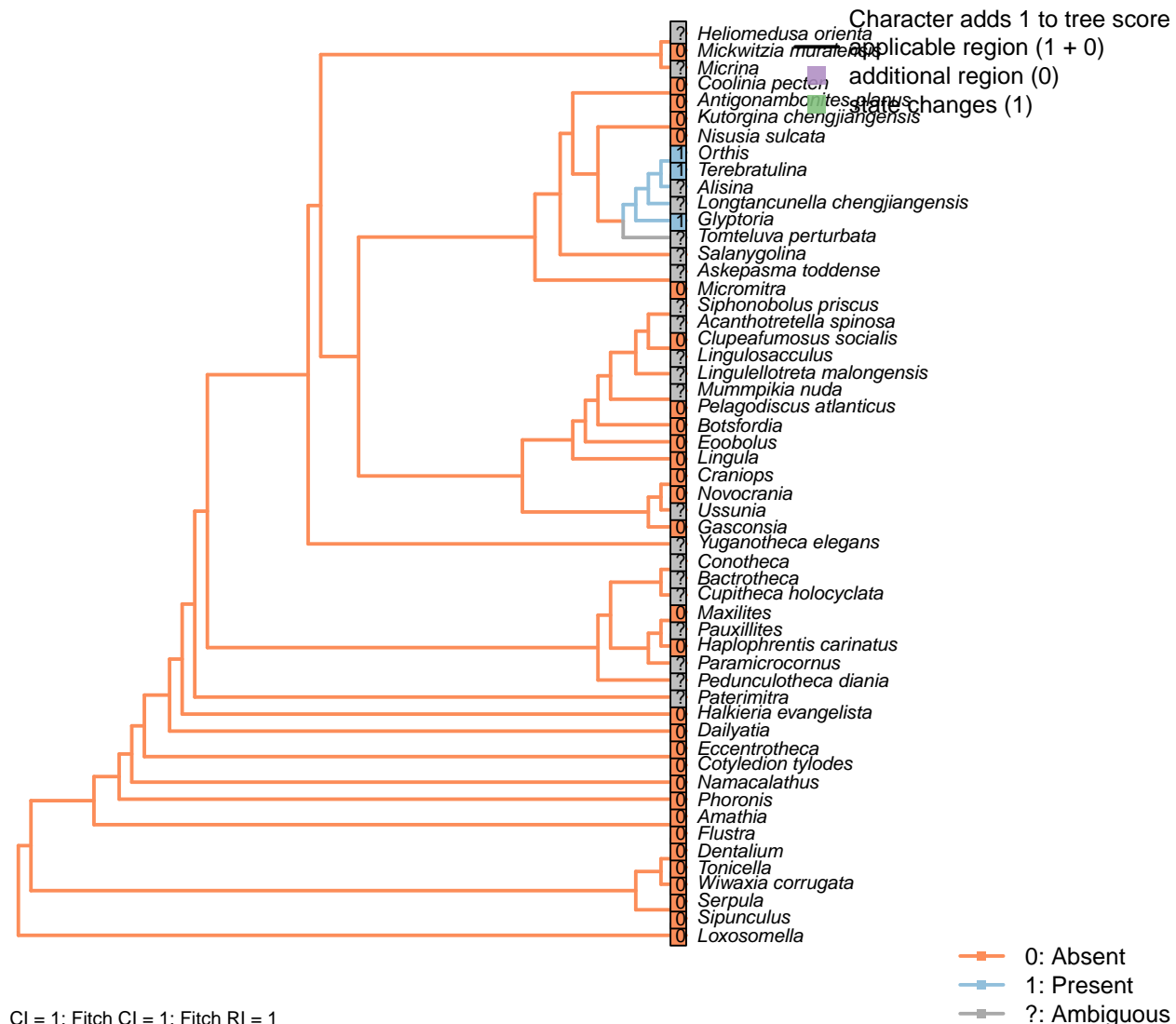
*Pelagodiscus atlanticus*: Inapplicable as vascular system not directly equivalent to the canonical; see. fig 6b in Balthasar (2009).

*Salanygolina*: Ventral musculature not clearly constrained (Holmer *et al.*, 2009).

*Siphonobolus priscus*: Coded following general siphonotretid condition described by Popov (1992, p. 407).

*Ussunia*: Internal anatomy not adequately preserved to evaluate (Nikitin and Popov, 1984).

## [84] Muscle scars: Adjustor

**Character 84: Sclerites: Bivalved: Muscle scars: Adjustor**

0: Absent

1: Present

Neomorphic character.

After Bassett *et al.* (2001) character 7.

This character is contingent on the presence of a pedicle. Extreme caution must be used in inferring an absent state, as adjustor scars can be extremely difficult to distinguish from the adductor scars.

*Alisina*: Muscle scars scored based on *Alisina comleyensis* (Bassett *et al.*, 2001). The presence of an adjustor is marked as not presently available, as it is not clear that a scar, if present, could be distinguished from the diminutive muscle scars present.

*Askepasma toddense*: Following the interpretation of the musculature presented by Williams *et al.* (2000),

fig. 81.

*Botsfordia*: Not described in Popov (1992).

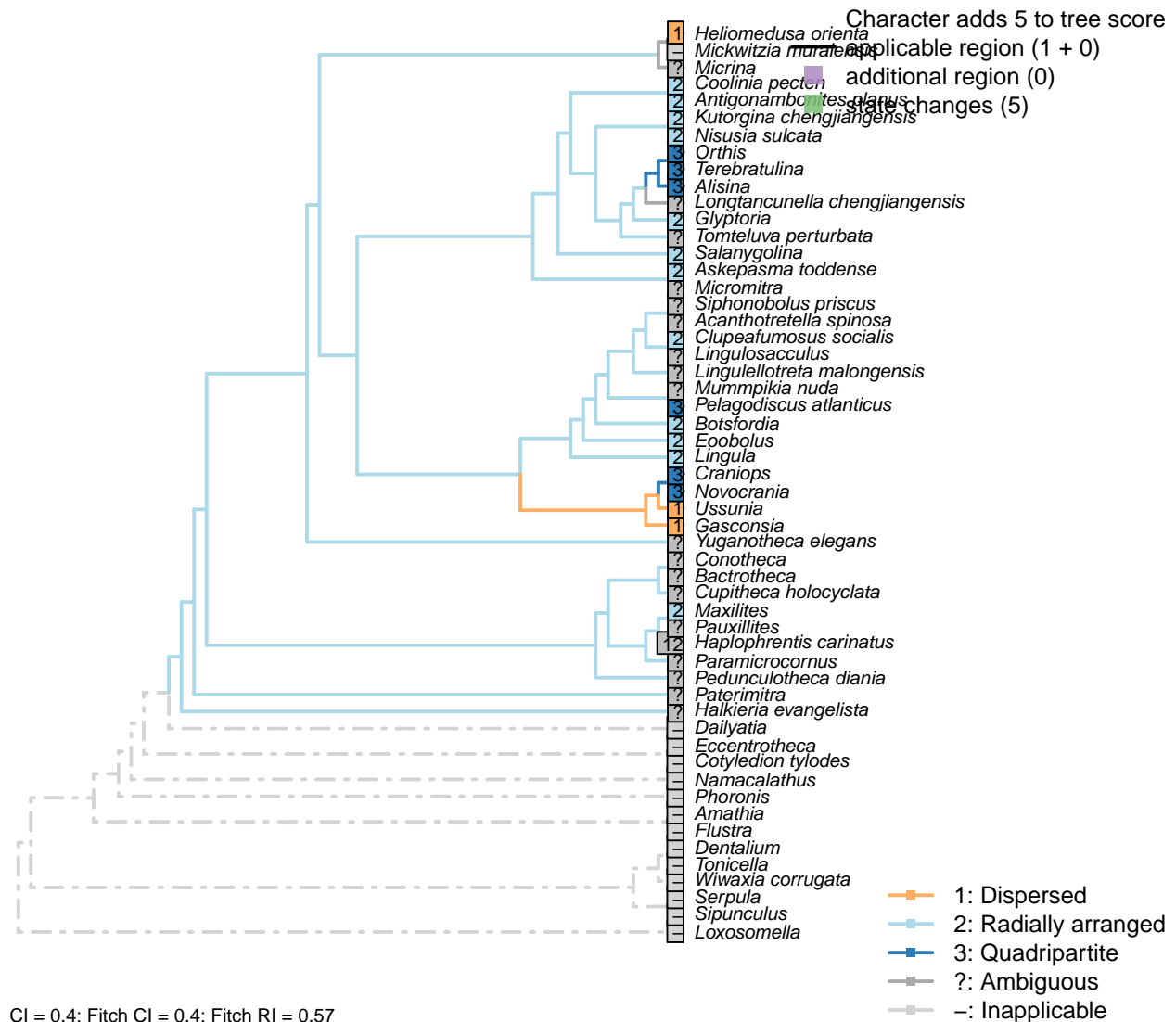
*Clupeafumosus socialis*: Not known in any acrotretid (Williams et al., 2000); not evident in *Clupeafumosus* (Topper et al., 2013a).

*Gasconsia*: No mention of an adjustor muscle in *Gasconsia* or Trimerellida more generally on pp. 184–185 of Williams et al. (2000), nor in discussion in Williams et al. (2007) (p. 2850). Coded as absent.

*Mickwitzia muralensis*: Scars absent; instead, cones ornament shell's internal surface.

*Siphonobolus priscus*: Ventral musculature poorly constrained (Williams et al., 2000; Popov et al., 2009).

## [85] Muscle scars: Dorsal adductors



### Character 85: Sclerites: Bivalved: Muscle scars: Dorsal adductors

1: Dispersed

2: Radially arranged

3: Quadripartite  
Transformational character.

After Bassett *et al.* (2001) character 8, and Williams *et al.* [Williams *et al.* (1996), character 35; 2000, p. 160, character 54]

In the dorsal valve, the anterior and posterior adductor scars of articulated brachiopods form a single (quadripartite) muscle field (Williams *et al.*, 2000, p. 201)

In contrast, the anterior and posterior scars of e.g. trimerellids have prominently separate attachment points, with anterior and posterior muscle fields clearly distinct, and coded as “dispersed”.

In e.g. kutorginates, adductor muscles are separated into left and right fields; the same is the case in lingulids, where there are more separate muscle groups and the left and right fields conspire to produce a radial arrangement; both of these configurations are scored as “radially arranged”.

*Alisina*: Following Williams *et al.* (2000) table 15 (their character 54).

*Antigonambonites planus*: Treatise.

*Askepasma toddense*: Separate left and right fields, so radially arranged – following the interpretation of the musculature presented by Williams *et al.* (2000), fig. 81.

*Botsfordia*: Following Williams *et al.* (1998b), appendix 2.

*Chupeafumosus socialis*: Following reconstruction of *Hadrotreta* by Williams (2000), fig. 51, which exhibits distinct left and right fields.

*Coolinia pecten*: “radially arranged adductor scars” – Bassett and Popov (2017), p1.

*Gasconsia*: Following the coding of Williams *et al.* (2000), table 15.

*Glyptoria*: Scored as “dispersed” by Williams *et al.* (1998b) ... but then so is *Kutorgina*, which Bassett *et al.* (2001) score as radial.

Williams *et al.* (2000) state, for superfamily Protorthida, “dorsal adductor scars probably linear”, which fits in the category of “radial” employed herein – so that’s what we follow.

*Halkieria evangelista*: It is unclear whether the paired muscle scars of *Oikozetetes* may be homologous to brachiopod adductors.

*Haplophrentis carinatus*: Moysiuk *et al.* (2017) reconstruct distinct left and right attachment scars, consistent with general situation in hyoliths (see Dzik, 1980); it is unclear whether additional smaller scars were present in a radial arrangement (as in e.g. *Gompholites*, Marek, 1967) or whether unseen scars were dispersed, hence the partially ambiguous coding.

*Helomedusa orienta*: Distinct anterior and posterior fields (Chen *et al.*, 2007); coded as “dispersed” by Williams *et al.* (2000) in table 15.

*Maxilites*: A pair of large oval muscle scars on the conical shield is complemented with smaller scars elsewhere on the operculum (Marek, 1972; Martí Mus and Bergström, 2005).

*Mickwitzia muralensis*: Scars absent; instead, cones ornament shell’s internal surface.

*Micromitra*: Williams *et al.* (1998b) code as “dispersed”, but have a less divided scheme of character states and disagree with other sources in some codings (e.g. Bassett *et al.*, 2001, in Kutorginates). Williams *et al.* (2000) do not describe *Micromitra* musculature and we were unable to find any reliable description of the scars, so we code as “not presently available”.

*Novocrania*: Craniids scored as “open, quadripartite” by Williams *et al.* (1996).

*Pelagodiscus atlanticus*: Discinids scored as “open, quadripartite” by Williams *et al.* (1996).

*Salanygolina*: “The dorsal valve of *Salanygolina* has a radial arrangement of adductor muscle scars and the scars of posteromedially placed internal oblique muscles, which are also characteristic of paterinates and

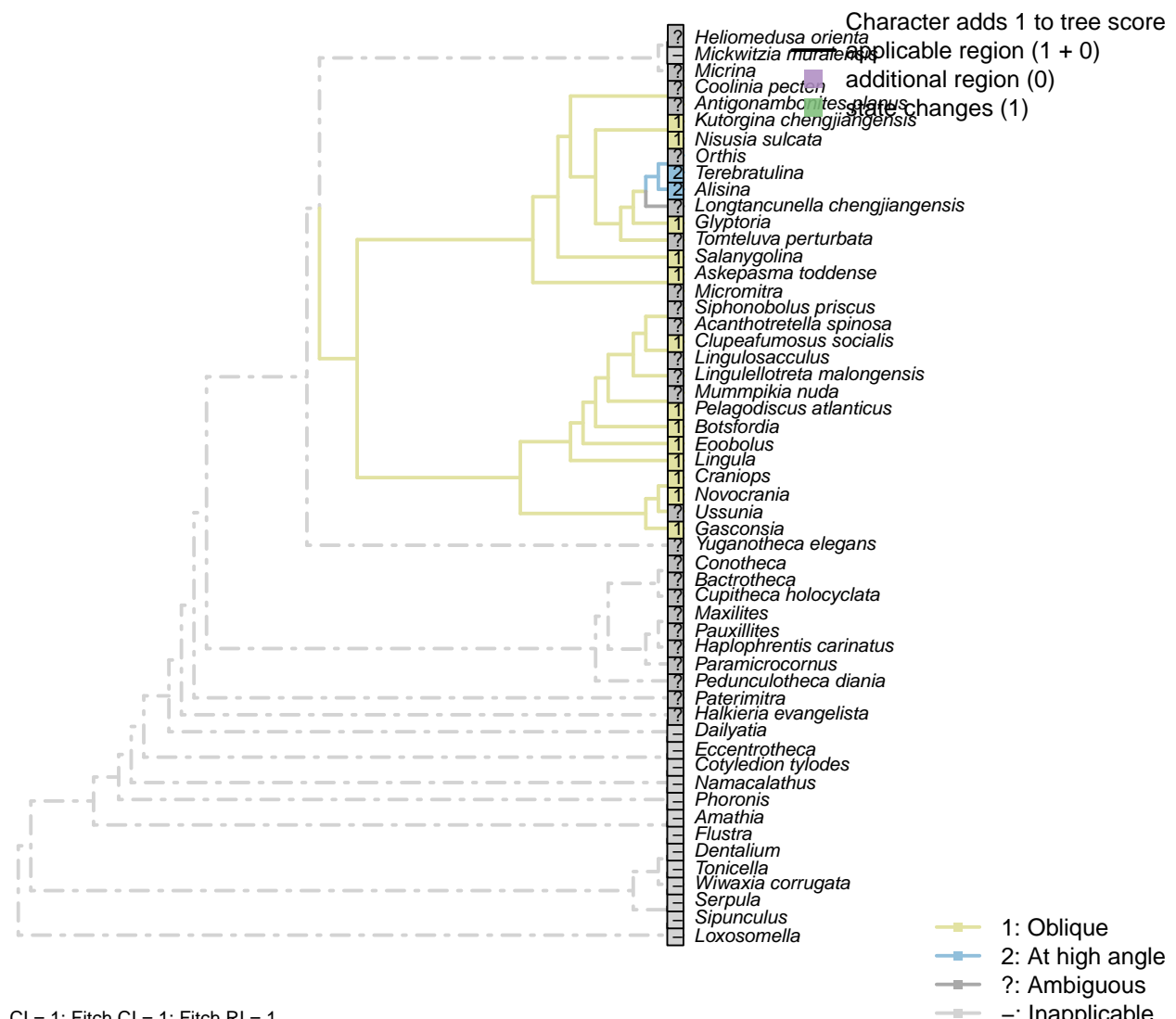
chileates” – Holmer *et al.* (2009).

*Siphonobolus priscus*: Ventral musculature poorly constrained (Williams *et al.*, 2000; Popov *et al.*, 2009).

*Terebratulina*: Coded as “grouped, quadripartite” by Williams *et al.* (1996).

*Ussunia*: Following coding with state 0 (dispersed) in table 15 in Williams *et al.* (2000).

## [86] Muscle scars: Adductors: Position



### Character 86: Sclerites: Bivalved: Muscle scars: Adductors: Position

1: Oblique

2: At high angle

Transformational character.

Position of adductor muscles relative to commissural plane.

After Bassett *et al.* (2001) character 11.

*Askepasma toddense*: Following the interpretation of the musculature presented by Williams *et al.* (2000),

fig. 81.

*Botsfordia*: Following description of Popov (1992).

*Coolinia pecten*: Not reported by Williams *et al.* (2000), nor Bassett & Popov (2017), nor explicitly by Dewing (2001).

*Eoobolus*: “*Eoobolus* should have anterior and posterior adductors and a variety of oblique muscles which were probably arranged in criss-crossing pairs” – Balthasar (2009).

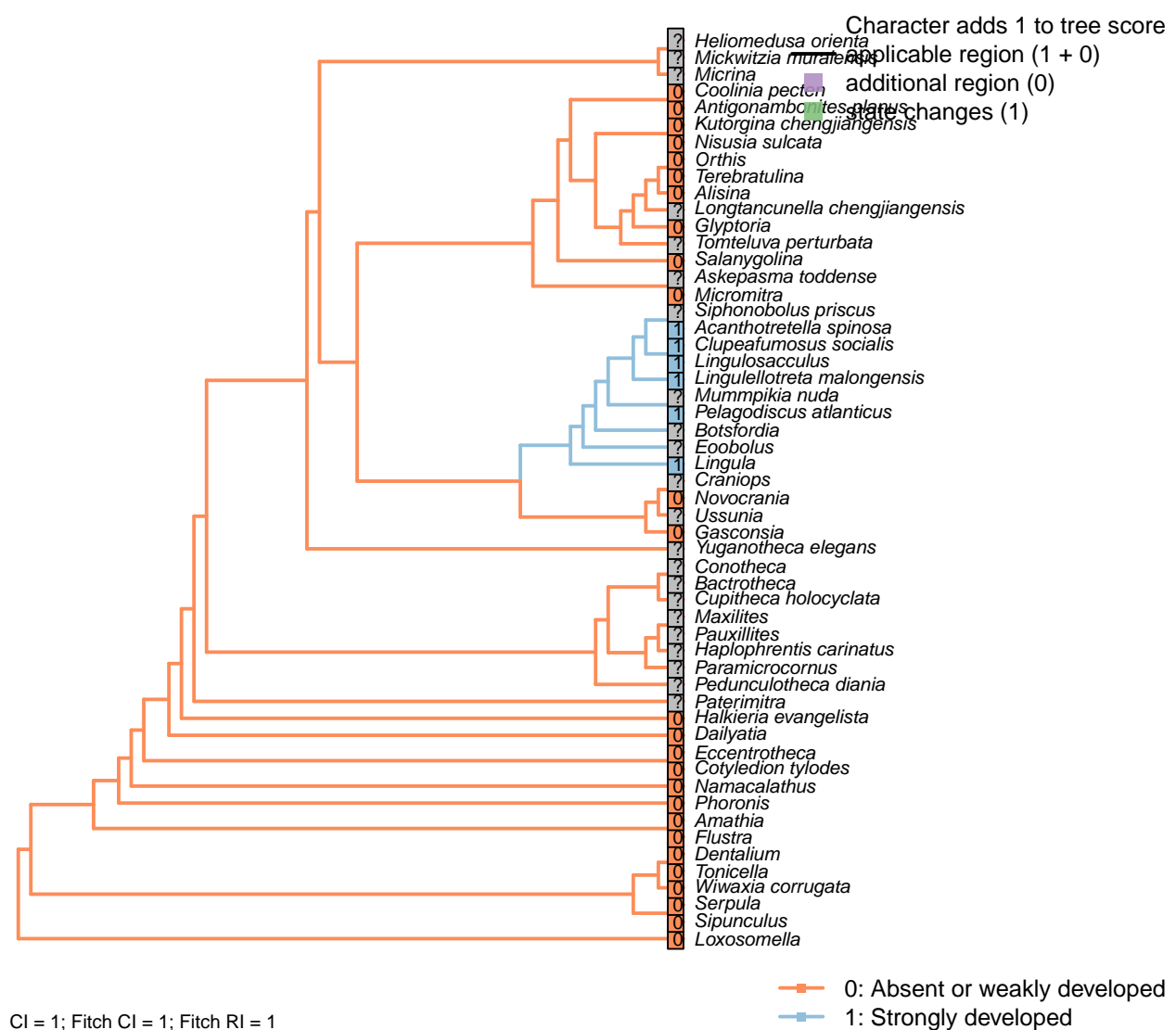
*Gasconsia*: See discussion under Trimerellida in Williams *et al.* (2000).

*Mickwitzia muralensis*: Scars absent; instead, cones ornament shell’s internal surface.

*Pelagodiscus atlanticus*: Musculature considered essentially equivalent to *Lingula* by Williams *et al.* (2000), so *Lingula* coding followed here.

*Siphonobolus priscus*: Ventral musculature poorly constrained (Williams *et al.*, 2000; Popov *et al.*, 2009).

## [87] Muscle scars: Dermal muscles



**Character 87: Sclerites: Bivalved: Muscle scars: Dermal muscles**

- 0: Absent or weakly developed
  - 1: Strongly developed
- Neomorphic character.

Based on character 11 in Zhang *et al.* (2014).

Well developed dermal muscles present in the body wall of recent lingulates, which are absent in all calcareous-shelled brachiopods. These muscles are responsible for the hydraulic shell-opening mechanism, and possibly present in all organophosphatic-shelled brachiopods, with the possible exception of the paterinates (Williams *et al.*, 2000, p. 32).

*Alisina, Antigonambonites planus, Gasconsia, Glyptoria, Nisusia sulcata, Orthis, Salanygolina:* According to the statement of Williams *et al.* (2000, p. 32) that these muscle are absent in all carbonate- shelled brachiopods.

*Askepasma toddense:* According to the statement of Williams *et al.* (2000, p. 32) that the presence of these muscles in paterinates is uncertain.

*Botsfordia:* Implicitly taken as present in Popov (1992), though not marked in diagrams – suggesting not strongly developed.

*Clupeafumosus socialis:* This character is coded based on the score of Acrotreta in Zhang *et al.* (2014), and statement in Williams *et al.* (2000, P.32).

*Coolinia pecten:* According to the statement of Williams *et al.* (2000, p. 32) that these muscle are absent in all carbonate-shelled brachiopods.

*Eoobolus:* Not remarked upon by Balthasar (2009).

*Kutorgina chengjiangensis:* According to the statement of Williams *et al.* (2000, p. 32) that these muscle are absent in all carbonate- shelled brachiopods, and the coding for kutorginids in Zhang *et al.* (2014).

*Micromitra:* Williams *et al.* (2000, p. 32) are uncertain about the presence of these muscles in the paterinates. Zhang *et al.* (2014) code absence in Paterinida, but without specifying evidence; we follow their coding here.

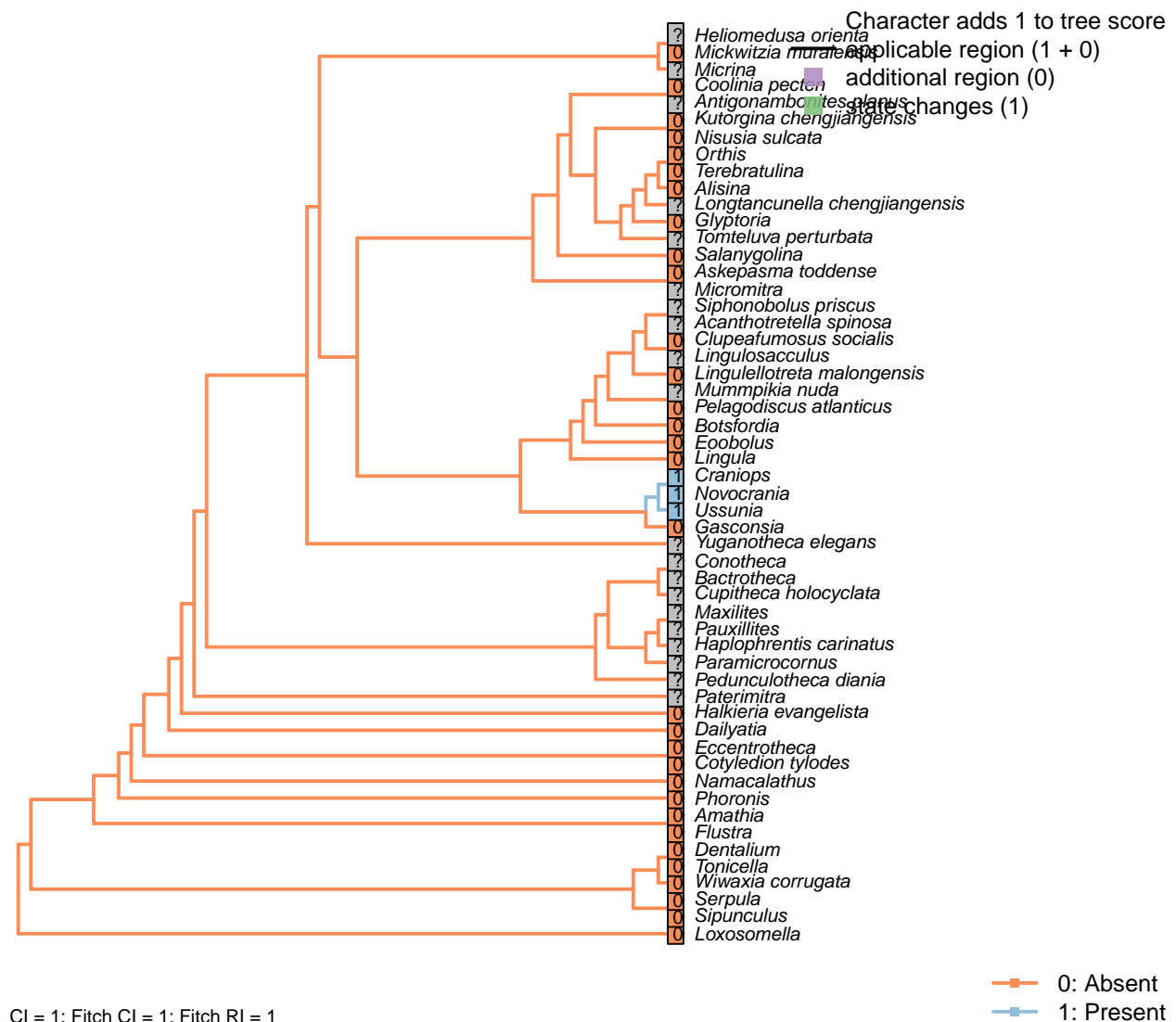
*Mummpikia nuda, Tomteluva perturbata:* Though Williams *et al.* (2000, p. 32) state that these muscles are absent in all carbonate-shelled brachiopods, their existence cannot be discounted with certainty in this taxon, which is therefore coded not presently available.

*Novocrania:* Following Zhang *et al.* (2014), and the statement of Williams *et al.* (2000) that such muscles are absent in all calcite-shelled brachiopods.

*Pelagodiscus atlanticus:* Musculature considered essentially equivalent to *Lingula* by Williams *et al.* (2000), so *Lingula* coding followed here.

*Siphonobolus priscus:* Ventral musculature poorly constrained (Williams *et al.*, 2000; Popov *et al.*, 2009).

*Terebratulina:* Williams *et al.* (2000, p. 32) state that these muscles are absent in all carbonate-shelled brachiopods.

[88] Muscle scars: Unpaired median (*levator ani*)Character 88: Sclerites: Bivalved: Muscle scars: Unpaired median (*levator ani*)

0: Absent

1: Present

Neomorphic character.

The *levator ani* is a diminutive unpaired medial muscle found in certain calcitic brachiopods [Williams et al. (2000); see fig. 89, character 34 in table 13].

*Alisina*, *Kutorgina chengjiangensis*, *Nisusia sulcata*: Following table 13 in Williams et al. (2000).

*Coolinia pecten*: Not reported in Dewing (2001).

*Craniops*: See fig. 90 in Williams et al. (2000).

*Gasconsia*: Williams et al. (2000) code an unpaired medial muscle scar as present in their table 13, but give no reference for this coding, which perhaps arises from their interpretation of the taxon as a trimerellid. Hanken and Harper (1985, p. 249 and text-fig. 2) explicitly identify a pair of central muscles, so we code a

*levator ani* as absent.

*Heliomedusa orienta*: Poor preservation of minor muscle scars noted by Chen *et al.* (2007).

*Mickwitzia muralensis*: Scars absent; instead, cones ornament shell's internal surface.

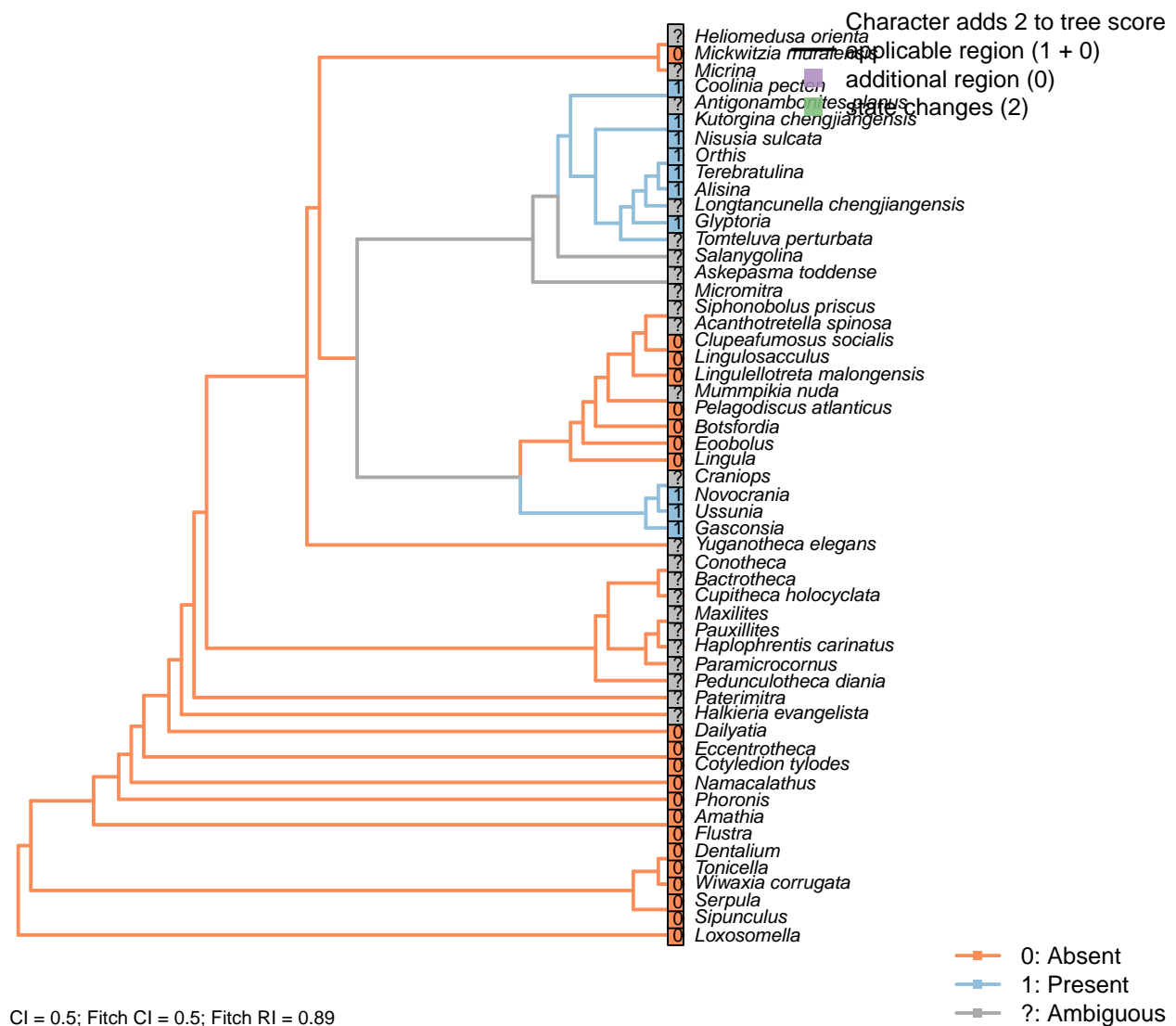
*Novocrania*: Following table 13 in Williams *et al.* (2000) (for *Novocrania*).

*Pelagodiscus atlanticus*: Musculature considered essentially equivalent to *Lingula* by Williams *et al.* (2000), so *Lingula* coding followed here.

*Siphonobolus priscus*: Ventral musculature poorly constrained (Williams *et al.*, 2000; Popov *et al.*, 2009).

*Ussunia*: Following table 15 in Williams *et al.* (2000).

## [89] Muscle scars: Dorsal diductor



CI = 0.5; Fitch CI = 0.5; Fitch RI = 0.89

### Character 89: Sclerites: Bivalved: Muscle scars: Dorsal diductor

0: Absent

1: Present

Neomorphic character.

After Bassett *et al.* (2001) character 9.

*Acanthotretella spinosa*: Not observable in *Acanthotretella* itself, so coded as ambiguous – though it is likely based on the anticipated phylogenetic affinities of *Acanthotretella* that the muscles are absent.

*Askepasma toddense*: Possible diductor scar could instead correspond to discinoid posterior adductors (Williams *et al.*, 1998b); coded as uncertain. Not reconstructed in the interpretation of the musculature presented by Williams *et al.* (2000), fig. 81.

*Clupeafumosus socialis*: Not reported by Topper *et al.* (2013a), nor reconstructed in generic acrotretid by Williams *et al.* (2000).

*Gasconsia*: Internal oblique muscles serve as diductors.

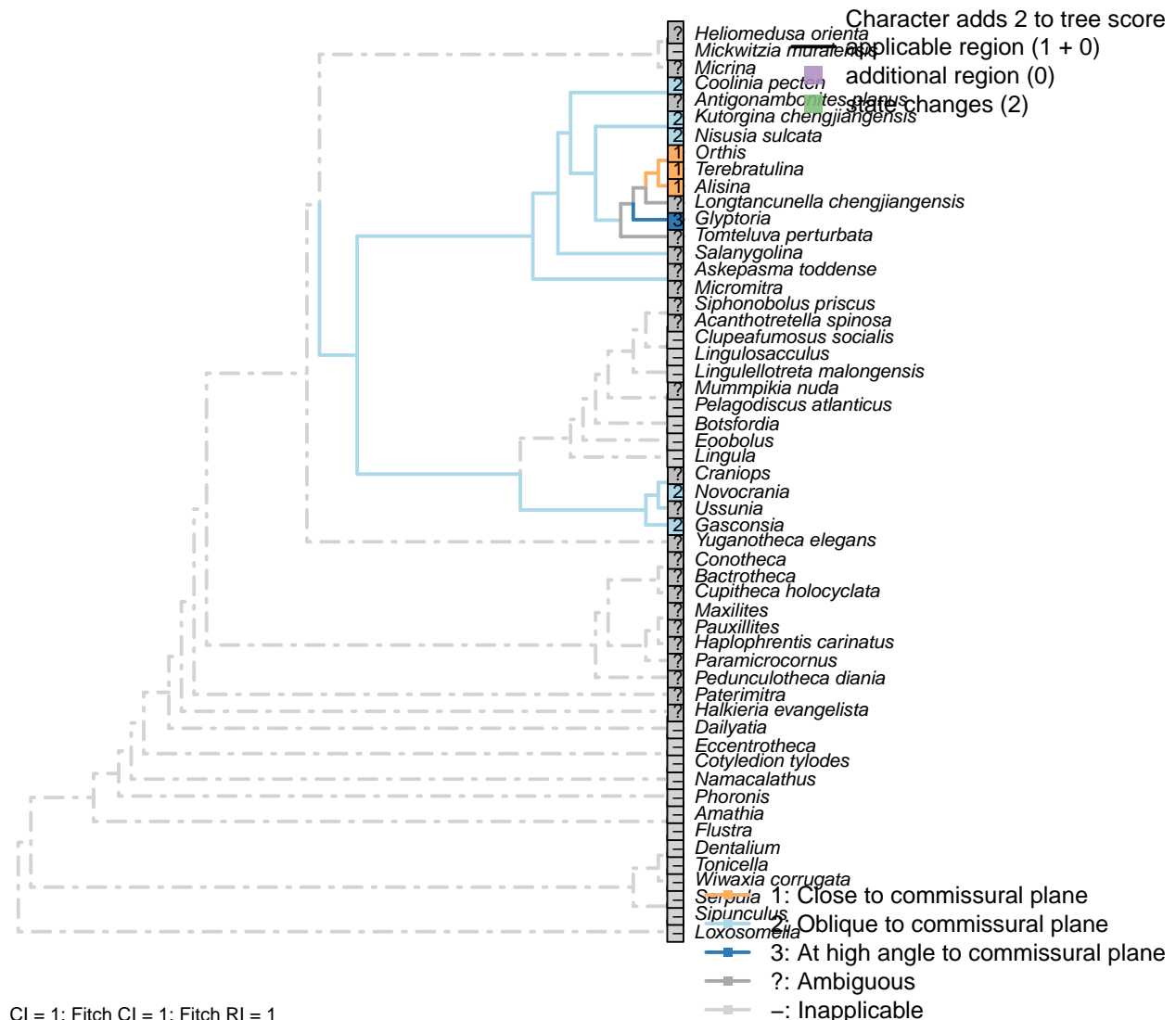
*Halkieria evangelista*: It is unclear whether the paired muscle scars of *Oikozetetes* are homologous to brachiopod diductors.

*Micromitra*: Possible diductor scar could instead correspond to discinoid posterior adductors (Williams *et al.*, 1998b); coded as uncertain.

*Siphonobolus priscus*: Ventral musculature poorly constrained (Williams *et al.*, 2000; Popov *et al.*, 2009).

*Ussunia*: Internal oblique muscles present (Nikitin and Popov, 1984) and taken to serve as diductors by analogy with *Gasconsia*.

### [90] Muscle scars: Dorsal diductor: Position



#### Character 90: Sclerites: Bivalved: Muscle scars: Dorsal diductor: Position

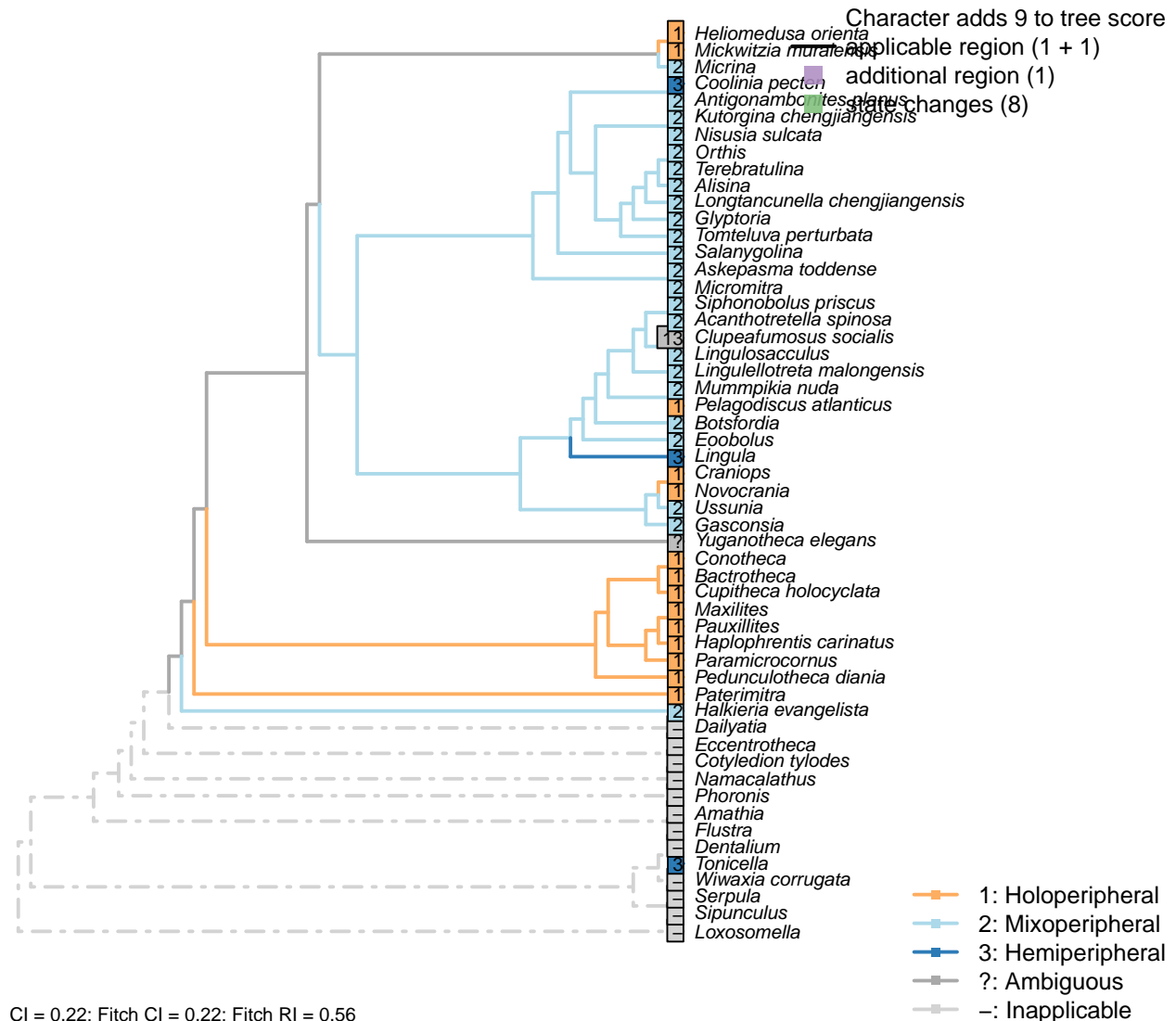
- 1: Close to commissural plane
  - 2: Oblique to commissural plane
  - 3: At high angle to commissural plane
- Transformational character.

After Bassett *et al.* (2001) character 10.

*Siphonobolus priscus*: Ventral musculature poorly constrained (Williams *et al.*, 2000; Popov *et al.*, 2009).

## 5.12 Sclerites: Dorsal valve

### [91] Growth direction



See Fig. 284 in Williams *et al.* (1997).

The growth direction dictates the attitude of the cardinal area relative to the hinge, which does not therefore represent an independent character.

Crudely put, if, viewed from a dorsal position, the umbo falls within the outer margin of the shell, growth is holoperipheral; if it falls outside the margin, it is mixoperipheral; if it falls exactly on the margin, it is hemiperipheral.

*Clupeafumosus socialis*: Appears hemiperipheral in fig. 3 in Topper *et al.* (2013a), though bordering on

holoperipheral, so scored as ambiguous.

*Craniops*: “Both valves with growth holoperipheral” – Williams et al. (2000), p. 164.

*Heliomedusa orienta*: “holoperipheral growth in dorsal valve” – Williams et al. (2007).

Zhang et al. (2009) conclude that Chen et al. (2007) misidentify the dorsal valve as the ventral valve.

*Micrina*: See Holmer et al. (2008).

*Paterimitra*: S2 and L sclerites are clearly holoperipheral. See Larsson et al. (2014), fig. 2.

*Tonicella*: For the purposes of this analysis, we must treat polyplacophoran and brachiopod valves as potentially homologous.

In brachiopods, the dorsal valve bears the lophophore, which arises from the anterior lobe of the larva (Altenburger et al., 2013) – indicating that the dorsal shell field is associated with the anterior lobe.

In polyplacophorans, the head valve arises from a shell field on the anterior (pre-prototroch) lobe of the larva (Wanninger and Haszprunar, 2002a), which we therefore treat as homologous with the brachiopod dorsal valve.

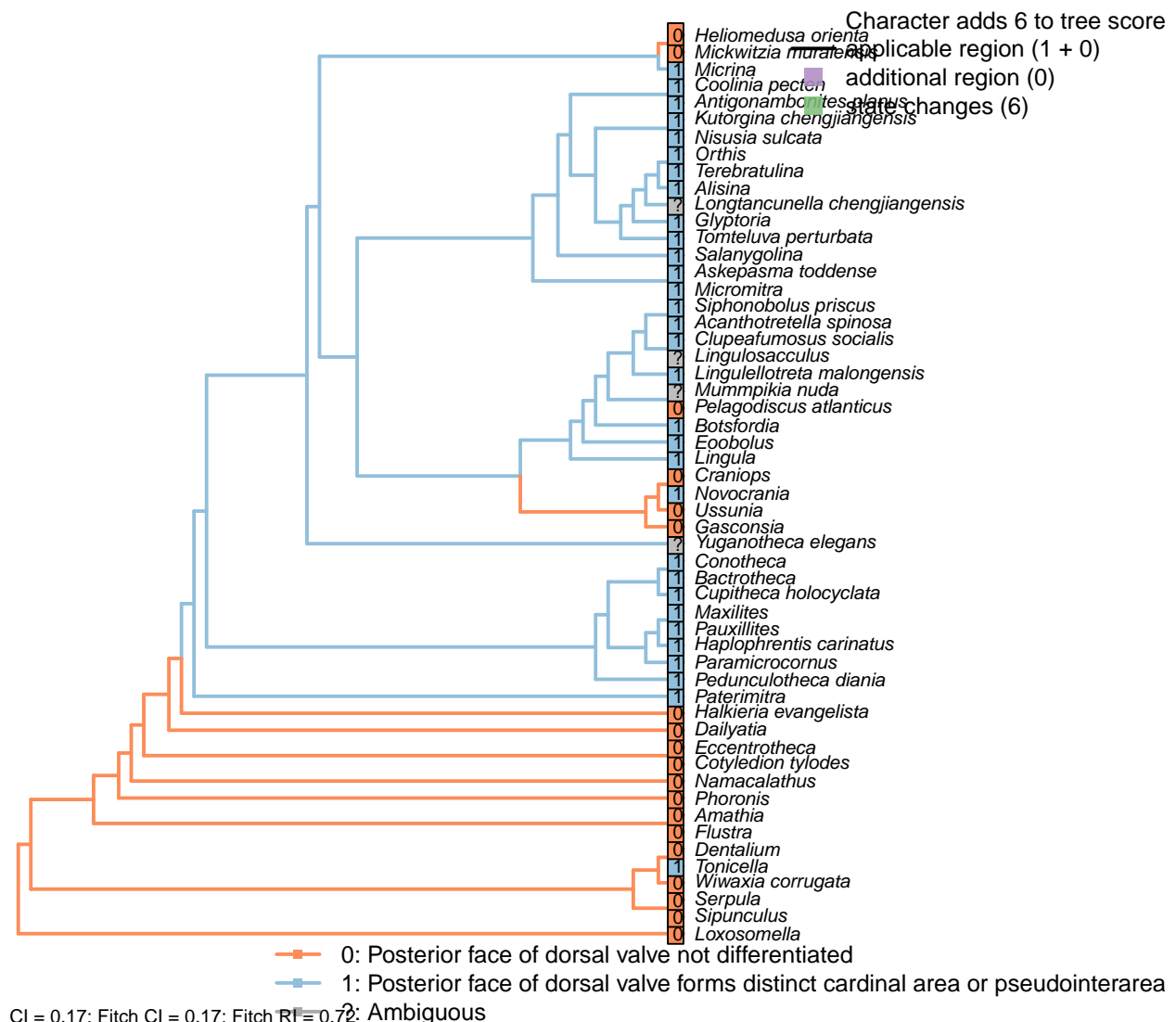
In support of this hypothesis, we note that the posterior (but not anterior) valves of chitons bear apophyses (Schwabe, 2010; Connors et al., 2012), which are most prominent in the ventral (but not dorsal) valves of brachiopods (Williams et al., 1997, fig. 322), and which occur in the morph A shell of *Oikozetetes*, which is interpreted as the posterior valve of a halkieriid (Paterson et al., 2009).

As the single posterior shell field of polyplacophorans subdivides to give rise to the six intermediate valves plus the tail valve (Wanninger and Haszprunar, 2002a), we prefer to consider the intermediate valves as representing “subdivisions” of a single valve rather than additional valves added to the body plan.

Growth is hemiperipheral in the anterior valve of polyplacophorans and holoperipheral in the posterior valves (Schwabe, 2010; Connors et al., 2012).

*Ussunia*: Growth “mixoperipheral in both valves” in trimerellids (Williams et al., 2000; Popov et al., 1997).

## [92] Posterior surface: Differentiated

**Character 92: Sclerites: Dorsal valve: Posterior surface: Differentiated**

0: Posterior face of dorsal valve not differentiated

1: Posterior face of dorsal valve forms distinct cardinal area or pseudointerarea

Neomorphic character.

In shells that grow by mixoperipheral growth, the triangular area subtended between each apex and the posterior ends of the lateral margins is termed the cardinal area. In shells with holoperipheral growth, a flattened surface on the posterior margin of the valve is termed a pseudointerarea (paraphrasing Williams et al., 1997).

In order for this character to be independent of a shell's growth direction, we do not distinguish between a "cardinal area", "interarea" or "pseudointerarea".

*Acanthotretella spinosa*: Pseudointerarea present, following Siphonotretidae coding in Williams et al. (2000), table 6.

*Alisina*, *Antigonambonites planus*, *Coolinia pecten*, *Glyptoria*, *Kutorgina chengjiangensis*, *Orthis*, *Salany-*

*golina*, *Tomteluva perturbata*: Cardinal area (interarea) present.

*Askepasma toddense*: Well-defined pseudointerarea (Williams et al., 2000, p153).

*Botsfordia*: “dorsal pseudointerarea vestigial, divided by median groove” – Williams et al. (2000).

*Clupeafumosus socialis*: Pseudointerarea present; figured by Topper et al. (2013a), fig. 3j.

*Craniops*: “Only some craniopsids (Lingulapholis, Pseudopholidops [not *Craniops*]) have well-developed pseudointerareas.” – Williams et al. (2000).

*Gasconsia*: Absent: the dorsal (branchial) pseudointerarea of *G. schucherti* is “reduced or obsolete”; that of *G. worsleyi* “short, virtually obsolete” (Hanken and Harper, 1985).

*Haplophrentis carinatus*: A very short pseudointerarea appears to be present (Moysiuk et al., 2017).

*Helio medusa orienta*: Pseudointerarea in ventral valve, but not dorsal valve (Williams et al., 2000, 2007).

*Lingula*, *Lingulellotreta malongensis*: Pseudointerarea present, following Williams et al. (2000), table 6.

*Lingulosacculus*: Unclear from fossil material.

*Longtancunella chengjiangensis*: Zhang et al. (2011a) note that “all evidence of a pseudointerarea is lacking”, but the two-dimensional preservation style of Chengjiang material makes details of dorsal valve difficult to distinguish, and the possibility of a diminutive pseudointerarea cannot be excluded with total confidence.

*Mickwitzia muralensis*: Shell flat.

*Micrina*: = Sellate sclerite duplicature (Holmer et al., 2008).

*Micromitra*: “Dorsal pseudointerarea usually well defined, low, anacline to catacline” – Williams et al. (2000).

*Mummpikia nuda*: “Information on the dorsal interarea is inconclusive [...] no obvious interarea is recognisable; whether or not this is the primary state or a taphonomic artefact is difficult to assess” – Balthasar (2008), p. 276.

*Nisusia sulcata*: Cardinal area (interarea) present – with reference to Holmer et al. (2018a).

*Pedunculotheca diana*, *Novocrania*, *Paterimitra*: Pseudointerarea.

*Pauxillites*: Marek (1966).

*Pelagodiscus atlanticus*: Absent, following entry for Discinidae in Williams et al. (2000), table 6.

*Siphonobolus priscus*: “Dorsal pseudointerarea weakly anacline, undivided, elevated above the valve floor” – Popov et al. (2009).

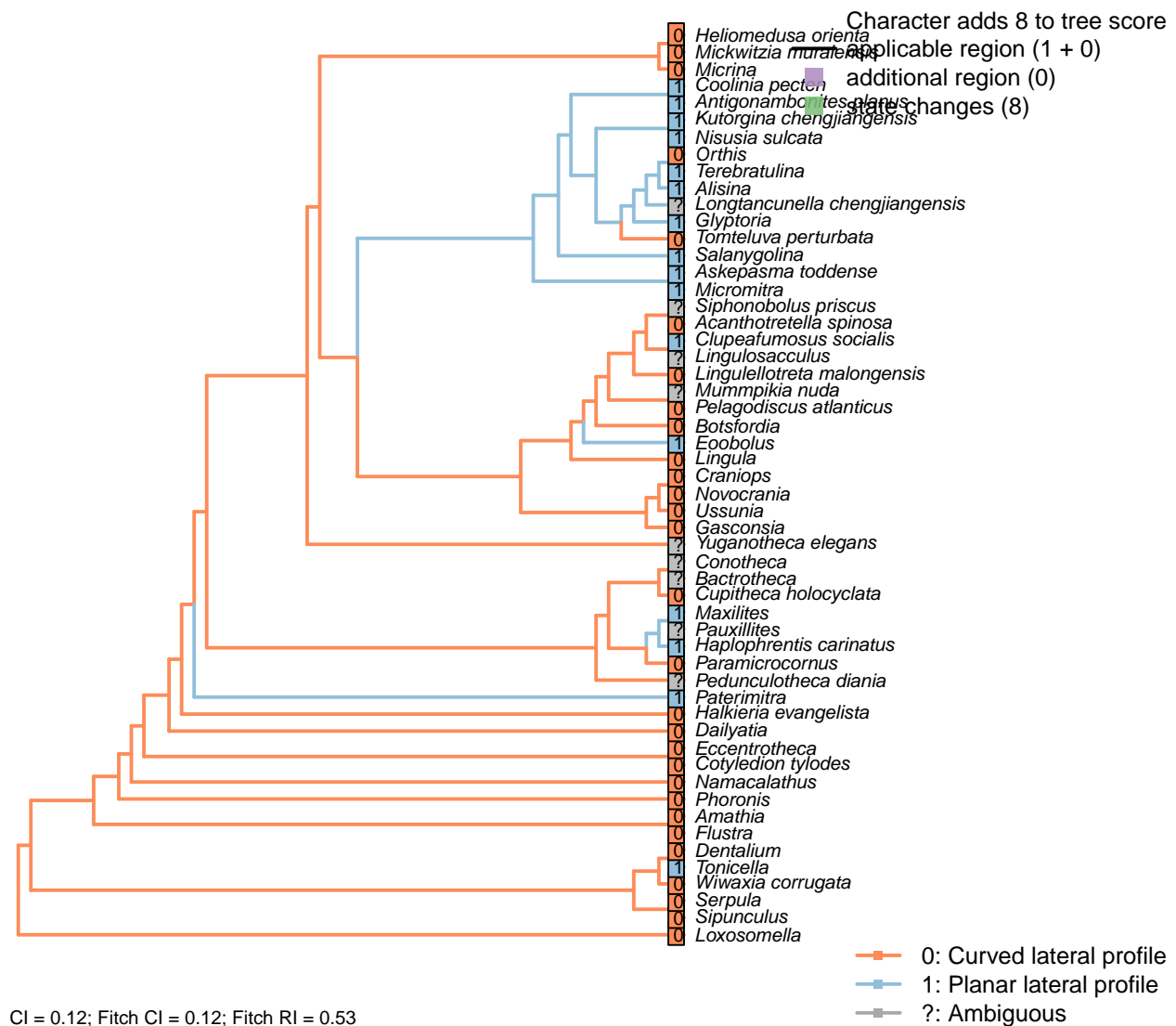
*Terebratulina*: Interarea present.

*Tonicella*: V-shaped notch in anterior valve (Schwabe, 2010).

*Ussunia*: Following table 15 in Williams et al. (2000).

*Yuganotheca elegans*: A differentiated region is not obvious in fossil material or its reconstruction (Zhang et al., 2014), but the two-dimensional preservation style of Chengjiang material makes details of dorsal valve difficult to distinguish, and the possibility of a diminutive pseudointerarea cannot be excluded with confidence.

### [93] Differentiated posterior surface: Morphology



#### Character 93: Sclerites: Dorsal valve: Differentiated posterior surface: Morphology

0: Curved lateral profile

1: Planar lateral profile

Neomorphic character.

It is possible for a cardinal area or pseudointerarea to be distinct from the anterior part of the shell, yet to remain curved in lateral profile.

Taking an undifferentiated posterior margin as primitive, the primitive condition is curved – flattening of the posterior margin represents an additional modification that can only occur once the posterior margin is differentiated.

*Bactrotheca*: The short aspect of the cardinal interarea (Valent et al., 2012) makes it difficult to evaluate

whether it is planar or curved.

*Botsfordia*: “Curved pseudointerarea” – Skovsted et al. (2017).

*Clupeafumosus socialis*: Truncated but essentially planar surface; see e.g. p196 of Topper et al. (2013a).

*Conotheca*: Difficult to establish from material figured in Devaere et al. (2014) due to low elevation of operculum.

*Cupitheca holocyclata*: Curved (Sun et al., 2018a).

*Eoobolus*: Essentially planar; see Balthasar (2009), fig. 4a.

*Pelagodiscus atlanticus*, *Gasconsia*, *Heliomedusa orienta*, *Mickwitzia muralensis*, *Ussunia*: Posterior surface cannot be flat if it is not differentiated.

*Maxilites*: Approximately planar (Marek, 1972).

*Micromitra*: Essentially straight; see fig. 3.7 in Ushatinskaya (2016).

*Paramicrocornus*: Zhang et al. (2018).

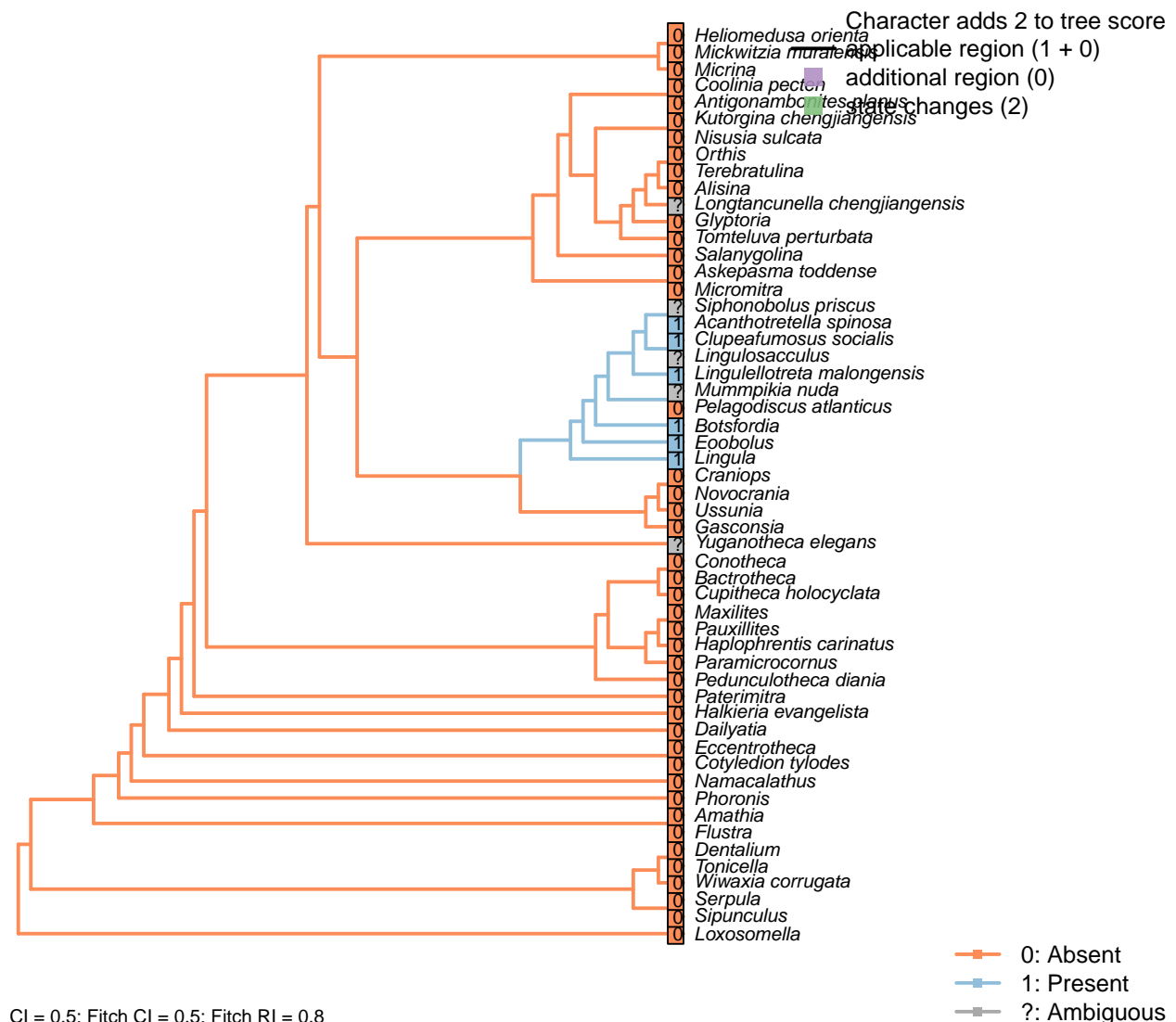
*Pauxillites*: Not clear from published material.

*Pedunculotheca diania*: Difficult to evaluate based on present material, given low nature of valve and compressed preservation.

*Siphonobolus priscus*: The short interarea appears planar (see for example Popov et al. 2009 fig. 6A), but its short length makes it difficult to establish whether slight curvature is present.

*Tonicella*: Essentially planar, though open in aspect (following Chiton in Schwabe, 2010).

## [94] Posterior surface: Medial groove



## Character 94: Sclerites: Dorsal valve: Posterior surface: Medial groove

0: Absent

1: Present

Neomorphic character.

Following character 29 in Williams *et al.* (2000), table 9 (which relates to pseudointerarea).

*Acanthotretella spinosa*: The dorsal pseudointerarea is poorly preserved, but appears to have a median groove (Holmer and Caron, 2006).

*Botsfordia*: “dorsal pseudointerarea vestigial, divided by median groove” – Williams *et al.* (2000).

*Clupeafumosus socialis*: Present; figured by Topper *et al.* (2013a), fig. 3j.

*Foobolus*: Prominent medial groove (Balthasar, 2009).

*Heliomedusa orienta*: “A posteriorly protruding dorsal pseudointerarea with no median groove and no flexure

lines” – Chen et al. (2007).

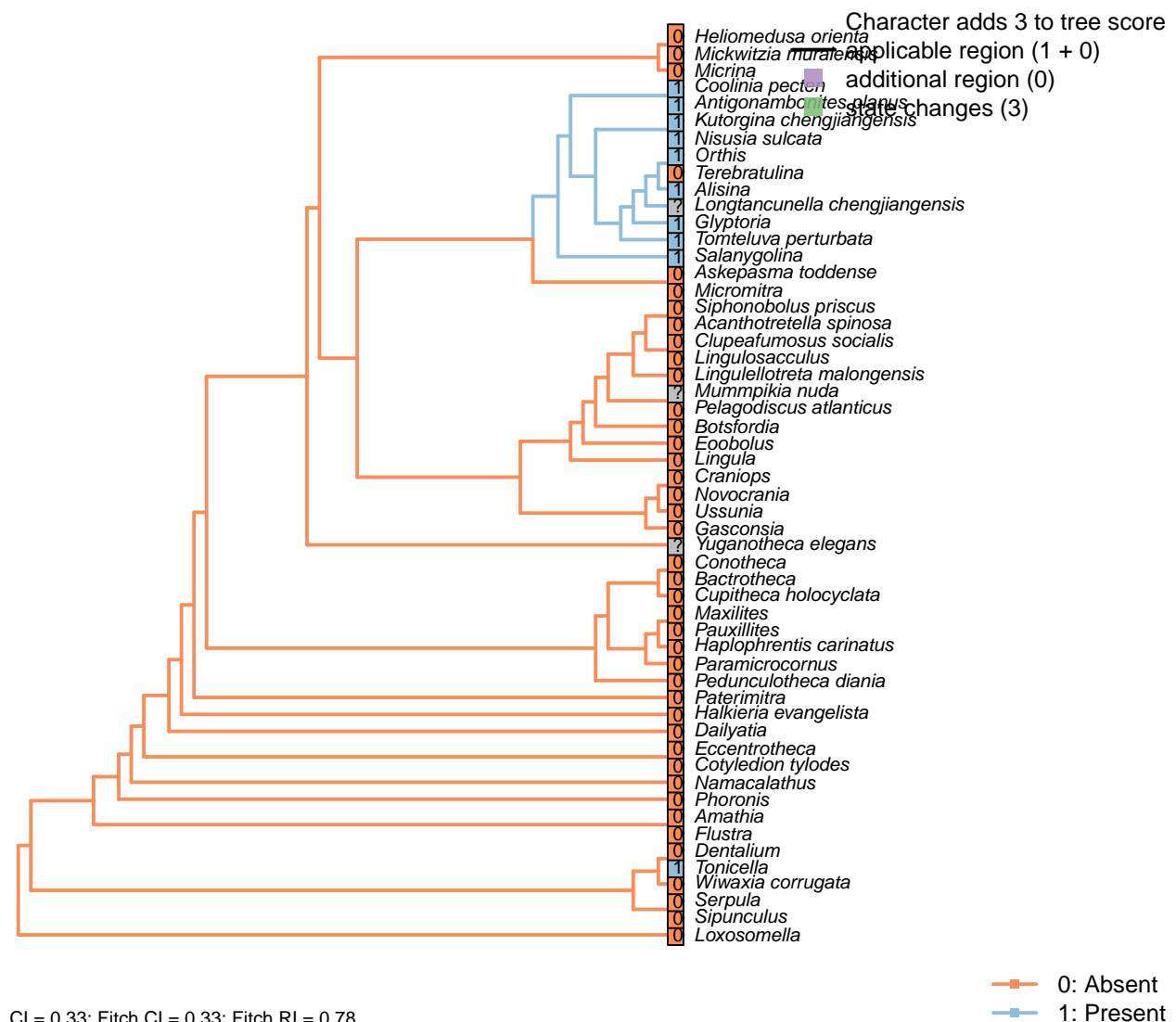
*Lingulellotreta malongensis*: Dorsal pseudointerarea with wide, concave median groove and short propareas” – Williams et al. (2000).

*Maxilites*: Marek (1972).

*Paramicrocornus*: Zhang et al. (2018).

*Siphonobolus priscus*: The dorsal pseudointerarea of *S. priscus* is undivided (Popov et al., 2009), but in other species it is divided by a “wide, poorly defined median groove” (Williams et al., 2000). Coded, therefore, as polymorphic.

## [95] Posterior surface: Notothyrium



### Character 95: Sclerites: Dorsal valve: Posterior surface: Notothyrium

0: Absent

1: Present

Neomorphic character.

A notothyrium is an opening in an interarea that accommodates the pedicle, and may be filled with plates.

*Botsfordia*: Following Williams et al. (1998b), appendix 2.

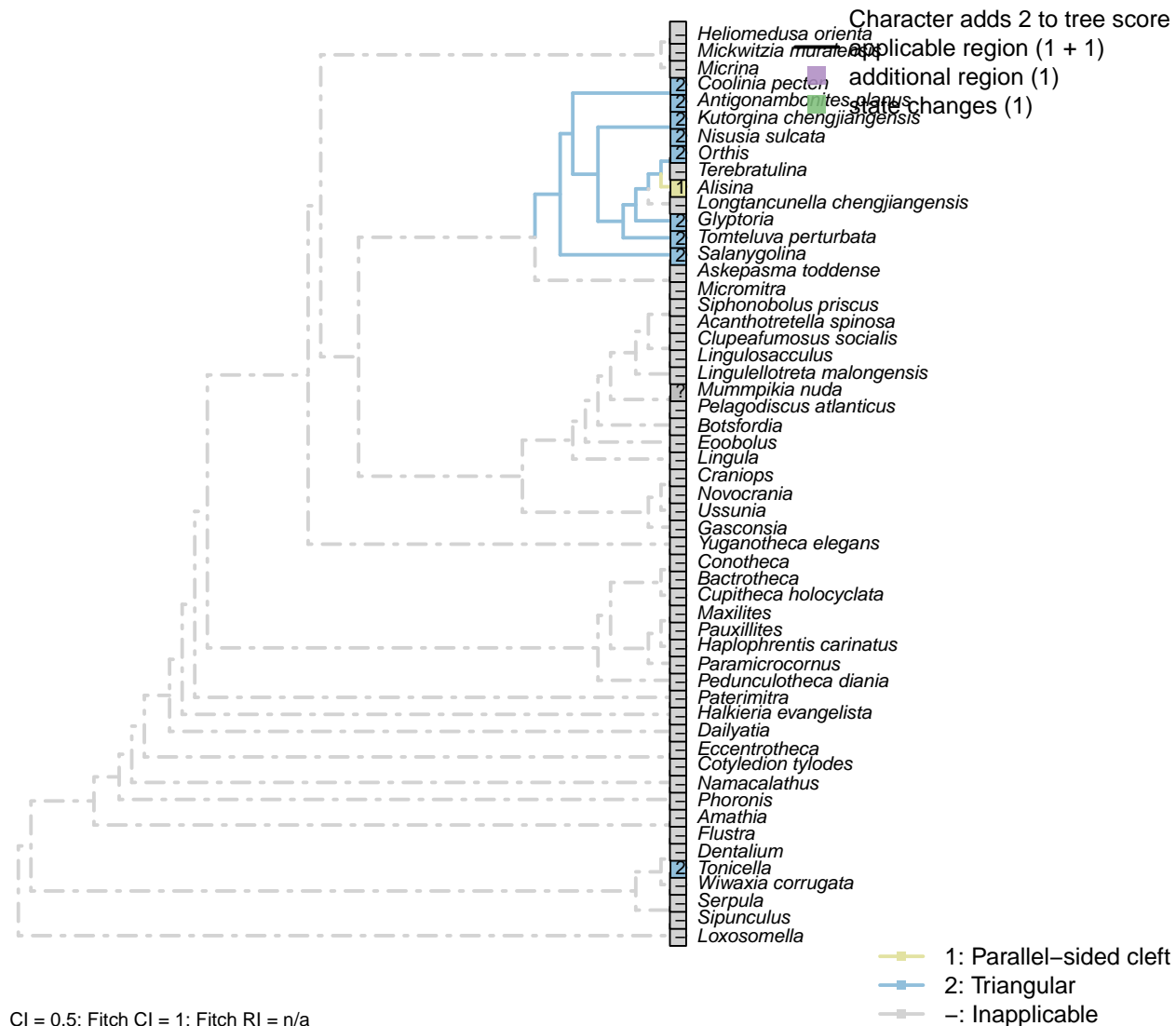
*Longtancunella chengjiangensis*: No evidence or report of an opening at the hinge line in fossil material in Zhang et al. (2007c) or Zhang et al. (2011a).

*Maxilites*: Marek (1972).

*Paramicrocornus*: Zhang et al. (2018).

*Tonicella*: The deep V-shaped notch (Schwabe, 2010, fig. 8) is positionally equivalent to the brachiopod notothyrium.

## [96] Posterior surface: Notothyrium: Shape



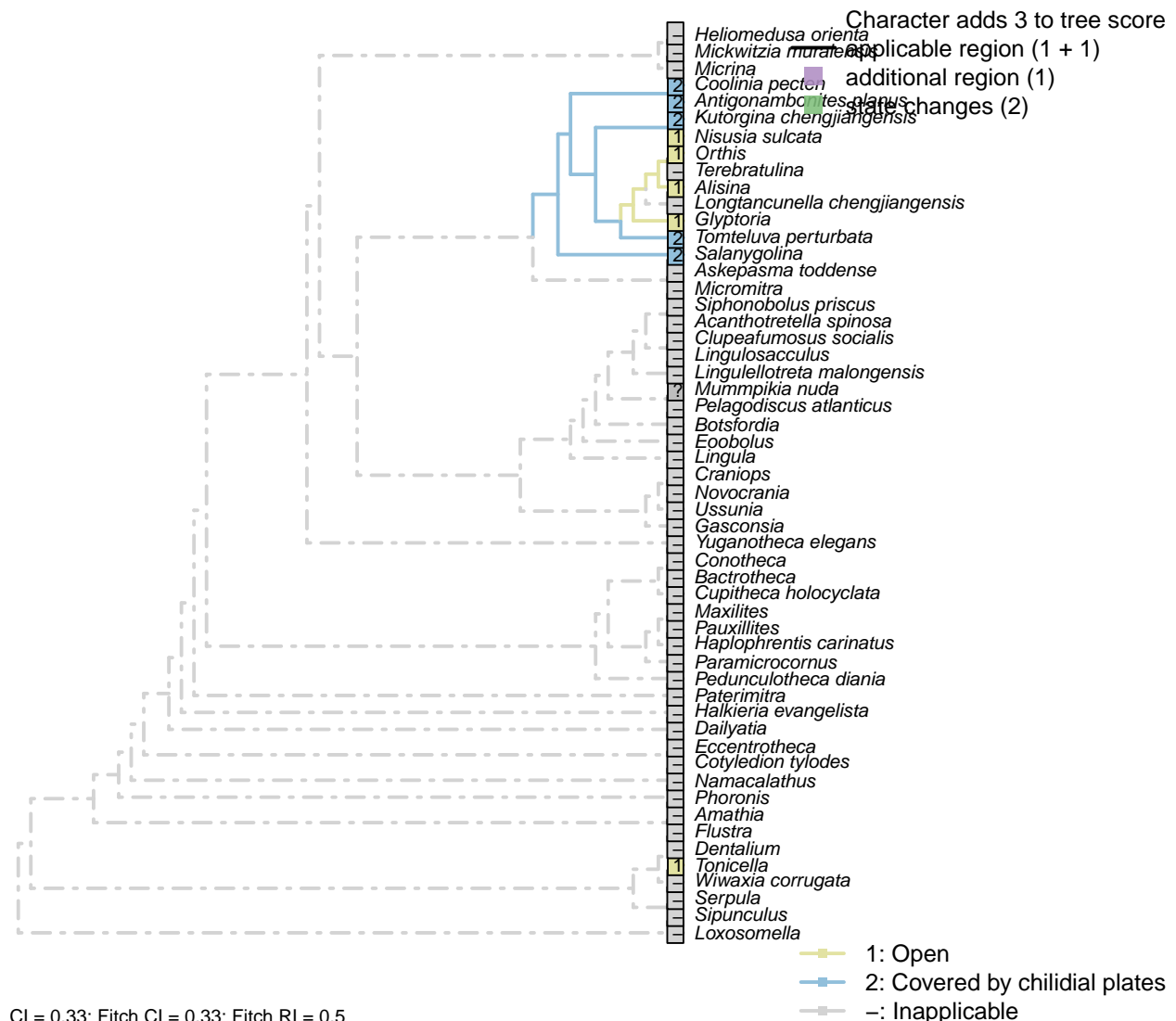
CI = 0.5; Fitch CI = 1; Fitch RI = n/a

### Character 96: Sclerites: Dorsal valve: Posterior surface: Notothyrium: Shape

- 1: Parallel-sided cleft
- 2: Triangular
- Transformational character.

A notothyrium is an opening in an interarea that accommodates the pedicle, and may be filled with plates. A simplification of character 5 in Bassett et al. (2001).

### [97] Posterior surface: Notothyrium: Chilidial plates



CI = 0.33; Fitch CI = 0.33; Fitch RI = 0.5

### Character 97: Sclerites: Dorsal valve: Posterior surface: Notothyrium: Chilidial plates

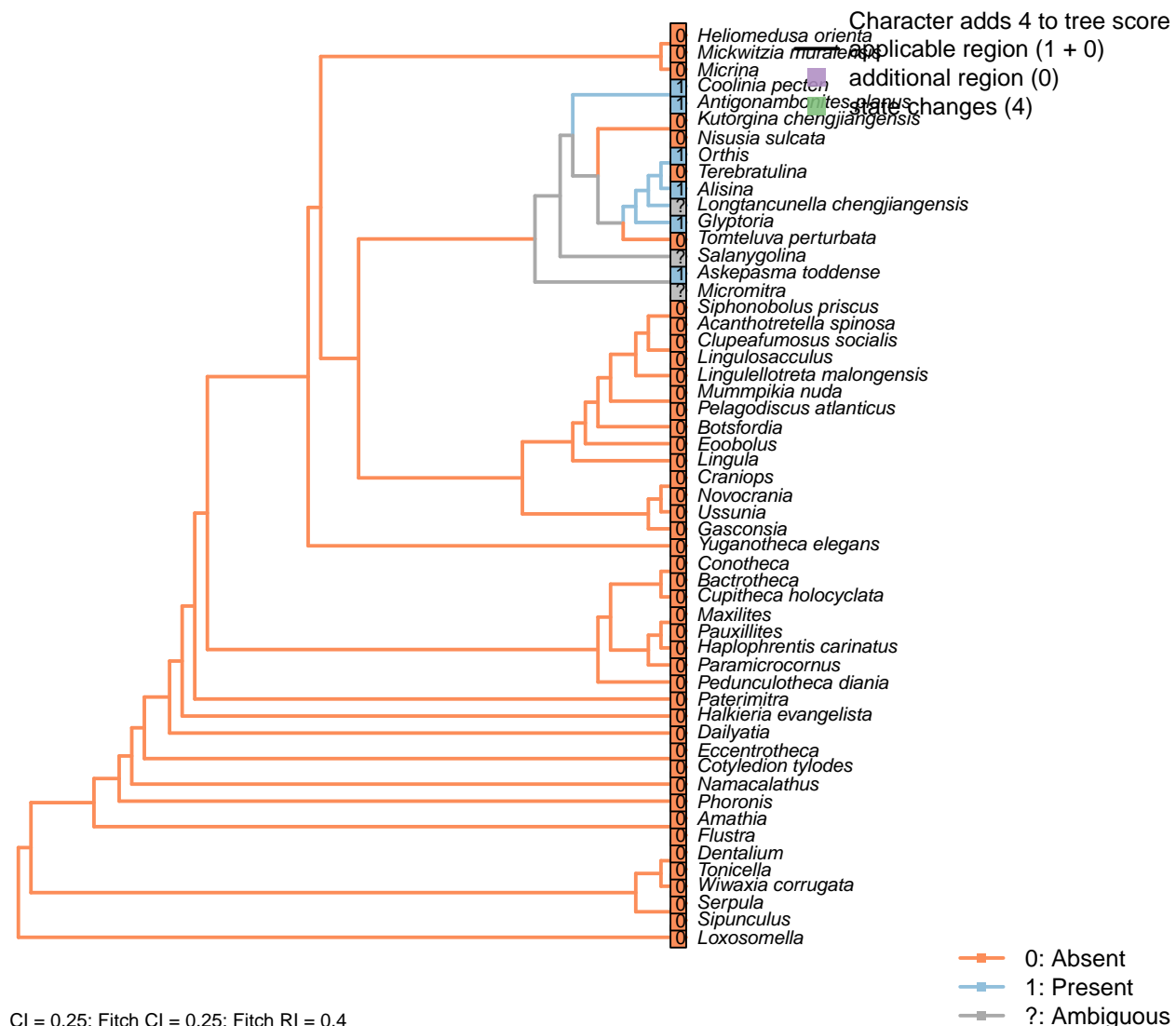
- 1: Open
- 2: Covered by chilidial plates
- Transformational character.

A notothyrium may be open or covered by a chilidium or two chilidial plates.

No included taxa exhibit more than one chilidial plate.

Transformational as it is not self-evident whether the ancestral taxon had an open or closed notothyrium.

## [98] Notothyrial platform



## Character 98: Sclerites: Dorsal valve: Notothyrial platform

0: Absent

1: Present

Neomorphic character.

After Bassett *et al.* (2001) character 12.

The presence or absence of a notothyrial platform, which often serves as an attachment point for the diductors in a similar fashion to the cardinal processes, is independent of the presence of a notothyrium.

*Alisina, Glyptoria*: Bassett *et al.* (2001) score as present in Table 18.1.*Askepasma toddense*: Raised notothyrial platform (Williams *et al.*, 1998b).*Coolinia pecten*: Referred to as the “posterior platform” in Dewing (2001).*Kutorgina chengjiangensis*: “Dorsal diductor scars impressed on floor of notothyrial cavity”: Williams *et al.* (2000), regarding Kutorginata.

Bassett *et al.* (2001) score as absent in Table 18.1.

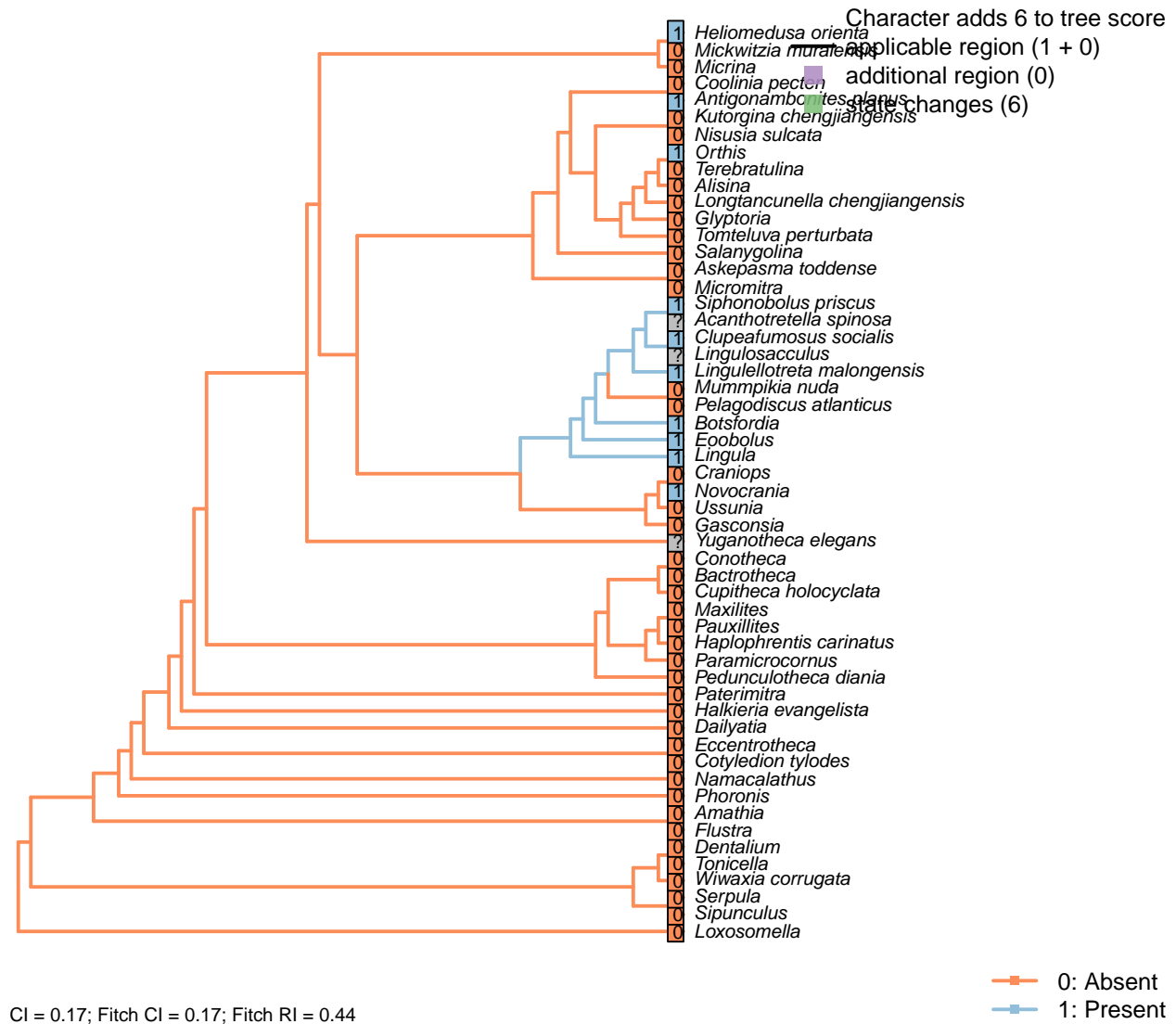
*Micromitra*: A low notothyrial plate (Williams *et al.*, 1998b) conceivably correspond to the raised notothyrial platform of *Askepasma*; coded ambiguous accordingly.

*Nisusia sulcata*: Bassett *et al.* (2001) score as absent in Table 18.1.

“Dorsal diductor scars impressed on floor of notothyrial cavity”: Williams *et al.* (2000), regarding Kutorginata.

*Ussunia*: “Visceral platforms absent in both valves” – Williams *et al.* (2000), p. 192.

## [99] Medial septum



### Character 99: Sclerites: Dorsal valve: Medial septum

0: Absent

1: Present

Neomorphic character.

The dorsal valve of many taxa exhibits a septum or process (or myophragm) along the medial line. See character 25 in Benedetto (2009).

*Acanthotretella spinosa*: Not described by Holmer & Caron (2006), but an unannotated linear feature corresponds to the position of a median septum. Without detailed study of the specimen, we opt to score this as ambiguous.

*Antigonambonites planus*: Weakly developed septum evident in internal cast: Williams et al. (2000), fig. 508.2e.

*Botsfordia*: “dorsal interior with narrow anterior projection extending to midvalve, bisected by median ridge” – Williams et al. (2000).

*Clupeafumosus socialis*: Prominent process evident (Topper et al., 2013a).

*Eoobolus*: A “median projection” is present (fig. 4g in Balthasar, 2009).

*Glyptoria*: Neither evident nor reported in Williams et al. (2000).

*Heliomedusa orienta*: Reported on ‘ventral’ valve by Chen et al. (2007); we consider their ‘ventral’ valve to be the dorsal valve.

The structure is unambiguously figured (e.g. fig. 5.1 in Chen et al., 2007), contra its coding as absent in Williams et al. (2000) and its lack of mention in Williams et al. (2007) or Zhang et al. (2009).

*Kutorgina chengjiangensis*: Absent – fig. 129.1f in Williams et al. (2000).

*Lingulellotreta malongensis*: Very weakly developed but seemingly present between muscle scars in *Lingulellotreta*, more prominent in *Aboriginella* (also Lingulellotretidae) (Williams et al., 2000, fig. 34).

*Lingulosacculus*: It is not possible to determine, based on the material presented in Balthasar & Butterfield (2009), whether the anterior projection of the visceral area in the dorsal valve corresponds to a medial septum in the underlying shell.

*Mummpikia nuda*: See pl. 2 panel 6 in Balthasar (2008).

*Nisusia sulcata*: Fig. 125 in Williams et al. (2000).

*Novocrania*: Median process evident: Williams et al. (2000) fig. 100.2a, d.

*Orthis*: Short medial process (“low median ridge”, p. 724) present in dorsal valve; see Fig. 523.3b in Williams et al. (2000).

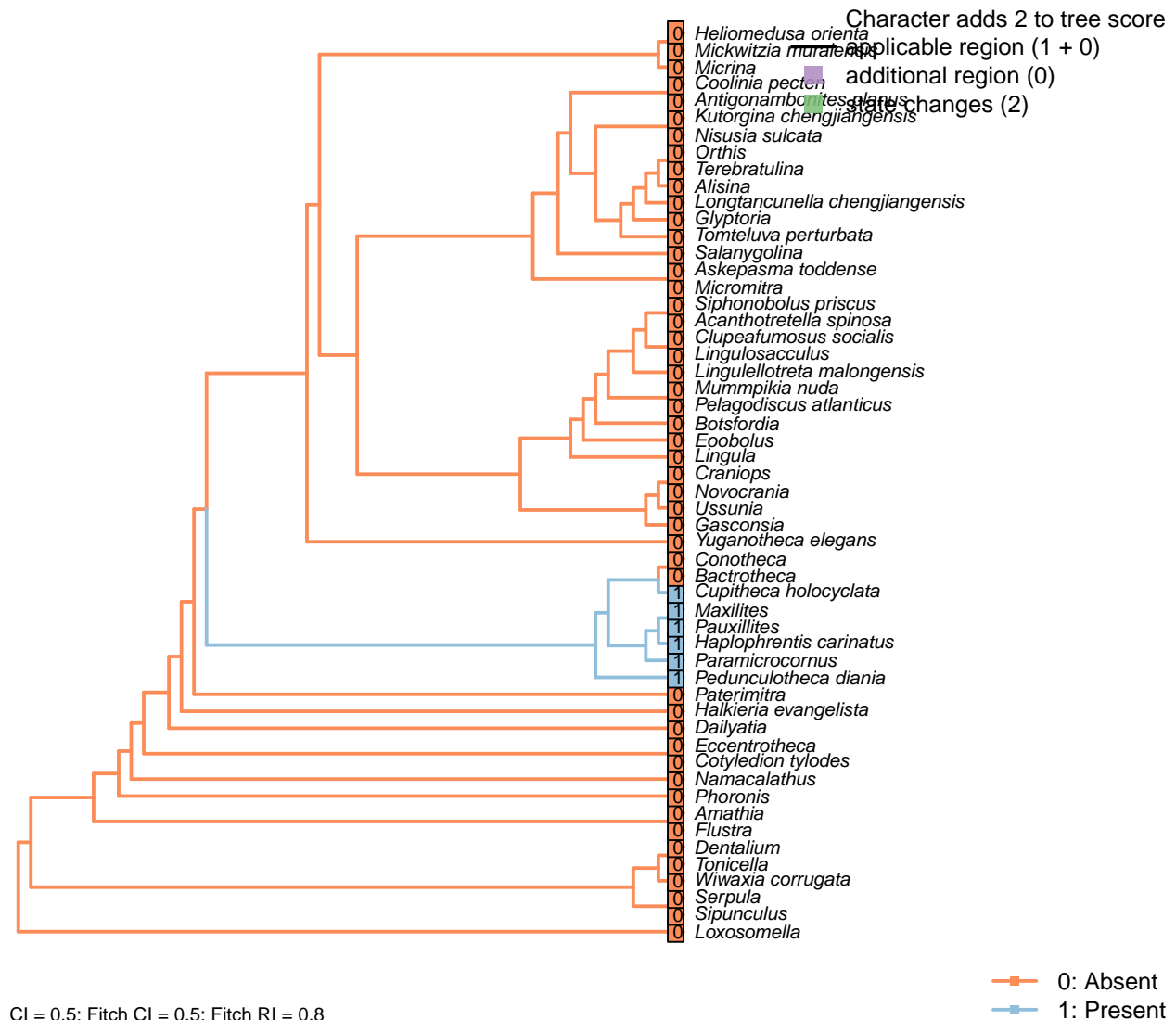
*Paramicrocornus*: Zhang et al. (2018).

*Pauxillites*: Marek (1966).

*Siphonobolus priscus*: “Dorsal interior [...] bisected by a short median ridge.” – Popov et al. (2009).

*Ussunia*: Following char 42 in table 15 in Williams et al. (2000).

## [100] Cardinal shield



### Character 100: Sclerites: Dorsal valve: Cardinal shield

0: Absent

1: Present

Neomorphic character.

The hyolithid operculum is divided into a cardinal and conical shield (Zhang et al., 2018), separated by furrows corresponding to the position of the helens. See Marek (1976) (fig. 2) or Martí Mus and Bergström (2005) (fig. 1) for schematic.

With no obvious sites for muscle attachment, the shields are unlikely to be homologous to the notothyrial

platform.

*Bactrotheca*: No differentiation between the cardinal and conical shields.

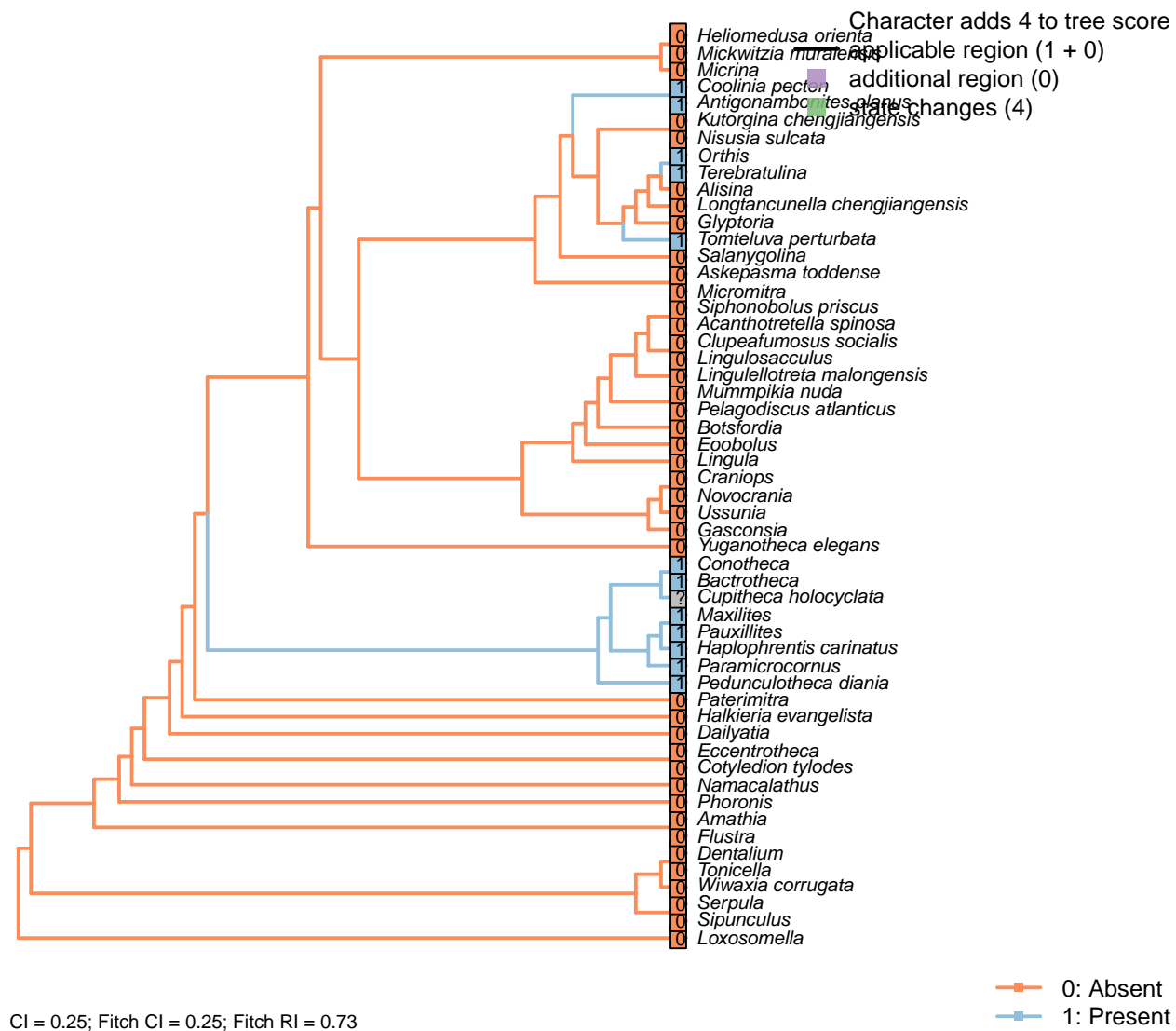
*Conotheca*: No differentiation between cardinal shield and conical shield (Wrona, 2003; Devaere et al., 2014).

*Cupitheca holocyclata*: Narrow cardinal shield (Skovsted et al., 2016).

*Maxilites*: Marek (1972).

*Paramicrocornus*: Zhang et al. (2018).

## [101] Cardinal processes



### Character 101: Sclerites: Dorsal valve: Cardinal processes

0: Absent

1: Present

Neomorphic character.

After Bassett *et al.* (2001) character 13. See Martí Mus and Bergström (2005) for an illustration. Cardinal processes are unlikely to be homologous with the notothyrial platform, even if their function is similar.

*Bactrotheca*: “Narrow broadly diverging cardinal processes with subparallel edges” – Valent *et al.* (2012).

*Clupeafumosus socialis*: Not reported by Topper *et al.* (2013a).

*Conotheca*: Present (Wrona, 2003).

*Cupitheca holocyclata*: Well-defined (Skovsted *et al.*, 2016).

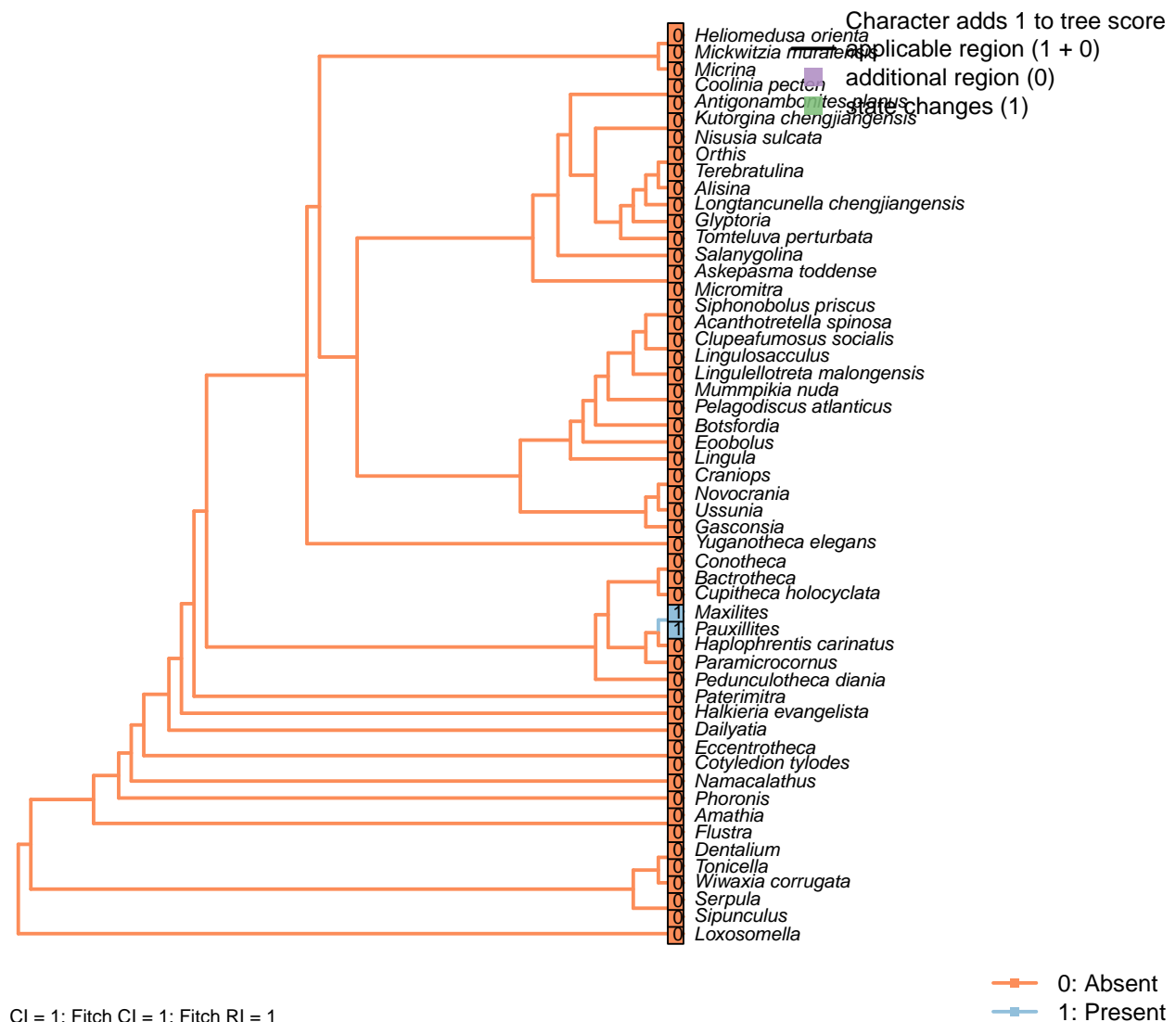
*Longtancunella chengjiangensis*: Not evident, and ought arguably to be discernable if present given the quality of preservation.

*Maxilites*: Narrow cardinal processes (Marek, 1972).

*Paramicrocornus*: Present (Zhang *et al.*, 2018).

*Pauxillites*: Marek (1966).

## [102] Cardinal teeth

**Character 102: Sclerites: Dorsal valve: Cardinal teeth**

0: Absent

1: Present

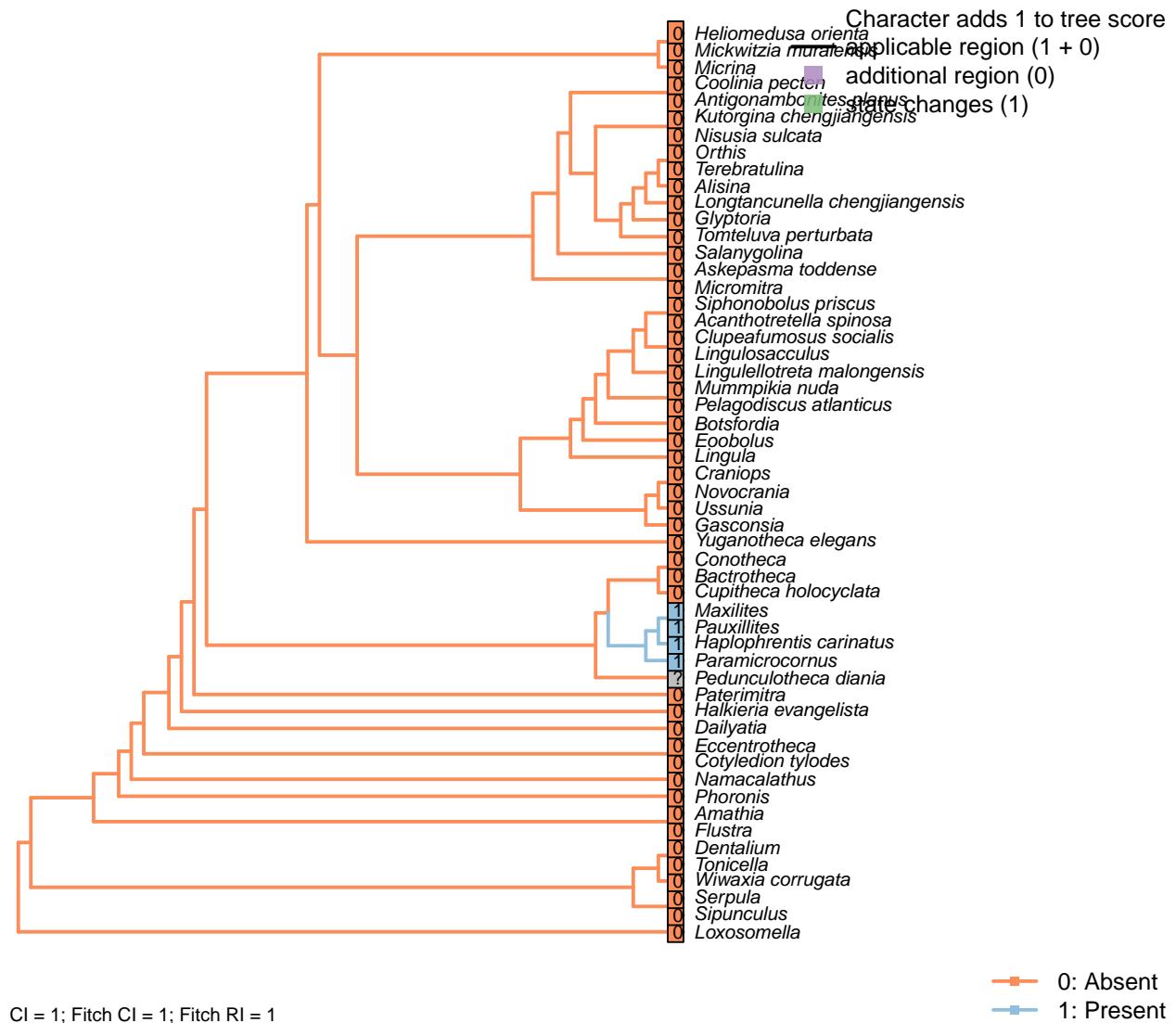
Neomorphic character.

Radially arranged teeth, separated by furrows, adorn the cardinal margin of the operculum of certain hyolithids (Marek, 1963). The absence of corresponding tooth sockets indicates that they do not serve to articulate the valves; Marek (1967) does not consider the teeth to be homologous with brachiopod cardinal teeth.

*Maxilites*: Dorsal teeth figured in Martí Mus and Bergström (2005).

*Pauxillites*: Present (Marek, 1966).

## [103] Clavicles

**Character 103: Sclerites: Dorsal valve: Clavicles**

0: Absent

1: Present

Neomorphic character.

Prominent symmetrical ridges on the inner surface of the hyolith operculum.

*Conotheca*: “Processes and clavicle-like structures are absent” – Devaere et al. (2014).

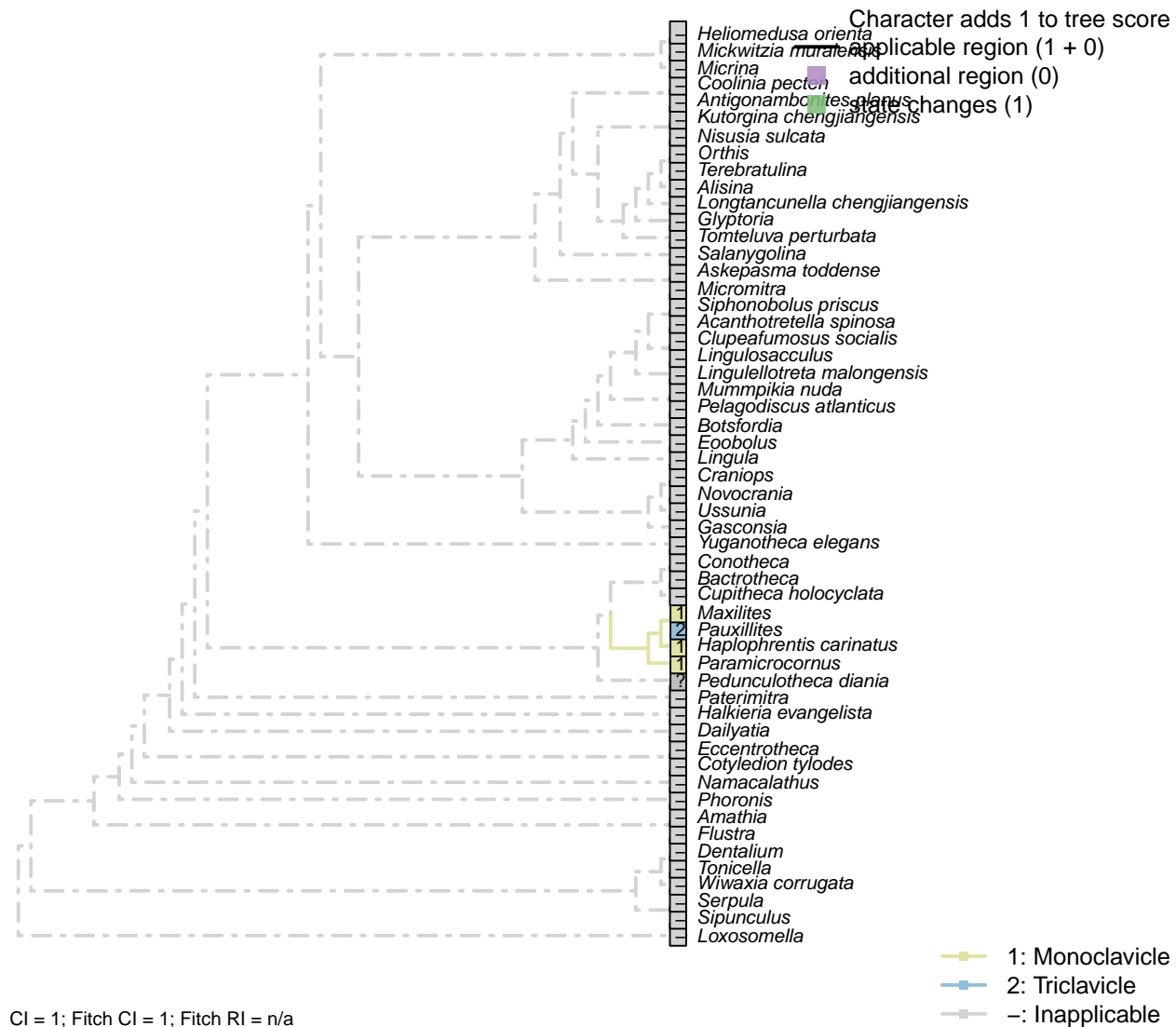
*Cupitheca holocyclus*: “No traces of clavicles” (Skovsted et al., 2016).

*Maxilites*: Single pair (Marek, 1972).

*Paramicrocornus*: Zhang et al. (2018).

*Pauxillites*: Marek (1966).

## [104] Clavicles: Type of clavicles



CI = 1; Fitch CI = 1; Fitch RI = n/a

**Character 104: Sclerites: Dorsal valve: Clavicles: Type of clavicles**

1: Monoclavicle

2: Triclavicle

Transformational character.

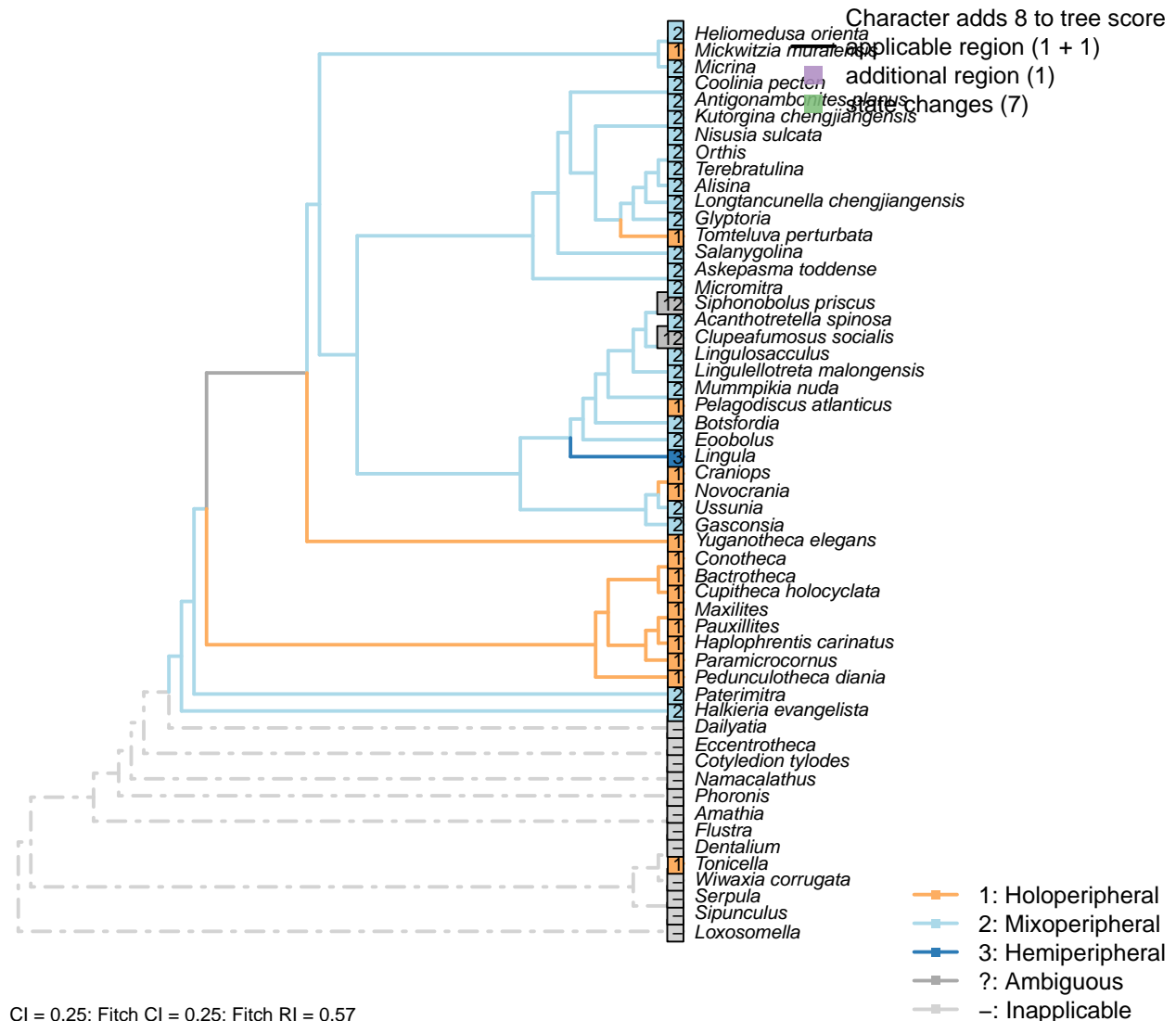
Usually the operculum of hyoliths has one pair of clavicles, but in some taxa of hyolithida there are more than one pair of clavicles, which can be divided into six types (Marek, 1967). The included taxa either exhibit a single pair of monoclavicles, or three pairs of clavicles.

*Paramicrocornus*: Zhang et al. (2018).

*Pauxillites*: Three pairs of clavicles (Marek, 1966).

## 5.13 Sclerites: Ventral valve

### [105] Growth direction



#### Character 105: Sclerites: Ventral valve: Growth direction

- 1: Holoperipheral
- 2: Mixoperipheral
- 3: Hemiperipheral
- Transformational character.

See Fig. 284 in Williams *et al.* (1997) for depiction of terms.

The growth direction dictates the attitude of the cardinal area relative to the hinge, which does not therefore represent an independent character.

Crudely put, if, viewed from a dorsal position, the umbo falls within the outer margin of the shell, growth is holoperipheral; if it falls outside the margin, it is mixoperipheral; if it falls exactly on the margin, it is

hemiperipheral.

*Clupeafumosus socialis*: Inferred from Topper *et al.* (2013a).

*Craniops*: “Both valves with growth holoperipheral” – Williams *et al.* (2000), p. 164.

*Heliomedusa orienta*: Williams *et al.* (2000, 2007) reconstruct mixoperipheral growth in the ventral valve [though Chen *et al.* (2007) reconstruct the valves the other way round, i.e. it is the ventral valve that grows holoperipherally, and the dorsal mixoperipherally].

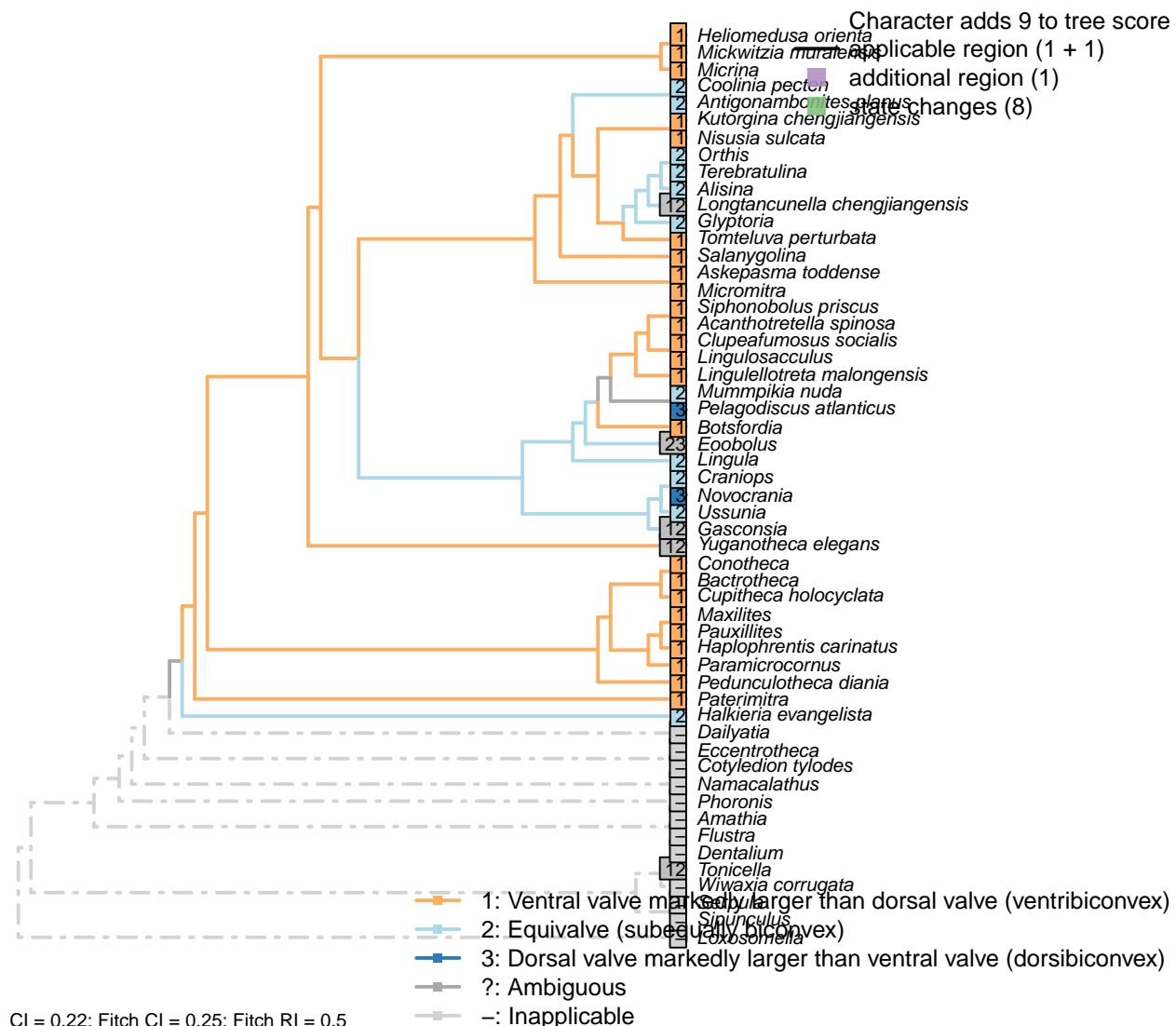
*Paterimitra*: The apical flange notwithstanding, the umbo of the S1 sclerite is posterior of the hinge line and the posterior edge of the lateral plate – see Larsson *et al.* (2014), fig. 2a, c.

*Siphonobolus priscus*: Initially holoperipheral (Popov *et al.*, 2009, p. 159), then on the brink of being mixoperipheral in adulthood, so coded as polymorphic.

*Tonicella*: Growth is hemiperipheral in the anterior valve of polyplacophorans and holoperipheral in the posterior valves (Schwabe, 2010; Connors *et al.*, 2012).

*Ussunia*: Growth “mixoperipheral in both valves” in trimerellids (Williams *et al.*, 2000; Popov *et al.*, 1997).

## [106] Relative size

**Character 106: Sclerites: Ventral valve: Relative size**

- 1: Ventral valve markedly larger than dorsal valve (ventribiconvex)
  - 2: Equivalve (subequally biconvex)
  - 3: Dorsal valve markedly larger than ventral valve (dorsibiconvex)
- Transformational character.

In many brachiopods, the valves are closely similar in size; in others, the ventral valve is markedly larger than the dorsal, on account of being more convex. Marginal cases are treated as ambiguous for the relevant states.

*Antigonambonites planus*: Broadly equivalve – see Williams *et al.* (2000) fig. 508.2c.

*Botsfordia*: After table 8 in Williams *et al.* (2000).

*Craniops*: “Shell subequally biconvex” – Williams *et al.* (2000).

*Eoobolus*: “*Eoobolus* is biconvex”, but in his amended diagnosis, Balthasar (2009) described it as “shell

inequivaled, dorsibiconvex".

*Gasconsia*: Equivalve as juveniles, becoming "convexiplane" (Williams et al., 2000, p. 187) as adults (Hanken and Harper, 1985).

*Heliomedusa orienta*: Ventral valve larger than the dorsal valve (Zhang et al., 2009, p. 659).

*Kutorgina chengjiangensis*: Ventral valve larger (see Williams et al., 2000, fig. 125.).

*Longtancunella chengjiangensis*, *Yuganotheca elegans*: The ventral valve is somewhat, but not markedly, larger than the dorsal; as such, this character is coded ambiguous for equivalve/ventral valve larger.

*Mummpikia nuda*: Aside from hinge, valves similar in convexity and size (Balthasar, 2008).

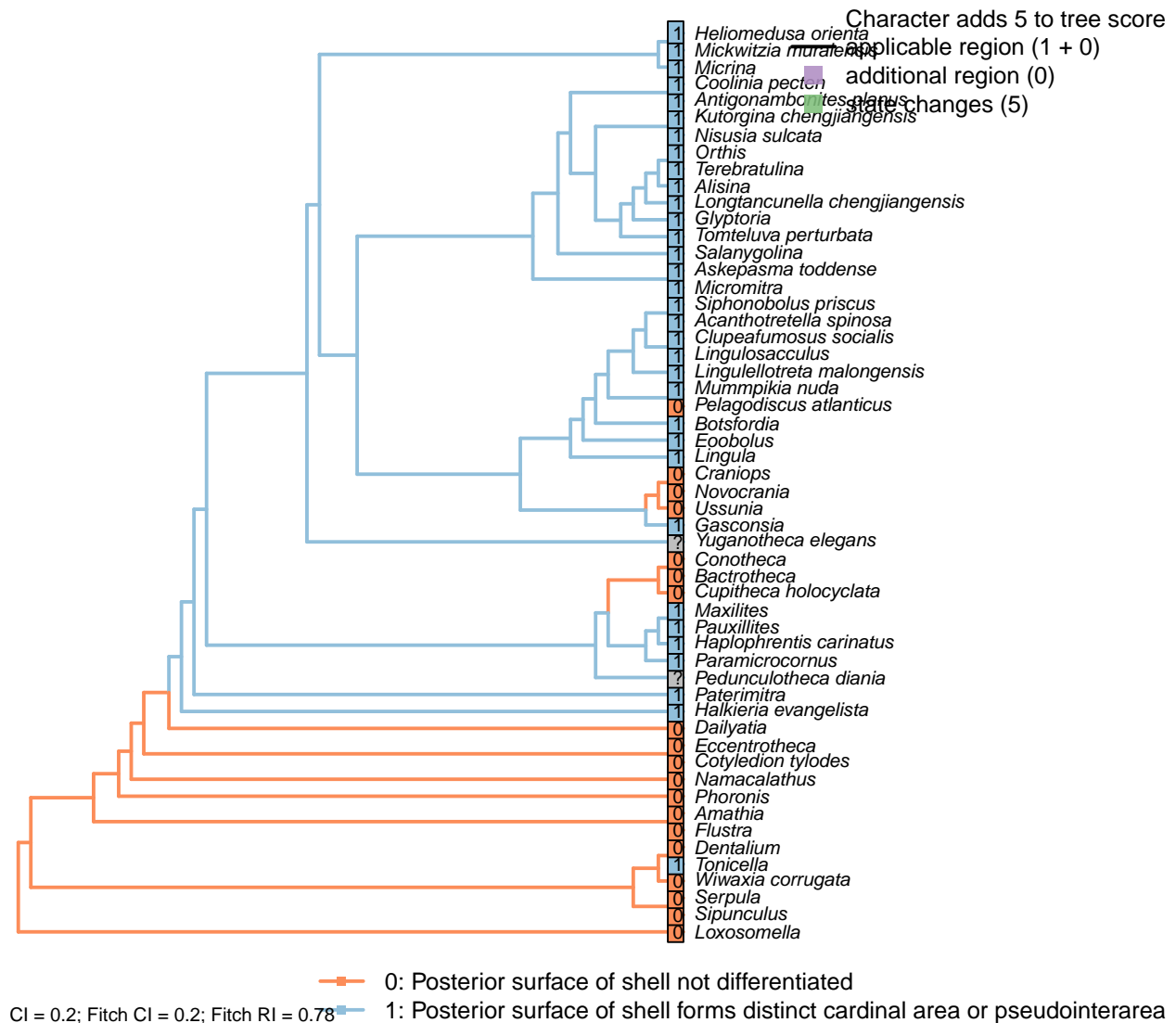
*Nisusia sulcata*: Ventral valve larger (see Williams et al., 2000, fig. 126.).

*Siphonobolus priscus*: Ventribiconvex (Popov et al., 2009).

*Tonicella*: Coded as ambiguous for equivalve/ventral valve larger: the posterior embryonic shell field, treated herein as equivalent to the ventral valve,.

*Ussunia*: Subequally biconvex (Williams et al., 2000, p. 192).

### [107] Posterior surface: Differentiated



#### Character 107: Sclerites: Ventral valve: Posterior surface: Differentiated

0: Posterior surface of shell not differentiated

1: Posterior surface of shell forms distinct cardinal area or pseudointerarea

Neomorphic character.

In shells that grow by mixoperipheral growth, the triangular area subtended between each apex and the posterior ends of the lateral margins is termed the cardinal area. In shells with holoperipheral growth, a flattened surface on the posterior margin of the valve is termed a pseudointerarea (paraphrasing Williams et al., 1997).

In order for this character to be independent of a shell's growth direction, we do not distinguish between a "cardinal area", "interarea" or "pseudointerarea".

*Alisina, Antigonambonites planus, Coolinia pecten, Glyptoria, Kutorgina chengjiangensis, Nisusia sulcata,*

*Orthis, Salanygolina, Tomteluva perturbata*: Interarea present.

*Bactrotheca*: No clear delineation of posterior (functionally dorsal) surface.

*Clupeafumosus socialis*: Described by Topper *et al.* (2013a).

*Conotheca*: Round in cross-section, with no clear delineation of posterior (functionally dorsal) surface (Devlaere *et al.*, 2014).

*Cupitheca holocyclata*: No evidence of differentiation; circular cross-section (Vendrasco *et al.*, 2017).

*Gasconsia*: The region corresponding to the ventral (pseudo)interarea is described as a “trimerellid ventral cardinal area” by Williams *et al.* (2000, p.162), who code both an interarea and a pseudointerarea as absent in trimerellids.

*Heliomedusa orienta*: Zhang *et al.* (2009) report a moderate to somewhat developed ventral pseudointerarea, confirmed by Williams *et al.* (2007).

*Lingulosacculus*: The conical valve is interpreted as the ventral valve with an extended pseudointerarea.

*Longtancunella chengjiangensis*: Though “all evidence of a pseudointerarea is lacking” – Zhang *et al.* (2011a) – the region of the shell between the strophic hinge line and the colleplax (fig. 2 in Zhang *et al.*, 2011a) is distinct from the rest of the shell; the ends of the strophic hinge line are marked by prominent nicks in the shell margin. *Longtancunella* is therefore coded as having a differentiated posterior surface.

*Mickwitzia muralensis*: Termed an interarea by Balthasar (2004).

*Mummpikia nuda*: Balthasar (2008) interprets a pseudointerarea as being present – e.g. p273, “Of particular interest is the vault that bridges the most anterior portion of the ventral pseudointerarea and raises it above the visceral platform.”; “This pattern is reversed in the ventral valves of *M. nuda*, where the anterior projection of the pedicle groove is raised above the valve floor whereas the lateral parts of pseudointerarea are not”.

*Paterimitra*: Triangular notch and subapical flange.

*Pedunculotheca diania*: Lateral lines suggest differentiation of posterior surface, but difficult to discern a change in morphology of this region. Coded ambiguous.

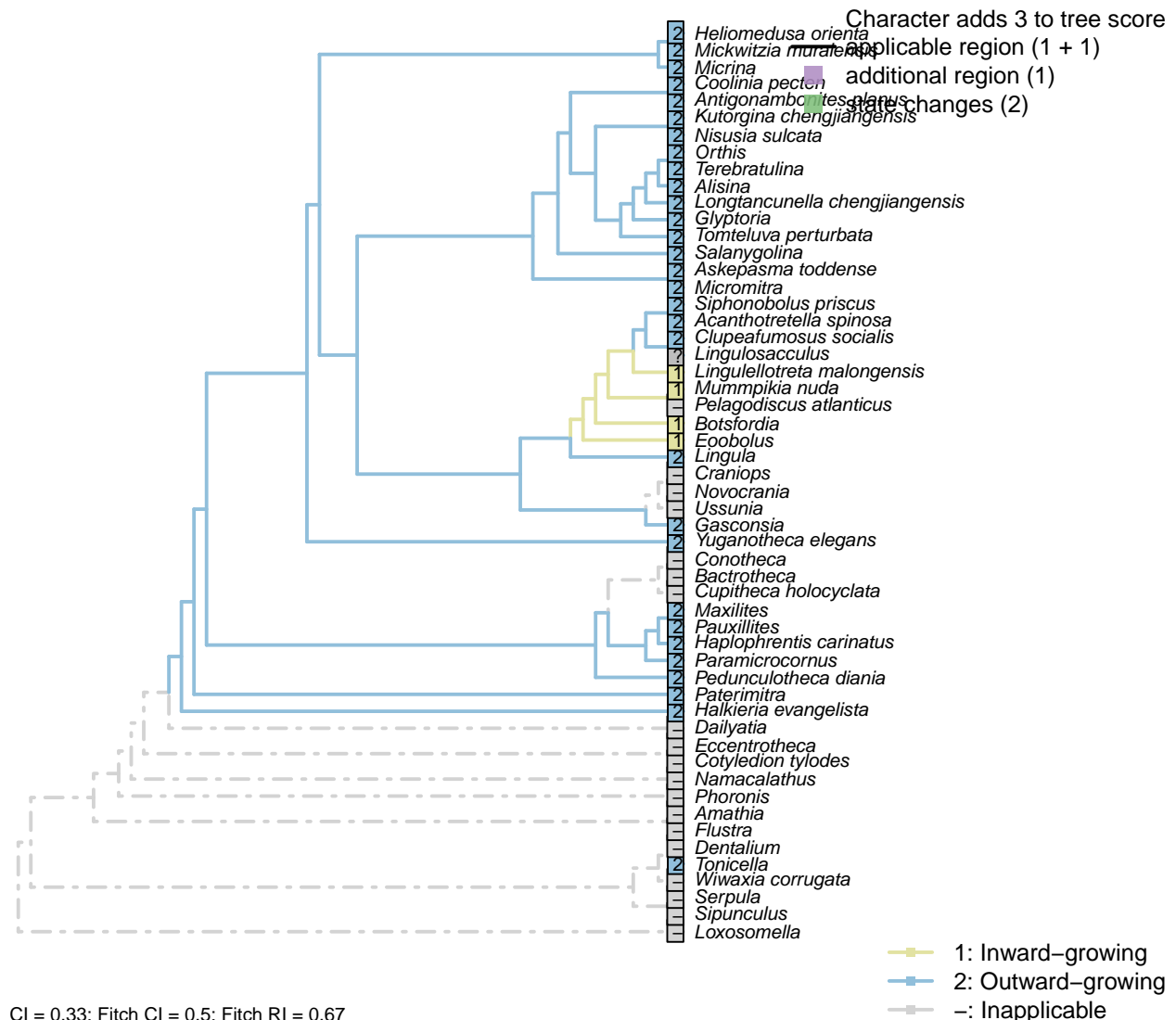
*Siphonobolus priscus*: “Ventral pseudointerarea, low, undivided, poorly defined” – Williams *et al.* (2000).

*Terebratulina*: Interarea.

*Tonicella*: Following the proposed homology model between the posterior valve of polyplacophorans and the ventral valve of brachiopods, the “posterior” surface of the polyplacophoran valve is taken to be the surface that would articulate with the anterior valve, which is anatomically anterior on the living organism.

*Ussunia*: Following char 17 in table 15 of Williams *et al.* (2000).

### [108] Posterior margin growth direction



#### Character 108: Sclerites: Ventral valve: Posterior margin growth direction

- 1: Inward-growing
- 2: Outward-growing
- Transformational character.

Balthasar (2008) notes an inward-growing posterior margin of the pseudointerarea as potentially linking *Mummpikia* with the linguliform brachiopods.

Coded as inapplicable in taxa without a differentiated posterior margin: the posterior margin can only grow

inwards if it is differentiated from the anterior margin; else the entire shell would grow in on itself.

*Botsfordia*: Inward-growing; see Skovsted & Holmer (2005), pl. 4.

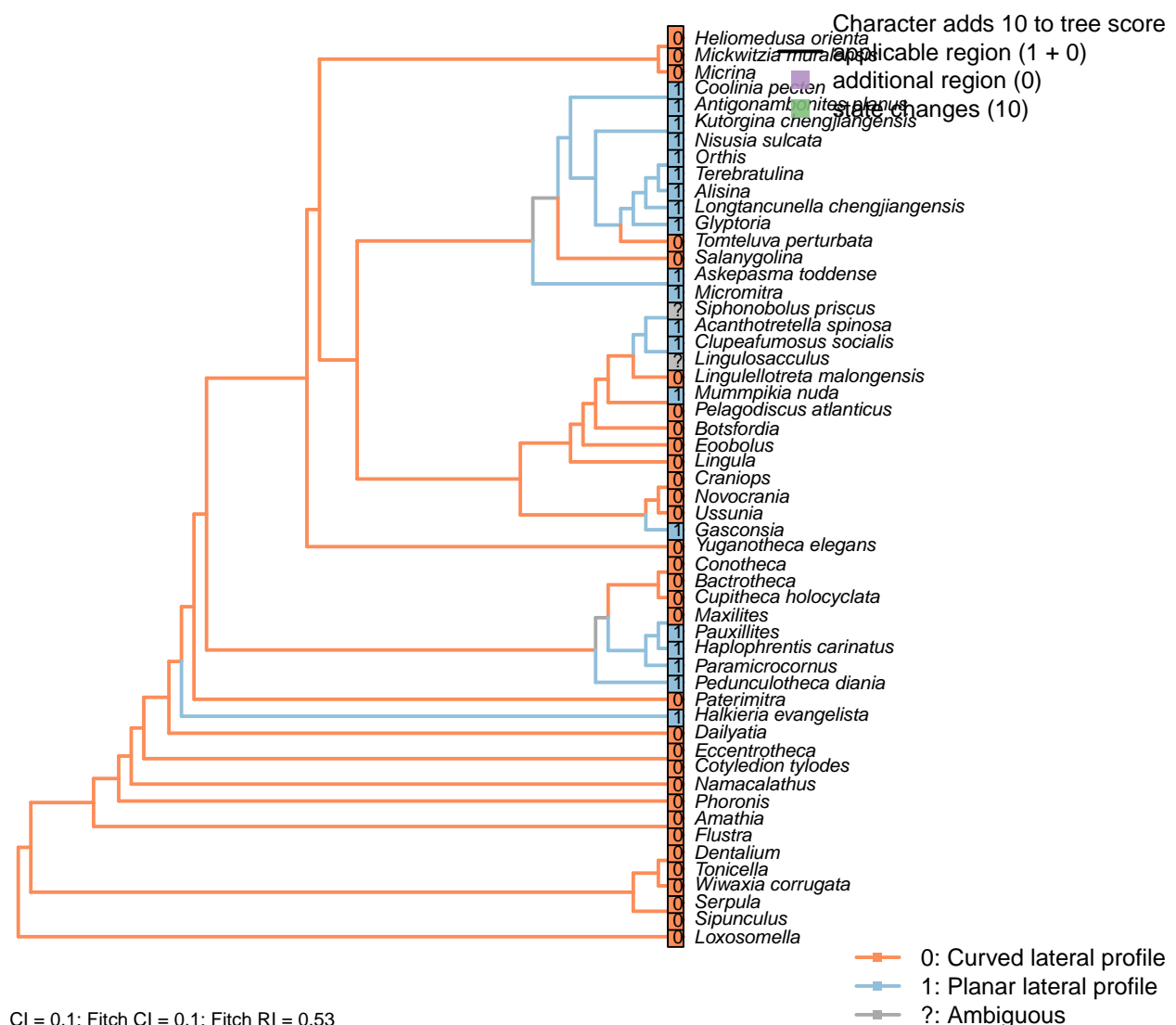
*Clupeafumosus socialis*: See Topper *et al.* (2013a).

*Eoobolus*: See for example Skovsted & Holmer (2005), pl. 3.

*Lingulellotreta malongensis*: Transverse cross section of ventral pseudointerarea concave.

*Mummpikia nuda*: Balthasar (2008) interprets an inward-growing posterior margin of the pseudointerarea – e.g. p273, “Of particular interest is the vault that bridges the most anterior portion of the ventral pseudointerarea and raises it above the visceral platform [...] An inward-growing posterior margin is otherwise known only from the pseudointerareas of linguliform brachiopods”.

### [109] Posterior surface: Planar



#### Character 109: Sclerites: Ventral valve: Posterior surface: Planar

0: Curved lateral profile

1: Planar lateral profile

Neomorphic character.

It is possible for a cardinal area or pseudointerarea to be distinct from the anterior part of the shell, yet to remain curved in lateral profile.

Taking an undifferentiated posterior margin as primitive, the primitive condition is curved – flattening of the posterior margin represents an additional modification that can only occur once the posterior margin is differentiated.

A flat and triangular interarea links *Mummpikia* with the Obolellidae (Balthasar, 2008) – but all included taxa have triangular interareas, so this is not listed as a separate character.

*Acanthotretella spinosa*: ventral pseudointerareas are most similar to those found within the Order Siphonotretida.

*Botsfordia*: See Skovsted & Holmer (2005), pl. 3, fig. 14.

*Clupeafumosus socialis*: “Ventral pseudointerarea is gently procline and is flat in lateral profile”. — (Topper et al., 2013a).

*Conotheca*: Strongly curved in some species (Wrona, 2003).

*Eoobolus*: Some curvature retained.

*Haplophrentis carinatus*: Dorsal surface essentially linear (Moysiuk et al., 2017, fig ed6a, ed7a).

*Lingulellotreta malongensis*: Transverse cross section of ventral pseudointerarea concave.

*Longtancunella chengjiangensis*: Flattened, reflecting the strophic hinge line.

*Maxilites*: Gently sinuous (Martí Mus and Bergström, 2005).

*Micromitra*: Essentially planar; see fig. 6 in Ushatinskaya (2016).

*Paramicrocornus*: Posterior (functionally dorsal) surface is linear in adults (though slightly curving in juveniles) (Zhang et al., 2018).

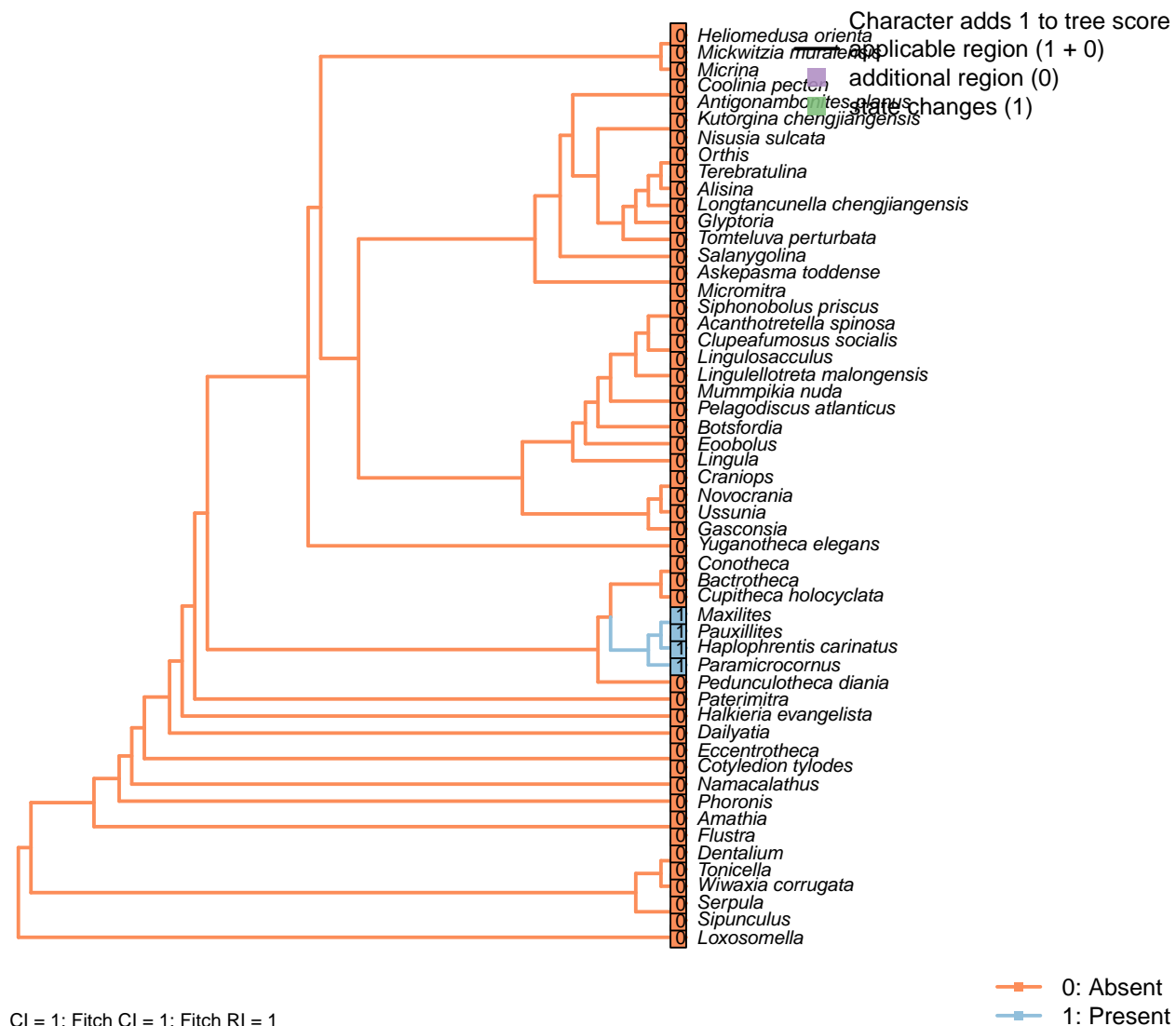
*Pauxillites*: Reconstructed as linear by Marek (1976).

*Pedunculotheca diania*: Essentially linear.

*Siphonobolus priscus*: ‘Almost’ planar – see Popov et al. (2009, fig. 4). Coded as ambiguous.

*Tonicella*: (Schwabe, 2010).

## [110] Ligula



CI = 1; Fitch CI = 1; Fitch RI = 1

**Character 110: Sclerites: Ventral valve: Ligula**

0: Absent

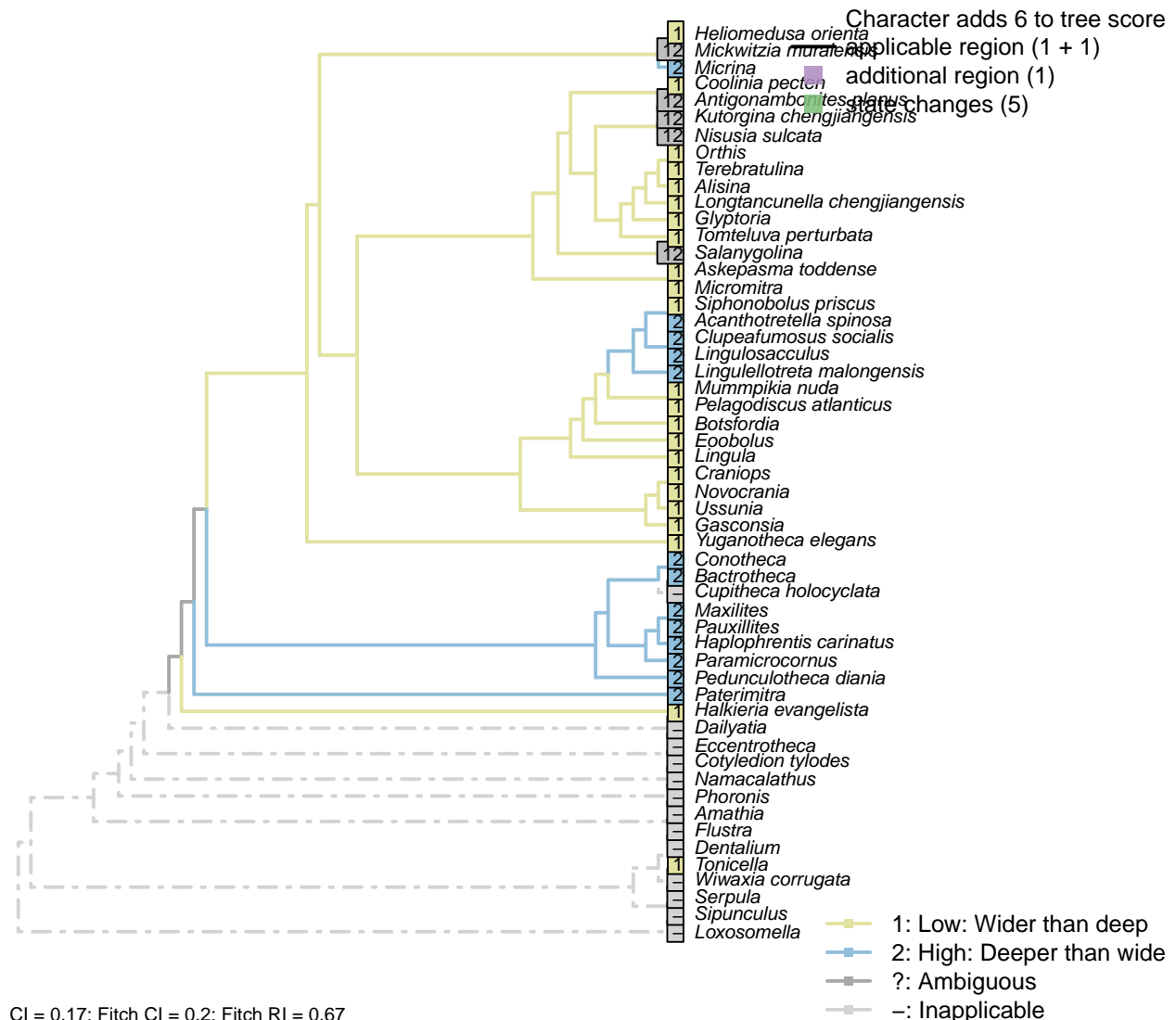
1: Present

Neomorphic character.

The aperture of many hyolithid hyoliths is characterised by a ligula, a tongue-like protruding shelf on the functionally ventral surface of conical shell (Martí Mus and Bergström, 2005). This can be recognized by an acute angle in the lateral profile of the commissure (see second figure on p. 91 of Marek, 1966). No brachiopods display an equivalent feature.

*Paramicrocornus*: “Very short” semicircular ligula (Zhang et al., 2018).

### [111] Posterior surface: Extent



Distinguishes taxa whose ventral valve is essentially flat from those that are essentially conical.

*Antigonambonites planus*: Though scored High in data matrix of Benedetto (2009), this taxon (see Williams et al., 2000, fig. 508) does not express the deeply conical ventral valve that this character is intended to reflect. It is charitably coded as ambiguous.

*Clupeafumosus socialis*: Entire valve length – see schematic in Williams et al. (1997), fig. 286.

*Coolinia pecten*: See fig. 485 in Williams et al. (2000).

*Gasconsia*: “ventral cardinal interarea low, apsacline, with narrow, poorly defined homeodeltidium” – Williams et al. (2000), p. 186.

*Kutorgina chengjiangensis*: This taxon (see Williams et al., 2000, fig. 129; Popov, 1992, fig. 1) comes close

to expressing the deeply conical ventral valve that this character is intended to reflect, though this is not always so pronounced (e.g. Williams et al., 2000, fig. 125). It is therefore coded as ambiguous.

*Mickwitzia muralensis*: Often not prominently high (Skovsted and Holmer, 2003; Balthasar, 2004), though in some cases (e.g. Butler et al., 2015) the ventral valve approaches the conical shape that this character is intended to capture. Coded as polymorphic.

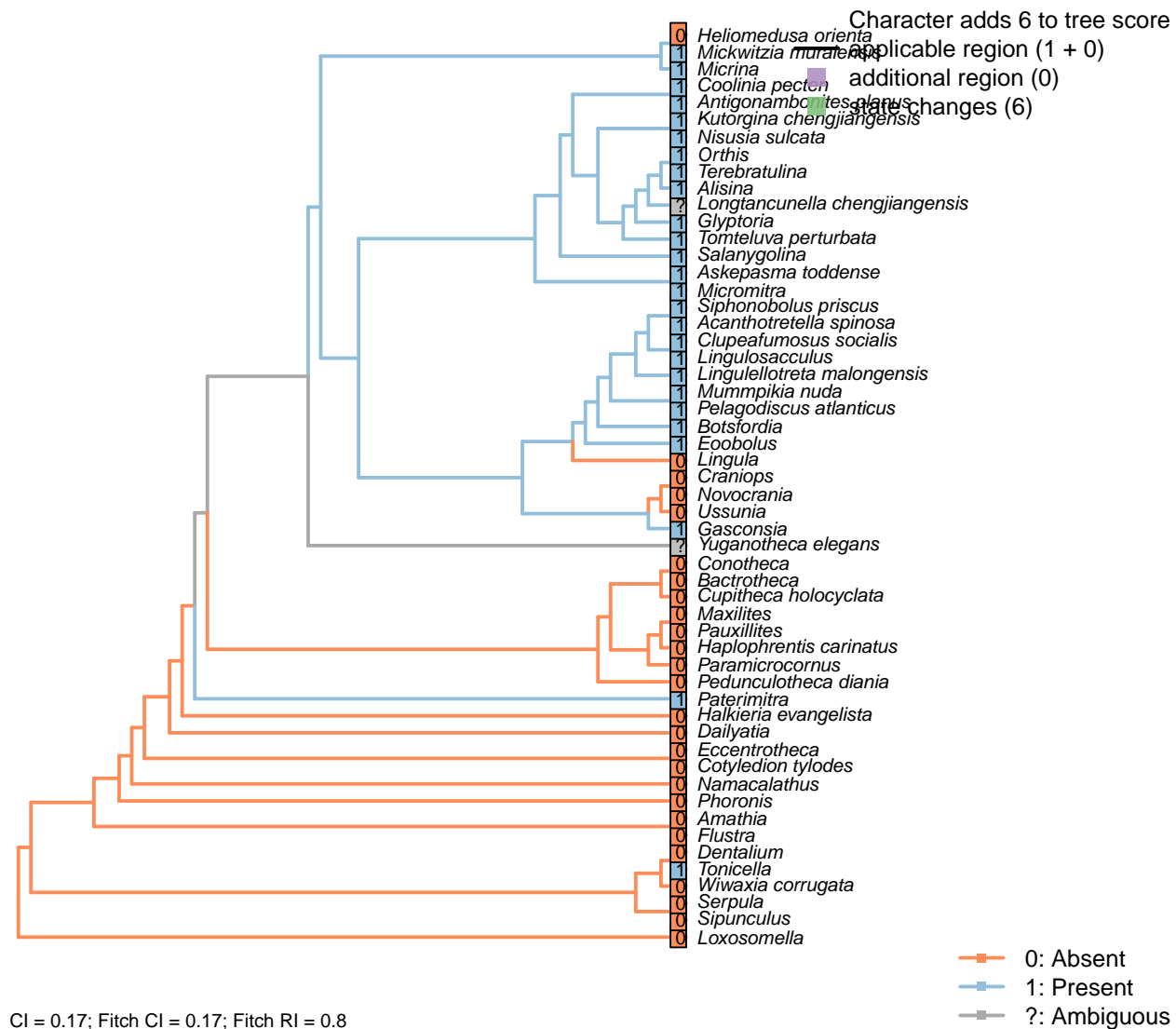
*Nisusia sulcata*: Scored as high in data matrix of Benedetto (2009), and depicted as such in Williams et al. (2000, fig. 125) and Popov (1992, fig. 1); but not high in all specimens (e.g. Williams et al., 2000, fig. 126). It is therefore coded as polymorphic.

*Novocrania*: Low cone.

*Orthis*: Scored ‘Low’ for *Eoorthis* by Benedetto (2009); assumed same in *Orthis*.

*Salanygolina*: Whereas Williams et al. (2000, p. 156) describe the ventral pseudointerarea as high, the shell lacks the deeply conical aspect that this character is intended to capture; we thus code the taxon as ambiguous.

## [112] Posterior surface: Delthyrium



**Character 112: Sclerites: Ventral valve: Posterior surface: Delthyrium**

0: Absent

1: Present

Neomorphic character.

A delthyrium is an opening in an interarea or pseudointerarea that accommodates the pedicle, and may be filled with plates.

The homology of the pedicle in the pseudointerarea of obolellids and botsfordiids with the umbonal pedicle foramen of acrotretids was proposed by Popov (1992), and seemingly corroborated by observations of Ushatinskaya & Korovnikov (2016), who note that the propareas of the *Botsfordia* ventral valve sometimes merge to form an elongate teardrop-shaped pedicle foramen.

*Acanthotretella spinosa*: Origin modelled on *Siphonobolus*.

*Askepasma toddense*: Homeodeltidium absent (Williams et al., 2000, p. 153); deltidium is open (see Topper et al., 2013b, fig. 4).

*Botsfordia*: The homology of the triangular notch or groove in the pseudointerarea with the umbonal pedicle foramen of acrotretids was proposed by Popov (1992), and seemingly corroborated by observations of Ushatinskaya & Korovnikov (2016), who note that the propareas of the *Botsfordia* ventral valve sometimes merge to form an elongate teardrop-shaped pedicle foramen.

*Clupeafumosus socialis*: Following Popov (1992), the larval delthyrium is sealed in adults by outgrowths of the posterolateral margins of the shell.

*Eoobolus*: See for example fig. 5 in Balthasar (2009).

*Glyptoria*: “Delthyrium and notothyrium open, wide” – Cooper (1976).

*Longtancunella chengjiangensis*: Unclear: a narrow ridge that may correspond to a pseudodeltidium evident in fig 2a and sketched in fig. 2c is not discussed in the text of Zhang et al. (2011a), so the delthyrial region is coded as ambiguous.

*Mickwitzia muralensis*: A delthyrium is present in young individuals (Balthasar, 2004).

*Micrina*: Opening inferred by Holmer et al. (2008).

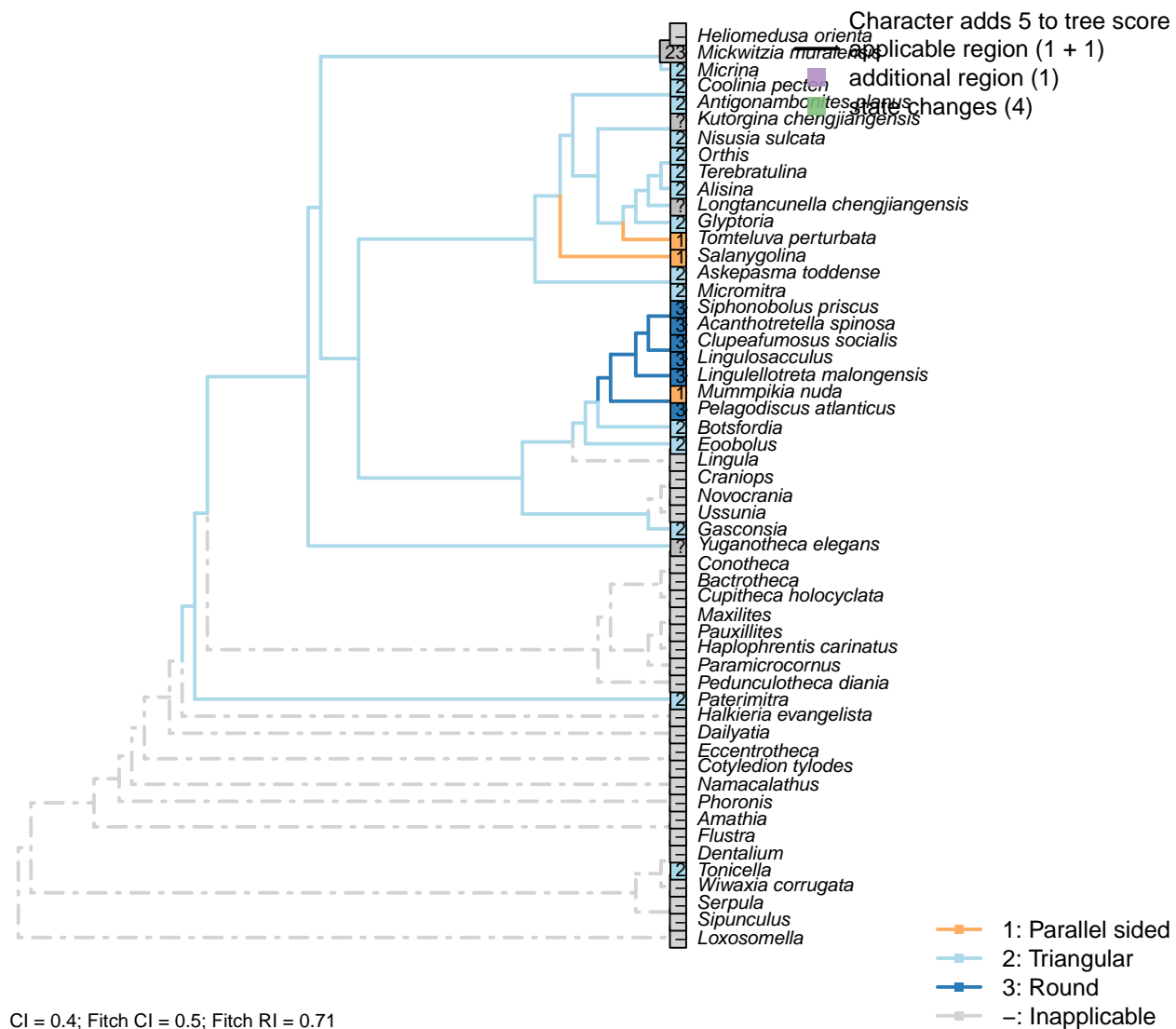
*Pelagodiscus atlanticus*: The listrum (pedicle opening) is interpreted as originating via a similar mechanism to that of acrotretids (Popov, 1992), and hence corresponding to a basally sealed delthyrium.

*Siphonobolus priscus*: Ontogeny presumed to resemble that of acrotretids.

*Tonicella*: The antemucronal area (Schwabe, 2010) is treated as equivalent to the brachiopod delthyrium.

*Yuganotheca elegans*: Details of the hinge region are unclear due to the flattened and overprinted nature of fossil preservation.

## [113] Posterior surface: Delthyrium: Shape



## Character 113: Sclerites: Ventral valve: Posterior surface: Delthyrium: Shape

1: Parallel sided

2: Triangular

3: Round

Transformational character.

A parallel-sided delthyrium links *Mummipikia* with the Obolellidae (Balthasar, 2008).

Following Popov (1992), the larval delthyrium of acrotretids and allied taxa is understood to be sealed in adults by outgrowths of the posterolateral margins of the shell. The resultant round or teardrop-shaped foramen corresponds to the delthyrium.

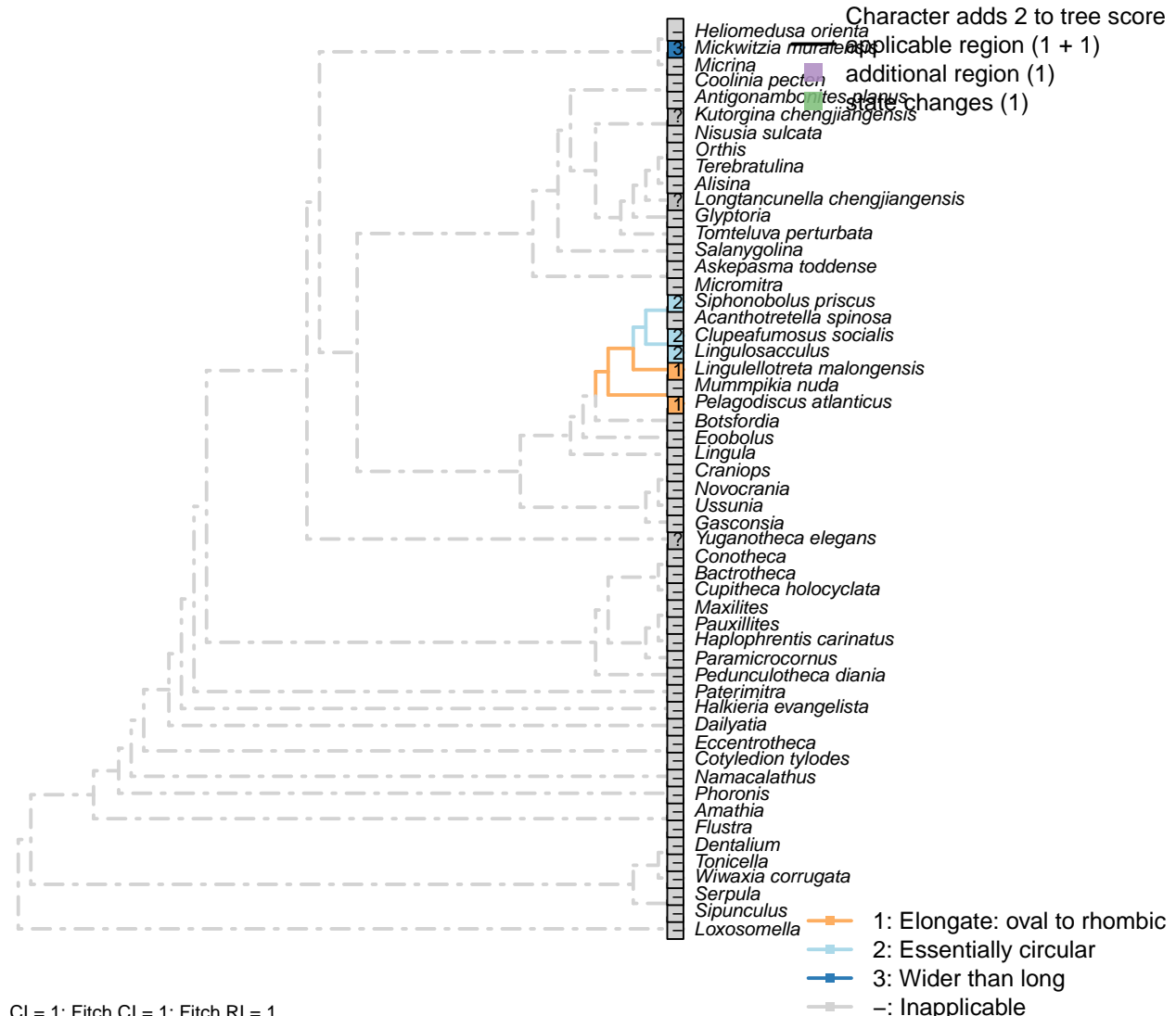
*Askepasma toddense*: Prominently triangular (see Topper et al., 2013b, fig. 2).

*Clupeafumosus socialis*: Following the model of Popov (1992).

*Mickwitzia muralensis*: An opening is incorporated at the base of the homeodeltidium when the organism switches from early to late maturity (fig. 10 in Balthasar, 2004). This opening is conceivably homologous

with the pedicle foramen of acrotretid brachiopods and their ilk. To reflect this possible homology, *Mickwitzia* is coded as polymorphic (triangular/round).

### [114] Posterior surface: Delthyrium: Shape: Aspect of rounded opening



CI = 1; Fitch CI = 1; Fitch RI = 1

#### Character 114: Sclerites: Ventral valve: Posterior surface: Delthyrium: Shape: Aspect of rounded opening

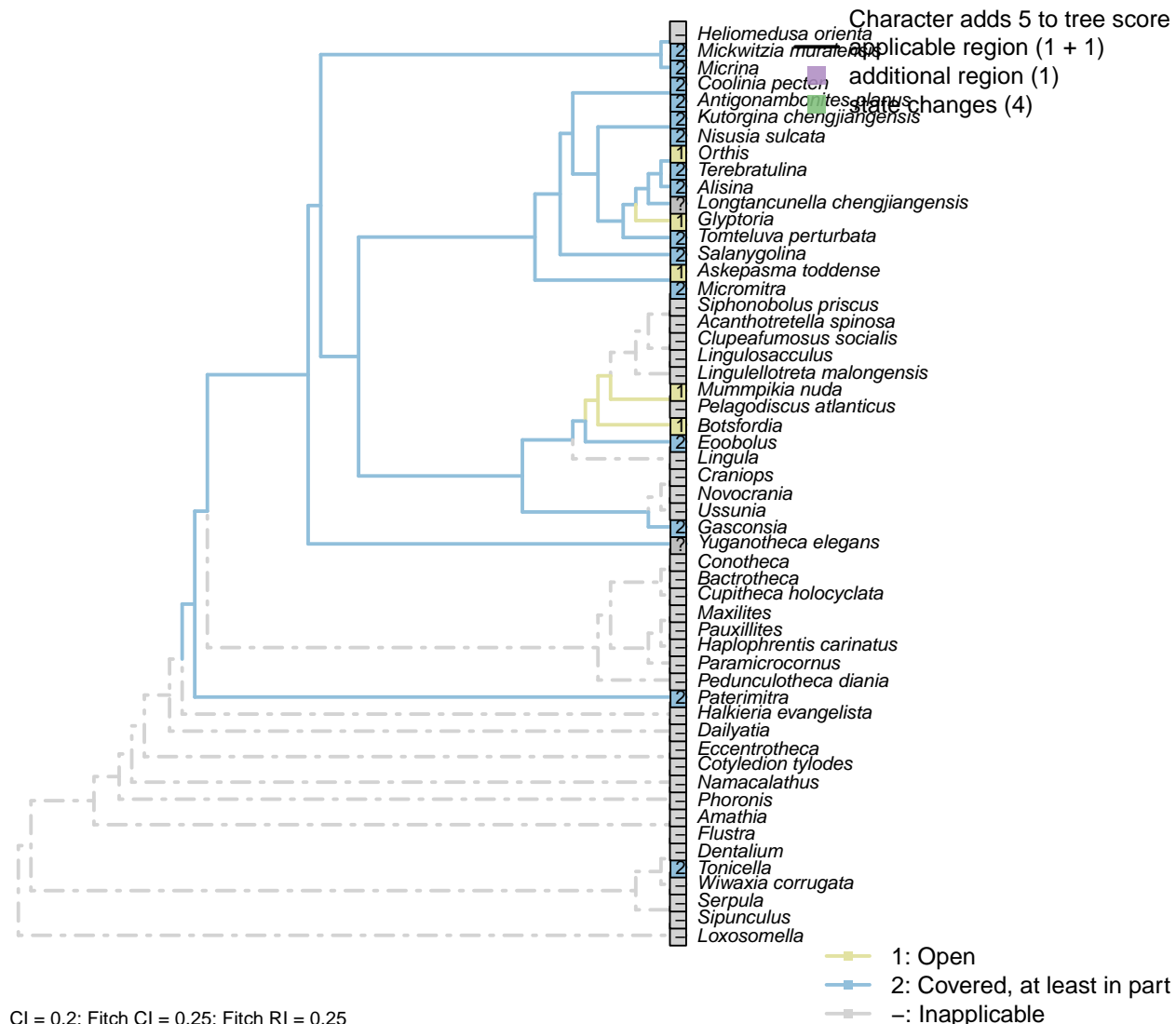
- 1: Elongate: oval to rhombic
- 2: Essentially circular
- 3: Wider than long
- Transformational character.

Chen *et al.* (2007) propose that an oval to rhombic foramen characterises the discinids [and *Heliomedusa*, though the foramen in this taxon has since been reinterpreted by Zhang *et al.* (2009) as an impression of internal tissue].

*Lingulellotreta malongensis*: Oval (Williams *et al.*, 2000).

*Mickwitzia muralensis*: Wider than long: see fig. 10 in Balthasar (2004).

## [115] Posterior surface: Delthyrium: Cover

**Character 115: Sclerites: Ventral valve: Posterior surface: Delthyrium: Cover**

- 1: Open
- 2: Covered, at least in part
- Transformational character.

An open delthyrium links *Mummipikia* with the Obolellidae (Balthasar, 2008).

The delthyrial opening can be covered by one or more deltidial plates, or a pseudodeltitium.

Inapplicable in taxa with a round delthyrium (generated by overgrowth of the delthyrial opening by postero-

lateral parts of the shell, per Popov, 1992).

*Askepasma toddense*: Open (Topper et al., 2013b).

*Botsfordia*: See pl. 3 fig. 15 in Skovsted & Holmer (2005).

*Coolinia pecten*: A convex pseudodeltidium completely covers the delthyrium in *Coolinia*.

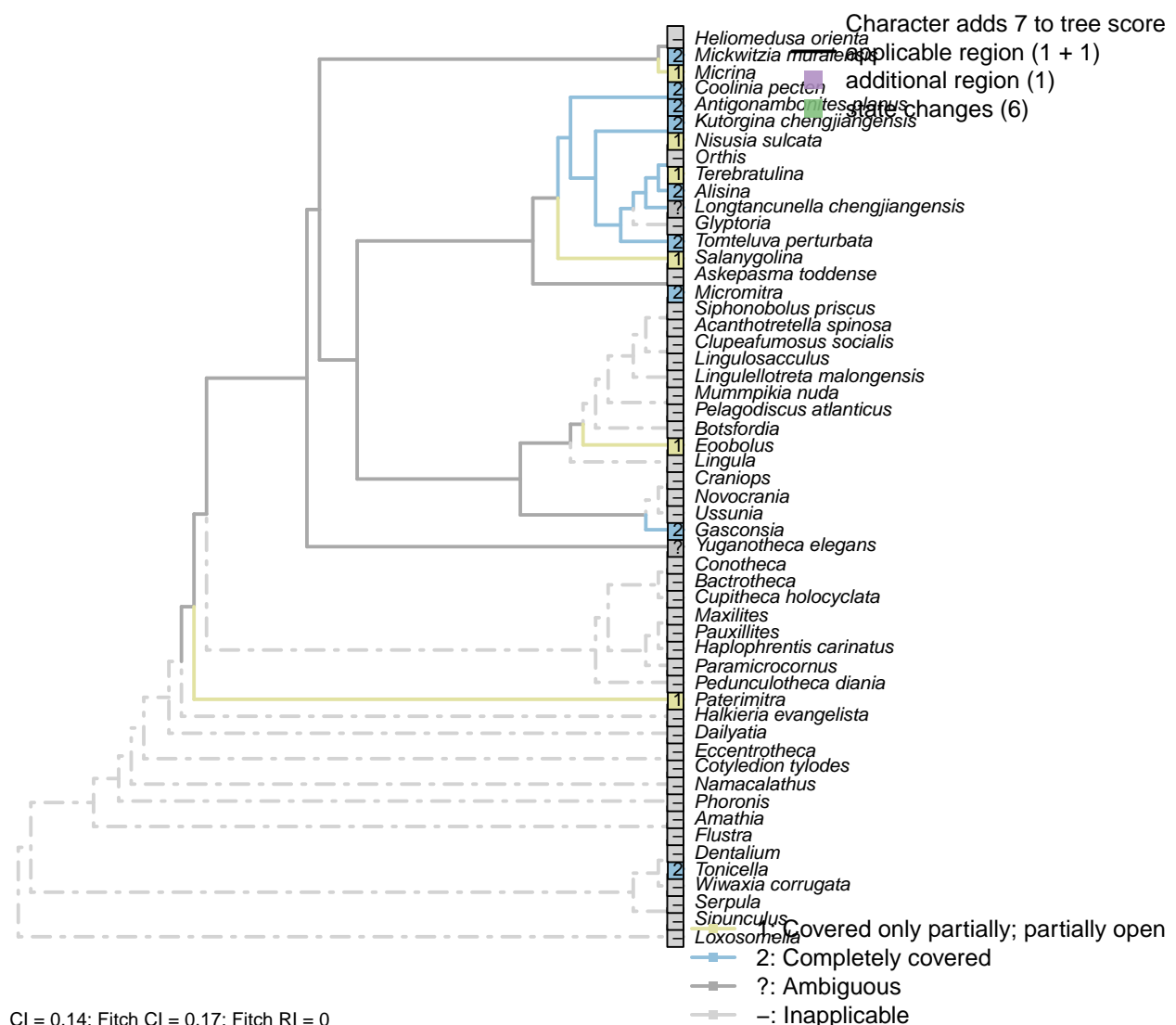
*Glyptoria*: Coded as open by Williams et al. (1998b).

*Micromitra*: Williams et al. (2000), fig. 83.3.

*Nisusia sulcata*: “Covered only apically by a small convex pseudodeltitium” – Holmer et al. (2018a).

*Paterimitra*: Covered by subaical flange, in part.

### [116] Posterior surface: Delthyrium: Cover: Extent



CI = 0.14; Fitch CI = 0.17; Fitch RI = 0

**Character 116: Sclerites: Ventral valve: Posterior surface: Delthyrium: Cover: Extent**

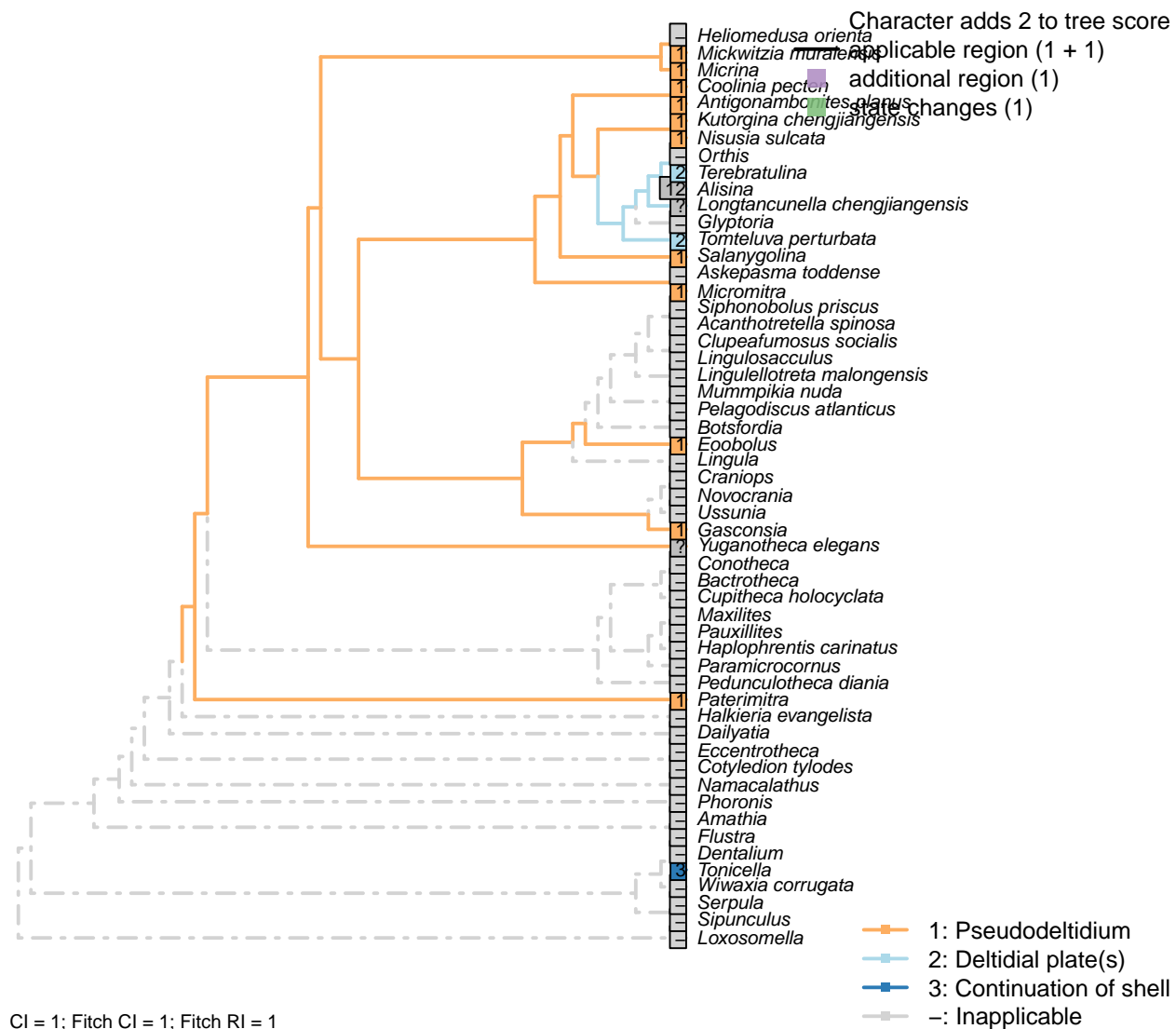
- 1: Covered only partially; partially open  
 2: Completely covered  
 Transformational character.

*Micrina*: Remains somewhat open.

*Micromitra*: Completely covered (Williams et al., 2000, fig. 83.3).

*Nisusia sulcata*: A well-defined pseudo-deltidium [...] closes only the apical part of the delthyrium (Rowell and Caruso, 1985).

### [117] Posterior surface: Delthyrium: Cover: Identity



**Character 117: Sclerites: Ventral valve: Posterior surface: Delthyrium: Cover: Identity**

- 1: Pseudodeltidium  
 2: Deltidial plate(s)  
 3: Continuation of shell  
 Transformational character.

This character has the capacity for further resolution (one or more deltidial plates), but this is unlikely to affect the results of the present study.

The pseudodelthyrium is also referred to as a homeodeltidium.

The antemucronal area of Polyplacophora is treated as equivalent to the brachiopod delthyrium, but is not depositionally distinct to the rest of the shell, so is coded with a distinct character state.

*Alisina*: Stated as “concave pseudodeltidium with median plication” – Williams et al. (2000)  
Coded as “Pseudodeltidium: Covered by concave plate” by Bassett *et al.* (2001).

*Askepasma toddense*: No pseudodeltidium (Williams et al., 2000, p. 153).

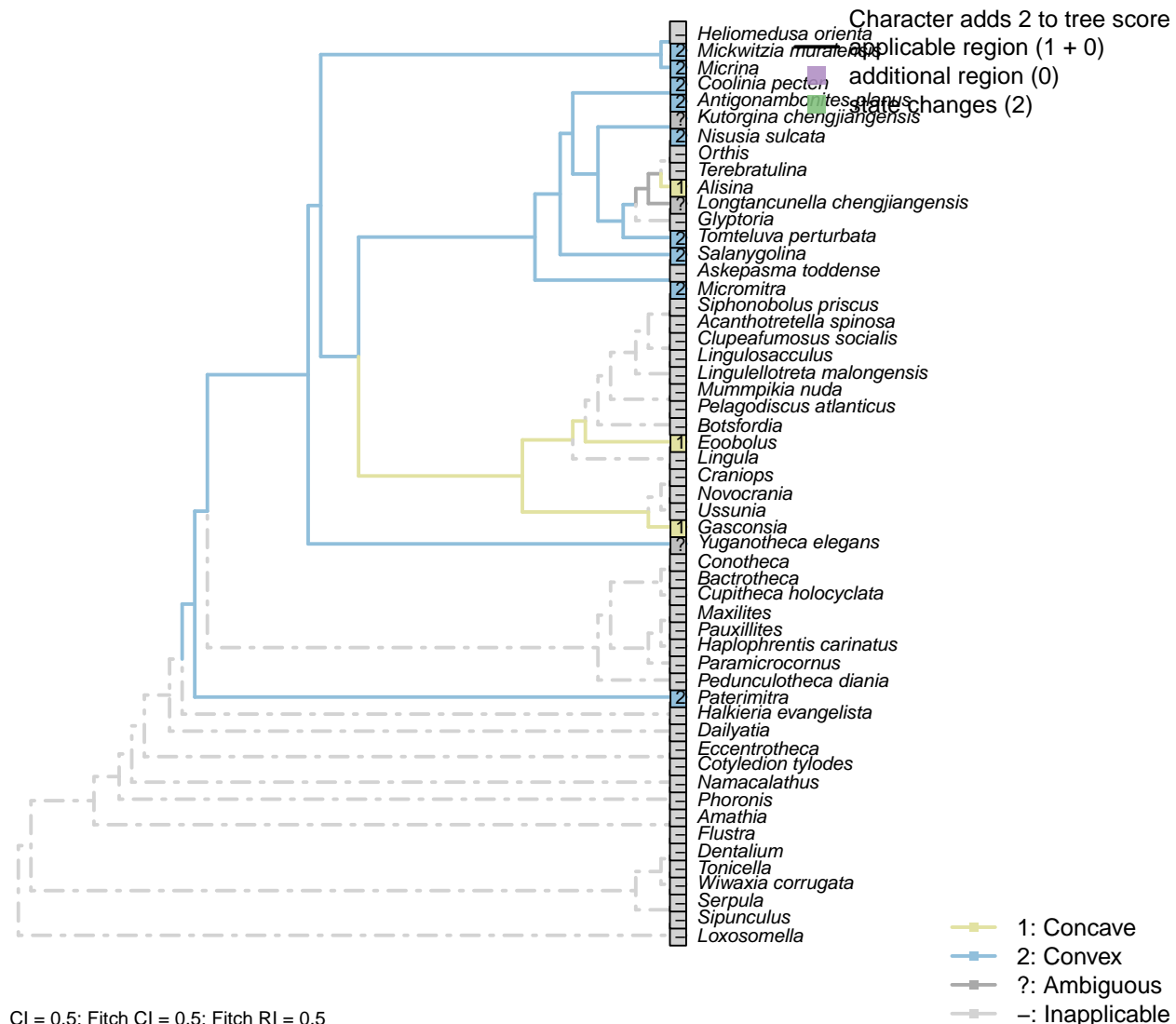
*Gasconsia*: A homeodeltidium is illustrated by Hanken and Harper (1985).

*Lingulellotreta malongensis*: The subapical flange of the *Paterimitra* S1 sclerite has been homologised with the ventral homeodeltidium of *Micromitra* (Larsson et al., 2014).

*Mickwitzia muralensis*: Termed a homoedeltidium by Balthasar (2004).

*Micrina*: “Ventral valve convex with apsacline interarea bearing delthyrium, covered by a convex pseudodeltidium” – Holmer et al. (2008).

## [118] Posterior surface: Delthyrium: Pseudodeltidium: Shape



CI = 0.5; Fitch CI = 0.5; Fitch RI = 0.5

**Character 118: Sclerites: Ventral valve: Posterior surface: Delthyrium: Pseudodeltidium: Shape**

1: Concave

2: Convex

Transformational character.

A ridge-like (i.e. convex) pseudodeltidium unites *Salanygolina* with *Coolinia* and other Chileata (Holmer et al., 2009, p. 6).

*Alisina*: “concave pseudodeltidium with median plication” – Williams et al. (2000)  
Coded as “Pseudodeltidium: Covered by concave plate” by Bassett et al. (2001).

*Antigonambonites planus*: Convex (Williams et al., 2000, fig. 508).

*Gasconsia*: “Narrow depressed homeodeltidium” – Hanken and Harper (1985).

*Kutorgina chengjiangensis*: Difficult to determine based on material presented in Zhang et al. (2007b), or indeed for other species in the genus (e.g. Williams et al., 2000; Skovsted and Holmer, 2005; Holmer et al.,

2018b).

*Mickwitzia muralensis*: Convex (see Balthasar, 2004, fig. 4B).

*Micrina*: Convex deltoid (Holmer et al., 2008).

*Micromitra*: Gently convex (see Williams et al., 2000, fig. 83.3).

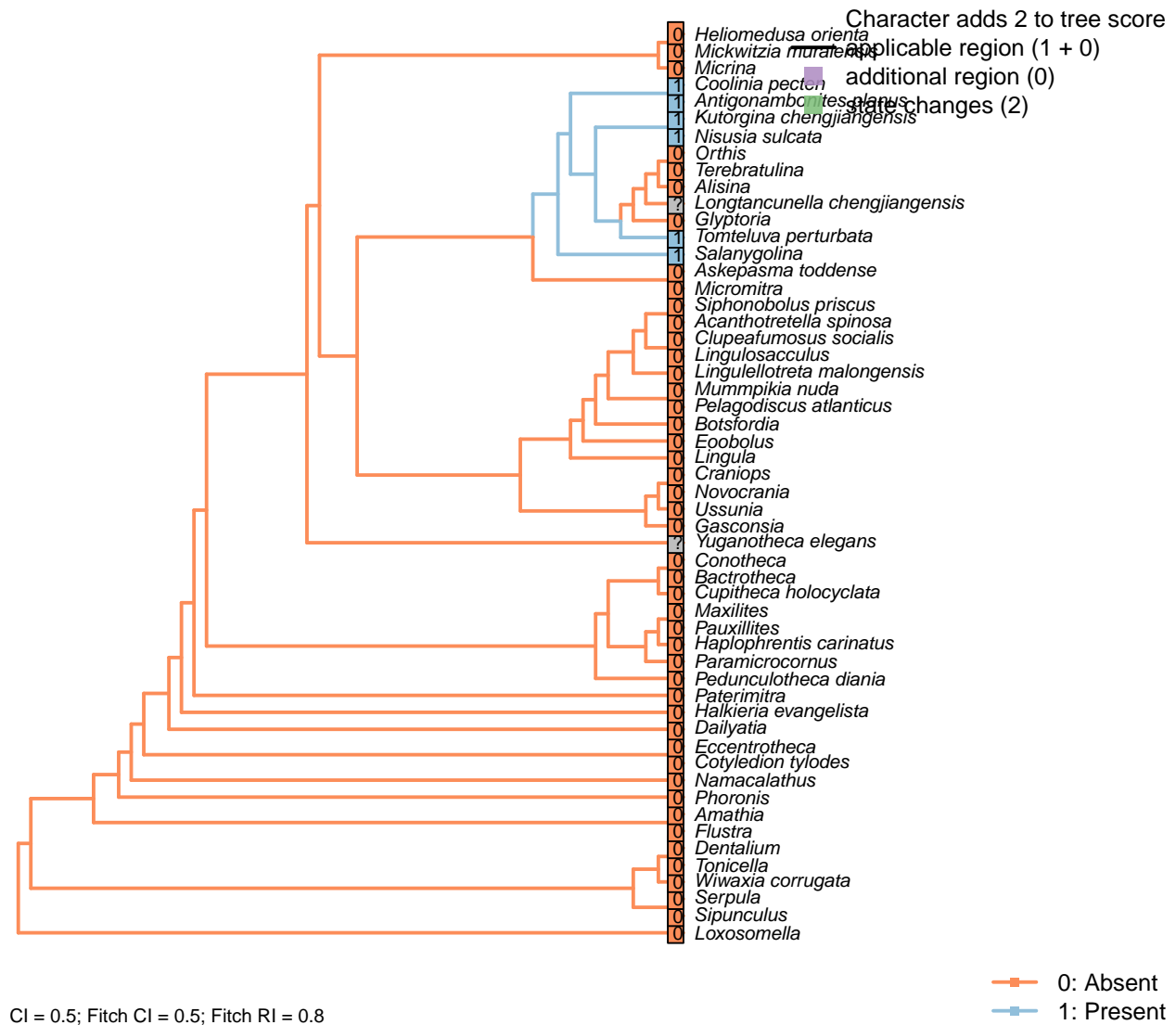
*Nisusia sulcata*: Convex in *Nisusia* (see Rowell and Caruso, 1985, fig. 8.4).

*Paterimitra*: Gently convex (see Williams et al., 2000, fig. 83.1).

*Salanygolina*: “The presence of [...] a narrow delthyrium covered by a convex pseudodeltidium, places Salanygolinidae outside the Class Paterinata and strongly suggests affinity to the Cambrian Chileida” – Holmer et al. (2009), p. 9.

*Tomteluva perturbata*: Convex (Streng et al., 2016).

### [119] Posterior surface: Delthyrium: Pseudodeltidium: Hinge furrows



**Character 119: Sclerites: Ventral valve: Posterior surface: Delthyrium: Pseudodeltidium: Hinge furrows**

0: Absent

1: Present

Neomorphic character.

After Bassett *et al.* (2001) character 18, "Hinge furrows on lateral sides of pseudodeltidium".

*Bactrotheca, Conotheca, Haplophrentis carinatus, Maxilites, Pauxillites, Pedunculotheca diania, Novocrania, Pelagodiscus atlanticus, Lingula, Terebratulina, Phoronis, Dailyatia, Acanthotretella spinosa, Askepasma toddense, Micromitra, Clupeafumosus socialis, Eccentrotheca, Heliomedusa orienta, Lingulosacculus, Lingulellotreta malongensis, Micrina, Mumppikia nuda, Orthis, Paterimitra*: Absent due to inapplicability of neomorphic character.

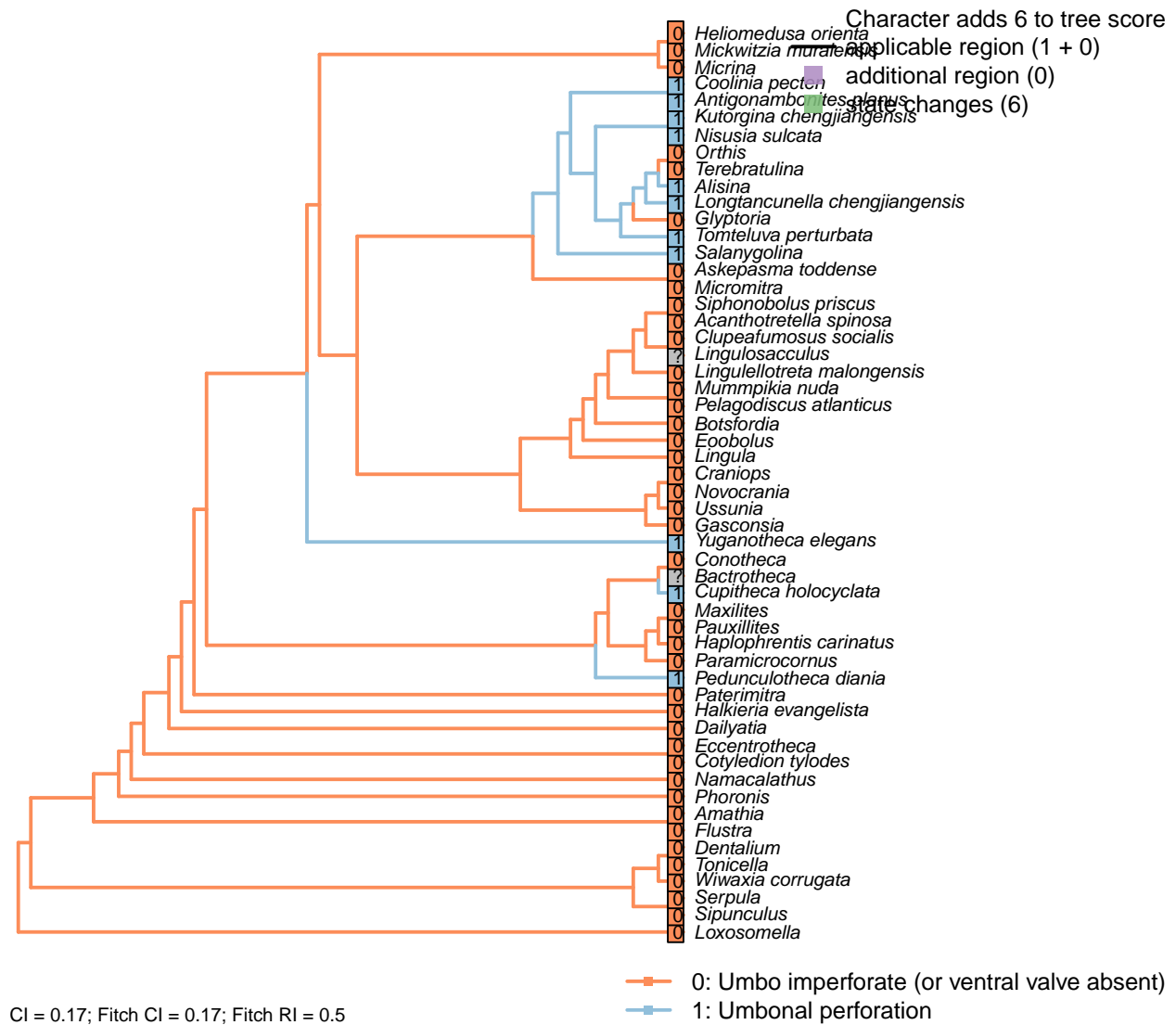
*Gasconsia*: Not evident or illustrated (Hanken and Harper, 1985).

*Glyptoria*: Coded as absent in Bassett *et al.* (2001) (table 18.1).

*Kutorgina chengjiangensis, Nisusia sulcata*: Coded as present in Bassett *et al.* (2001) (table 18.1).

*Salanygolina*: The presence of this feature is impossible to determine based on the available material.

## [120] Umbonal perforation



### Character 120: Sclerites: Ventral valve: Umbonal perforation

0: Umbo imperforate (or ventral valve absent)

1: Umbonal perforation

Neomorphic character.

Certain taxa, particularly those with a colleplax, exhibit a perforation at the umbo of the ventral valve. This opening is sometimes associated with a pedicle sheath, which emerges from the umbo of the ventral valve without any indication of a relationship with the hinge.

In contrast, the pedicle of acrotretids and similar brachiopods is situated on the larval hinge line, but is later surrounded by the posterolateral regions of the growing shell to become separated from the hinge line, and encapsulated in a position close to (or with resorption of the benthic shell, at) the umbo (see Popov, 1992, pp. 407–411 and fig. 3 for discussion). In some cases, an internal pedicle tube attests to this origin – potentially corresponding to the pedicle groove of lingulids. As such, the pedicle foramen of acrotretids and

allies is not originally situated at the umbo; it is instead understood to represent a basally sealed delthyrium.

*Bactrotheca*: The apical termination of the conical valve is not preserved (Valent et al., 2012).

*Clupeafumosus socialis*: The presumed pedicle foramen reported by Topper et al. (2013a) is at the ventral valve umbo. No evidence of an internal pedicle tube is present, but we follow Popov (1992) in inferring the encapsulation of the pedicle foramen.

*Cupitheca holocyclata*: Decollation generates open umbo, sealed secondarily with septum.

*Dalyatia*: The B and C sclerites of *Dalyatia* bear small umbonal perforations (Skovsted et al., 2015), but these are not considered to be homologous with the ventral valve, so this character is coded as inapplicable – though the possibility that the perforations are equivalent is intriguing.

A1 sclerites typically have a pair of perforations, which are conceivably equivalent to the setal tubes of *Micrina* (Holmer et al., 2011). The A1 sclerite of *D. bacata* has a structure that is arguably similar to the ‘colleplax’ of *Paterimitra*. But the homology of any of these structures to the umbonal aperture of brachiopods is difficult to establish.

*Eccentrotheca*: The sclerites of *Eccentrotheca* form a ring that surrounds the inferred attachment structure; the attachment structure does not emerge from an aperture within an individual sclerite. Thus no feature in *Eccentrotheca* is judged to be potentially homologous with the apical perforation in bivalved brachiopods.

*Heliomedusa orienta*: There is “compelling evidence to demonstrate that the putative pedicle illustrated by Chen et al. (2007, Figs. 4, 6, 7) in fact is the mold of a three-dimensionally preserved visceral cavity” – Zhang et al. (2009).

*Lingulosacculus*: The apical termination of the fossil is unknown.

*Mickwitzia muralensis*: The umbo itself is imperforate (Balthasar, 2004).

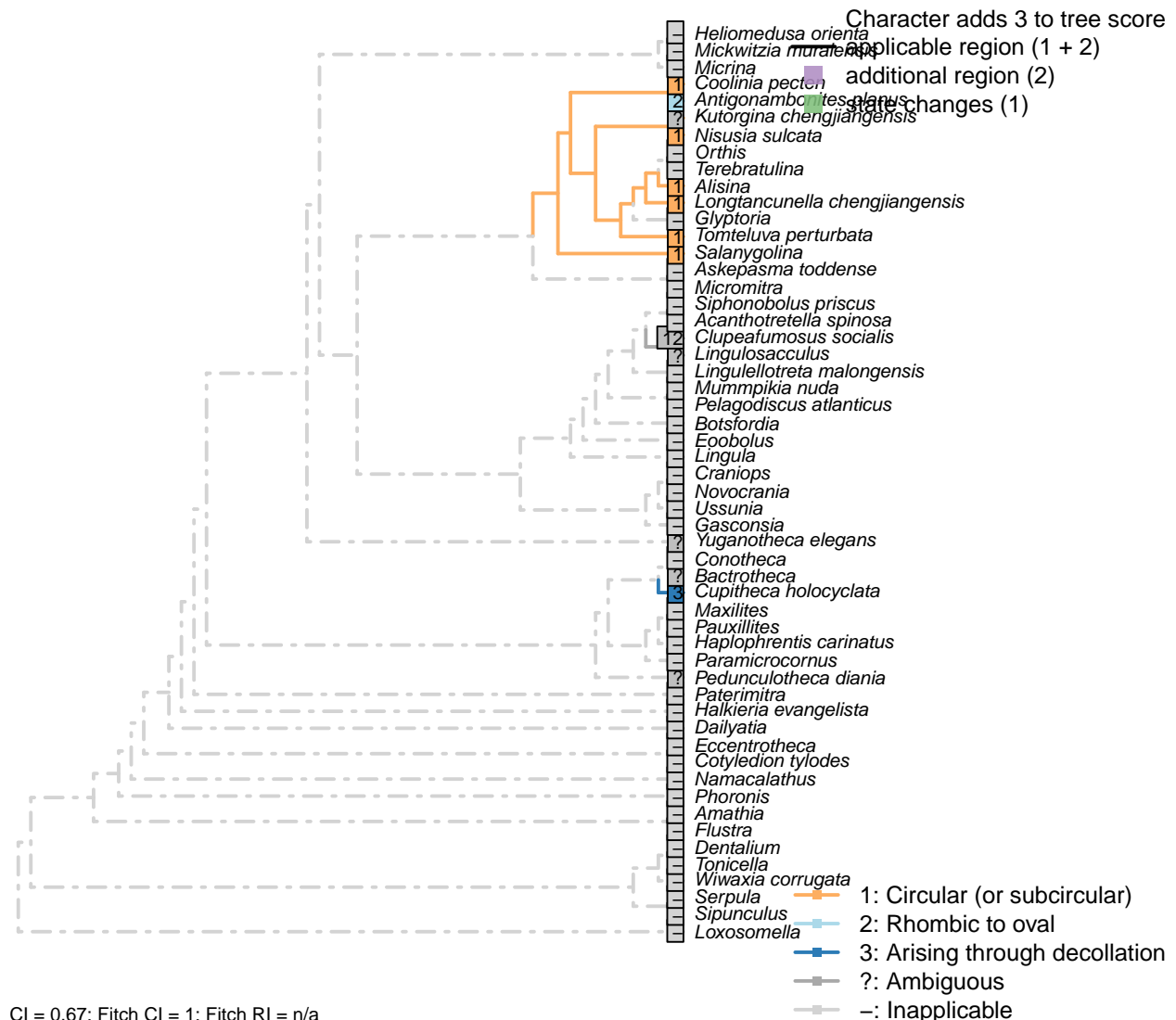
*Paramicrocornus*: Zhang et al. (2018).

*Paterimitra*: The presumed pedicle foramen is an opening between the S1 and S2 sclerites, neither of which are perforated (Skovsted et al., 2009).

*Siphonobolus priscus*: Prominent subcircular perforation at umbo associated with an internal pedicle tube (Popov et al., 2009), thus presumed to share an origin with the acrotretid pedicle foramen.

*Tomteluva perturbata*: Streng et al. (2016) observe “an internal tubular structure probably representing the ventral end of the canal within the posterior wall of the pedicle tube”, but do not consider this tomteluvid dube to be homologous with the pedicle tube of acrotretids and their ilk, stating (p. 274) that it appears to be unique within Brachiopoda.

### [121] Umbonal perforation: Shape



#### Character 121: Sclerites: Ventral valve: Umbonal perforation: Shape

- 1: Circular (or subcircular)
  - 2: Rhombic to oval
  - 3: Arising through decollation
- Transformational character.

The perforation in *Cupitheca* seems to have a distinct origin, arising through decollation; as such, the shape simply reflects the outline of the shell. This reflects a distinct origin of the perforation and is therefore provided as a separate state.

*Acanthotretella spinosa*: Too small to observe given quality of preservation (Holmer and Caron, 2006).

*Alisina*: Seemingly circular (Zhang et al., 2011b).

*Antigonambonites planus*: Based on p.92, fig.4B.

*Clupeafumosus socialis*: Taller than wide in some cases, but very nearly circular in others; see Topper et al.

(2013a).

*Coolinia pecten*: Bassett and Popov write “a dominant feature of the ventral umbo is a sub-oval perforation about 270 µm long and 250 µm wide”: the width and height of this structure are almost identical, and we score it as (sub) circular.

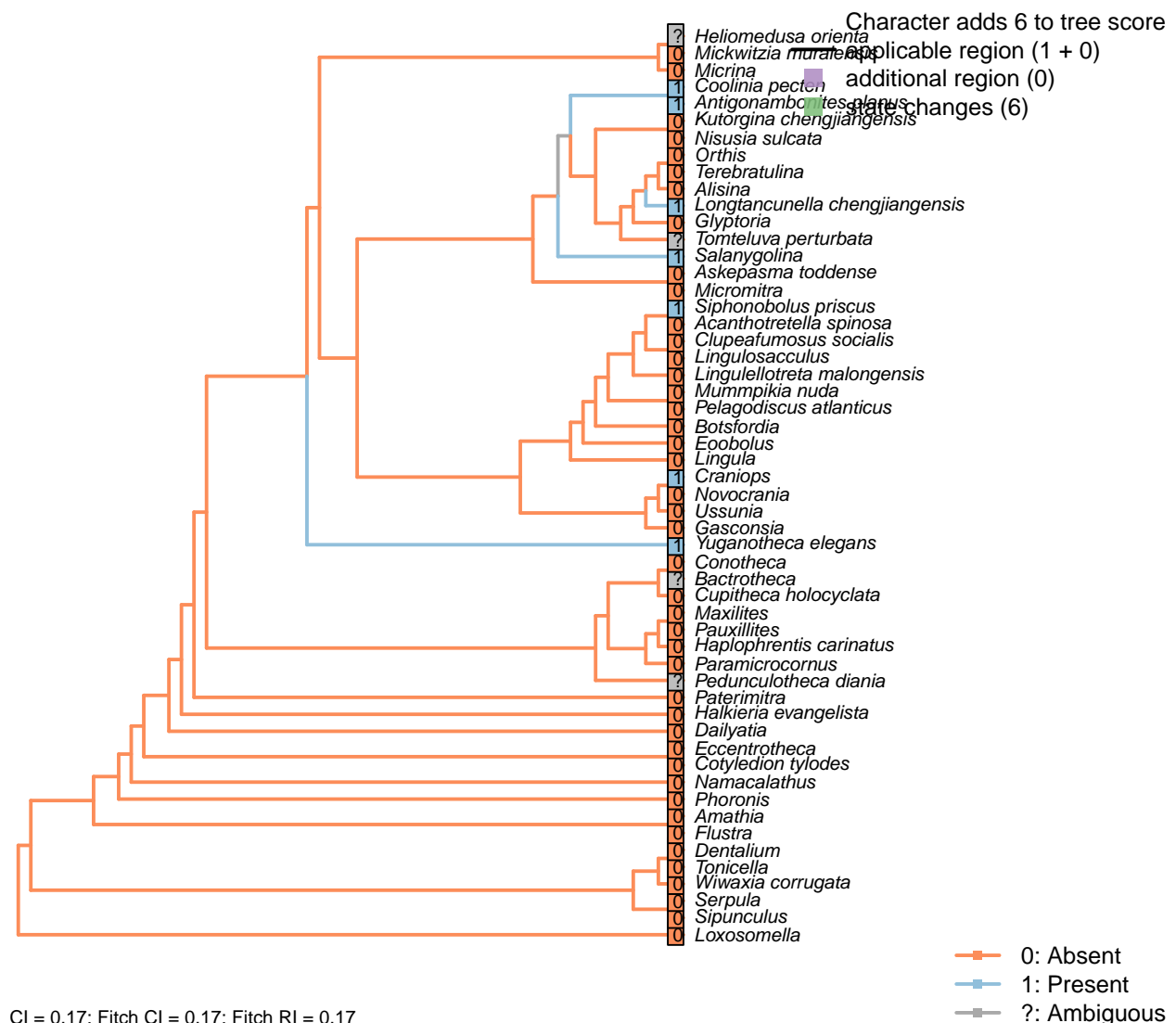
*Heliomedusa orienta*: Rhombic to oval – seen as evidence for a discinid affinity (Chen et al., 2007).

*Kutorgina chengjiangensis*: The exact size and shape of the apical perforation is obscured by the emerging pedicle.

*Nisusia sulcata*: “close to circular” (Holmer et al., 2018a).

*Salanygolina*: Essentially circular (Holmer et al., 2009, fig. 4).

## [122] Colleplax, cicatrix or pedicle sheath



**Character 122: Sclerites: Ventral valve: Colleplax, cicatrix or pedicle sheath**

0: Absent

1: Present

Neomorphic character.

In certain taxa, the umbo of the ventral valve bears a colleplax, cicatrix or pedicle sheath; Bassett *et al.* (2008) consider these structures as homologous.

*Bactrotheca*: The apical termination of the conical valve is not preserved (Valent *et al.*, 2012).

*Botsfordia*: Following Williams *et al.* (1998b), appendix 2.

*Clupeafumosus socialis*: Not reported by Topper *et al.* (2013a).

*Craniops*: *Paracraniops* is “externally similar to *Craniops*, but lacking cicatrix” – indicating that *Craniops* bears a cicatrix (Williams *et al.*, 2000). Also coded as present in their table 15.

*Heliomedusa orienta*: A cicatrix was reconstructed by Jin and Wang (1992) (figs 6b, 7), but has not been reported by later authors; possibly, as with the ‘pedicle foramen’ of Chen *et al.* (2007), this structure represents internal organs rather than a cicatrix proper (Zhang *et al.*, 2009); as such it has been recorded as ambiguous.

*Kutorgina chengjiangensis*: The umbonal region of kutorginides “clearly lacks a pedicle sheath” (Holmer *et al.*, 2018b).

*Lingulellotreta malongensis*: The pedicle is identified as such (rather than a pedicle sheath) by the internal pedicle tube.

*Longtancunella chengjiangensis*: A ring-like structure surrounding the pedicle is interpreted as a colleplax (Zhang *et al.*, 2011a), though the authors make no comparison with the pedicle capsule exhibited by extant terebratulids (see Holmer *et al.*, 2018a).

*Micrina*: Absent in *Micrina* (Holmer *et al.*, 2011).

*Pedunculotheeca diania*: The flat apical termination of juvenile individuals possibly functioned as colleplax for attachment, but may simply represent the benthic shell; we treat it as ambiguous to reflect this potential homology.

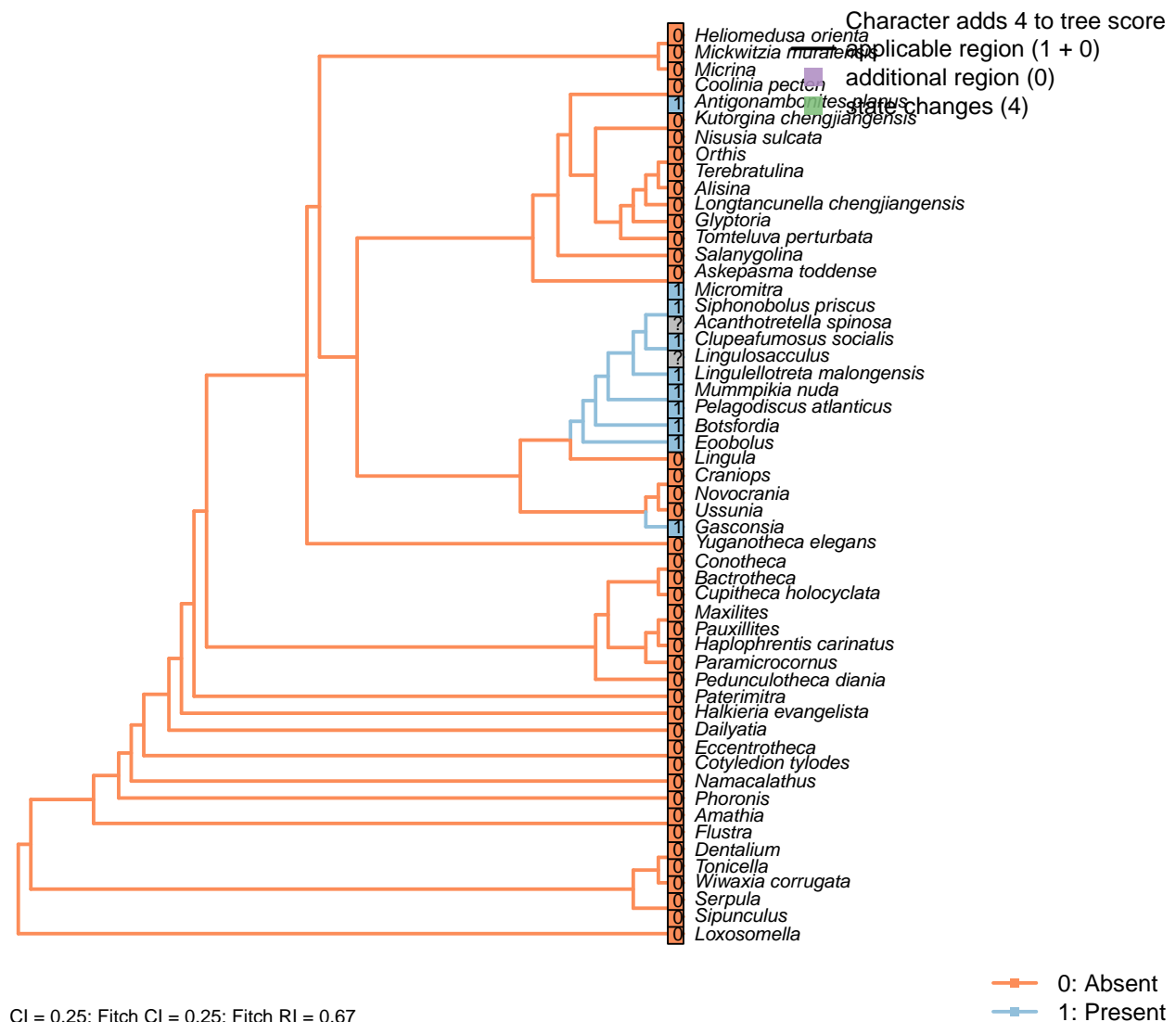
*Siphonobolus priscus*: Coded as present in view of the attachment scar, which has been considered homologous with the “adult colleplax and foramen with attachment pad” in *Salanygolina* (Popov *et al.*, 2009).

*Tomteluva perturbata*: The internal canal associated with the pedicle is unique to the tomteluvids, and has an uncertain identity (Streng *et al.*, 2016). It could conceivably correspond to an internalized pedicle sheath or an equivalent structure, so this feature is coded as ambiguous here.

*Ussunia*: Following table 15 in Williams *et al.* (2000).

*Yuganotheca elegans*: The median collar or conical tube is conceivably homologous with the pedicle sheath.

## [123] Median septum



CI = 0.25; Fitch CI = 0.25; Fitch RI = 0.67

**Character 123: Sclerites: Ventral valve: Median septum**

0: Absent

1: Present

Neomorphic character.

Chen *et al.* (2007) observe a median septum in what they interpret as the ventral valve of *Heliomedusa*, and the ventral valve of *Discinisca*, which they propose points to a close relationship.

*Acanthotretella spinosa*: Carbonaceous preservation confounds the identification of internal shell structures;

it is possible that this feature is present, but not observable in the Burgess Shale material.

*Botsfordia*: Following Williams et al. (1998b), appendix 2.

*Clupeafumosus socialis*: A short medial ridge (septum) is present in the ventral valve (Topper et al., 2013a).

*Eoobolus*: Prominent median septum (fig. 4d, e in Balthasar, 2009).

*Gasconsia*: Evident in moulds of ventral valve (Hanken and Harper, 1985; Watkins, 2002).

*Glyptoria*: Neither evident nor reported in Williams et al. (2000).

*Haplophrentis carinatus*: The carina of *H. carinatus* is an angular elevation of the ventral valve surface, rather than a septum growing inward on the interior of shell.

*Helomedusa orienta*: Reported on ‘ventral’ valve by Chen et al. (2007); we consider the ‘ventral’ valve to be the dorsal valve.

*Lingulellotreta malongensis*: Medial septum visible in ventral valve in Williams et al. (2000), fig. 34.1c.

*Micromitra*: Ventral ridge characteristic of *Micromitra* (Skovsted and Peel, 2010).

*Mummpikia nuda*: “Some specimens also reveal that the vault had a slight median septum, which is now visible as a notch or a groove dividing the right from the left part” – Balthasar (2008).

*Novocrania*: Valve thin and often unmineralized.

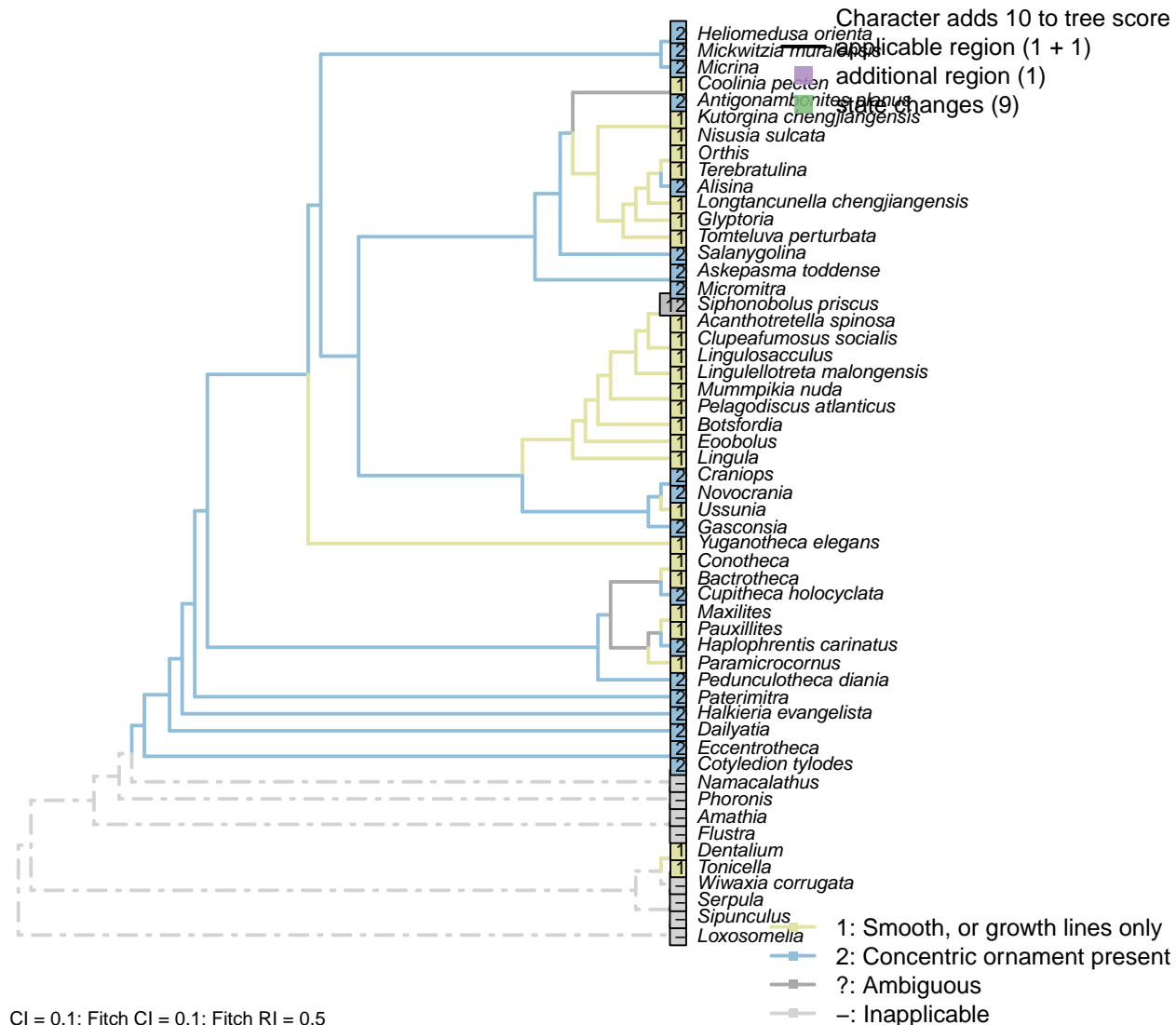
*Pelagodiscus atlanticus*: Described as present in *Discinisca* by Chen et al. (2007); assumed present also in *Pelagodiscus*.

*Siphonobolus priscus*: Present; see Popov et al. (2009), fig. 5J.

*Ussunia*: Following char. 42 in table 15 in Williams et al. (2000).

## 5.14 Sclerites: Ornament

### [124] Concentric ornament



#### Character 124: Sclerites: Ornament: Concentric ornament

- 1: Smooth, or growth lines only
- 2: Concentric ornament present
- Transformational character.

After character 11 in Williams *et al.* (1998b). Coded as transformational as it is possible that maintaining a smooth shell without occasional prominent ridges requires greater secretory control.

*Askepasma toddense*, *Micromitra*, *Glyptoria*, *Kutorgina chengjiangensis*, *Salanygolina*: Following appendix 2 in Williams *et al.* (1998b).

*Bactrotheca*: Both valves with fine growth lines only (Valent *et al.*, 2012).

*Botsfordia*: Following Williams *et al.* (1998b), appendix 2.

Pustules are arranged along concentric growth lines (Skovsted and Holmer, 2005), so are not treated as a

distinct ornamentation.

*Conotheca*: Both valves covered with concentric growth lines (Devaere et al., 2014), but no further ornament (Wrona, 2003).

*Cotyledion tylodes*: Zhang et al. (2013).

*Cupitheca holocyphata*: Broad symmetric ridges in some specimens (Vendrasco et al., 2017).

*Eccentrotheca*: More or less concentric ridges occur on *Eccentrotheca* sclerites (Skovsted et al., 2011).

*Halkieria evangelista*: Ridges in shell parallel, but are more prominent than, growth lines.

*Haplophrentis carinatus*: A series of regularly spaced concentric ridges adorn both valves (Moysiuk et al., 2017); these are more pronounced than mere growth lines.

*Helomedusa orienta*: The ornament on shell exterior is described as concentric fila (Chen et al., 2007, P.43), and also scored as it in Williams et al. (2000, pp.160–163).

*Maxilites*: Surfaces of both valves covered with concentric growth lines (Marek, 1972; Martí Mus and Bergström, 2005).

*Mickwitzia muralensis*: Symmetric fila.

*Novocrania*: Irregular ridges externally (Williams et al., 2000).

*Pauxillites*: Ventral side of ventral valve and whole dorsal valve covered with faint growth lines (Valent and Corbacho, 2015).

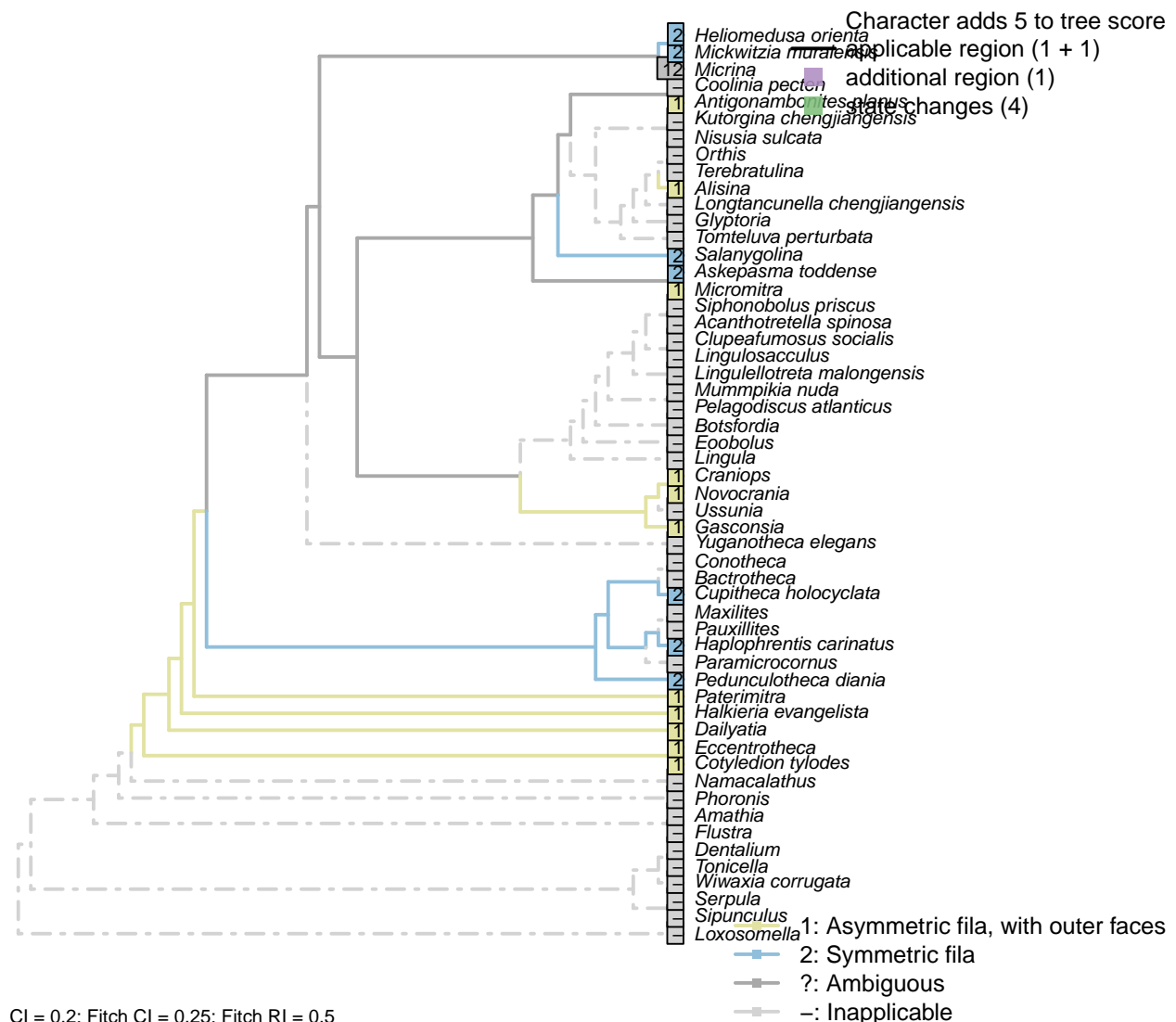
*Pedunculotheca diania*: A series of regularly spaced concentric ridges adorn the ventral valve; comparatively less regular lines ornament the operculum.

*Pelagodiscus atlanticus*: Only growth lines evident (Williams et al., 2000).

*Terebratulina*: Single ridge evident in Williams et al. (2006) fig. 1425.1a interpreted as interruption of growth rather than inherent feature, so coded as absent (i.e. smooth).

*Tonicella*: No prominent ornamentation in *Tonicella* (Connors et al., 2012).

## [125] Concentric ornament: Symmetry

**Character 125: Sclerites: Ornament: Concentric ornament: Symmetry**

1: Asymmetric fila, with outer faces

2: Symmetric fila

Transformational character.

After character 11 in Williams *et al.* (1998b).*Alisina*: Seemingly asymmetric (Williams *et al.*, 2000, fig. 122.3c; Zhang *et al.*, 2011b, Fig. 1).*Askepasma toddense*, *Micromitra*, *Glyptoria*, *Kutorgina chengjiangensis*, *Salanygolina*: Following appendix 2

in Williams *et al.* (1998b).

*Dailyatia*: Clear asymmetry (Skovsted *et al.*, 2015).

*Eccentrotheca*: Ornament, such as it is, is asymmetric, with prominent outer faces (Skovsted *et al.*, 2011).

*Gasconsia*: Assymmetric (Hanken and Harper, 1985, fig. 3).

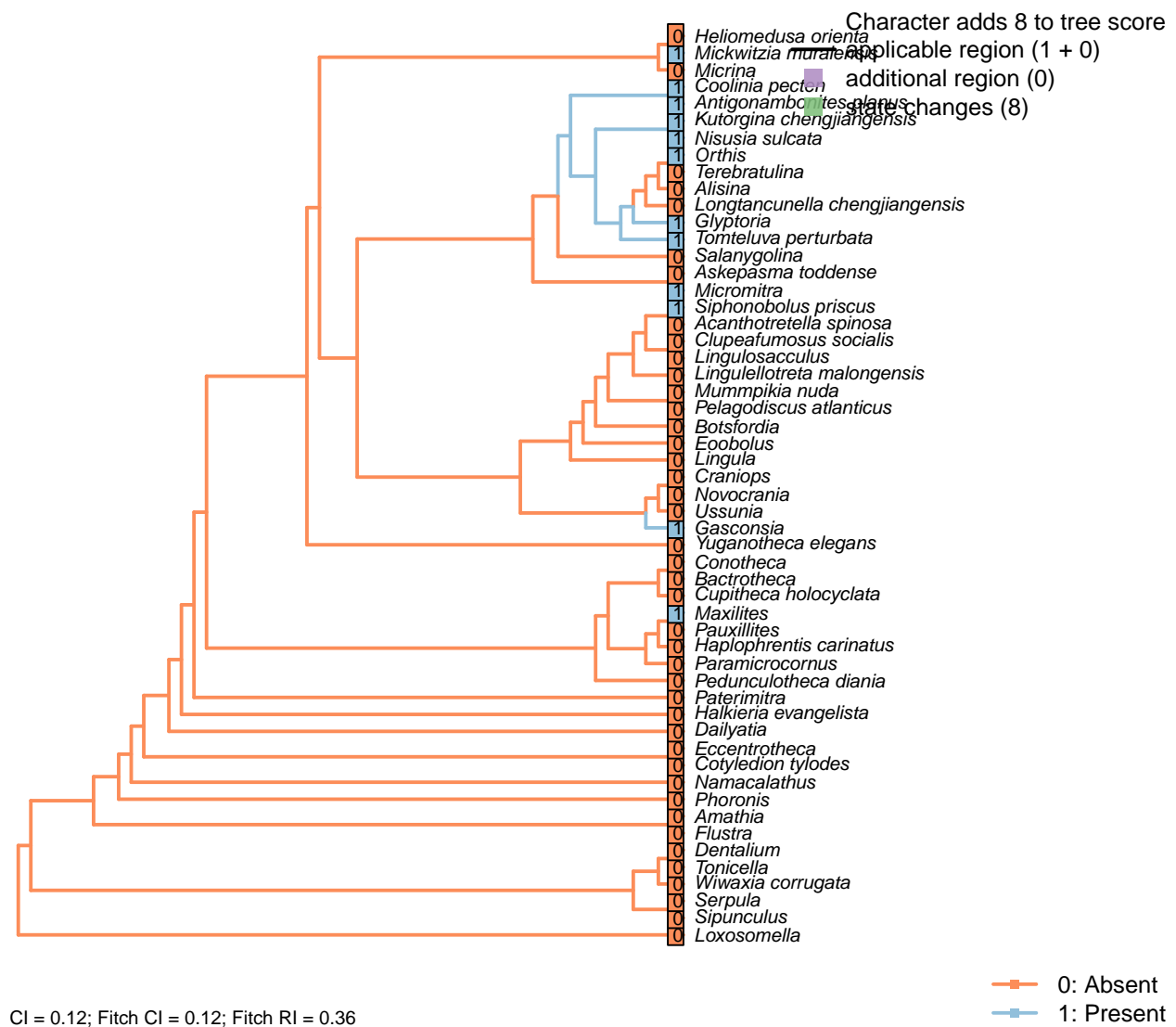
*Heliomedusa orienta*: See fig. 1715 in Williams *et al.* (2007).

*Mickwitzia muralensis*: Symmetric fila (Balthasar, 2004).

*Micrina*: No obvious asymmetry, even if not obviously symmetric either (Holmer *et al.*, 2008). Coded as ambiguous.

*Novocrania*: Clear outer faces (Williams *et al.*, 2000, fig. 100.2b).

## [126] Radial ornament



Character 126: Sclerites: Ornament: Radial ornament

0: Absent

1: Present

Neomorphic character.

Ridges radiating from umbo, i.e. ribs.

*Askepasma toddense*: “Ornament of irregularly developed, concentric growth lamellae; microornamentation of irregularly arranged, polygonal pits” – Williams et al. (2000), p153; figs on p.155.

*Botsfordia*: Following Williams et al. (1998b), Appendix 2.

*Eoobolus*: Very faint costellae in some specimens but coded absent.

*Gasconsia*: “Ornament of indistinct low radial ribs” – Williams et al. (2000, p167).

*Glyptoria*: “Coarsely costate” – Williams et al. (2000, p710).

*Heliomedusa orienta*: See fig. 1715 in Williams et al. (2007).

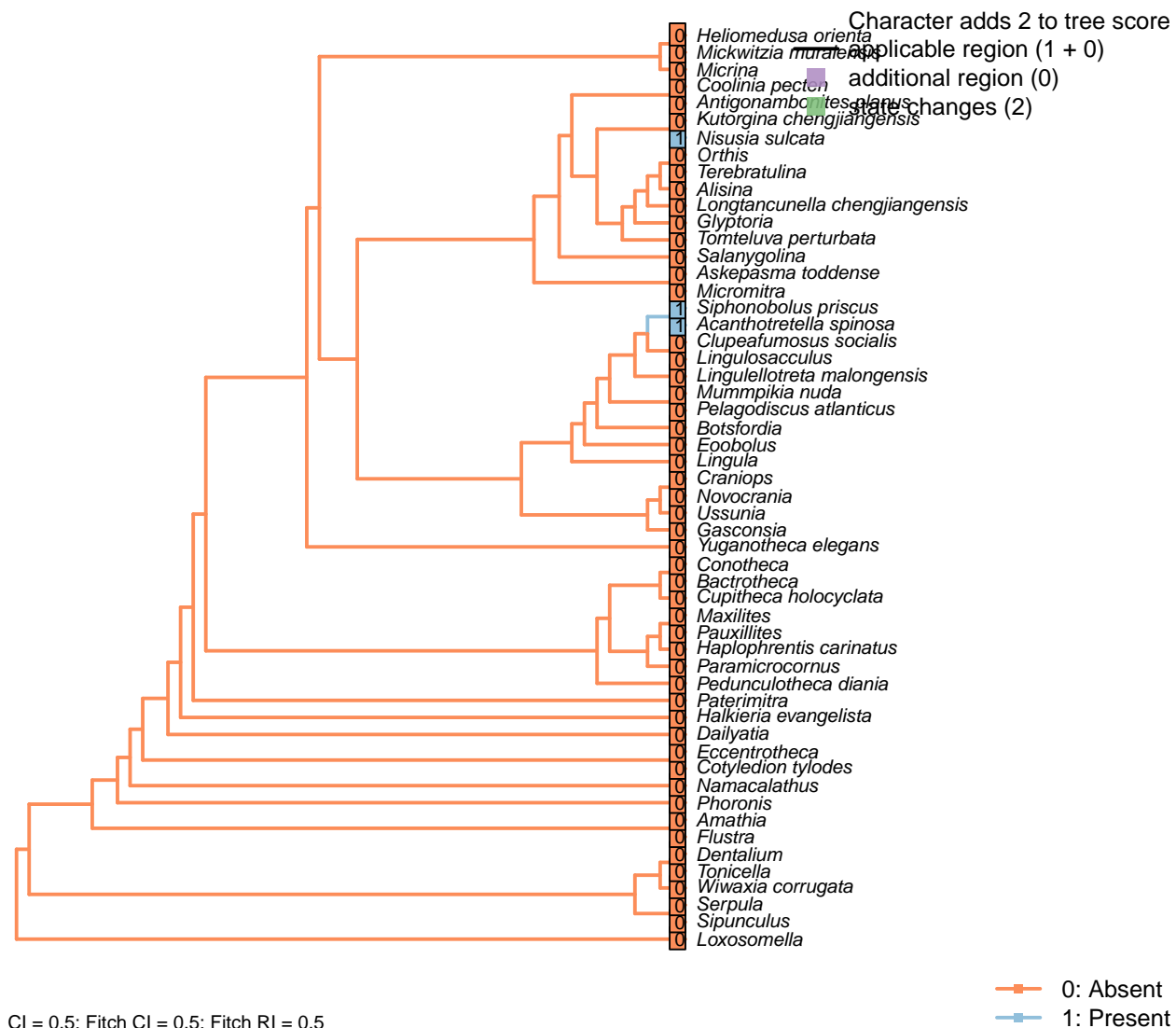
*Maxilites*: Lines radiate from the apex of the operculum (Marek, 1972, pl.2 fig. 5) and ornament the conical valve (Marek, 1972, pl. 2. fig. 3).

*Paramicrocornus*: Zhang et al. (2018).

*Siphonobolus priscus*: “Indistinct radial ribs accentuated by radial rows of tubercles” – Popov et al. (2009).

*Ussunia*: Unornamented.

## [127] Shell-penetrating spines



## Character 127: Sclerites: Ornament: Shell-penetrating spines

0: Absent

1: Present

Neomorphic character.

Mineralized or partly mineralized spines are observed in *Heliomedusa* and *Acanthotretella*.

*Glyptoria*: Neither evident nor reported in Williams *et al.* (2000).

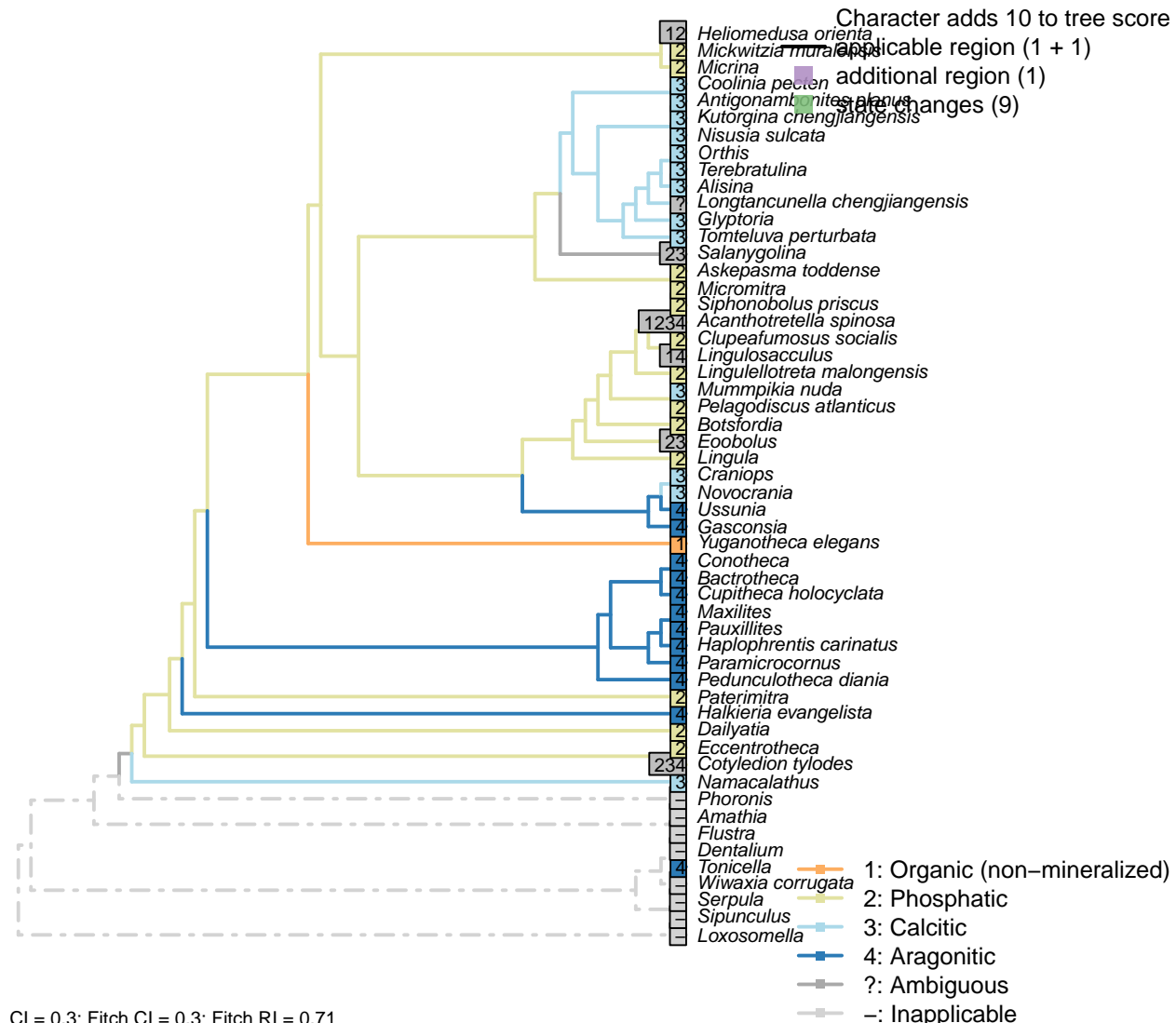
*Heliomedusa orienta*: The ‘spines’ reported by Chen *et al.* (2007) are pyritized spinelike setae – see pp. 2580–2590 in Williams *et al.* (2007).

*Nisusia sulcata*: Bears numerous small, hollow spines (Williams *et al.*, 2000).

*Tonicella*: Aesthete canals penetrate the main valves of certain chitons, but are not equivalent to the shell-penetrating spines of brachiopods.

## 5.15 Sclerites: Composition

### [128] Mineralogy



#### Character 128: Sclerites: Composition: Mineralogy

- 1: Organic (non-mineralized)
- 2: Phosphatic
- 3: Calcitic
- 4: Aragonitic

Transformational character.

*Acanthotretella spinosa*: Holmer & Caron (2006) note the absence of brittle breakage, interpreted as indicating the absence of a material mineralized component to the shells. The preservation is strikingly different from that of other Burgess Shale brachiopods, ruling out a primarily calcitic or phosphatic composition. The two-dimensional nature of the preservation also differs from that of co-occurring aragonitic taxa (hyoliths; Holmer and Caron, 2006, p. 273), indicating that any mineralization was minor at best.

Holmer & Caron (2006, p. 286) suggest that it is more likely that a (minor) mineral component was present

than that it was not, though without providing an uncontested rationale. To be as conservative as possible, we therefore code this taxon as ambiguous.

*Clupeafumosus socialis*: Phosphatic – hence the conventional placement within Linguliformea.

*Cotyledion tylodes*: The extensive relief and association with pyrite framboids indicates original mineralization, but the identity of the biomineral remains uncertain (Zhang et al., 2013).

*Craniops*: Shell calcitic.

*Cupitheca holocyclus*: Reconstructed as aragonitic from microstructural fabrics (Vendrasco et al., 2017).

*Eoobolus*: “the original shell of *Eoobolus* contained small calcareous grains that were incorporated into organic-rich layers alongside apatite” (Balthasar, 2007).

*Gasconsia*: Confirmed in Trimerella by Balthasar et al. (2011).

*Heliomedusa orienta*: “Shell originally organophosphatic, but may generally have been poorly mineralized” – Williams et al. (2007) – cf. ibid, p. 2889, “These strong similarities to discinoids in soft-part anatomy imply that the *Heliomedusa* shell was chitinous or chitinophosphatic, not calcareous.”

*Lingulellotreta malongensis*: Coded as phosphatic by Zhang et al. (2014), but with no explanation. Cracks within shells of Chengjiang specimens (e.g. Zhang et al., 2007a, fig. 3) demonstrate that the shells were originally mineralized, but not the identity of the original biomineral. This said, phosphatized material from Kazakhstan (Holmer et al., 1997) is attributed to the same species; presuming this phosphate to be original and the material to be conspecific, *L. malongensis* is coded as having phosphatic shells.

*Lingulosacculus*: The absence of relief in *Lingulosacculus* rules out a phosphatic or calcitic composition, but co-occurring (and presumably aragonitic) hyolithids are preserved in the same fashion. Its constitution was thus either organic or aragonitic (Balthasar and Butterfield, 2009).

*Longtancunella chengjiangensis*: “The original composition of the shell cannot be determined with certainty”, though it was “most probably entirely soft and organic” – Zhang et al. (2011a).

*Mickwitzia muralensis*: Calcite and silica deemed diagenetic by Balthasar (2004).

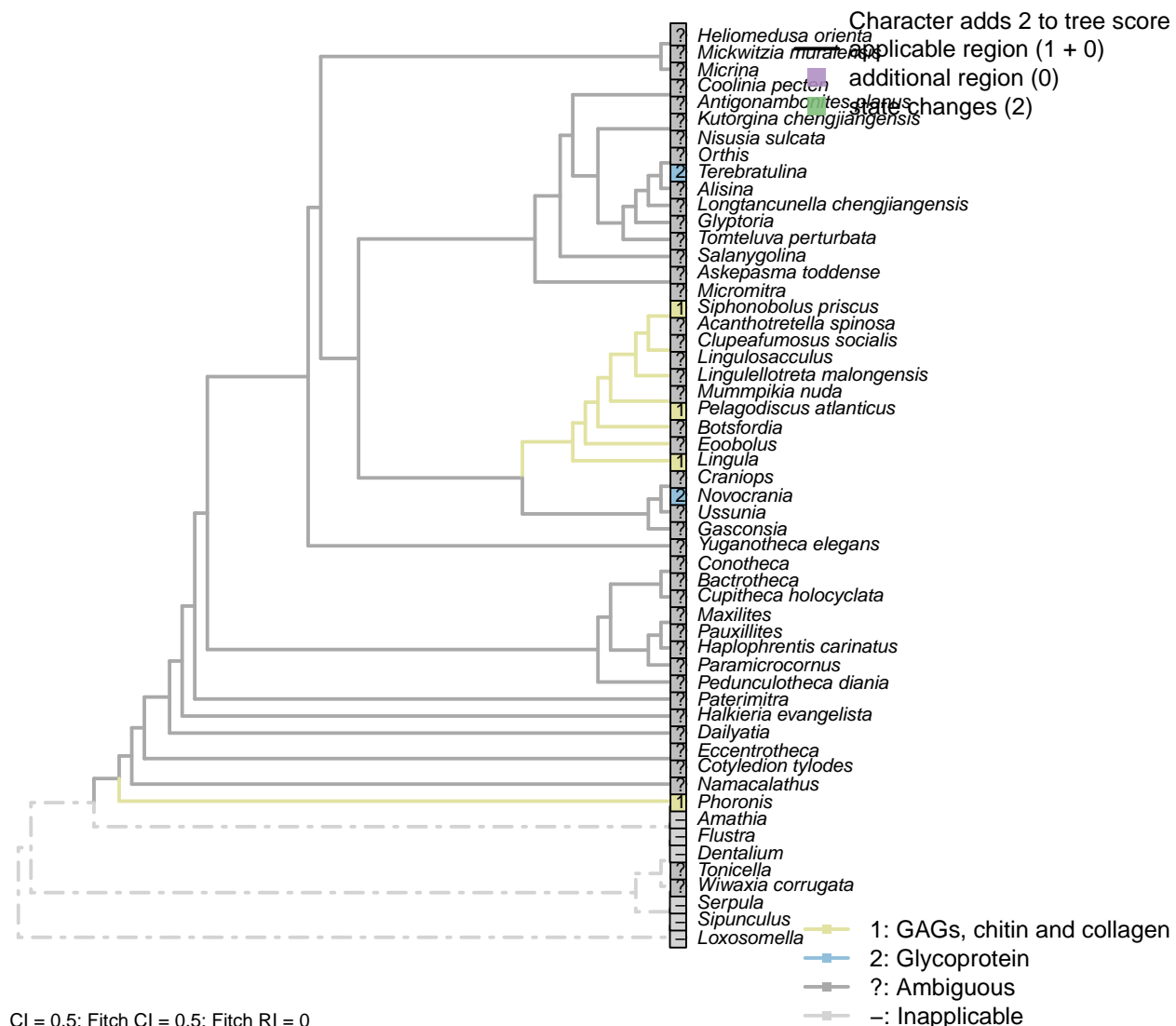
*Mummpikia nuda*: Identified as calcareous by preservational criteria, and description “primary calcitic shells of *M. nuda*” (Balthasar, 2008).

*Novocrania*: Ventral valve uncalcified in extant forms or sometimes thin (Williams et al., 2000), but coded as calcitic as calcite-mineralizing pathways are present.

*Salanygolina*: Original mineralogy unknown, but known to be mineralised and anticipated to be phosphatic (Holmer et al., 2009).

*Ussunia*: Trimerellids were probably aragonitic (Williams et al., 2000).

## [129] Cuticle or organic matrix

**Character 129: Sclerites: Composition: Cuticle or organic matrix**

1: GAGs, chitin and collagen

2: Glycoprotein

Transformational character.

Williams *et al.* (1996) identify glycoprotein-based organic scaffolds as distinct from those comprising glycosaminoglycans (GAGs), chitin and collagen. This character can only be scored for extant taxa.

*Lingula*: Coded as GAGs, chitin and collagen in lingulids by Williams *et al.* (1996).

*Novocrania*: Coded as glycoprotein for craniids by Williams *et al.* (1996).

*Pelagodiscus atlanticus*: Coded as GAGs, chitin and collagen in discinids by Williams *et al.* (1996).

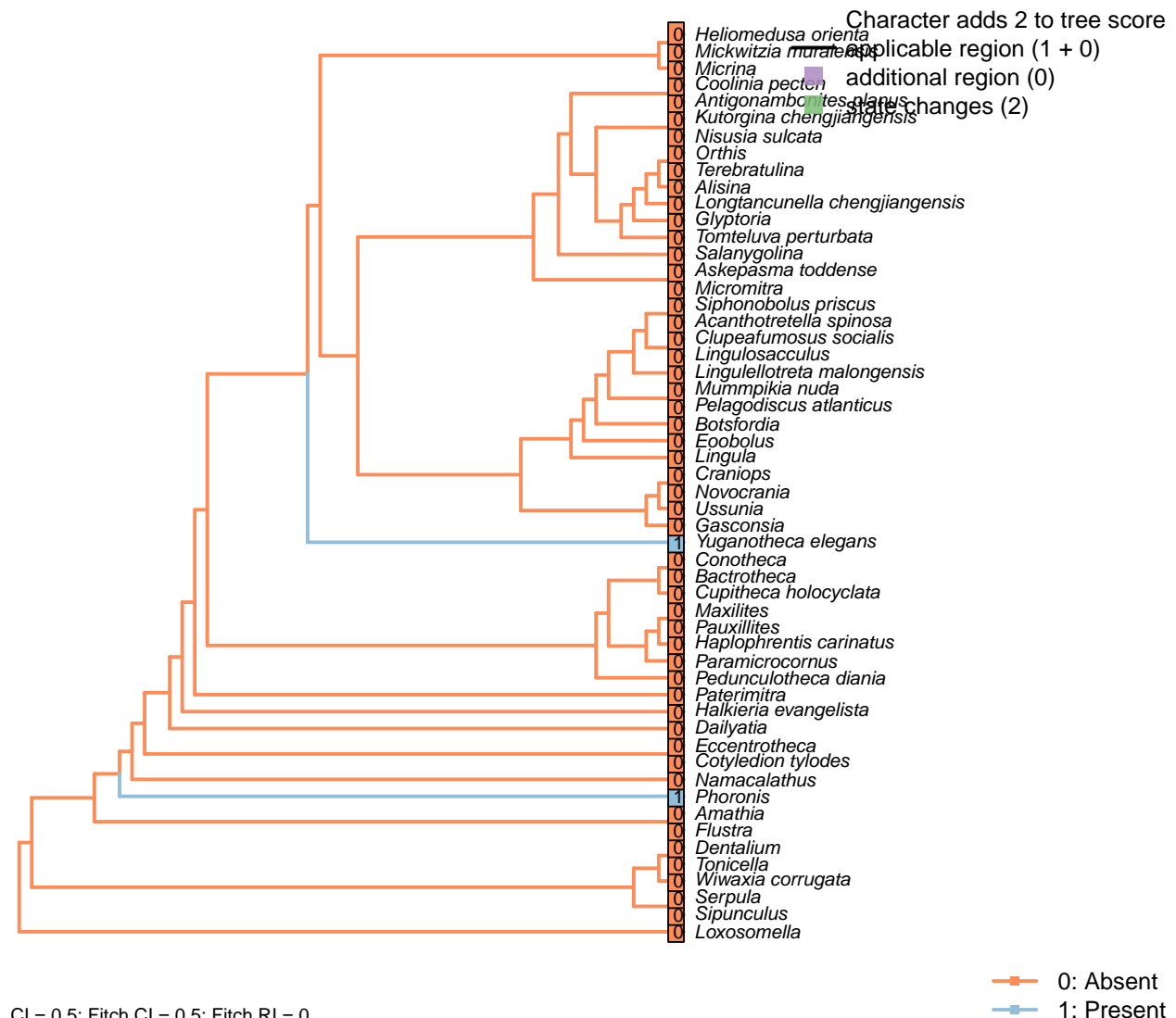
*Phoronis*: “The presence of sulphated glycosaminoglycans (GAGs) in the chitinous cuticle of *Phoronis* (Hermann, 1997, p. 215) would suggest a link with linguliforms, as GAGs are unknown in rhynchonelliform shells (Fig. 1891, 1896)” – Williams *et al.* (2007), p. 2830.

*Siphonobolus priscus*: Lenticular chambers in siphonotretid shells interpreted as degraded GAG residue

(Williams et al., 2004).

*Terebratulina*: Coded as glycoprotein for terebratulids by Williams *et al.* (1996).

### [130] Incorporation of sedimentary particles



CI = 0.5; Fitch CI = 0.5; Fitch RI = 0

#### Character 130: Sclerites: Composition: Incorporation of sedimentary particles

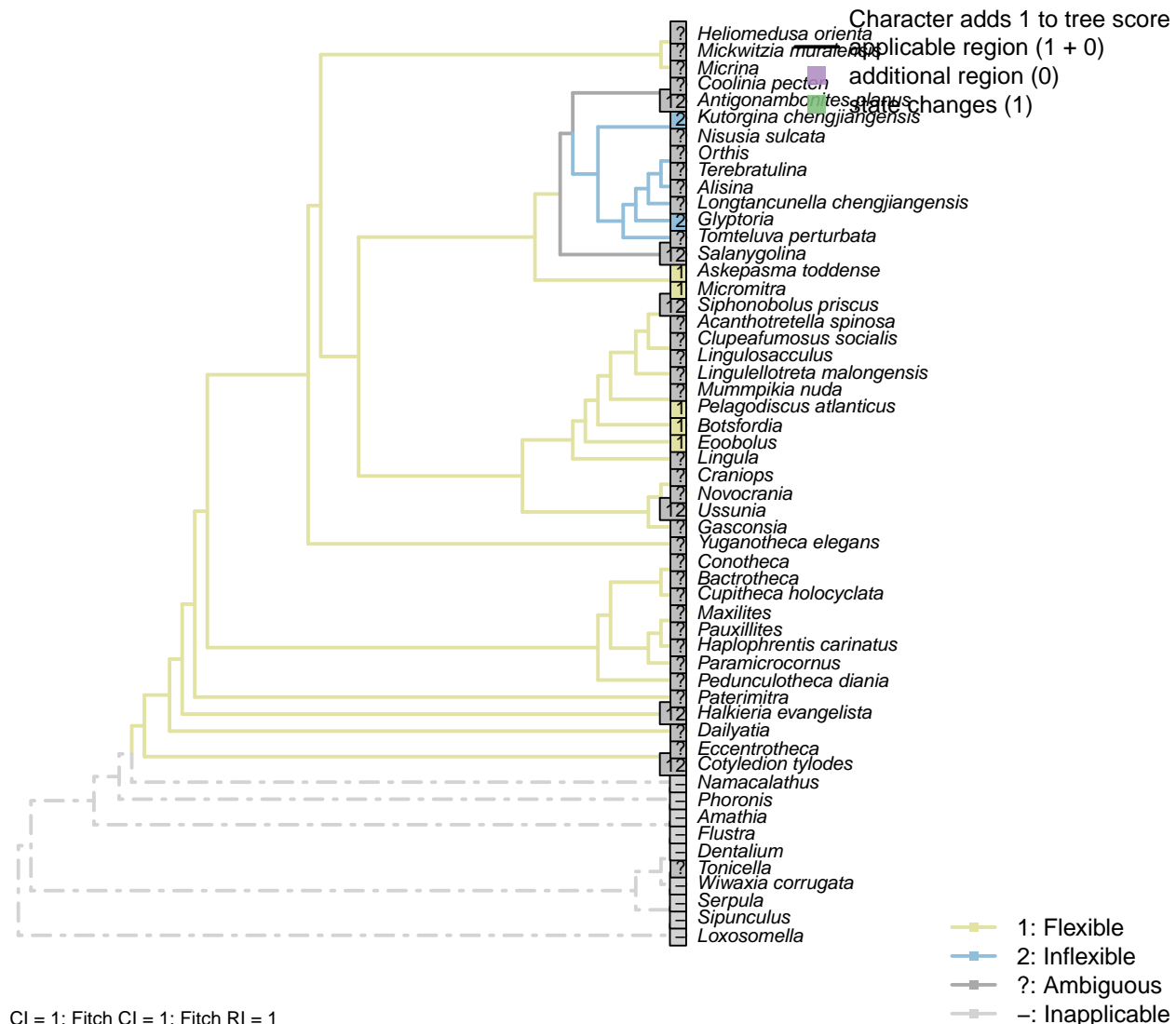
0: Absent

1: Present

Neomorphic character.

Phoronids and *Yuganotheca* agglutinate particles into their sclerites.

### [131] Periostracum: Flexibility



#### Character 131: Sclerites: Composition: Periostracum: Flexibility

1: Flexible

2: Inflexible

Transformational character.

Following character 9 in Williams *et al.* (1998b); see their p228–230 for a discussion of how this might be inferred from fossil material.

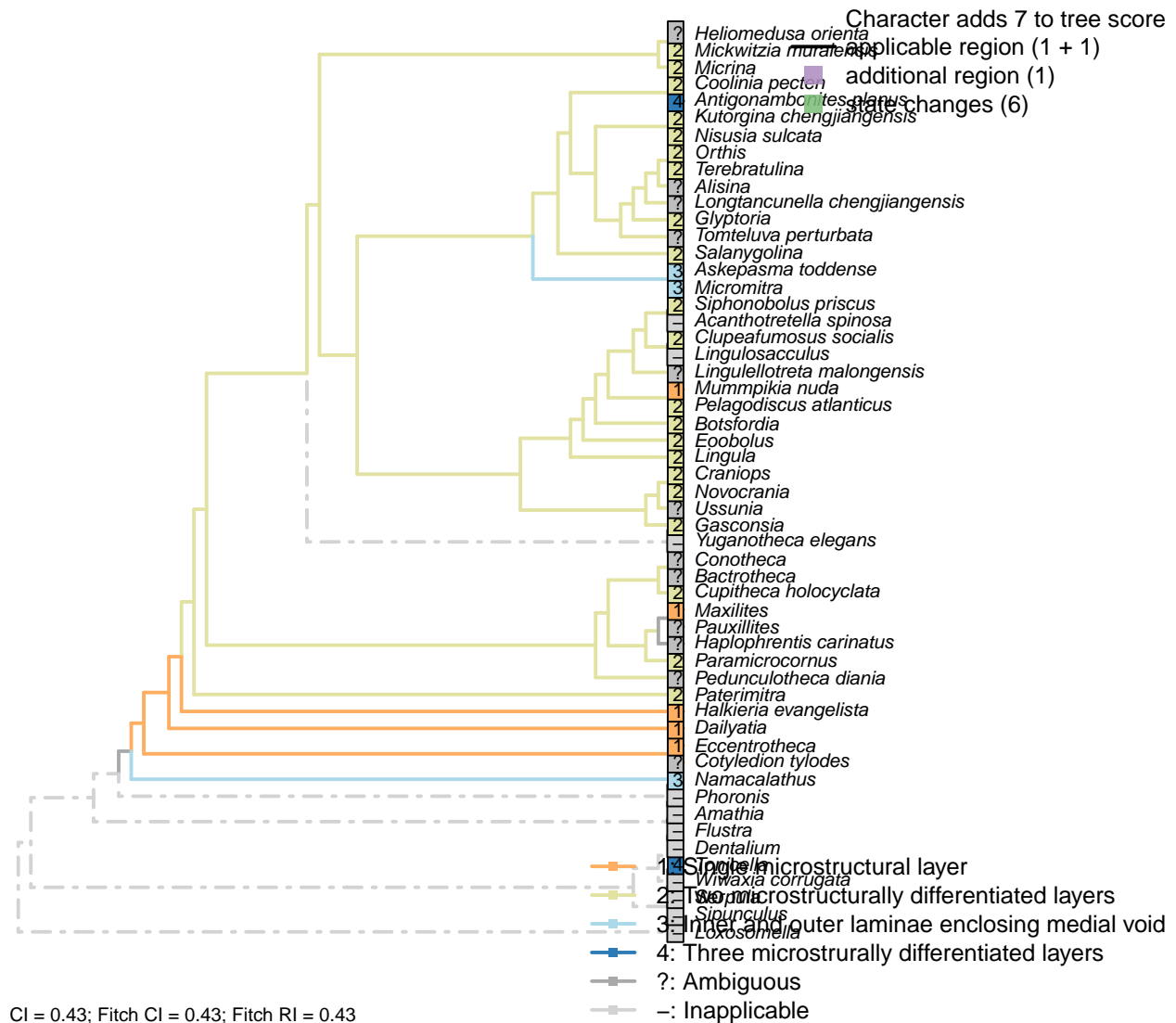
*Askepasma toddense*, *Micromitra*, *Glyptoria*, *Kutorgina chengjiangensis*: Following appendix 2 in Williams *et al.* (1998b).

*Botsfordia*, *Eoobolus*: Coded as flexible in Williams *et al.* (1998b), Appendix 2.

*Pelagodiscus atlanticus*: Flexible (Williams *et al.*, 1998b).

*Salanygolina*: Coded as uncertain in appendix 2 in Williams *et al.* (1998b).

### [132] Microstructure: Number of distinct layers



#### Character 132: Sclerites: Composition: Microstructure: Number of distinct layers

- 1: Single microstructural layer
  - 2: Two microstructurally differentiated layers
  - 3: Inner and outer laminae enclosing medial void
  - 4: Three microstrurally differentiated layers
- Transformational character.

Hyolith conchs comprise two mineralized layers of fibrous bundles. Bundles are measure 5–15 µm across; their constituent fibres are each 0.1–1.0 µm wide. In the inner layer, the fibres are transverse; in the outer layer, the bundles are inclined towards the umbo, becoming longitudinal on the outermost margin.

Coded as non-additive as there is no clear necessity to add layers sequentially: for example, three layers could arise by the addition of a void within a single pre-existing layer.

Stratiform laminae, shell-penetrating canals and other features above the scale of crystal organization are not considered as contributing to the mineralogical microstructure and are coded separately.

Inapplicable in taxa with a non-mineralized shell.

*Bactrotheca*: Taxon known only from moulds (Valent et al., 2012).

*Botsfordia*: “Composed of a thin primary layer and a laminate secondary shell exhibiting baculate shell structure” – Skovsted & Holmer (2005), with reference to Skovsted and Holmer (2003).

*Clupeafumosus socialis*: General acrotretid structure taken from Zhang *et al.* (2016).

*Cupitheca holocyclata*: Inner and outer layers (Vendrasco et al., 2017).

*Eoobolus*: “*Eoobolus* shells exhibit the general characteristics of modern linguliform shells, i.e. they were composed of alternating sets of organic and apatite-rich layers that were separated by thin sheets of recalcitrant organic layers.” – Balthasar (2007).

*Halkieria evangelista*: Single layer of fibrous aragonite (Porter, 2008).

*Maxilites*: Coded following helen microstructure described in the similar material of ‘*Hyolithes*’ (Martí Mus and Bergström, 2007).

*Mickwitzia muralensis*: “the shell structure of *Mickwitzia* [...] is closely similar to the columnar shell of linguliform acrotretoid brachiopods as well as to the linguloid *Lingulellotreta*, in that it has slender columns in the laminar succession” – Williams et al. (2007).

*Micrina*: Identical to *Mickwitzia* and more derived linguliforms (Holmer et al., 2011).

*Mummpikia nuda*: Balthasar (2008) considers the single mineralogical layer, which comprises phosphatic rods and laminae, to characterize Obolellata.

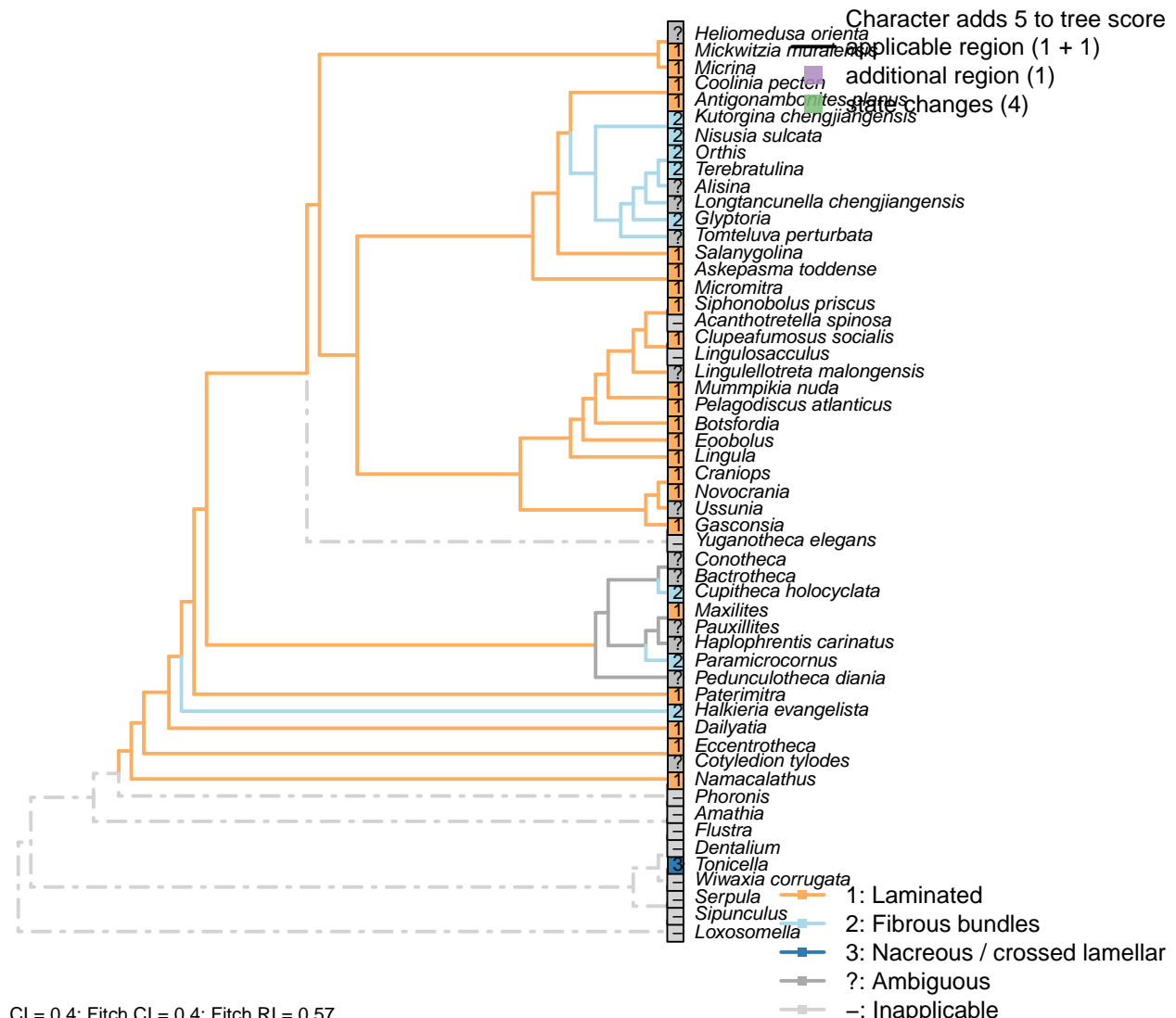
*Namacalathus*: *Namacalathus* exhibits three layers, none of which have any obvious correspondence with those of brachiopods.

*Paramicrocornus*: “The shells of both skeletal components show very similar structures and are composed of two layers” – Zhang et al. (2018).

*Siphonobolus priscus*: “Orthodoxly secreted primary and secondary layers” – Williams et al. (2004).

*Tonicella*: From periostracum inwards, Chiton bears three microstructural layers: fine-grained, nacreous, and regular crossed lamellar.

### [133] Microstructure: Format



#### Character 133: Sclerites: Composition: Microstructure: Format

- 1: Laminated
  - 2: Fibrous bundles
  - 3: Nacreous / crossed lamellar
- Transformational character.

Hyolith conchs comprise two mineralized layers of fibrous bundles. Bundles measure 5–15 µm across; their constituent fibres are each 0.1–1.0 µm wide. In the inner layer, the fibres are transverse; in the outer layer, the bundles are inclined towards the umbo, becoming longitudinal on the outermost margin.

Stratiform laminae, shell-penetrating canals and other features above the scale of crystal organization are not considered as contributing to the mineralogical microstructure and are coded separately.

The pervasive (not just superficial) polygonal structures in *Paterimitra* are distinct, and characterize *Askepasma*, *Salanygolina*, *Eccentrotheca* and *Paterimitra* (Larsson et al., 2014)

Williams et al. (2000) identify cross-bladed laminae as diagnostic of Strophomenata, with the exception of

some older groups that contain fibres or laminar laths.

*Antigonambonites planus*: Tabular laminae, not fibrous as previously thought (Madison, 2017).

*Askepasma toddense*: Lamination present (Balthasar et al., 2009), with imprints of presumed mantle cells (following Williams et al., 1998b, appendix 2).

*Botsfordia*: “Composed of a thin primary layer and a laminate secondary shell exhibiting baculate shell structure” – Skovsted & Holmer (2005), with reference to Skovsted and Holmer (2003).

Williams et al. (1998b, appendix 2) code lamination as present, with no imprints of presumed mantle cells.

*Coolinia pecten*: Dewing (2004).

*Craniops*: (Williams et al., 1997, fig. 249.1).

*Cupitheca holocyphata*: Fibrous bundles (Vendrasco et al., 2017).

*Eccentrotheca, Paterimitra*: Laminated (Balthasar et al., 2009).

*Micromitra, Eoobolus*: Lamination present, with no imprints of presumed mantle cells (following Williams et al., 1998b, appendix 2).

*Gasconsia*: Laminated relict shell structure visible, indicating original constitution from “sheet-like laminae” (Hanken and Harper, 1985).

*Glyptoria, Kutorgina chengjiangensis*: Lamination absent (following Williams et al., 1998b, appendix 2).

*Lingula*: Lingulid laminae are thicker than those of tommotiids or paterinids, but construed as homologous (Balthasar et al., 2009).

*Maxilites*: Coded following helen microstructure described in the similar material of ‘*Hyolithes*’ (Martí Mus and Bergström, 2007).

*Mickwitzia muralensis*: Alternation of layers (Balthasar, 2004).

*Micrina*: *Micrina* exhibits polygonal imprints on the internal surfaces of successive second-order laminae, suggesting the existence of a polygonal organization of these layers (Balthasar et al., 2009).

*Mummpikia nuda*: Balthasar (2008) considers the single mineralogical layer, which comprises phosphatic rods and laminae, to characterize Obolellata.

*Namacalathus*: The inner and outer layer are foliated. The columnar inflections lack canals, and as such we do not consider them to bear any obvious homology with the hollow pillars of tommotiids and certain brachiopods, their superficial similarity to strophomenid pseudopunctae notwithstanding.

*Novocrania*: Laminar secondary layer (Parkinson et al., 2005).

*Orthis*: Orithidina have impunctate shells with a fibrous secondary layer (Williams et al., 2000, p. 724).

*Paramicrocornus*: Fibrous (Zhang et al., 2018).

*Salanygolina*: “Apatitic crystals of varying shapes and dimensions” – Holmer et al. (2009).

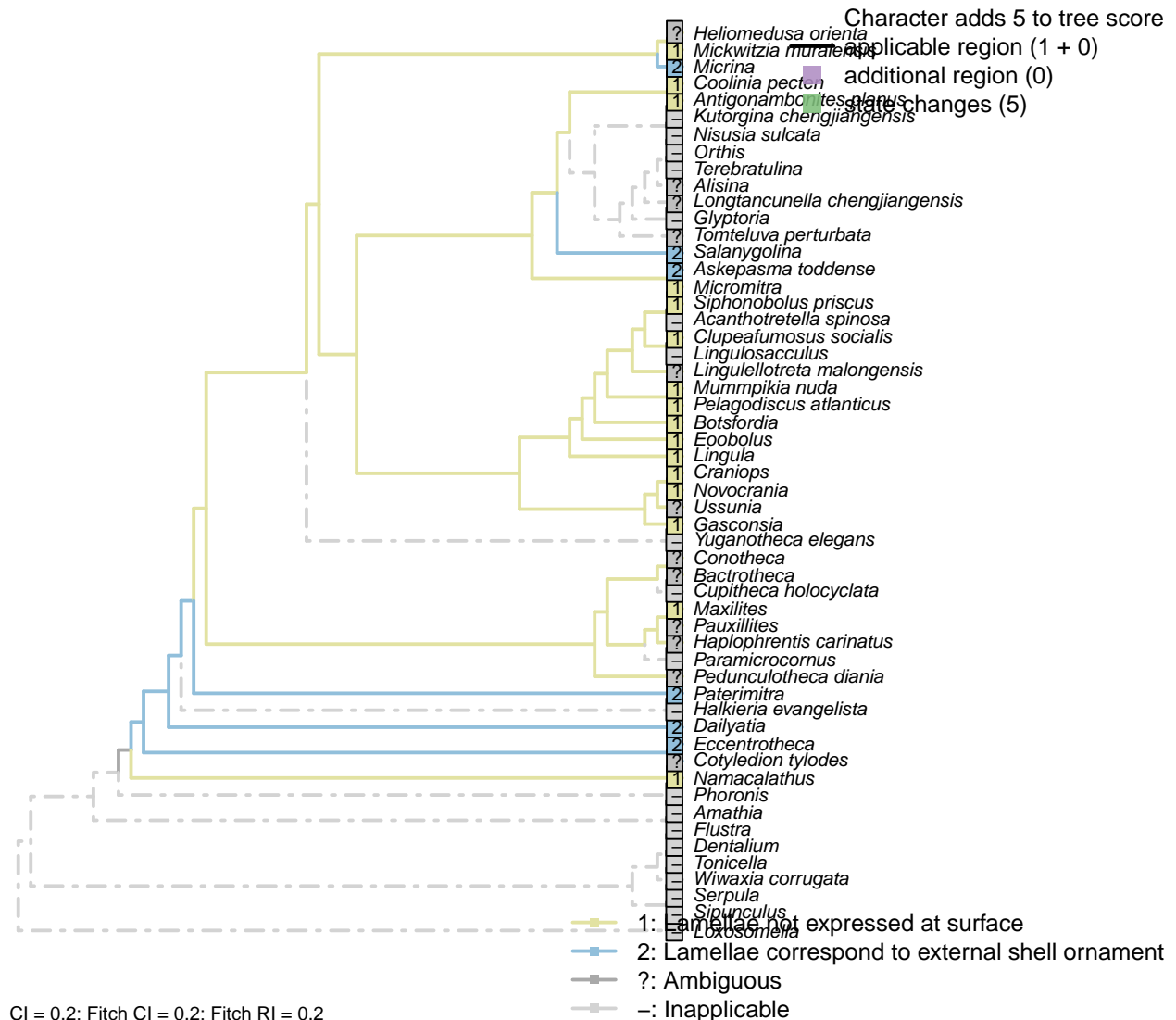
*Siphonobolus priscus*: Cleaved stratified platy laminae, best preserved in canal walls (Williams et al., 2004).

*Terebratulina*: Parkinson et al. (2005).

*Tomteluva perturbata*: No original structural details evident (Streng et al., 2016).

## 5.16 Sclerites: Structure

### [134] Stratiform lamellae expressed at surface



#### Character 134: Sclerites: Structure: Stratiform lamellae expressed at surface

- 1: Lamellae not expressed at surface
- 2: Lamellae correspond to external shell ornament
- Transformational character.

In tommotiids, the shell simply comprises a stack of stratiform lamellae, each corresponding to a circumferential rib at the shell surface. This is particularly apparent in *Dailytia* (Skovsted et al., 2015) and *Paterimitra*

(Larsson et al., 2014).

*Askepasma toddense*: Topper et al. (2013b).

*Coolinia pecten*: Dewing (2004).

*Dailyatia*: Each lamina corresponds to a ridge on the surface (Skovsted et al., 2015).

*Eoobolus*: Balthasar (2007).

*Maxilites*: Coded following helen microstructure described in the similar material of '*Hyolithes*' (Martí Mus and Bergström, 2007).

*Novocrania*: Parkinson et al. (2005).

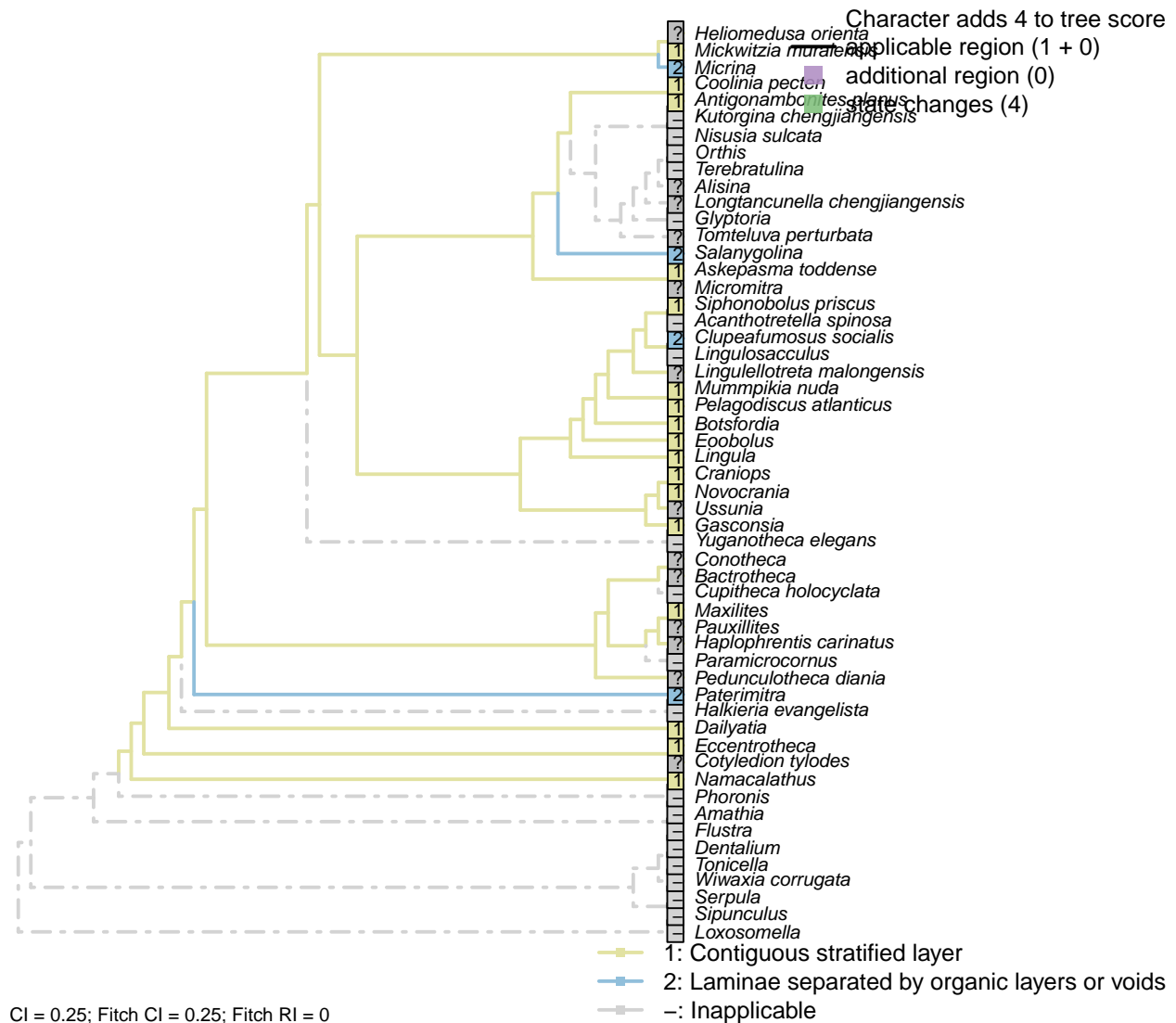
*Paterimitra*: Particularly apparent (Larsson et al., 2014).

*Pelagodiscus atlanticus*: Williams et al. (1998a).

*Salanygolina*: Laminae seem to terminate at superficial ridges (Holmer et al., 2009).

*Siphonobolus priscus*: (Williams et al., 2004).

## [135] Stratiform laminae separated

**Character 135: Sclerites: Structure: Stratiform laminae separated**

- 1: Contiguous stratified layer
  - 2: Laminae separated by organic layers or voids
- Transformational character.

Laminae within, for example, *Salanygolina* are separated by voids that may originally have contained organic material (e.g. Holmer et al., 2009). In contrast, tommotiids and paterinids exhibit stratification without voids,

perhaps representing periodic fluctuations in phosphate availability (Balthasar et al., 2009).

*Askepasma toddense*, *Eccentrotheca*: Contiguous (Balthasar et al., 2009).

*Botsfordia*: Skovsted and Holmer (2003).

*Clupeafumosus socialis*: Acrotretid laminae are separated by column-supported voids.

*Coolinia pecten*: Dewing (2004).

*Craniops*: (Williams et al., 1997, fig. 249.1).

*Dailyatia*: Contiguous (Skovsted et al., 2015, figs. 54–55).

*Eoobolus*: Essentially contiguous, notwithstanding occasional laminae of calcite/chlorite (Balthasar, 2007).

*Gasconsia*: Hanken and Harper (1985).

*Maxilites*: Coded following helen microstructure described in the similar material of ‘*Hyolithes*’ (Martí Mus and Bergström, 2007).

*Mickwitzia muralensis*: (Balthasar, 2004).

*Micrina*: Matrix filled chambers (Balthasar et al., 2009, fig. DR1).

*Mummpikia nuda*: Seemingly contiguous (Balthasar, 2008).

*Novocrania*: Not in *Novocrania*, though possibly present in *Neoancistrocrania* (Parkinson et al., 2005).

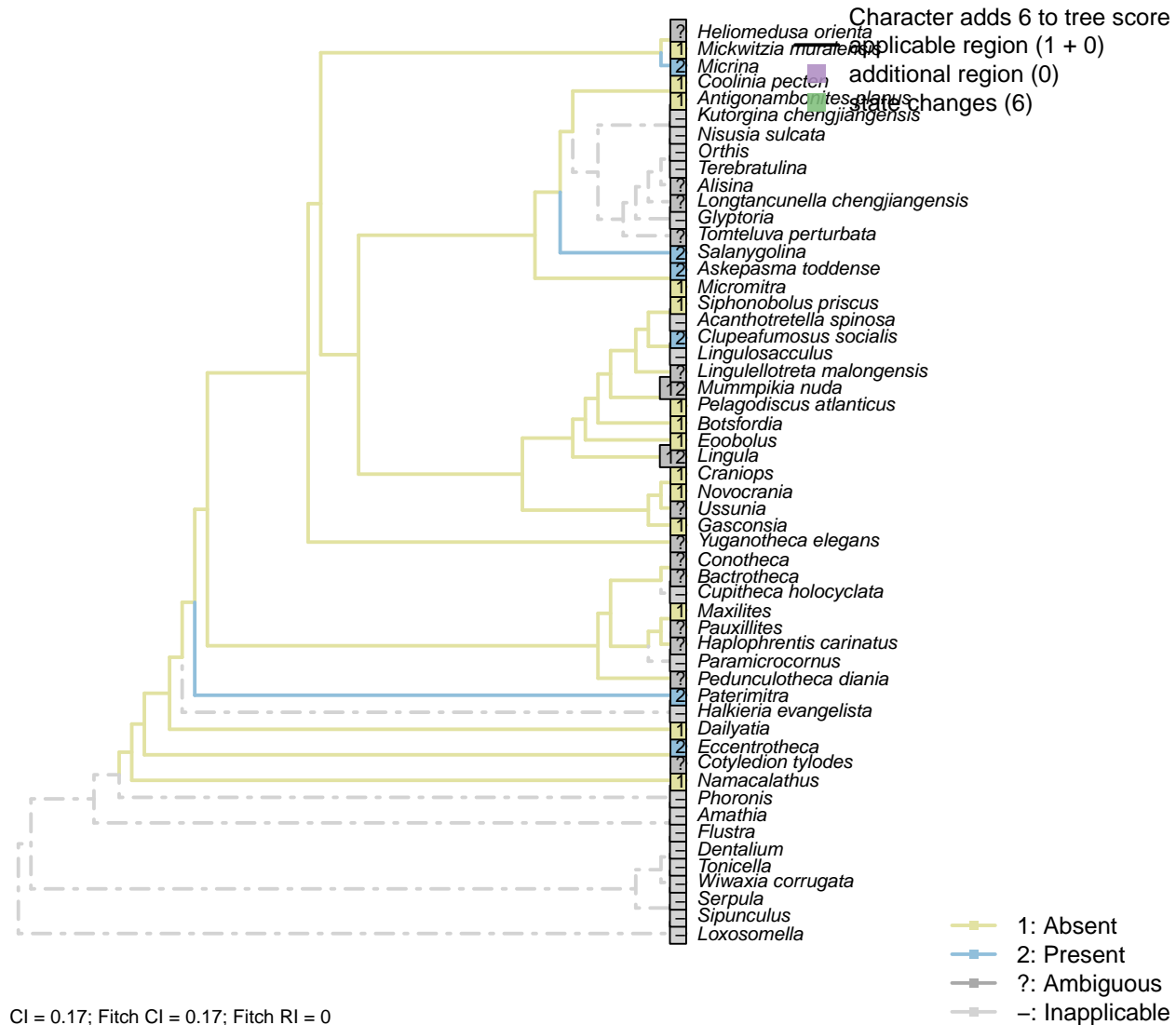
*Paterimitra*: Contiguous in some regions, but large internal cavities present [Balthasar et al. (2009); see fig. DR3].

*Pelagodiscus atlanticus*: Williams et al. (1998a).

*Salanygolina*: Polygonally-filled voids (Holmer et al., 2009).

*Siphonobolus priscus*: (Williams et al., 2004).

### [136] Stratiform laminae with polygonal ornament



#### Character 136: Sclerites: Structure: Stratiform laminae with polygonal ornament

1: Absent

2: Present

Transformational character.

See character 37 in Williams et al. (1998b).

“A distinct primary layer [...] is characterized by a polygonal ornament that is mineralized from the polygon walls inward, while the rest of the shell and/or sclerite is secreted by basal accretion” – Balthasar et al. (2009). Distinguished from epithelial cell moulds in lingulids, which do not form an integral part of the shell structure (Balthasar et al., 2009).

Treated as transformational as ancestral condition is ambiguous.

*Askepasma toddense, Eccentrotheca, Paterimitra*: Present (Balthasar et al., 2009).

*Micromitra, Botsfordia, Eoobolus*: Lamination present, with no imprints of presumed mantle cells (following

Williams et al., 1998b, appendix 2).

*Chupeafumosus socialis*: Epithelial cell moulds present on inner shell layer in acrotretids (Zhang et al., 2016).

*Coolinia pecten*: Dewing (2004).

*Craniops*: (Williams et al., 1997, fig. 249.1).

*Dailyatia*: Polygonal structures on external surface of sclerites only (Skovsted et al., 2015); not reported from other camenellans (Balthasar et al., 2009).

*Gasconsia*: Hanken and Harper (1985).

*Lingula*: Absent in *Lingula*, though potentially equivalent, if superficial (Balthasar et al., 2009), features adorn *Lingulella* (Curry and Williams, 1983).

*Maxilites*: Coded following helen microstructure described in the similar material of ‘*Hyolithes*’ (Martí Mus and Bergström, 2007).

*Micrina*: *Micrina* exhibits polygonal imprints on the internal surfaces of successive second-order laminae, suggesting the existence of a polygonal organization of these layers (Balthasar et al., 2009).

*Mummpikia nuda*: It is conceivable that the rods (Balthasar, 2008) correspond to the polygonal ornament observed in other taxa; coded as ambiguous.

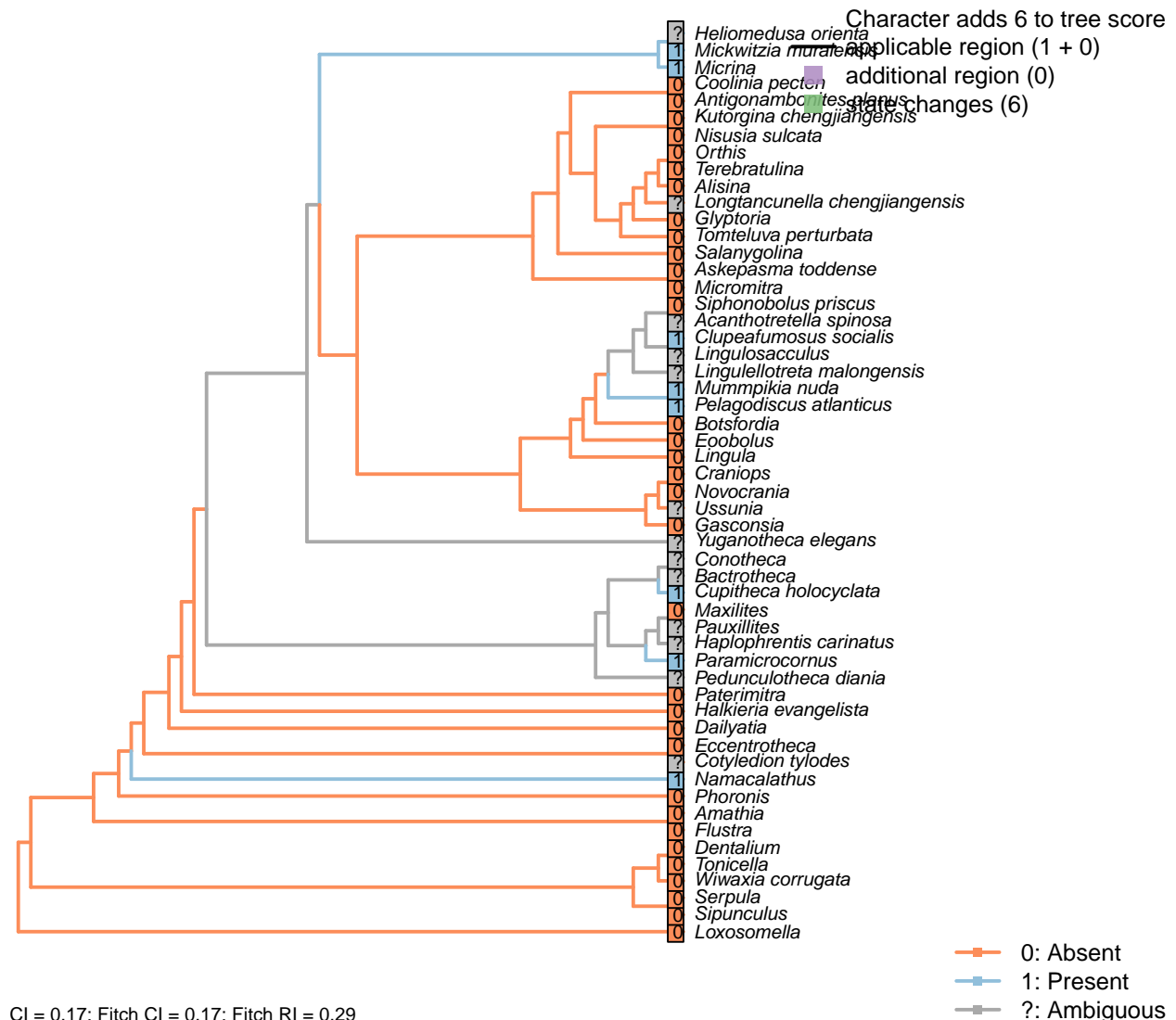
*Novocrania*: Parkinson et al. (2005).

*Pelagodiscus atlanticus*: Williams et al. (1998a).

*Salanygolina*: Prominently present (Holmer et al., 2009).

*Siphonobolus priscus*: (Williams et al., 2004).

## [137] Canals



## Character 137: Sclerites: Structure: Canals

0: Absent

1: Present

Neomorphic character.

A caniculate microstructure occurs in lingulids; canals are narrower (< 1 µm) than punctae, may branch, and do not fully penetrate the shell, terminating just within the boundaries of a microstructural layer. See Williams et al. (1997), p303ff, and Balthasar (2008), p273, for discussion.

Tubules described in hyoliths by Kouchinsky (2000) measure around 10 µm in diameter, making them an order of magnitude wider than lingulid canals.

This said, Balthasar (2008) considers the rod-like tubules within the columnar shell microstructure of *Mickwitzia* cf. *occidens* (1–3 µm wide, Skovsted and Holmer, 2003), acrotretides (1 µm wide, see Holmer, 1989, Zhang et al. (2016)) and lingulellotretids (100 nm wide, Cusack et al., 1999) as equivalent to lingulid canals.

*Micrina* exhibits both punctae and canals (Harper et al., 2017), challenging Carlson's contention (in Williams

et al., 2007) that the structures are potentially homologous as shell perforations.

*Bactrotheca*: Taxon known only from moulds (Valent et al., 2012).

*Botsfordia*: Not evident in section presented by Skovsted & Holmer (2003).

*Clupeafumosus socialis*: Acrotretid laminae bear characteristic columns (e.g. Zhang et al., 2016).

Balthasar (2008) considers these columns as homologous with tubules within the columnar shell microstructure *Mummpikia*, *Mickwitzia* and lingulellotretids.

*Cupitheca holocyclata*: Orthogonal tubules (Vendrasco et al., 2017).

*Halkieria evangelista*: The chambers in halkieriid sclerites do not correspond in morphology or dimension to the brachiopod-like canals documented by this character.

*Longtancunella chengjiangensis*: Preservational resolution not sufficient to evaluate.

*Maxilites*: Coded following helen microstructure described in the similar material of ‘*Hyolithes*’ (Martí Mus and Bergström, 2007).

*Mickwitzia muralensis*: Coded as present to reflect similarity of columnar microstructure remarked on by, among others, Balthasar (2008); Williams et al. (2007); Skovsted & Holmer (2003).

*Micrina*: Acrotretid laminae bear characteristic columns (e.g. Zhang et al., 2016); a similar fabric has been reported, and assumed homologous, in *Micrina* (Butler et al., 2012).

A similar columnar shell microstructure also occurs in the closely related *Mickwitzia* (Balthasar, 2008).

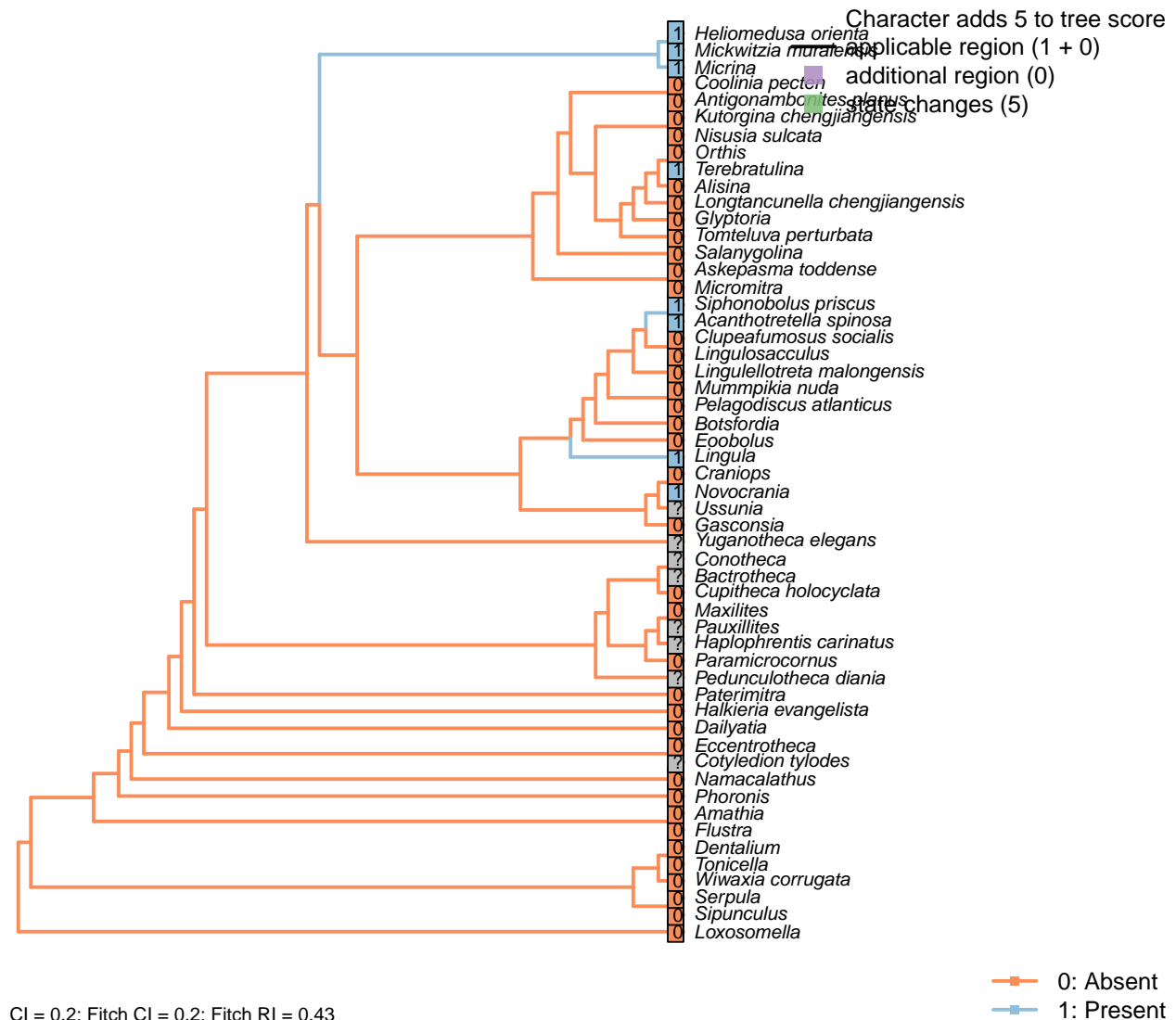
*Namacalathus*: Canal-like structures have been reported in *Namacalathus* (Zhuravlev et al., 2015), and interpreted as evidence for a Lophophorate affinity. Though the structures are not necessarily directly equivalent, the hypothesis of homology is followed here.

*Paramicrocornus*: Columns, replicated in phosphate and present in both layers of the shell, have been interpreted as potential homologues to acrotretid columns (Zhang et al., 2018).

*Siphonobolus priscus*: The ‘canals’ through the shell have a diameter of c. 20 µm (Williams et al., 2004, text-fig. 2a), falling within the definition of punctae (rather than canals) used herein.

*Tonicella*: Aesthete canals do not fall within the definition of this character.

### [138] Punctae



#### Character 138: Sclerites: Structure: Punctae

0: Absent

1: Present

Neomorphic character.

Punctae are 10–20 µm wide canals created by multicellular extensions of the outer epithelium. They penetrate the full depth of the shell.

Balthasar (2008) writes:

“Vertical shell penetrating structures, such as punctae, pseudopunctae, extropunctae and canals, are common in many groups of brachiopods and are distinguished based on their geometry and size (Williams et al., 1997). Punctae are 10–20 µm wide and represent multicellular extensions of the outer epithelium (Owen and Williams, 1969). Pseudopunctae and extropunctae are similar in diameter but, instead of canals, are vertical stacks of conical deflections of individual shell layers (Williams and Brunton, 1993). None of these three types of vertical shell structure, all of which are confined to calcitic-shelled brachiopods, compares with the much smaller canals (< 1 µm in diameter) of *M. nuda*. The only type of vertical structure that fits the

size and nature of the canals of the Mural obbolellids are the canals of linguliform brachiopods, which range in width from 180 to 740 nm and are occupied by proteinaceous strands in extant taxa (Williams et al., 1992, 1994, 1997). In contrast to obbolellid canals, however, linguliform canals are not known to penetrate the entire shell but terminate in organic-rich layers (Williams et al., 1997). Based on these considerations it would, therefore, be misleading to call obbolellid shells punctate (they are as much "punctate" as acrotretids or other linguliforms); rather their shell structure should be called canalicate (Williams et al., 1997)."

*Bactrotheca*: Taxon known only from moulds (Valent et al., 2012).

*Craniops*: "impunctate".

*Haplophrentis carinatus*: The tubules within the centre of the bundles of hyolith shells (Kouchinsky, 2000) are c. 10 µm wide, making them an order of magnitude larger than the canals that characterize lingulid valves, and a similar scale to punctae. This said, they have only been reported in a putative allathecid, so the presence of equivalent structures in hyolithids has never been demonstrated.

*Helomedusa orienta*: 'Identical' to those in *Mickwitzia* – see Williams et al. (2007).

*Maxilites*: Coded following helen microstructure described in the similar material of 'Hyolithes' (Martí Mus and Bergström, 2007).

*Mickwitzia muralensis*: Coded as present to reflect that the chambers contained setae; following Carlson in Williams et al. (2007), the punctae may or may not be homologous as punctae, but are likely homologous as shell perforations; both these perforations and those of *Micrina* were associated with setae, even if their equivalence be with juvenile vs adult setal structures in modern brachiopods (Balthasar, 2004, p. 397).

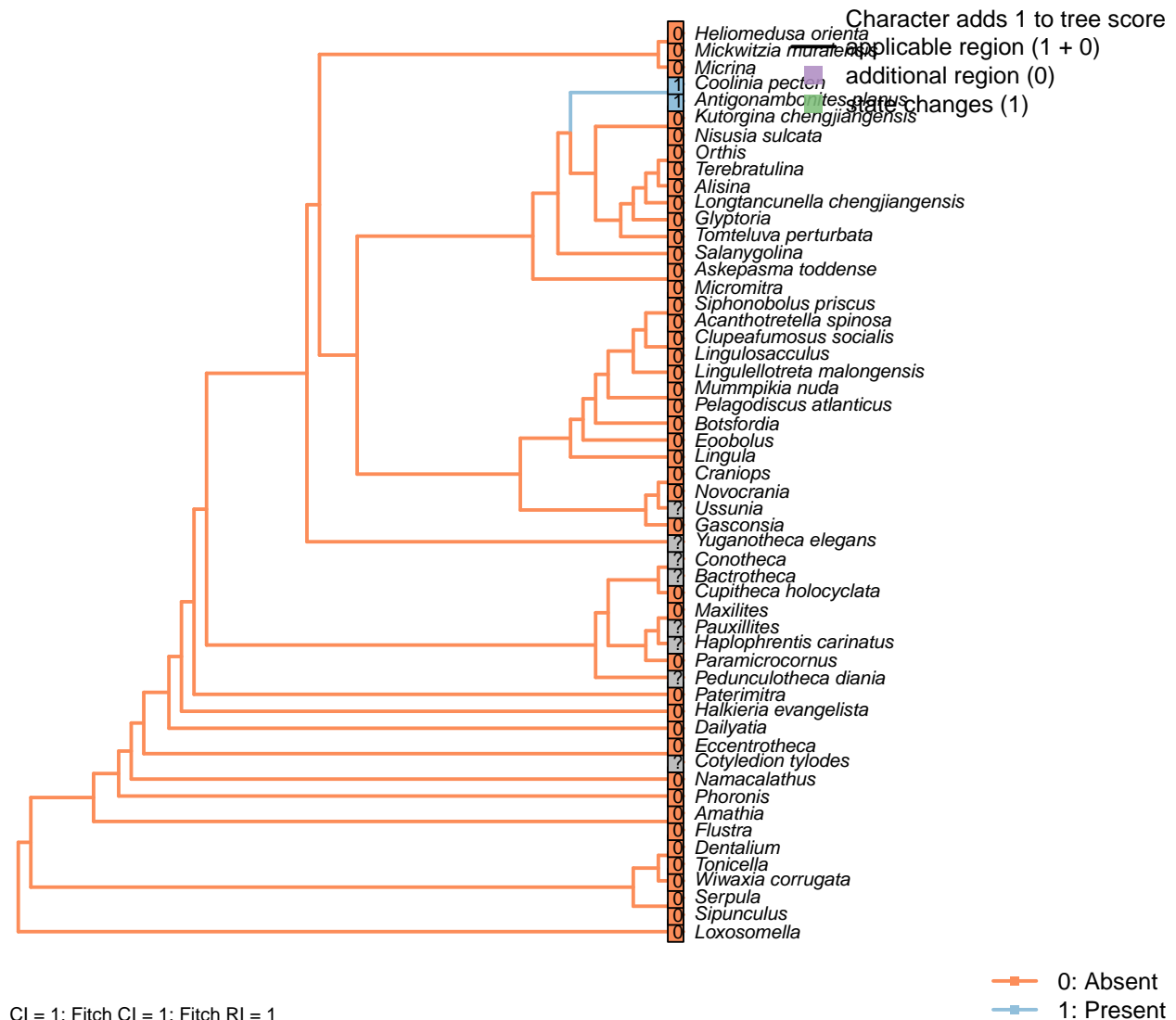
*Mummpikia nuda*: "Vertical shell penetrating structures, such as punctae, pseudopunctae, extropunctae and canals, are common in many groups of brachiopods and are distinguished based on their geometry and size (Williams et al., 1997). Punctae are 10–20 µm wide and represent multicellular extensions of the outer epithelium (Owen and Williams, 1969). [...] None of these three types of vertical shell structure, all of which are confined to calcitic-shelled brachiopods, compares with the much smaller canals (< 1 µm in diameter) of *M. nuda*. The only type of vertical structure that fits the size and nature of the canals of the Mural obbolellids are the canals of linguliform brachiopods, which range in width from 180 to 740 nm and are occupied by proteinaceous strands in extant taxa (Williams et al., 1992, 1994; Williams et al., 1997)." – Balthasar (2008).

*Paramicrocornus*: Not evident despite excellent preservation; interpreted as absent (Zhang et al., 2018).

*Siphonobolus priscus*: The 'canals' through the shell have a diameter of c. 20 µm (Williams et al., 2004, text-fig. 2a), falling within the definition of punctae used herein.

*Terebratulina*: Endopunctae are relatively large canals, diameter vary greatly from 5–20 µm.

### [139] Pseudopunctae



#### Character 139: Sclerites: Structure: Pseudopunctae

0: Absent

1: Present

Neomorphic character.

Pseudopunctae are not punctae, but deflections of shell laminae. They characterise Strophomenata in particular.

*Antigonambonites planus*, *Glyptoria*, *Nisusia sulcata*: Scored absent in data matrix of Benedetto (2009).

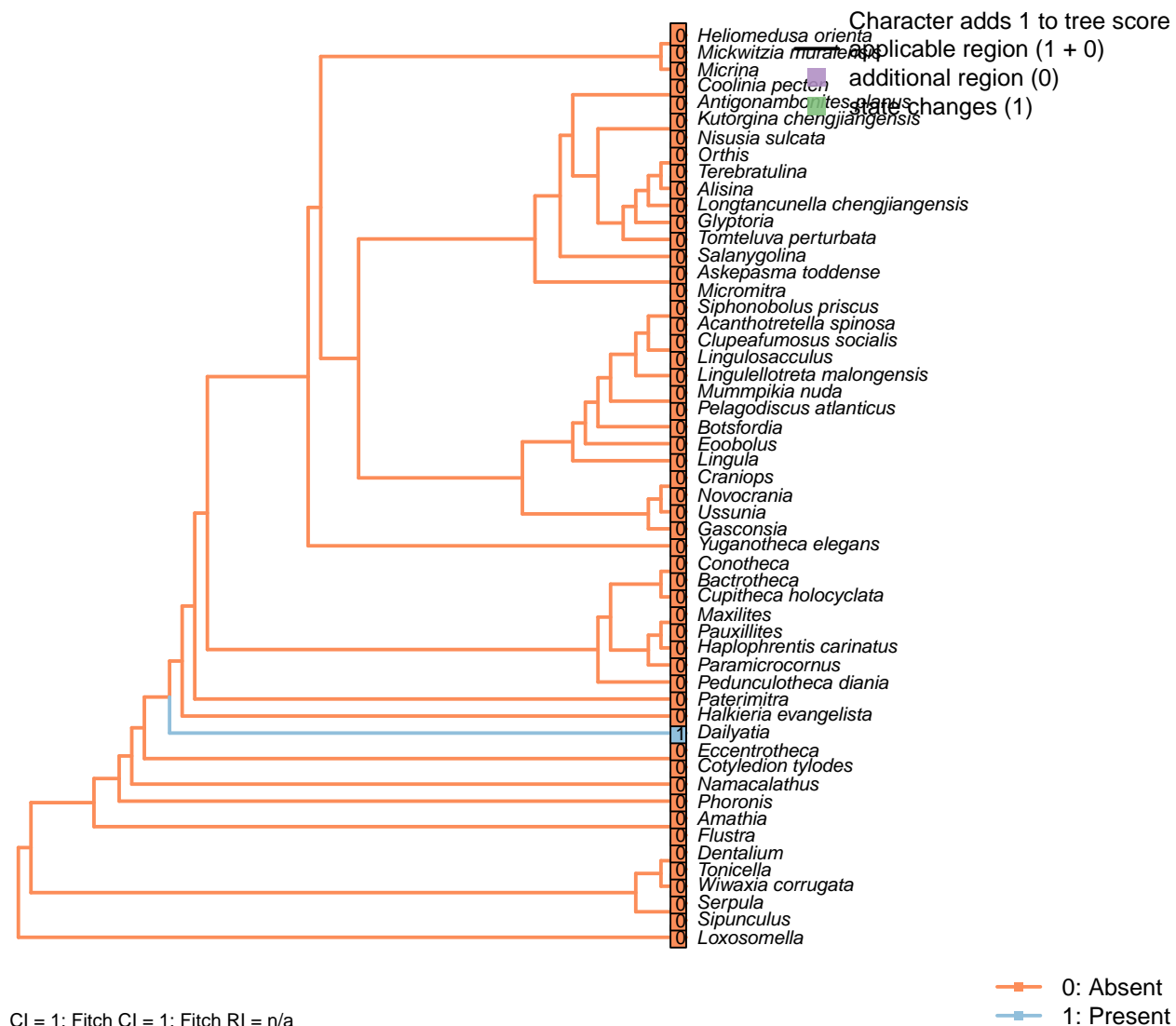
*Bactrotheca*: Taxon known only from moulds (Valent et al., 2012).

*Maxilites*: Coded following helen microstructure described in the similar material of ‘*Hyolithes*’ (Martí Mus and Bergström, 2007).

*Orthis*: Scored absent (in *Eoorthis*) in data matrix of Benedetto (2009).

*Paramicrocornus*: Absent (Zhang et al., 2018).

## [140] External polygonal ornament

**Character 140: Sclerites: Structure: External polygonal ornament**

0: Absent

1: Present

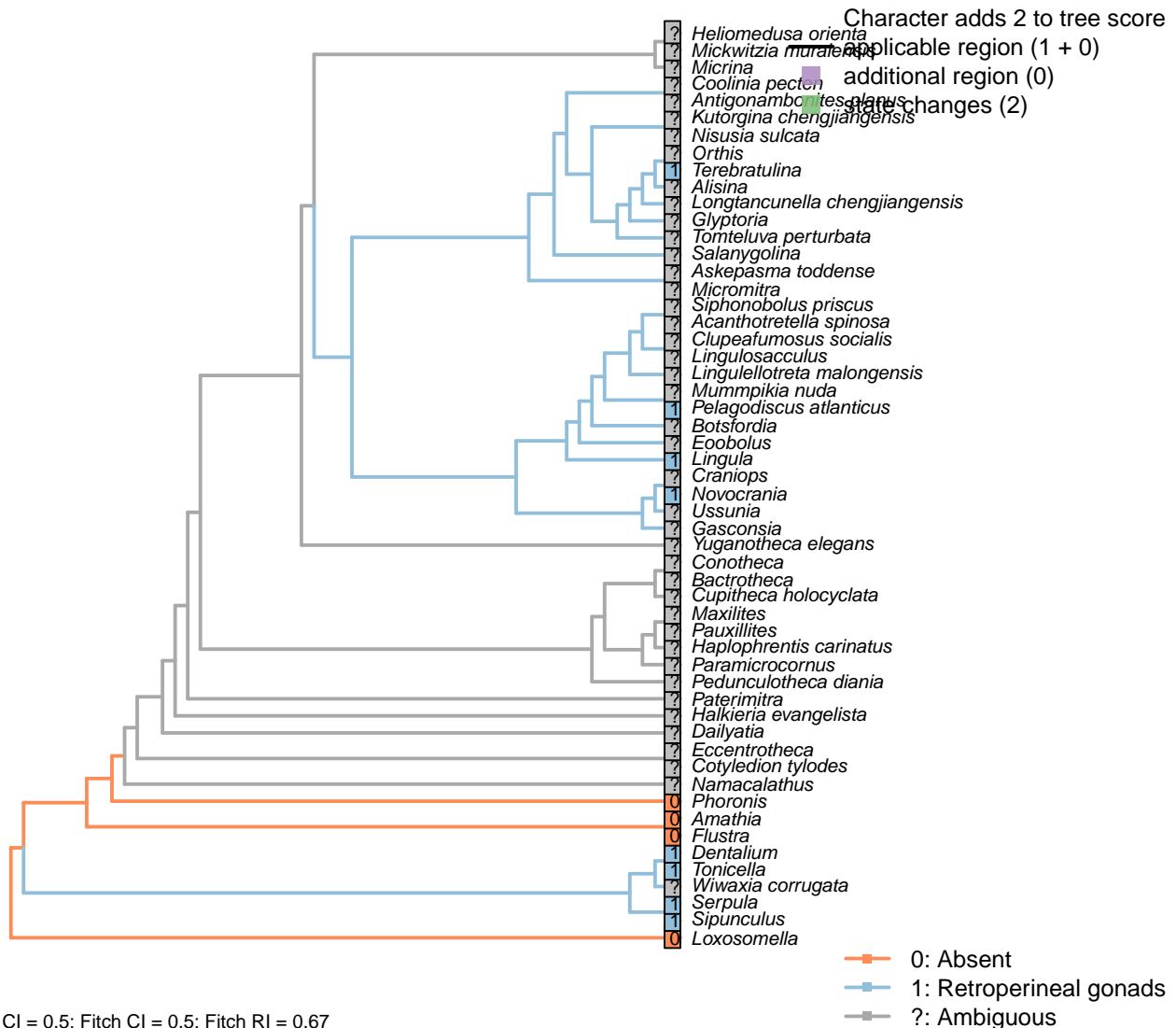
Neomorphic character.

Regular polygonal compartments, around 10 µm in diameter, characterise *Paterimitra*. Walls between compartments have the cross-section of an anvil. An external polygonal structure (possible imprints of epithelial tissue) occurs in *Dailyatia*, but it is a surface pattern, which is different from the polygonal prisms in the body wall of other paterinid-like groups.

*Clupeafumosus socialis*: The polygonal ornament reported in acrotretids by Zhang *et al.* (2016) is on the internal surface of the shell.

## 5.17 Gametes

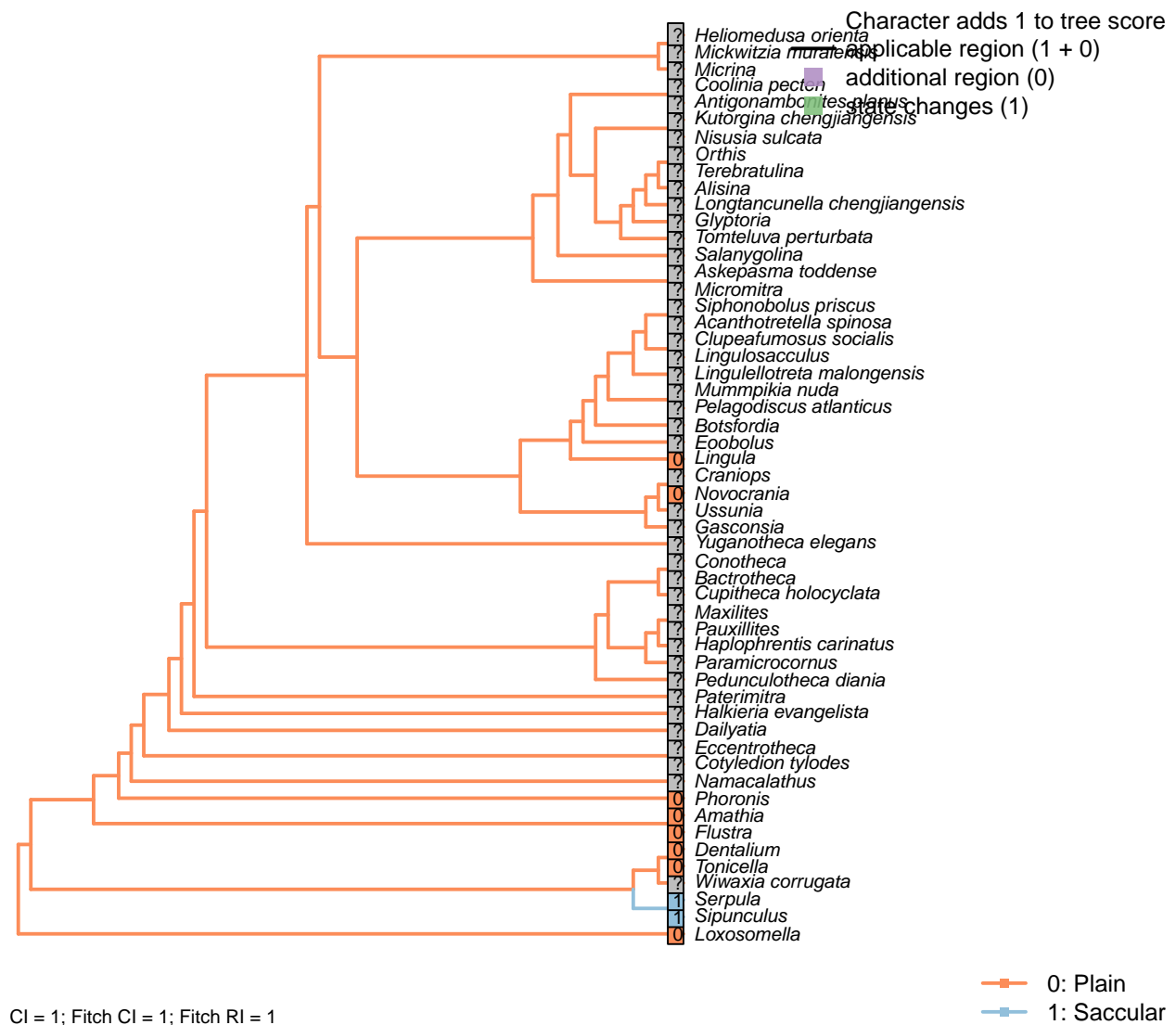
[141] Gonocoel



CI = 0.5; Fitch CI = 0.5; Fitch RI = 0.67

Character 27 in Haszprunar (1996).

## [142] Ovary wall saccular



## Character 142: Gametes: Ovary wall saccular

0: Plain

1: Saccular

Neomorphic character.

After character 31 in Haszprunar (1996).

## [143] Testis wall saccular

## Character 143: Gametes: Testis wall saccular

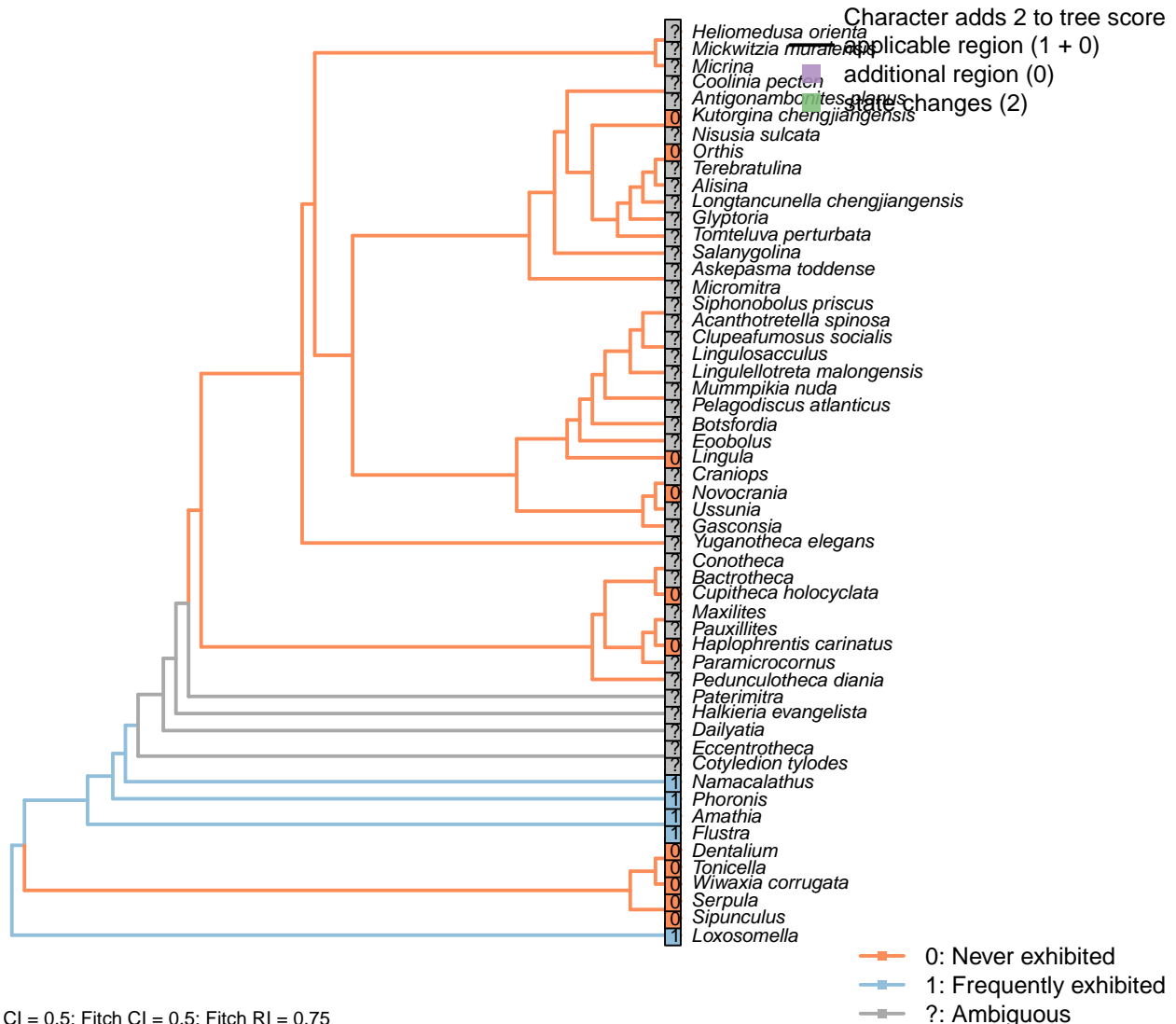
0: Plain

1: Saccular

Neomorphic character.

After character 31 in Haszprunar (1996).

### [144] Asexual reproduction



CI = 0.5; Fitch CI = 0.5; Fitch RI = 0.75

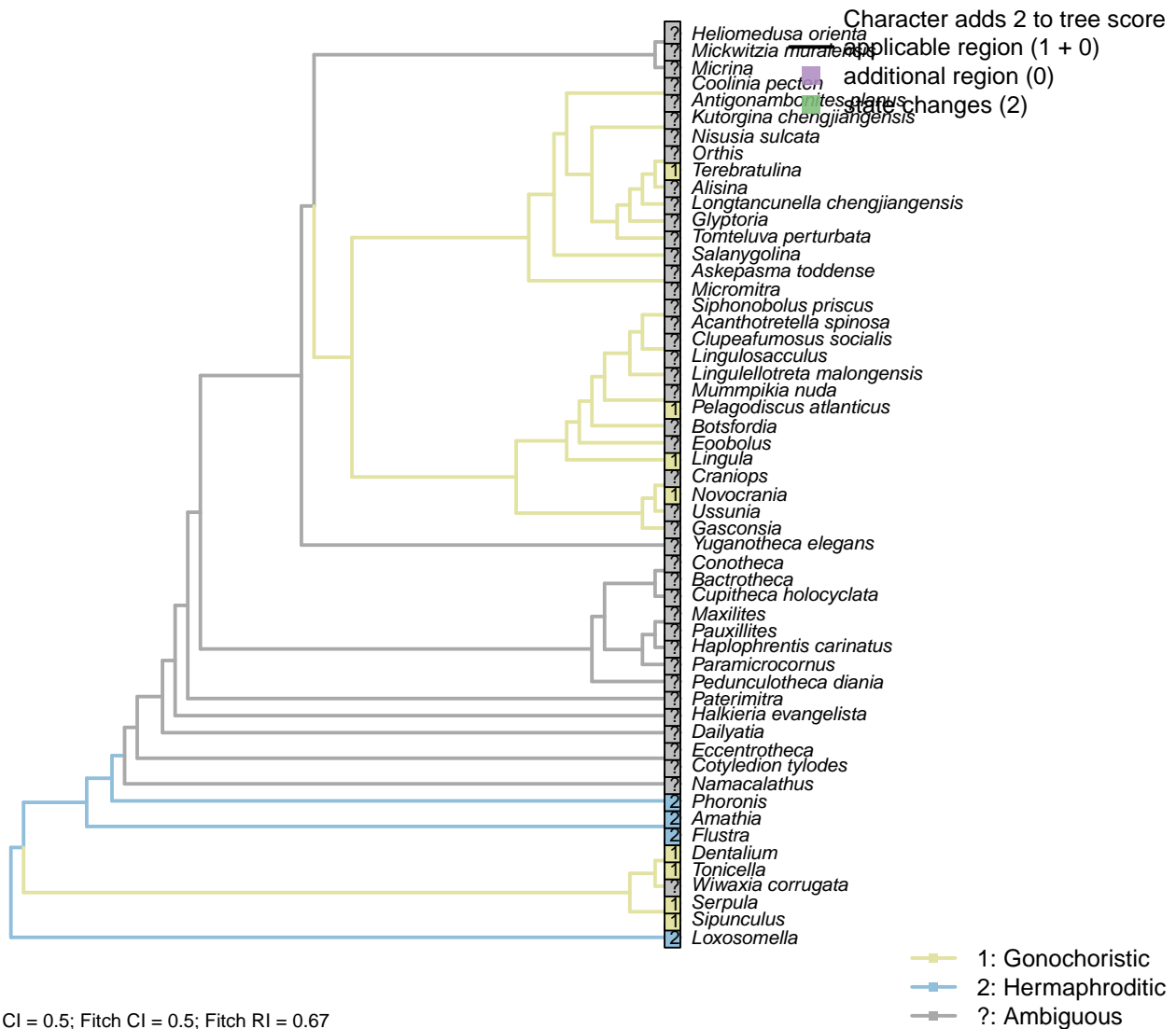
#### Character 144: Gametes: Asexual reproduction

- 0: Never exhibited
- 1: Frequently exhibited
- Neomorphic character.

After character 30 in Haszprunar (1996).

*Namacalathus*: Budding well documented (e.g. Zhuravlev et al., 2015).

## [145] Sexes



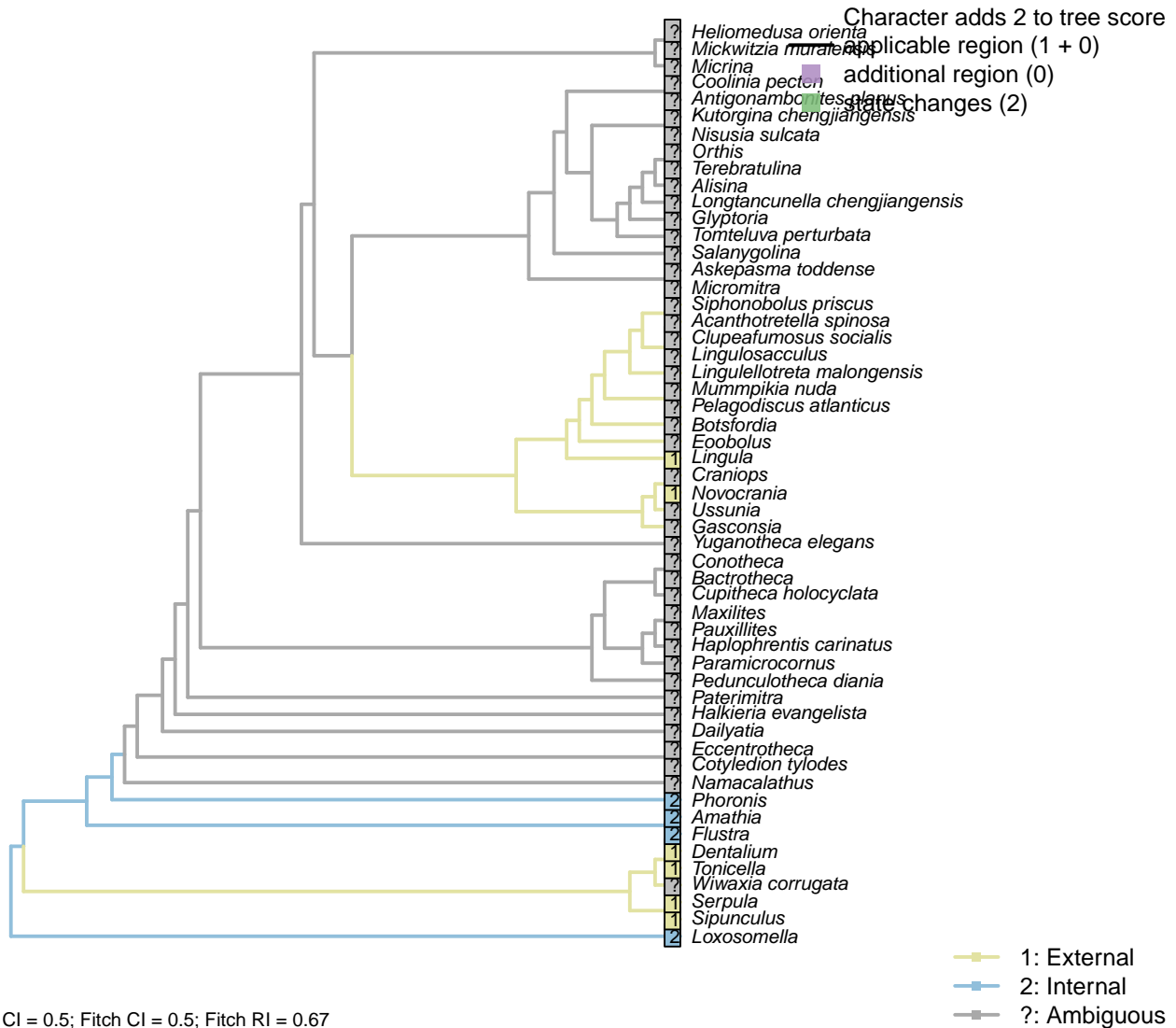
## Character 145: Gametes: Sexes

- 1: Gonochoristic  
 2: Hermaphroditic  
 Transformational character.

After characters 1.61 and 2.54 in von Salvini-Plawen and Steiner (1996).

*Amathia*: Hermaphroditic (Reed, 1988).

## [146] Fertilization



## Character 146: Gametes: Fertilization

1: External

2: Internal

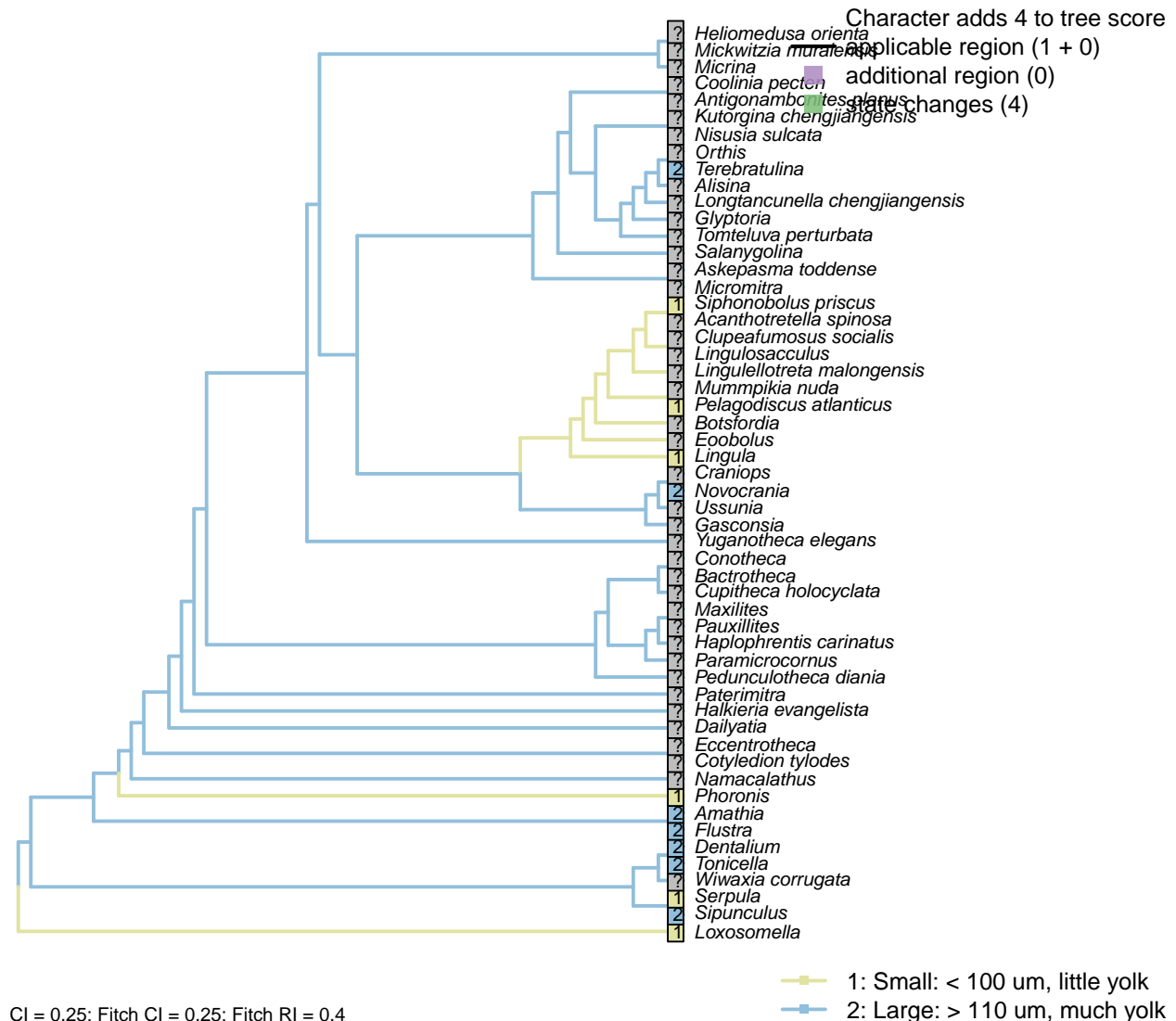
Transformational character.

After character 62 in Haszprunar (2000).

*Amathia*: Brood pouches in abandoned lophophore.

## 5.18 Gametes: Egg

[147] Size



### Character 147: Gametes: Egg: Size

1: Small: < 100 um, little yolk

2: Large: > 110 um, much yolk

Transformational character.

Following Carlson (1995), character 7. This character is only possible to code in extant taxa. It is not considered independent of Carlson's character 11, number of gametes released per spawning, as it is possible to produce more small eggs than large eggs – thus this latter character is not reproduced in the present study. The same goes for Carlson's character 12, gamete dispersal mode; brooders will tend to brood large eggs.

*Amathia*: "Mature eggs commonly measure about 200 μm in diameter" (Franzén, 1977); the larva is a similar size (Reed and Cloney, 1982).

*Dentalium*: Egg size can vary from 60–200 μm in scaphopods, but in *Dentalium* the eggs are large (Dufresne-

Dube et al., 1983).

*Flustra*: “Mature eggs commonly measure about 200 µm in diameter” – Franzén (1977).

*Novocrania*, *Pelagodiscus atlanticus*, *Lingula*, *Terebratulina*: Following coding for class in Carlson (1995) appendix 1, character 7.

*Loxosomella*: Tiny (Nielsen, 1966).

*Phoronis*: *Phoronis* has planktotrophic larvae. indicating a small egg size (Ruppert et al., 2004). Carlson (1995) codes phoronids as polymorphic, as some members of the phylum have eggs of each size.

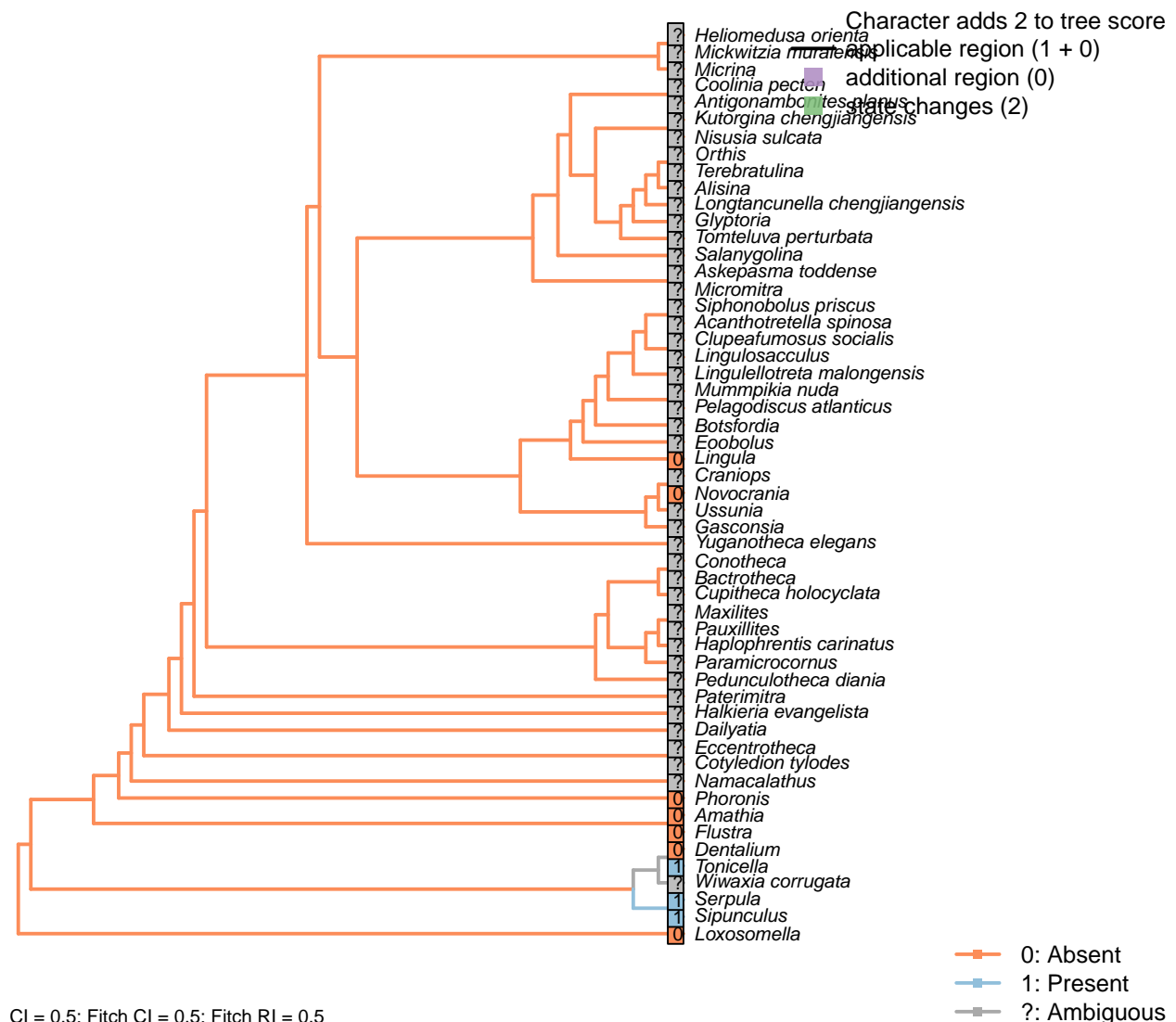
*Serpula*: c. 50 µm in *Hydroides* (Miles et al., 2007).

*Siphonobolus priscus*: “the ventral brephic valve [was] 50 µm across, [which] is close to the known lower limit of the brachiopod egg size” – Popov et al. (2009).

*Sipunculus*: c. 200 µm in diameter (Rice, 1988).

*Tonicella*: Buckland-Nicks et al. (1988).

## [148] Protective membrane



## Character 148: Gametes: Egg: Protective membrane

0: Absent

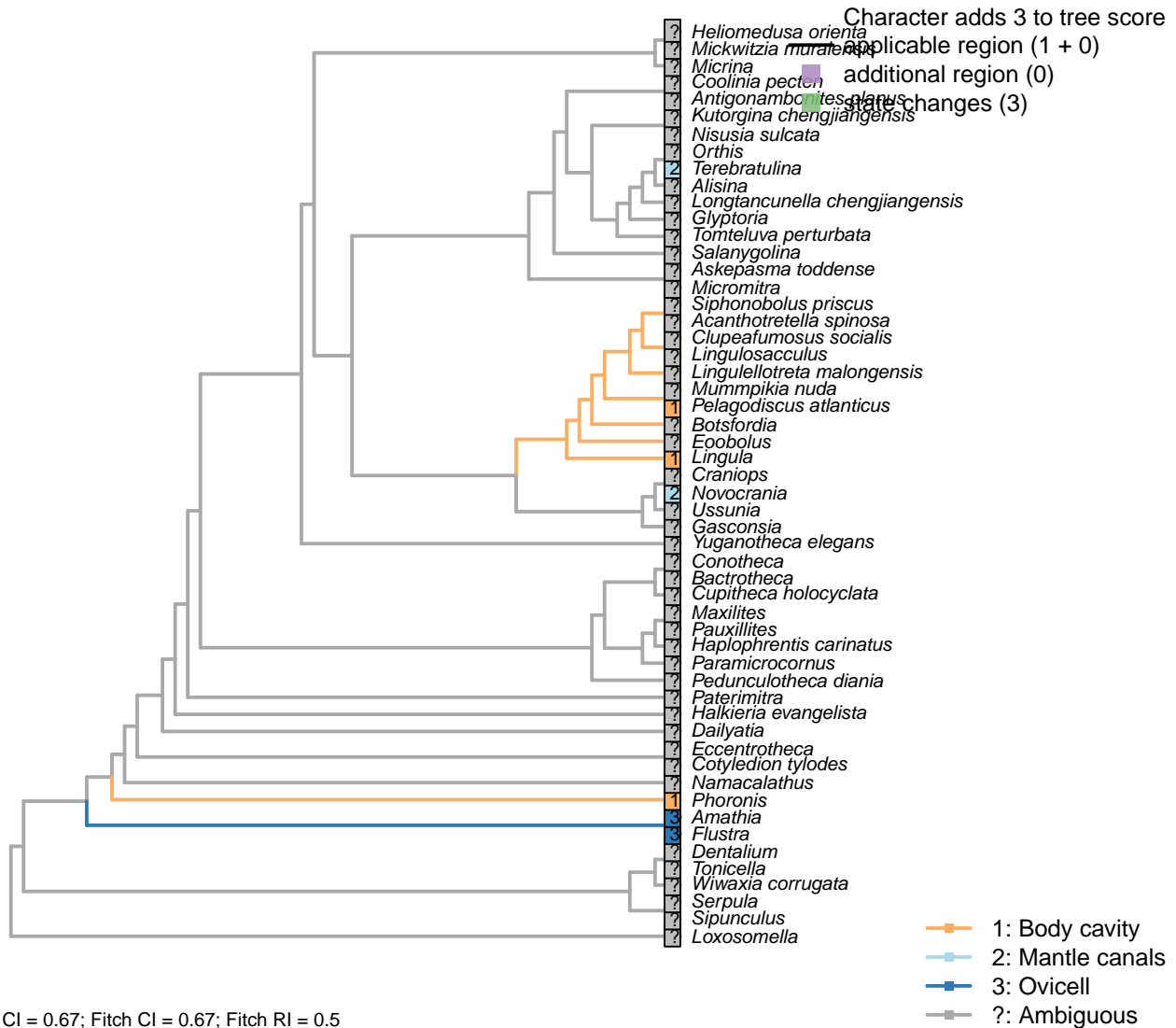
1: Present

Neomorphic character.

After character 4.69 in von Salvini-Plawen and Steiner (1996).

*Flustra, Amathia*: "Eggs have a loose consistency and are capable of changing form" (Franzén, 1977).*Phoronis*: Eggs "are surrounded by a delicate fertilization membrane" (Pennerstorfer and Scholtz, 2012).

## [149] Site of maturation

**Character 149: Gametes: Egg: Site of maturation**

1: Body cavity

2: Mantle canals

3: Ovicell

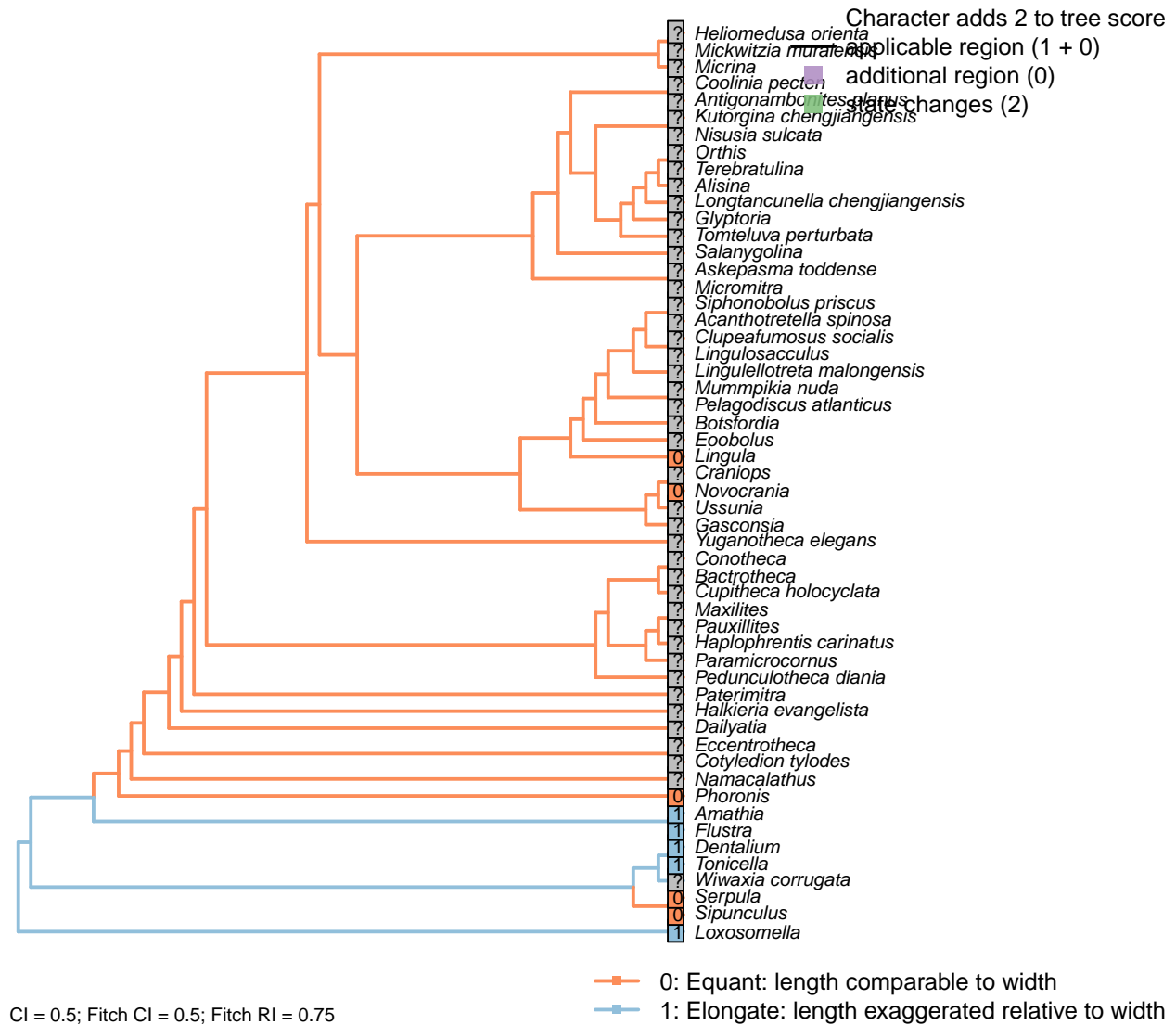
Transformational character.

After Carlson (1995), character 9. Only possible to code in extant taxa.

*Flustra, Amathia*: Ovicell (Franzén, 1977).*Novocrania, Pelagodiscus atlanticus, Lingula, Terebratulina*: Following Hodgson & Reunov (1994).*Phoronis*: Following coding for class in Carlson (1995) Appendix 1, character 9.

## 5.19 Gametes: Spermatozoa

### [150] Nucleus: Shape



0: Equant: length comparable to width

1: Elongate: length exaggerated relative to width

Neomorphic character.

After character 41 in Ponder and Lindberg (1997).

*Flustra, Amathia*: Elongate (Franzén, 1981).

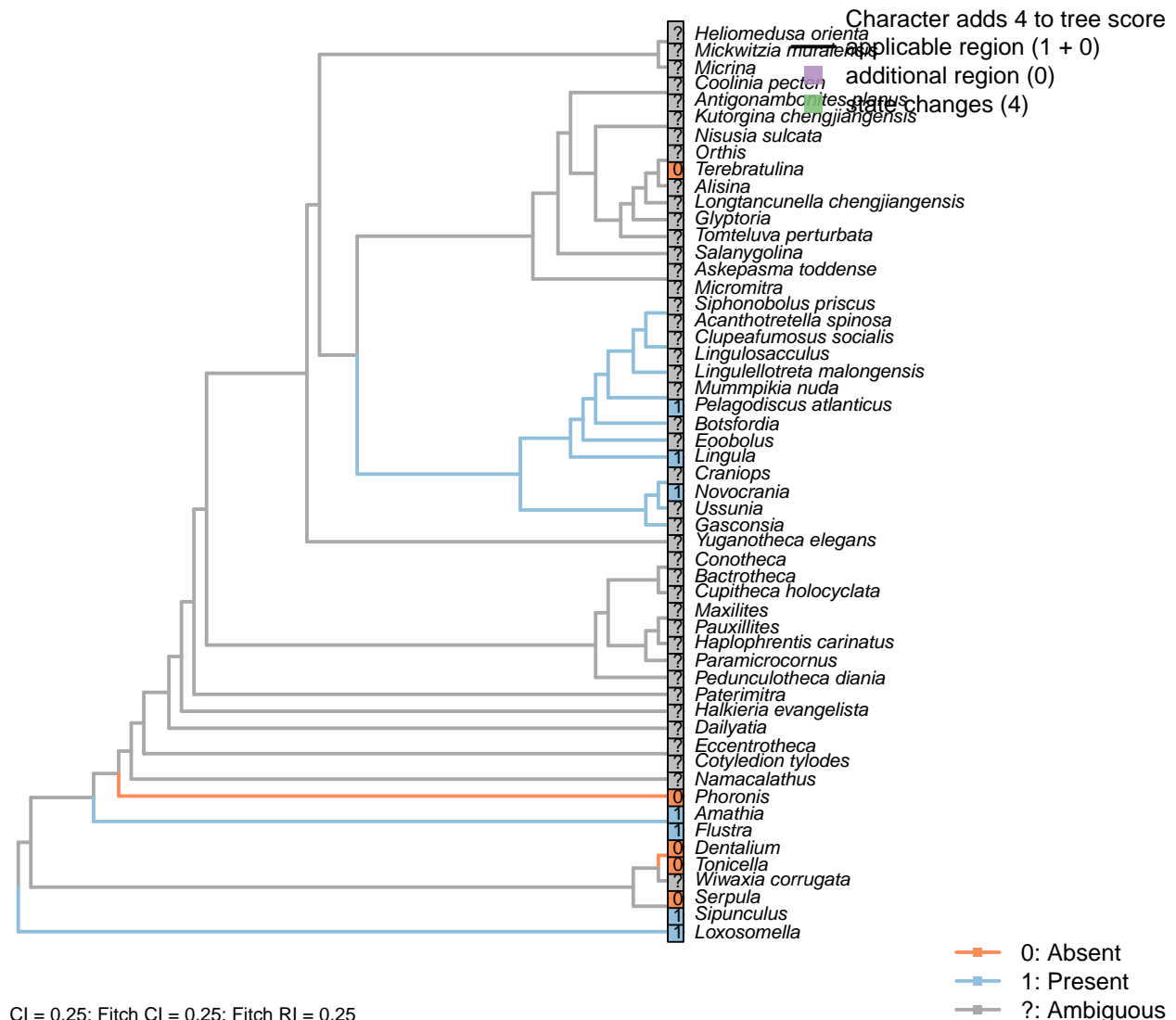
*Dentalium*: Elongate nucleus, 4–6 times longer than wide (Dufresne-Dube et al., 1983).

*Loxosomella*: Elongate in *Loxosoma* (Franzén, 2000).

*Serpula*: Gherardi et al. (2011).

*Tonicella*: Profoundly elongated nucleus (Buckland-Nicks et al., 1988).

## [151] Anterior nuclear fossa



## Character 151: Gametes: Spermatozoa: Anterior nuclear fossa

0: Absent

1: Present

Neomorphic character.

Following Smith (2012a), after character 160 in Giribet and Wheeler (2002). A fossa (latin: ditch) is a dent

or impression.

*Flustra, Amathia*: Present (in *Tubulipora*; Franzén, 1984).

*Dentalium*: Dufresne-Dube et al. (1983).

*Loxosomella*: Present in *Loxosoma* (Franzén, 2000).

*Pelagodiscus atlanticus*: Present in *Discinisca tenuis* (Hodgson and Reunov, 1994).

*Phoronis*: Nucleus “almost round” (Reunov and Klepal, 2004).

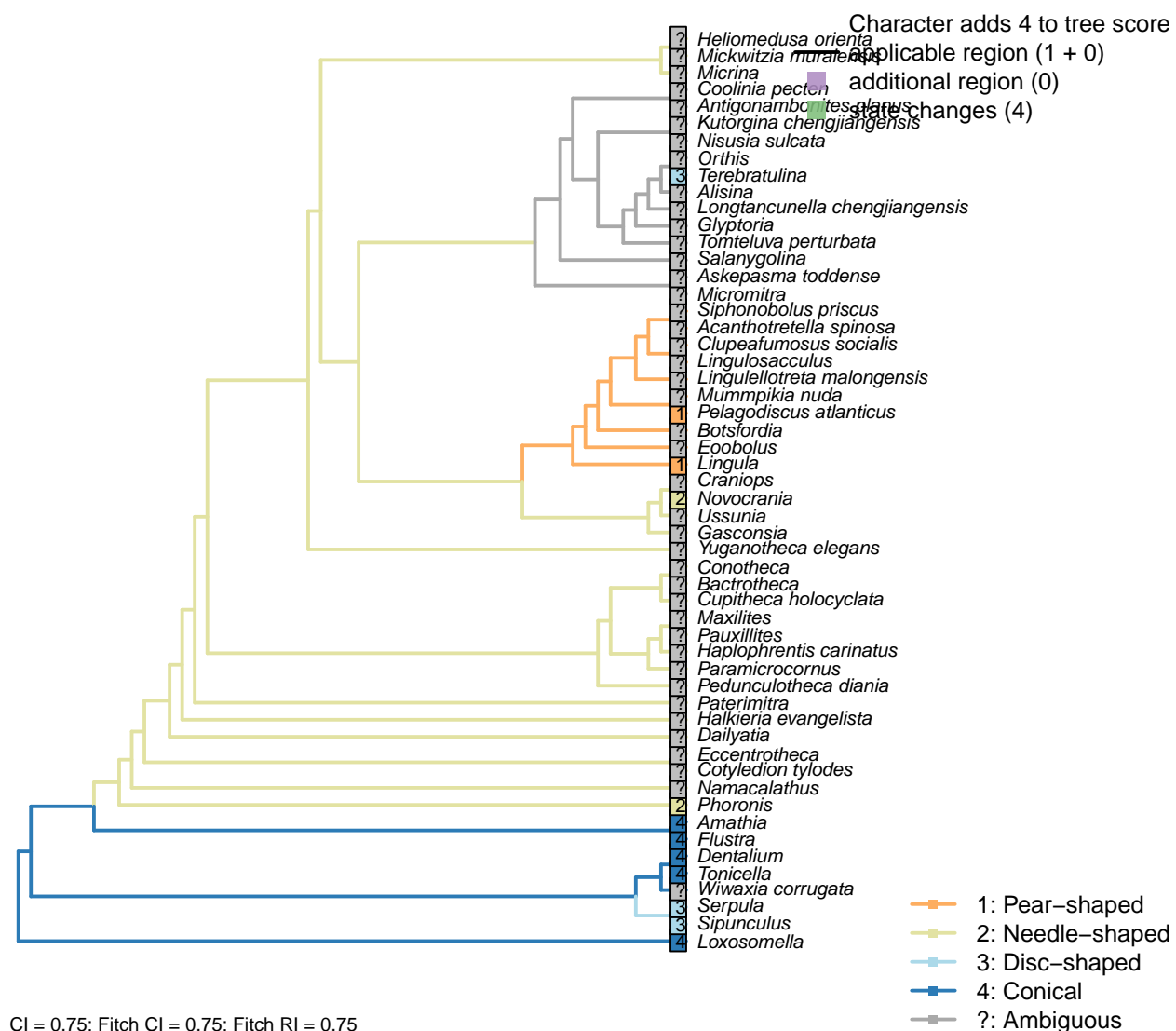
*Serpula*: Absent: subacrosomal space does not impinge on nuclear envelope (Gherardi et al., 2011).

*Sipunculus*: Prominent in *Phascolion* (Rice, 1993).

*Terebratulina*: No anterior invagination (Hodgson and Reunov, 1994).

*Tonicella*: Buckland-Nicks et al. (1988).

## [152] Acrosome: Shape



**Character 152: Gametes: Spermatozoa: Acrosome: Shape**

- 1: Pear-shaped
- 2: Needle-shaped
- 3: Disc-shaped
- 4: Conical

Transformational character.

*Flustra, Amathia*: Conical (in *Tubulipora*; Franzén, 1984).

*Dentalium*: Low conical aspect (Dufresne-Dube et al., 1983).

*Lingula*: Pear-shaped (Fukumoto, 2003).

*Loxosomella*: Conical/cylindrical acrosome-like extension in *Loxosoma* (Franzén, 2000).

*Novocrania*: Needle-shaped (Afzelius and Ferraguti, 1978).

*Pelagodiscus atlanticus*: Pear-shaped (Hodgson and Reunov, 1994).

*Phoronis*: Needle-shaped (Reunov and Klepal, 2004).

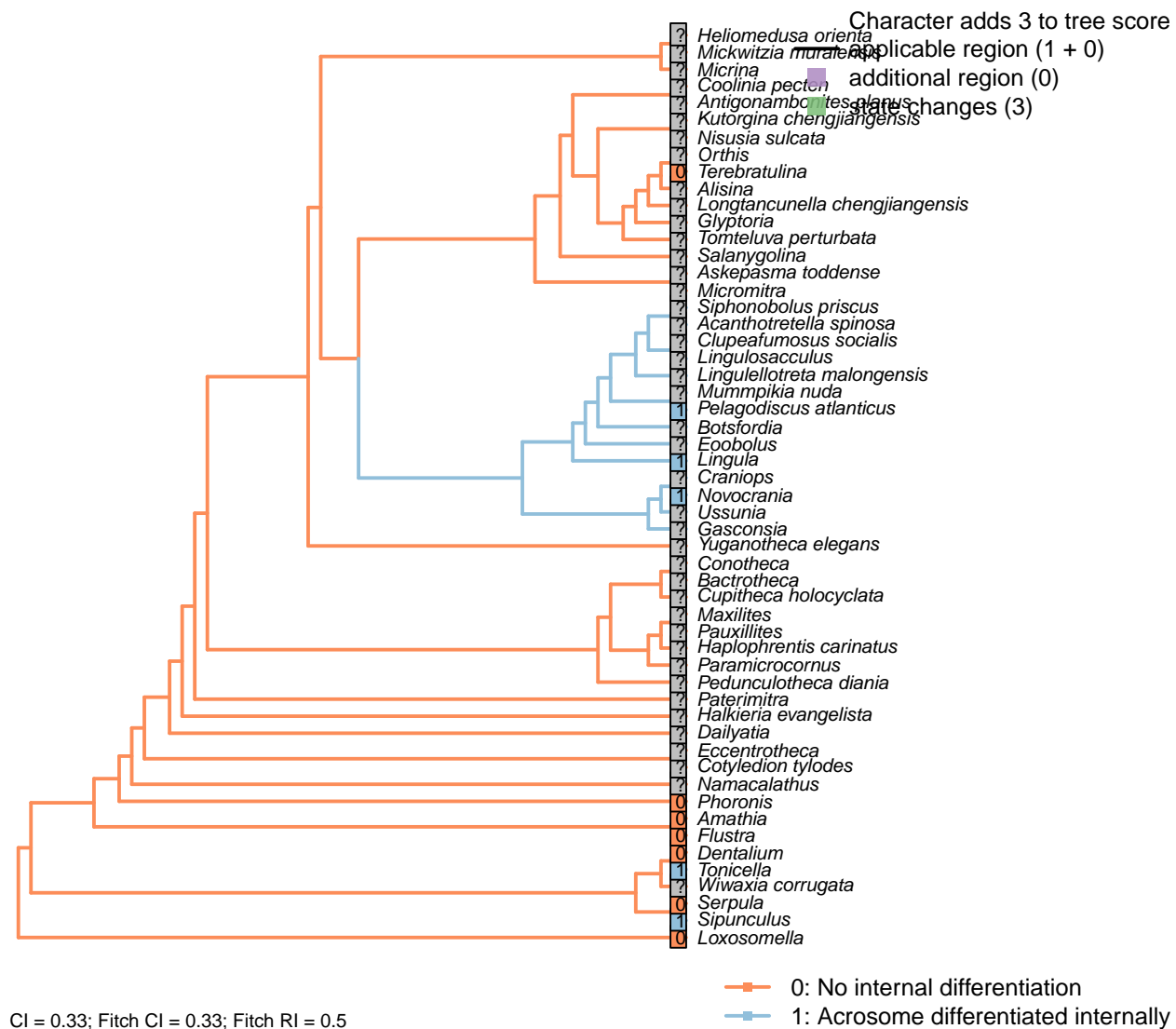
*Serpula*: Gherardi et al. (2011).

*Sipunculus*: A peaked disc in *Phascolion* (Rice, 1993).

*Terebratulina*: Disc-shaped (in *Kraussina*) (Hodgson and Reunov, 1994).

*Tonicella*: Elongate: cylindrical to conical (Buckland-Nicks et al., 1988).

## [153] Acrosome: Differentiated internally

**Character 153: Gametes: Spermatozoa: Acrosome: Differentiated internally**

0: No internal differentiation

1: Acrosome differentiated internally

Neomorphic character.

Hodgson and Reunov (1994) describe the *Discinisca* acrosome as having “an electron-lucent centre and an electron-dense outer region”, and state that this trait is characteristic of inarticulate brachiopods.

*Flustra, Amathia*: No evidence of internal differentiation (in *Tubulipora*; Franzén, 1984).

*Dentalium*: Differentiated membrane only (Dufresne-Dube et al., 1983).

*Lingula*: Clear differentiation of marginal area (Fukumoto, 2003).

*Loxosomella*: Not evident in *Loxosoma* (Franzén, 2000).

*Novocrania*: “Along the inner and outer margins there are periodically banded layers, and between them

there is a less dense layer" – Afzelius and Ferraguti (1978).

*Pelagodiscus atlanticus*: Following *Discinisca tenuis*, described in Hodgson & Reunov (1994).

*Phoronis*: Acrosome-like structure; no internal division or surrounding membrane, with possibility that much of the acrosome is secondarily lost (Reunov and Klepal, 2004).

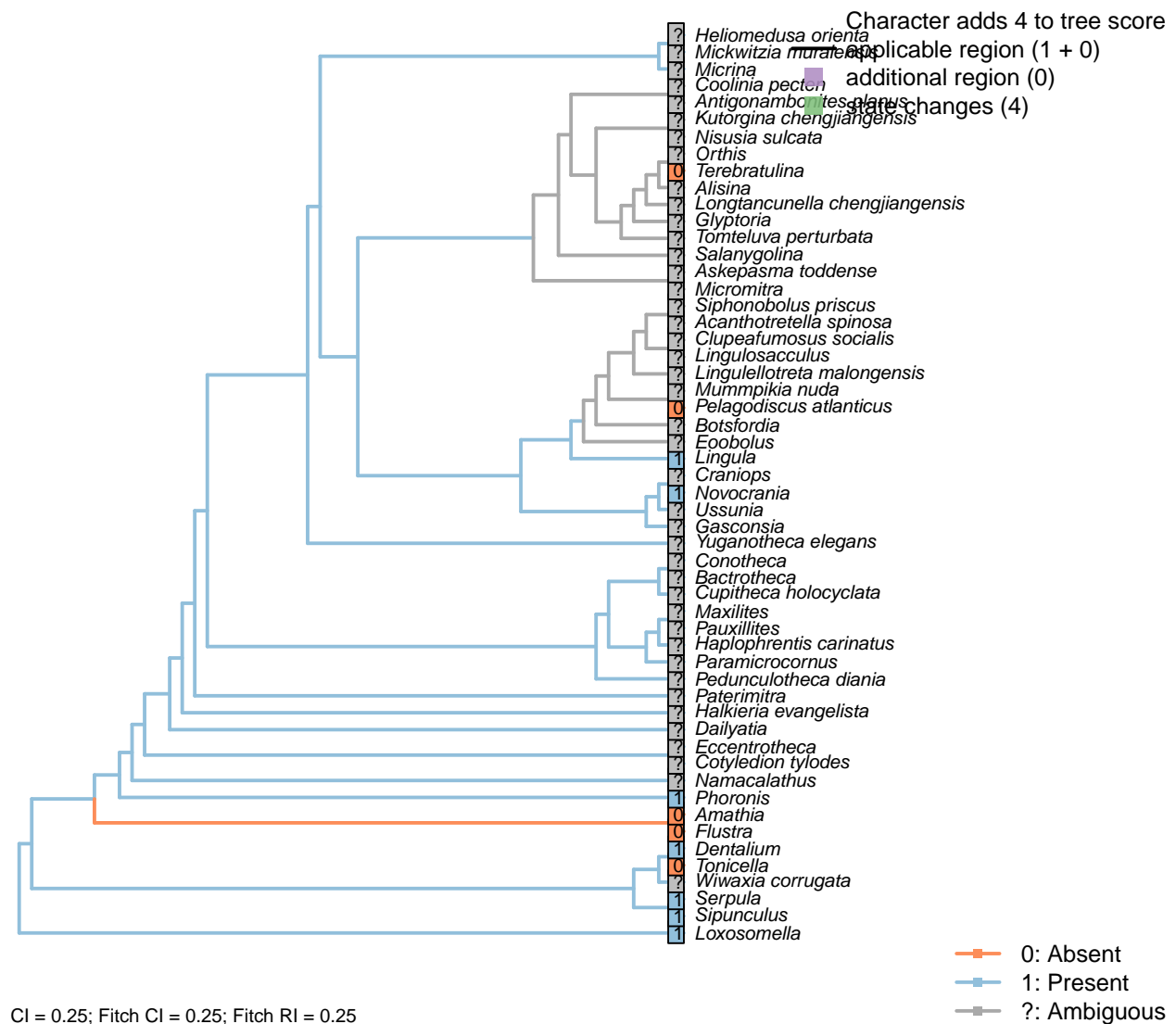
*Serpula*: Gherardi et al. (2011).

*Sipunculus*: No differentiation within acrosomal vesicle (Rice, 1993).

*Terebratulina*: Following Hodgson & Reunov (1994).

*Tonicella*: "One can distinguish two components in the acrosome, an apical and a basal granule" – Buckland-Nicks et al. (1988).

## [154] Acrosome: Sub-acrosomal space



0: Absent

1: Present

Neomorphic character.

*Flustra, Amathia*: No distinct space (in *Tubulipora*; Franzén, 1984).

*Dentalium*: Dufresne-Dube et al. (1983).

*Lingula*: Filled with sub-acrosomal substance (Fukumoto, 2003).

*Loxosomella*: Present in *Loxosoma* (Franzén, 2000).

*Novocrania*: Prominent (Afzelius and Ferraguti, 1978).

*Pelagodiscus atlanticus*: Subacrosomal material (in *Discinisca*) but no subacrosomal space (Hodgson and Reunov, 1994).

*Phoronis*: The filament-like acrosome continues backwards as a tube-like structure (Franzén and Ahlfors, 1980, summarized in Jamieson (1991)).

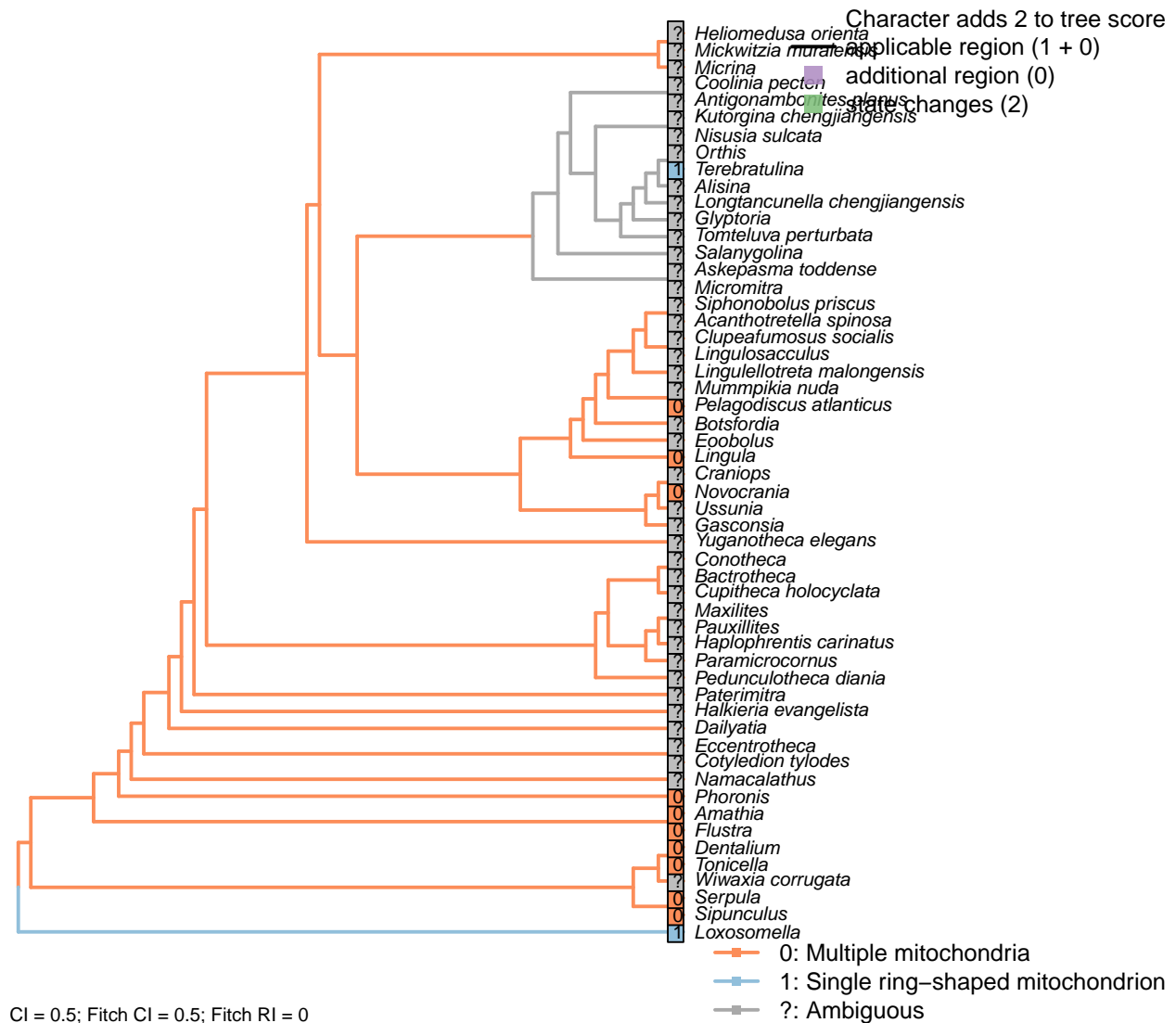
*Serpula*: Gherardi et al. (2011).

*Sipunculus*: Rice (1993).

*Terebratulina*: No subacrosomal material, let alone a subacrosomal space (e.g. Hodgson and Reunov, 1994).

*Tonicella*: Not evident (Buckland-Nicks et al., 1988).

## [155] Mid-piece

**Character 155: Gametes: Spermatozoa: Mid-piece**

- 0: Multiple mitochondria
- 1: Single ring-shaped mitochondrion
- Neomorphic character.

Following Hodgson & Reunov (1994).

*Flustra, Amathia*: Two mitochondrial derivatives in *Flustra* (Franzén, 1981, 1977); four in *Tubulipora* (Franzén, 1984).

*Dentalium*: Dufresne-Dube et al. (1983).

*Lingula, Terebratulina*: Following Hodgson & Reunov (1994).

*Loxosomella*: “The midpiece consists of two long mitochondrial rods connected with each other by a thin mitochondrial lamella” (Franzén, 2000, in *Loxosoma*); these are essentially a single organelle surrounding a

central rod of electron-dense material.

*Novocrania*: Four mitochondria (Afzelius and Ferraguti, 1978).

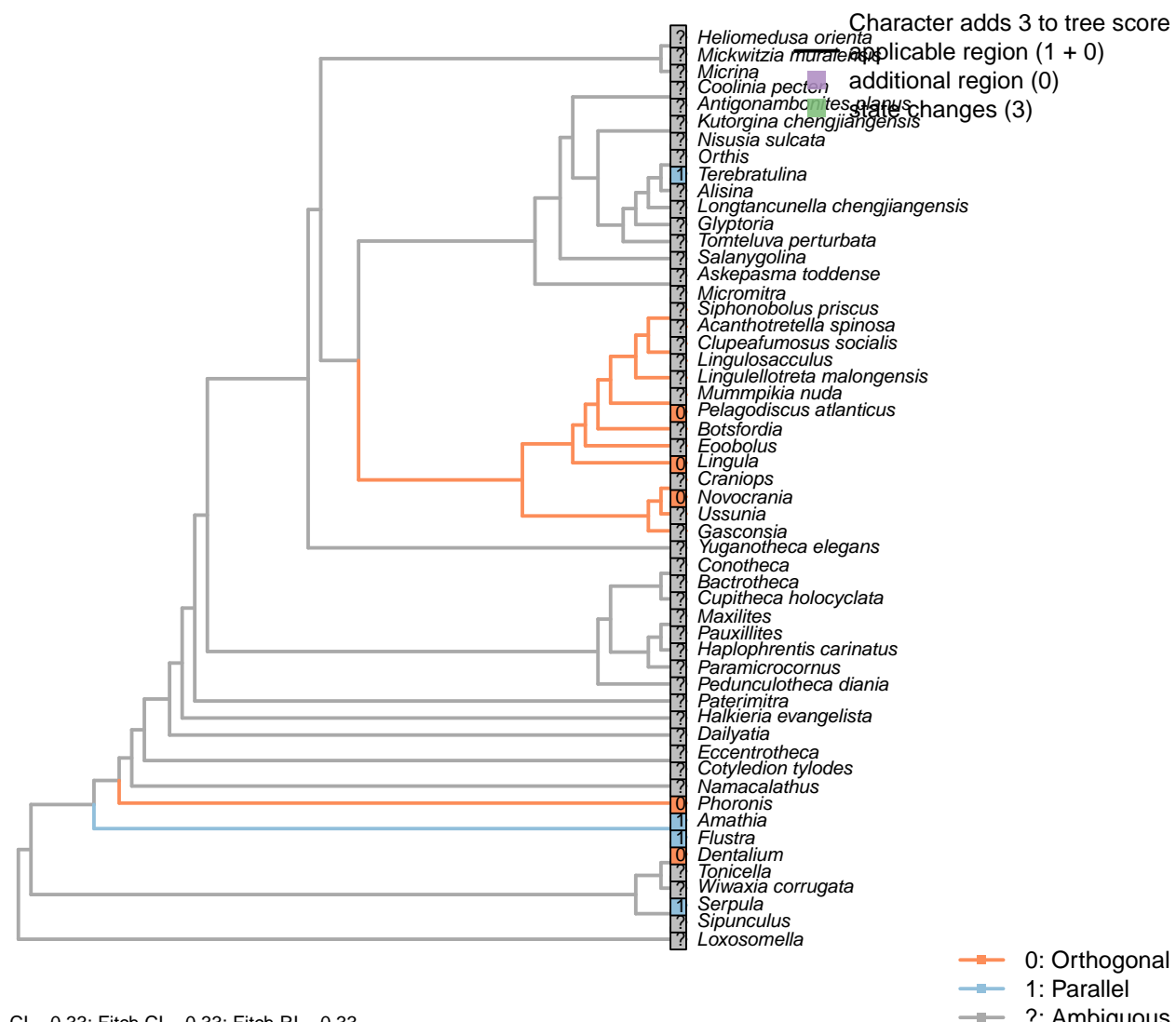
*Pelagodiscus atlanticus*: Following *Discinisca tenuis*, described in Hodgson & Reunov (1994).

*Phoronis*: The mitochondria fuse in the middle stage of spermiogenesis to become a pair of mitochondria (Reunov and Klepal, 2004).

*Serpula*: Five mitochondria in ring (Gherardi et al., 2011).

*Sipunculus*: Ring of five mitochondria around the central centriole (Rice, 1993).

## [156] Centrioles: Orientation



CI = 0.33; Fitch CI = 0.33; Fitch RI = 0.33

### Character 156: Gametes: Spermatozoa: Centrioles: Orientation

0: Orthogonal

1: Parallel

Neomorphic character.

Following Hodgson and Reunov (1994).

*Flustra, Amathia*: (Franzén, 1981).

*Dentalium*: Dufresne-Dube et al. (1983).

*Lingula, Terebratulina*: Following Hodgson & Reunov (1994).

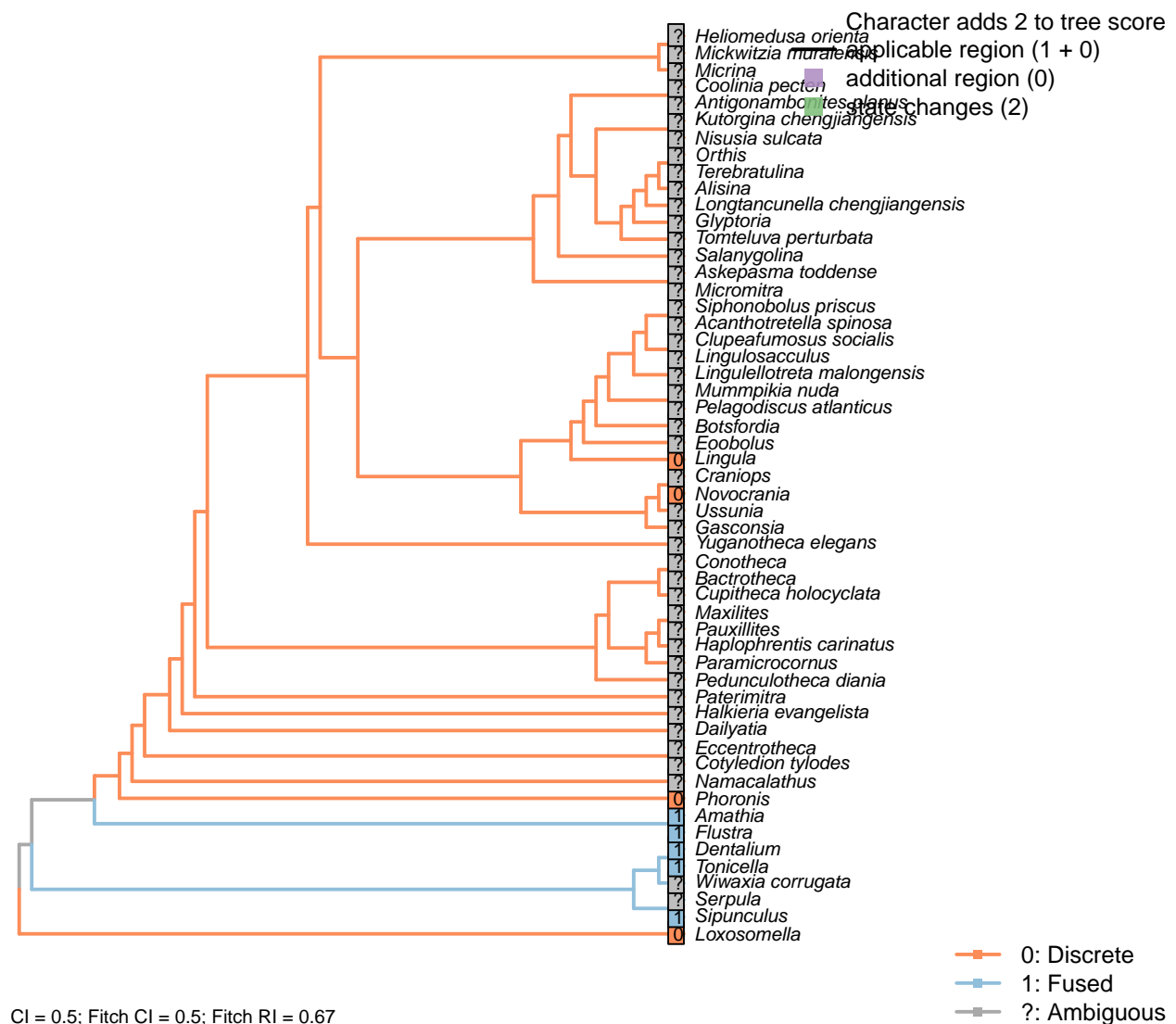
*Novocrania*: Two orthogonal centrioles (Afzelius and Ferraguti, 1978).

*Pelagodiscus atlanticus*: Following *Discinisca tenuis*, described in Hodgson & Reunov (1994).

*Phoronis*: Only one centriole in spermatzoon (Reunov and Klepal, 2004, p. 7), but centrioles are perpendicularly oriented in spermatogonia (*ibid.*, p. 2).

*Serpula*: The proximal centriole is parallel to the flagellum (Gherardi et al., 2011).

## [157] Centrioles: Fusion



Character 157: Gametes: Spermatozoa: Centrioles: Fusion

- 0: Discrete  
 1: Fused  
 Neomorphic character.

Following Smith (2012a); see Buckland-Nicks (2008).

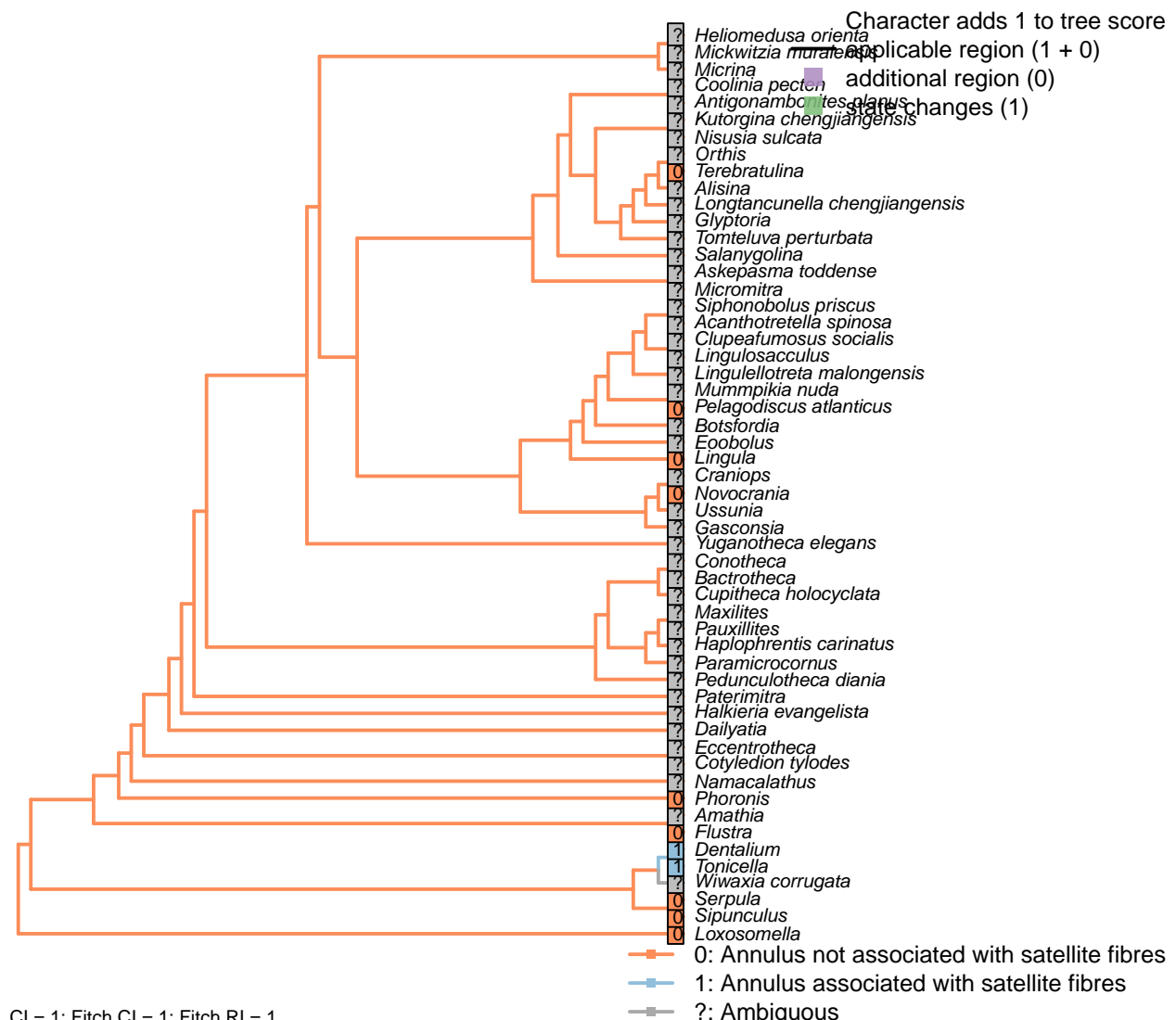
*Flustra, Amathia, Sipunculus*: Proximal centriole fused anterior to distal centriole.

*Dentalium*: Proximal centriole fused anterior to distal centriole (Dufresne-Dube et al., 1983).

*Loxosomella, Novocrania, Lingula, Phoronis*: Basal body in deep nuclear fossa.

*Tonicella*: Proximal centriole fused lateral to distal centriole and offset.

## [158] Satellite fibre complex



### Character 158: Gametes: Spermatozoa: Satellite fibre complex

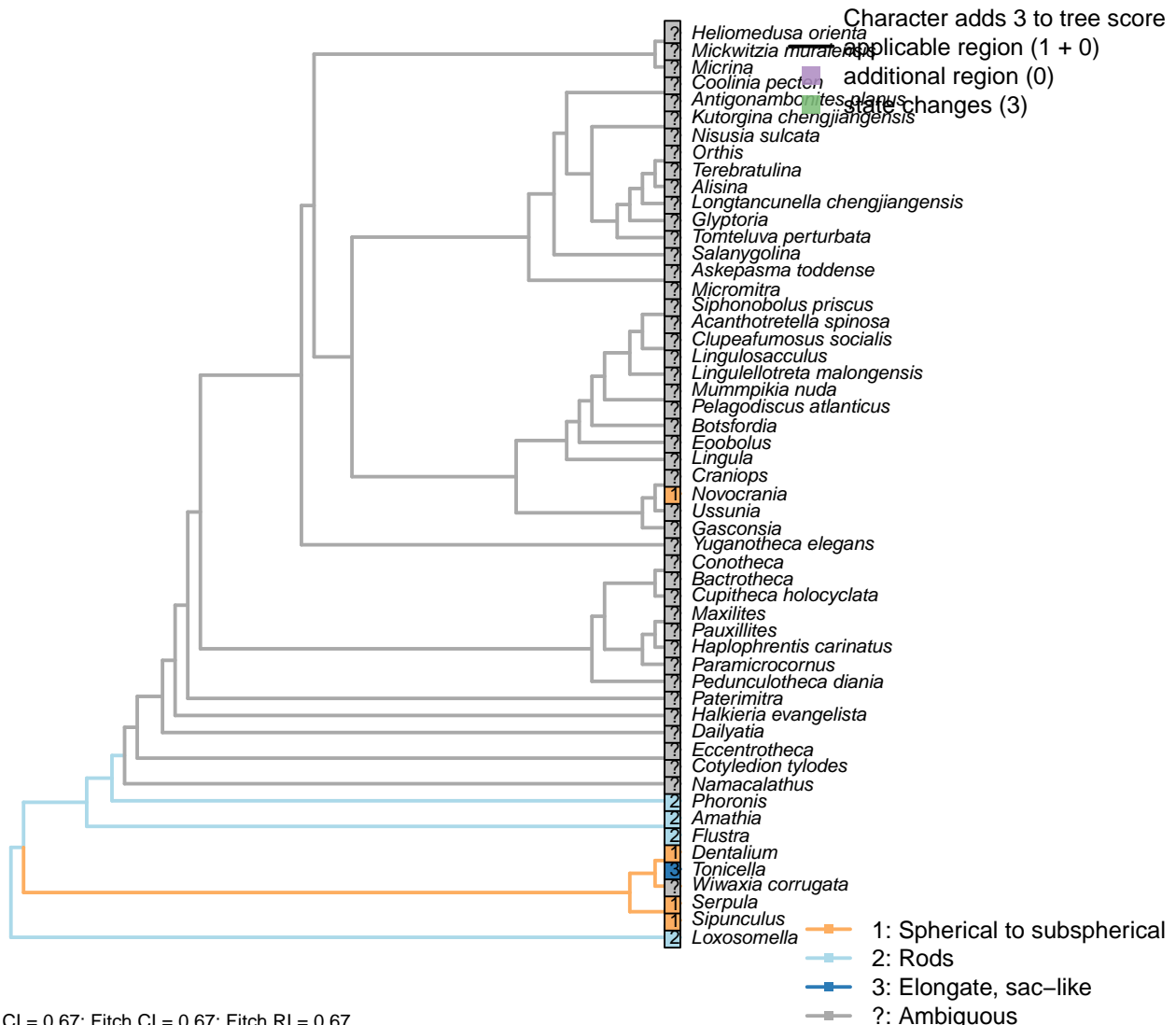
- 0: Annulus not associated with satellite fibres

- 1: Annulus associated with satellite fibres

- Neomorphic character.

Following Smith (2012a), after character 48 in Ponder and Lindberg (1997).

### [159] Mitochondria: Shape



#### Character 159: Gametes: Spermatozoa: Mitochondria: Shape

1: Spherical to subspherical

2: Rods

3: Elongate, sac-like

Transformational character.

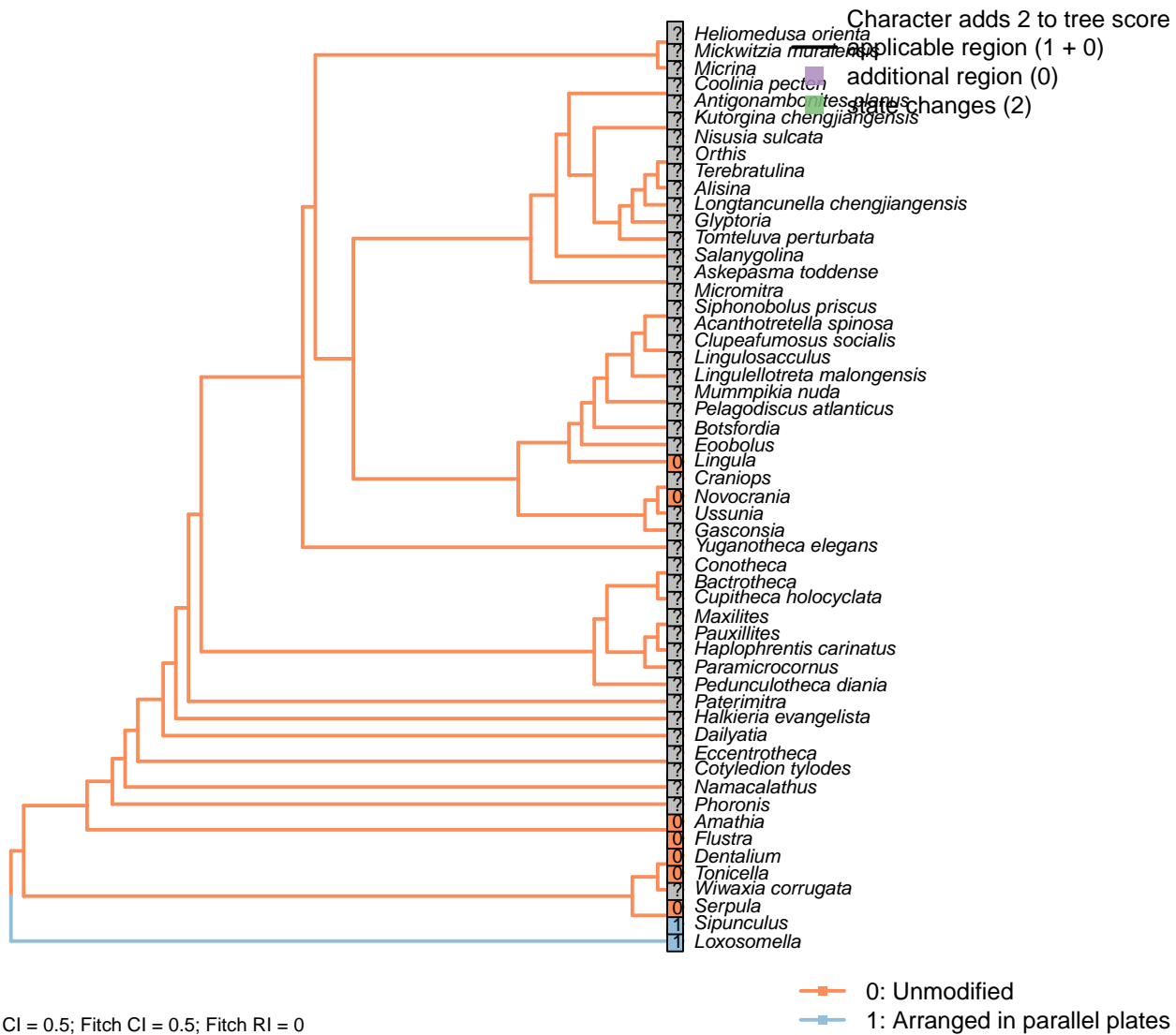
After character 5 in Buckland-Nicks (2008); see also character 43 in Ponder and Lindberg (1997).

*Flustra, Amathia*: Rods (Franzén, 1981).

*Loxosomella*: Elongate rods in *Loxosoma* (Franzén, 2000).

*Tonicella*: See Buckland-Nicks et al. (1988).

## [160] Mitochondria: Cristae: Configuration

**Character 160: Gametes: Spermatozoa: Mitochondria: Cristae: Configuration**

0: Unmodified

1: Arranged in parallel plates

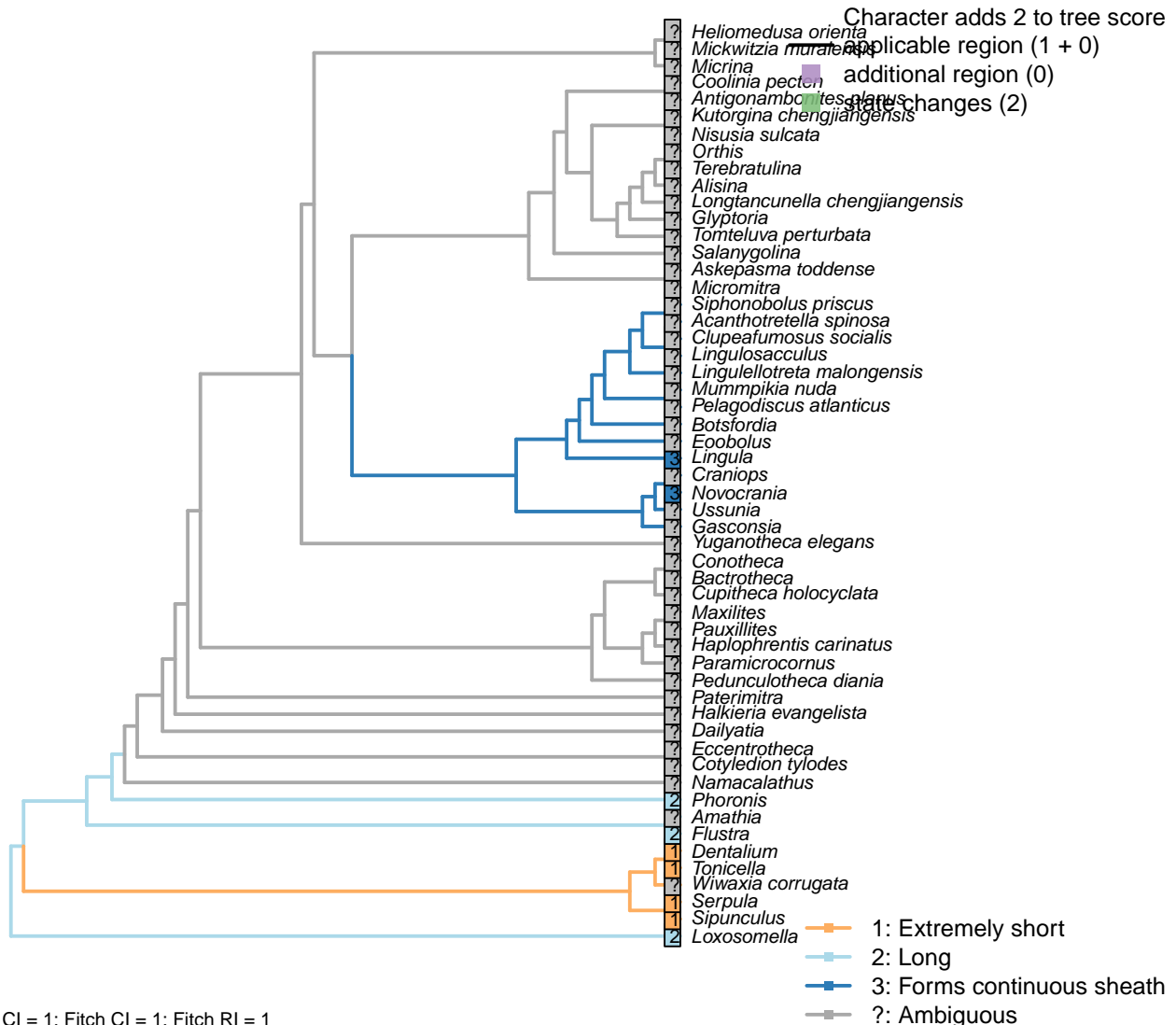
Neomorphic character.

After character 44 in Ponder and Lindberg (1997). Cristae are internal compartments formed by inner mitochondrial membranes.

*Flustra, Amathia*: “Typical cristae”; “Randomly oriented” – Franzén (1984) (in *Tubulipora*).

*Loxosomella*: in *Loxosoma* (Franzén, 2000).

### [161] Mitochondria: Midpiece



#### Character 161: Gametes: Spermatozoa: Mitochondria: Midpiece

- 1: Extremely short
  - 2: Long
  - 3: Forms continuous sheath
- Transformational character.

After Smith (2012a); see also character 43 in Ponder and Lindberg (1997); character 164 in Giribet and Wheeler (2002).

*Flustra, Amathia*: Long (Franzén, 1981).

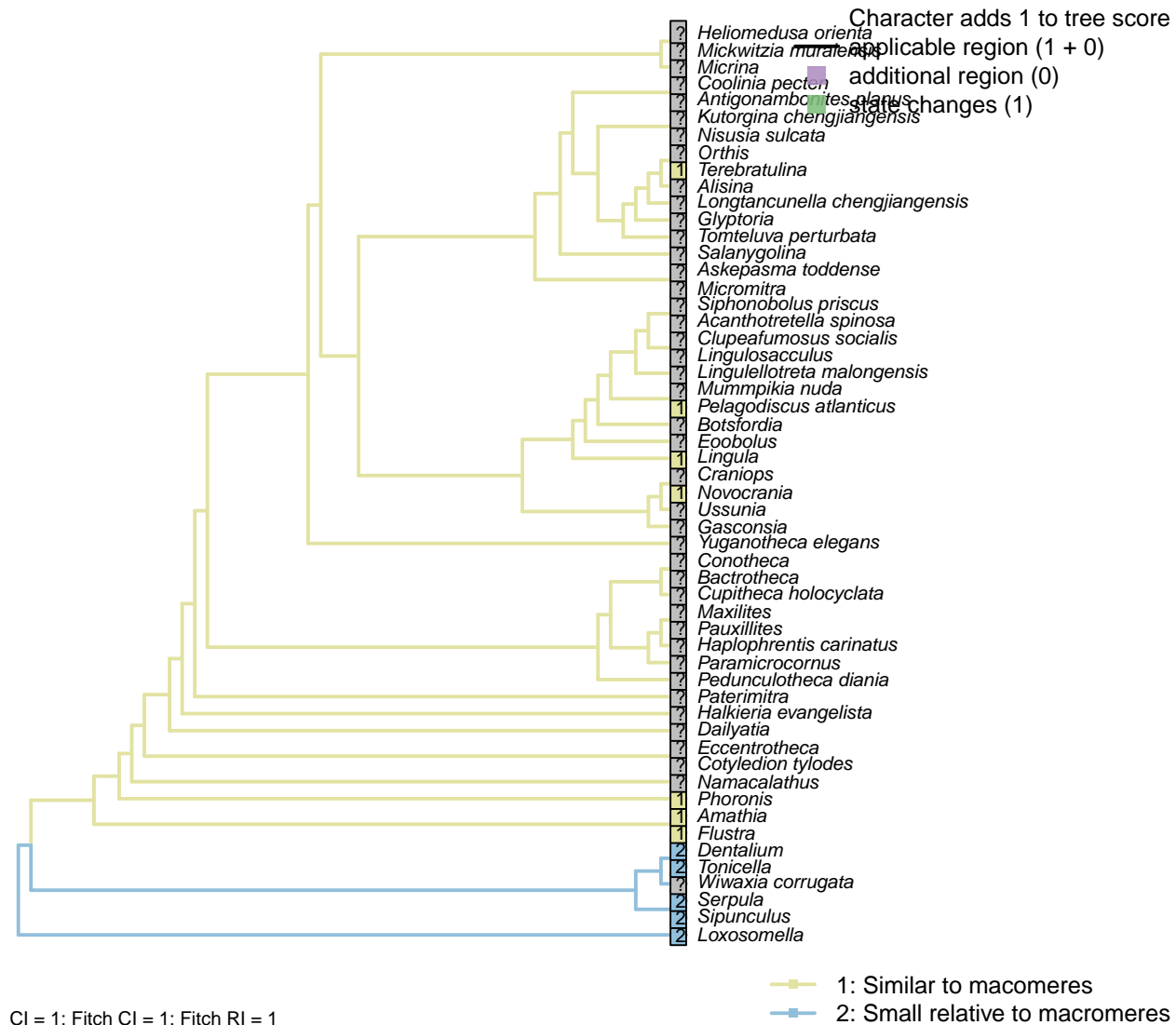
*Loxosomella*: As long as the flagellum in *Loxosoma* (Franzén, 2000).

*Serpula*: Five mitochondria surround the base of the flagellum in short midpiece, comparable to that of *Sipunculus* and *Dentalium* (Gherardi et al., 2011).

*Sipunculus*: Short ring of five mitochondria around the central centriole (Rice, 1993).

## 5.20 Embryo

### [162] Micromere size



#### Character 162: Embryo: Micromere size

- 1: Similar to macromeres
- 2: Small relative to macromeres
- Transformational character.

Following Hejnol (2010). Blastomeres may undergo significant size differentiation, generating macromeres and micromeres of prominently different sizes.

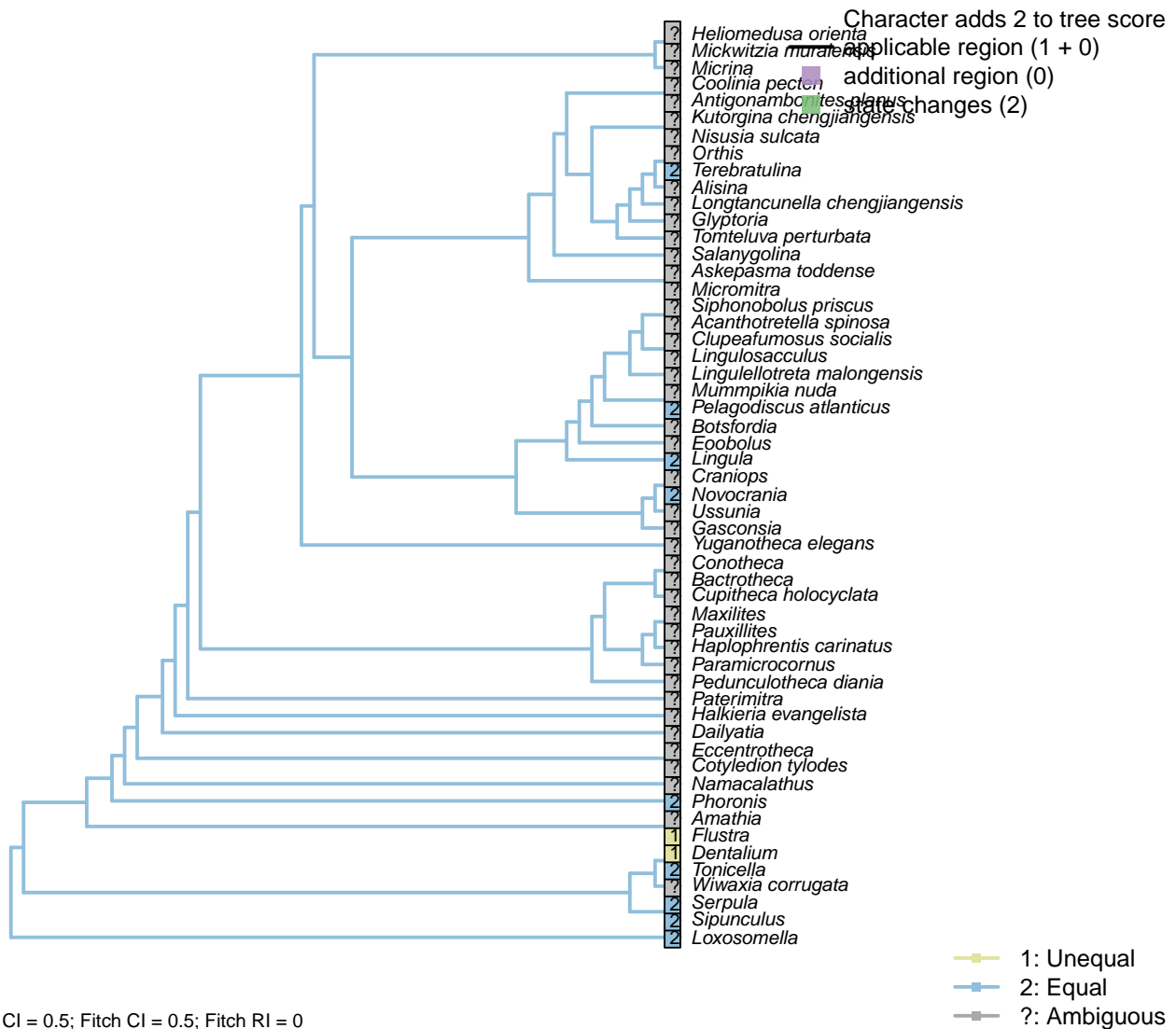
*Flustra, Amathia*: In *Membranipora*, “cleavage is slightly unequal resulting in little larger central blastomeres” (Gruhl, 2010b).

*Lingula, Terebratulina*: Williams et al. (1997).

*Phoronis*: Uniform size (Pennerstorfer and Scholtz, 2012).

*Sipunculus*: Prominent differentiation in *Phascolosoma* (Adrianov et al., 2011).

## [163] Equal

**Character 163: Embryo: Cleavage: Equal**

1: Unequal

2: Equal

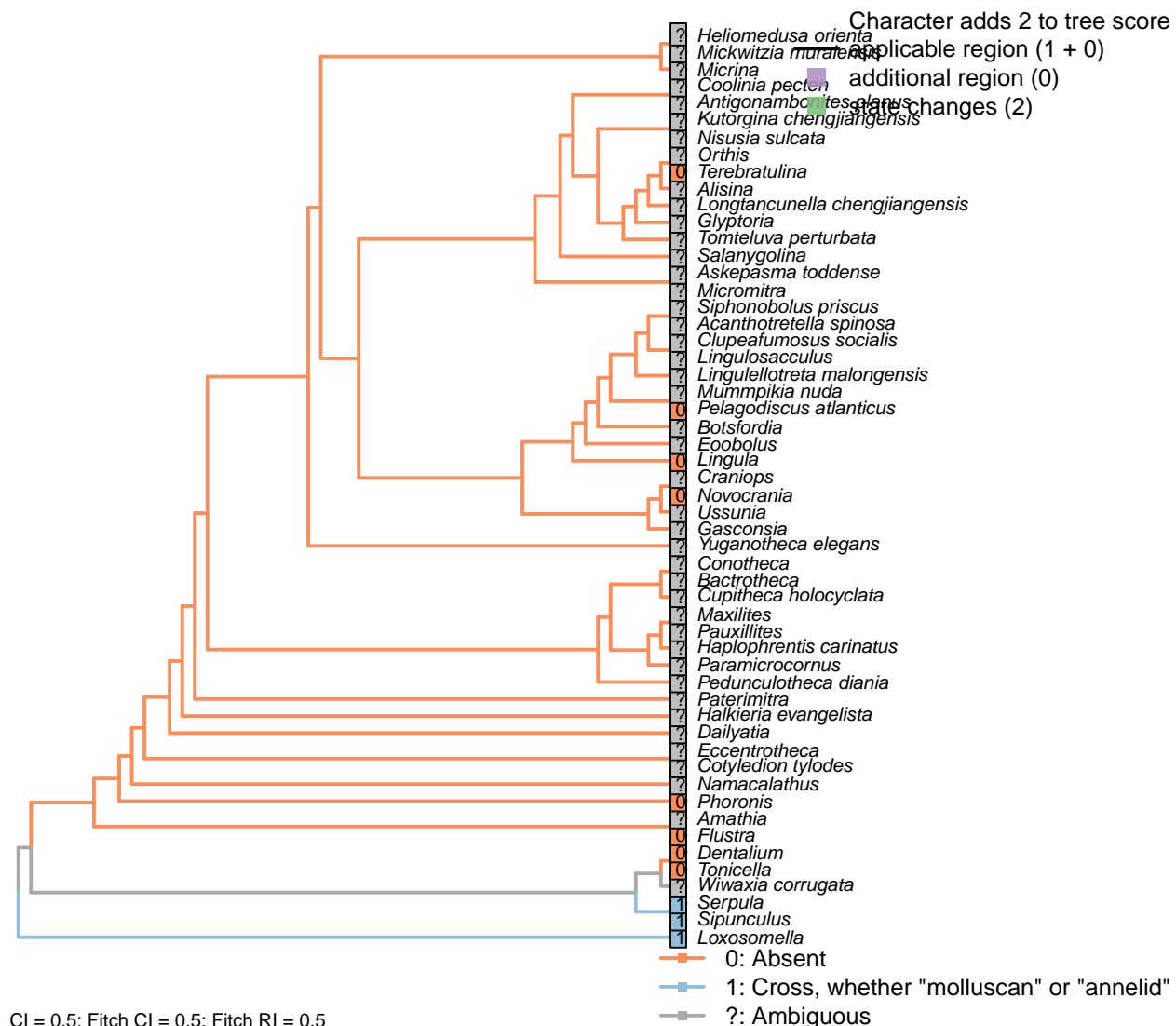
Transformational character.

Following character 170 in Giribet and Wheeler (2002).

*Novocrania*, *Pelagodiscus atlanticus*, *Lingula*, *Terebratulina*: Equal, in all brachiopods (Williams et al., 1997).

*Phoronis*: “Cleavage is holoblastic and results in approximately equal sized, or adequate, blastomeres.” – Pennerstorfer and Scholtz (2012).

## [164] Cross pattern

**Character 164: Embryo: Cleavage: Cross pattern**

0: Absent

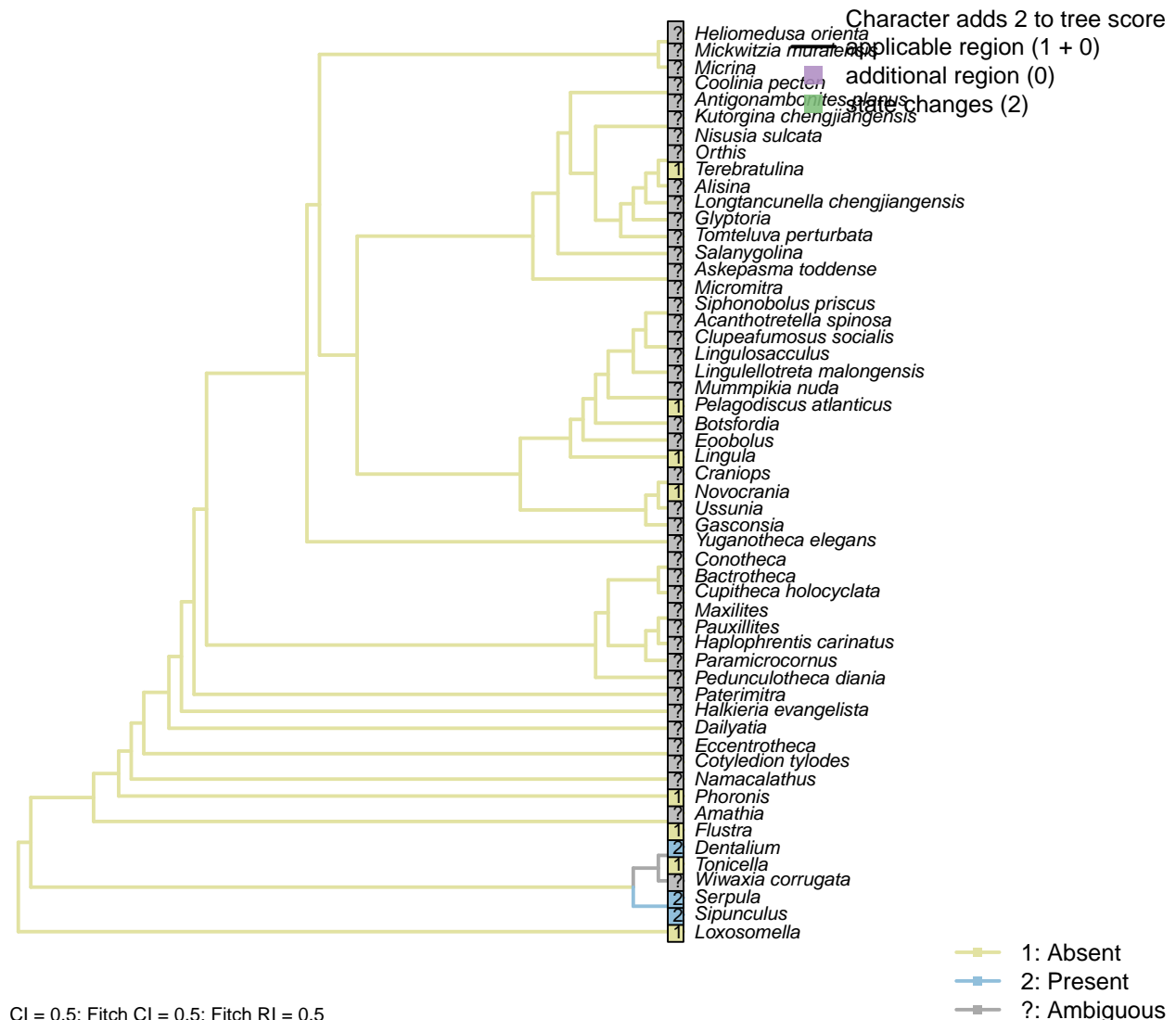
1: Cross, whether "molluscan" or "annelid"

Neomorphic character.

The "molluscan cross" and "annelid cross" cannot be systematically discriminated from one another, so are treated as a single state.

See characters 127 & 128 in Rouse (1999); 1.49 in von Salvini-Plawen and Steiner (1996); character 34 in Haszprunar (1996); 35 in Haszprunar (2000); 172 in Giribet and Wheeler (2002).

## [165] Polar lobe formation



## Character 165: Embryo: Cleavage: Polar lobe formation

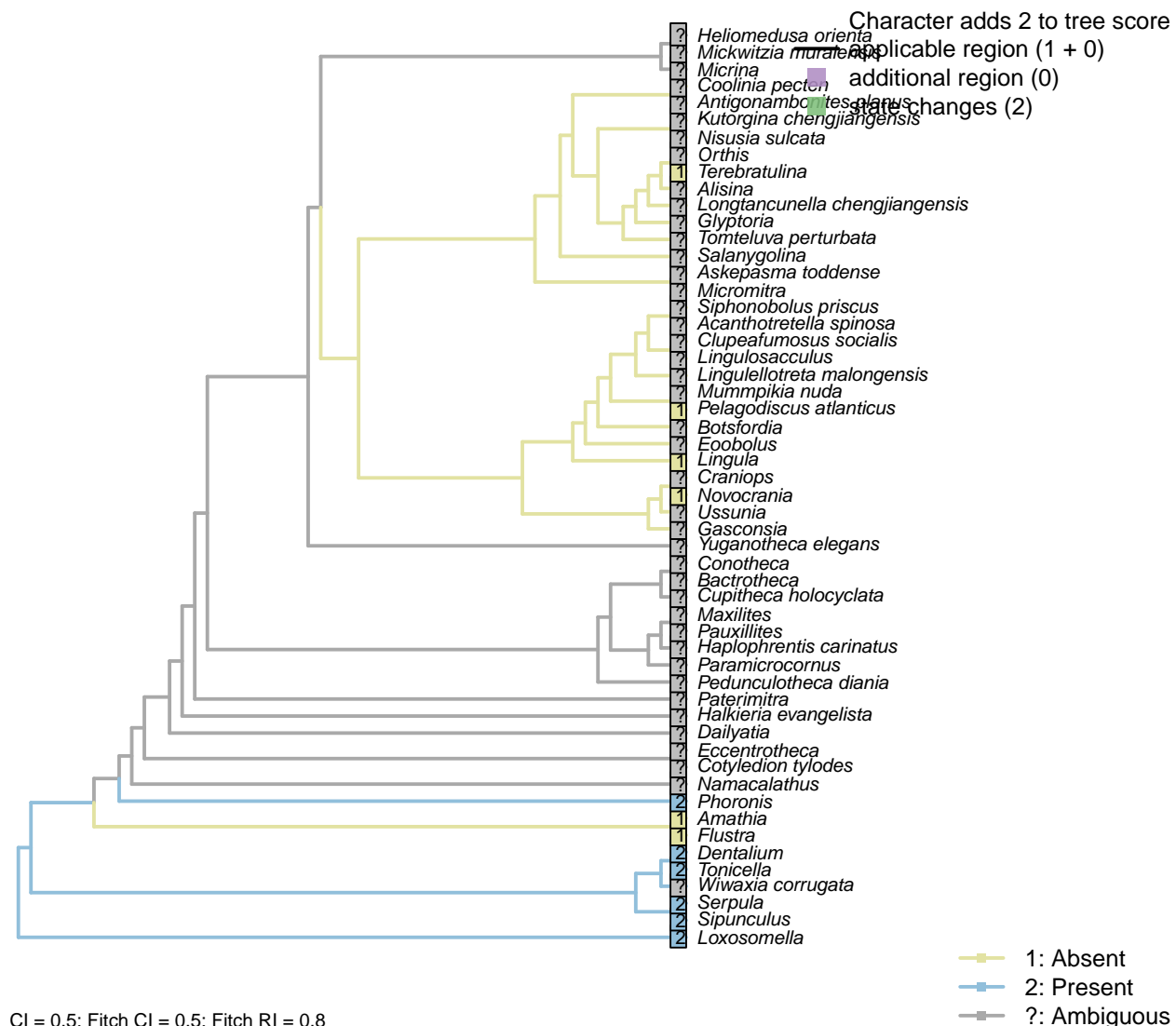
1: Absent

2: Present

Transformational character.

Following character 171 in Giribet and Wheeler (2002).

## [166] Spiral



## Character 166: Embryo: Cleavage: Spiral

1: Absent

2: Present

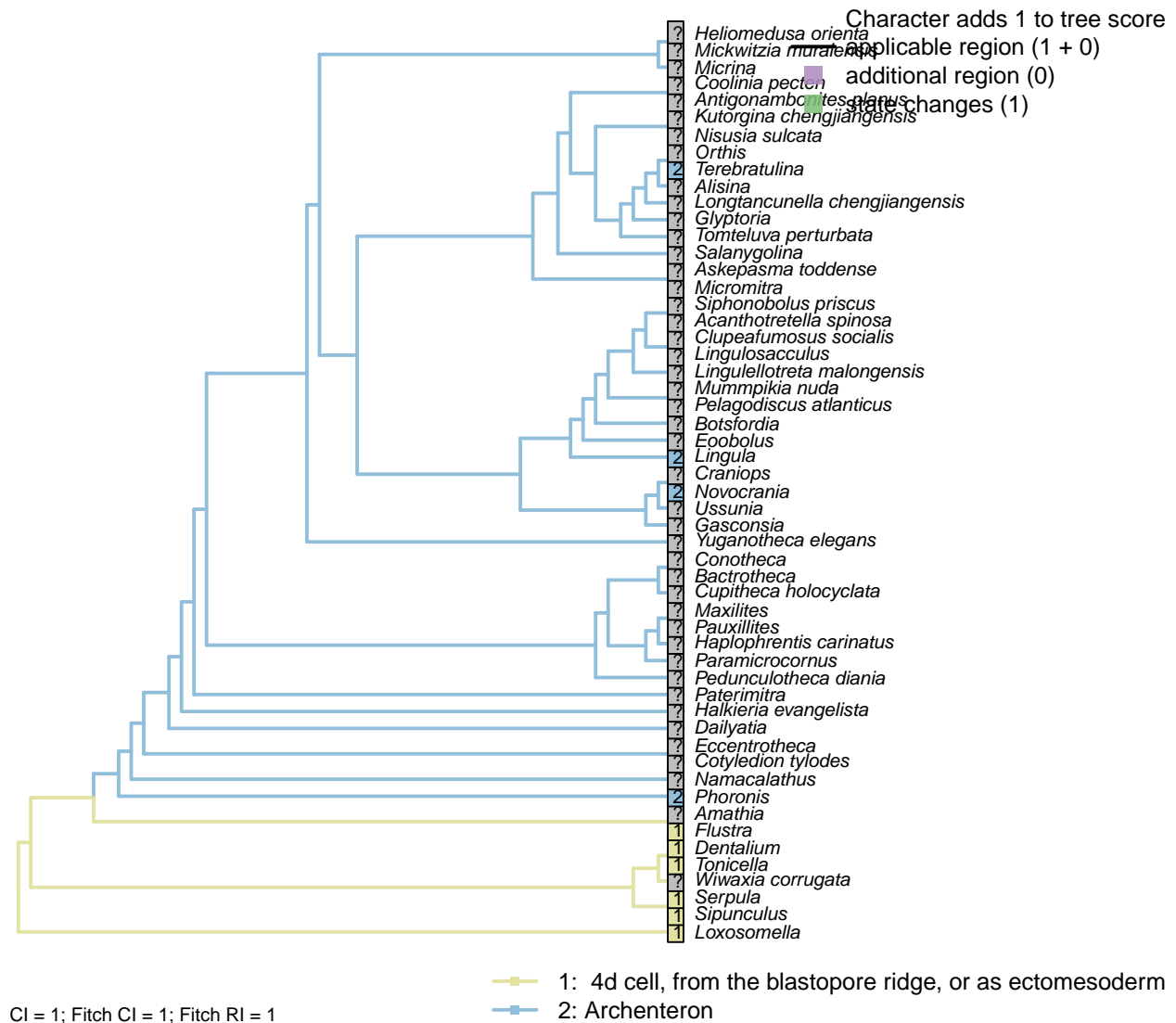
Transformational character.

See characters 32–33 in Haszprunar (1996); character 1.48 in von Salvini-Plawen and Steiner (1996); character 29 in Glenner et al. (2004).

*Flustra, Amathia*: “While entoprocts are spiral cleavers, ectoprocts show a radial cleavage pattern” – Fuchs and Wanninger (2008).

*Phoronis*: “The observed cleavage displays several characters consistent with the pattern of spiral cleavage” (Pennerstorfer and Scholtz, 2012).

### [167] Origin of mesoderm



#### Character 167: Embryo: Origin of mesoderm

1: 4d cell, from the blastopore ridge, or as ectomesoderm

2: Archenteron

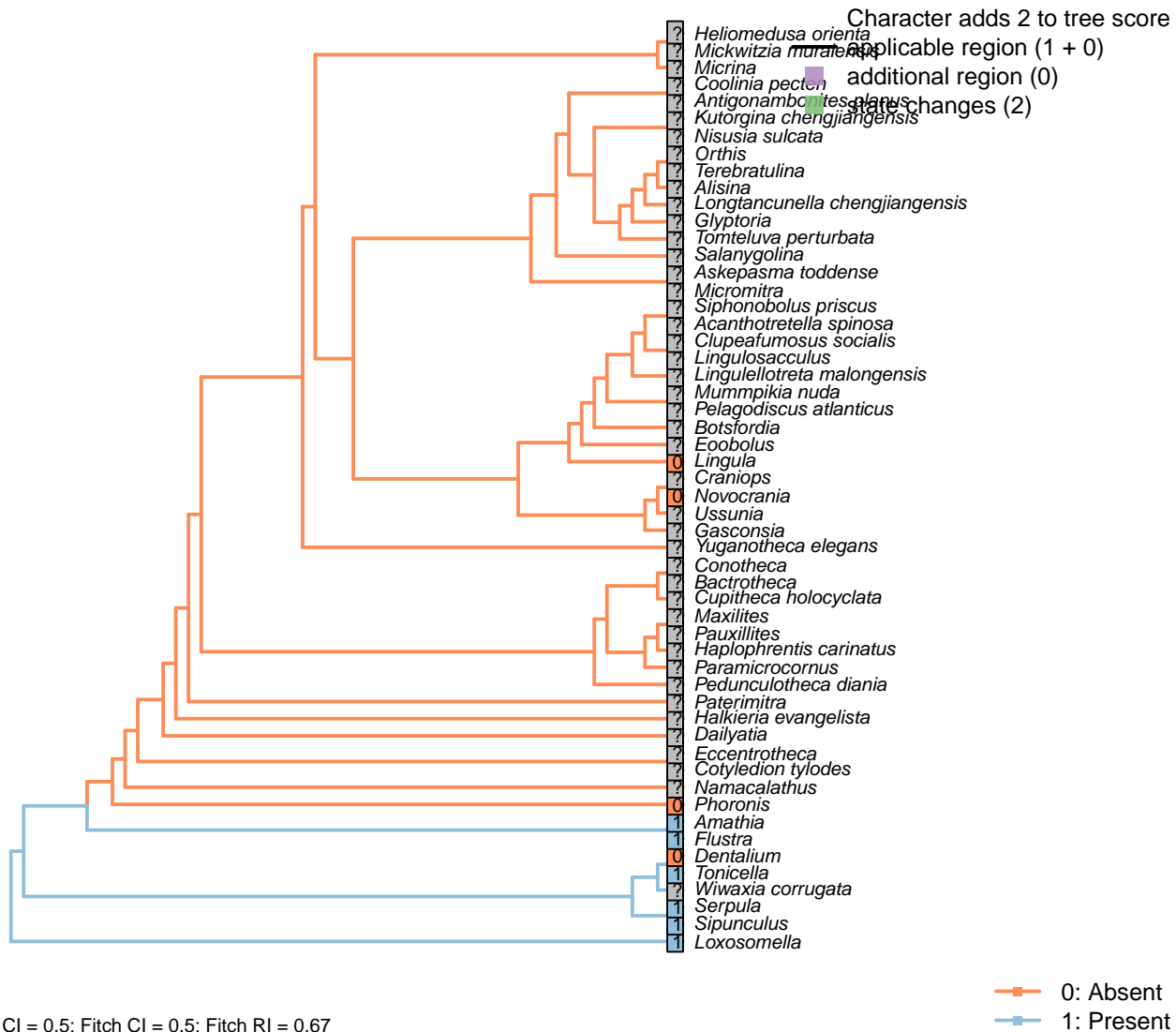
Transformational character.

After characters 32 in Grobe (2007) and 36–37 in Glenner et al. (2004).

*Terebratulina*: Williams et al. (1997).

## 5.21 Larva: Apical organ

### [168] Muscles extending to the hyposphere



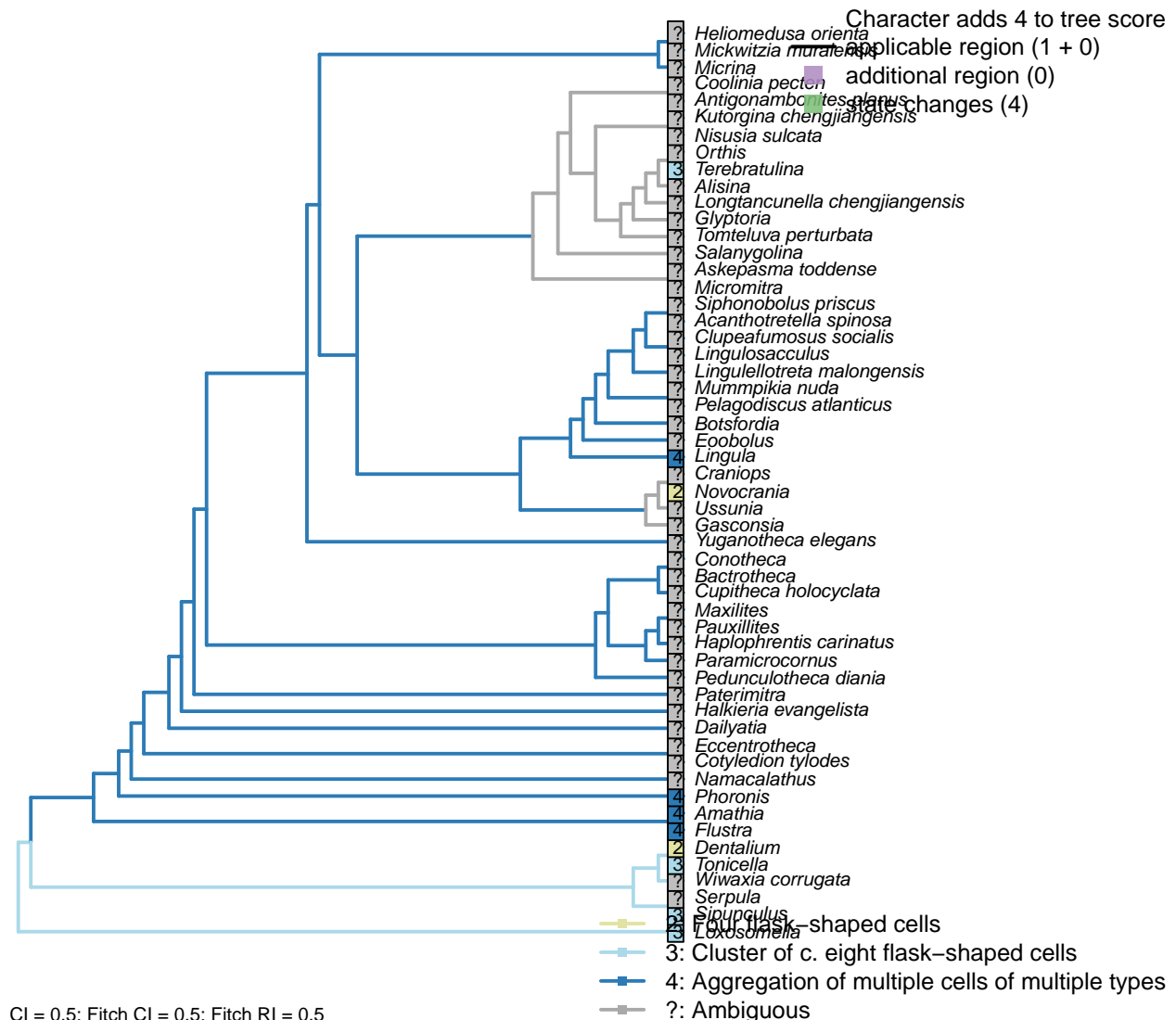
Character 8 in Vinther et al. (2008).

*Flustra, Amathia*: Median muscles extending from apical organ (Gruhl, 2008).

*Dentalium*: Apical organ has disappeared before musculature is set in place (Wanninger and Haszprunar, 2002b).

*Phoronis*: Not evident (Santagata, 2004, fig. 2C).

## [169] Serotonergic cells



### Character 169: Larva: Apical organ: Serotonergic cells

- 1: Two flask-shaped cells
  - 2: Four flask-shaped cells
  - 3: Cluster of c. eight flask-shaped cells
  - 4: Aggregation of multiple cells of multiple types
- Transformational character.

Character 8 in Haszprunar and Wanninger (2008).

*Flustra, Amathia*: Concentration of 30–40 serotonergic perikarya (in *Fredericella*; Gruhl, 2010a).

*Lingula*: Cluster of “numerous” serotonergic cells (Hay-Schmidt, 1992; Altenburger and Wanninger, 2010); more than, but probably equivalent to, the flask-shaped cells of *Terebratula* (Lüter, 2016).

*Loxosomella*: Six to eight apical cells; eight peripheral cells (Wanninger et al., 2007), indicating a probable

equivalence to polyplacophorans (Haszprunar and Wanninger, 2008).

*Novocrania*: Four flask-shaped cells (Altenburger and Wanninger, 2010).

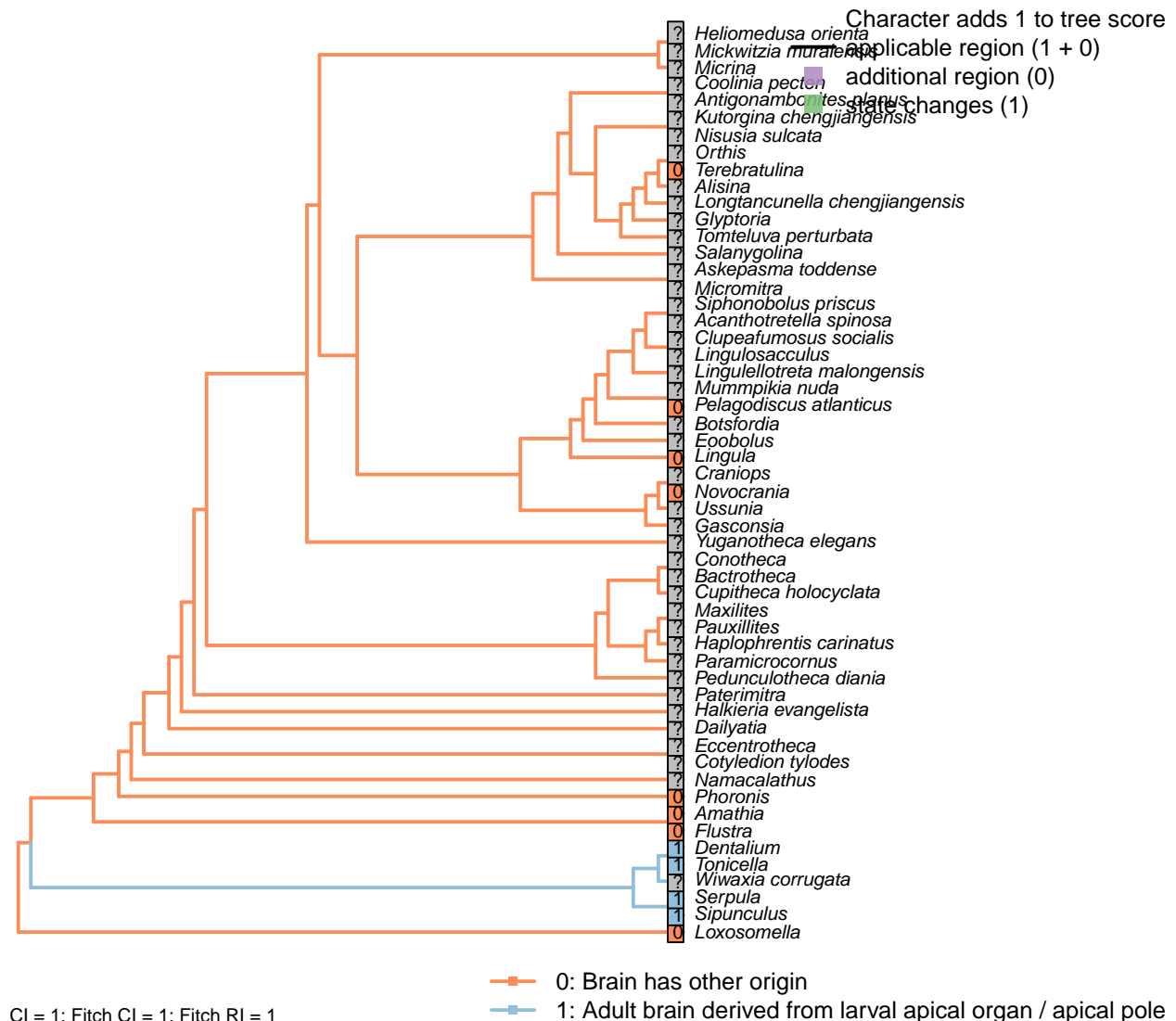
*Phoronis*: Multiple shapes of cells present (Santagata, 2002); resembles the linguliform arrangement (Altenburger and Wanninger, 2010).

*Sipunculus*: Cluster of around eight cells, though not quite countable (Wanninger et al., 2005).

*Terebratulina*: Eight in *Terebratalia* (Lüter, 2016).

*Tonicella*: Eight in *Ischnochiton* and *Mopalia* (Wanninger et al., 2007).

## [170] Develops into adult brain



### Character 170: Larva: Apical organ: Develops into adult brain

0: Brain has other origin

1: Adult brain derived from larval apical organ / apical pole

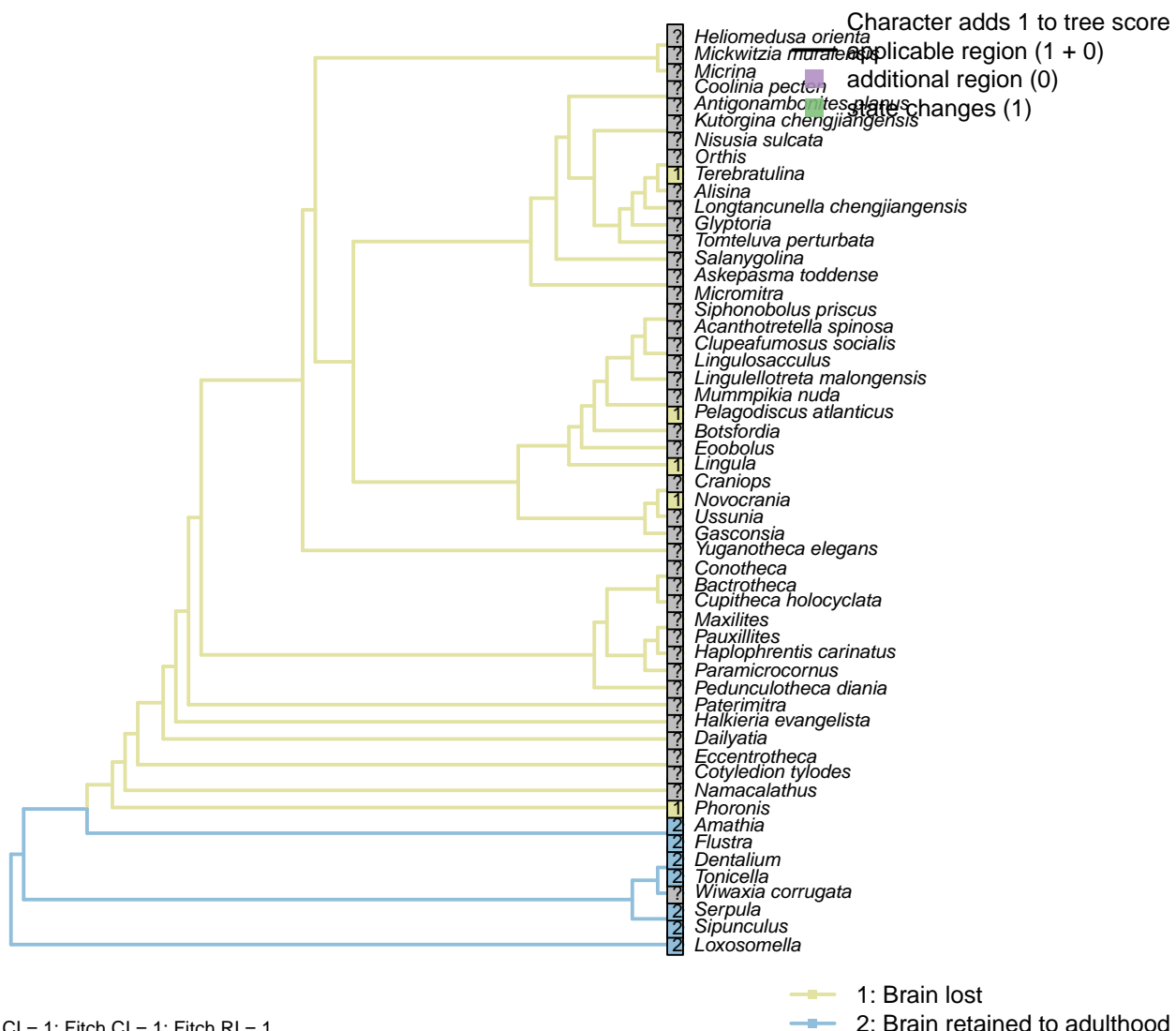
2:

Neomorphic character.

Character 79 in Glenner et al. (2004).

*Lingula*: “both the larval apical ganglion and the ventral ganglion must be retained as the adult nervous system” (Hay-Schmidt, 1992), but not necessarily as the brain.

### [171] Brain persists into adulthood



#### Character 171: Larva: Brain persists into adulthood

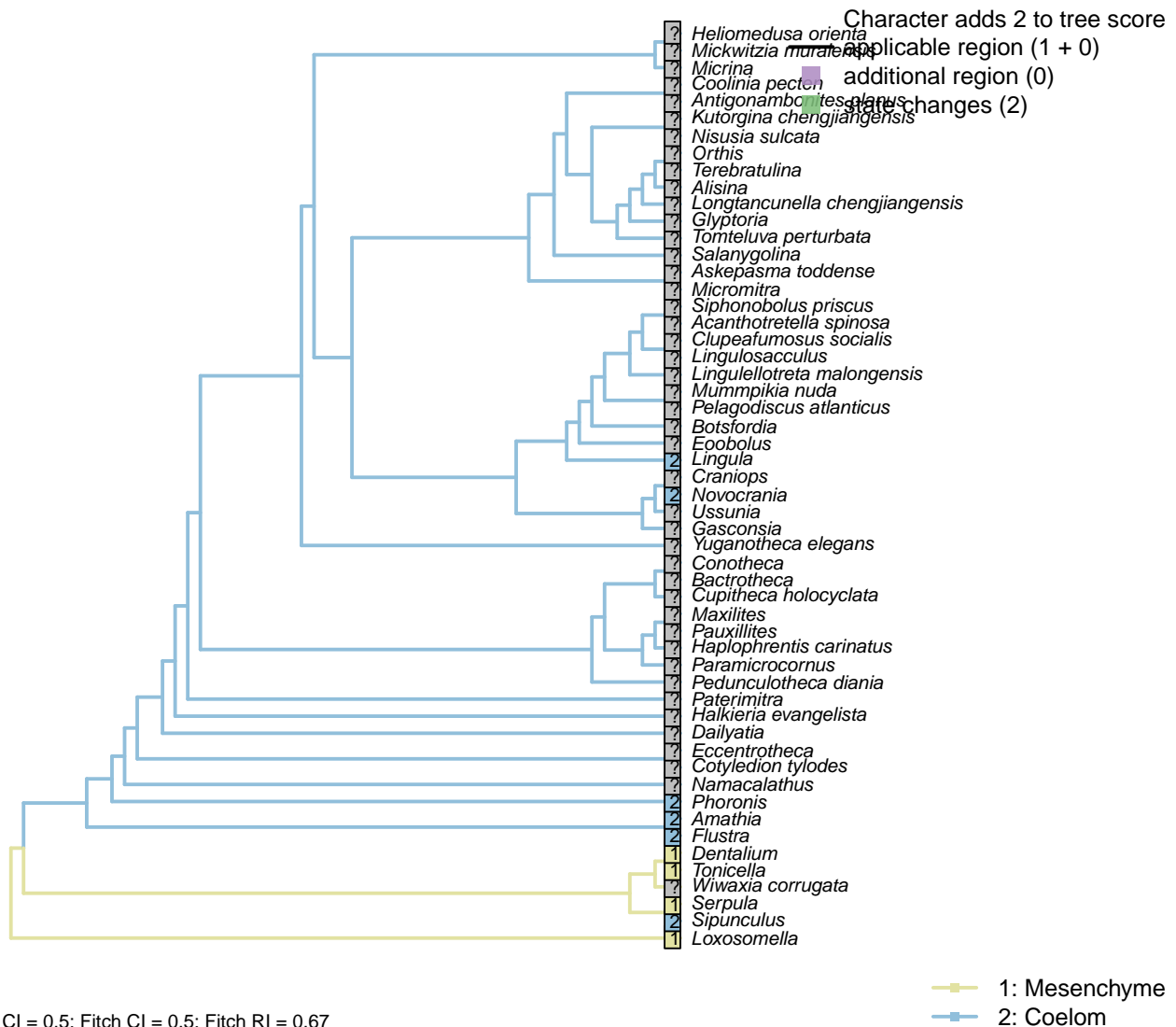
1: Brain lost

2: Brain retained to adulthood

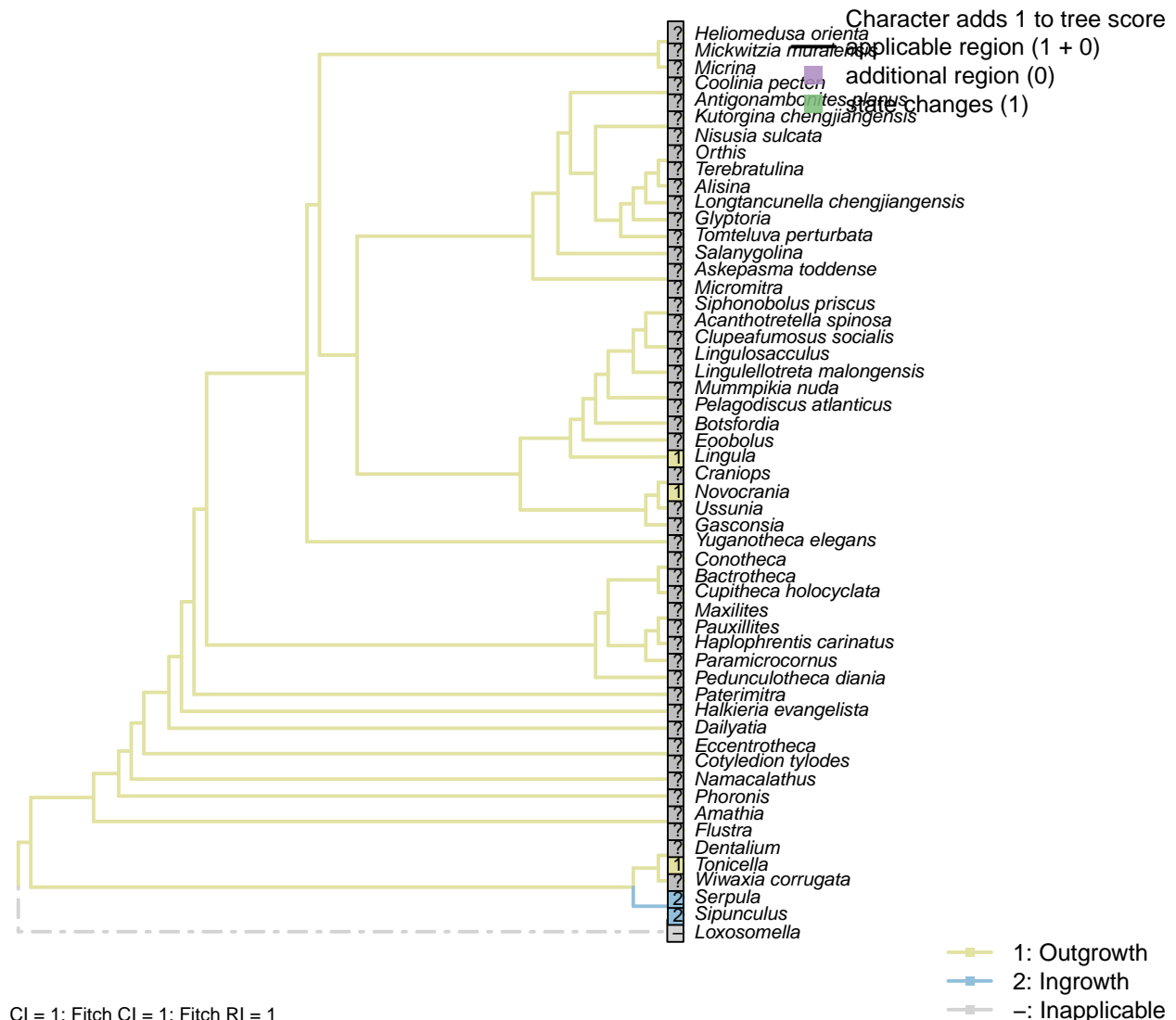
Transformational character.

After character 3 in Richter et al. (2010).

## [172] Origin of body cavity



### [173] Formation of coelomoducts



#### Character 173: Larva: Formation of coelomoducts

1: Outgrowth

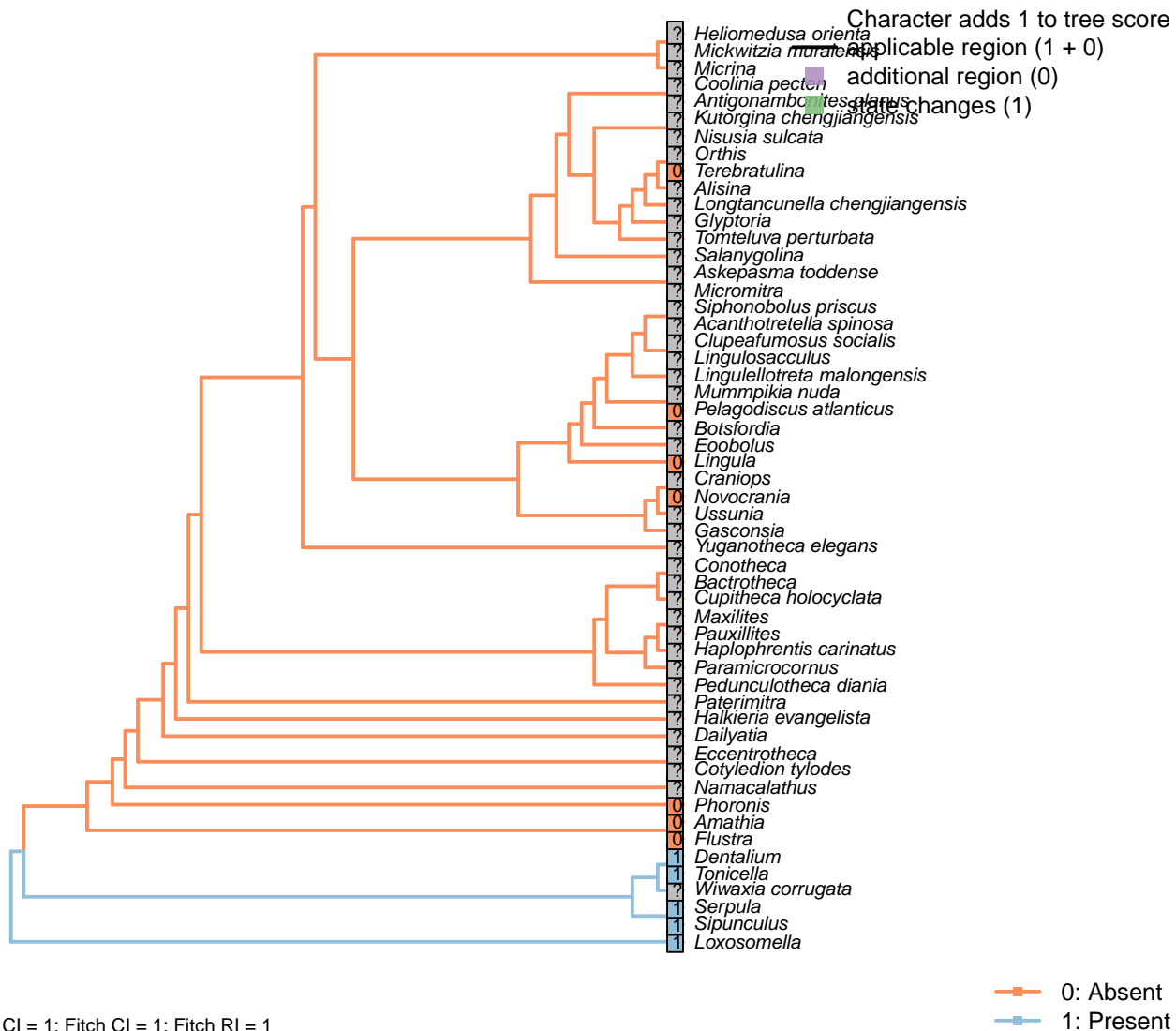
2: Ingrowth

Transformational character.

Character 26 in Haszprunar (2000).

*Loxosomella*: Coelomoducts absent (Haszprunar, 2000).

## [174] Foot



CI = 1; Fitch CI = 1; Fitch RI = 1

**Character 174: Larva: Foot**

0: Absent

1: Present

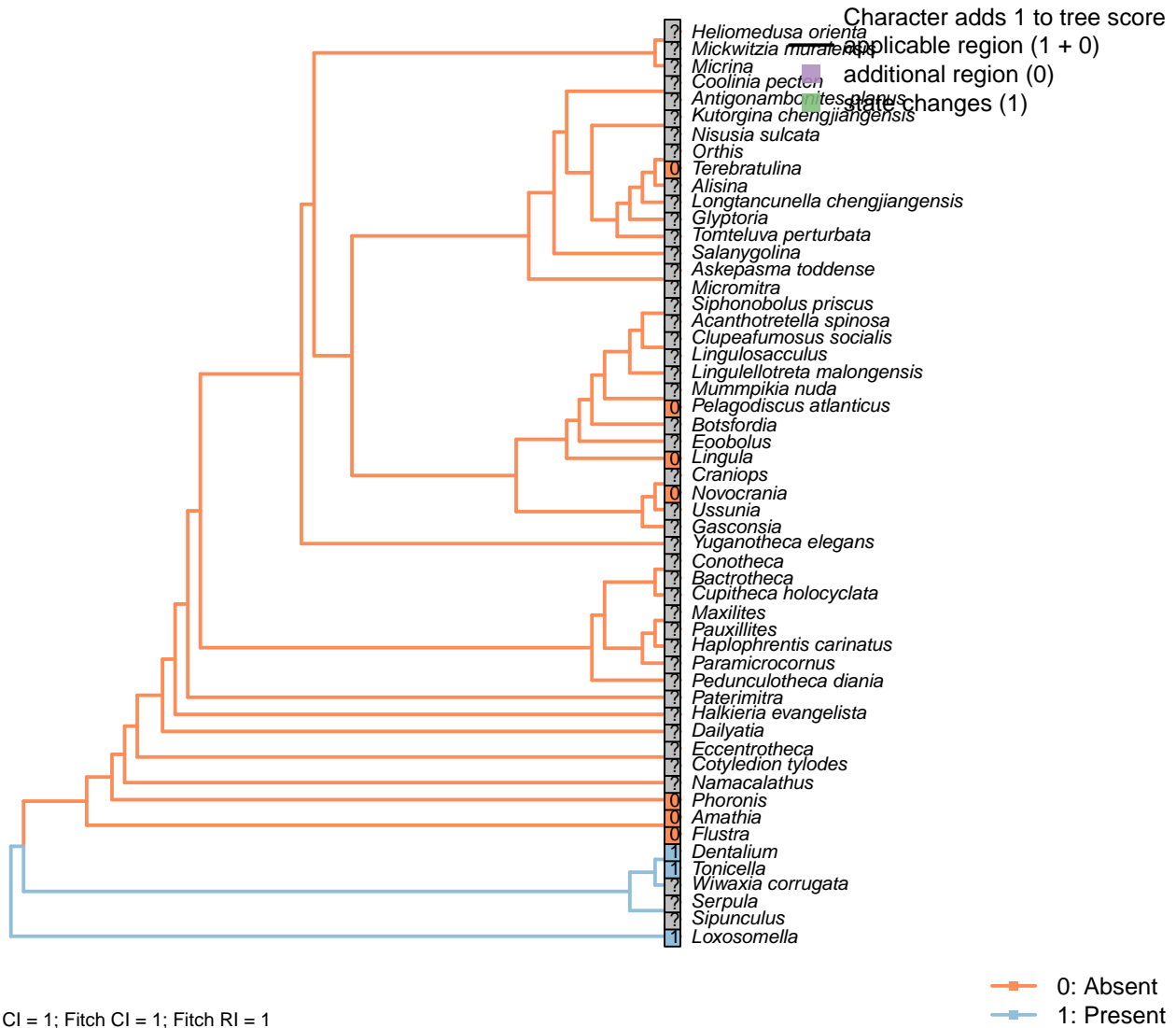
Neomorphic character.

Foot or neurotroch present in larval stage, whether or not it is also present in mature individuals. Following Wingstrand (1985).

*Loxosomella*: A foot is present in the creeping-type larva of *Loxosomella murmanica*, though absent in *L. atkinsae* and the many other entoprocts that have swimming-type larvae (Fuchs and Wanninger, 2008).

*Sipunculus*, *Serpula*: Wingstrand (1985) considers the annelid neurotroch to be potentially homologous with the molluscan and entoproct foot.

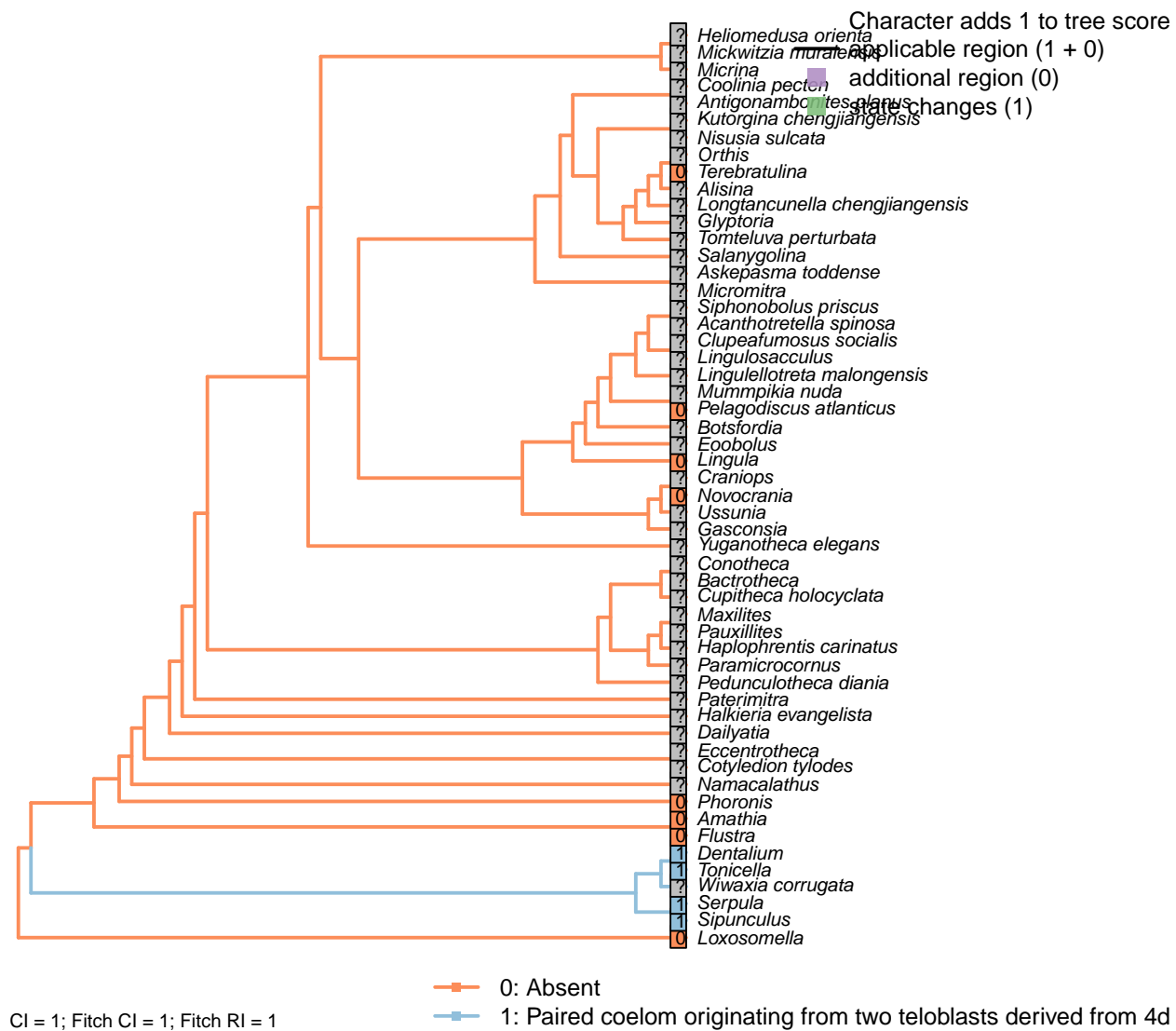
## [175] Pedal gland



A pedal gland is considered evidence for homology between the molluscan and entoproct foot (Haszprunar and Wanninger, 2008).

*Amathia*: Ciliated clef corresponds to position of foot (Reed and Cloney, 1982), but dedicated foot not present.

## [176] Paired

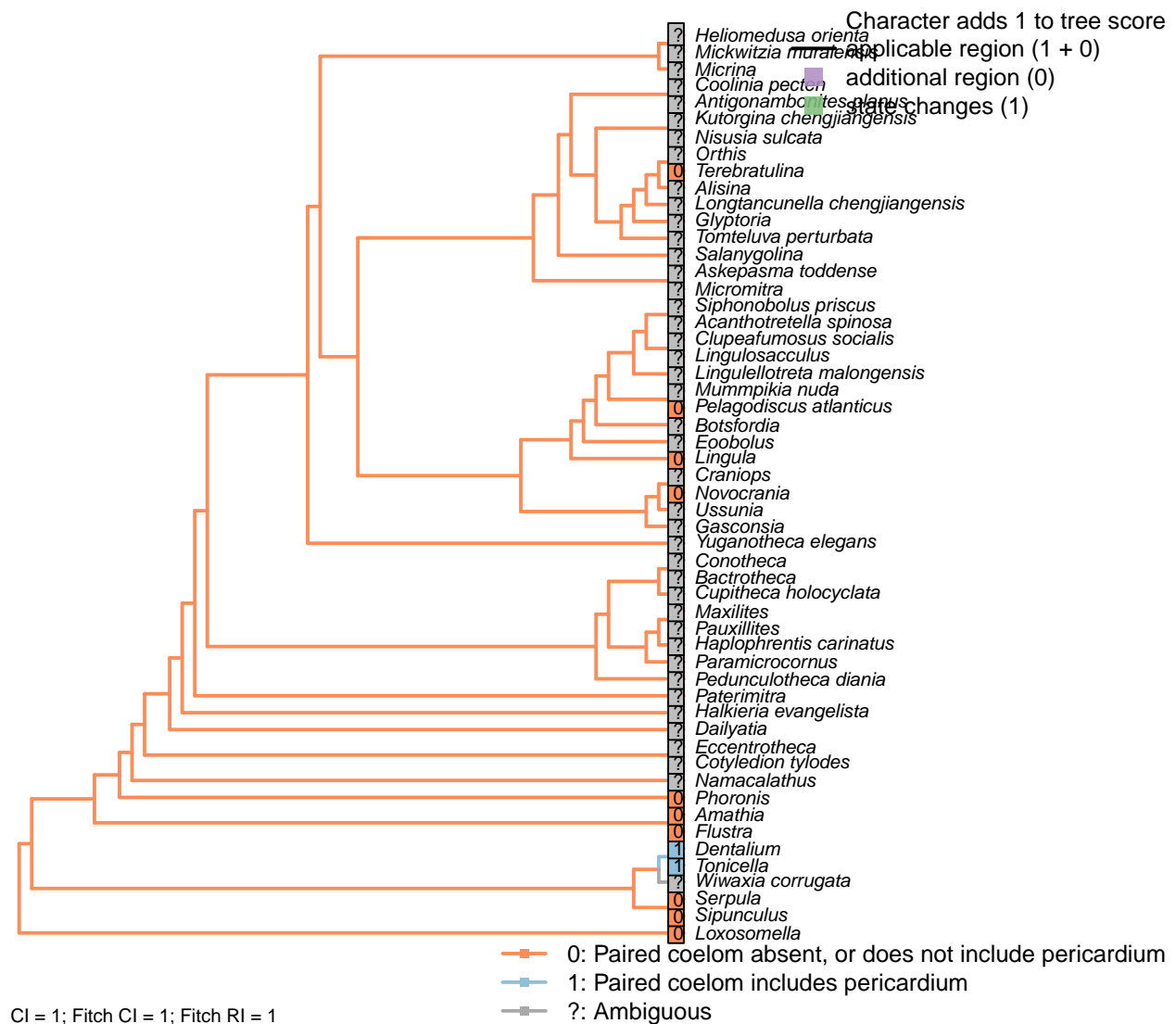


Character 2.02 in Scheltema (1993).

*Amathia*: No evidence of pairing (Reed and Cloney, 1982).

*Flustra*: Hypostegal coelom separated from principal (perigastric) body cavity in cheilostomata – but this is not clearly equivalent to the paired coelom intended by this character. The coelom of *Fredericella* is not paired (Gruhl, 2010a).

## [177] Paried: Includes pericardium

**Character 177: Larva: Coelom: Paried: Includes pericardium**

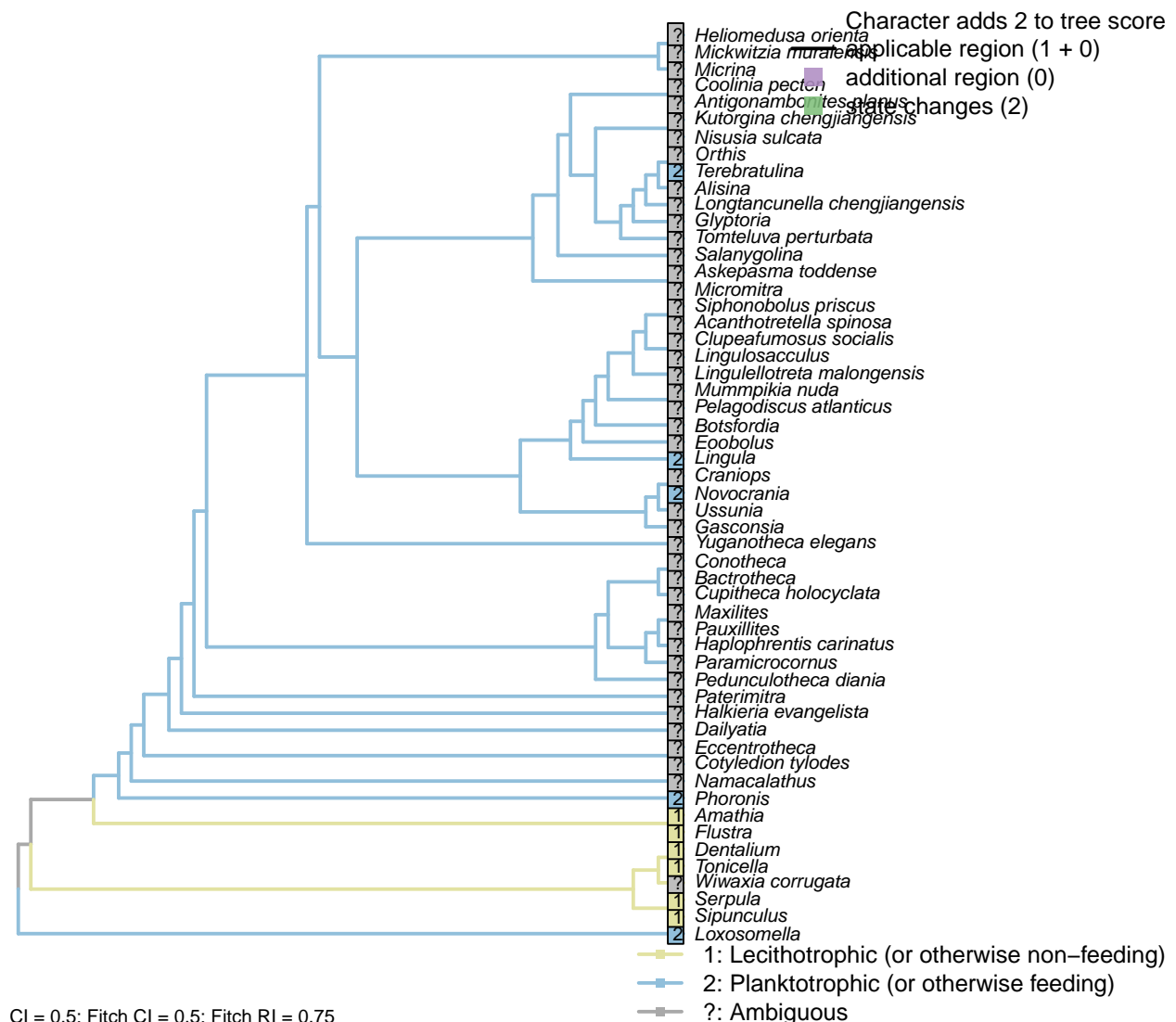
0: Paired coelom absent, or does not include pericardium

1: Paired coelom includes pericardium

Neomorphic character.

Character 1.03 in Scheltema (1993).

## [178] Feeding



## Character 178: Larva: Feeding

1: Lecithotrophic (or otherwise non-feeding)

2: Planktotrophic (or otherwise feeding)

Transformational character.

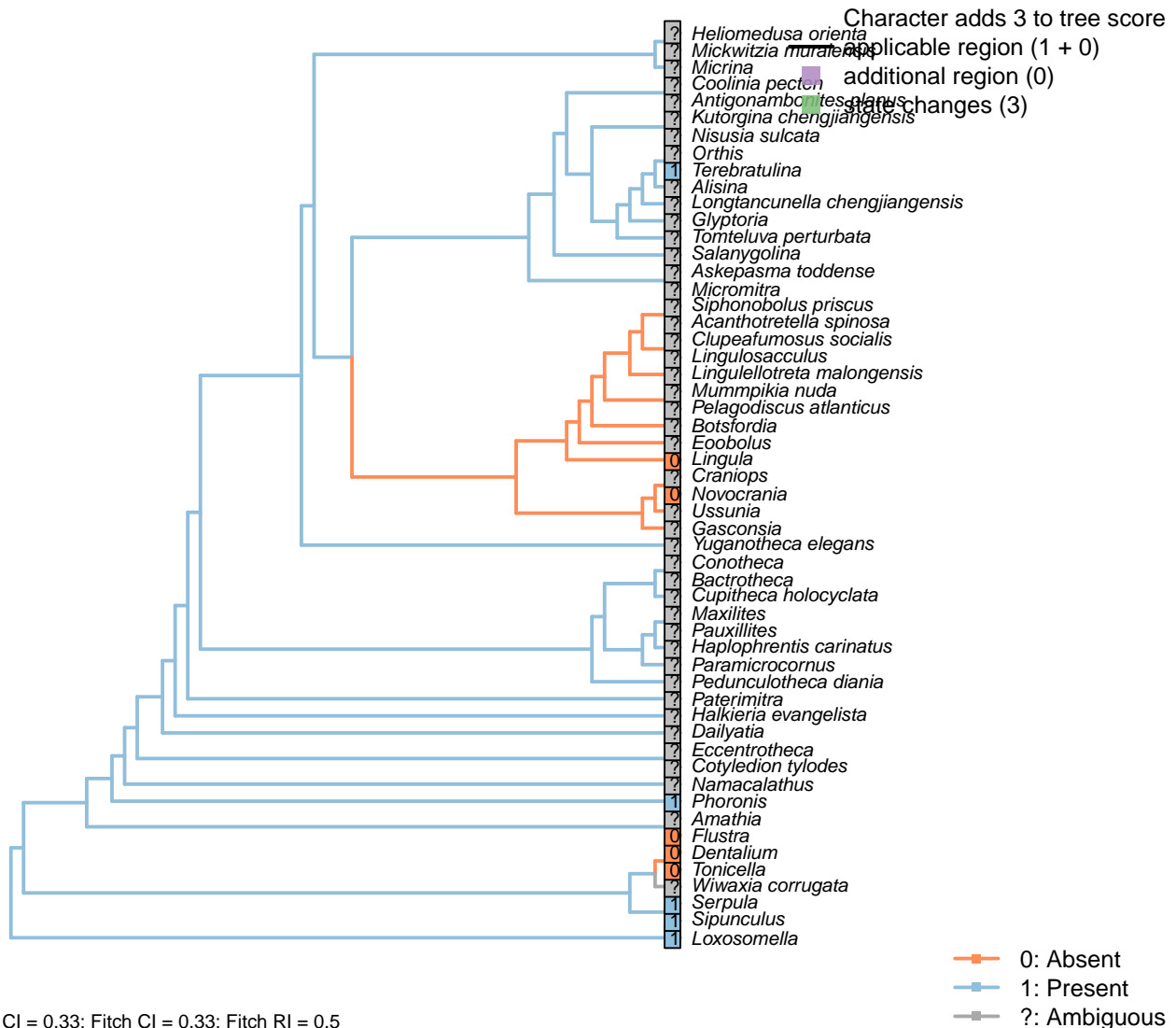
Character 140 in Rouse (1999). See also character 2.66 in von Salvini-Plawen and Steiner (1996); 153 in Giribet and Wheeler (2002).

*Amathia*: Lecithotrophic (Reed and Cloney, 1982).

*Flustra*: Metamorphose almost immediately after release from gonozoid (Zimmer and Woollacott, 2013); most bryozoans are lecithotrophic (Reed and Cloney, 1982).

## 5.22 Larva: Cilia

### [179] Metatroch



#### Character 179: Larva: Cilia: Metatroch

0: Absent

1: Present

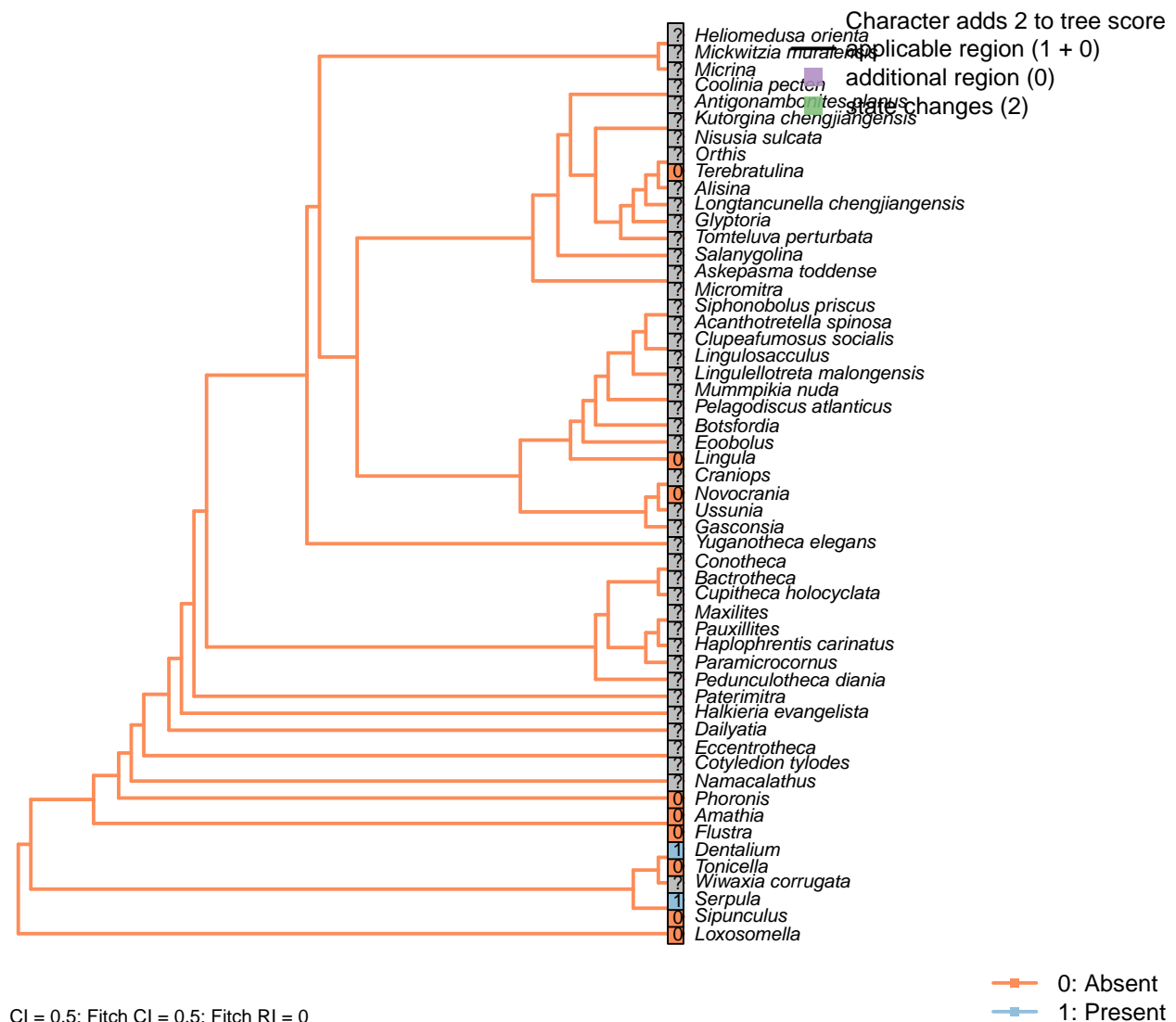
Neomorphic character.

See characters 129 and 131 in Rouse (1999); 40 in Haszprunar (1996).

A prototroch is the defining character of a trochophore larva; a metatroch is a secondary ciliary ring (Rouse, 1999).

*Terebratulina*: Williams et al. (1997).

## [180] Telotroch



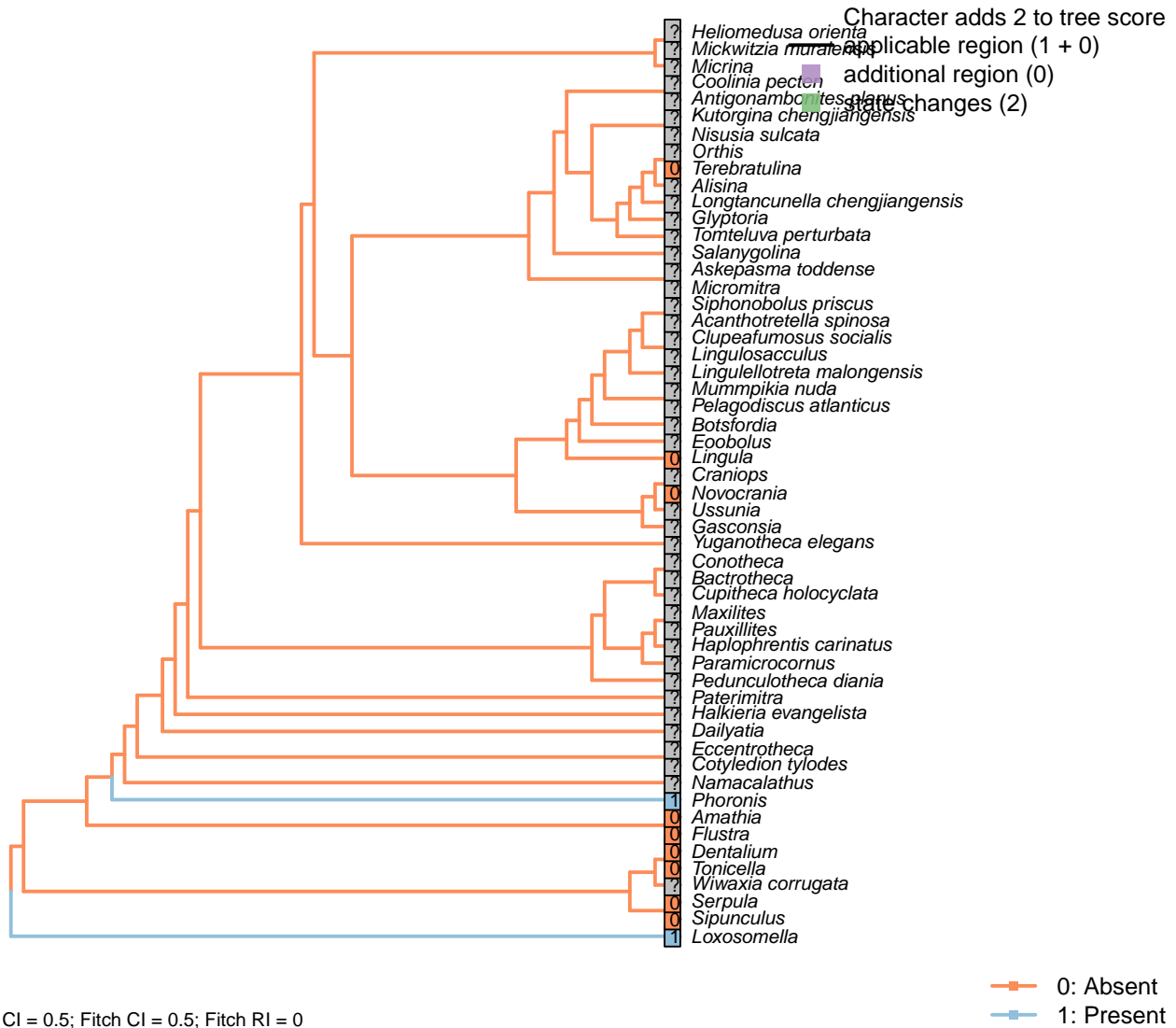
A posterior ciliary band. Character 136 in Rouse (1999).

*Amathia*: Absent; single ciliary field lacks telotroch equivalent (Reed and Cloney, 1982).

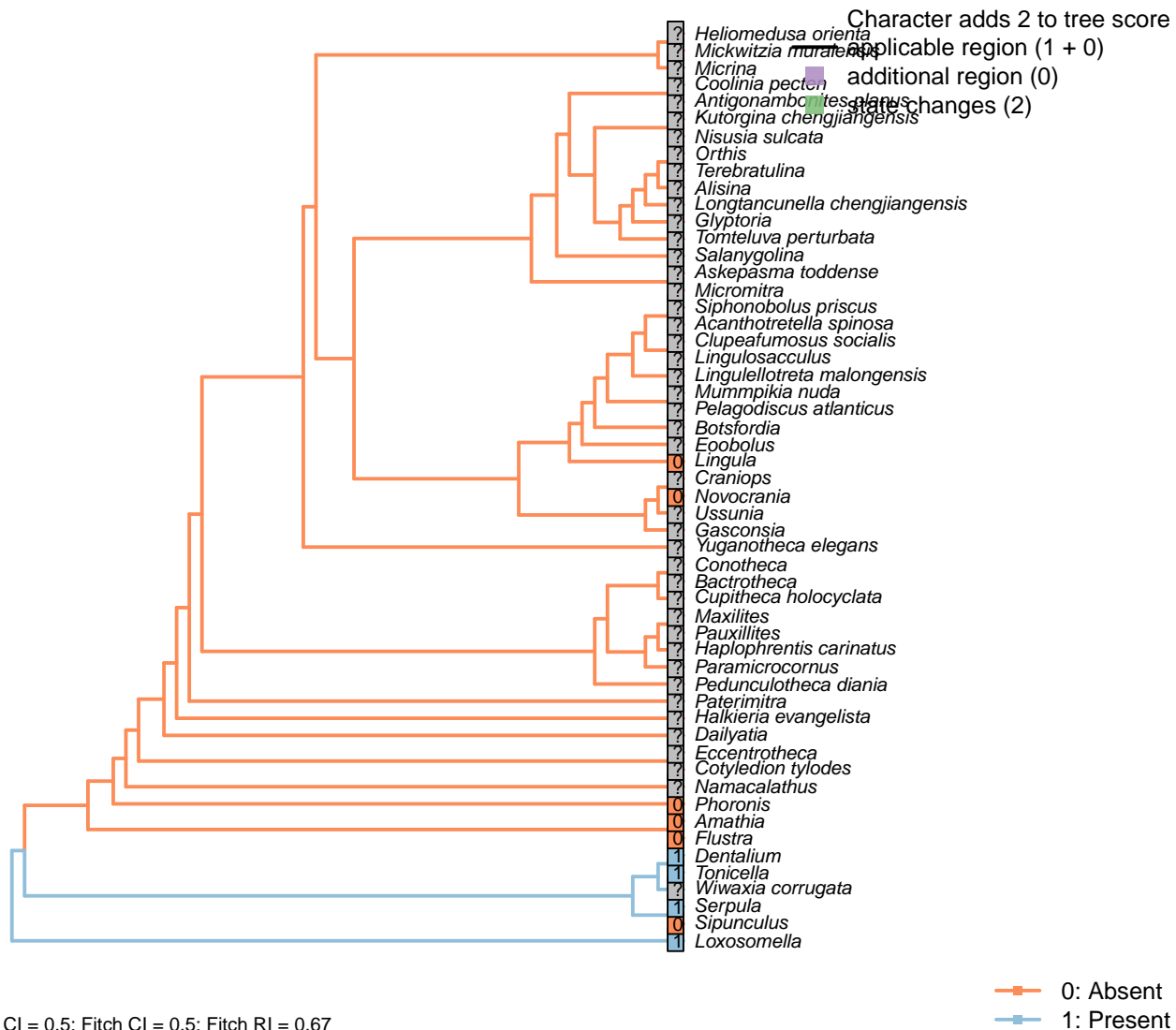
*Flustra*: Absent (Zimmer and Woollacott, 2013).

*Terebratulina*: Williams et al. (1997).

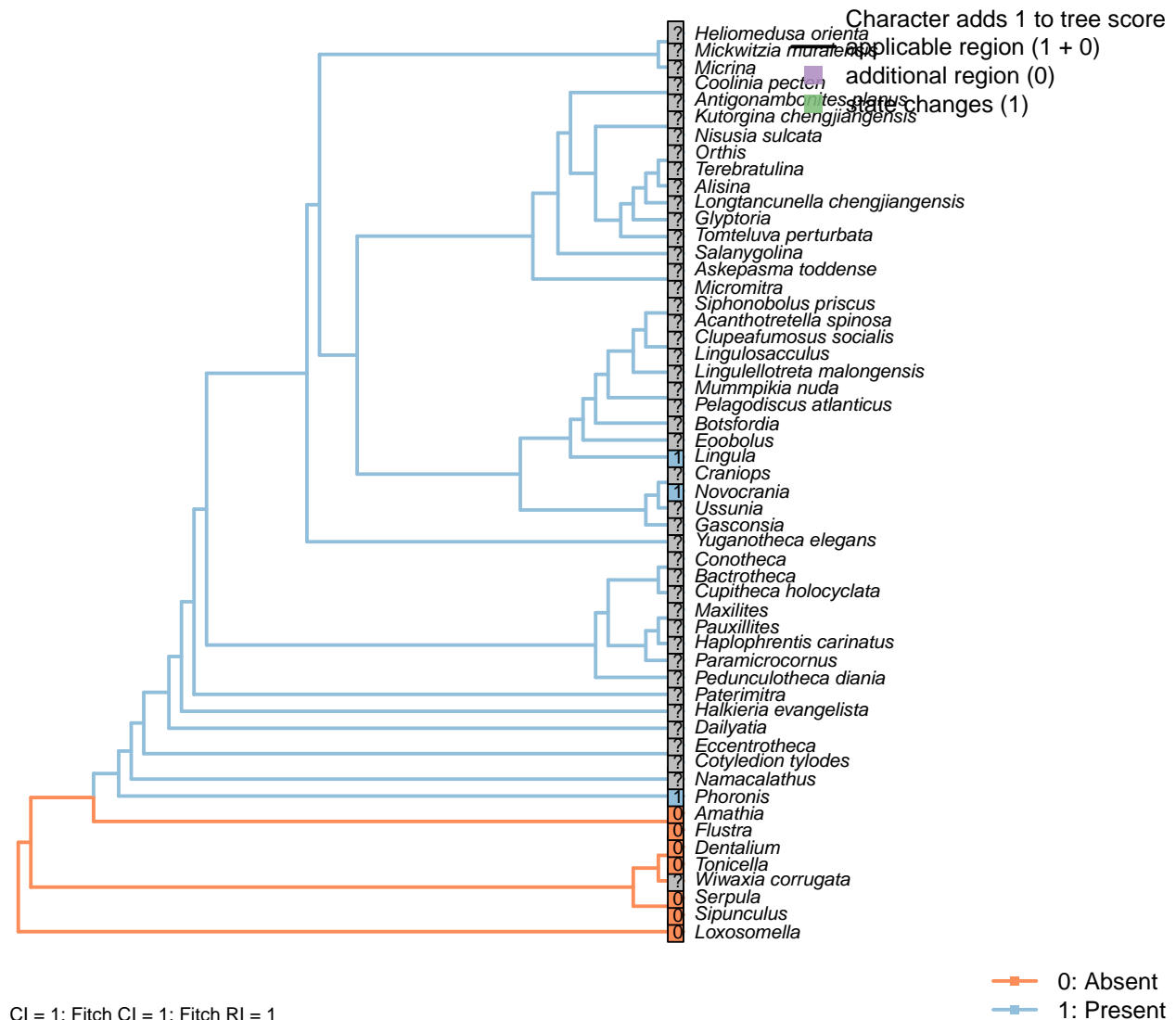
## [181] Ciliated food groove



## [182] Ciliary bands: Downstream



## [183] Ciliary bands: Upstream



## Character 183: Larva: Cilia: Ciliary bands: Upstream

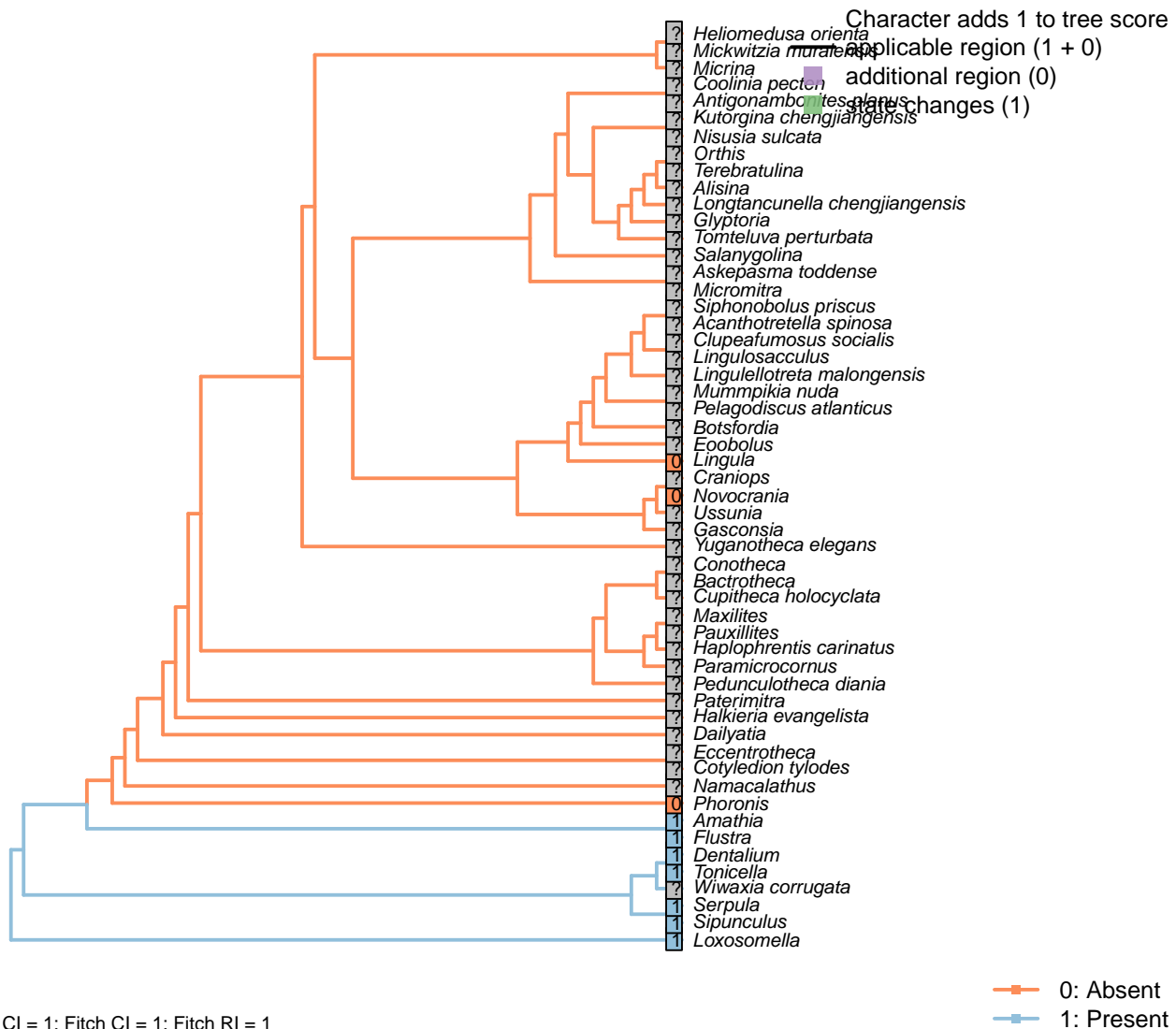
0: Absent

1: Present

Neomorphic character.

Upstream-collecting ciliary bands with single cilia on monociliated cells. See character 32 in Glenner et al. (2004).

## [184] Adoral ciliary band



## Character 184: Larva: Cilia: Adoral ciliary band

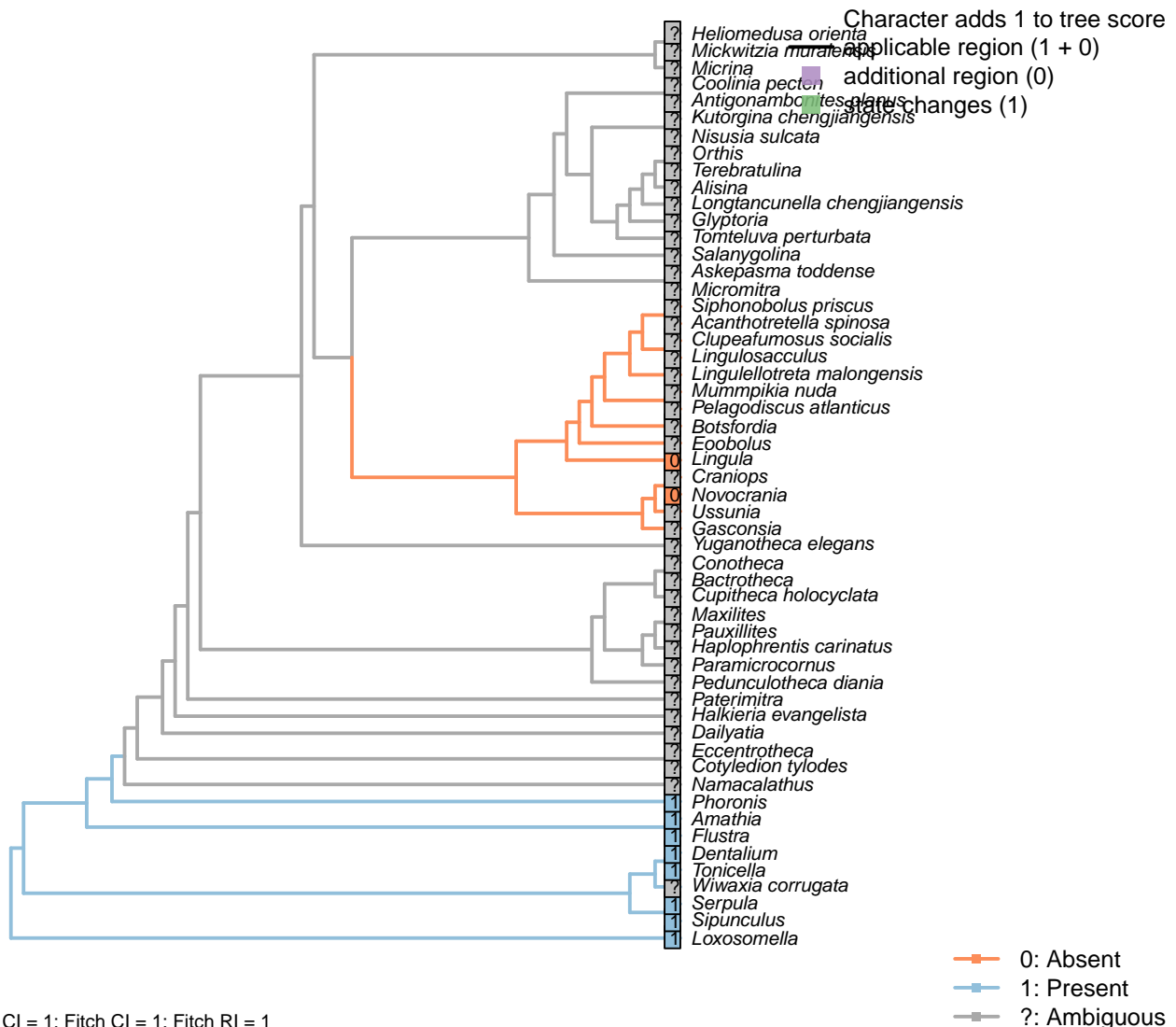
0: Absent

1: Present

Neomorphic character.

Characters 1.50, 2.66 and 4.68 in von Salvini-Plawen and Steiner (1996); 2 in Vinther et al. (2008). See also characters 39 in Haszprunar (1996) and 153 in Giribet and Wheeler (2002).

## [185] Nerve ring underlying ciliated larval swimming organ

**Character 185: Larva: Cilia: Nerve ring underlying ciliated larval swimming organ**

0: Absent

1: Present

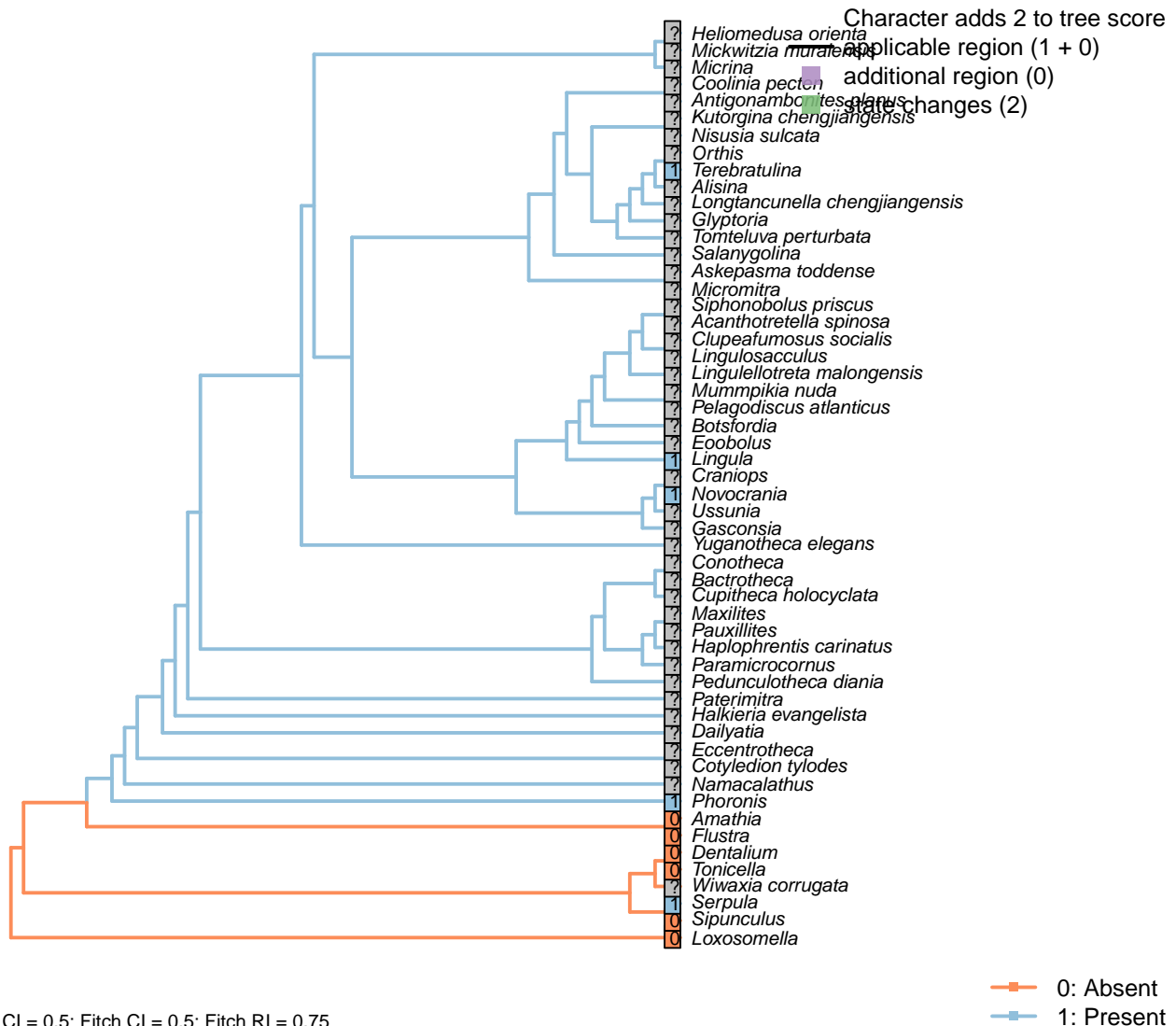
Neomorphic character.

Following Wanninger (2009).

*Amathia*: Nodular nerve ring underlies corona (Reed and Cloney, 1982).*Flustra*: Present, following schematic in Gruhl and Schwaha (2016).

## 5.23 Ciliary ultrastructure

### [186] Accessory centriole



CI = 0.5; Fitch CI = 0.5; Fitch RI = 0.75

#### Character 186: Ciliary ultrastructure: Accessory centriole

0: Absent

1: Present

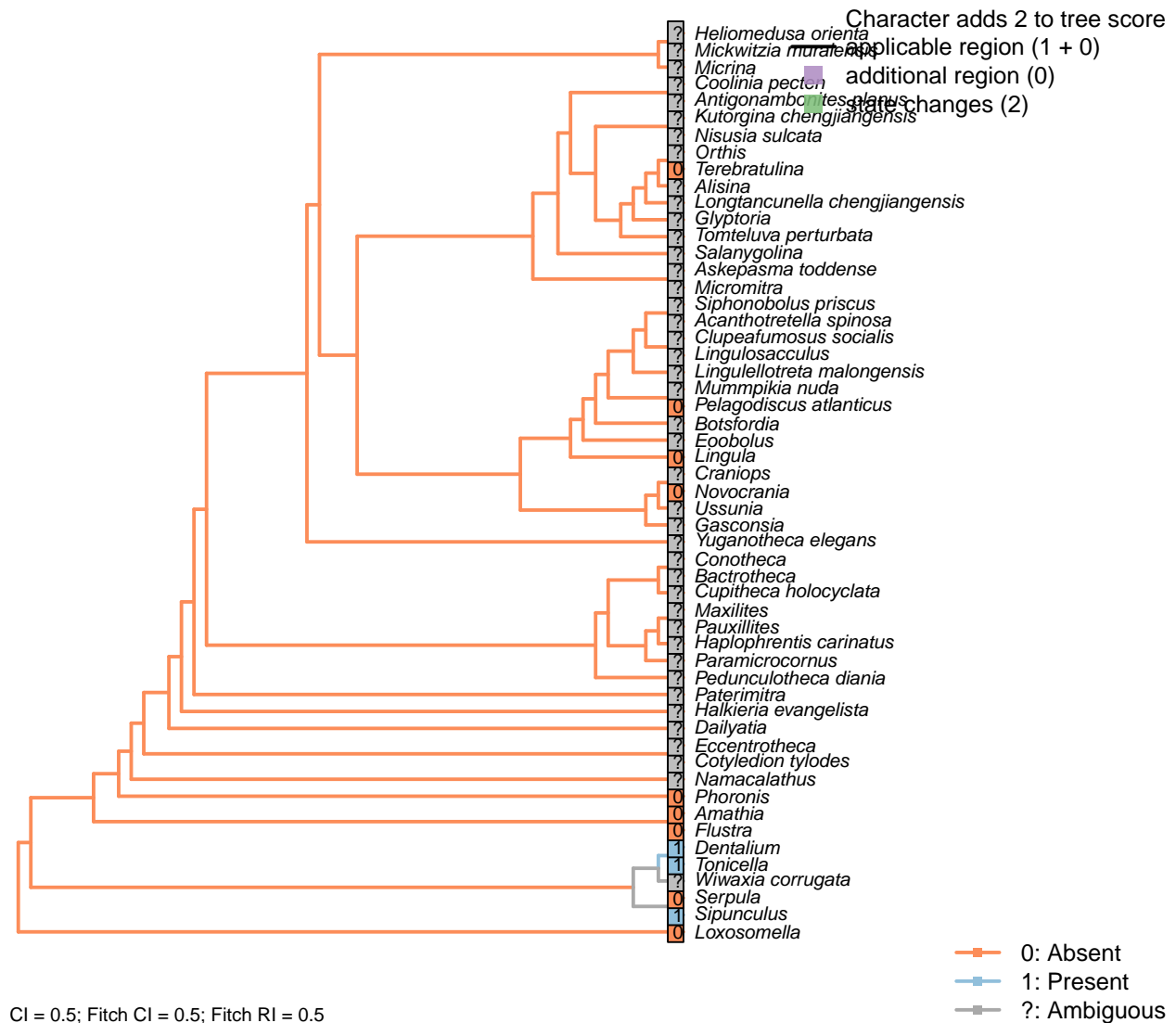
Neomorphic character.

After Lundin et al. (2009).

*Serpula*: Present in certain annelids; not verified in *Serpula*.

*Terebratulina*: Present (Lüter, 1995).

[187] Aggregation of granules below basal plate



**Character 187: Ciliary ultrastructure: Aggregation of granules below basal plate**

0: Absent

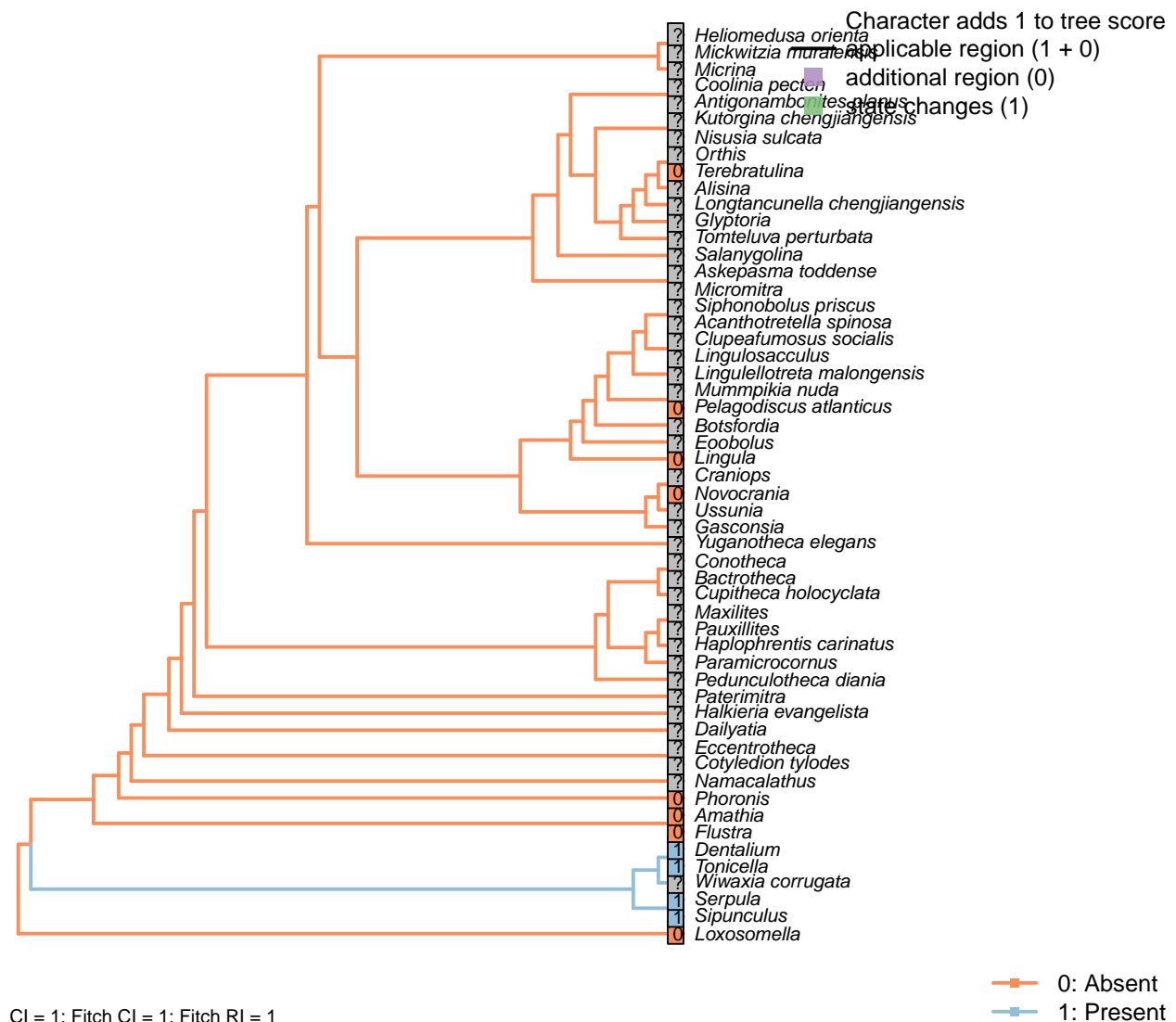
1: Present

Neomorphic character.

After Lundin et al. (2009).

*Serpula*: Following *Harmothoe* (Holborow et al., 1969).

## [188] Radiating tubular fibres

**Character 188: Ciliary ultrastructure: Basal foot: Radiating tubular fibres**

0: Absent

1: Present

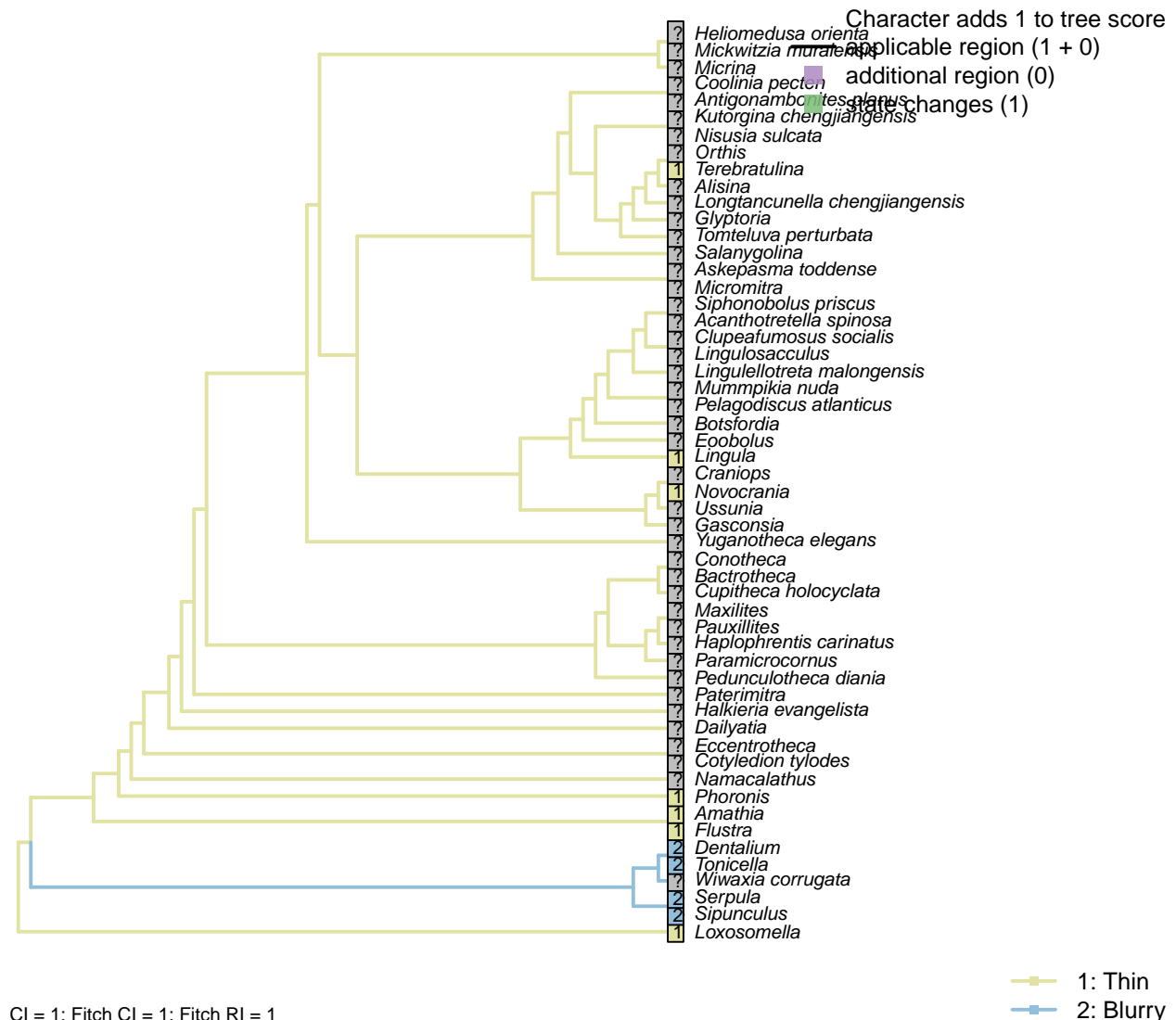
Neomorphic character.

After Lundin et al. (2009). Fibres radiate from the distal end of the basal foot of the cilia in certain taxa.

*Amathia*: Reed and Cloney (1982).

*Serpula*: Basal foot in *Magelona* is connected to cytoplasmic microtubules (Bartolomaeus, 1995).

### [189] Basal plate



#### Character 189: Ciliary ultrastructure: Basal plate

1: Thin

2: Blurry

Transformational character.

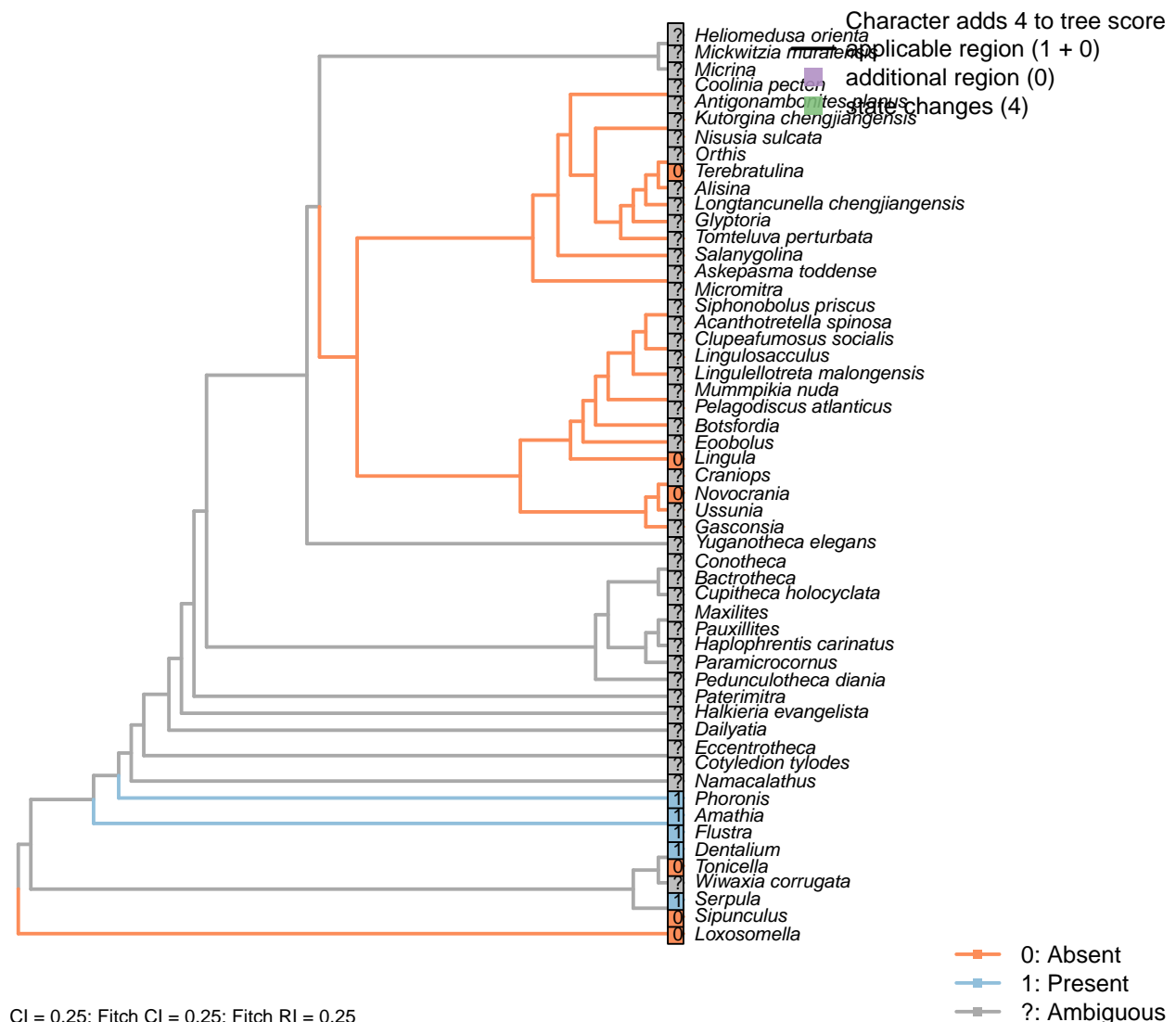
After Lundin et al. (2009). Also termed “dense plate”.

*Amathia*: Reed and Cloney (1982).

*Serpula*: Broad and ‘blurry’ in *Magelona* (Bartolomaeus, 1995).

*Terebratulina*: Thin to thick, but not blurry (Lüter, 1995).

## [190] Brushborder of microvilli



CI = 0.25; Fitch CI = 0.25; Fitch RI = 0.25

**Character 190: Ciliary ultrastructure: Brushborder of microvilli**

0: Absent

1: Present

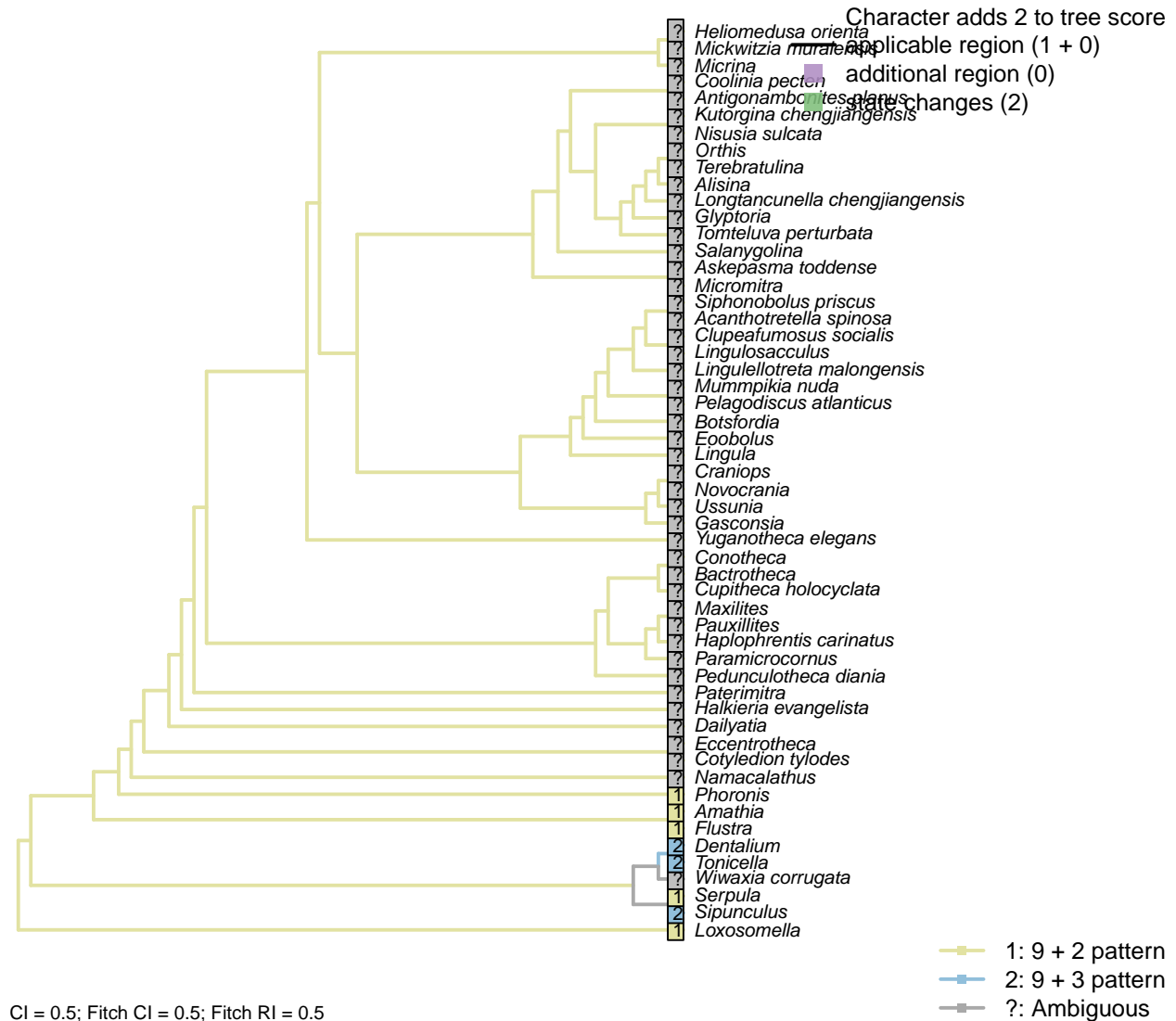
Neomorphic character.

After Lundin et al. (2009); coded following Smith (2012a).

*Amathia*: Present (Reed and Cloney, 1982).

*Terebratulina*: Absent (Lüter, 1995).

### [191] Centriolar triplet derivative in basal body



CI = 0.5; Fitch CI = 0.5; Fitch RI = 0.5

#### Character 191: Ciliary ultrastructure: Centriolar triplet derivative in basal body

1: 9 + 2 pattern

2: 9 + 3 pattern

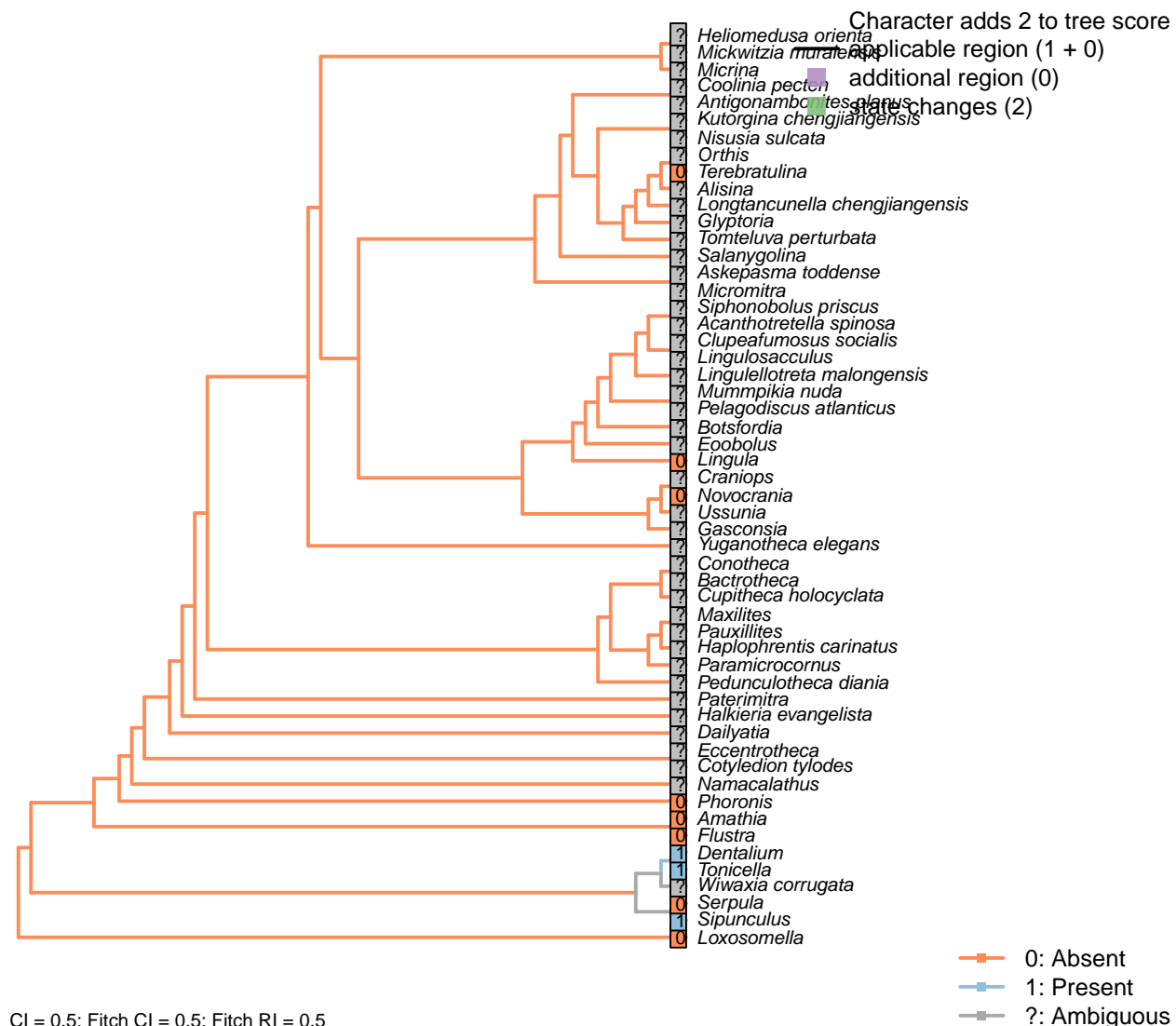
Transformational character.

After Lundin et al. (2009).

*Amathia*: Reed and Cloney (1982).

*Serpula*: Following *Enchytraeus* (Reger, 1967), *Magelona* (Bartolomaeus, 1995) and *Harmothoe* (Holborow et al., 1969).

## [192] Ciliary necklace with connecting strands

**Character 192: Ciliary ultrastructure: Ciliary necklace with connecting strands**

0: Absent

1: Present

Neomorphic character.

After Lundin et al. (2009).

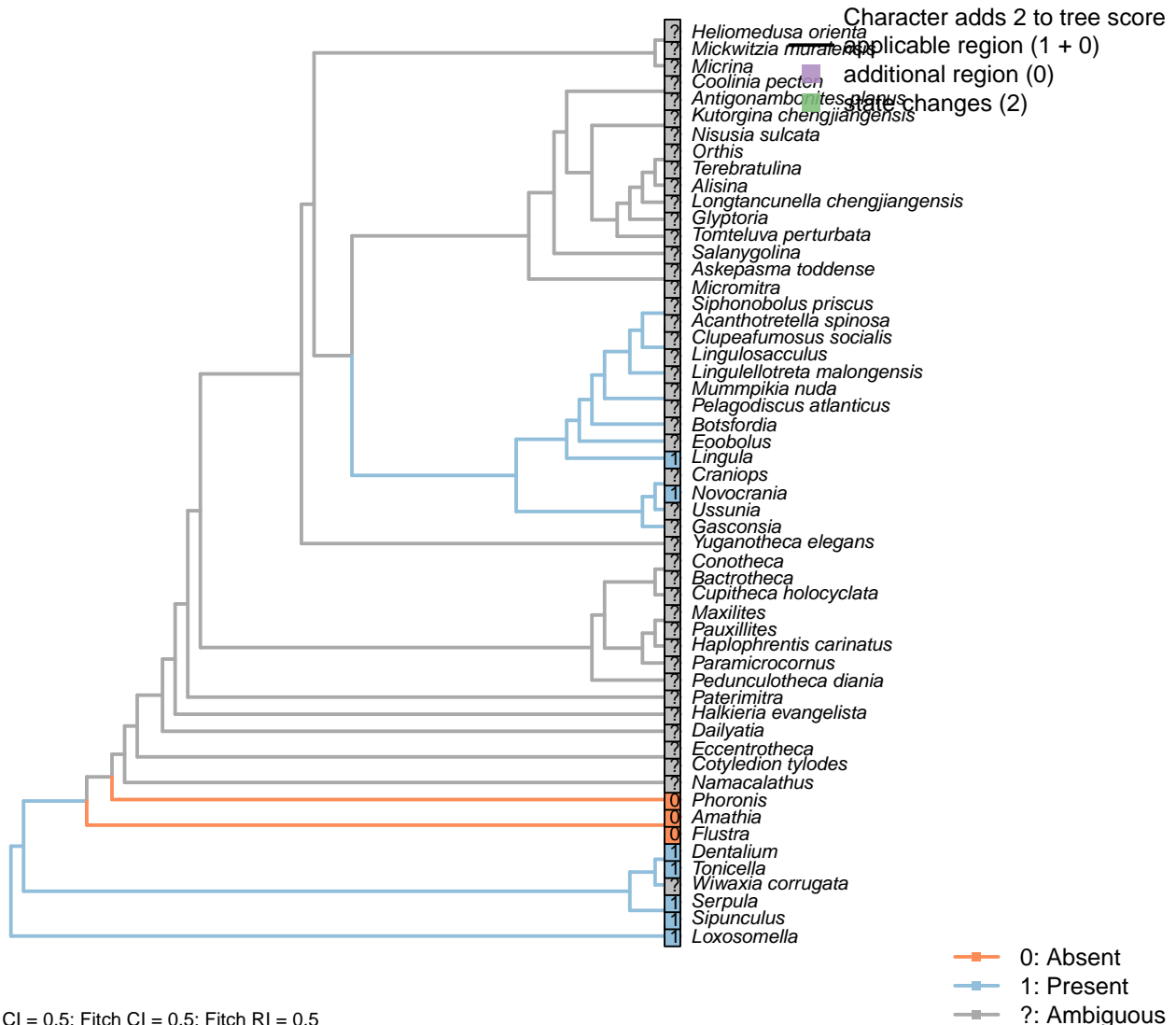
The ciliary necklace is defined by Gilula and Satir (1972) as “Well-defined rows or strands of membrane particles that encircle the ciliary shaft”. It occurs immediately below the basal plate, and comprises three beaded circles of on the circumference of the cilia membrane.

*Amathia*: Reed and Cloney (1982).

*Serpula*: Not evident in *Enchytraeus* (Reger, 1967), *Magelona* (Bartolomaeus, 1995) or *Harmothoe* (Holborow et al., 1969).

*Terebratulina*: (Lüter, 1995).

## [193] Presence



## Character 193: Ciliary ultrastructure: Compound cilia: Presence

0: Absent

1: Present

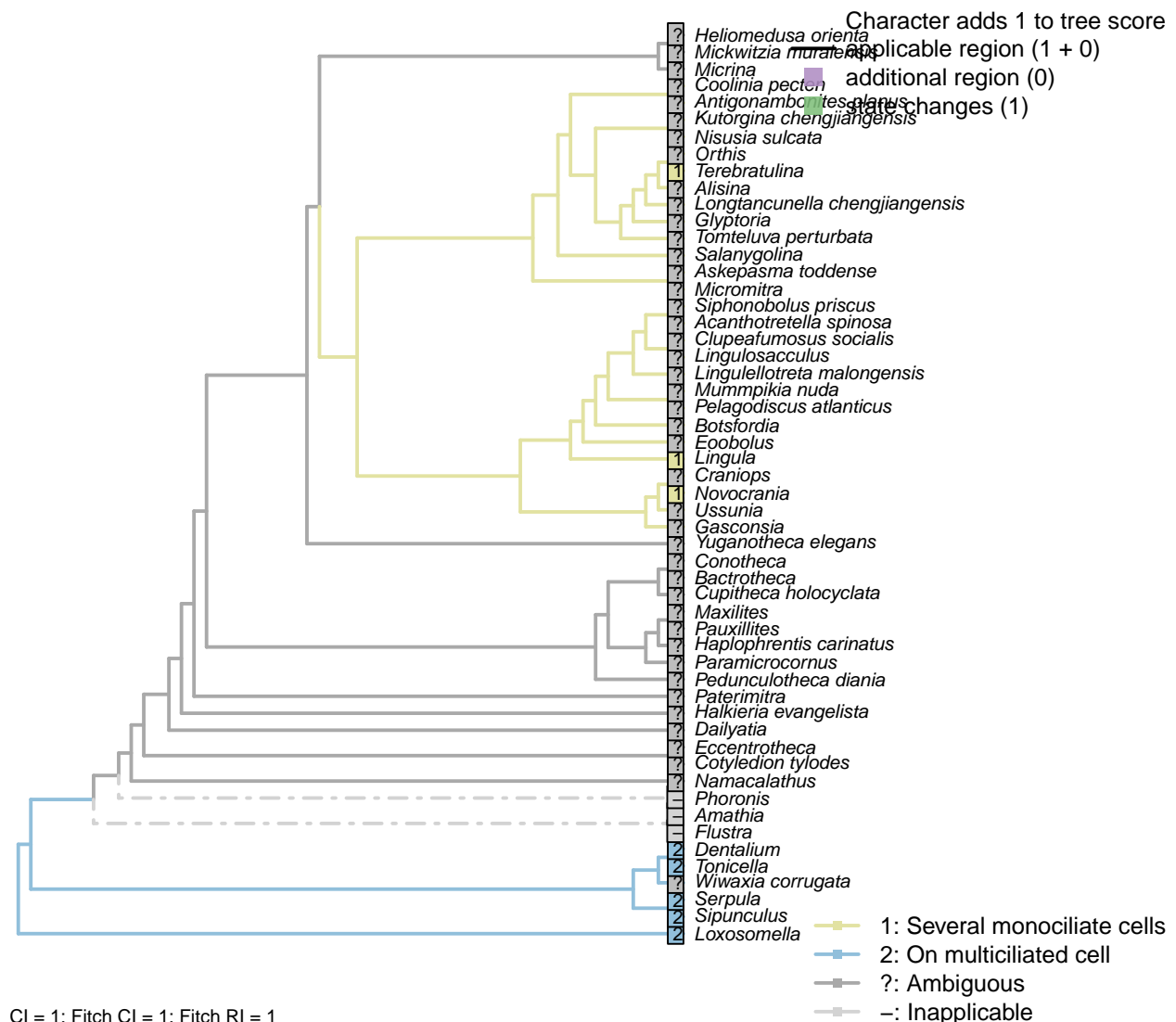
Neomorphic character.

After Lundin et al. (2009). Compound cilia are motile structures composed of 10–100 regular cilia used in locomotion or feeding.

*Amathia*: Reed and Cloney (1982).

*Serpula*: Nielsen (1987).

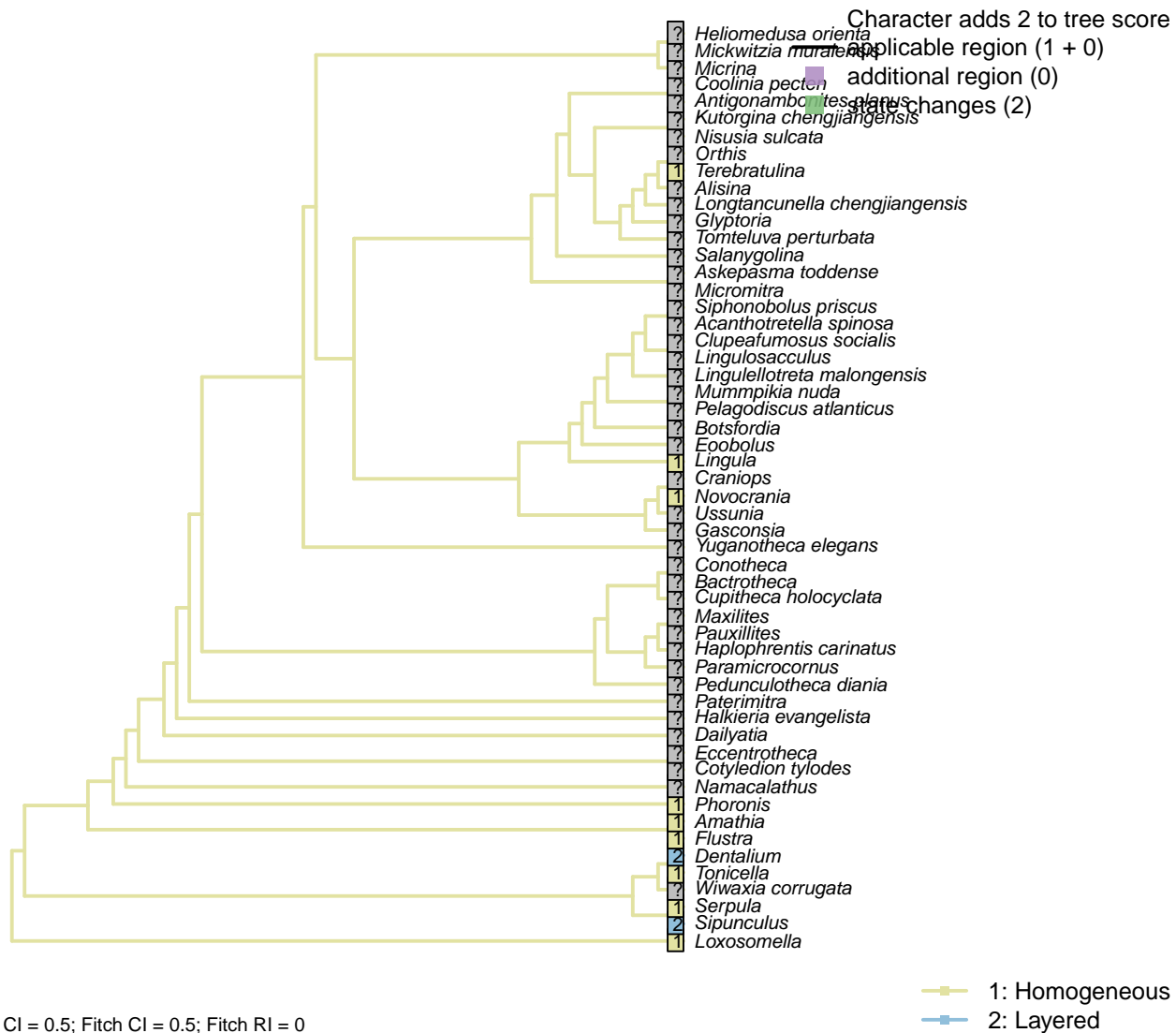
## [194] Origin



Character 14 in Glenner et al. (2004). Compound cilia can be produced by the aggregation of cilia from multiple monociliate cells, or from a single cell bearing multiple cilia (Nielsen, 1987).

*Terebratulina*: “The coelothelial cells of the metacoel are monociliated”; “even some epithelial muscle cells are monociliated” – Lüter (1995).

## [195] Glycocalyx ultrastructure



### Character 195: Ciliary ultrastructure: Glycocalyx ultrastructure

1: Homogeneous

2: Layered

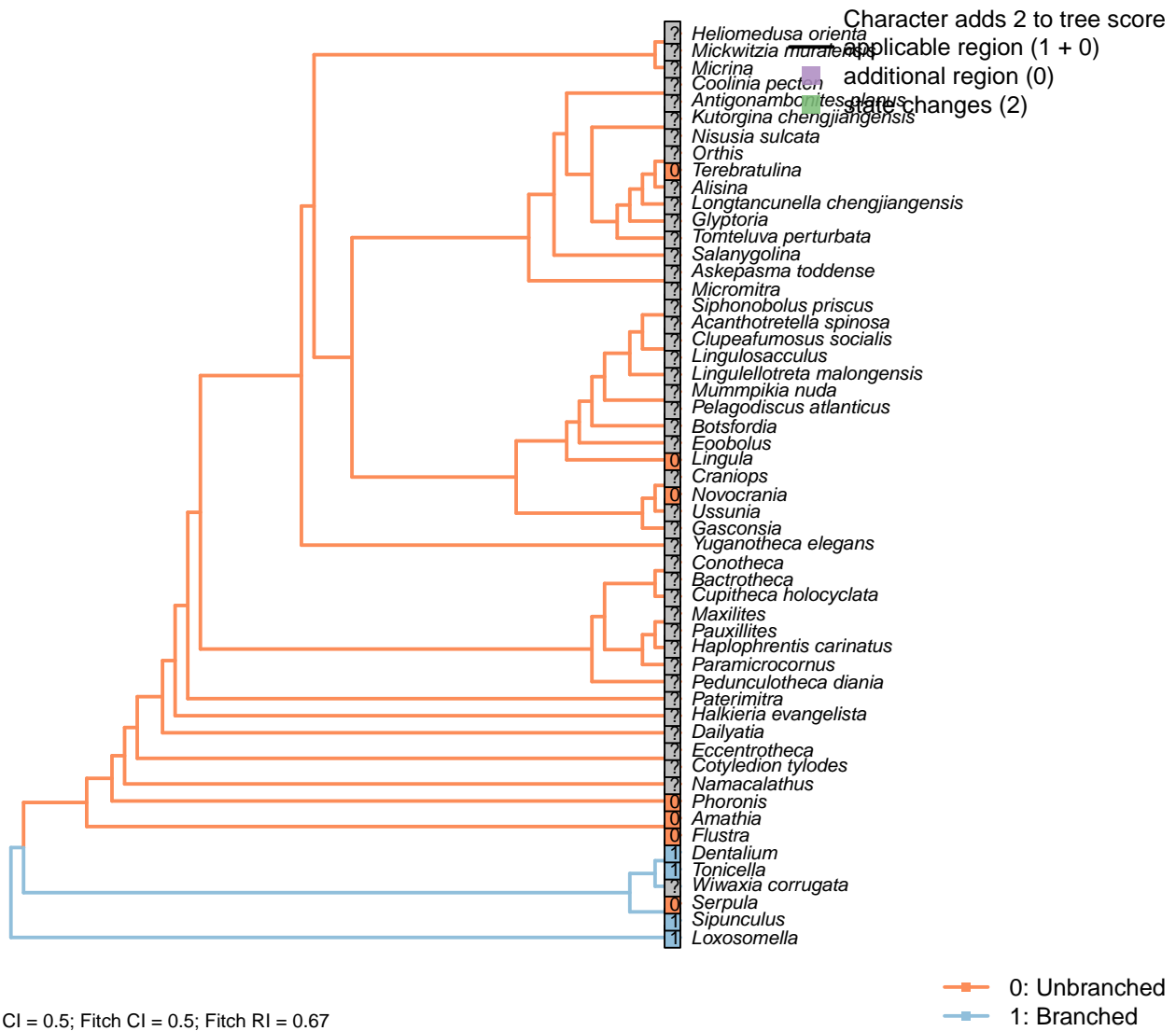
Transformational character.

After Lundin et al. (2009).

*Amathia*: Reed and Cloney (1982).

*Terebratulina*: Homogeneous (Lüter, 1995).

## [196] Branched



**Character 196: Ciliary ultrastructure: Microvilli on epidermal surface: Branched**

0: Unbranched

1: Branched

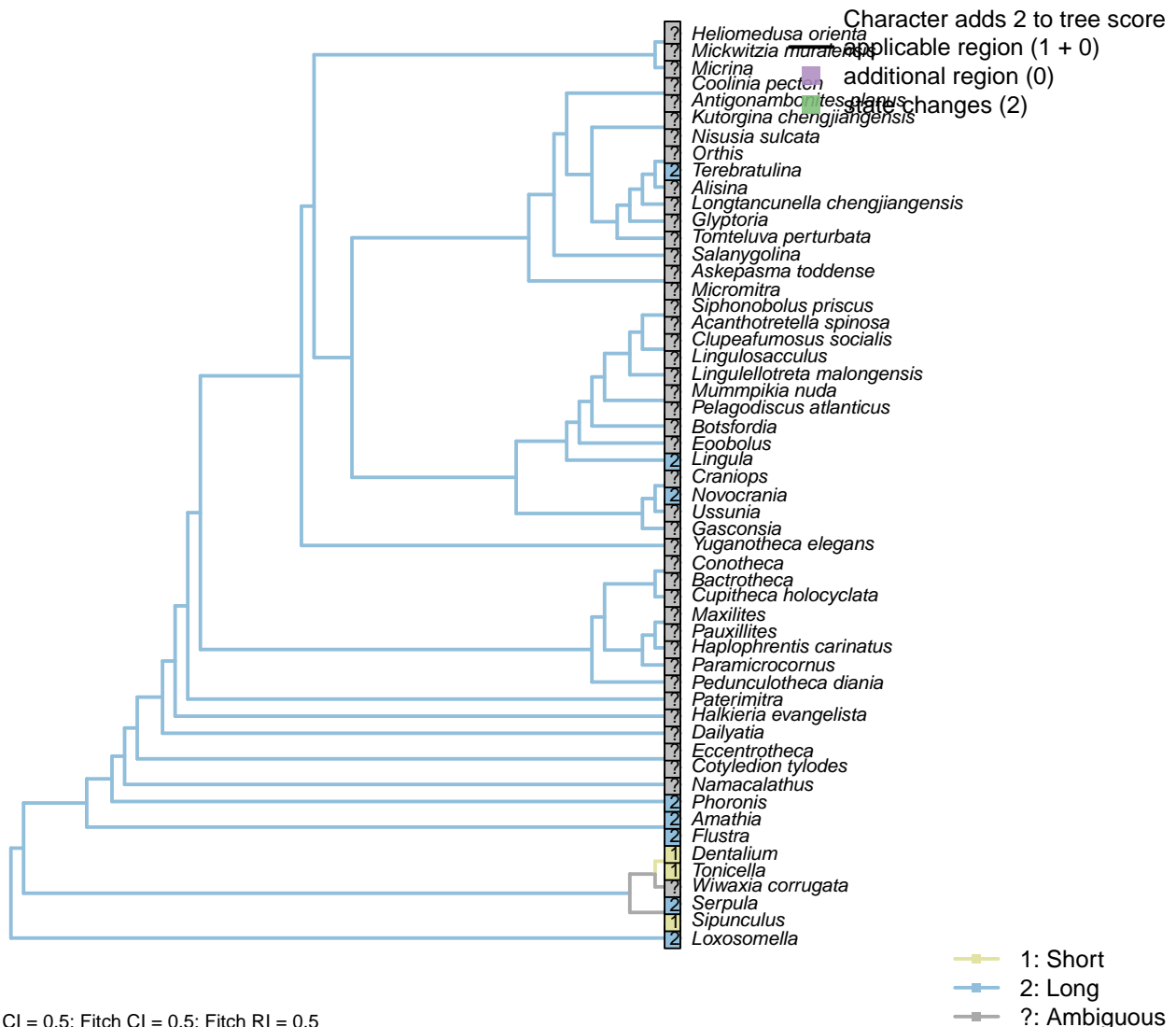
Neomorphic character.

After Lundin et al. (2009).

*Amathia*: Reed and Cloney (1982).

*Terebratulina*: (Lüter, 1995).

## [197] Length



## Character 197: Ciliary ultrastructure: Vertical ciliary rootlet: Length

1: Short

2: Long

Transformational character.

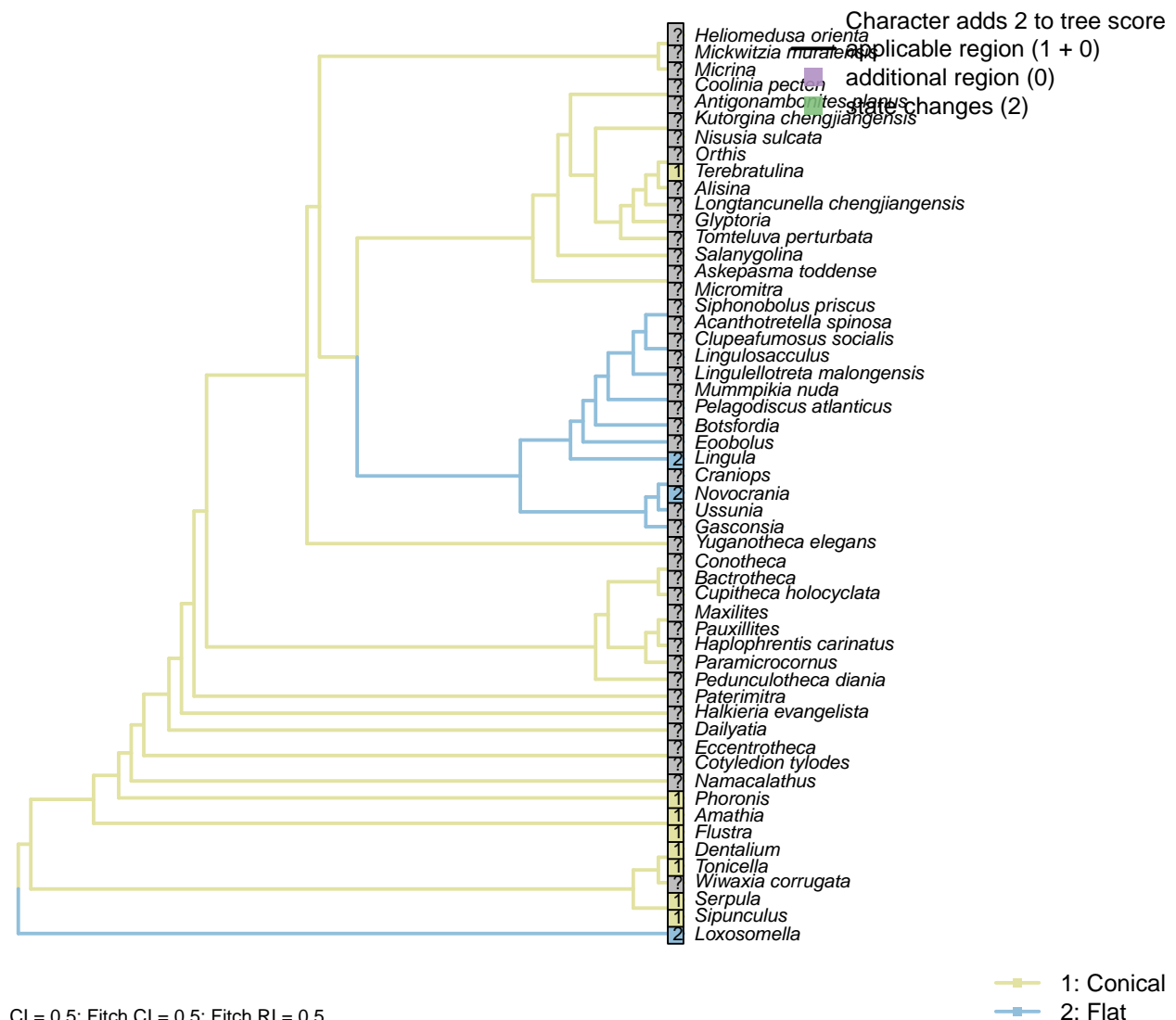
After Lundin et al. (2009). The vertical ciliary rootlet is also termed the posterior rootlet.

*Amathia*: Reed and Cloney (1982).

*Loxosomella*: Details of ciliary ultrastructure are illustrated in Nielsen and Rostgaard (1976).

*Terebratulina*: Long (Lüter, 1995).

## [198] Shape

**Character 198: Ciliary ultrastructure: Vertical ciliary rootlet: Shape**

1: Conical

2: Flat

Transformational character.

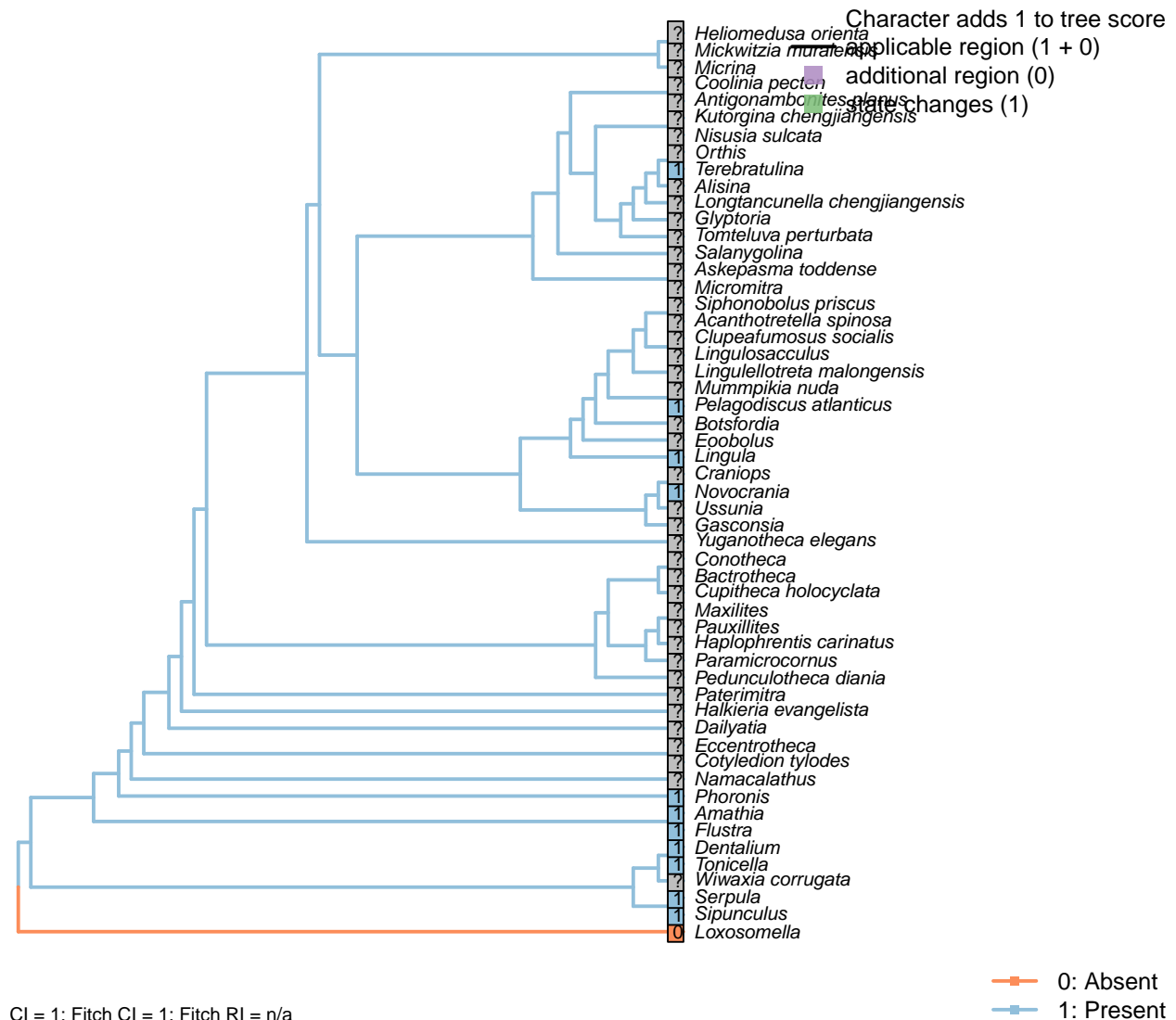
After Lundin et al. (2009). The vertical ciliary rootlet is also termed the posterior rootlet.

*Amathia*: Reed and Cloney (1982).

*Serpula*: Conical in *Enchytraeus* (Reger, 1967) and *Magelona* (Bartolomaeus, 1995).

*Terebratulina*: Conical: tapering to a point (Lüter, 1995).

## [199] Presence



## Character 199: Ciliary ultrastructure: Secondary ciliary rootlet: Presence

0: Absent

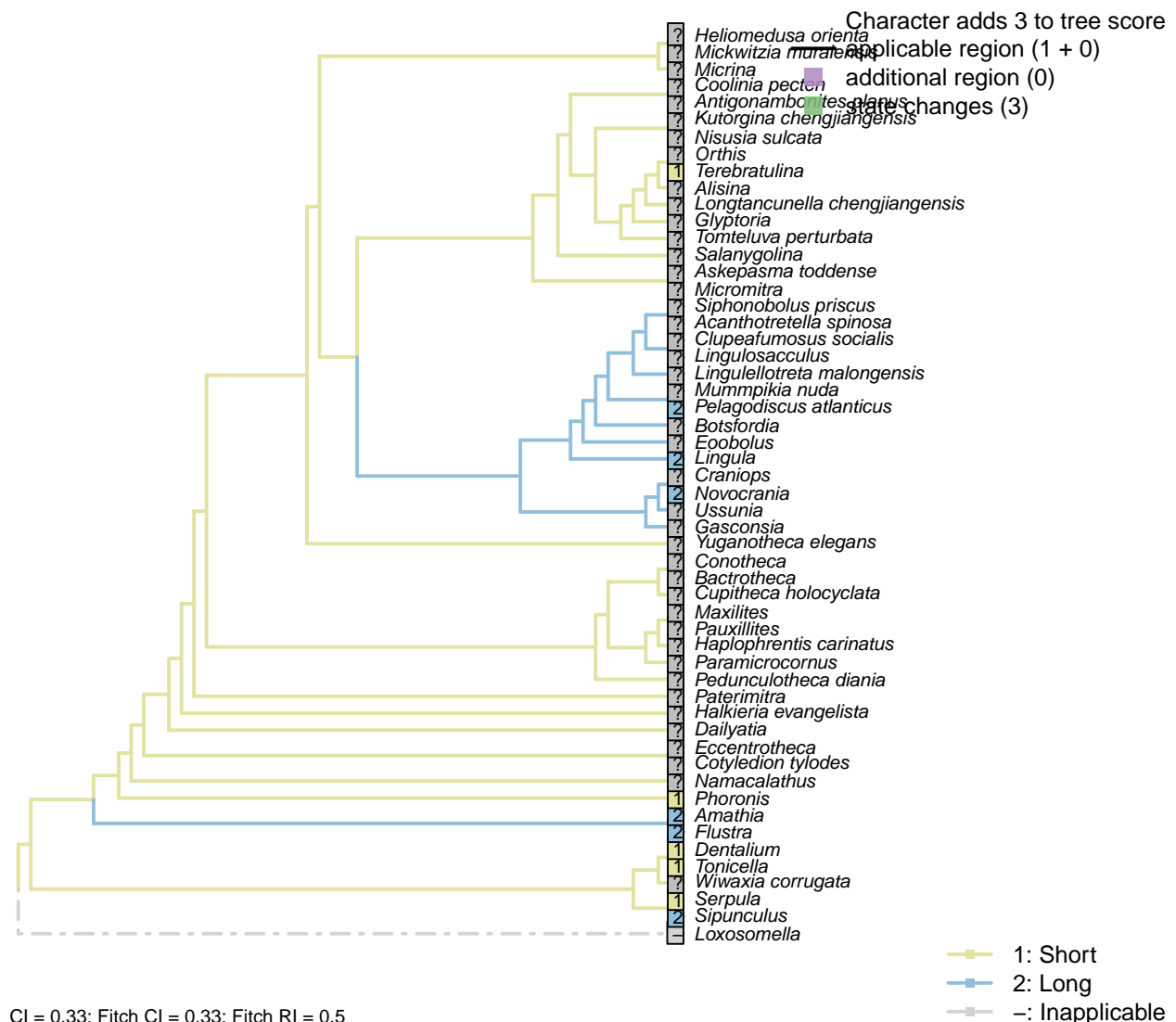
1: Present

Neomorphic character.

After Lundin et al. (2009). The secondary ciliary rootlet is also termed the anterior ciliary rootlet.

*Amathia*: Reed and Cloney (1982).

## [200] Length

**Character 200: Ciliary ultrastructure: Secondary ciliary rootlet: Length**

1: Short

2: Long

Transformational character.

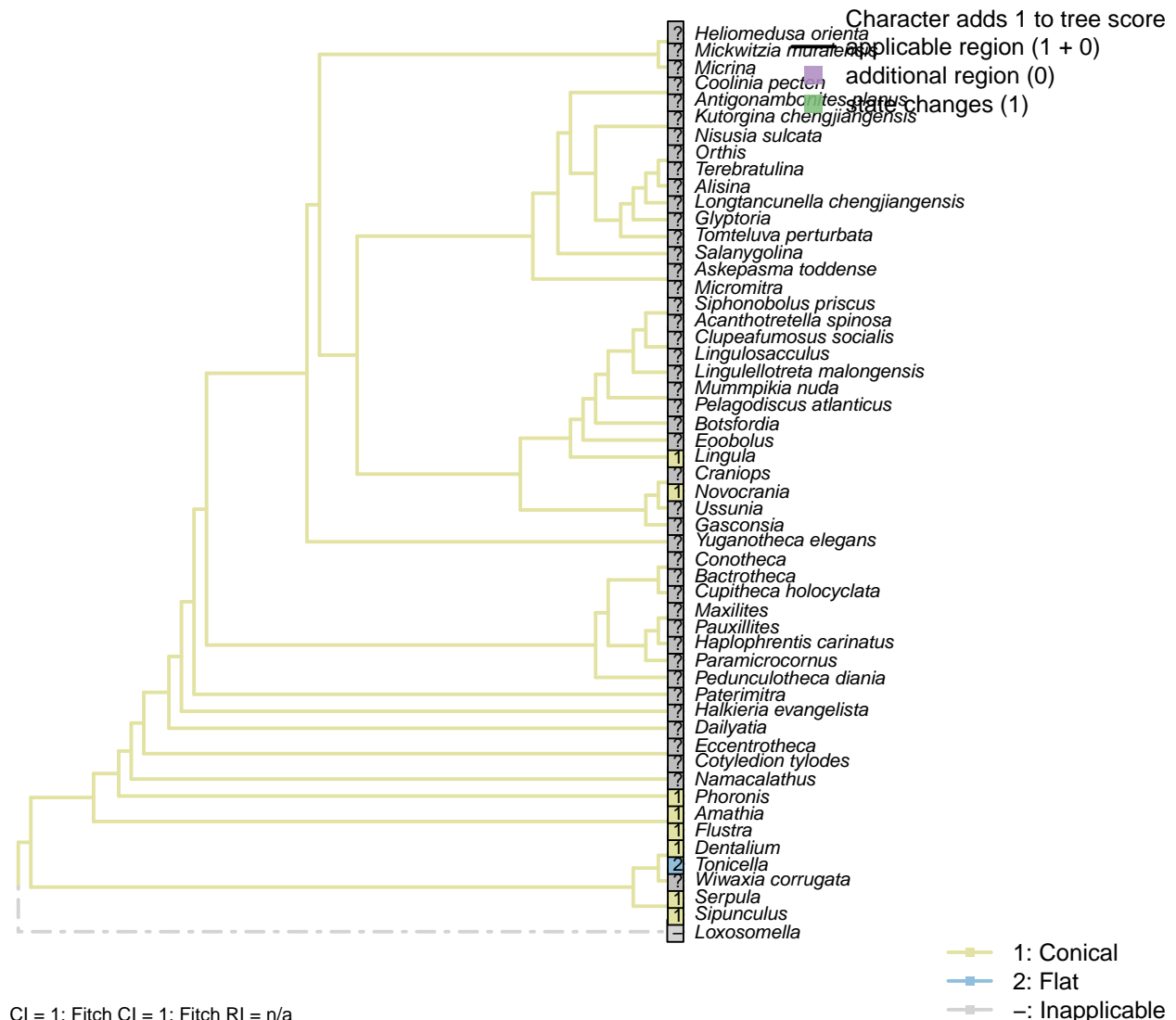
After Lundin et al. (2009). The secondary ciliary rootlet is also termed the anterior ciliary rootlet.

*Amathia*: Reed and Cloney (1982).

*Serpula*: Short in *Enchytraeus* (Reger, 1967), *Magelona* (Bartolomaeus, 1995) and *Harmothoe* (Holborow et al., 1969).

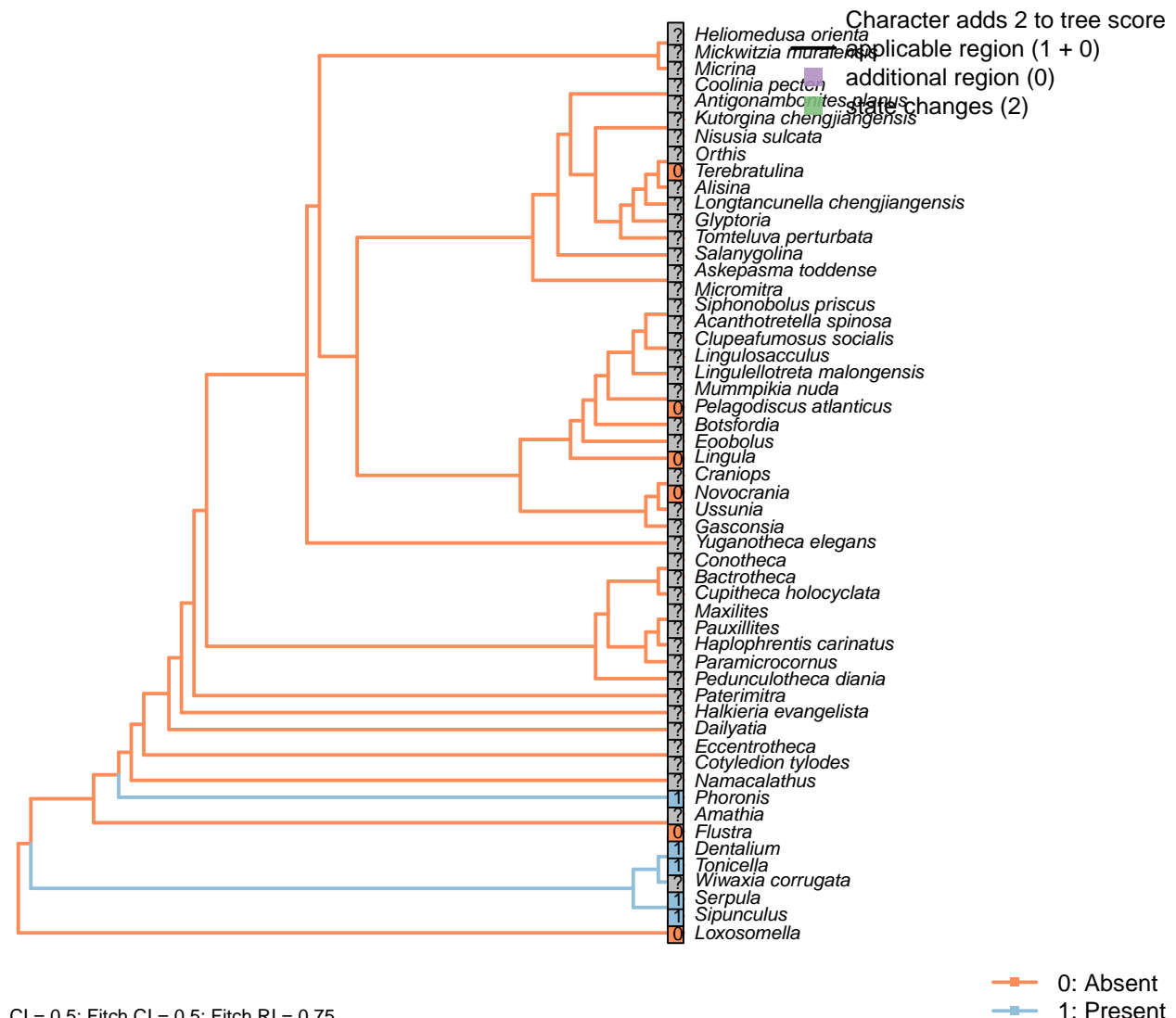
*Terebratulina*: “Very small” – Lüter (1995).

## [201] Shape

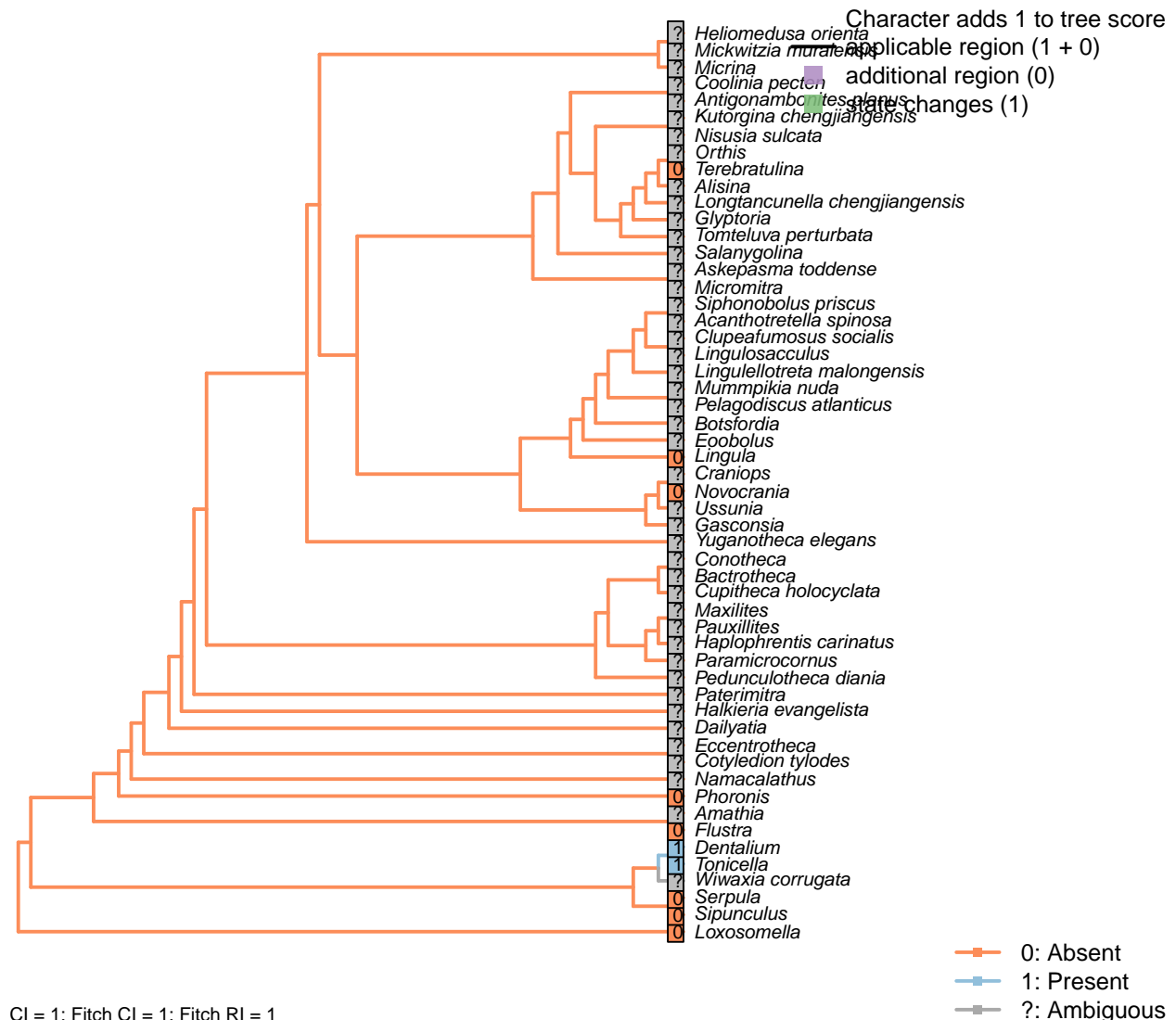


## 5.24 Nephridia

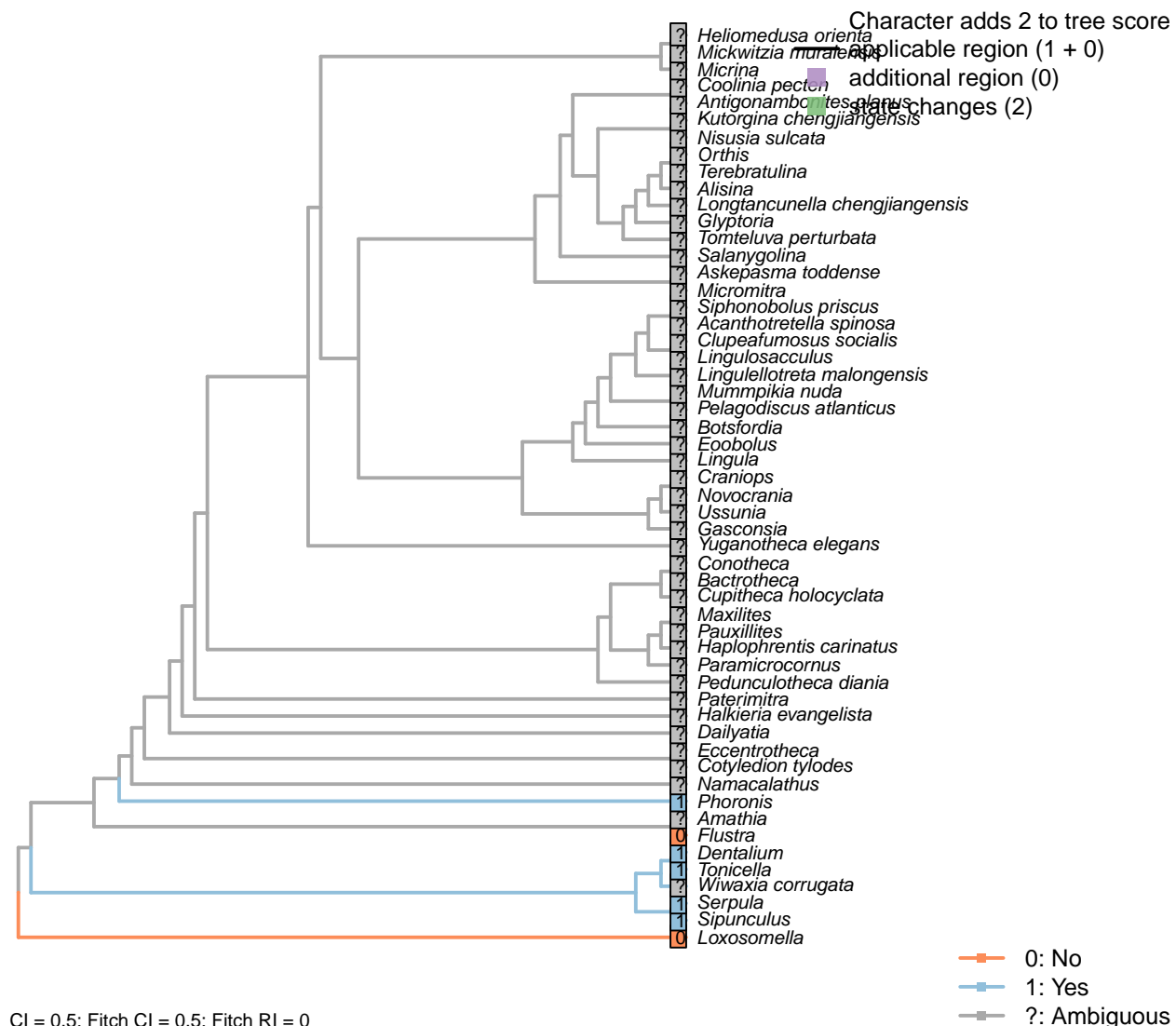
### [202] Podocytes



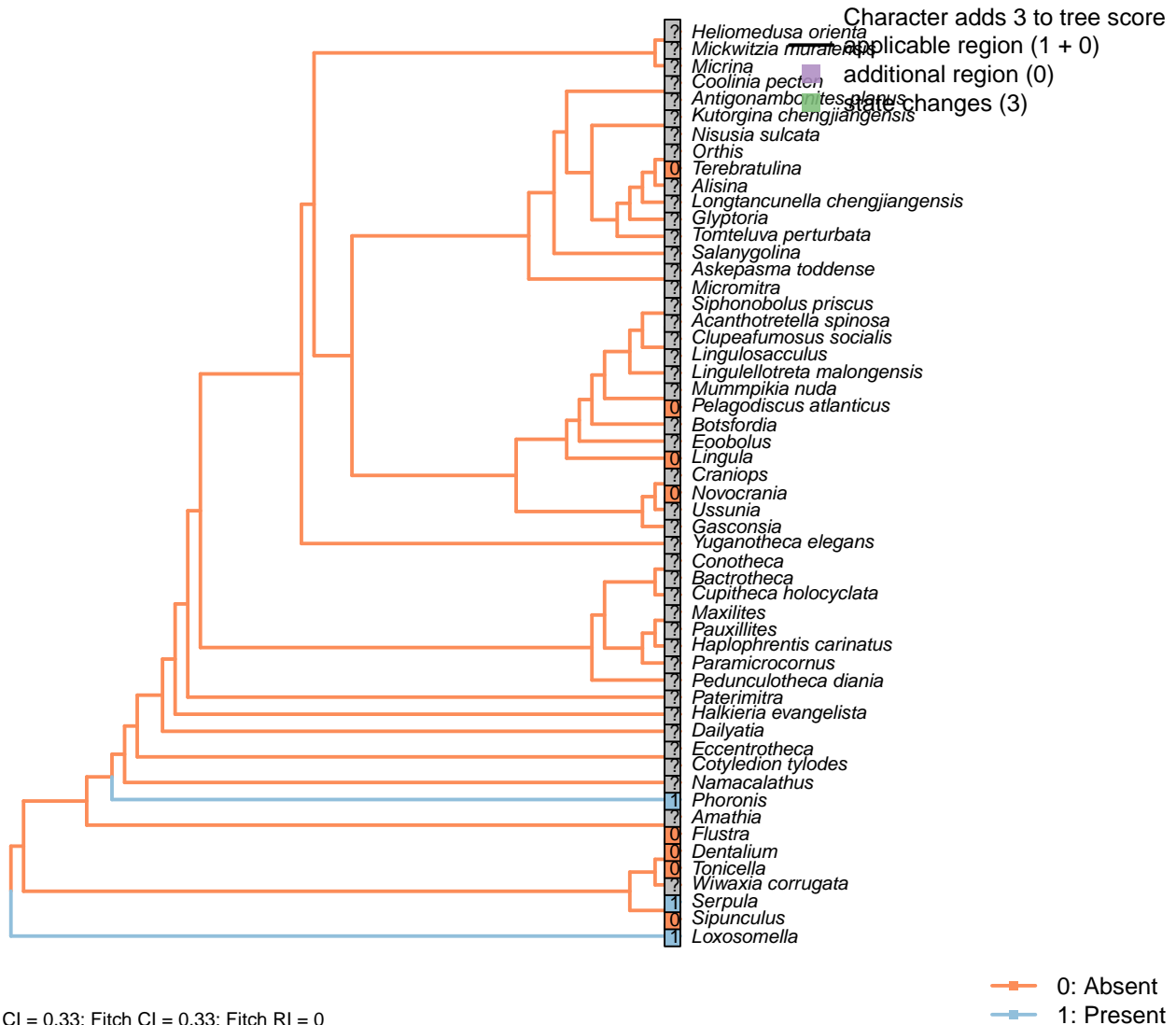
## [203] Rhogocytes



## [204] Serve as excretory organs

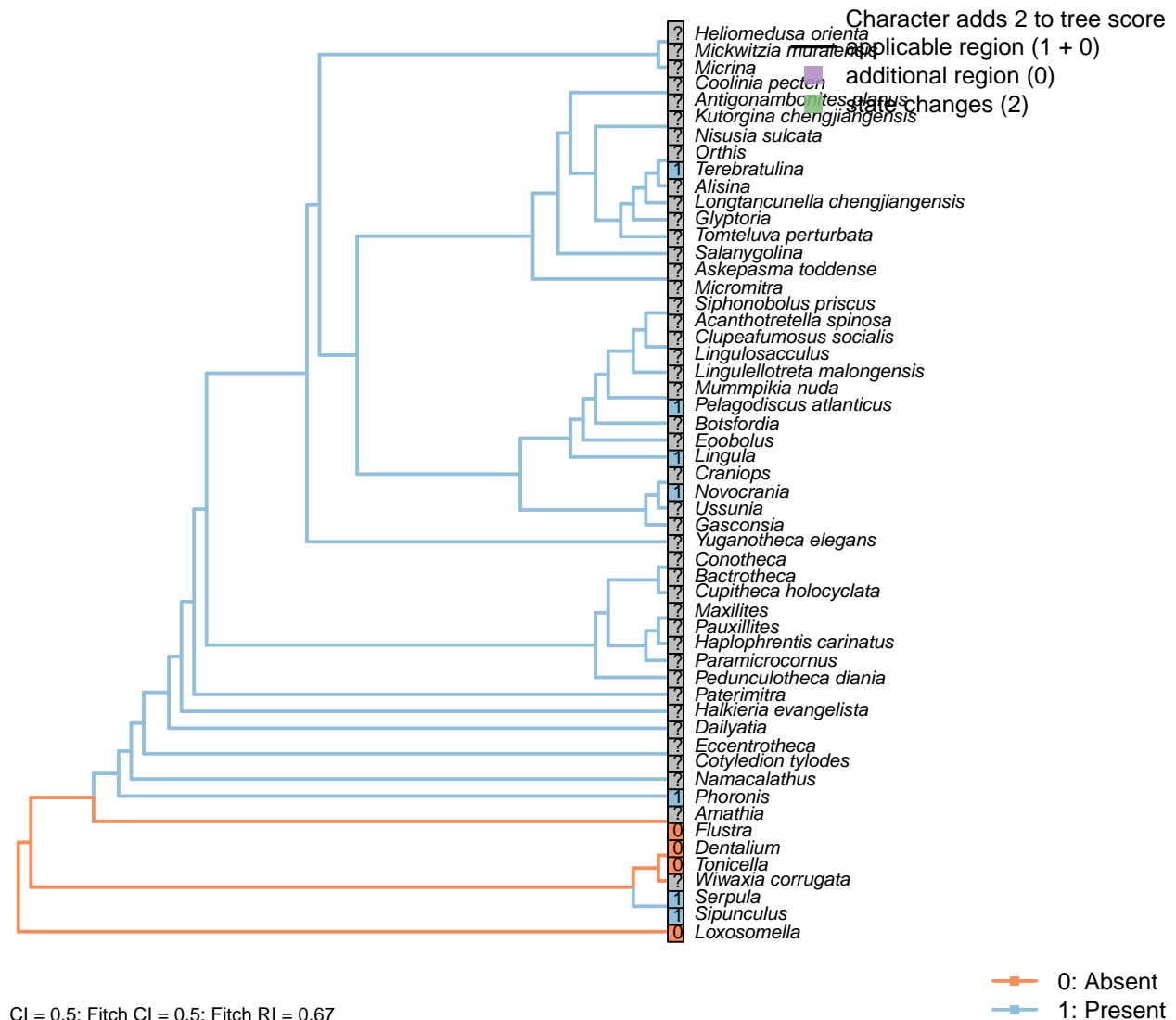


## [205] Protonephridia



Also termed cyrtocytes. Character 21 in Grobe (2007); 1.47 in von Salvini-Plawen and Steiner (1996); 138 in Rouse (1999); 20 in Haszprunar (1996); 90 in Glenner et al. (2004).

## [206] Metanephridia



## Character 206: Nephridia: Metanephridia

0: Absent

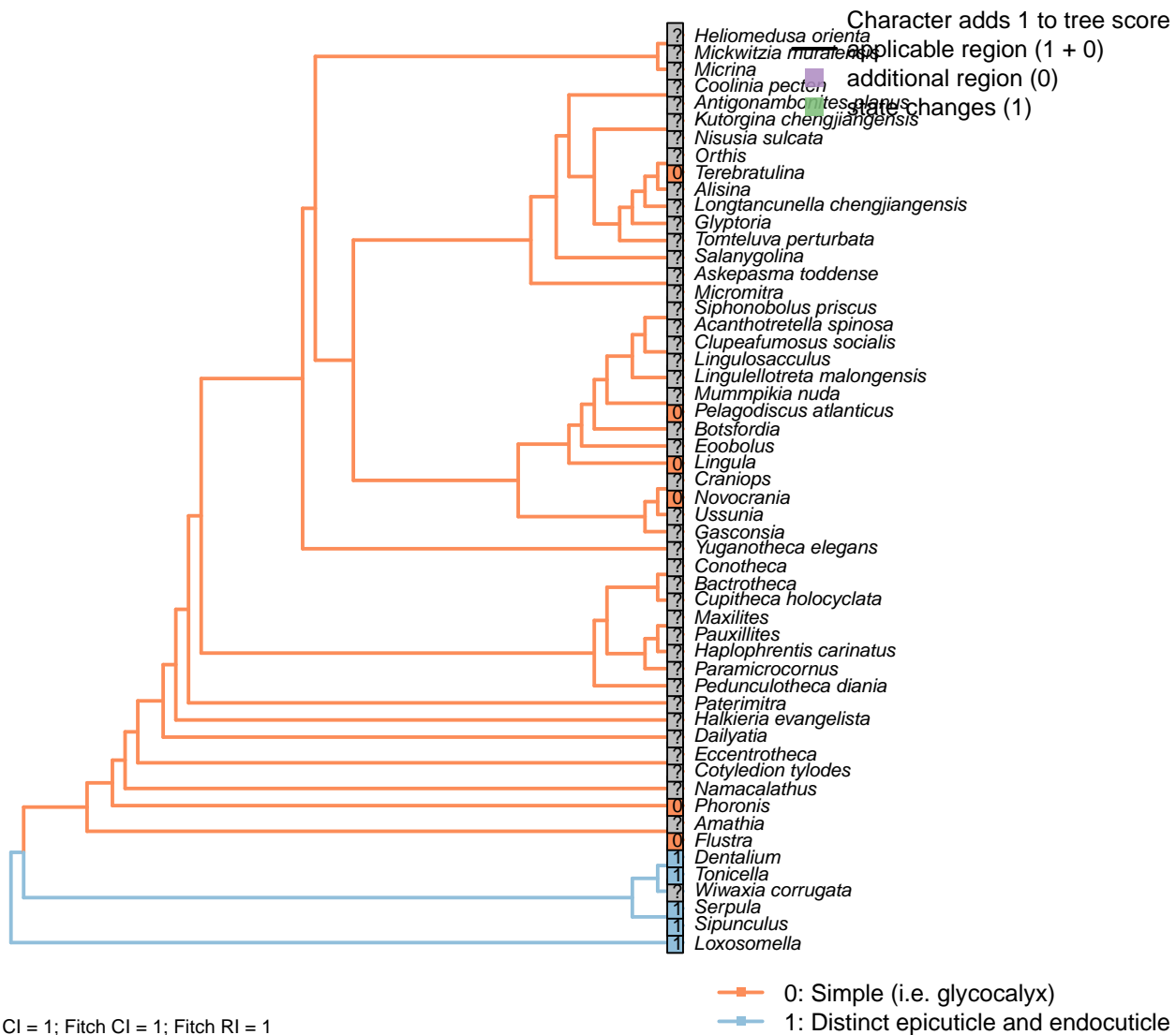
1: Present

Neomorphic character.

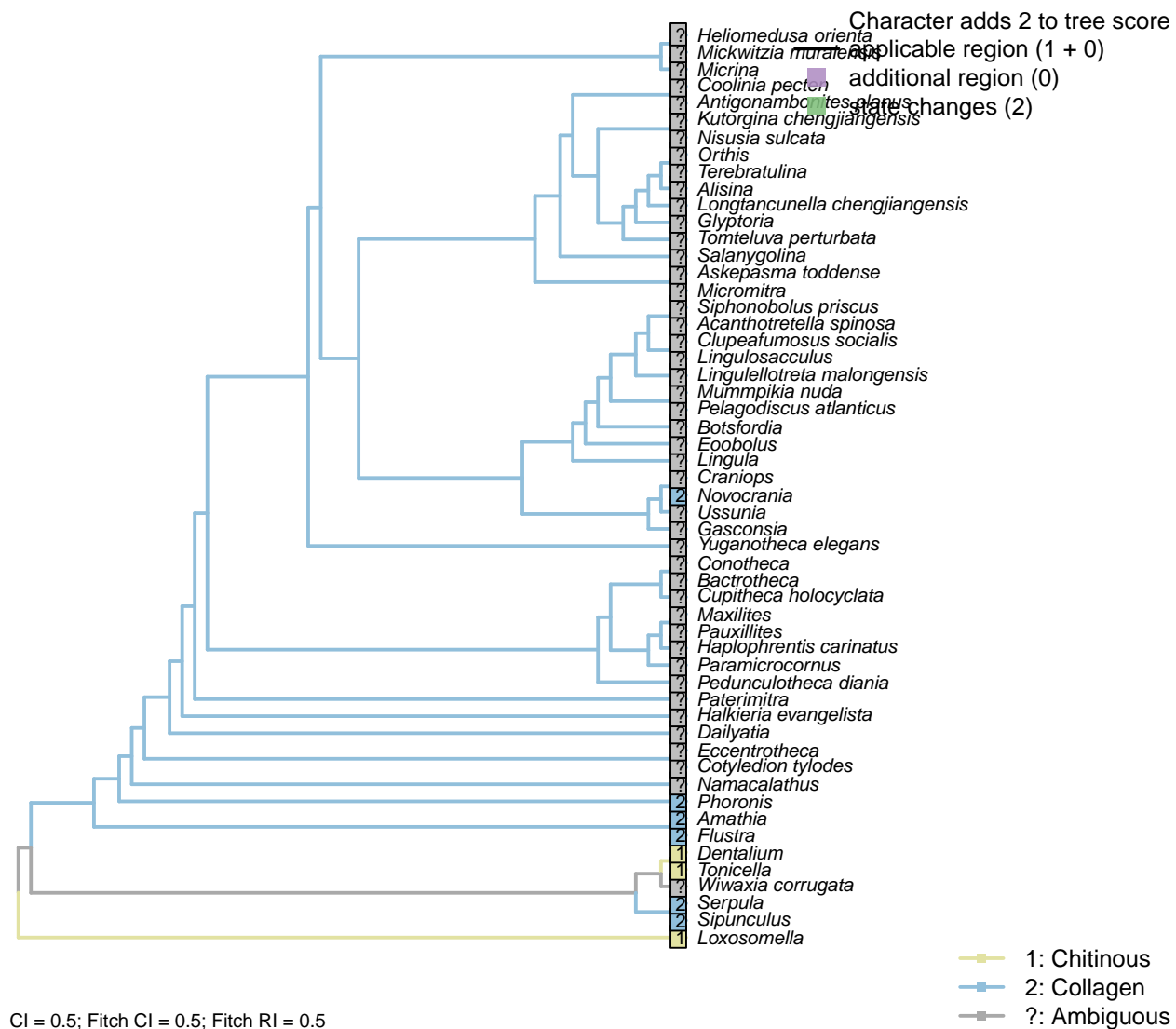
See characters 35 in Rouse (1999); 28 in Haszprunar (2000); 93 in Glenner et al. (2004); 1.47 in von Salvini-Plawen and Steiner (1996); 21 in Grobe (2007); 138 in Rouse (1999); 20 in Haszprunar (1996).

## 5.25 Cuticle

[207] Layers



## [208] Composition



## Character 208: Cuticle: Composition

1: Chitinous

2: Collagen

Transformational character.

Character 2 in Haszprunar and Wanninger (2008).

*Flustra, Amathia*: Collagenous (Schopf and Manheim, 1967), though chitin is associated with the exoskeleton (Hunt, 1972).*Tonicella, Dentalium*: Haszprunar and Wanninger (2008).*Pelagodiscus atlanticus, Lingula, Terebratulina*: The brachiopod pedicle has a chitinous cuticle (Williams et al., 1997; MacKay and Hewitt, 1978), but the tentacles are associated with collagen (Williams et al., 1997); marked as polymorphic.*Loxosomella*: Absent (Haszprunar and Wanninger, 2008). Chitin is occasionally present in certain species,

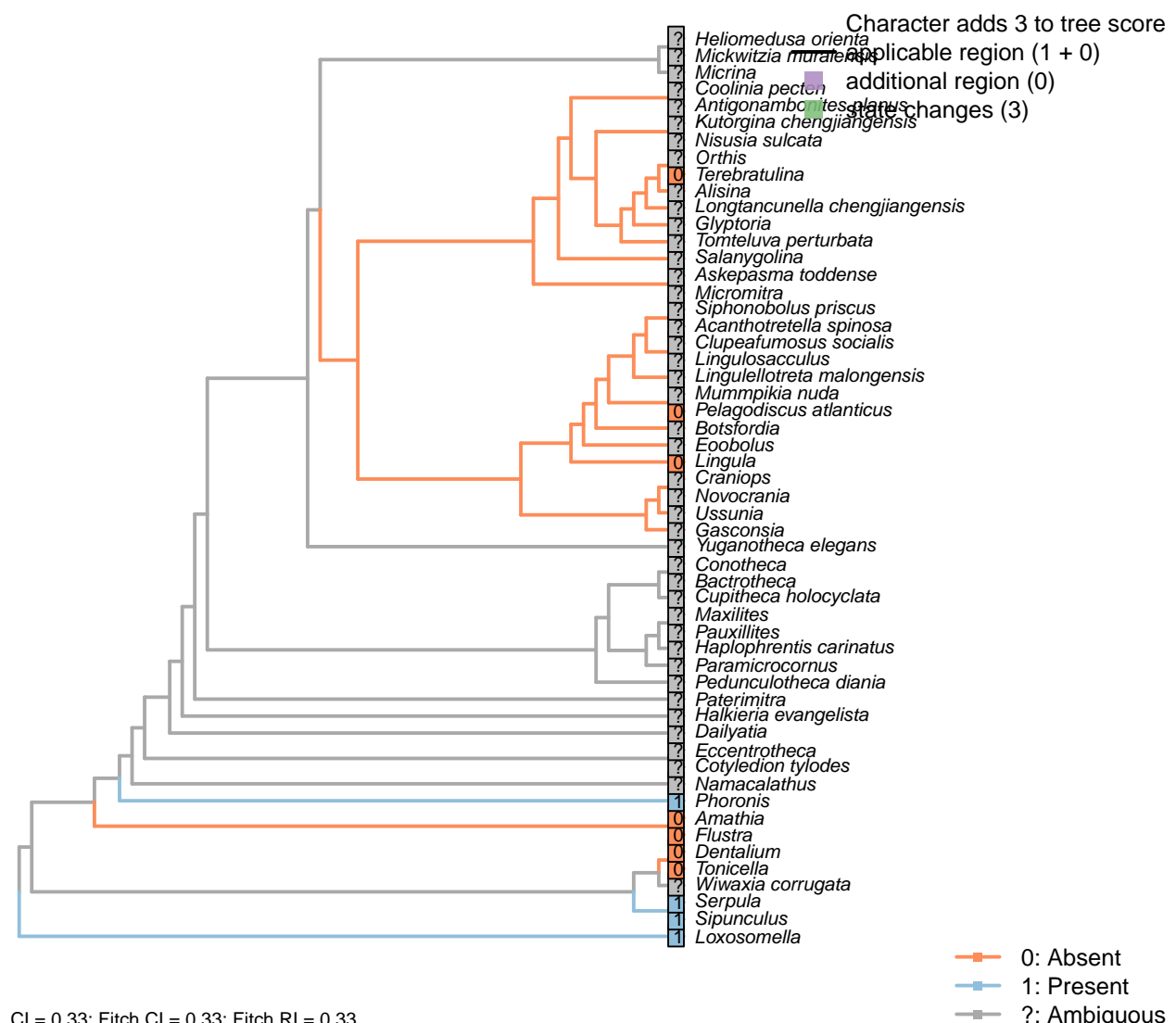
perhaps in regions where rigidity is necessary (Borisanova et al., 2015).

*Novocrania*: No (chitinous) pedicle, so only collagenous cuticle present (Williams et al., 1997).

*Phoronis*: Collagen fibres in tentacle cuticle (Bartolomaeus, 2001); chitin only present in tubes (Jeuniaux, 1971).

*Sipunculus*: Collagenous (Goffinet et al., 1978).

## [209] Fibrous layer with thick fibrils



### Character 209: Cuticle: Fibrous layer with thick fibrils

0: Absent

1: Present

Neomorphic character.

After Borisanova et al. (2015).

*Loxosomella, Flustra, Amathia, Serpula, Tonicella, Dentalium:* Following table 2 in Borisanova et al. (2015).

*Lingula:* Pedicle cuticle entirely homogeneous (Williams et al., 1997).

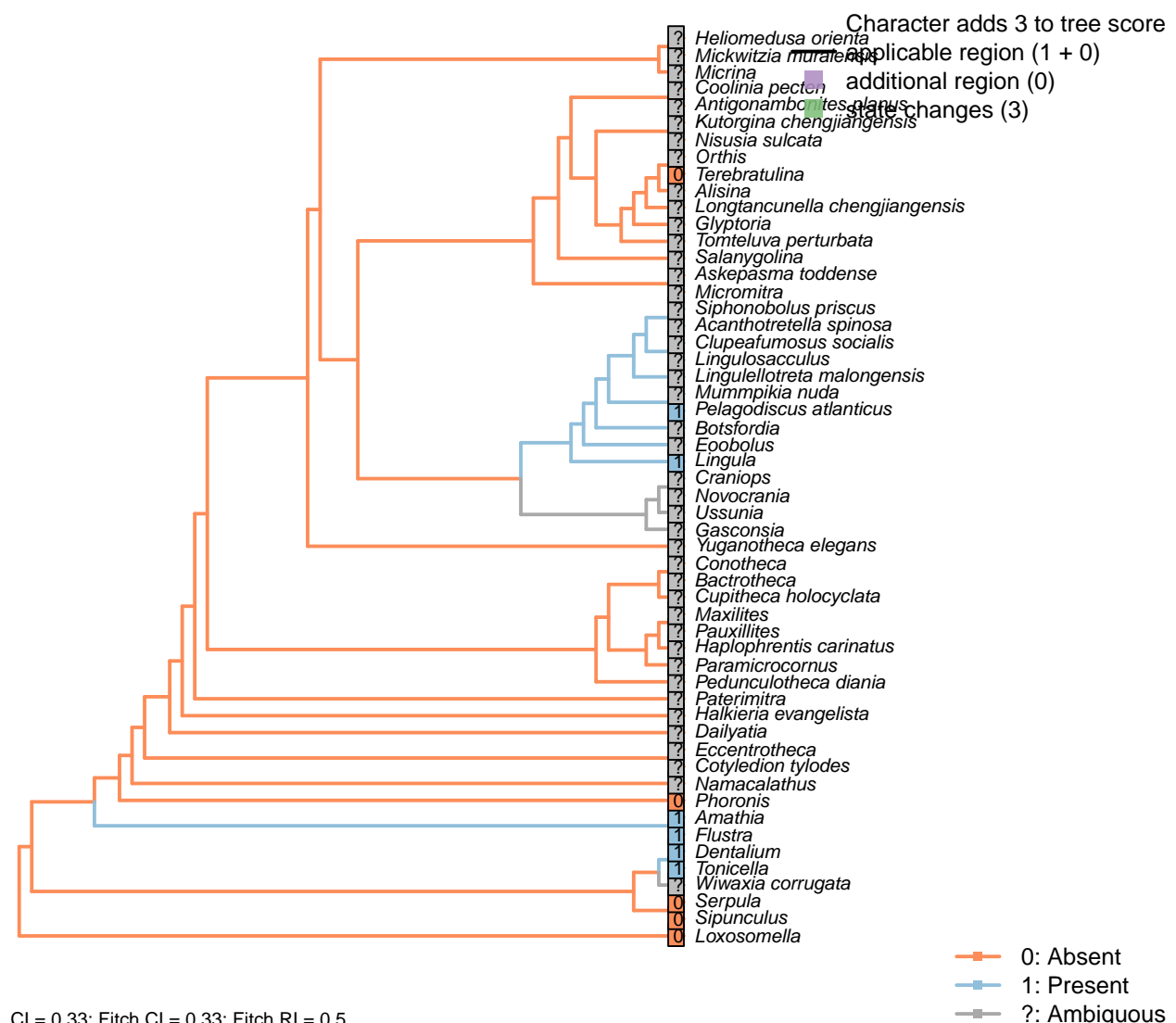
*Pelagodiscus atlanticus:* Microvilli in otherwise homogeneous epidermis (Williams et al., 1997).

*Phoronis:* Outer layer seemingly fibrous (Bereiter-Hahn et al., 1984).

*Sipunculus:* Fibrous collagen only (Bereiter-Hahn et al., 1984).

*Terebratulina:* Not evident in *Notosaria* (Bereiter-Hahn et al., 1984; Williams et al., 1997).

## [210] Homogeneous layer



0: Absent

1: Present

Neomorphic character.

After Borisanova et al. (2015).

*Loxosomella, Flustra, Amathia, Serpula, Tonicella, Dentalium:* Following table 2 in Borisanova et al. (2015).

*Lingula:* Pedicle cuticle entirely homogeneous (Williams et al., 1997).

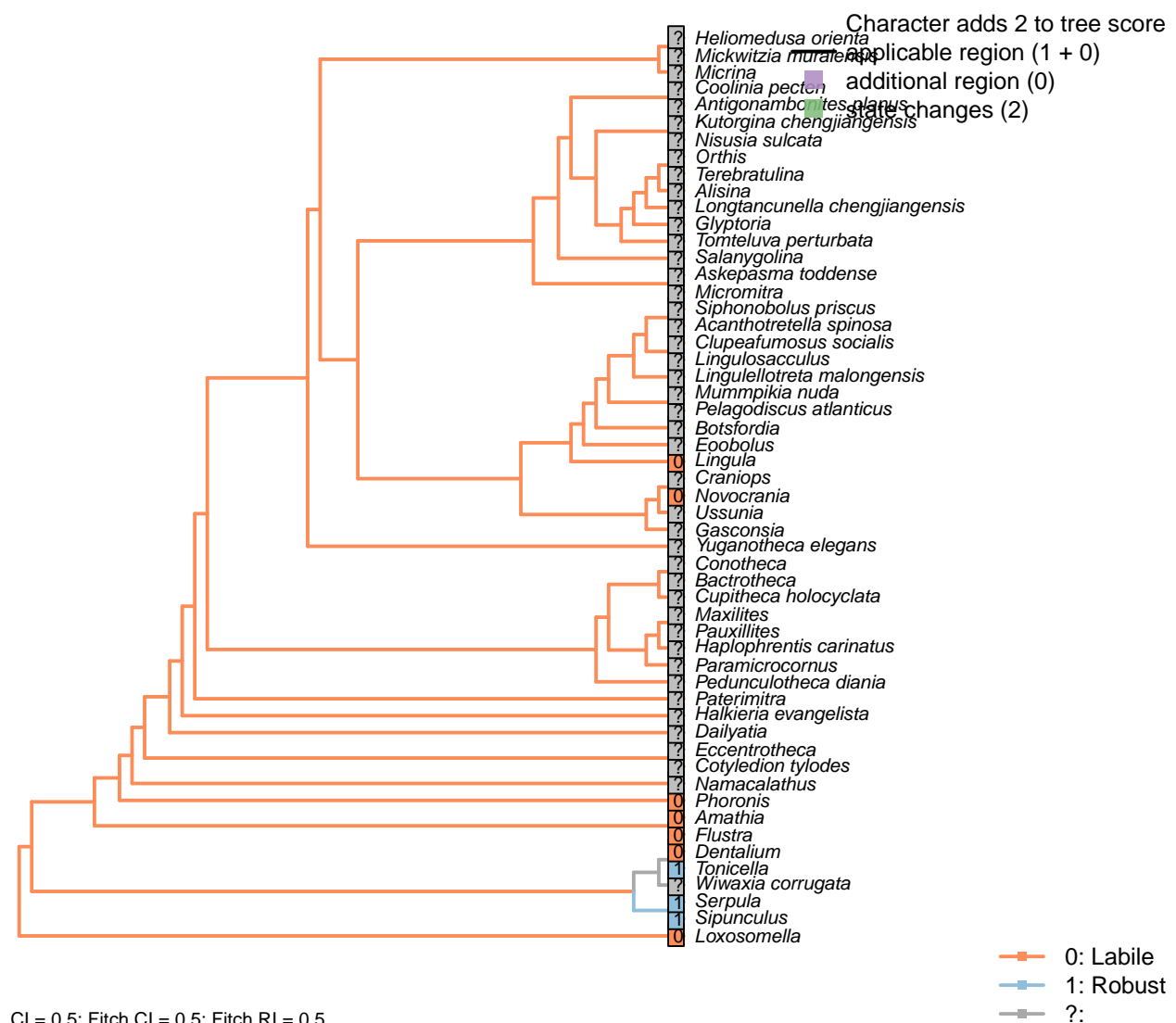
*Pelagodiscus atlanticus:* Microvilli in otherwise homogeneous epidermis (Williams et al., 1997).

*Phoronis:* Not evident (Bereiter-Hahn et al., 1984).

*Sipunculus:* Fibrous collagen only (Bereiter-Hahn et al., 1984).

*Terebratulina:* Cuticle is homogeneous in *Notosaria* (Bereiter-Hahn et al., 1984; Williams et al., 1997).

## [211] Resilience



### Character 211: Cuticle: Resilience

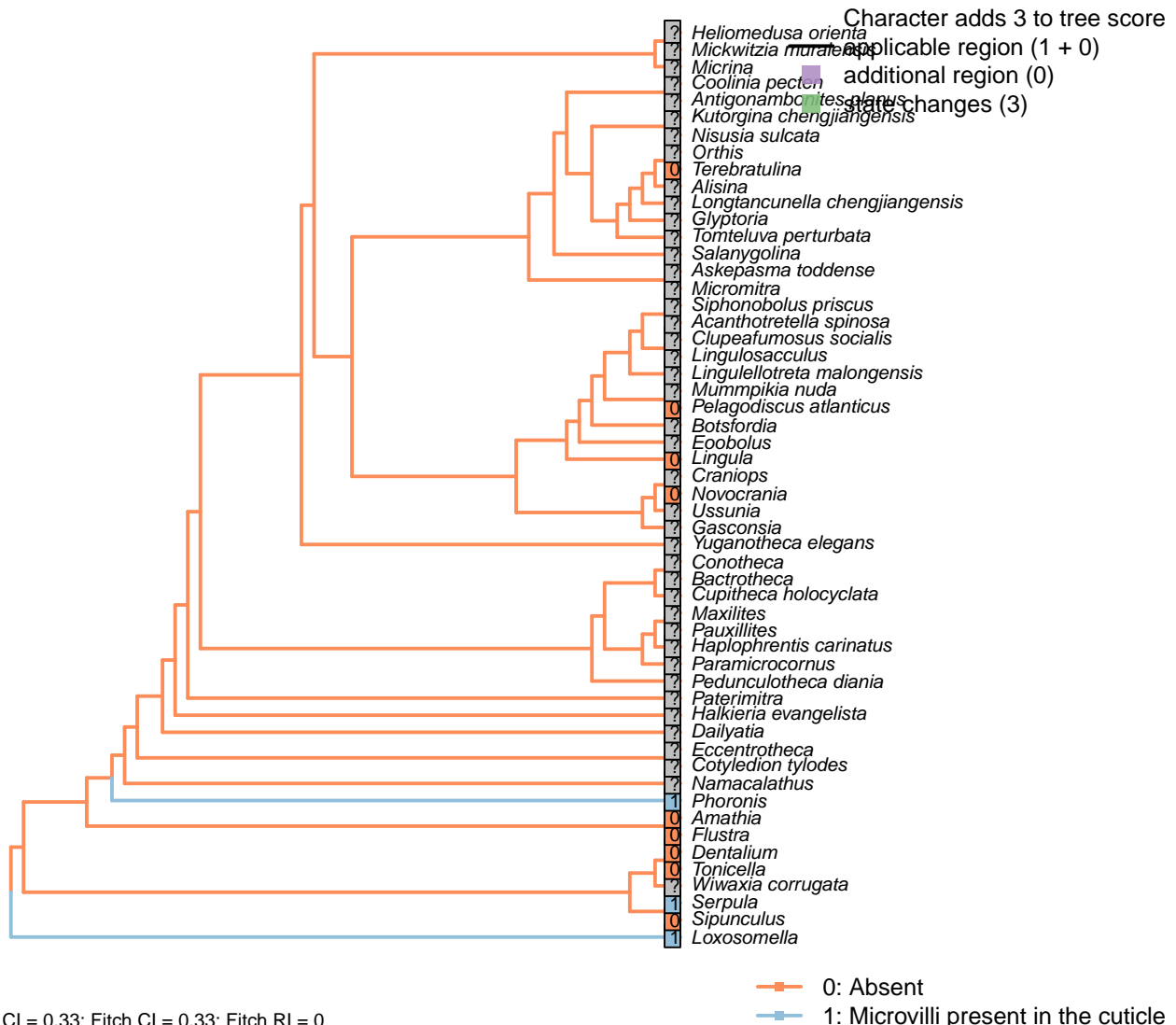
0: Labile

1: Robust

2:  
Neomorphic character.

Character 1 in Haszprunar (2000).

## [212] Microvilli



### Character 212: Cuticle: Microvilli

- 0: Absent
  - 1: Microvilli present in the cuticle
- Neomorphic character.

After Borisanova et al. (2015).

*Loxosomella, Flustra, Amathia, Serpula, Tonicella, Dentalium:* Following table 2 in Borisanova et al. (2015).

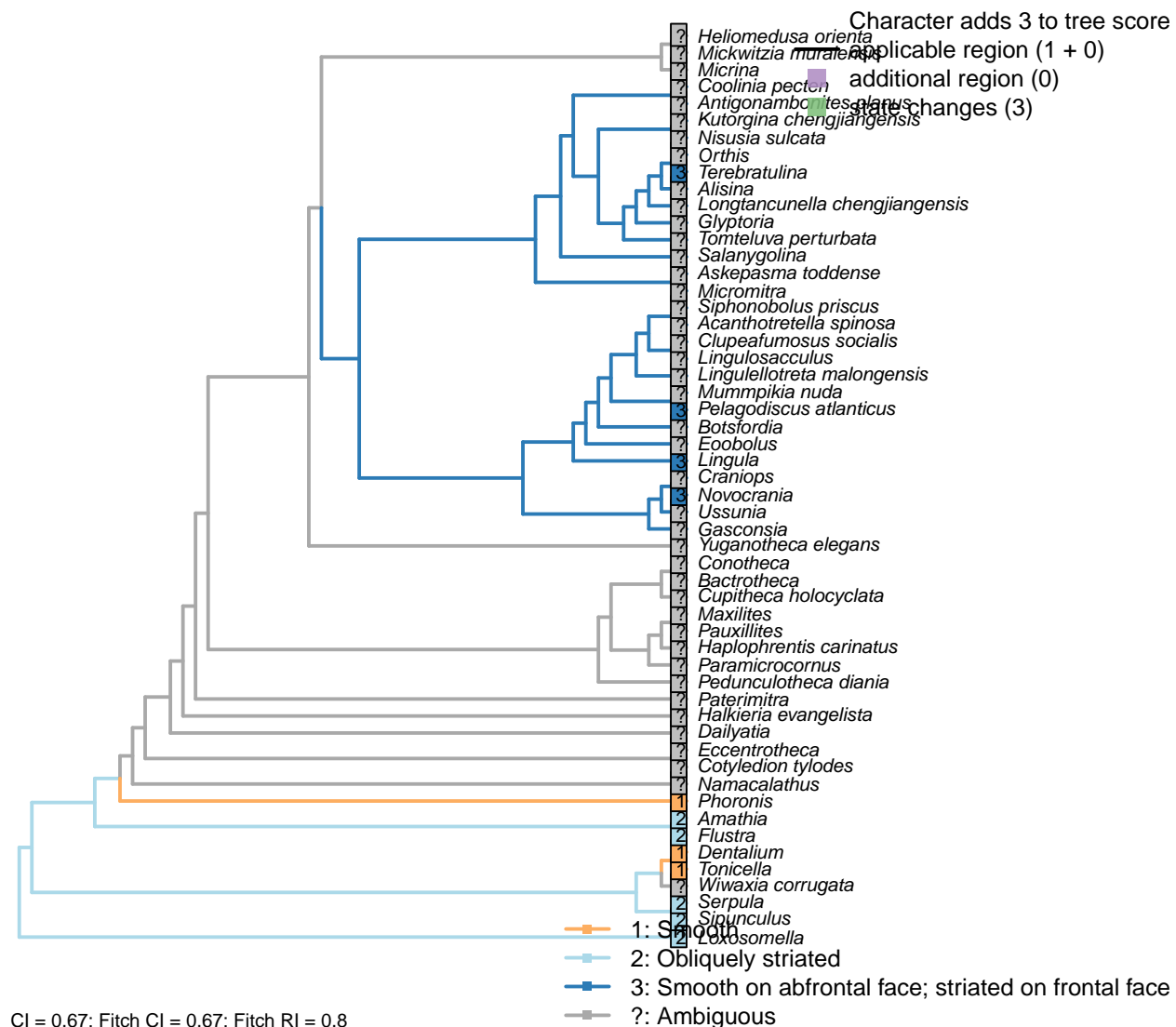
*Pelagodiscus atlanticus:* Microvillios inner epithelium in Discina (Williams et al., 1997).

*Phoronis:* Present on outer epithelium (Bereiter-Hahn et al., 1984).

*Sipunculus:* Fibrous collagen only (Bereiter-Hahn et al., 1984).

## 5.26 Muscles

### [213] Cytology



#### Character 213: Muscles: Cytology

1: Smooth

2: Obliquely striated

3: Smooth on abfrontal face; striated on frontal face  
Transformational character.

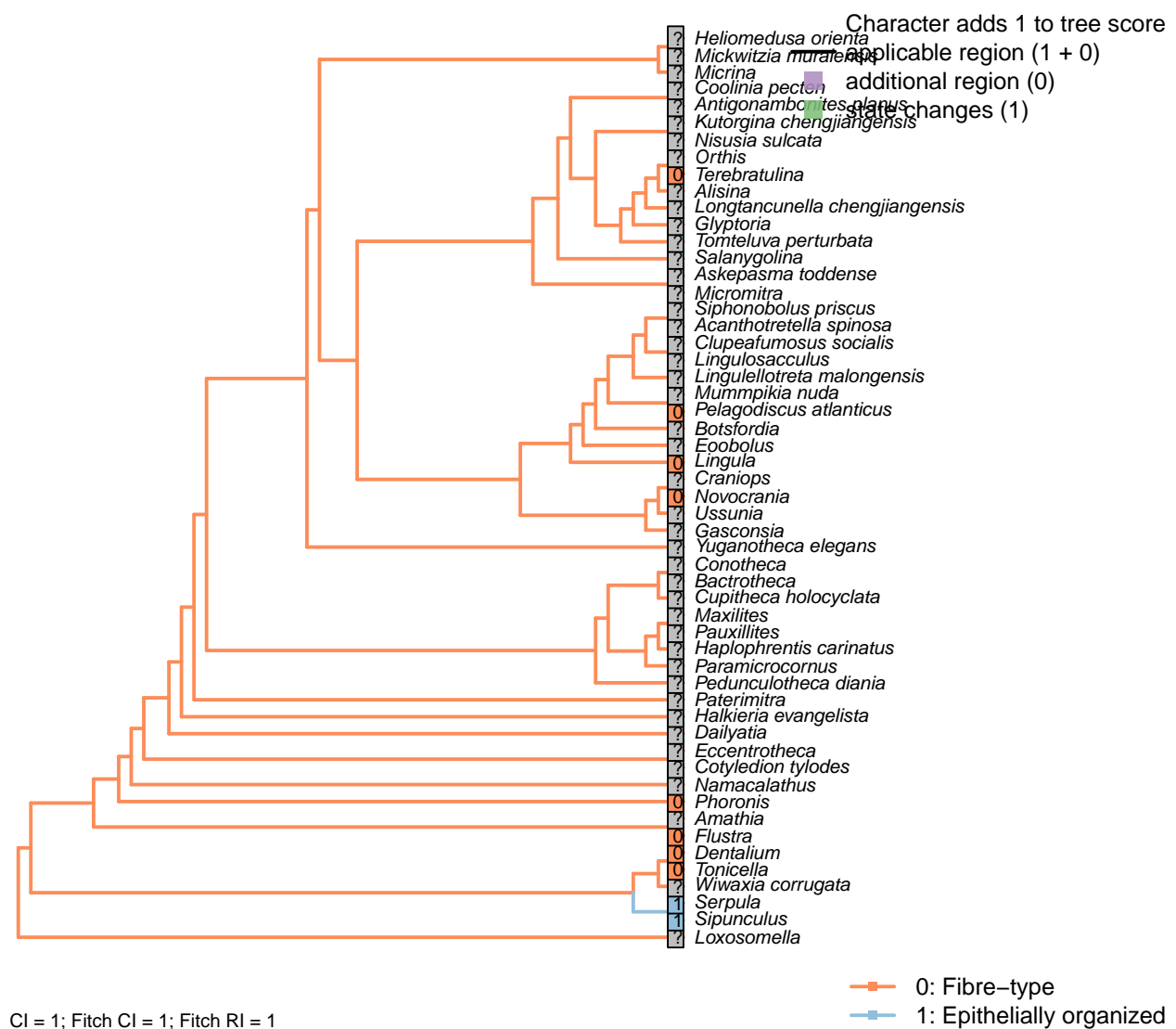
Character 19 in Haszprunar (1996); see also character 13 in Haszprunar (2000).

*Flustra, Amathia*: In Bryozoa, myofibrils are “all striated” (Pardos et al., 1991).

*Novocrania, Pelagodiscus atlanticus, Lingula, Terebratulina*: In brachiopods, myofibrils “are striated on the frontal face and smooth on the abfrontal face” (Pardos et al., 1991).

*Phoronis*: “In *P. australis* [...] all the myofibrils belong to the smooth type” – Pardos et al. (1991).

## [214] Histology



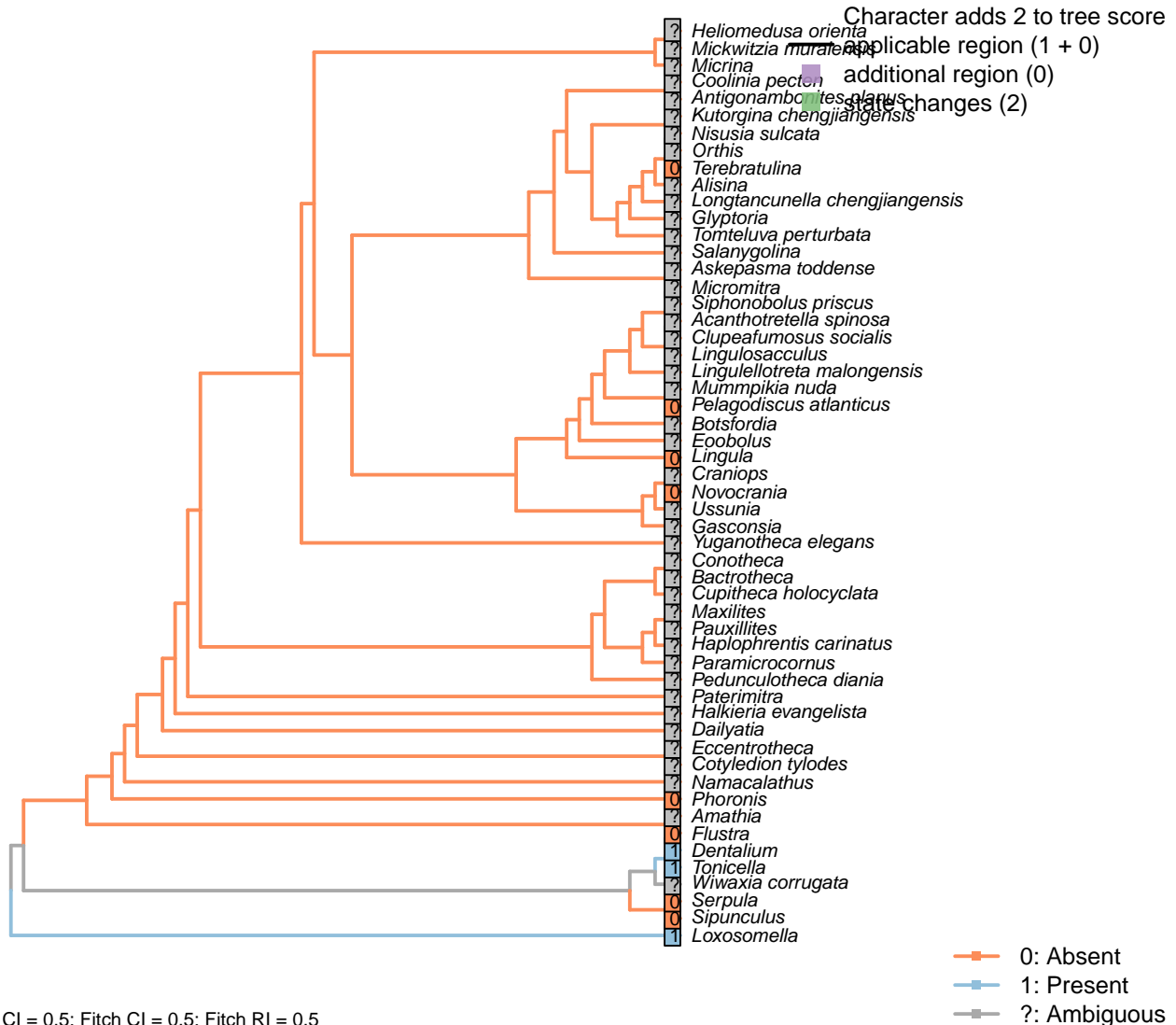
### Character 214: Muscles: Histology

- 0: Fibre-type
- 1: Epithelially organized
- 2:  
Neomorphic character.

See character 18 in Haszprunar (1996).

## 5.27 Glands

### [215] Pedal gland



CI = 0.5; Fitch CI = 0.5; Fitch RI = 0.5

#### Character 215: Glands: Pedal gland

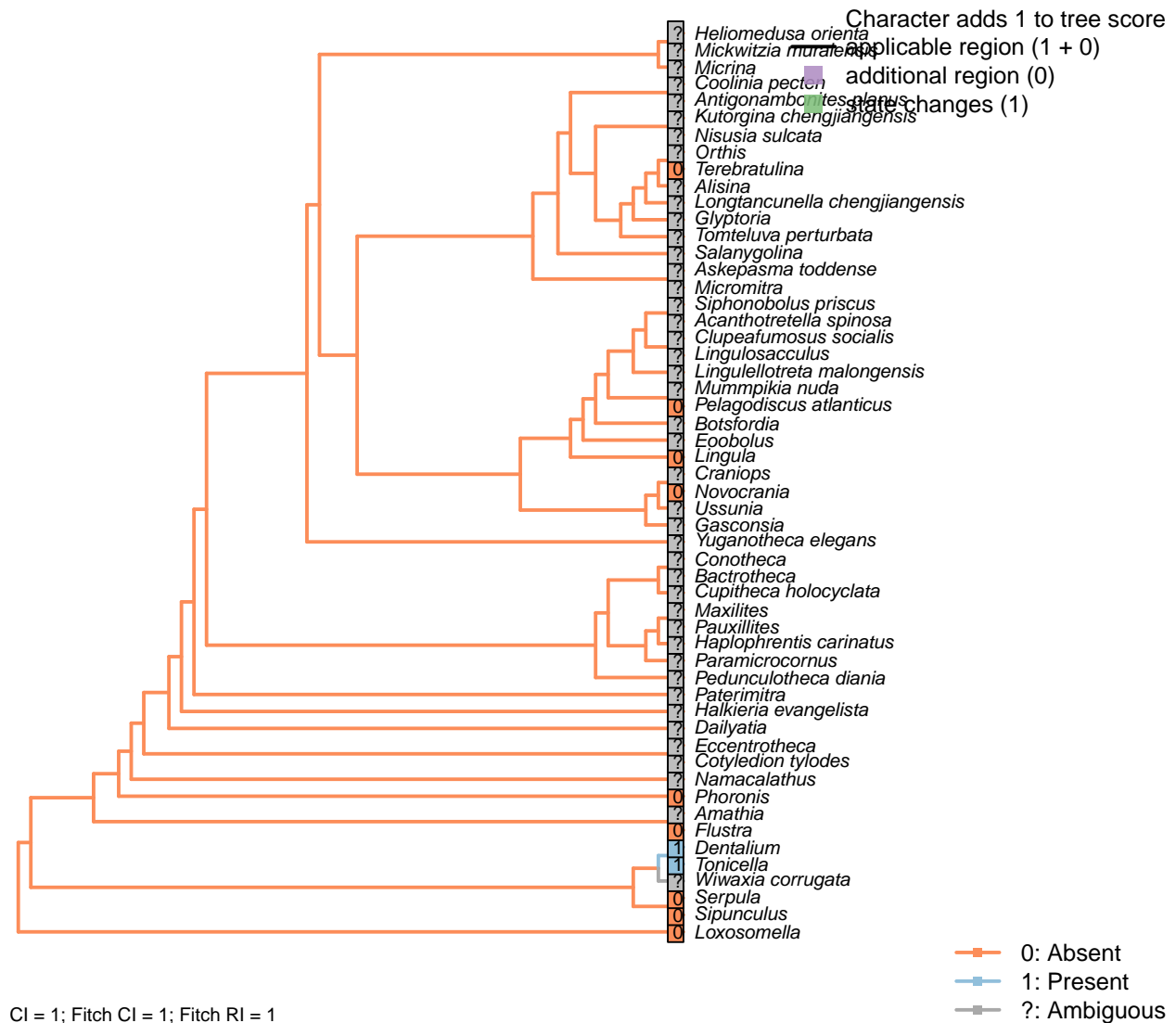
0: Absent

1: Present

Neomorphic character.

Characters 1.13, 1.40 & 2.08 in Scheltema (1993); 114 in Giribet and Wheeler (2002); 1.53 in von Salvini-Plawen and Steiner (1996); 9 in Haszprunar (1996).

## [216] Paired pharyngeal diverticulae



CI = 1; Fitch CI = 1; Fitch RI = 1

## Character 216: Glands: Paired pharyngeal diverticulae

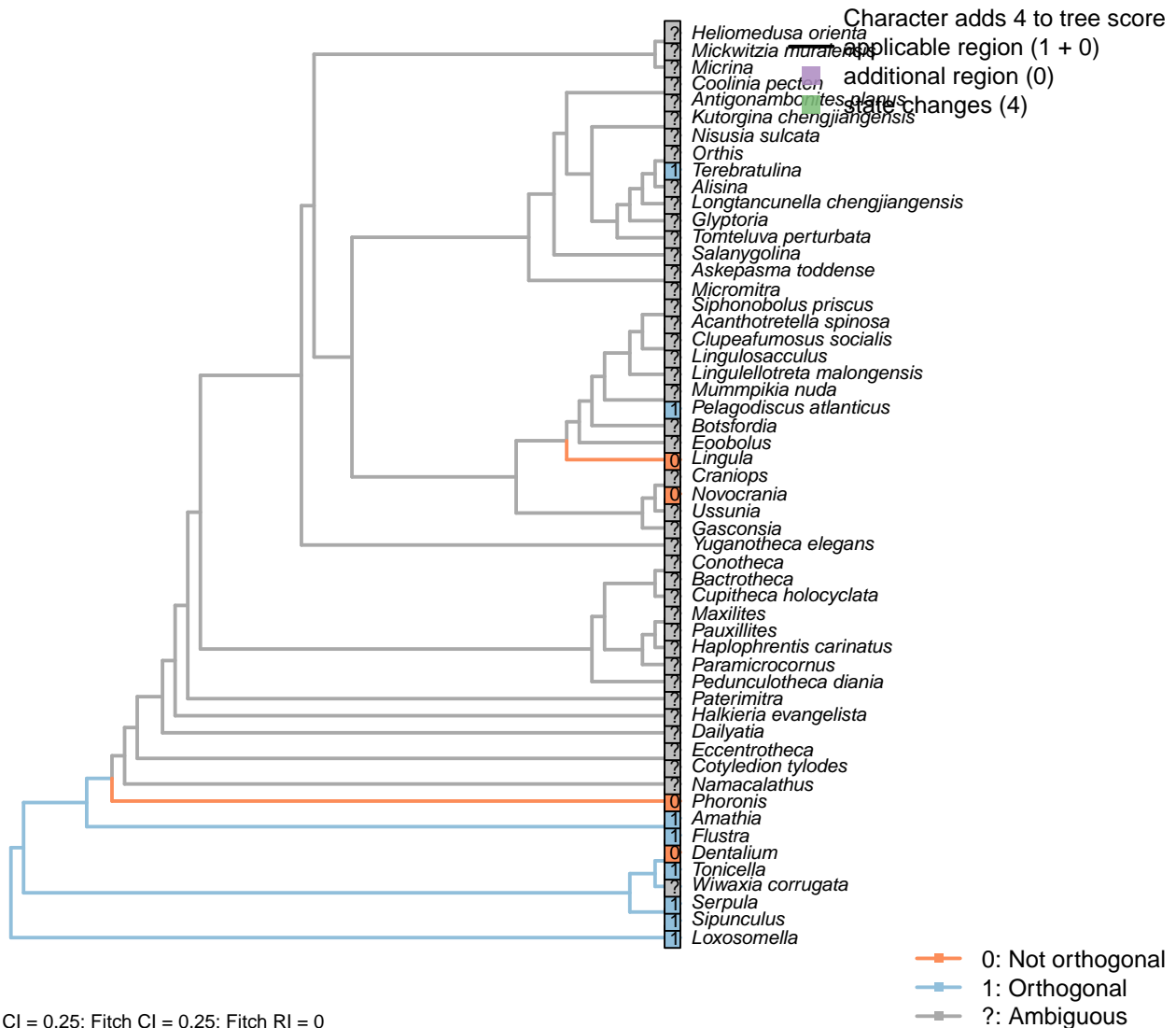
0: Absent

1: Present

Neomorphic character.

## 5.28 Nervous system

### [217] Orthogonal



#### Character 217: Nervous system: Orthogonal

0: Not orthogonal

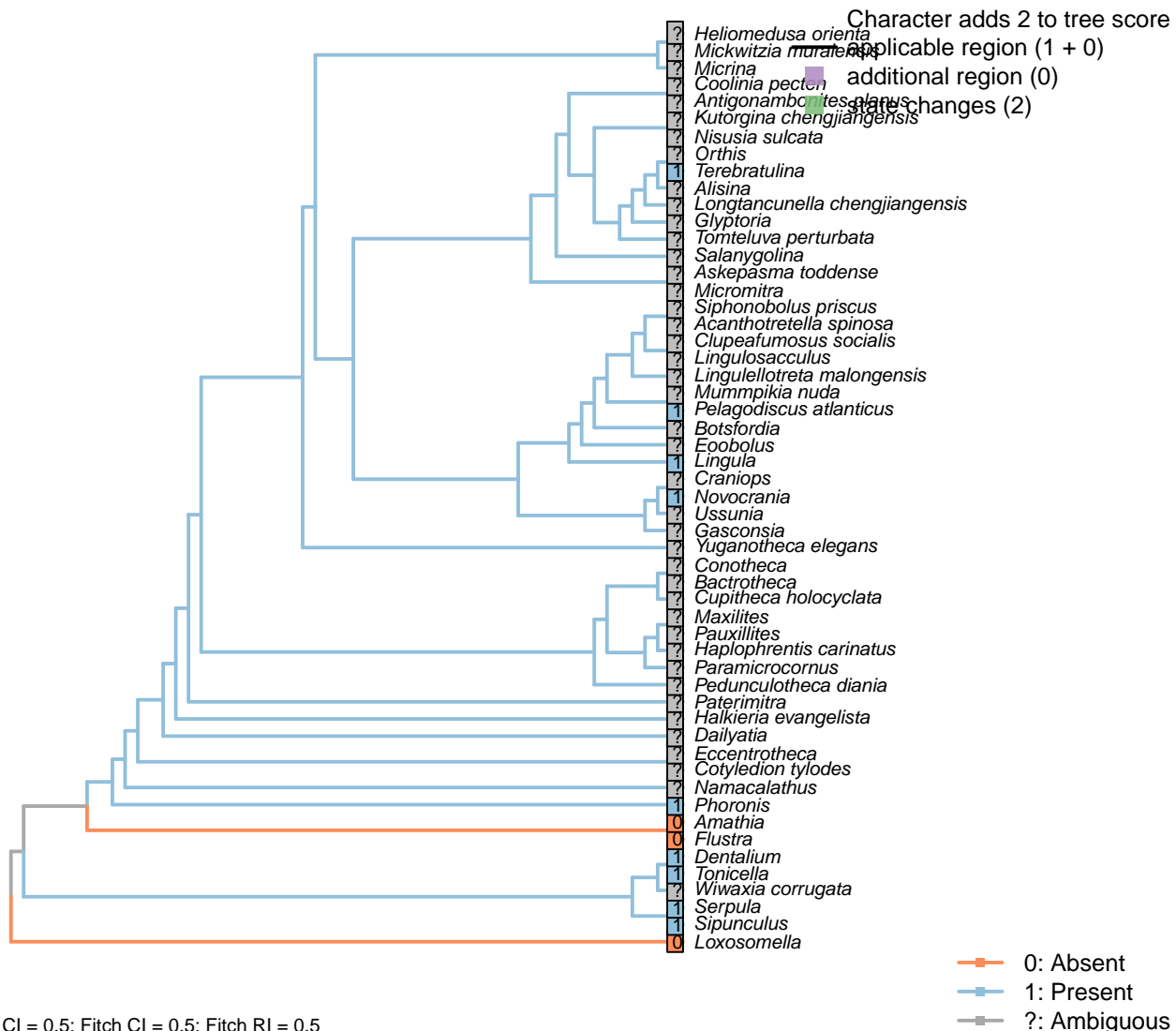
1: Orthogonal

Neomorphic character.

Character 14 in Haszprunar (1996). Paired longitudinal nerve cords regularly interconnected by transversal commissures to form a rectangular pattern.

*Amathia*: Temereva and Kosevich (2016).

## [218] Glial system



CI = 0.5; Fitch CI = 0.5; Fitch RI = 0.5

### Character 218: Nervous system: Glial system

0: Absent

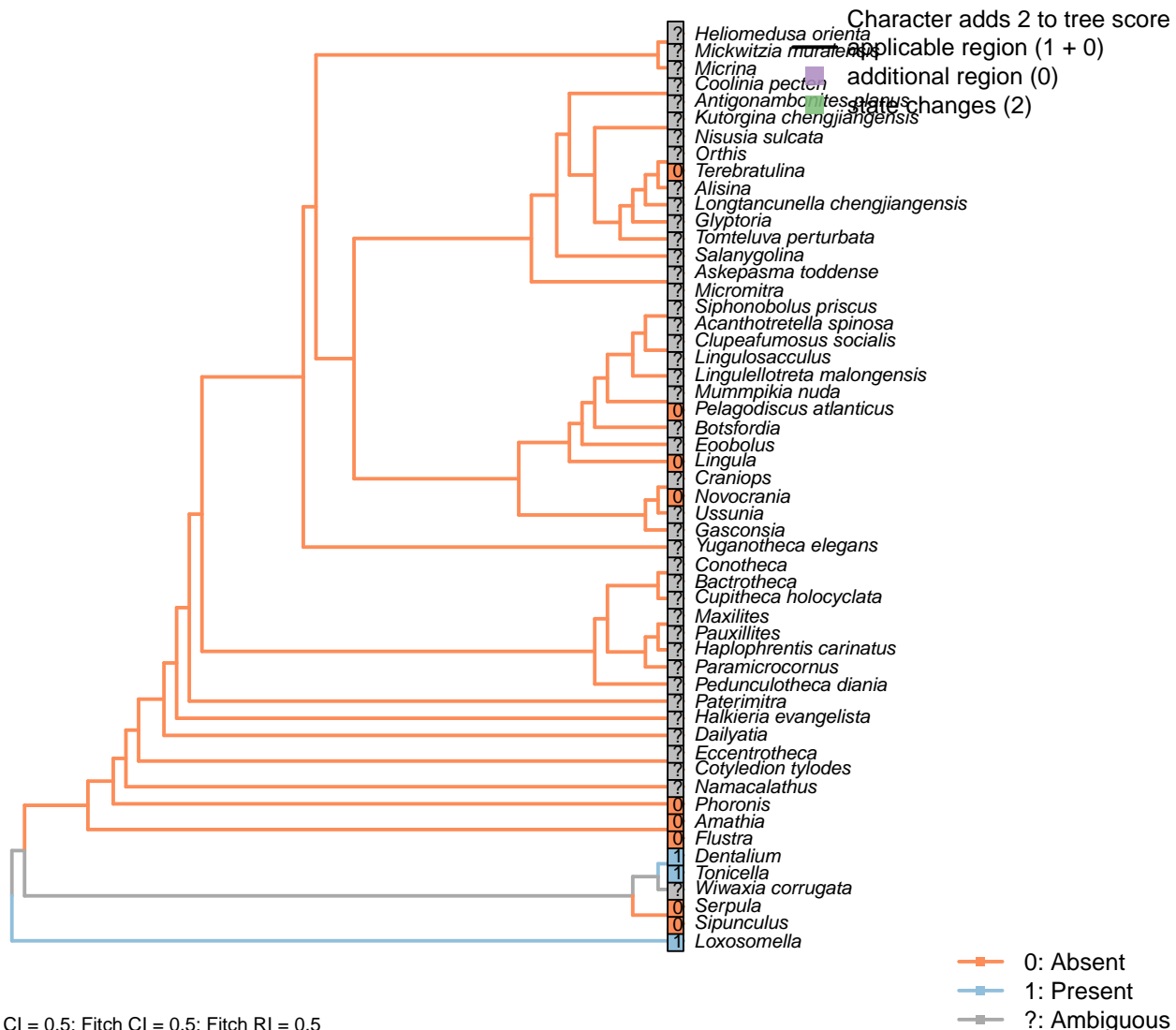
1: Present

Neomorphic character.

Character 16 in Haszprunar (1996). The Glial system interconnects the nervous and muscle systems.

*Phoronis*: Glial cells are “abundant” (Temereva, 2016).

### [219] Buccal nerve ring



CI = 0.5; Fitch CI = 0.5; Fitch RI = 0.5

#### Character 219: Nervous system: Buccal nerve ring

0: Absent

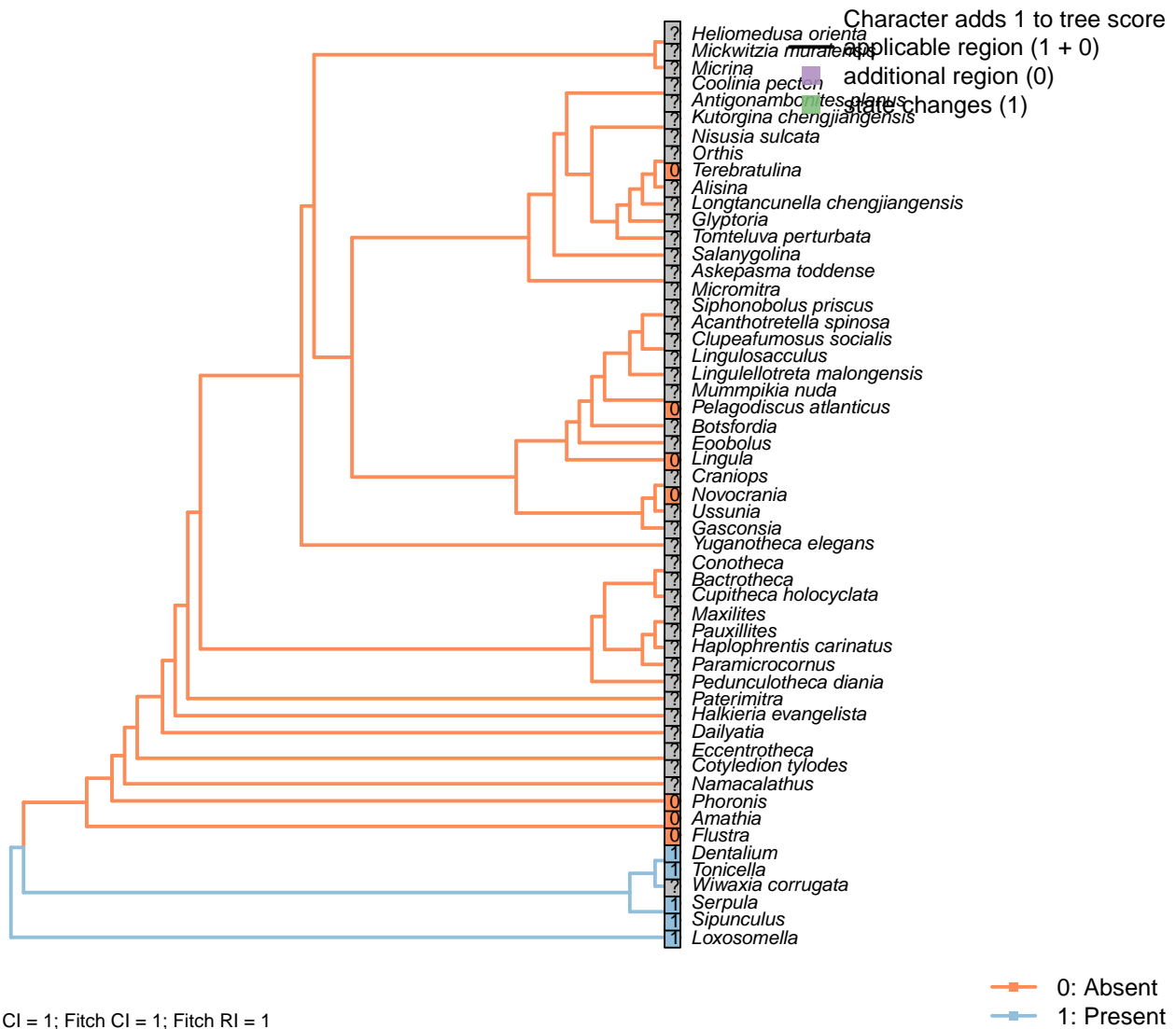
1: Present

Neomorphic character.

Character 7b in Haszprunar and Wanninger (2008).

*Amathia*: Temereva and Kosevich (2016).

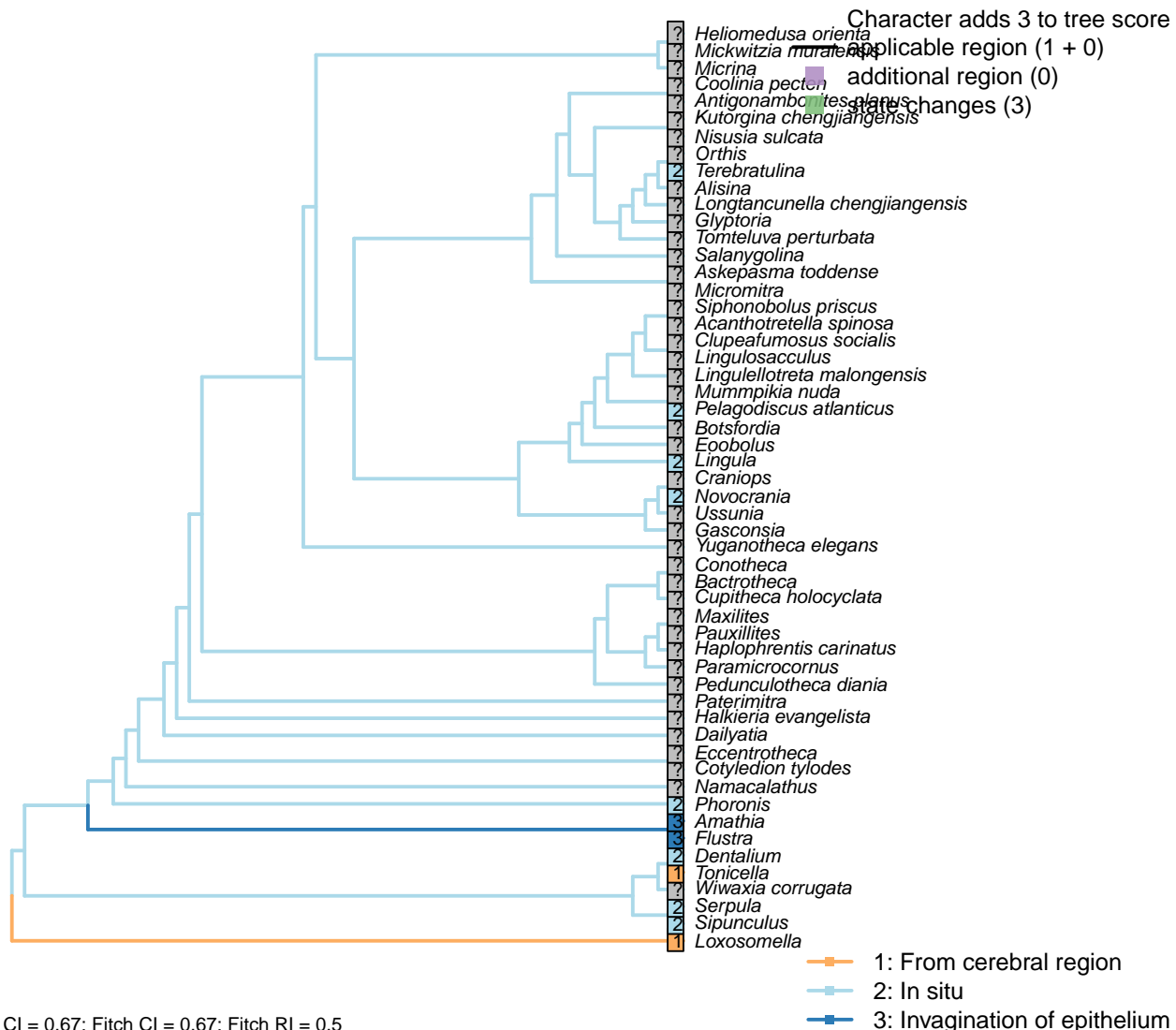
## [220] Anterior nerve loop



Character 7c in Haszprunar and Wanninger (2008). A pre-oral nerve loop is present in molluscs, *Loxosomella* and certain annelids (Wanninger et al., 2007).

*Amathia*: Temereva and Kosevich (2016).

## [221] Formation of ganglia



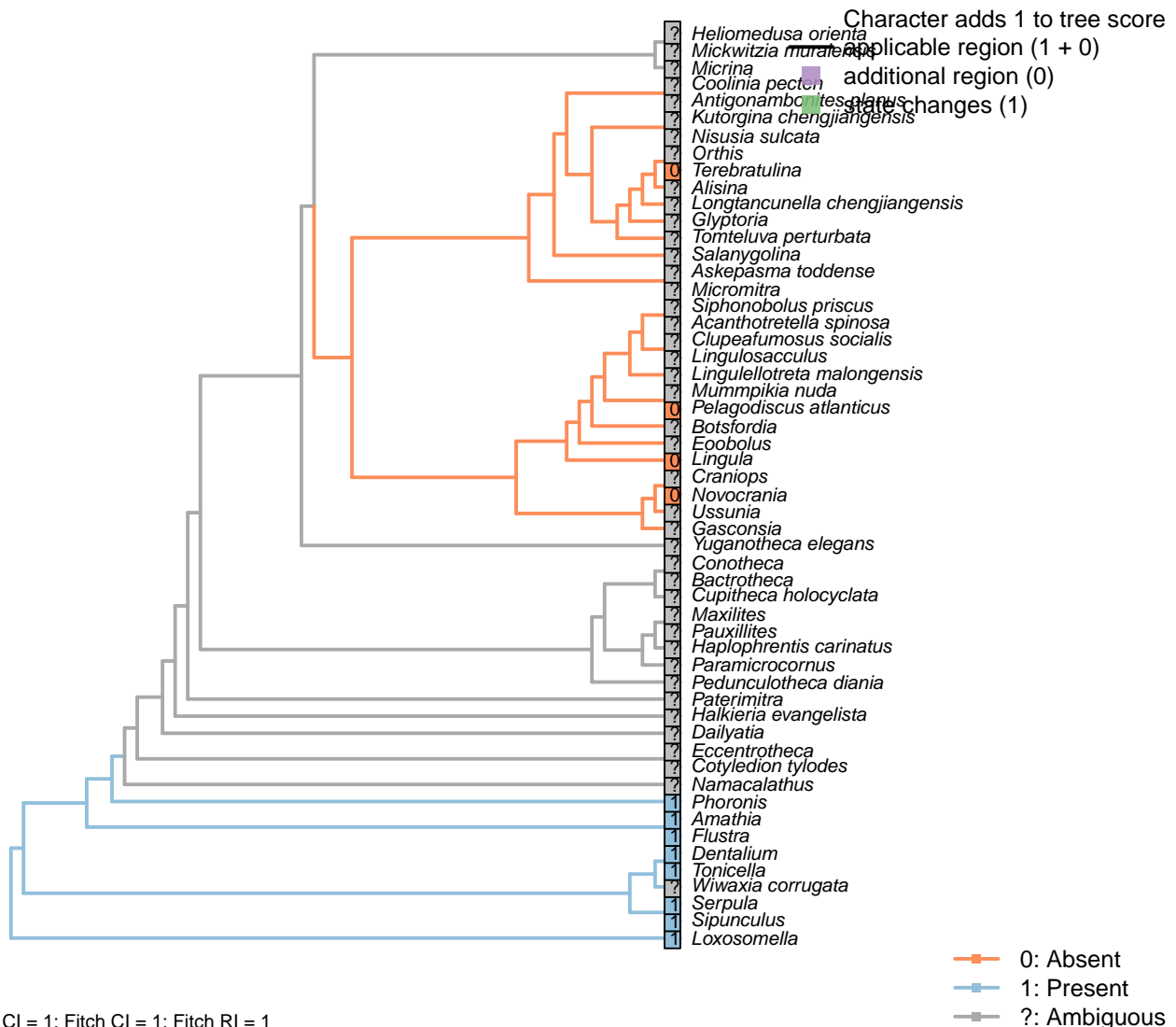
### Character 221: Nervous system: Formation of ganglia

- 1: From cerebral region
  - 2: In situ
  - 3: Invagination of epithelium
- Transformational character.

Character 1.22 in von Salvini-Plawen and Steiner (1996).

*Flustra, Amathia*: “The cerebral ganglion in all bryozoans is formed as an invagination of a portion of epithelium” – Temereva and Kosevich (2016).

## [222] Presence



## Character 222: Nervous system: Cerebral ganglia: Presence

0: Absent

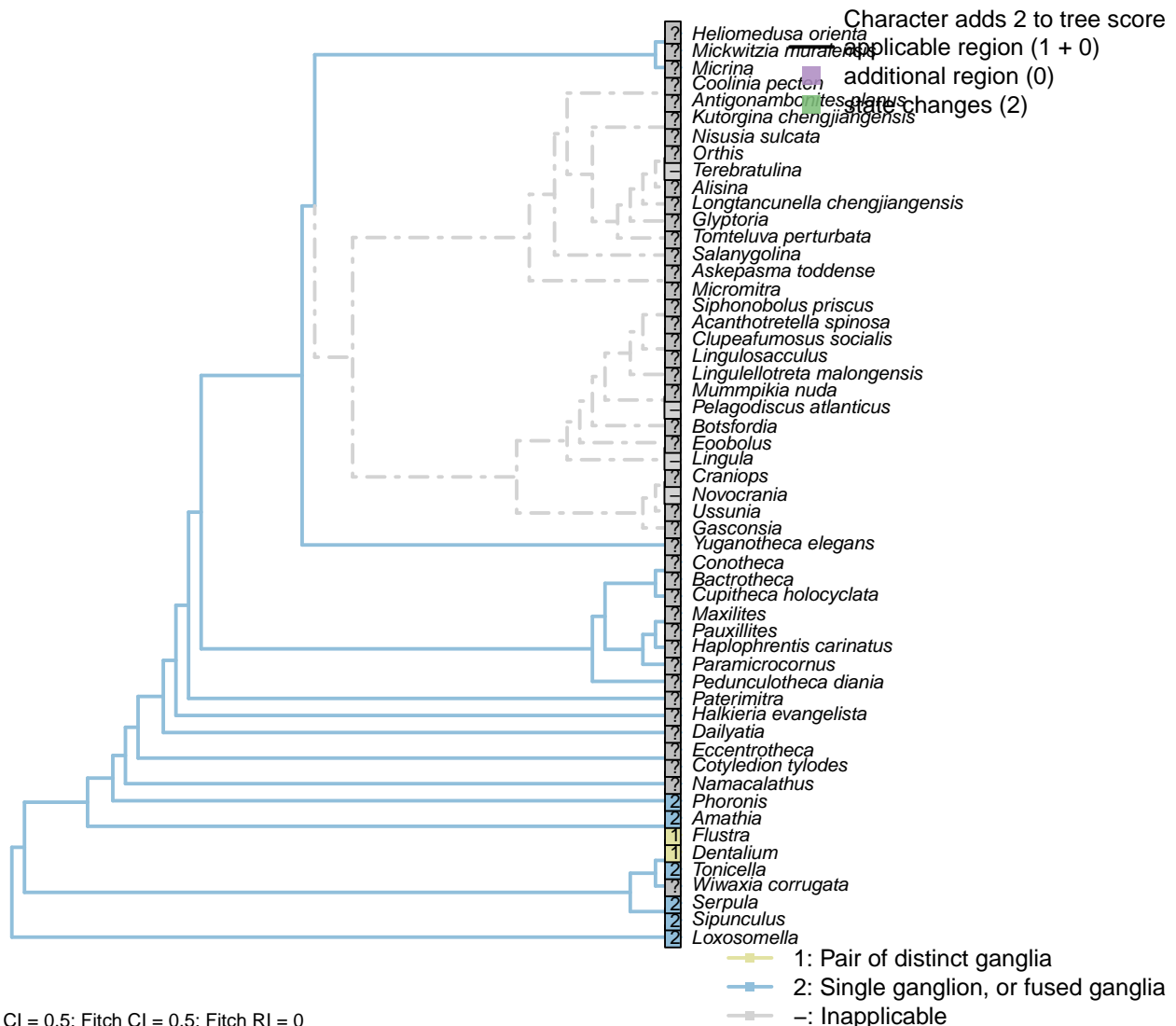
1: Present

Neomorphic character.

After character 13 in Haszprunar (1996).

*Amathia*: Temereva and Kosevich (2016).*Phoronis*: We treat the dorsal ganglion, which is formed by two ends of the tentacular nerve ring (Temereva, 2016), as cerebral.

## [223] Fused

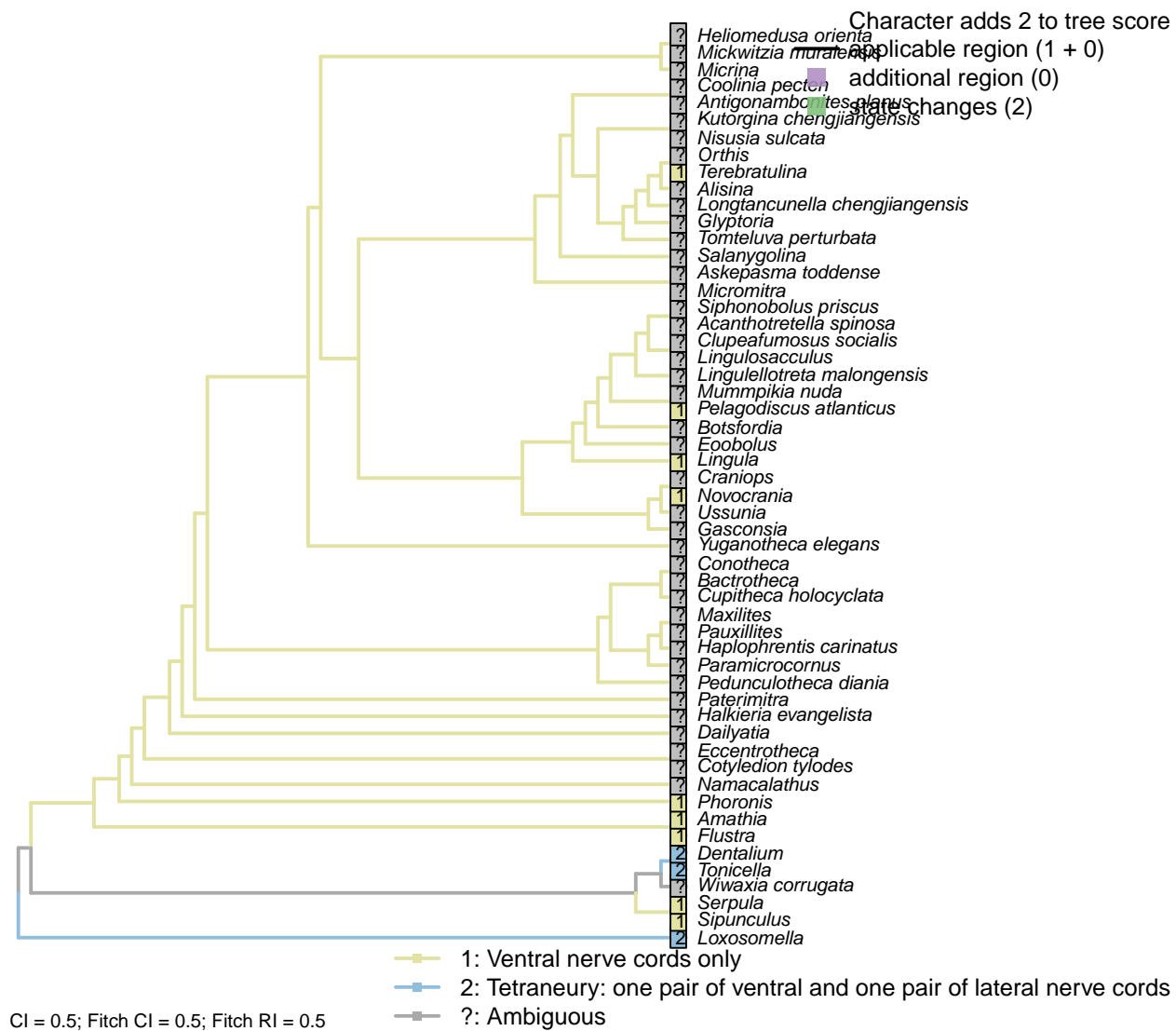
**Character 223: Nervous system: Cerebral ganglia: Fused**

- 1: Pair of distinct ganglia
  - 2: Single ganglion, or fused ganglia
- Transformational character.

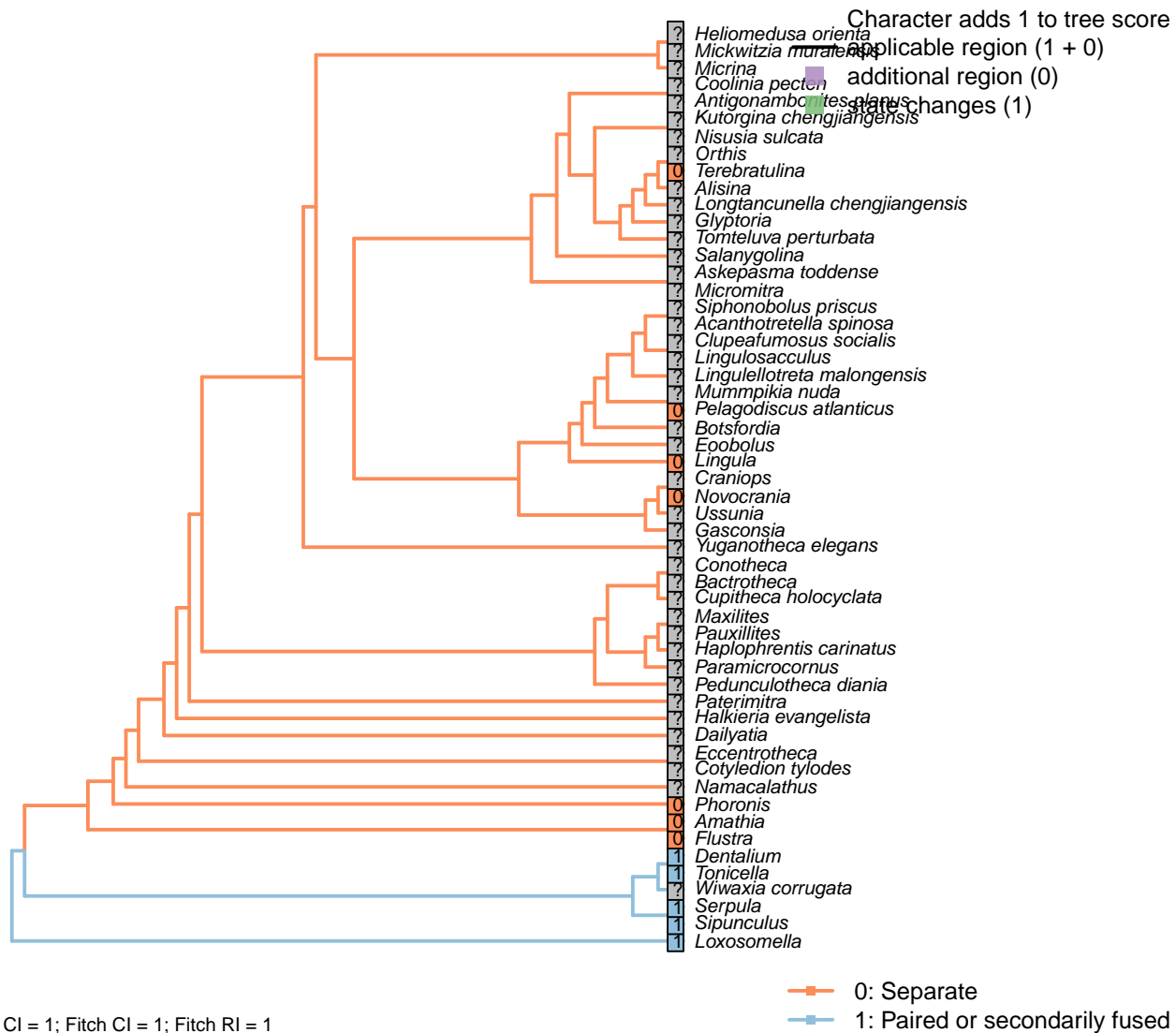
After character 13 in Haszprunar (1996).

*Amathia*: Fused (Temereva and Kosevich, 2016).

## [224] Nerve cords



## [225] Ventral longitudinal nerves

**Character 225: Nervous system: Ventral longitudinal nerves**

0: Separate

1: Paired or secondarily fused

Neomorphic character.

Character 80 in Glenner et al. (2004); see also character 6 in Vinther et al. (2008).

*Amathia*: Temereva and Kosevich (2016).

# Chapter 6

## Taxonomic implications

This section briefly places key features of our results in the context of previous phylogenetic hypotheses.

**Outgroup** We advise caution in the interpretation of outgroup relationships. Outgroup taxa include single representatives of diverse and ancient phyla, and are thus prone to long branch error (Parks and Goldman, 2014). The relationships of the lophotrochozoan phyla were not the primary object of this study, and have long resisted elucidation; this said, we have attempted to incorporate all morphological evidence that has been interpreted as informing relationships between these groups.

**Brachiopod crown and stem group** Crown- and stem-group terminology has great value in clarifying the early evolution of major lineages (Budd and Jensen, 2000; Carlson and Cohen, 2009). The crown group of a lineage is defined as the last common ancestor of all living members of a group, and all its descendants; the stem group as all taxa more closely related to the crown group than to any other extant taxon. In our selection of taxa, the brachiopod crown group corresponds to the last common ancestor of *Terebratulina*, *Novocrania*, *Pelagodiscus* and *Lingula*; the brachiopod stem group comprises anything between this node and the branching point of *Phoronis*, which marks the base of the Brachiozoan crown group.

**Craniiforms** Trimerellids are reconstructed as paraphyletic with respect to Craniiforms. This is consistent with the affinity commonly drawn between these groups (e.g. Williams et al., 2000), and helps to account for the stratigraphically late (Ordovician) appearance of Craniids in the fossil record. (Aragonite is underrepresented in early Palaeozoic strata due to taphonomic bias.)

The position of the craniiforms is not conclusively resolved; shell characters point to a relationship with the Rhynchonelliforms, which is countered by similarities between the spermatozoa of phoronids and terebratulids, indicating a craniiform + linguliform clade. This latter relationship is preferred by the majority of parsimony analyses, though a small subset of weighting parameters places the craniiform clade within the rhynchonelliforms instead.

The Bayesian results offer a more surprising interpretation that places the craniiforms as paraphyletic with respect to all other brachiopods, with *Gasconsia* representing the basalmost member of the Rhynchonellid lineage, upholding suggestions (Holmer et al., 2014) of a chileid rather than trimerellid affinity. To our knowledge, the hypothesis of a paraphyletic craniiform+trimerellid grade has never been proposed, and represents a poor fit to stratigraphic data; potentially it represents an artefact resulting from the incorrect handling of inapplicable data within the Mk model.

**Rhynchonelliforms** The position of kutoarginids within the rhynchonelliform stem lineage has been tricky to resolve (Holmer et al., 2018b); our results agree that they form a clade, but differ on their closest relatives; Fitch parsimony places them as sister to the Chileids; correcting for inapplicables places them sister to Rhynchonelliforms; and Bayesian analysis fails to distinguish between these two possibilities. These results are broadly in accord with previous proposals (Holmer et al., 2018a). The protorthid *Glyptoria* is the earliest diverging of the included rhynchonelliform lineages.

*Salanygolina* has been interpreted as a stem-group rhynchonelliform based on its combination of paterinid and chileate features (Holmer et al., 2009). Our results position *Salanygolina* as sister either to the Chileids or the Chileids + Rhynchonelliforms, corroborating this interpretation.

Basal rhynchonellids are characterized by a circular umbonal perforation in the ventral valve, associated with a colleplax. Partly on this basis, the aberrant taxa *Yuganotheca* and *Tomteluva* tend to plot close to the chileids under Fitch and Bayesian analysis, though a variety of positions in this region of the tree are equally plausible. The BGS method, in contrast, supports the interpretation of *Yuganotheca* as a stem-group brachiopod (Zhang et al., 2014).

**Linguliforms** The reconstruction of Linguloformea comprising Linguloidea as sister to Discinoidea is as expected. Lingulellotretids also sit within this linguliform grouping; a position in the phoronid stem lineage (advocated by Balthasar and Butterfield, 2009) is not upheld. Acrotretids and Siphonotretids form a clade with *Lingulosacculus*.

More novel is the reconstruction of the calcitic obolellid *Mummpikia* in the linguliform total group: a rhynchonelliform affinity has been assumed based on its calcitic mineralogy. This said, Balthasar (2008) has highlighted the similarities between obolellids and linguliform brachiopods, including sub- $m$  vertical canals and the detailed configuration of the posterior shell margin. Our analysis upholds the case for a linguliform affinity for *Mummpikia*; a calcitic shell seemingly arose through an independent change within this taxon. As such, *Mummpikia* has no direct bearing on the origin of ‘Calciata’, save that shell mineralogy is perhaps less static than commonly assumed.

More generally, our results identify Class Obolellata as polyphyletic: *Alisina* (Trematobolidae) plots within Rhynchonellata; *Tomteluva* is harder to place, but tends to group with *Salanygolina* stemwards of the chileids.

**Paterinids** Paterinids have traditionally been placed within the Linguliforms on the basis of their phosphatic shell (Williams et al., 2007), which we identify as ancestral within the brachiopod crown group; consequently, our analysis places the paterinids within the Rhynchonelliforms instead. Characters supporting this position include the strophic hinge line, planar cardinal area, the absence of a pedicle nerve impression, and the morphology of the mantle canals.

More generally, although some lingulids can be found which share more generic characters (e.g. shell growth direction) with paterinids, the particular combination of characters exhibited in paterinids does not occur anywhere in the linguliform lineage, but is more similar to that of basal rhynchonelliforms, particularly *Salanygolina* (as noted by Holmer et al., 2009).

**Tommotiids** Tommotiids represent a basal grade, paraphyletic to phoronids and crown-group brachiopods, in line with previous interpretations.

*Mickwitzia* is consistently the most crownwards of the tommotiids, falling as sister to the brachiopod crown group (except in the Bayesian results, where they fall within the paraphyletic craniiform grade). *Mickwitzia* is closely related to *Micrina* and *Heliomedusa*, though the exact nature of this relationship varies from analysis to analysis. The latter affiliation reflects similarities emphasized by Holmer and Popov in Williams et al. (2007).

*Dailyatia* tends to plot closely with *Halkieria*, reflecting the similarity in the form of their proposed scleritome (Skovsted et al., 2015). Bayesian analysis recovers this pair as sister to annelids and molluscs; Fitch parsimony places them in the molluscan stem group. Inapplicable-corrected parsimony instead places these taxa as sister to hyoliths + brachiopods (cf. Zhao et al., 2017).

**Hyoliths** Within the hyoliths, orthothecids are consistently recovered as a grade that is paraphyletic to the hyolithids. Hyoliths as a whole are interpreted as stem-group Brachiopods, which refines the broader phylogenetic position proposed by Moysiuk et al. (2017). This is to say, they sit closer to brachiopods than the phoronids do, but no analysis places them within the Brachiopod crown group.

Tommotiids lie both stemwards (e.g. *Eccentrotheca*) and crownwards (*Mickwitzia*) of hyoliths, which thus represent derived tommotiids.

# Supplementary Figures

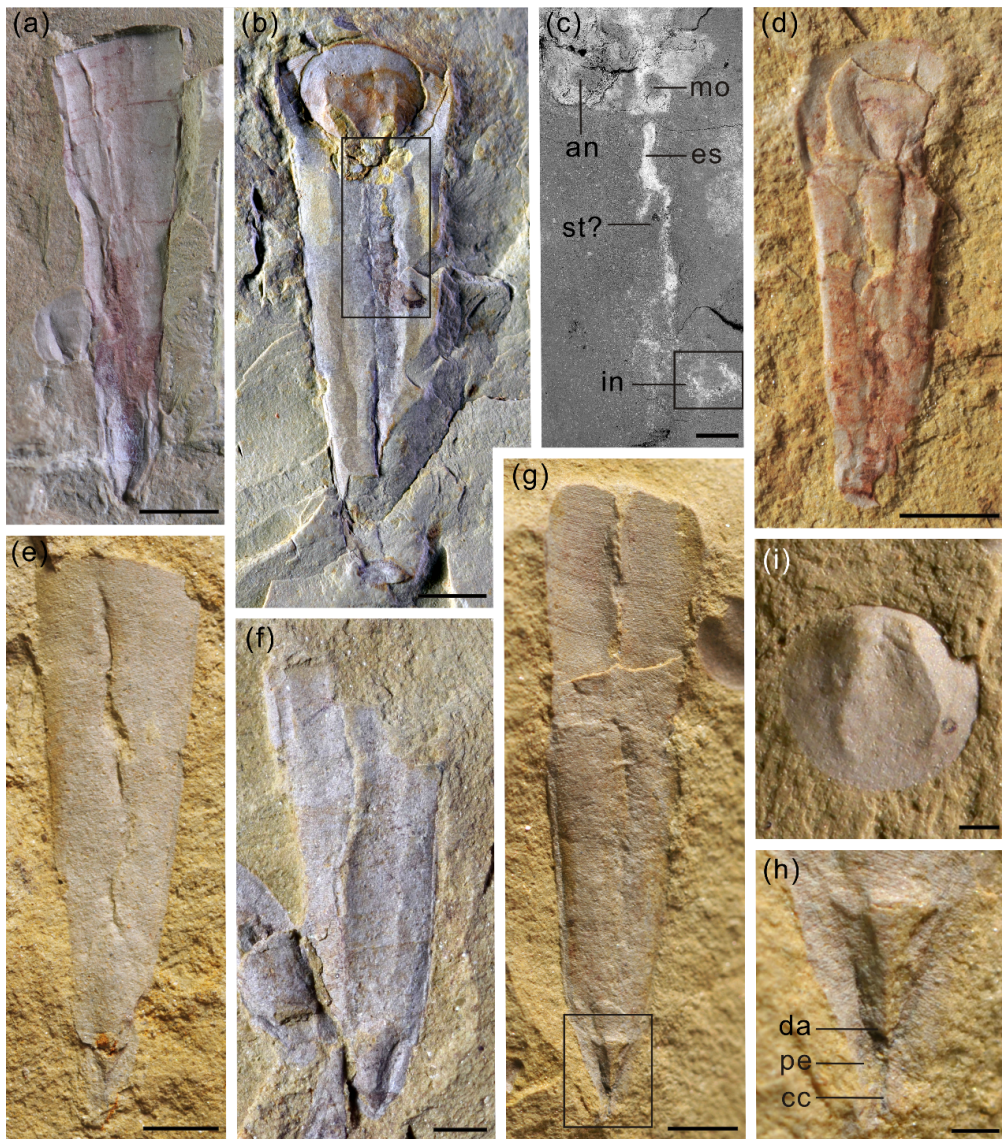


**Fig. S1.** *Pedunculotheca diania* Sun, Zhao et Zhu gen. et sp. nov. from the Chengjiang Biota, Yunnan Province, China. (a) NIGPAS 166601, external mould of dorsum with dorsal apex and pedicle foramen. (b) NIGPAS 166597, preserving conical shell, operculum and internal soft tissue, showing a compressed elliptic cross-section; backscatter electron micrograph of boxed region shown in (c). (d) NIGPAS 166599b, counterpart, juvenile conical shell with operculum showing two longitudinal ventral grooves and

circular larval shell. (e) NIGPAS 166602, conical shell with incomplete attachment structure. (f) NIGPAS 166598, broken shell with two ventral furrows and incomplete attachment structure. (g) NIGPAS 166596, incomplete shell with one medial ventral furrow and short attachment structure with coelomic cavity; detail of boxed region shown in (h). (i) NIGPAS 166603, exterior of operculum. Scale bars: 2mm (for a, b and e-g); 500 µm (for c, h and i).

Abbreviations: an = anus, cc = coelomic cavity, da = dorsal apex, es = esophagus, in = intestine, mo = mouth, pe = pedicle, st = stomach.

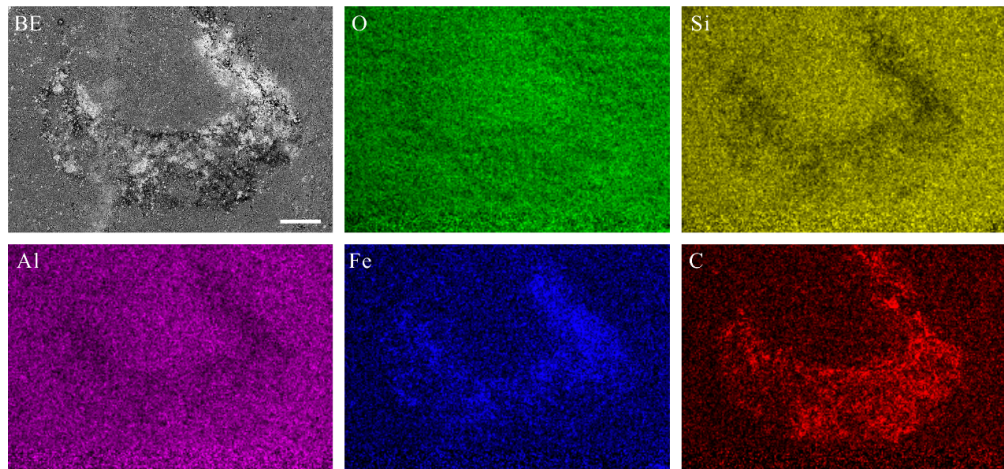


**Fig. S2. Elemental distribution in the gut of *Pedunculotheca diania* Sun, Zhao et Zhu gen. et sp. nov. NIGPAS 166597.** Region corresponds to boxed region in Fig. S1c. Scale bar = 100 µm.

Abbreviations: BE = backscatter electron image, O = Oxygen, Si = Silicon, Al = Aluminium, Fe = Iron, C = Carbon.

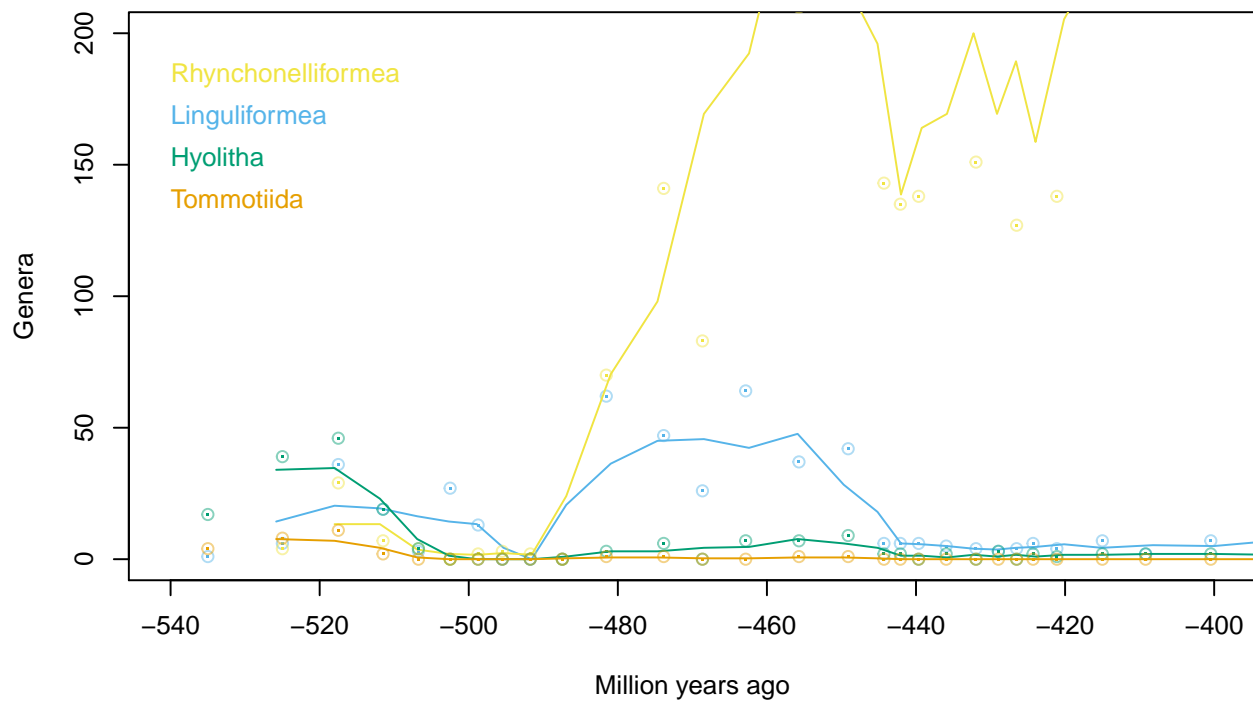


**Fig. S3. Global diversity of brachiopods through the Paleozoic.** Points represent number of genera reported in each time bin; lines represent rolling mean diversity over three consecutive time bins. Data from Paleobiology database.

# Supplementary Table

NIGPAS Specimen numbers	Fossil locality	Coordinates
166593, 166617	Shankou Village, Anning	24°49'53" N, 102°24'47.9" E
166594, 166595	Yaoying Village, Wuding	25°36'01.2" N, 102°20'04.6" E
166596–166616	Ma'anshan Village, Chengjiang	24°40'37.2" N, 102°58'40.2" E

**Table S1. Provenance of fossil material.** Individuals from the Yaoying section are usually bigger, with a thicker body wall, and have a smaller ratio of apertural width to shell length than specimens from other areas. In the absence of other differentiating features, we consider these deviations to represent ecophenotypical variation within a single species, perhaps reflecting the increased energetics and predation pressure that accompany the shallower water depth reported at the Yaoying section (Zhao et al., 2012).

# Bibliography

- Adrianov, A. V., Maiorova, A. S., and Malakhov, V. V. (2011). Embryonic and larval development of the peanut worm *Phascolosoma agassizii* (Keferstein 1867) from the Sea of Japan (Sipuncula: Phascolosomatidea). *Invertebrate Reproduction and Development*, 55(1):22–29, doi:10.1080/07924259.2010.548638.
- Adrianov, A. V., Malakhov, V. V., and Maiorova, A. S. (2006). Development of the tentacular apparatus in sipunculans (Sipuncula): I. *Thysanocardia nigra* (Ikeda, 1904) and *Themiste pyroides* (Chamberlin, 1920). *Journal of Morphology*, 267(5):569–583, doi:10.1002/jmor.10423.
- Afzelius, B. A. and Ferraguti, M. (1978). Fine structure of brachiopod spermatozoa. *Journal of Ultrastructure Research*, 63(3):308–315, doi:10.1016/s0022-5320(78)80054-9.
- Altenburger, A. and Wanninger, A. (2010). Neuromuscular development in *Novocrania anomala*: evidence for the presence of serotonin and a spiralian-like apical organ in lecithotrophic brachiopod larvae. *Evolution and Development*, 12(1):16–24, doi:10.1111/j.1525-142X.2009.00387.x.
- Altenburger, A., Wanninger, A., and Holmer, L. E. (2013). Metamorphosis in Craniiformea revisited: *Novocrania anomala* shows delayed development of the ventral valve. *Zoomorphology*, 132(4):379–387, doi:10.1007/s00435-013-0194-3.
- Balthasar, U. (2004). Shell structure, ontogeny, and affinities of the Lower Cambrian bivalved problematic fossil *Mickwitzia muralensis* Walcott, 1913. *Lethaia*, 37(4):381–400, doi:10.1080/00241160410002090.
- Balthasar, U. (2007). An early Cambrian organophosphatic brachiopod with calcitic granules. *Palaeontology*, 50(6):1319–1325, doi:10.1111/j.1475-4983.2007.00729.x.
- Balthasar, U. (2008). *Mummpikia* gen. nov. and the origin of calcitic-shelled brachiopods. *Palaeontology*, 51(2):263–279, doi:10.1111/j.1475-4983.2008.00754.x.
- Balthasar, U. (2009). The brachiopod *Eobolus* from the early Cambrian Mural Formation (Canadian Rocky Mountains). *Paläontologische Zeitschrift*, 83(3):407–417, doi:10.1007/s12542-009-0026-4.
- Balthasar, U. and Butterfield, N. J. (2009). Early Cambrian soft-shelled brachiopods as possible stem-group phoronids. *Acta Palaeontologica Polonica*, 54(2):307–314, doi:10.4202/app.2008.0042.
- Balthasar, U., Cusack, M., Faryma, L., Chung, P., Holmer, L. E., Jin, J., Percival, I. G., and Popov, L. E. (2011). Relic aragonite from Ordovician–Silurian brachiopods: Implications for the evolution of calcification. *Geology*, 39(10):967–970, doi:10.1130/g32269.1.
- Balthasar, U., Skovsted, C. B., Holmer, L. E., and Brock, G. A. (2009). Homologous skeletal secretion in tommotiids and brachiopods. *Geology*, 37:1143–1146, doi:10.1130/g30323a.1.
- Bartolomaeus, T. (1995). Secondary monociliarity in the Annelida: monociliated epidermal cells in larvae of *Magelona mirabilis* (Magelonida). *Microfauna Marina*, 10(January 1995):327–332.
- Bartolomaeus, T. (2001). Ultrastructure and formation of the body cavity lining in *Phoronis muelleri* (Phoronida, Lophophorata). *Zoomorphology*, 120(3):135–148, doi:10.1007/s004350000030.

- Bartolomaeus, T. and Quast, B. (2005). Structure and development of nephridia in Annelida and related taxa. *Hydrobiologia*, 535:139–165, doi:10.1007/s10750-004-1840-z.
- Bassett, M. G. and Popov, L. E. (2017). Earliest ontogeny of the Silurian orthotetide brachiopod *Coolinia* and its significance for interpreting strophomenate phylogeny. *Lethaia*, 50(4):504–510, doi:10.1111/let.12204.
- Bassett, M. G., Popov, L. E., and Egerquist, E. (2008). Early ontogeny of some Ordovician–Silurian strophomenate brachiopods: Significance for interpreting evolutionary relationships within early Rhynchonelliformea. *Fossils and Strata*, 54:13–20.
- Bassett, M. G., Popov, L. E., and Holmer, L. E. (2001). Functional morphology of articulatory structures and implications for patterns of musculature in Cambrian rhynchonelliform brachiopods. In Brunton, H., Cocks, R. M., and Long, S. L., editors, *Brachiopods, Past and Present*, pages 163–176. CRC Press.
- Benedetto, J. L. (2009). *Chaniella*, a new lower Tremadocian (Ordovician) brachiopod from northwestern Argentina and its phylogenetic relationships within basal rhynchonelliforms. *Paläontologische Zeitschrift*, 83(3):393–405, doi:10.1007/s12542-009-0023-7.
- Bereiter-Hahn, J., Matoltsy, A. G., and Sylvia Richards, K. (1984). *Biology of the Integument*. Springer.
- Borisanova, A. O., Yushin, V. V., Malakhov, V. V., and Temereva, E. N. (2015). The fine structure of the cuticle of kamptozoans is similar to that of annelids. *Zoomorphology*, 134(2):165–181, doi:10.1007/s00435-015-0261-z.
- Brazeau, M. D., Guillerme, T., and Smith, M. R. (2018). An algorithm for morphological phylogenetic analysis with inapplicable data. *Systematic Biology*, doi:10.1101/209775.
- Brazeau, M. D., Smith, M. R., and Guillerme, T. (2017). MorphyLib: a library for phylogenetic analysis of categorical trait data with inapplicability. *Zenodo*, doi:10.5281/zenodo.815371.
- Buckland-Nicks, J. A. (2008). Fertilization biology and the evolution of chitons. *American Malacological Bulletin*, 25(1):97–111.
- Buckland-Nicks, J., Koss, R., and Chia, F. . (1988). Fertilization in a chiton: Acrosome-mediated sperm-egg fusion. *Gamete Research*, 21(3):199–212, doi:10.1002/mrd.1120210302.
- Budd, G. E. and Jensen, S. (2000). A critical reappraisal of the fossil record of the bilaterian phyla. *Biological Reviews*, 75(2):253–295, doi:10.1111/j.1469-185X.1999.tb00046.x.
- Butler, A. D., Streng, M., Garwood, R., Lowe, T., and Holmer, L. E. (2012). Constructing Cambrian body-plans: critical evaluation of tommotiid and stem-brachiopod character homologies [Exceptional preservation of *Micrina* setae and 3D MicroCT reconstruction confirm the tommotiid stem-group brachiopod link]. In *Palaeontological Association Annual Meeting*, volume 56, page 61. The Palaeontological Association.
- Butler, A. D., Streng, M., Holmer, L. E., and Babcock, L. E. (2015). Exceptionally preserved *Mickwitzia* from the Indian Springs Lagerstätte (Cambrian Stage 3), Nevada. *Journal of Paleontology*, 89(6):933–955, doi:10.1017/jpa.2016.8.
- Butterfield, N. J. (1990). A reassessment of the enigmatic Burgess Shale fossil *Wiwaxia corrugata* (Matthew) and its relationship to the polychaete *Canadia spinosa* Walcott. *Paleobiology*, 16(3):287–303, doi:10.2307/2400789.
- Byrum, C. A. and Ruppert, E. E. (1994). The ultrastructure and functional morphology of a captacula-lum in *Graptacme calamus* (Mollusca, Scaphopoda). *Acta Zoologica*, 75(1):37–46, doi:10.1111/j.1463-6395.1994.tb00960.x.
- Carlson, S. J. (1995). Phylogenetic relationships among extant brachiopods. *Cladistics*, 11:131–197, doi:10.1111/j.1096-0031.1995.tb00084.x.

- Carlson, S. J. and Cohen, B. L. (2009). Separating the crown from the stem: defining Brachiopoda and Pan-Brachiopoda delineates stem-brachiopods. *Geological Society of America Annual Meeting Abstract Program*, 41:562.
- Chen, J.-Y., Huang, D.-Y., and Chuang, S.-H. (2007). Reinterpretation of the Lower Cambrian brachiopod *Heliomedusa orienta* Sun and Hou, 1987a as a discinid. *Journal of Paleontology*, 81(1):38–47, doi:10.1666/0022-3360(2007)81[38:rotlcb]2.0.co;2.
- Connors, M. J., Ehrlich, H., Hog, M., Godeffroy, C., Araya, S., Kallai, I., Gazit, D., Boyce, M., and Ortiz, C. (2012). Three-dimensional structure of the shell plate assembly of the chiton *Tonicella marmorea* and its biomechanical consequences. *Journal of Structural Biology*, 177(2):314–328, doi:10.1016/j.jsb.2011.12.019.
- Cooper, G. A. (1976). Lower Cambrian brachiopods from the Rift Valley (Israel and Jordan). *Journal of Paleontology*, 50(2):269–289.
- Curry, G. B. and Williams, A. (1983). Epithelial moulds on the shells of the early Palaeozoic brachiopod Lingulella. *Lethaia*, 16(2):111–118, doi:10.1111/j.1502-3931.1983.tb01706.x.
- Cusack, M., Williams, A., and Buckman, J. O. (1999). Chemico-structural evolution of linguloid brachiopod shells. *Palaeontology*, 42(5):799–840, doi:10.1111/1475-4983.00098.
- Devaere, L., Clausen, S., Álvaro, J. J., Peel, J. S., and Vachard, D. (2014). Terreneuvian orthothecid (Hyolitha) digestive tracts from northern Montagne Noire, France; taphonomic, ontogenetic and phylogenetic implications. *PLoS ONE*, 9(2), doi:10.1371/journal.pone.0088583.
- Dewing, K. (2001). Hinge modifications and musculature of strophomenoid brachiopods: examples across the Ordovician–Silurian boundary, Anticosti Island, Quebec. *Canadian Journal of Earth Sciences*, 38:125–141, doi:10.1139/e00-027.
- Dewing, K. (2004). Shell structure and its bearing on the phylogeny of Late Ordovician-Early Silurian Strophomenoid Brachiopods from Anticosti Island, Quebec. *Journal of Paleontology*, 78(2):275–286, doi:10.1666/0022-3360(2004)078<0275:SSAIBO>2.0.CO;2.
- Dufresne-Dube, L., Picheral, B., and Guerrier, P. (1983). An ultrastructural analysis of *Dentalium vulgare* (Mollusca, Scaphopoda) gametes with special reference to early events at fertilization. *Journal of Ultrastructure Research*, 83(3):242–257, doi:10.1016/S0022-5320(83)90132-6.
- Dzik, J. (1978). Larval development of hyolithids. *Lethaia*, 11(4):293–299, doi:10.1111/j.1502-3931.1978.tb01884.x.
- Dzik, J. (1980). Ontogeny of *Bactrotheca* and related hyoliths. *Geologiska Föreningen i Stockholm Förhandlingar*, 102(3):223–233, doi:10.1080/11035898009455162.
- Emig, C. C. (1992). Functional disposition of the lophophore in living Brachiopoda. *Lethaia*, 25(3):291–302, doi:10.1111/j.1502-3931.1992.tb01398.x.
- Fischer, F. P., Maile, W., and Renner, M. (1980). Die Mantelpapillen und Stacheln von *Acanthochiton fascicularis* L. (Mollusca, Polyplacophora). *Zoomorphologie*, 94(2):121–131, doi:10.1007/BF01081929.
- Fitch, W. M. (1971). Toward defining the course of evolution: minimum change for a specific tree topology. *Systematic Biology*, 20(4):406–416, doi:10.1093/sysbio/20.4.406.
- Franzén, Å. (1977). Gametogenesis of Bryozoans. In Woollacott, R. M. and Zimmer, R. L., editors, *Biology of Bryozoans*, pages 1–22. Elsevier.
- Franzén, Å. (1981). Comparative ultrastructural studies of spermatids and spermatozoa in Bryozoa and Entoprocta. In Larwood, G. P. and Nielsen, C., editors, *Recent and Fossil Bryozoans*, pages 83–92. Olsen & Olsen.

- Franzén, Å. (1984). Ultrastructure of spermatids and spermatozoa in the cyclostomatous bryozoan *Tubulipora* (Bryozoa, Cyclostomata). *Zoomorphology*, 104(3):140–146, doi:10.1007/BF00312132.
- Franzén, Å. (2000). Spermiogenesis, sperm ultrastructure and sperm transport in *Loxosoma pectinaricola* (Entoprocta). *Invertebrate Reproduction and Development*, 37(2):129–136, doi:10.1080/07924259.2000.9652411.
- Franzén, Å. and Ahlfors, K. (1980). Ultrastructure of spermatids and spermatozoa in *Phoronis*, Phylum Phoronida. *Journal of Submicroscopic Cytology*, 12(4):585–597.
- Freeman, G. and Lundelius, J. W. (1999). Changes in the timing of mantle formation and larval life history traits in linguliform and craniiform brachiopods. *Lethaia*, 32:197–217, doi:10.1111/j.1502-3931.1999.tb00539.x.
- Fuchs, J., Bright, M., Funch, P., and Wanninger, A. (2006). Immunocytochemistry of the neuromuscular systems of *Loxosomella vivipara* and *L. parguerensis* (Entoprocta: Loxosomatidae). *Journal of Morphology*, 267(7):866–83, doi:10.1002/jmor.10446.
- Fuchs, J. and Wanninger, A. (2008). Reconstruction of the neuromuscular system of the swimming-type larva of *Loxosomella atkinsae* (Entoprocta) as inferred by fluorescence labelling and confocal microscopy. *Organisms Diversity and Evolution*, 8(4):325–335, doi:10.1016/jоде.2008.05.002.
- Fukumoto, M. (2003). The acrosome reaction of the spermatozoa of the inarticulate brachiopod *Lingula anatina*. In Brunton, H., Cocks, R. M., and Long, S. L., editors, *Brachiopods, Past and Present*, pages 40–45. Taylor & Francis.
- Gherardi, M., Lepore, E., Sciscioli, M., Mercurio, M., Licciano, M., and Giangrande, A. (2011). A study on spermatogenesis of three Mediterranean serpulid species. *Italian Journal of Zoology*, 78(2):174–181, doi:10.1080/11250003.2010.529468.
- Gilula, N. B. and Satir, P. (1972). The ciliary necklace. *The Journal of Cell Biology*, 53(2):494–509, doi:10.1083/jcb.53.2.494.
- Giribet, G. and Wheeler, W. C. (2002). On bivalve phylogeny: a high-level analysis of the Bivalvia (Mollusca) based on combined morphology and DNA sequence data. *Invertebrate Biology*, 121(4):271–324, doi:10.1111/j.1744-7410.2002.tb00132.x.
- Glenner, H., Hansen, A. J., Sørensen, M. V., Ronquist, F., Huelsenbeck, J. P., and Willerslev, E. (2004). Bayesian inference of the metazoan phylogeny; a combined molecular and morphological approach. *Current Biology*, 14(18):1644–9, doi:10.1016/j.cub.2004.09.027.
- Goffinet, G., Voss-Foucart, M.-F., and Barzin, S. (1978). Ultrastructure of the cuticle of the sipunculans *Golfingia vulgaris* and *Sipunculus nudus*. *Transactions of the American Microscopical Society*, 97(4):512–523, doi:10.2307/3226167.
- Goloboff, P. A. (1997). Self-weighted optimization: tree searches and character state reconstructions under implied transformation costs. *Cladistics*, 13(3):225–245, doi:10.1111/j.1096-0031.1997.tb00317.x.
- Goloboff, P. A. (1999). Analyzing large data sets in reasonable times: solutions for composite optima. *Cladistics*, 15(4):415–428, doi:10.1006/clad.1999.0122.
- Goloboff, P. A. (2014). Extended implied weighting. *Cladistics*, 30(3):260–272, doi:10.1111/cla.12047.
- Goloboff, P. A. and Catalano, S. A. (2016). TNT version 1.5, including a full implementation of phylogenetic morphometrics. *Cladistics*, 32(3):221–238, doi:10.1111/cla.12160.
- Goodrich, E. S. (1945). The study of nephridia and genital ducts since 1895. *The Quarterly Journal of Microscopical Science*, 86(344):113–392.

- Gordon, D. P. (1975). The resemblance of bryozoan gizzard teeth to "annelid-like" setae. *Acta Zoologica*, 56(4):283–289, doi:10.1111/j.1463-6395.1975.tb00105.x.
- Gorjansky, V. Y. and Popov, L. E. (1986). On the origin and systematic position of the calcareous-shelled inarticulate brachiopods. *Lethaia*, 19:223–240, doi:10.1111/j.1502-3931.1986.tb00737.x.
- Grobe, P. (2007). *Larval development, the origin of the coelom and the phylogenetic relationships of the Phoronida*. PhD thesis, Free University, Berlin, Berlin.
- Gruhl, A. (2008). Muscular systems in gymnolaemate bryozoan larvae (Bryozoa: Gymnolaemata). *Zoomorphology*, 127:143–159, doi:10.1007/s00435-008-0059-3.
- Gruhl, A. (2010a). Neuromuscular system of the larva of *Fredericella sultana* (Bryozoa: Phylactolaemata). *Zoologischer Anzeiger - A Journal of Comparative Zoology*, 249(3-4):139–149, doi:10.1016/j.jcz.2010.06.001.
- Gruhl, A. (2010b). Ultrastructure of mesoderm formation and development in *Membranipora membranacea* (Bryozoa: Gymnolaemata). *Zoomorphology*, 129(1):45–60, doi:10.1007/s00435-009-0099-3.
- Gruhl, A. and Schwaha, T. F. (2016). Bryozoa (Ectoprocta). In Schmidt-Rhaesa, A., Harzsch, S., and Purschke, G., editors, *Structure and Evolution of Invertebrate Nervous Systems*, pages 324–340. Oxford University Press, Oxford.
- Gustus, R. M. and Cloney, R. A. (1972). Ultrastructural similarities between setae of brachiopods and polychaetes. *Acta Zoologica*, 53(2):229–233, doi:10.1111/j.1463-6395.1972.tb00590.x.
- Gustus, R. M. and Cloney, R. A. (1973). Ultrastructure of the larval compound setae of the polychaete *Nereis vexillosa* Grube. *Journal of Morphology*, 140(3):355–366, doi:10.1002/jmor.1051400308.
- Hanken, N.-M. and Harper, D. A. T. (1985). The taxonomy, shell structure, and palaeoecology of the trimerellid brachiopod *Gasconsia* Northrop. *Palaeontology*, 28(2):243–254.
- Hanson, J. (1949). Observation on the branchial crown of the Serpulidae (Annelida, Polychaeta). *Quarterly Journal of Microscopical Science*, 90(3):221–233.
- Harper, D. A. T., Popov, L. E., and Holmer, L. E. (2017). Brachiopods: origin and early history. *Palaeontology*, 60:609–631, doi:10.1111/pala.12307.
- Haszprunar, G. (1996). The Mollusca: coelomate turbellarians or mesenchymate annelids? In Taylor, J. D., editor, *Origin and Evolutionary Radiation of the Mollusca*, pages 29–51. The Malacological Society of London, London.
- Haszprunar, G. (2000). Is the Aplacophora monophyletic? A cladistic point of view. *American Malacological Bulletin*, 15:115–130.
- Haszprunar, G. and Wanninger, A. (2008). On the fine structure of the creeping larva of *Loxosomella murmanica*: additional evidence for a clade of Kamptozoa (Entoprocta) and Mollusca. *Acta Zoologica*, 89(2), doi:10.1111/j.1463-6395.2007.00301.x.
- Hausen, H. (2005). Chaetae and chaetogenesis in polychaetes (Annelida). *Hydrobiologia*, 535–536(1):37–52, doi:10.1007/s10750-004-1836-8.
- Havlicek, M. (1982). Lingulacea, Paterinacea, and Siphonotretacea (Brachiopoda) in the Lower Ordovician sequence of Bohemia. *Sbornik geologickych ved, Paleontologie*, 25:9–82, pl. 1–16.
- Hay-Schmidt, A. (1992). Ultrastructure and immunocytochemistry of the nervous system of the larvae of *Lingula anatina* and *Glottidia* sp. (Brachiopoda). *Zoomorphology*, 112(4):189–205, doi:10.1007/BF01632817.
- Hejnol, A. (2010). A twist in time—the evolution of spiral cleavage in the light of animal phylogeny. *Integrative and Comparative Biology*, 50(5):695–706, doi:10.1093/icb/icq103.

- Herrmann, K. (1997). Phoronida. In Harrison, F. W. and Woollacott, R. M., editors, *Microscopic Anatomy of Invertebrates, 13: Lophophorates, Entoprocta, and Cycliophora*, pages 207–236. Wiley-Blackwell.
- Hodgson, A. N. and Reunov, A. A. (1994). Ultrastructure of the spermatozoon and spermatogenesis of the brachiopods *Discinisca tenuis* (Inarticulata) and *Kraussina rubra* (Articulata). *Invertebrate Reproduction & Development*, 25(1):23–31, doi:10.1080/07924259.1994.9672365.
- Holborow, P. L., Laverack, M. S., and Barber, V. C. (1969). Cilia and other surface structures of the trochophore of *Harmothoë imbricata* (Polychaeta). *Zeitschrift für Zellforschung und Mikroskopische Anatomie*, 98(2):246–261, doi:10.1007/BF00338328.
- Holmer, L. E. (1989). Middle Ordovician phosphatic inarticulate brachiopods from Västergötland and Dalarna, Sweden. *Fossils and Strata*, 26:1–172.
- Holmer, L. E. and Caron, J.-B. (2006). A spinose stem group brachiopod with pedicle from the Middle Cambrian Burgess Shale. *Acta Zoologica*, 87:273–290, doi:10.1111/j.1463-6395.2006.00241.x.
- Holmer, L. E., Pettersson Stolk, P. S., Skovsted, C. B., Balthasar, U., and Popov, L. E. (2009). The enigmatic early Cambrian *Salanygolina* – A stem group of rhynchonelliform chileate brachiopods? *Palaeontology*, 52(1):1–10, doi:10.1111/j.1475-4983.2008.00831.x.
- Holmer, L. E., Popov, L. E., and Bassett, M. G. (2014). Ordovician–Silurian Chileida—first post-Cambrian records of an enigmatic group of Brachiopoda. *Journal of Paleontology*, 88(3):488–496, doi:10.1666/13-104.
- Holmer, L. E., Popov, L. E., Koneva, S. P., and Rong, J.-Y. (1997). Early Cambrian Lingulellotreta (Lingulata, Brachiopoda) from south Kazakhstan (Malyi Karatau Range) and South China (eastern Yunnan). *Journal of Paleontology*, 71(4):577–584, doi:10.1017/s0022336000040063.
- Holmer, L. E., Popov, L. E., Pour, M. G., Claybourn, T., Zhang, Z.-L., Brock, G. A., and Zhang, Z.-F. (2018a). Evolutionary significance of a middle Cambrian (Series 3) *in situ* occurrence of the pedunculate rhynchonelliform brachiopod *Nisusia sulcata*. *Lethaia*, doi:10.1111/let.12254.
- Holmer, L. E., Skovsted, C. B., Brock, G. A., Valentine, J. L., and Paterson, J. R. (2008). The Early Cambrian tommotiid *Micrina*, a sessile bivalved stem group brachiopod. *Biology Letters*, 4:724–728, doi:10.1098/rsbl.2008.0277.
- Holmer, L. E., Skovsted, C. B., Larsson, C. M., Brock, G. A., and Zhang, Z.-F. (2011). First record of a bivalved larval shell in Early Cambrian tommotiids and its phylogenetic significance. *Palaeontology*, 54(2):235–239, doi:10.1111/j.1475-4983.2010.01030.x.
- Holmer, L. E., Zhang, Z.-F., Topper, T. P., Popov, L. E., and Claybourn, T. M. (2018b). The attachment strategies of Cambrian kutoarginate brachiopods: the curious case of two pedicle openings and their phylogenetic significance. *Journal of Paleontology*, 92(1):33–39, doi:10.1017/jpa.2017.76.
- Hou, X.-G., Siveter, D. J., Siveter, D. J., Aldridge, R. J., Cong, P.-Y., Gabbott, S. E., and Purnell, M. A. (2017). Brachiopoda. In *The Cambrian Fossils of Chengjiang, China: The Flowering of Early Animal Life*. Blackwell.
- Hu, S.-X., Zhang, Z.-F., Holmer, L. E., and Skovsted, C. B. (2010). Soft-part preservation in a linguliform brachiopod from the lower Cambrian Wulongqing Formation (Guanshan Fauna) of Yunnan, South China. *Acta Palaeontologica Polonica*, 55(3):495–505, doi:10.4202/app.2009.1106.
- Hunt, S. (1972). Scleroprotein and chitin in the exoskeleton of the ectoproct *Flustra foliacea*. *Comparative Biochemistry and Physiology Part B: Comparative Biochemistry*, 43(3):571–574, doi:10.1016/0305-0491(72)90140-X.
- Jacquet, S. M., Brock, G. A., and Paterson, J. R. (2014). New data on *Oikozetetes* (Mollusca, Halkieriidae) from the lower Cambrian of South Australia. *Journal of Paleontology*, 88(5):1072–1084, doi:10.1666/13-137.

- Jamieson, B. G. M. (1991). *Fish Evolution and Systematics: Evidence from Spermatozoa: With a Survey of Lophophorate, Echinoderm and Protochordate Sperm and an Account of Gamete Cryopreservation*. Cambridge University Press.
- Jeuniaux, C. (1971). Chitinous structures. *Comprehensive biochemistry*, 26(C):595–632.
- Jin, Y.-G. and Wang, H.-Y. (1992). Revision of the Lower Cambrian brachiopod *Heliomedusa* Sun & Hou, 1987. *Lethaia*, 24:35–49, doi:10.1111/j.1502-3931.1992.tb01790.x.
- Keay, J. (2007). Larval development of the polychaete annelid, *Serpula vermicularis*. Technical report, Oregon Institute of Marine Biology.
- Kopuchian, C. and Ramírez, M. J. (2010). Behaviour of resampling methods under different weighting schemes, measures and variable resampling strengths. *Cladistics*, 26(1):86–97, doi:10.1111/j.1096-0031.2009.00269.x.
- Kouchinsky, A. V. (2000). Skeletal microstructures of hyoliths from the Early Cambrian of Siberia. *Alcheringa: An Australasian Journal of Palaeontology*, 24(2):65–81, doi:10.1080/03115510008619525.
- Larsson, C. M., Skovsted, C. B., Brock, G. A., Balthasar, U., Topper, T. P., and Holmer, L. E. (2014). *Paterimitra pyramidalis* from South Australia: scleritome, shell structure and evolution of a lower Cambrian stem group brachiopod. *Palaeontology*, 57(2):417–446, doi:10.1111/pala.12072.
- Laurie, J. (1987). The musculature and vascular systems of two species of Cambrian Paterinide (Brachiopoda). *Bureau of Mineral Resources Journal of Australian Geology and Geophysics*, 10:261–265.
- Leise, E. M. (1988). Sensory organs in the hairy girdles of some mopaliid chitons. *American Malacological Bulletin*, 6(1):141–151.
- Leise, E. M. and Cloney, R. (1982). Chiton integument: ultrastructure of the sensory hairs of *Mopalia muscosa* (Mollusca: Polyplacophora). *Cell and Tissue Research*, 223(1):43–59, doi:10.1007/BF00221498.
- Lewis, P. O. (2001). A likelihood approach to estimating phylogeny from discrete morphological character data. *Systematic Biology*, 50(6):913–925, doi:10.1080/106351501753462876.
- Li, G.-X. and Holmer, L. E. (2004). Early Cambrian lingulate brachiopods from the Shaanxi Province, China. *GFF*, 126(2):193–211, doi:10.1080/11035890401262193.
- Lundin, K., Schander, C., and Todt, C. (2009). Ultrastructure of epidermal cilia and ciliary rootlets in Scaphopoda. *Journal of Molluscan Studies*, 75(1):69–73, doi:10.1093/mollus/eyn042.
- Lüter, C. (1995). Ultrastructure of the metanephridia of *Terebratulina retusa* and *Crania anomala* (Brachiopoda). *Zoomorphology*, 115(2):99–107, doi:10.1007/BF00403258.
- Lüter, C. (2000). Ultrastructure of larval and adult setae of Brachiopoda. *Zoologischer Anzeiger*, 239(1):75–90.
- Lüter, C. (2003). Brachiopod larval setae – a key to the phylum's ancestral life cycle? In *Brachiopods Past and Present*, pages 46–55. CRC Press, London.
- Lüter, C. (2016). Brachiopoda. In Schmidt-Rhaesa, A., Harzsch, S., and Purschke, G., editors, *Structure and Evolution of Invertebrate Nervous Systems*, pages 341–350. Oxford University Press, Oxford.
- MacKay, S. and Hewitt, R. A. (1978). Ultrastructural studies on the brachiopod pedicle. *Lethaia*, 11(4):331–339, doi:10.1111/j.1502-3931.1978.tb01891.x.
- Maddison, W. P. (1993). Missing data versus missing characters in phylogenetic analysis. *Systematic Biology*, 42(4):576–581, doi:10.1093/sysbio/42.4.576.
- Madison, A. (2017). Laminar shell structure of *Antigonambonites planus* (Pander, 1830) (Brachiopoda, Billingsellida). *Estonian Journal of Earth Sciences*, 66:183–187, doi:10.3176/earth.2017.17.

- Malinky, J. M. (1987). Taxonomic revision of lower and middle Paleozoic Orthothecida (Hyolitha) from North America and China. *Journal of Paleontology*, 61(05):942–959, doi:10.1017/S0022336000029310.
- Marek, L. (1963). New knowledge on the morphology of *Hyolithes*. *Sborník geologických věd: Paleontologie*, 1:53–73, pls 1–4.
- Marek, L. (1966). New hyolithid genera from the Ordovician of Bohemia [Nové rody hyolitů z Českého ordoviku]. *Časopis Národního Muzea, Oddíl přírodovědný*, 135:89–92.
- Marek, L. (1967). The Class Hyolitha in the Caradoc of Bohemia. *Sborník Geologických věd. Paleontologie*, 9:51–112, pls 1–10.
- Marek, L. (1972). Middle Cambrian Hyolithes: *Maxilites* gen. n. [*Maxilites* gen. n. ze středního kambria (Hyolitha)]. *Časopis Národního Muzea, Oddíl přírodovědný*, 141(1-2):69–72.
- Marek, L. (1976). The distribution of the Mediterranean Ordovician Hyolitha. In Bassett, M. G., editor, *The Ordovician System: Proceedings of a Palaeontological Association Symposium*, pages 491–499. University of Wales Press and National Museum of Wales, Cardiff.
- Martí Mus, M. and Bergström, J. (2005). The morphology of hyolithids and its functional implications. *Palaeontology*, 48(6):1139–1167, doi:10.1111/j.1475-4983.2005.00511.x.
- Martí Mus, M. and Bergström, J. (2007). Skeletal microstructure of helens, lateral spines of hyolithids. *Palaeontology*, 50(5):1231–1243, doi:10.1111/j.1475-4983.2007.00700.x.
- Miles, C. M., Hadfield, M. G., and Wayne, M. L. (2007). Heritability for egg size in the serpulid polychaete *Hydroides elegans*. *Marine Ecology Progress Series*, 340(May 2014):155–162, doi:10.3354/meps340155.
- Morton, J. E. (1959). The habits and feeding organs of *Dentalium entalis*. *Journal of the Marine Biological Association of the United Kingdom*, 38(2):225–238, doi:10.1017/S0025315400006032.
- Moysiuk, J., Smith, M. R., and Caron, J.-B. (2017). Hyoliths are Palaeozoic lophophorates. *Nature*, 541(7637):394–397, doi:10.1038/nature20804.
- Nielsen, C. (1966). On the life-cycle of some Loxosomatidae (Entoprocta). *Ophelia*, 3(1):221–247, doi:10.1080/00785326.1966.10409644.
- Nielsen, C. (1971). Entoproct life-cycles and the entoproct/ectoproct relationship. *Ophelia*, 9(2):209–341, doi:10.1080/00785326.1971.10430095.
- Nielsen, C. (1987). Structure and function of metazoan ciliary bands and their phylogenetic significance. *Acta Zoologica*, 68(4):205–262, doi:10.1111/j.1463-6395.1987.tb00892.x.
- Nielsen, C. (1991). The development of the brachiopod *Crania (Neocrania) anomala* (O. F. Müller) and its phylogenetic significance. *Acta Zoologica*, 72(1):7–28, doi:10.1111/j.1463-6395.1991.tb00312.x.
- Nielsen, C. and Rostgaard, J. (1976). Structure and function of an entoproct tentacle with a discussion of ciliary feeding types. *Ophelia*, 15(2):115–140, doi:10.1080/00785326.1976.10425453.
- Nikitin, I. F. and Popov, L. E. (1984). Brachiopods and biostratigraphy of the Middle and Upper Ordovician of the Chingiz Range. In *Brachiopods and biostratigraphy of the Middle and Upper Ordovician of the Chingiz Range, Part II: Brachiopods from the Bestamak and Sargaldak Formations (Middle Ordovician)*, pages 126–166. Nauka, Alma-Ata.
- Nixon, K. C. (1999). The Parsimony Ratchet, a new method for rapid parsimony analysis. *Cladistics*, 15(4):407–414, doi:10.1111/j.1096-0031.1999.tb00277.x.
- Orrhage, L. (1971). Light and electron microscope studies of some annelid setae. *Acta Zoologica*, 52(1):157–169, doi:10.1111/j.1463-6395.1971.tb00555.x.

- Orrrage, L. and Müller, M. C. M. (2005). Morphology of the nervous system of Polychaeta (Annelida). *Hydrobiologia*, 535-536(1):79–111, doi:10.1007/s10750-004-4375-4.
- Owen, G. and Williams, A. (1969). The caecum of articulate Brachiopoda. *Proceedings of the Royal Society B: Biological Sciences*, 172:187–201, doi:10.1098/rspb.1969.0019.
- Pardos, F., Roldán, C., Benito, J., and Emig, C. C. (1991). Fine structure of the tentacles of *Phoronis australis* Haswell (Phoronida, Lophophorata). *Acta Zoologica*, 72(2):81–90, doi:10.1111/j.1463-6395.1991.tb00320.x.
- Parkinson, D., Curry, G. B., Cusack, M., and Fallick, A. E. (2005). Shell structure, patterns and trends of oxygen and carbon stable isotopes in modern brachiopod shells. *Chemical Geology*, 219(1-4):193–235, doi:10.1016/j.chemgeo.2005.02.002.
- Parks, S. L. and Goldman, N. (2014). Maximum Likelihood inference of small trees in the presence of long branches. *Systematic Biology*, 63(5):798–811, doi:10.1093/sysbio/syu044.
- Paterson, J. R., Brock, G. A., and Skovsted, C. B. (2009). *Oikozetetes* from the early Cambrian of South Australia: implications for halkieriid affinities and functional morphology. *Lethaia*, 42(2):199–203, doi:10.1111/j.1502-3931.2008.00132.x.
- Pennerstorfer, M. and Scholtz, G. (2012). Early cleavage in *Phoronis muelleri* (Phoronida) displays spiral features. *Evolution and Development*, 14(6):484–500, doi:10.1111/ede.12002.
- Pilger, J. F. (1982). Ultrastructure of the tentacles of *Themiste lageniformis* (Sipuncula). *Zoomorphology*, 100(2):143–156, doi:10.1007/BF00310360.
- Ponder, W. F. and Lindberg, D. R. (1997). Towards a phylogeny of gastropod molluscs: an analysis using morphological characters. *Zoological Journal of the Linnean Society*, 119(2):83–265, doi:10.1111/j.1096-3642.1997.tb00137.x.
- Popov, L. E. (1992). The Cambrian radiation of brachiopods. In Lipps, J. H. and Signor, P. W., editors, *Origin and Early Evolution of Metazoa*, pages 399–423. Pergamon.
- Popov, L. E., Bassett, M. G., Holmer, L. E., and Ghobadi Pour, G. M. (2009). Early ontogeny and soft tissue preservation in siphonotretide brachiopods: new data from the Cambrian-Ordovician of Iran. *Gondwana Research*, 16(1):151–161, doi:10.1016/j.gr.2009.01.009.
- Popov, L. E., Bassett, M. G., Holmer, L. E., Skovsted, C. B., and Zuykov, M. A. (2010). Earliest ontogeny of Early Palaeozoic Craniiformea: Implications for brachiopod phylogeny. *Lethaia*, 43(3):323–333, doi:10.1111/j.1502-3931.2009.00197.x.
- Popov, L. E., Holmer, L. E., and Gorjansky, V. J. (1997). Late Ordovician and Early Silurian trimerellide brachio-pods from Kazakhstan. *Journal of Paleontology*, 71(4):584–598, doi:10.1017/S0022336000040075.
- Porter, S. M. (2008). Skeletal microstructure indicates chancelloriids and halkieriids are closely related. *Palaeontology*, 51(4):865–879, doi:10.1111/j.1475-4983.2008.00792.x.
- Rannala, B., Zhu, T.-Q., and Yang, Z.-H. (2012). Tail paradox, partial identifiability, and influential priors in Bayesian branch length inference. *Molecular Biology and Evolution*, 29(1):325–335, doi:10.1093/molbev/msr210.
- Reed, C. G. (1988). The reproductive biology of the gymnolaemate bryozoan *Bowerbankia gracilis* (Ctenostomata: Vesiculariidae). *Ophelia*, 29(1):1–23, doi:10.1080/00785326.1988.10430816.
- Reed, C. G. and Cloney, R. A. (1982). The larval morphology of the marine bryozoan *Bowerbankia gracilis* (Ctenostomata: Vesicularioidea). *Zoomorphology*, 100(1):23–54, doi:10.1007/BF00312198.
- Reger, J. F. (1967). A fine structure study on the organization and innervation of pharyngeal glands and associated ciliated epithelium in the annelid *Enchytraeus albidus*. *Journal of Ultrastructure Research*, 20:451–461, doi:10.1016/S0022-5320(67)80112-6.

- Reunov, A. A. and Klepal, W. (2004). Ultrastructural study of spermatogenesis in *Phoronopsis harmeri* (Lophophorata, Phoronida). *Helgoland Marine Research*, 58(1):229, doi:10.1007/s10152-003-0153-3.
- Rice, M. E. (1988). Observations on development and metamorphosis of *Siphonosoma cumanense* with comparative remarks on *Sipunculus nudus* (Sipuncula, Sipunculidae). *Bulletin of Marine Science*, 42(1):1–15.
- Rice, M. E. (1993). Sipuncula. In Harrison, F. W. and Rice, M. E., editors, *Microscopic anatomy of invertebrates, volume 12: Onychophora, Chilopoda, and Lesser Protostomata*, volume 12, pages 237–326. Wiley-Liss, New York.
- Richter, S., Loesel, R., Purschke, G., Schmidt-Rhaesa, A., Scholtz, G., Stach, T., Vogt, L., Wanninger, A., Brenneis, G., Döring, C., Faller, S., Fritsch, M., Grobe, P., Heuer, C. M., Kaul, S., Møller, O. S., Müller, C. H., Rieger, V., Rothe, B. H., Stegner, M. E., and Harzsch, S. (2010). Invertebrate neurophylogeny: suggested terms and definitions for a neuroanatomical glossary. *Frontiers in Zoology*, 7:29, doi:10.1186/1742-9994-7-29.
- Robinson, J. (2014). The muscles, body wall and valve-opening mechanism of extant craniid (inarticulated) brachiopods. *Journal of Natural History*, 48:1231–1252, doi:10.1080/00222933.2013.840941.
- Robson, S. P. and Pratt, B. R. (2001). Cambrian and Ordovician linguliform brachiopods from the Shallow Bay Formation (Cow Head Group), western Newfoundland. *75(2):241–260*, doi:10.1017/s0022336000018060.
- Ronquist, F., Teslenko, M., van der Mark, P., Ayres, D. L., Darling, A., Hohna, S., Larget, B., Liu, L., Suchard, M. A., and Huelsenbeck, J. P. (2012). MrBayes 3.2: efficient Bayesian phylogenetic inference and model choice across a large model space. *Systematic Biology*, 61(3):539–42, doi:10.1093/sysbio/sys029.
- Rouse, G. W. (1999). Trochophore concepts: ciliary bands and the evolution of larvae in spiralian Metazoa. *Biological Journal of the Linnean Society*, 66(4):411–464, doi:10.1111/j.1095-8312.1999.tb01920.x.
- Rouse, G. W. (2000). Bias? What bias? The evolution of downstream larval-feeding in animals. *Zoologica Scripta*, 29(3):213–236, doi:10.1046/j.1463-6409.2000.00040.x.
- Rowell, A. J. and Caruso, N. E. (1985). The evolutionary significance of *Nisusia sulcata*, an early articulate brachiopod. *Journal of Paleontology*, 59(5):1227–1242.
- Ruppert, E. E. and Carle, K. J. (1983). Morphology of metazoan circulatory systems. *Zoomorphology*, 103(3):193–208, doi:10.1007/BF00310477.
- Ruppert, E. E., Fox, R. S., and Barnes, R. D. (2004). *Invertebrate zoology: a functional evolutionary approach*, volume 53. Thompson Learning.
- Ruppert, E. E. and Rice, M. E. (1995). Functional organization of dermal coelomic canals in *Sipunculus nudus* (Sipuncula) with a discussion of respiratory designs in sipunculans. *Invertebrate Biology*, 114(1):51–63, doi:10.2307/3226953.
- Santagata, S. (2002). Structure and metamorphic remodeling of the larval nervous system and musculature of *Phoronis pallida* (Phoronida). *Evolution and Development*, 4(1):28–42, doi:10.1046/j.1525-142x.2002.01055.x.
- Santagata, S. (2004). Larval development of *Phoronis pallida* (Phoronida): implications for morphological convergence and divergence among larval body plans. *Journal of Morphology*, 259(3):347–358, doi:10.1002/jmor.10205.
- Scheltema, A. H. (1993). Aplacophora as progenetic aculiferans and the coelomate origin of mollusks as the sister taxon of Sipuncula. *Biological Bulletin*, 184(1):57–78, doi:10.2307/1542380.
- Schopf, T. J. M. and Manheim, F. T. (1967). Chemical composition of Ectoprocta (Bryozoa). *Journal of Paleontology*, 41(5):1197–1225, doi:10.2307/1302092.

- Schulze, A., Cutler, E. B., and Giribet, G. (2005). Reconstructing the phylogeny of the Sipuncula. *Hydrobiologia*, 535-536(1):277–296, doi:10.1007/s10750-004-4404-3.
- Schwabe, E. (2010). Illustrated summary of chiton terminology. *Spixiana*, 3(2):171–194.
- Schwaha, T. F. and Wanninger, A. (2015). The serotonin-lir nervous system of the Bryozoa (Lophotrochozoa): a general pattern in the Gymnolaemata and implications for lophophore evolution of the phylum Evolutionary developmental biology and morphology. *BMC Evolutionary Biology*, 15(1):223, doi:10.1186/s12862-015-0508-9.
- Sereno, P. C. (2007). Logical basis for morphological characters in phylogenetics. *Cladistics*, 23(6):565–587, doi:10.1111/j.1096-0031.2007.00161.x.
- Shimek, R. L. (1988). The functional morphology of scaphopod captacula. *The Veliger*, 30(3):213–221.
- Shunkina, K. V., Zaytseva, O. V., Starunov, V. V., and Ostrovsky, A. N. (2015). Comparative morphology of the nervous system in three phylactolaemate bryozoans. *Frontiers in Zoology*, 12:28, doi:10.1186/s12983-015-0112-2.
- Simmons, M. P. and Freudenstein, J. V. (2011). Spurious 99% bootstrap and jackknife support for unsupported clades. *Molecular Phylogenetics and Evolution*, 61(1):177–191, doi:10.1016/j.ympev.2011.06.003.
- Skovsted, C. B., Betts, M. J., Topper, T. P., and Brock, G. A. (2015). The early Cambrian tommotiid genus *Dailyatia* from South Australia. *Memoirs of the Association of Australasian Palaeontologists*, 48(1):1–117.
- Skovsted, C. B., Brock, G. A., Paterson, J. R., Holmer, L. E., and Budd, G. E. (2008). The scleritome of *Eccentrotheca* from the Lower Cambrian of South Australia: Lophophorate affinities and implications for tommotiid phylogeny. *Geology*, 36:171–174, doi:10.1130/g24385a.1.
- Skovsted, C. B., Brock, G. A., Topper, T. P., Paterson, J. R., and Holmer, L. E. (2011). Scleritome construction, biofacies, biostratigraphy and systematics of the tommotiid *Eccentrotheca helenia* sp. nov. from the early Cambrian of South Australia. *Palaeontology*, 54:253–286, doi:10.1111/j.1475-4983.2010.01031.x.
- Skovsted, C. B. and Holmer, L. E. (2003). Early Cambrian (Botomian) stem group brachiopod *Mickwitzia* from Northeast Greenland. *Acta Palaeontologica Polonica*, 48(1):1–20.
- Skovsted, C. B. and Holmer, L. E. (2005). Early Cambrian brachiopods from north-east Greenland. *Palaeontology*, 48(2):325–345, doi:10.1111/j.1475-4983.2005.00450.x.
- Skovsted, C. B., Holmer, L. E., Larsson, C. M., Höglström, A. E. S., Brock, G. A., Topper, T. P., Balthasar, U., Stolk, S. P., and Paterson, J. R. (2009). The scleritome of *Paterimitra*: an Early Cambrian stem group brachiopod from South Australia. *Proceedings of the Royal Society B: Biological Sciences*, 276:1651–1656, doi:10.1098/rspb.2008.1655.
- Skovsted, C. B., Knight, I., Balthasar, U., and Boyce, W. D. (2017). Depth related brachiopod faunas from the lower Cambrian Forteau Formation of southern Labrador and western Newfoundland, Canada. *Palaeontologia Electronica*, 20.3.54A:1–52, doi:10.26879/775.
- Skovsted, C. B., Pan, B., Topper, T. P., Betts, M. J., Li, G., and Brock, G. A. (2016). The operculum and mode of life of the lower Cambrian hyolith *Cupitheca* from South Australia and North China. *Palaeogeography, Palaeoclimatology, Palaeoecology*, 443:123–130, doi:10.1016/j.palaeo.2015.11.042.
- Skovsted, C. B. and Peel, J. S. (2010). Early Cambrian brachiopods and other shelly fossils from the basal Kinzers Formation of Pennsylvania. *Journal of Paleontology*, 84(4):754–762, doi:10.1666/09-123.1.
- Smith, M. R. (2012a). *Morphology, ecology, and affinity of soft-bodied ‘molluscs’ from Cambrian Burgess Shale-type deposits*. PhD thesis, University of Toronto, Toronto, Ontario.
- Smith, M. R. (2012b). Mouthparts of the Burgess Shale fossils *Odontogriphus* and *Wiwaxia*: implications for the ancestral molluscan radula. *Proceedings of the Royal Society B: Biological Sciences*, 279(1745):4287–4295, doi:10.1098/rspb.2012.1577.

- Smith, M. R. (2014). Ontogeny, morphology and taxonomy of the soft-bodied Cambrian 'mollusc' *Wiwaxia*. *Palaeontology*, 57(1):215–229, doi:10.1111/pala.12063.
- Smith, M. R. (2017). Quantifying and visualising divergence between pairs of phylogenetic trees: implications for phylogenetic reconstruction. *bioRxiv*, doi:10.1101/227942.
- Smith, M. R. (2018). TreeSearch: phylogenetic tree search using custom optimality criteria.
- Steiner, G. (1992). Phylogeny and classification of Scaphopoda. *Journal of Molluscan Studies*, 58(4):385–400, doi:10.1093/mollus/58.4.385.
- Storch, V. and Herrmann, K. (1978). Podocytes in the blood vessel linings of *Phoronis muelleri* (Phoronida, Tentaculata). *Cell and Tissue Research*, 190(3):553–556, doi:10.1007/bf00219564.
- Streng, M., Butler, A. D., Peel, J. S., Garwood, R. J., and Caron, J.-B. (2016). A new family of Cambrian rhynchonelliform brachiopods (Order Naukatida) with an aberrant coral-like morphology. *Palaeontology*, 59(2):269–293, doi:10.1111/pala.12226.
- Sumner-Rooney, L. H., Schrödl, M., Lodde-Bensch, E., Lindberg, D. R., Heß, M., Brennan, G. P., and Sigwart, J. D. (2015). A neurophylogenetic approach provides new insight to the evolution of Scaphopoda. *Evolution and Development*, 17(6):337–346, doi:10.1111/ede.12164.
- Sun, H.-J., Malinky, J. M., Zhu, M.-Y., and Huang, D.-Y. (2018a). Palaeobiology of orthothecide hyoliths from the Cambrian Manto Formation of Hebei Province, North China. *Acta Palaeontologica Polonica*, 63(1):87–101, doi:10.4202/app.00413.2017.
- Sun, H.-J., Smith, M. R., Zeng, H., Zhao, F.-C., Li, G.-X., and Zhu, M.-Y. (2018b). Hyoliths with pedicles constrain the origin of the brachiopod body plan. page submitted.
- Sun, Y. and Qiu, J.-W. (2012). Serpulidae (Annelida: Polychaeta) from Hong Kong. *Zootaxa*, 3423:1–42.
- Sutton, M. D., Briggs, D. E. G., Siveter, D. J., and Siveter, D. J. (2005). Silurian brachiopods with soft-tissue preservation. *Nature*, 436(7053):1013–1015, doi:10.1038/nature03846.
- Sutton, M. D. and Sigwart, J. D. (2012). A chiton without a foot. *Palaeontology*, 55(2):401–411, doi:10.1111/j.1475-4983.2011.01126.x.
- Temereva, E. N. (2016). Phoronida. In Schmidt-Rhaesa, A., Harzsch, S., and Purschke, G., editors, *Structure and Evolution of Invertebrate Nervous Systems*, pages 351–359. Oxford University Press, Oxford.
- Temereva, E. N. (2017). Innervation of the lophophore suggests that the phoronid *Phoronis ovalis* is a link between phoronids and bryozoans. *Scientific Reports*, 7:14440, doi:10.1038/s41598-017-14590-8.
- Temereva, E. N. and Kosevich, I. A. (2016). The nervous system of the lophophore in the ctenostome *Amathia gracilis* provides insight into the morphology of ancestral ectoprocts and the monophyly of the lophophorates. *BMC Evolutionary Biology*, 16(1):181, doi:10.1186/s12862-016-0744-7.
- Temereva, E. N. and Kuzmina, T. V. (2017). The first data on the innervation of the lophophore in the rhynchonelliform brachiopod *Hemithiris psittacea*: what is the ground pattern of the lophophore in lophophorates? *BMC Evolutionary Biology*, 17(1):172, doi:10.1186/s12862-017-1029-5.
- Topper, T. P., Harper, D. A. T., and Ahlberg, P. (2013a). Reappraisal of the brachiopod *Acrotreta socialis* von Seebach, 1865: clarifying 150 years of confusion. *GFF*, 135(2):191–203, doi:10.1080/11035897.2013.811440.
- Topper, T. P., Holmer, L. E., Skovsted, C. B., Brock, G. A., Balthasar, U., Larsson, C. M., Petterson Stolk, P. S., and Harper, D. A. T. (2013b). The oldest brachiopods from the lower Cambrian of South Australia. *Acta Palaeontologica Polonica*, 58(1):93–109, doi:10.4202/app.2011.0146.
- Torrey, H. B. (1901). On *Phoronis pacifica* sp. nov. *Biological Bulletin*, 2(6):282–288, doi:10.2307/1535705.

- Ushatinskaya, G. T. (2016). Protegulum and brephic shell of the earliest organophosphatic brachiopods. *Paleontological Journal*, 50(2):141–152, doi:10.1134/s0031030116020088.
- Ushatinskaya, G. T. and Korovnikov, I. V. (2016). Revision of the superfamily Acrotheloidea (Brachiopoda, class Linguliformea, order Lingulida) from the Lower and Middle Cambrian of the Siberian Platform. *Paleontological Journal*, 50(5):450–462, doi:10.1134/s0031030116050130.
- Valent, M. and Corbacho, J. (2015). *Pauxillites thaddei* a new Lower Ordovician hyolith from Morocco. *Acta Musei Nationalis Pragae, Series B - Historia Naturalis*, 71(1-2):51–54, doi:10.14446/AMNP.2015.51.
- Valent, M., Fatka, O., Szabad, M., Micka, V., and Marek, L. (2012). Two new orthothecids from the Cambrian of the Barrandian area (Hyolitha, Skryje-Týřovice Basin, Czech Republic). *Bulletin of Geosciences*, 87(2):241–248, doi:10.3140/bull.geosci.1142.
- Vendrasco, M. J., Checa, A. G., and Porter, S. M. (2017). Periostracum and fibrous shell microstructure in the unusual Cambrian hyolith *Cupitheca*. *Spanish Journal of Palaeontology*, 32(1):95–108.
- Vinther, J. and Nielsen, C. (2005). The Early Cambrian *Halkieria* is a mollusc. *Zoologica Scripta*, 34(1):81–89, doi:10.1111/j.1463-6409.2005.00177.x.
- Vinther, J., Van Roy, P., and Briggs, D. E. G. (2008). Machaeridians are Palaeozoic armoured annelids. *Nature*, 451(7175):185–188, doi:10.1038/nature06474.
- Vogt, L. (2017). The logical basis for coding ontologically dependent characters. *Cladistics*, doi:10.1111/cla.12209.
- von Salvini-Plawen, L. and Steiner, G. (1996). Synapomorphies and plesiomorphies in higher classification of Mollusca. In Taylor, J. D., editor, *Origin and Evolutionary Radiation of the Mollusca*, pages 29–51. The Malacological Society of London, London.
- Wanninger, A. (2009). Shaping the things to come: ontogeny of lophotrochozoan neuromuscular systems and the tetraneuralia concept. *Biological Bulletin*, 216(3):293–306, doi:10.1086/bblv216n3p293.
- Wanninger, A., Fuchs, J., and Haszprunar, G. (2007). Anatomy of the serotonergic nervous system of an entoproct creeping-type larva and its phylogenetic implications. *Invertebrate Biology*, 126(3):268–278, doi:10.1111/j.1744-7410.2007.00097.x.
- Wanninger, A. and Haszprunar, G. (2001). The expression of an engrailed protein during embryonic shell formation of the tusk-shell, *Antalisentalis* (Mollusca, Scaphopoda). *Evolution & Development*, 3(5):312, doi:10.1046/j.1525-142X.2001.01034.x.
- Wanninger, A. and Haszprunar, G. (2002a). Chiton myogenesis: perspectives for the development and evolution of larval and adult muscle systems in molluscs. *Journal of Morphology*, 251(2):103–113, doi:10.1002/jmor.1077.
- Wanninger, A. and Haszprunar, G. (2002b). Muscle development in *Antalisentalis* (Mollusca, Scaphopoda) and its significance for scaphopod relationships. *Journal of Morphology*, 254(1):53–64, doi:10.1002/jmor.10004.
- Wanninger, A., Koop, D., Bromham, L., Noonan, E., and Degnan, B. M. (2005). Nervous and muscle system development in *Phascolionstrombus* (Sipuncula). *Development Genes and Evolution*, 215(10):509–518, doi:10.1007/s00427-005-0012-0.
- Watkins, R. (2002). New record of the trimerellid brachiopod *Gasconsia*, a rare Silurian Lazarus taxon. *Journal of Paleontology*, 76(1):185–186, doi:10.1666/0022-3360(2002)076<0185:nottb>2.0.co;2.
- Wiens, J. J. (1998). Does adding characters with missing data increase or decrease phylogenetic accuracy? *Systematic Biology*, 47(4):625–640, doi:10.1080/106351598260635.

- Wiens, J. J. (2003). Missing data, incomplete taxa, and phylogenetic accuracy. *Systematic Biology*, 52(4):528–538, doi:10.1080/10635150390218330.
- Williams, A. and Brunton, C. H. C. (1993). Role of shell structure in the classification of the orthotetidine brachiopods. *Palaeontology*, 36:931–966.
- Williams, A., Carlson, S. J., Brunton, C. H. C., Holmer, L. E., and Popov, L. E. (1996). A supra-ordinal classification of the Brachiopoda. *Philosophical Transactions of the Royal Society B: Biological Sciences*, 351(1344):1171–1193, doi:10.1098/rstb.1996.0101.
- Williams, A., Carlson, S. J., Brunton, C. H. C., Holmer, L. E., Popov, L. E., Mergl, M., Laurie, J. R., Bassett, M. G., Cocks, L. R. M., Rong, J.-Y., Lazarev, S. S., Grant, R. E., Racheboeuf, P. R., Jin, Y.-G., Wardlaw, B. R., Harper, D. A. T., and Wright, A. D. (2000). Linguliformea, Craniiformea, and Rhynchonelliformea (part). In *Treatise on Invertebrate Paleontology, Part H, Brachiopoda (Revised)*, volume 2 & 3, pages 1–919. Geological Society of America & Paleontological Institute.
- Williams, A., Cusack, M., and Buckman, J. O. (1998a). Chemico-structural phylogeny of the discinoid brachiopod shell. *Philosophical Transactions of the Royal Society B: Biological Sciences*, 353(1378):2005–2038, doi:10.1098/rstb.1998.0350.
- Williams, A., Cusack, M., and Mackay, S. (1994). Collagenous chitino-phosphatic shell of the brachiopod *Lingula*. *Philosophical Transactions of the Royal Society B: Biological Sciences*, 346:223–266, doi:10.1098/rstb.1994.0143.
- Williams, A., Holmer, L. E., and Cusack, M. (2004). Chemico-structure of the organophosphatic shells of siphonotretide brachiopods. *Palaeontology*, 47(5):1313–1337, doi:10.1111/j.0031-0239.2004.00404.x.
- Williams, A., James, M. A., Emig, C. C., Mackay, S., Rhodes, M. C., Cohen, B. L., Gawthrop, A. B., Peck, L. S., Curry, G. B., Ansell, A. D., Cusack, M., Walton, D., Brunton, C. H. C., MacKinnon, D. I., and Richardson, J. R. (1997). Introduction. In *Treatise on Invertebrate Paleontology, Part H, Brachiopoda (Revised)*, volume 1, pages 1–539. Geological Society of America & Paleontological Institute.
- Williams, A., Mackay, S., and Cusack, M. (1992). Structure of the organo-phosphatic shell of the brachiopod *Discina*. *Philosophical Transactions of the Royal Society B: Biological Sciences*, 337:83–104, doi:10.1098/rstb.1992.0086.
- Williams, A., Popov, L. E., Holmer, L. E., and Cusack, M. (1998b). The diversity and phylogeny of the paterinate brachiopods. *Palaeontology*, 41:221–262.
- Williams, A., Racheboeuf, P. R., Savage, N. M., Lee, D. E., Popov, L. E., Carlson, S. J., Logan, A., Lüter, C., Cusack, M., Curry, G. B., Wright, A. D., Harper, D. A. T., Cohen, B. L., Cocks, L. R. M., MacKinnon, D. I., Smirnova, T. N., Baker, P. G., Carter, J. L., Gourvennec, R., Mancenido, M. O., Brunton, C. H. C., Dong-Li, D.-S., Boucot, A. J., Bassett, M. G., Alvarez, F., Holmer, L. E., Mergl, M., Emig, C. C., Rubel, M., and Jia-Yu, J.-R. (2007). Supplement. In *Treatise on Invertebrate Paleontology, Part H, Brachiopoda (Revised)*, volume 6, pages 2321–3226. Geological Society of America & Paleontological Institute.
- Williams, A., Sandy, M. R., Carlson, S. J., Lee, D. E., Johnson, J. G., Smirnova, T. N., Jin, Y.-G., Hou, H.-F., Carter, J. L., Gourvennec, R., Racheboeuf, P. R., Brunton, C. H. C., Dagys, A. S., Curry, G. B., Baker, P. G., Sun, D.-L., and MacKinnon, D. I. (2006). Rhynchonelliformea (part). In *Treatise on Invertebrate Paleontology, Part H, Brachiopoda (Revised)*, volume 5, pages 1689–2320. Geological Society of America & Paleontological Institute.
- Wingstrand, K. G. (1985). On the anatomy and relationships of Recent Monoplacophora. *Galathea Report*, 16:7–94.
- Wrona, R. (2003). Early Cambrian molluscs from glacial erratics of King George Island, West Antarctica. *Polish Polar Research*, 24(3-4):181–216.

- Yang, Z. and Zhu, T. (2018). Bayesian selection of misspecified models is overconfident and may cause spurious posterior probabilities for phylogenetic trees. *Proceedings of the National Academy of Sciences*, 115(8):1854–1859, doi:10.1073/pnas.1712673115.
- Young, C. M. (2002). *Atlas of Marine Invertebrate Larvae*. Academic Press, New York.
- Zhang, C., Rannala, B., and Yang, Z.-H. (2012). Robustness of compound Dirichlet priors for Bayesian inference of branch lengths. *Systematic Biology*, 61(5):779–84, doi:10.1093/sysbio/sys030.
- Zhang, Z.-F., Han, J., Zhang, X.-L., Liu, J.-N., Guo, J.-F., and Shu, D.-G. (2007a). Note on the gut preserved in the Lower Cambrian *Lingulellotreta* (Lingulata, Brachiopoda) from southern China. *Acta Zoologica*, 88(1):65–70, doi:10.1111/j.1463-6395.2007.00252.x.
- Zhang, Z.-F., Holmer, L. E., Ou, Q., Han, J., and Shu, D.-G. (2011a). The exceptionally preserved Early Cambrian stem rhynchonelliform brachiopod *Longtancunella* and its implications. *Lethaia*, 44(4):490–495, doi:10.1111/j.1502-3931.2011.00261.x.
- Zhang, Z.-F., Holmer, L. E., Popov, L. E., and Shu, D.-G. (2011b). An obolellate brachiopod with soft-part preservation from the Early Cambrian Chengjiang fauna of China. *Journal of Paleontology*, 85(3):460–463, doi:10.1666/10-121.1.
- Zhang, Z.-F., Holmer, L. E., Skovsted, C. B., Brock, G. A., Budd, G. E., Fu, D., Zhang, X.-L., Shu, D.-G., Han, J., Liu, J.-N., Wang, H., Butler, A., and Li, G.-X. (2013). A sclerite-bearing stem group entoproct from the early Cambrian and its implications. *Scientific Reports*, 3:1066, doi:10.1038/srep01066.
- Zhang, Z.-F., Li, G.-X., Emig, C. C., Han, J., Holmer, L. E., and Shu, D.-G. (2009). Architecture and function of the lophophore in the problematic brachiopod *Heliomedusa orienta* (Early Cambrian, South China). *Geobios*, 42(5):649–661, doi:10.1016/j.geobios.2009.04.001.
- Zhang, Z.-F., Li, G.-X., Holmer, L. E., Brock, G. A., Balthasar, U., Skovsted, C. B., Fu, D.-J., Zhang, X.-L., Wang, H.-Z., Butler, A. D., Zhang, Z.-L., Cao, C.-Q., Han, J., Liu, J.-N., and Shu, D.-G. (2014). An early Cambrian agglutinated tubular lophophorate with brachiopod characters. *Scientific Reports*, 4:4682, doi:10.1038/srep04682.
- Zhang, Z.-F., Shu, D.-G., Emig, C. C., Zhang, X.-L., Han, J., Liu, J.-N., Li, Y., and Guo, J.-F. (2007b). Rhynchonelliformean brachiopods with soft-tissue preservation from the early Cambrian Chengjiang Lagerstätte of South China. *Palaeontology*, 50:1391–1402, doi:10.1111/j.1475-4983.2007.00725.x.
- Zhang, Z.-F., Shu, D.-G., Han, J., and Liu, J.-N. (2004). New data on the lophophore anatomy of Early Cambrian linguloids from the Chengjiang Lagerstätte, Southwest China. *Carnets de géologie (Notebooks on geology)*, 4:1–7, doi:10.4267/2042/310.
- Zhang, Z.-F., Shu, D.-G., Han, J., and Liu, J.-N. (2005). Morpho-anatomical differences of the Early Cambrian Chengjiang and Recent lingulids and their implications. *Acta Zoologica*, 86:277–288, doi:10.1111/j.1463-6395.2005.00211.x.
- Zhang, Z.-F., Shu, D.-G., Han, J., and Liu, J.-N. (2007c). A gregarious lingulid brachiopod *Longtancunella chengjiangensis* from the Lower Cambrian, South China. *Lethaia*, 40(1):11–18, doi:10.1111/j.1502-3931.2006.00002.x.
- Zhang, Z.-F., Smith, M. R., and Shu, D.-G. (2015). New reconstruction of the *Wiwaxia* scleritome, with data from Chengjiang juveniles. *Scientific Reports*, 5:14810, doi:10.1038/srep14810.
- Zhang, Z.-L., Skovsted, C. B., and Zhang, Z.-F. (2018). A hyolithid without helens preserving the oldest hyolith muscle scars; palaeobiology of *Paramicrocornus* from the Shujingtuo Formation (Cambrian Series 2) of South China. *Palaeogeography, Palaeoclimatology, Palaeoecology*, 489:1–14, doi:10.1016/j.palaeo.2017.07.021.

- Zhang, Z.-L., Zhang, Z.-F., and Wang, H.-Z. (2016). Epithelial cell moulds preserved in the earliest acrotretid brachiopods from the Cambrian (Series 2) of the Three Gorges area, China. *GFF*, 138(4):455–466, doi:10.1080/11035897.2016.1143528.
- Zhao, F.-C., Hu, S.-X., Caron, J.-B., Zhu, M.-Y., Yin, Z.-J., and Lu, M. (2012). Spatial variation in the diversity and composition of the Lower Cambrian (Series 2, Stage 3) Chengjiang Biota, Southwest China. *Palaeogeography, Palaeoclimatology, Palaeoecology*, 346–347:54–65, doi:10.1016/j.palaeo.2012.05.021.
- Zhao, F.-C., Smith, M. R., Yin, Z.-J., Zeng, H., Li, G.-X., and Zhu, M.-Y. (2017). *Orthrozanclus elongatus* sp. and the significance of sclerite-covered taxa for early trochozoan evolution. *Scientific Reports*, 7(1):16232, doi:10.1038/s41598-017-16304-6.
- Zhuravlev, A. Y., Wood, R. A., and Penny, A. M. (2015). Ediacaran skeletal metazoan interpreted as a lophophorate. *Proceedings of the Royal Society B: Biological Sciences*, 282(1818):20151860, doi:10.1098/rspb.2015.1860.
- Zimmer, R. L. and Woollacott, R. M. (2013). Metamorphosis, ancestrulae and coloniality in Bryozoan life cycles. In Woollacott, R. M. and Zimmer, R. L., editors, *Biology of Bryozoans*, pages 91–142. Elsevier.